Conf.-820940--

Proceedings of the Passive and Hybrid Solar Energy Update

September 15-17, 1982
Washington, D.C.

Sponsored by:
U.S. Department of Energy
Assistant Secretary, Conservation and Renewable Energy
Passive and Hybrid Solar Energy Division
Under Contract No. DE-AM03-76SF00700

November 1982

DO NOT MICROFILM
COVER

DISCLAIMER

This report has been reproduced directly from the best available copy.

Available from the National Technical Information Service, U. S. Department of Commerce, Springfield, Virginia 22161.

Price: Printed Copy A17
Microfiche A01

Codes are used for pricing all publications. The code is determined by the number of pages in the publication. Information pertaining to the pricing codes can be found in the current issues of the following publications, which are generally available in most libraries: *Energy Research Abstracts, (ERA); Government Reports Announcements* and Index (*GRA* and I); *Scientific and Technical Abstract Reports (STAR);* and publication, NTIS-PR-360 available from (NTIS) at the above address.

Conf.-820940
Dist. Category UC-59c

Proceedings of the Passive and Hybrid Solar Energy Update

CONF-820940--
DE83 007242

September 15-17, 1982
Washington, D.C.

Coordinated by:
MCC Associates, Inc.
Silver Spring, MD 20910

and

Rockwell International/ETEC
Canoga Park, CA 91304
Under Contract No. DE-AM03-76SF00700

Sponsored by:
U.S. Department of Energy
Assistant Secretary, Conservation and
Renewable Energy
Passive and Hybrid Solar Energy Division
Washington, D.C. 20585

November 1982

INTRODUCTION

Substantial progress is being made toward the development and utilization of passive and hybrid solar energy technologies through the combined efforts of the Federal government, the national laboratories, and private industry. The steady progress of the National Passive and Hybrid Solar Energy Program exhibited in the papers of these proceedings is important in realizing our national goal of conserving resources while meeting the energy needs of the United States.

This year's Update focused on five major topic areas of passive and hybrid solar technology. They were:

- Overview, Assessment & Planning
- Design & Analysis Tools
- Non-residential Buildings
- Residential Buildings
- Materials and Components

Significant progress was reported this year on fundamental heat transfer research concerning convective, radiative, and evaporative heating and cooling; on lighting technology; and on energy analysis tools such as the BLAST, DOE, and SERIRES computer programs. Advances in design methods, performance testing, manufactured buildings, materials and components, and information dissemination were also reported. On-going research and development efforts continue to address remaining technical challenges in the areas of passive cooling, improved collection and storage materials, and combined heating, cooling, and lighting systems in commercial buildings.

Appreciation is expressed to the many people whose dilligent efforts at all levels have contributed toward reaching the goals of this challenging national program.

The U. S. Department of Energy (DOE), Passive and Hybrid Solar Energy Division, gratefully acknowledges the efforts and support of key individuals, organizations, and contractors in the preparation for and conduct of the Passive & Hybrid Solar Energy Update and its proceedings.

Particular appreciation is expressed to Guy Ervin, III of Rockwell International/ETEC, whose organization was responsible for this year's Update, and to Marianne McCarthy and Janet Terner of MCC Associates, Inc., for their dedicated efforts in organizing the conference and preparing the proceedings for publication.

Special thanks is extended to all the speakers, moderators, and panelists who contributed their time and effort to the Update, and to all speakers and contractors who prepared papers for these proceedings.

Janet Neville
Program Manager
U. S. Department of Energy
San Francisco Operations

Blank Page

PROCEEDINGS

of the

PASSIVE & HYBRID SOLAR ENERGY UPDATE

September 15 - 17, 1982

Washington, D.C.

TABLE OF CONTENTS

SECTION 1: OVERVIEW, ASSESSMENT, AND PLANNING

SECTION 2: DESIGN & ANALYSIS TOOLS

SECTION 5: MATERIALS & COMPONENTS

ADDITIONAL PAPERS SUBMITTED FOR THE PROCEEDINGS

PROJECT SUMMARY

Project Title:	The Passive Solar Industries Council
Principal Investigators:	Robert Naismith Layne Ridley
Organization:	Potomac Energy Group 125 S. Royal Street Alexandria, Virginia 22314
Project Goals:	Provide a mechanism for dissemination of government and corporate-sponsored passive solar research results to building industry in format useable to various groups within the industry. Bring representatives of building industry together at meetings to evaluate and coordinate research and development programs of both industry and government. Widen industry knowledge and use of appropriate passive solar technology by distributing information and encouraging interaction among different sectors of the industry.
Project Status:	The Passive Solar Industries Council now includes 48 members from various sectors of the building industry, including major trade associations representing builders, designers, craftsmen, manufacturers, distributors and others; large private corporations now developing passive solar products or refining current products for passive solar applications; small businesses manufacturing and marketing passive solar products; and independent professionals involved in passive solar products and/or services. PSIC publishes a monthly newsletter reporting on passive solar projects, research, programs and issues, and an information series, Passive Solar Trends, consisting of reports on passive solar technology, markets, cost-and-performance studies, case histories, and analysis of issues of concern to passive solar industry. Most information in the series derives from government-sponsored research, and ensures the transfer of this information to a broad industry audience. PSIC has assembled a library of DOE-sponsored passive solar research results, as well as information about passive solar from a variety of sources. PSIC meetings bring together representatives from the many diverse sectors of the industry. The PSIC Membership Directory, now being updated, describes the passive solar involvement of Council members, and incorporates an Industry Status Report.
Contract Number:	DE-AC02-81C S30635
Contract Period:	September 25, 1981 through September 24, 1983
Funding Level:	$180,023
Funding Source:	Department of Energy through Chicago Operations Office

PROJECT SUMMARY

Project Title:	Potential Benefits of Fundamental Research for Passive Solar Heating and Cooling
Principal Investigator:	Donald A. Neeper
Organization:	Solar Energy Group, MS K571 Los Alamos National Laboratory Los Alamos, NM 87545
Project Goals:	Determine if it is physically reasonable to attempt to double the contribution that can now be derived from the natural environment for the energy needs of buildings. Determine if there is opportunity for fundamental effort on high-technology materials, control of radiation, and enhancement of heat transfer, the results of which could create a quantum advance in building science.
Project Status:	This project was conducted separately from our research efforts that will be reported in the proceedings of this conference. Although FY-82 efforts on this project are complete and the final report has been published, we expect to continue broad-based calculational studies of the type initiated in this project, in order to provide guidance to research. Los Alamos reviewed the environmental resources for heating and cooling skin-dominated buildings. We calculated the thermal performance benefits that could result from improved heat transfer, high-resistance glazings, optically switchable glazings, and thermal storage in interior wall surfaces. The results indicate that the environment provides an adequate resource for major energy needs of buildings, but that new materials and methods are needed for capture and control of the energy.
Contract Number:	W-7504-ENG-36
Contract Period:	October 1, 1981 through September 30, 1982
Funding Level:	This project not funded separately. The sum of all Los Alamos work in FY 82 was $1600 K.
Funding Source:	Division of Passive and Hybrid Solar Energy, U.S. Department of Energy

LOS ALAMOS NATIONAL LABORATORY SOLAR PROGRAM*

S. K. Reisfeld and D. A. Neeper
Los Alamos National Laboratory
Solar Energy Group
Los Alamos, New Mexico

ABSTRACT

Progress is reported for passive solar tasks performed at the Los Alamos National Laboratory during FY 1982. Passive Solar Design Handbook, Vol. Three is in publication and the cooperative project on Vol. Four, expected to be published as an American Society for Heating, Refrigerating, and Air-Conditioning Engineers (ASHRAE) manual, Passive Solar Heating Analysis, is nearly complete.

Results on test cell experiments for the 1981-82 winter are reported, as are Class A performance monitoring, passive cooling, both residential and commercial economic cooling assessments, and thermal effects of distributed mass in passive buildings.

SUMMARY

The new document, Passive Solar Heating Analysis, to be published and distributed by ASHRAE, is nearly ready for that organization's review. Important new material and graphics have been integrated with the text material from Passive Solar Design Handbook, Vol. Two and Vol. Three.

Test cell data from the 1981-82 heating season has been analyzed, evaluated, and will soon appear in report form. Important conclusions include the benefits of selective surfaces on thermal storage walls, promising new commercial glazing results, and comparison of forced and natural air convection.

A study was conducted to assess the impact of passive heating strategies on summer cooling load. We considered 15 passive systems, 4 building construction types, and 2 load collector ratios in 4 cities representing 4 distinct climate types.

Considering thermal performance of mass throughout a passive building, we find that the distribution of massive elements can have a significant effect on the building's performance, even if those elements are not sunlit. Viewed in terms of total heat capacity (thc) and diurnal heat capacity (dhc), directly illuminated by sunlight (direct) or in a remote area (indirect), we find that although thc is always greater than the dhc, in terms of annual heating energy savings, the dhc is two to four times as important as the thc.

Los Alamos, as coordinator of the Class A Performance Evaluation Program, has devised the plan for validation of data, for development and testing of a general validation technique, and for collection, analysis, and archiving of Class A data. Nine test facilities are included in the passive heating network; four facilities are a part of the passive cooling program. We have received and analyzed data from the NBS facility and from the Lo-Cal House; site manuals describing in detail the construction and instrumentation of these two sites have been written and will soon be available for distribution.

The Building Energy Design Tools Development Council, on which we serve as a cochairman, has written a proposal for funding by DOE to carry out its purpose of collaborative reivew, evaluation, and development of new building energy design tools.

We performed economic studies of residential cooling potential on both the microlevel and the macrolevel as a part of the Lawrence Berkeley Laboratory-led Commercial Buildings Cooling Assessment. Additional work in the commercial buildings cooling project included a technical assessment of the evaporative cooling strategy. We modified the DOE-2 building energy analysis code to simulate two office buildings (10,000 ft^2 and 100,000 ft^2) for 11 US climate zones.

INTRODUCTION

Los Alamos work in passive solar systems began in 1976 with the use of small test boxes and one pair of test rooms. The studies were undertaken to examine our conviction that age-old passive methods of heating and cooling buildings could become well understood, that performance could be optimized, and that the technology itself could be placed on a firm engineering foundation.

We use small test boxes and rooms to provide a simple, inexpensive means of evaluating individual concepts, techniques, geometries, materials, and entire systems. More recently our work has focused on

*Work sponsored by the US Department of Energy, Office of Solar Heat Technologies.

developing numerical models and computer codes by which builders and architects can predict the performance of many styles of passive buildings in any US location. Test room results provide the precise measured data against which we can validate these theoretical models.

PASSIVE SOLAR DESIGN HANDBOOK, VOL. FOUR

This task, despite its title, will not result in another passive design handbook. With the assistance of a technical writing subcontractor, the Los Alamos authors and a review committee from ASHRAE, have extracted the most valuable portions of Passive Solar Design Handbook Vol. Two and Vol. Three, added additional, new material and graphics, and developed a new, well ordered document. The result will be a manual, Passive Solar Heating Analysis, to be published and distributed by ASHRAE as a part of their collection of technical manuals.

SOLAR PERFORMANCE AND HEAT TRANSFER COEFFICIENTS OF ADVANCED SYSTEMS

Introduction

Los Alamos has been operating passive solar test cells since 1976 in its research program aimed at better understanding of and optimization of passive solar components and buildings. Previous data have been presented in Refs. 1-7. Research emphasis during the 1981-82 winter centered on strategies to reduce heat loss including selective surfaces, two commercially available "superglazings," a heat pipe system, and convection suppression baffles.

There are 14 test cells, built in 7 side-by-side pairs, with a dividing insulated wall. Deliberately designed to have little thermal mass of their own, the cells derive their thermal storage mass from the added solar feature: Trombe wall, water wall, or internal direct gain concrete blocks. Table 1 shows the configuration of each cell for the 1981-82 heating season.

TABLE 1

CONFIGURATION OF TEST CELLS
1981-82

Cell 1.	Reference flat black Trombe wall, double glazed. Unchanged from 1980-81.
Cell 2.	Selective surface Trombe wall. Rebuilt since last year with a commercial fiberglass-filled masonry plaster on the south face to provide a smooth surface for bonding to the selective foil.
Cell 3.	Sunspace with fan-forced circulation to the cell, controlled by thermostats.
Cell 4.	Sunspace with natural circulation through vents. The top vent had a backdraft damper.
Cell. 5.	Crimsco water wall, selective surface, single glazed. Unchanged since 1981-82.
Cell 6.	Absorbing wall of Boardman tubes of phase-change material, selective surface, double glazed.
Cell 7.	Flat black Trombe wall with Weathershield Quad pane® glazing (uses two layers of 3M high-transmission plastic film).
Cell 8.	Flat black Trombe wall with triple glazing of one layer of Heat Mirror® between two layers of glass (manufactured by Empire Glass of Spokane).
Cells 9 and 10.	US Navy experiment.
Cell 11.	Direct gain, double glazed. Half of the mass removed since 1980-1981, reducing the mass area/collector area ratio from 6 to 3.
Cell 12.	Unvented reference Trombe wall until February when sloped louvers of high-transmission film were added between Trombe wall and the glazing to suppress convection.
Cell 13.	Nonsolar reference cell.
Cell 14.	Battelle heat pipe collector, unchanged since 1980-1981. Two heat pipes inoperable; double glazed.

Operation

Approximately 179 data channels recorded measurements from thermocouples, pyranometers, auxiliary heat, and weather instruments. Hourly averages of each value and instantaneous data were recorded on tape, transferred to computer disk, and stored for analysis.

Because we required an accurate value of the net load coefficient (NLC) for each cell, at the end of the testing period, we covered the apertures of all cells except 9, 10, and 13 with 4 in. of expanded polystyrene insulation to measure heating loads simultaneously. NLC's were calculated from

$$NLC = (S)(AUX - CLC \cdot DTN)/(S)DTO,$$

where

(S) denotes hourly summation over the specified time period,
AUX is the auxiliary heat required for the hour,
CLC is the heat transfer coefficient between two adjacent cells (3.5 Btu/°F-h),
DTN is the difference between the globe temperatures of the cell in question and the adjacent cell, and
DTO is the difference between the globe temperature of the cell in question and the outside dry-bulb temperature.

The resulting NLC's are shown in Table 2. Units are Btu/°F-h.

TABLE 2

POSTSEASON MEASURED NLC'S

CELL	NLC	CELL	NLC	CELL	NCL
1	21.5	5	22.0	11	22.9
2	22.9	6	21.4	12	22.0
3	23.9	7	24.1	13	21.0
4	24.6	8	21.9	14	22.7

Auxiliary heat was provided by two 500 W light bulbs in each cell; each cell was allotted two data channels for auxiliary power measurements. An online computer turned on the auxiliary heat when the globe temperature fell below the set point temperature and one data channel indicated the amount of heating from the length of time the computer requested auxiliary power.

Analysis

We calculated front loss coefficients for the Trombe wall test cells using measured mass wall temperatures;[8,9] each loss coefficient (see Table 3) is an average of data from at least 75 days (including 11 nighttime hours per day).

TABLE 3

MEASURED LOSS COEFFICIENTS, 1981-1982
Units: Btu/ft^2-h-°F

Cell	Glazing and Surface	U Avg	U Theoretical	U Advertised
1	Double-FB	0.41	0.41 - 0.47	
12A	Double-FB	0.40	0.41 - 0.47	
2	Double-selective	0.28	0.26 - 0.29	
7	Quad pane®	0.34	0.24 - 0.41	0.26
8	Heat Mirror®	0.24	0.21 - 0.23	0.23
12B	Double-louver	0.34	0.36 - 0.41	

A summary of results for the 1981-82 heating season is shown in Table 4. The third performance measure is the discomfort index, described in Ref. 10. Units of discomfort index are °F • °F. Because this is a measure of discomfort, a zero value indicates that a person would be perfectly comfortable; a doubling of DI indicates that the individual would be roughly twice as uncomfortable. See Table 4 for efficiencies, solar fractions, and discomfort values, and Figs. 1 and 2 for average useful efficiencies. See Ref. 11 for a complete discussion of conclusions.

TABLE 4

RESULTS FOR 1981-82

Cell	Useful Efficiency, %			Useful Solar Fraction, %			Discomfort Index (°F)[2]		
	P1	P2	P3	P1	P2	P3	P1	P2	P3
1	21	24	23	26	48	42	1	8	11
2	33	31	31	40	57	54	1	4	5
3	–	30	32	–	54	53	–	16	19
4	–	30	30	–	51	50	–	21	16
5	38	32	32	48	62	59	3	10	5
6	40	34	34	51	67	63	5	9	5
7	35	32	33	41	56	55	2	3	3
8	23	26	25	28	51	45	1	3	2
11	21	22	21	25	39	36	49	50	36
12	25	–	25	32	–	47	2	–	11
14	37	27	26	45	48	45	2	5	4

[d]P1 refers to Period 1, etc.

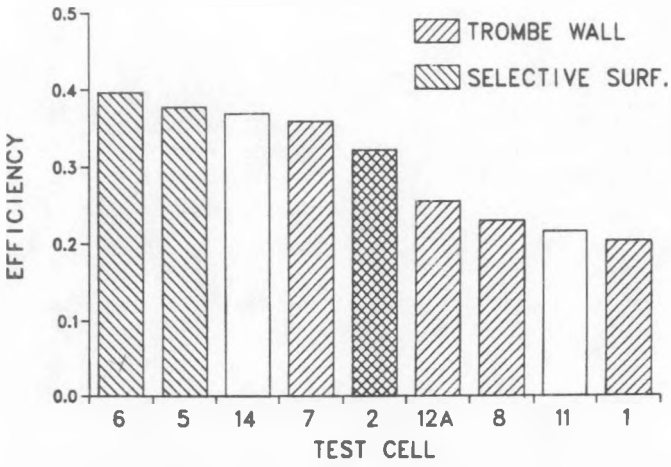

Fig. 1. Average useful efficiency, 1/12/82 to 2/25/82.

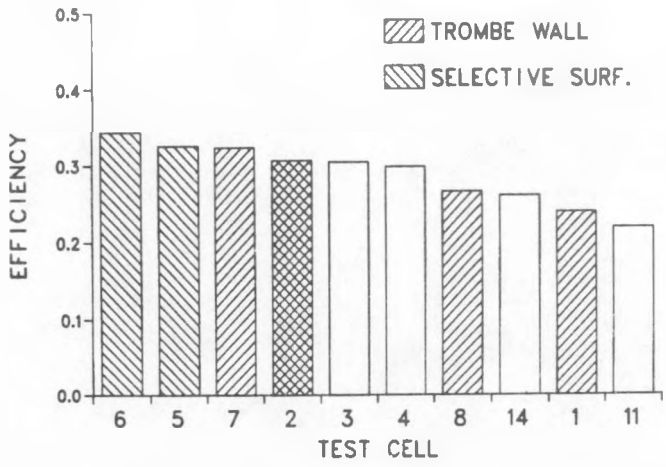

Fig. 2. Average useful efficiency, 2/26/82 to 3/22/82.

PASSIVE COOLING

We have undertaken this task to assess the impact of passive heating strategies on the summer cooling load and to evaluate the benefits of various schemes for control. The energy delivered passively to a building depends on other thermal energy flows in that building; we are focusing on the interactions between a passive solar system and the structure with which it is integrated. Before beginning this study, we investigated the general reduction of insolation on south-facing vertical walls by the use of fixed overhangs. The decrease in insolation correlates with the value L-D (latitude minus midmonth declination) and with the clearness index.

In the current study, we treat such passive system components as shades, drapes, overhangs, and vents in Trombe walls and sunspaces as features that reduce the incremental cooling load imposed by the passive heating system.

We considered 15 passive systems: 5 direct gain systems, 5 Trombe wall designs, and 5 sunspace systems. Four structural types -- low mass, frame construction with floor slab, high mass, and a reference house with no solar features and normal window area -- were covered. We use two load collector ratios obtained by varying the area of the solar aperture. Various combinations of these variables were studied in four cities, El Paso, Charleston, St. Louis, and Chicago, representing four climate zones. A typical output graph is seen in Fig. 3.

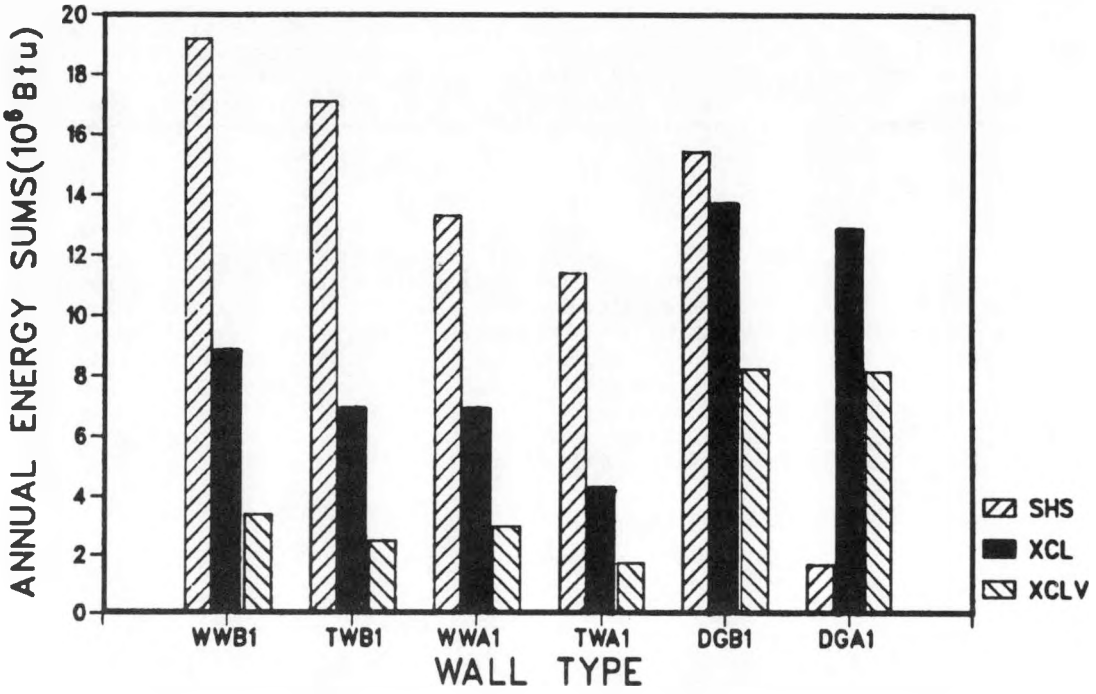

Fig. 3. Annual heating load reduction and cooling load penalties associated with a low mass passive solar building with fixed overhang in St. Louis.

For this case we have a low mass (frame construction) building with a fixed overhang located in St. Louis. The six cases represented on the graph are:

WWB1 - water wall with selective surface,
TWB1 - Trombe wall with selective surface,
WWA1 - water wall with flat black surface,
TWA1 - Trombe wall with flat black surface,
DGB1 - direct gain with night insulation,
DGA1 - direct gain with no night insulation.

The cross-hatched bar on the left in each set of three gives the amount of heat saved by the passive solar building relative to an identical reference building except for the passive solar features. The second bar, the solid one, gives the incremental cooling load caused by the presence of the passive solar features where no ventilation is allowed to occur. Finally, the cross-hatched bar on the right gives the incremental cooling load when ventilation is employed to reduce the indoor temperature whenever the outside ambient temperature is low enough. Note that the difference in height between the cross-hatched bar on the left and the cross-hatched bar on the right gives the net energy savings for the system represented by the bars. The systems presented in Fig. 3 are ranked from left to right in order of decreased energy savings. Note for example that the water wall with a selective surface has the highest net savings for a low mass building in St. Louis and that the direct gain building with no night insulation is a net loser, that is, the net savings is negative.

A comprehensive final report on the type of results presented in the section above will be available at the end of FY 1982.

THERMAL EFFECTS OF DISTRIBUTED MASS

We studied the effectiveness and performance contribution of mass that is distributed throughout a passive building in zones that are convectively coupled to passively heated or cooled zones. Quantitative estimation of these effects will help in measuring temperature swings in remote rooms and in determining the value of storage mass that is unlit by the sun.

Building elements have two types of heat capacity: total heat capacity (thc) and diurnal heat capacity (dhc). The thc represents the energy needed to raise the temperature of the entire buiding element (such as a wall) by one degree; the dhc is a measure of the ability of that same element to absorb and release heat during a 24-hour cycle.

The dhc is classified as direct if the surface is illuminated by direct or scattered solar radition or by reradiated infrared radiation from objects in the sunlight. If all heat transfer is by convection through air, the dhc is classified as indirect. Table 5 shows heat capacities (both dhc and thc) of concrete blocks with various cores.

We have found that the range of naturally occuring U-values (0.75 - 1.5 Btu/ft^2-°F-h) is adequate to permit use of indirect masonry surfaces up to 2 in. thick. U-values below 0.5 negate any benefit of such thermal storage. The dhc is always less than the thc and, likewise, indirect dhc is always less than direct dhc. However, viewed in terms of annual heating energy savings, the dhc is two to four times as important as the thc.

RESIDENTIAL BUILDING ANALYSIS

The objective of this task has been twofold: (1) to provide DOE, its contractors, and industry with a credible assessment of the economic and market potential for passive solar cooling technologies; and (2) to complete the economic analysis of optimal strategies for passive solar heating, cooling, and conservation, for a large number of geographic regions in the US. The approach has centered on several major subtasks: (1) revision of the existing region-specific housing data base to include information on cooling; (2) update of fuel prices to reflect 1981/82 conditions; (3) modification of the EASE III analysis code to include both conservation and cooling optimization capabilities; (4) collection of data on the physical performance of selected passive solar cooling technologies (rather unsuccessful to date); and (5) actual assessments of the economic feasibility and market attractiveness of passive solar strategies.

TABLE 5

HEAT CAPACITIES OF VARIOUS CONCRETE MASONRY UNITS

Case	Exterior or Interior Wall	Heat Capacity, Btu/°F-ft^2 Direct dhc	Indirect, dhc	Total, thc
Solid				
6 in.	Exterior	10.74	4.22	13.70
6 in.	Interior	6.72	4.04	6.85
8 in.	Exterior	10.79	4.06	18.58
8 in.	Interior	8.72	4.25	9.29
Hollow				
6 in.	Exterior	6.05	3.31	8.04
6 in.	Interior	3.99	3.01	4.02
8 in.	Exterior	6.07	3.27	9.28
8 in.	Interior	4.50	3.06	4.64
With Sand Fill				
6 in.	Exterior	7.25	3.59	11.52
6 in.	Interior	5.64	3.72	5.76
8 in.	Exterior	6.98	3.48	15.02
8 in.	Interior	6.83	3.83	7.51
With Grout Fill				
6 in.	Exterior	10.26	4.15	13.38
6 in.	Interior	6.56	4.00	6.69
8 in.	Exterior	10.11	3.98	18.04
8 in.	Interior	8.44	4.21	9.02

Assumptions: CMU density = 140 lb/ft^3.
Grout density = 130 lb/ft^3.

The actual thickness of a 6-in. wall is 5.62 in.
The actual thickness of an 8-in. wall is 7.62 in.

Figure 4 highlights the results of a preliminary examination of the cooling potential of a forced ventilation passive solar cooling concept of fixed design (water wall with a fan, for example). First year fuel savings in one's electric bill from reductions in cooling loads varies greatly, with the higher values generally in the southern portion of the country (higher cooling loads). However, when the heating contribution is taken into account, a different pattern emerges. Figure 5 portrays the per cent reduction in the annual aggregate fuel bill (electric for cooling, natural gas for heating) that would result from adoption of a forced ventilation technology. The reductions are substantial for many regions; allowable solar costs for such a system are shown in Fig. 6. These costs represent the maximum allowable solar add-on costs that would allow the home owner to recover his investment, with offset fuel savings, over a 30-year period.

CLASS A PERFORMANCE MONITORING

Background

A major objective of the Class A Performance Evaluation Program is to collect, analyze, and archive detailed test data for the rigorous validation of analysis/design tools used for passive solar research and design. In the fall of 1981, the Los Alamos National Laboratory assumed responsibility for coordinating and executing the Class A performance evaluation activities of the DOE Passive and Hybrid Solar Energy Program. Elements of the Class A validation plan can be seen in Ref. 12, Fig. 1, as well as a detailed description of the program. Although the initial thrust involves test cells, small unoccupied test buildings, and a residence, the program is expected to be expanded later to include commercial buildings and other test facilities.

Approach

The plan for Class a validation includes the following four elements.

(1) Data-needs definition and matching with available or needed test facilities;

(2) Development and testing of a general validation methodology;

(3) Collection, analysis, and archiving of Class A test data for

- full-program validation,
- component/algorithm validation,
- performance evaluation; and

(4) Program management.

Available and Needed Facilities. At present, nine test facilities or buildings are in the Class A network. Class A level data are being taken at several other facilties, both within and outside of DOE sponsorship. Data from these other facilities are being reviewed and compared with the data needs for a balanced program; those facilities found to be appropriate will later be

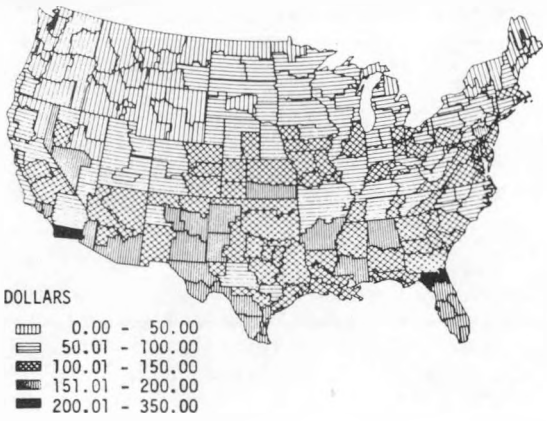

Fig. 4. Forced ventilation dollar value first year fuel savings.

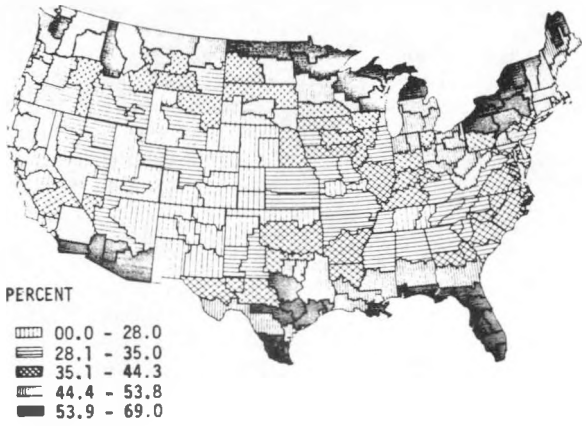

Fig. 5. Percent reduction in annual fuel bill displacement by natural/forced ventilation using electricity for cooling and natural gas for heating.

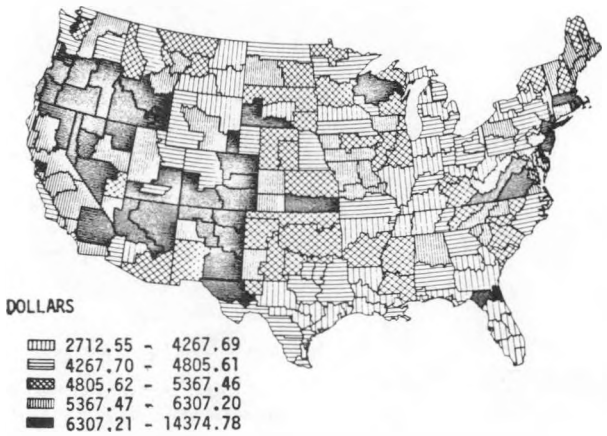

Fig. 6. Maximum allowable solar costs displacement by natural/forced ventilation using electricity for cooling and natural gas for heating.

included in an expanded Class A network. A complete list of the test facilities and detailed explanation of the entire program can be found in Ref. 12.

BUILDING ENERGY DESIGN TOOLS DEVELOPMENT COUNCIL

This council, made of up representatives from industry, professional, and research organizations, has as it's purpose the collaborative review, evaluation, and development of new building energy design tools. Los Alamos acts as cochairman of the technical review subcommittee; there are also subcommittees on developer/user interactions, information dissemination and operations and planning.

Three tasks have been undertaken by the Council:

(1) assessing the state of the art in building design tools;
(2) testing the technical capabilities of design tools by developing standard test procedures, testing selected tools, and reporting findings to DOE and to industry; and
(3) analyzing use of the tools through developing test problems, selecting expert users, and reporting guidelines.

The Council has written a proposal and submitted it to DOE for funding the program described here.

COMMERCIAL BUILDING COOLING ASSESSMENT

The objective of this work has been to provide DOE, its contractors, and the industry with a credible assessment of the economic and market potential for passive solar cooling technologies in the commercial buildings sector. In pursuit of this objective, major efforts were devoted to the Passive Solar Cooling Assessment (PSCA). Much of the analyses and supporting data bases are now part of the PSCA documents prepared by Lawrence Berkeley Laboratory and Whiddon and Associates for DOE. Detailed regional analysis of the economic attractiveness for each selected cooling technology and building application (office buildings only, at present) has been completed, with that analysis supporting some general observations on a national overview of both current and future passive solar cooling potential.

Figure 7 highlights the additional costs that may be incurred for small office buildings, for the given level of energy savings (expected dollar reductions in annual electric bills). The investment targets ($/ft^2 of building and set off by brackets) establish maximum expenditures for the passive solar cooling technology, night ventilation in this example. Considerable difference exists among the climate centers in both annual electric bill savings and the associated investment targets. The numbers in parentheses represent the percentage increase to recent building costs that these investment targets would add, if adopted. However, the fuel bill savings in concert with normal depreciation and the solar tax incentives (both income credits and accelerated state depreciation schedules) would just offset this amount. The relatively high values in California are caused by a rather healthy set of solar incentives.

Fig. 7. Map of measures of economic attractiveness for a nighttime ventilation cooling strategy in new one-story commercial office buildings.

PROGRAM ANALYSIS (COOLING ASSESSMENT)

This task, described in part in the section immediately above, was characterized by the assessment of various cooling systems and techniques by a multidisciplinary team assembled from several national laboratories and contractors. Systems under evaluation included load management, ventilative cooling, evaporative cooling, radiative cooling, earth-contact cooling, and dehumidification. In addition to the economic analyses, Los Alamos' efforts consisted of commercial buildings technical assessment for evaporative and earth-contact cooling systems at the individual building level; only the evaporative systems work is completed.

We simulated a single story (10,000 ft^2) and a multistory (100,000 ft^2) office building for 11 US climate zones including values for solar radiation, dry-bulb temperature, and humidity. The evaporatively cooled buildings have either a direct system (air washer type) or a combination direct and indirect system (heat exchanger); a vapor-compression system is used for auxiliary cooling. A maximum relative humidity of 70% was maintained in the occupied spaces; the greater of the energy savings resulting from a 55 or 60°F cold-deck temperature was reported. Results of the study are presented in Tables 6 and 7 for the single story and multistory buildings, respectively.

Preliminary economic benefit figures were computed for the energy saved by use of evaporative cooling. Assuming the cost for electricity to be \$15.00/10^6 Btu and ignoring electric demand, the evaporative cooling potential in 6 of the 11 climate zones for the single story office building justifies an investment of either \$1,500 or \$2,000 for the direct and direct/indirect evaporative cooling equipment, respectively. These investments yield a simple payback in less than 5 years. Similarly, the evaporative cooling potential for the 10-story building in 5 of the climate zones justifies an investment of either \$5,000 or \$7,500, respectively. Thus, evaporative cooling is a very promising technology if equipment costs are kept below the cost goals indicated above.

PASSIVE SOLAR PUBLICATIONS, FY 1982

R. W. Jones, "Summer Heat Gain Control in Passive Solar Heated Buildings: Fixed Horizontal Overhangs," International Passive and Hybrid Cooling Conference, Miami Beach, Florida, November 11-13, 1981. (LA-UR-81-2297)

J. D. Balcomb, "Heating Remote Rooms in Passive Solar Buildings," International Solar Energy Society Solar World Forum, Brighton, England, August 23-28, 1981. (LA-UR-81-2518)

J. C. Hyde, "Passive Test Cell Experiments During the Winter of 1979-80," Los Alamos National Laboratory report LA-9048-MS. (September 1981)

R. D. McFarland, W. O. Wray, J. D. Balcomb and R. W. Jones, "New Solar Load Ratio and Solar Radiation Correlations," presented at the Showcase for Technology, Albuquerque, New Mexico, October 28-30, 1981. (LA-UR-81-3114)

J. D. Balcomb, "Stratification in Hot Water Tanks," submitted to The Sunpaper of the New Mexico Solar Energy Association. (LA-UR-82-423)

J. D. Balcomb, R. W. Jones, R. D. McFarland, and W. O. Wray, "Performance Prediction of Passive Solar Heated Buildings by the Solar Load Ratio Method," submitted to Passive Solar Journal. (LA-UR-82-670 Revised)

J. D. Balcomb, "Passive Solar Concepts for Multistory Buildings," Proc. of the 1982 Annual Meeting, American Section of the International Solar Energy Society, Houston, Texas, June 1-5, 1982 (American Solar Energy Society, Newark, Delaware, 1982) (LA-UR-82-878).

G. J. Schoenau, "Thermal Performance of East-West Windows in Passive Solar Buildings," Los Alamos National Laboratory report internal report LA-UR-82-904 (May 1982).

J. D. Balcomb, "Heat Storage Effectiveness of Concrete Masonry Units," Concrete Masonry Solar Architecture Quarterly of the National Concrete Masonry Association, May 1982 (LA-UR-82-966).

B. D. Hunn, "Recommended Design Improvements for the Hunn Solar-Heated Residence," submitted to The Sunpaper of the New Mexico Solar Energy Association. (LA-UR-82-997)

R. D. McFarland, "Passive Test Cell Data for the Solar Laboratory, Winter 1980-81," Los Alamos National Laboratory report LA-9300-MS (May 1982).

J. L. Peterson and B. D. Hunn, "The Application of DOE-2 in the Predesign Phase of Commercial Building Design," Renewable Challenge Solar Technologies Conference and International Exposition, Houston, Texas, June 1-5, 1982. (LA-UR-82-989)

TABLE 6

EVAPORATIVE COOLING POTENTIAL
COLD DECK TEMPERATURE = 60°F RH = 70%
SINGLE-STORY OFFICE

City	Cooling Consumption Base Building (10^6 Btu)	Cooling of Energy Saved (10^6 Btu)		% Cooling Energy Saved	Electric Demand Base Building (kW)	Electric Demand Saved (kW)		% Electric Demand Saved
		Dir	Dir/Ind			Dir	Dir/Ind	
Atlanta	133.8	9.9	14.4	10.8	63.9	-0.3	-0.6	-0.9
Denver	71.0	25.1	29.7	41.8	53.9	0.9	2.3	4.3
Detroit	89.7	14.8	18.2	20.3	59.2	0.0	0.0	0.0
Fort Worth	158.0	20.9	25.2	15.9	66.8	-0.3	-0.3	-0.4
Fresno	146.8	22.8	38.5	26.2	63.0	0.0	-3.2	-5.1
Houston	189.7	4.7	7.0	3.7	67.1	0.9	0.0	0.0
Los Angeles	104.1	19.6	30.8	29.6	53.0	-0.9	3.8	7.2
Minneapolis	91.7	17.2	21.2	23.1	62.1	0.6	0.6	1.0
New York	93.4	11.8	16.2	17.3	59.5	-0.3	-0.3	-0.5
Phoenix	197.2	19.7	40.9	20.7	67.4	-0.3	-3.8	-5.6
Seattle	62.9	18.6	27.3	43.4	48.9	0.0	6.7	13.7

RH = relative humidity.

TABLE 7

EVAPORATIVE COOLING POTENTIAL
COLD DECK TEMPERATURE = 55°F RH = 70%
TEN-STORY OFFICE

City	Cooling Consumption Base Building (10^6 Btu)	Cooling of Energy Saved (10^6 Btu)		% Cooling Energy Saved	Electric Demand Base Building (kW)	Electric Demand Saved (kW)		% Electric Demand Saved
		Dir	Dir/Ind			Dir	Dir/Ind	
Atlanta	1119.7	22.9	58.2	5.2	642.3	-3.5	-3.5	-0.5
Denver	694.2	111.3	162.7	23.4	594.5	39.3	58.0	9.8
Detroit	840.4	66.8	105.0	12.5	641.4	0.9	2.1	0.3
Fort Worth*	1317.4	53.5	84.0	6.4	720.5	-26.1	-28.1	-3.9
Fresno*	1273.1	115.5	279.0	21.9	675.9	-32.2	-36.3	-5.4
Houston	1732.2	16.2	43.5	2.5	697.6	2.6	-23.1	-3.3
Los Angeles*	790.0	51.1	107.4	13.6	550.8	-18.2	25.8	4.7
Minneapolis	801.1	33.9	67.5	8.4	624.1	-0.6	0.0	0.0
New York	816.2	29.4	63.5	7.8	598.6	0.0	0.6	0.1
Phoenix	1902.8	154.6	349.6	18.4	755.6	-5.6	12.0	1.6
Seattle*	517.1	54.0	97.6	18.9	512.7	-6.4	56.8	11.1

*Cold deck temperature = 60°F.
RH = relative humidity.

B. D. Hunn, W. V. Turk, and W. O. Wray, "Validation of Passive Solar Analysis/Design Tools Using Class A Performance Evaluation Data," Seventh National Passive Solar Conference, Knoxville, Tennessee, August 29 - September 1, 1982. (LA-UR-82-1732)

R. W. Jones, "Passive Solar Design Handbook," submitted to the Newsletter of the New England Solar Energy Association. (LA-UR-82-1577)

R. W. Jones, "Monitored Passive Solar Buildings," Los Alamos National Laboratory report LA-9420-MS.

R. W. Jones, Ed., J. D. Balcomb, C. E. Kosiewicz, G. S. Lazarus, R. D. McFarland, and W. O. Wray, Passive Solar Design Handbook, Volume Three, (US Department of Energy, Washington, DC, 1982), in print.

E. F. Moore and R. D. McFarland, "Passive Solar Test Modules," Los Alamos National Laboratory report LA-9421-MS (June 1982).

D. A. Neeper and R. D. McFarland, "Some Potential Benefits of Fundamental Research for the Passive Solar Heating and Cooling of Buildings," Los Alamos National Laboratory report LA-9425-MS.

R. D. McFarland, R. W. Jones, and G. S. Lazarus, "Annual Performance of Sunspace-Type Passive Solar Collectors," Los Alamos National Laboratory report (in print).

J. D. Balcomb, "Passive Solar Heating Research," to be included in Advances in Solar Energy, edited by Donald Watson.

S. K. Reisfeld and D. A. Neeper, "Solar Energy Research at Los Alamos: January 1 - March 31, 1981," Los Alamos National Laboratory report LA-9470-PR.

S. K. Reisfeld and D. A. Neeper, "Solar Energy Research at Los Alamos: April 1 - September 30, 1981," Los Alamos National Laboratory report LA-9473-PR.

S. K. Reisfeld and D. A. Neeper, "Solar Energy Research at Los Alamos: October 1, 1981 - March 31, 1982," Los Alamos National Laboratory report LA-9474-PR.

REFERENCES

1. R. D. McFarland, "Passive Test Cell Data for the Solar Laboratory, Winter 1980-81," Los Alamos National Laboratory report LA-9300-MS (May 1982).

2. J. D. Balcomb, R. D. McFarland, and S. W. Moore, "Passive Testing at Los Alamos," Proc. of the Second National Passive Solar Conference, Philadelphia, Pennsylvania, March 16-18, 1978 (American Section of the International Solar Energy Society, Newark, Delaware, 1978), 2, pp. 602-609. (LA-UR-78-1158)

3. J. D. Balcomb, R. D. McFarland, and S. W. Moore, "Simulation Analysis of Passive Solar Heated Buildings - Comparison with Test Room Results," Proc. of the American Section of ISES, 1977 Annual Meeting, Orlando, Florida, June 6-19, 1977 (American Section of the International Solar Energy Society, Cape Canaveral, Florida, 1977), 1, Sec. 11, pp. 1-4. (LA-UR-77-939)

4. J. C. Hyde, "Passive Test Cell Experiments During the Winter of 1979-80," Los Alamos National Laboratory report LA-9048-MS (September 1981).

5. W. O. Wray and C. R. Miles, "A Passive Solar Retrofit Study for the United States Navy," Proc. of the Sixth National Passive Solar Conference, Portland, Oregon, September 8-12, 1981 (American Section of the International Solar Energy Society, Newark, Delaware, 1981), pp. 773-777. (LA-UR-81-2200)

6. W. O. Wray, C. R. Miles, and C. E. Kosiewicz, "A Passive Solar Retrofit Study for the United States Navy," Los Alamos National Laboratory report LA-9071-MS (November 1981).

7. R. D. McFarland and J. D. Balcomb, "Los Alamos Test Room Results," Proc. of the Seventh National Passive Solar Conference, Knoxville, Tennessee, August 29 - September 1, 1982 (American Solar Energy Society, Newark, Delaware, 1982), to be published. (LA-UR-82-1836)

8. J. D. Balcomb and J. C. Hedstrom, "Determining Heat Fluxes from Temperature Measurements in Massive Walls," Proc. of the Fifth National Passive Solar Conference, Amherst, Massachusetts, October 19-26, 1980 (American Section of the International Solar Energy Society, Newark, Delaware, 1981), pp. 136-149. (LA-UR-80-2231)

9. J. D. Balcomb, "Dynamic Measurements of Heat Loss Coefficients Through Trombe Wall Glazing Systems," Proc. of the Sixth National Passive Solar Conference, Portland, Oregon, September 8-12, 1981 (American Section of the International Solar Energy Society, Newark, Delaware, 1981), pp. 84-88. (LA-UR-81-2223)

10. J. A. Carroll, "An Index to Quantify Thermal Comfort in Homes," Proc. of the Fifth National Passive Solar Conference, Amherst, Massachusetts, October 19-26, 1980 (American Section of the International Solar Energy Society, Newark, Delaware, 1980), pp. 1210-1214.

11. R. D. McFarland, J. C. Hedstrom, J. D. Balcomb, and S. W. Moore, "Los Alamos Test Cell Results for the 1981-82 Winter," Los Alamos National Laboratory report in print.

12. B. D. Hunn, W. V. Turk, and W. O. Wray, "Validation of Passive Solar Analysis/Design Tools Using Class A Performance Evaluation Data," Proc. of the Seventh National Passive Solar Conference, Knoxville, Tennessee, August 29-September 1, 1982 (American Solar Energy Society, Newark, Delaware, 1982), to be published. (LA-UR-82-1732)

PROJECT SUMMARY

Project Title: Passive Cooling Technology Assessment

Principal Investigators: R. Kammerud, W. Place, M. Martin, W. Whiddon, G. Hart, B. Hunn, F. Roach

Organizations: Lawrence Berkeley Laboratory
University of California
Berkeley, California 94720

W.I. Whiddon and Associates
Bethesda, Maryland 20814

Los Alamos National Laboratory
University of California
Los Alamos, New Mexico 87545

Project Goals: To estimate the relative effectiveness of passive cooling technologies (ventilation, evaporation, natural lighting, radiation, dehumidification, and ground coupling) in reducing auxiliary energy requirements for office buildings. This study was intended to aid in establishing research program priorities for FY 1983 and beyond.

Project Status: This project has been completed, though additional related systems analyses of passive cooling strategies are continuing. The results of both the assessment and supplementary studies will be presented.

Passive cooling technologies have not been developed to a level of sophistication comparable to passive heating. The reasons for this disparity include the fact that the cooling resources have not been thoroughly characterized, the cooling resources are relatively weaker, and the mechanisms for coupling the cooling system to the resource are more complicated. During the past three years, the cooling resource has become better understood and the coupling mechanisms have been researched. This has provided a vastly improved basis for comparative evaluation of the various cooling technologies.

A baseline, nonpassive office building has been subjected to total energy analyses in eleven U.S. climates in order to provide a basis for comparison and evaluation of the technologies. The building architecture or mechanical system design was then altered as appropriate to incorporate individual passive cooling strategies. The modified building was re-analyzed to determine the impact of the strategy on (1) building boundary energy consumption, and (2) peak electricity demand. The energy performance results were subjected to preliminary economic analysis in order to estimate cost goals and national impacts of the individual strategies.

The baseline results indicate that there is substantial climate sensitivity of energy consumption for heating and lighting, even for large office buildings, and that the focus of the research program should be on strategies addressing electric energy consumption and demand. The passive cooling strategies have varying effectiveness: natural lighting is a clear topic for research emphasis, while radiative cooling, ventilation cooling, and advanced evaporative cooling show somewhat lesser potential. Dehumidification and conventional mechanical evaporative cooling strategies show relatively less energy savings potential.

Contract Number: DE-AC03-76SF00098

Contract Period: 1 October 1981 through 15 June 1982

Funding Level: $75,000

Funding Source: Office of Solar Heat Technologies, Passive and Hybrid Solar Energy Division, U. S Department of Energy

PASSIVE COOLING TECHNOLOGY ASSESSMENT: SYNTHESIS REPORT

W. L. Carroll, T. L. Webster, A. Mertol, B. Andersson,
R. C. Kammerud, W. Place, M. R. Martin
Passive Research and Development Group
Lawrence Berkeley Laboratory
University of California
Berkeley, CA 94720

J.L. Peterson
Solar Energy Group
Los Alamos National Laboratory
University of California
Los Alamos, NM 87545

C.A. Mangeng, F. Roach
Economics Group
Los Alamos National Laboratory
University of California
Los Alamos, NM 87545

W.I. Whiddon
W.I. Whiddon & Associates
Bethesda, MD 20814

G.K. Hart
Hart, McMurphy & Parks
Bethesda, MD 20814

EXECUTIVE SUMMARY

This summary attempts to distill from the research recommendations made in the body of this report the salient issues and suggested research directions for passive cooling. The suggestions are intentionally generalized and qualitative; they belie the depth and richness of the energy and economic data bases for office buildings that have been developed during the course of this project.

The results of the passive cooling technology assessment suggest that the national passive program should:

- Assign passive cooling research priorities as follows:

  Priority 1: Natural lighting and cooling load control

  Priority 2: Evaporative and ventilation cooling

  Priority 3: Dehumidification

- Conduct analyses of the potential of radiative and earth contact cooling in order to ascertain their research priorities relative to those for the other technologies stated above.

- Seek synergistic combinations of natural lighting, passive heating, passive cooling, building structure, and auxiliary heating and cooling systems.

- Conduct research specifically directed at quantification of occupant comfort requirements under cooling conditions and for illumination.

- Emphasize strategies which reduce electric consumption and electric peak power demand for both buildings and utilities.

- Include assessments of the nature summarized here as a continuing element of the passive program. Technology synergies and residential and other commercial building types should be considered in any future technology assessment. Market penetration and economic analysis must be performed to translate building-specific information into results suitable for national energy policy decisions.

Finally, it is suggested that the passive program provide an environment conducive to creative advances in the conceptual state-of-the-art so that the full potential of natural heating, cooling, and lighting resources can be explored and, in time, reduced to practice.

1. INTRODUCTION

This assessment of passive cooling technologies has been carried out in order to provide a technically sound basis for evaluation of the relative merits of research and development activities in the individual technologies. The results presented herein represent an overview of detailed systems analyses conducted for four passive cooling strategies: natural lighting, evaporation, ventilation, and dehumidification. It is anticipated that the analyses can be extended to two additional generic technologies, ground contact and sky radiation, in the near future. Illustrative results from the analyses are presented in this report and are synthesized into a set of recommendations for future research directions. Specific results upon which these recommendations are based are presented in an extensive technical appendix (attached), which will be the source of a series of in-depth technical reports intended to provide more specific guidance for future research activities.

Until recently the cooling technologies have not been the subject of a comprehensive and coordinated research program. Environmental resources and microclimatic effects are not as well understood for passive cooling as they are for passive solar heating. As a result, cooling research has focused heavily on the development of resource data bases and on a fundamental understanding of the heat transfer and fluid mechanics that allow access to the resource. While these generic cooling research problems have not been solved, they have advanced to a stage which allows preliminary evaluation of the relative potentials of several technologies. Within this context, the specific goals of this assessment are:

- Identify those combinations of passive cooling technologies, buildings types, and climates most likely to produce significant reductions in energy use.
- Develop recommendations for research projects directed at achievement of these potentials.
- Conduct economic analysis to establish a preliminary indicator of economic feasibility.

This assessment has investigated energy consumption reductions for individual technologies as applied to specific buildings in specific climates. Standard building energy analysis techniques have been used. The results have been subjected to preliminary economic analyses. The results have also been extrapolated to a national scope from the 11 basic climate sites for which results were generated. The study has not dealt with residential buildings, commercial buildings other than office buildings, combinations of passive cooling systems, potential synergisms between passive heating and cooling strategies, integration of passive and conventional strategies, nor retrofit concepts. The research recommendations described later fully acknowledge the limitations inherent in the analysis.

II. METHODOLOGY

The cooling assessment investigated the interaction of three key variables: Passive Technology, Building Type, and Climate.

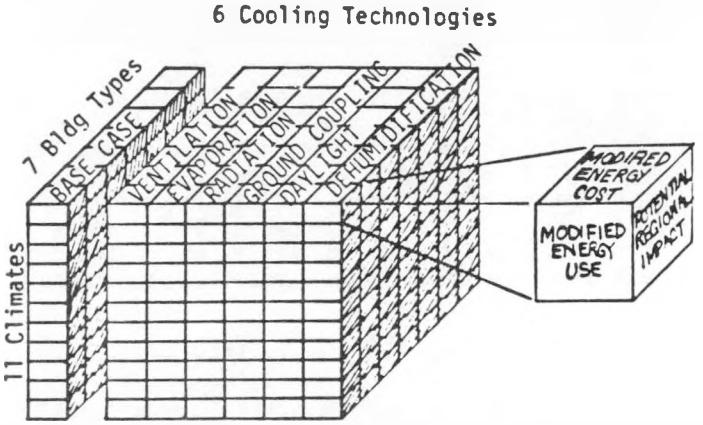

77 BASE CASE CELLS + 462 TECHNOLOGY CELLS = 539 TOTAL CELLS
(1 × 7 × 11) (6 × 7 × 11)

The purpose of the passive cooling assessment is to identify high-potential combinations of three key variables: passive solar phenomena, building type, and climate. It is essential to consider each technology's potential within the context of the U.S. building stock and climate characteristics.

Each cell of the matrix shown above holds the results of the various analyses carried out in the assessment. For each base case cell, three important pieces of information are generated:

- Base case energy use: The amount of energy a typical building type uses in the specified climate (both consumption and peak rate).
- Base case energy cost: The cost of the energy for both consumption and demand (based on typical utility rates, $\$/ft^2yr$).
- Regional energy use: Total site energy use for all buildings of the same type (consumption only).

For each cell on the technology side of the matrix, similar information was generated: energy use, cost, and aggregate regional use as modified by the particular technology.

The current assessment is based on the evaluation of four passive cooling technologies by detailed, computerized energy performance simulations of one-story (10,000 ft^2) and 10-story (100,000 ft^2) office buildings.

SUMMARY DESCRIPTION OF PASSIVE COOLING STRATEGIES

Daylighting:
- Clear view glazing of the base case building replaced by reflective glazing (τ = .15).
- Illumination glazing consists of clear, south-facing tilted glass mounted in closely spaced roof monitors.
- Lighting controls modified to dynamically reduce power input to lights in a manner proportional to the illumination available from the daylighting apertures.

Daytime Ventilation:
- Utilize outside air as much as possible during occupied hours to reduce cooling load by modulated ventilation.
- Assume that the ventilating requires no energy.

Nighttime Ventilation:
- Existing interior partitions in baseline changed from frame construction to 4-inch concrete.
- Additional concrete partitions added to subdivide the interior into one office per occupant.
- During unoccupied hours, the building was ventilated whenever the outside air temperature was less than the inside air temperature, but greater than the heating setpoint temperature.
- Assume that the ventilating requires no energy.

Evaporative Cooling:
- Direct: Employ a conventional air-wash type evaporative cooling device directly in the supply air stream.
- Direct/Indirect: Employ both a convectional air-wash type evaporative cooler and an evaporative heat recovery device in the exhaust air stream to provide indirect (sensible only) precooling for the outside air supply.

Dehumidification:
- An idealistic device is installed in the mixed air stream upstream from the cooling coil. This device removes just enough moisture from the mixed air stream that there is no condensation from the air stream onto the cooling coil.
- It is assumed that this device requires no energy.

Eleven regions were used to describe the range of climatic conditions for cooling in the U.S.

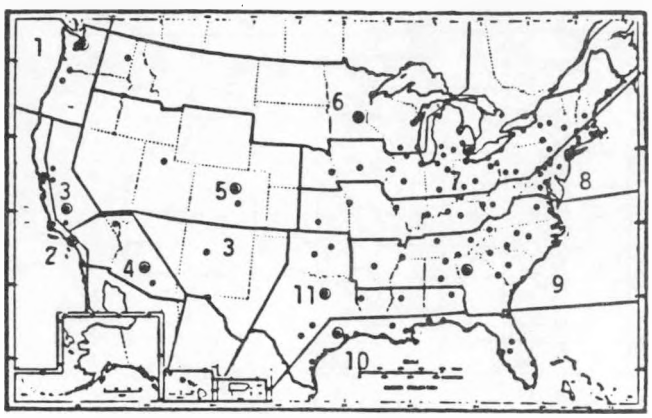

CLIMATE REGION	ANALYZED CITY	POPULATION (Millions)
1. Pacific Northwest	Seattle	5.4
2. California Coast	Los Angeles	18.2
3. Fresno/El Paso	Fresno	7.0
4. Desert Southwest	Phoenix	4.6
5. Central Mountain	Denver	6.8
6. Northern Tier	Minneapolis	12.6
7. Great Lakes	Detroit	50.6
8. Northeast	New York	58.8
9. South	Atlanta	28.7
10. Gulf Coast	Houston	18.3
11. Central Texas	Fort Worth	14.3

A similarity analysis of four climate characteristics (heating and cooling degree days, solar measure $\bar{K}_T$, and latent enthalpy hours) was performed for annual climate data summaries from all 226 U.S. weather stations. Based on estimates of the maximum allowable variation of each climate parameter across a region, the analysis suggested that 11 regions could be used to represent the entire nation. Minor shifts of region boundaries were tolerated to maintain geographic integrity. In the future, the sensitivity of assessment results will be tested against variations of climate parameters within each region.

This assessment has investigated only a portion (about 20%) of all possible combinations of the three key variables.

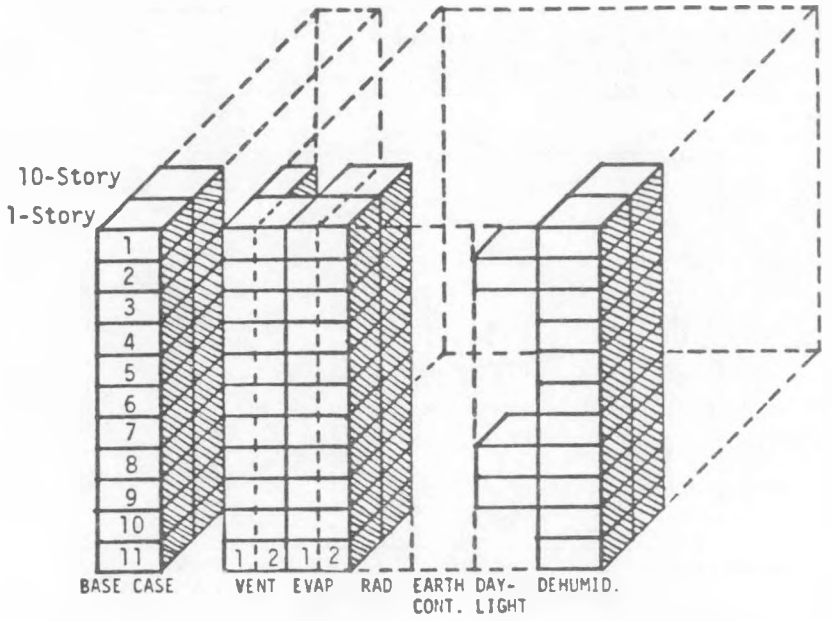

22 BASE CASE CELLS + 102 TECHNOLOGY CELLS = 124 CELLS

The diagram above illustrates a number of decisions about what portions of the cooling assessment could be accomplished within the time frame and budget allocated. Because of the effort needed to specify a prototype, only two building types could be defined and analyzed in the current assessment. Office buildings were selected for this assessment because they represent a large fraction of the floor area and energy consumption of the non-residential sector and are relatively easily characterized. One-story and 10-story office buildings were selected, each having 10,000 ft^2 per story, and similar occupancy, architecture, and mechanical systems. Selection of these building characteristics was based on existing knowledge and understanding of current practice. Two potential passive cooling technologies (radiation and earth contact) were omitted from the assessment because of scheduling difficulties. The investigations of day ventilation (vent 2) and daylighting were limited to one-story buildings.

This assessment was constrained by a number of limitations in the methodology, simulation tools, and available data.

- Because the level of engineering development varies widely among passive cooling technologies, a mixture of "realistic" and "ideal" systems were analyzed in this assessment. Therefore, direct comparison of passive technologies must be made with caution.

- Existing capabilities of energy simulation tools limited some aspects of the analysis.

- There is a critical lack of detailed information about the past, present, and projected building stock in the U.S. This lack of information has been a significant barrier to previous investigations. Part of this assessment effort was devoted to development of a preliminary characterization for office buildings--one of the more easily grasped sectors of the stock. The problem will be amplified for other building types.

- Care was taken to avoid conclusions which might be invalidated by uncertainties inherent in the results. Detailed, quantitative estimates of the uncertainties have not yet been made.

- The economic analyses made to date are preliminary, and since no direct estimates of the cost of strategy implementation have been made, definitive cost-benefit analyses could not be conducted.

- Thermal control was provided by an air temperature (drybulb) thermostat. Owing to a lack of information regarding comfort in cooling conditions, some technologies may not have been given the benefit of the doubt.

RECOMMENDATION: Continue efforts to conceptualize and evaluate advanced passive cooling systems.

RECOMMENDATION: Continue simulation tool development and refinement.

RECOMMENDATION: Initiate development of a comprehensive buildings data base, employing secondary sources and structuring the data for consistent comparative investigation across building types.

RECOMMENDATION: Develop uncertainty estimates for the analysis results, and improve the reliability of supporting data wherever possible.

RECOMMENDATION: Conduct research specifically directed at quantification of occupant comfort requirements under cooling conditions.

III. BASE CASE RESULTS

FINDING: Both heating and cooling in one-story and 10-story buildings are climate sensitive.

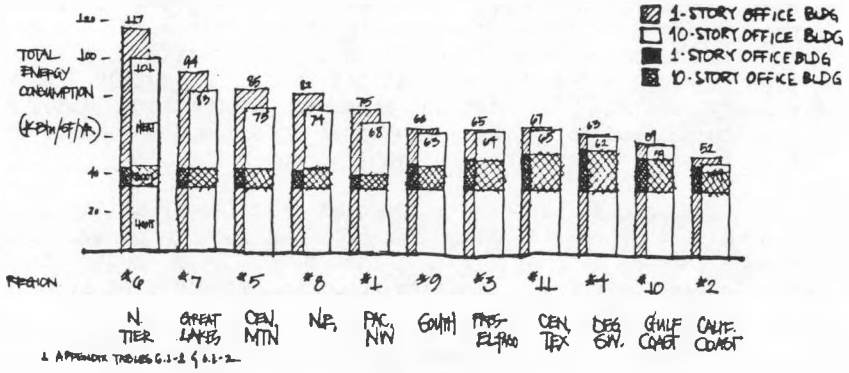

1 APPENDIX TABLES G.1-1 & G.1-2

The figure shows total energy consumption as an index (in kBtu/ft^2-yr) for both one-story and 10-story buildings over all eleven climate regions. Note that this is site (not primary) energy use. If primary energy were shown, the importance of cooling would be greater. It is also important to realize that this total consumption estimate is based on a simulation and is useful for comparing across building types within the context of the analysis (actual building usage may differ). The figure also shows the relationship of heating fuel consumption to total electric consumption (with divisions of each bar).

As expected, the one-story building tends to use more energy than the 10-story building (per square foot), especially in more severe climates. However, it is interesting to note that in each of these climates there is less than 20% difference in total energy use between the two buildings, and even less difference for cooling. It is also interesting to note that the heating energy requirements are substantial, even in the 10-story building.

RECOMMENDATION: Review assumptions and perform parametric analysis to see to what extent this result is an artifact of the prototypical building's characteristics.

FINDING: Lighting dominates the electric consumption in all climate regions examined.

TOTAL ELECTRICAL CONSUMPTION

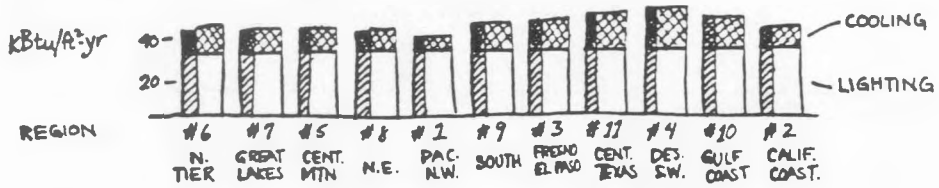

The figure shows total electric consumption divided into two end uses. The climate regions have been arranged as on the previous page, which illustrates the increasing importance of electric consumption in moving from colder to hotter climates. Cooling consumption is represented by the shaded area. Lighting ranges from roughly 60 to 75% of total electric consumption. Note, however, that these results are very sensitive to assumptions about the performance of both cooling and lighting equipment.

The base case building assumed an installed lighting capacity of 2.5 W/ft^2. New lighting technologies soon to be available could reduce this requirement by up to 50%. Even under these circumstances, electric lighting requirements would be at least equal to electricity requirements for all other end uses.

RECOMMENDATION: Research aimed at reducing electric consumption should focus on lighting as a key issue.

FINDING: Cooling is the dominant cause of peak electric power.

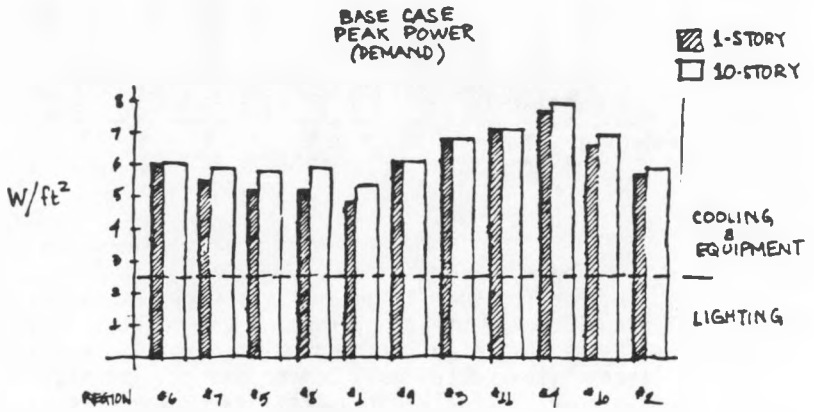

The figure shows peak electric power rate as an index (W/ft^2) for both 10-story and one-story office buildings over all climate regions, based on simulations. The figure also shows the relationship between the power for lighting and the power for cooling and equipment. The equipment peak electric power is nominal (0.35 W/ft^2).

Contrary to the situation for total electric consumption, cooling is the most significant cause of the peak power. The benefits of reducing peak power are significant in reducing both HVAC equipment size and utility capacity.

It is also interesting to note that the variations in peak cooling power are similar to variations in total cooling electric consumption (previous page) across climates. The ratio of the peak power to total consumption tends to be higher in northern climates, suggesting that the most promising strategies in northern climates will be those that have the biggest influence on peak power.

RECOMMENDATION: Research aimed at reducing peak electric power should focus on cooling issues.

FINDING: In office buildings, total electricity costs (including consumption and demand charges) far outweigh the importance of heating fuel costs. Demand charges alone typically account for 30-45% of total electrical cost.

FINDING: The regional variation in energy use does not correlate with the regional variation in energy costs.

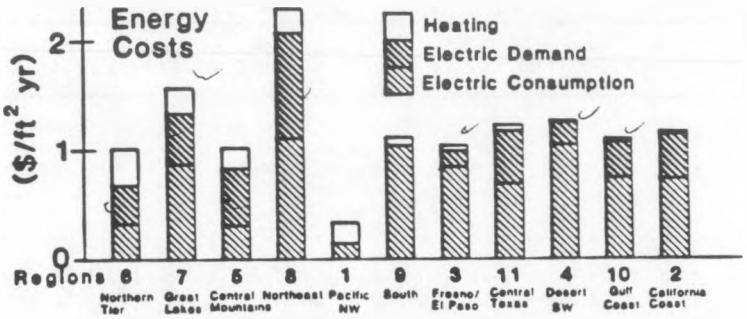

The cost of heating fuel is generally a very small portion of the total annual energy bill, reinforcing the point that electrical consumption is the most significant problem to be addressed in both small and large office buildings. Demand charges are significant in most regions, and vary widely across regions. The overall importance of demand charges and their potential for being affected both positively and negatively by the application of a passive cooling technology appear to be significant findings of the assessment. There is less difference between one-story and 10-story building types than was originally expected. The lack of correlation between energy use and cost shows the importance of local utility rate structure.

RECOMMENDATION: Focus R&D on reducing consumption and demand charges.

- Increase understanding of how building systems (architectural and engineering) can reduce demand.
- Investigate effects of consumption and demand reduction on utility load.

FINDING: Large buildings are predominant in the current office building stock--based on estimate of floor area (square footage)--and will become more dominant over the next two decades.

ESTIMATE of CURRENT (1980) OFFICE BUILDING STOCK

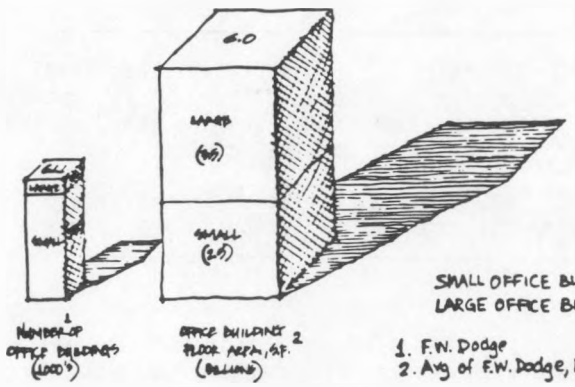

For the sake of the assessment, small office buildings are defined as less than 25,000 square feet and large as greater than 25,000 square feet. The basic division into large and small buildings is based on the assumption that the application of a potential passive cooling technology and the effects of the application will differ due to the scale of a building. Large buildings account for less than 10% of the number of buildings, but over 60% of the floor area in 1980, nearly 70% by 2000.

RECOMMENDATION: Focus R&D resources on proportions roughly equal to the allocation of square footage in the building stock--not on the number of buildings in the stock.

FINDING: By 2000, approximately 60-70% of aggregate office building energy use (at site) will be in buildings built after 1980.

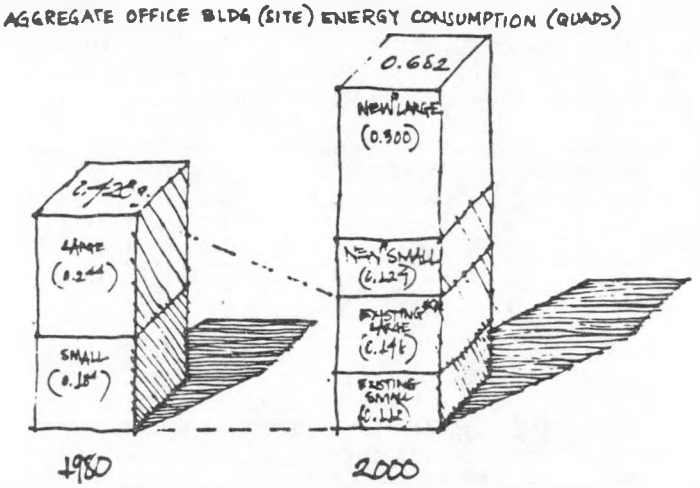

Aggregate energy consumption in office buildings in 2000 is based on the projected growth and replacement of U.S. office building stock multiplied by base case building energy consumption. Extrapolating construction trends of the last several years, construction of new buildings will be about 5% of the existing stock annually, with about 2% going to replace old stock and about 3% contributing to overall growth in the office building stock.

Growth of the building stock will have two important effects in 2000: the building stock will contain a majority of "new" buildings (those built since 1980) and aggregate energy use will have grown by about 50%. Therefore, it is important that research goals be established with the knowledge that the potential market for passive cooling technologies will be in a growing stock of newer buildings (generally better buildings in terms of energy use) rather than in a declining stock of poorer buildings. It should also be noted that the estimates of potential energy savings in this assessment are based on reasonably energy-conservative buildings as of 1980. These estimates of potential are therefore more conservative than if based on earlier, less conservative building stock energy use. It would be possible to draw a similar figure illustrating the reduction in peak electric power.

RECOMMENDATION: Focus R&D on buildings built after 1980 (i.e., compatible with current and emerging construction practices).

FINDING: There are two distinctly different opportunities for the application of a passive technology: during building design and after construction. Both opportunities can lead to large aggregate savings.

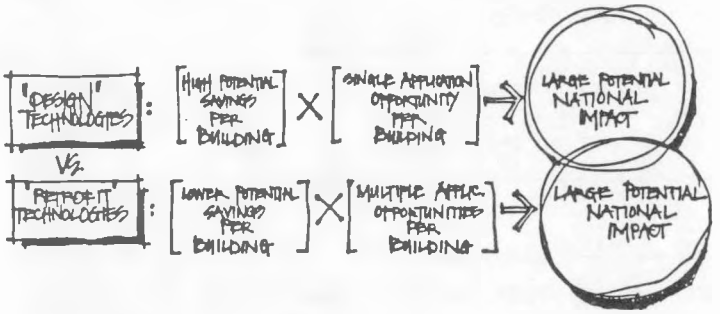

The greatest potential for saving energy in buildings occurs during building design. Furthermore, these savings usually continue over the life of the building. Unfortunately, this design opportunity occurs only once and, if lost, cannot be revisited. If a significant number of design opportunities can be taken advantage of, the resulting national impact would be substantial.

On the other hand, potential savings from modifications of a building after construction (retrofit) are generally lower than the potential during design. However, the opportunity to retrofit a building occurs over the entire life of a building. If passive cooling technologies can be developed for retrofit applications, the potential national impact can be substantial--of the same order of magnitude as in design applications.

The passive cooling concepts developed to date are most relevant to buildings still under design. Any of the technologies discussed in this assessment would require substantial change in buildings, greater than might typically be undertaken in a retrofit application. In order for these concepts to be generalizable to the entire building stock, a better understanding and description of the current and projected building stock in the U.S. is essential.

RECOMMENDATION: Continue development of passive cooling concepts for buildings in design.

RECOMMENDATION: Generate and evaluate concepts that address retrofit requirements.

RECOMMENDATION: Develop a structured description of existing building stock to facilitate generation of retrofit concepts.

IV. PASSIVE COOLING TECHNOLOGY RESULTS

A. NATURAL LIGHTING

FINDING: A realistically simulated natural lighting system (for a one-story building) produced energy consumption reductions and energy cost savings substantially greater than those of all the other technologies investigated, including those technologies that were simulated as thermodynamically ideal systems.

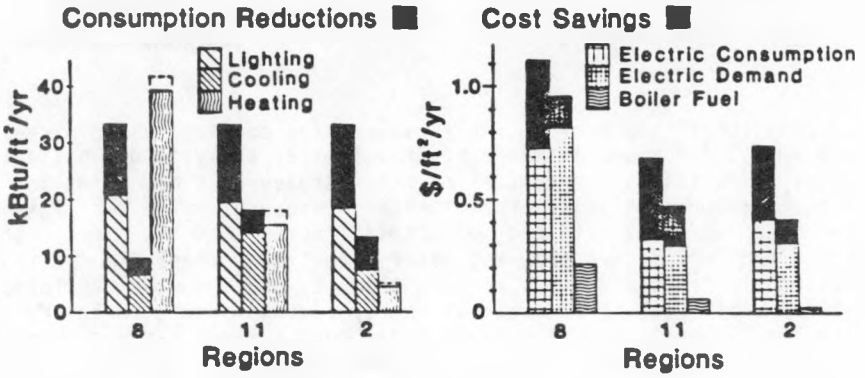

This figure shows the results for the three climates for which daylit buildings were analyzed, and which are representative of all climates in the assessment. For simplicity, the daylighting system used in the parametric analyses used a tilted, south-facing roof aperture of fixed opening. As a consequence, some of the advantages which could be achieved with multiple aperture orientations or variable aperture area were not fully realized. Even for this simple system, with an aperture area equal to only 2.5% of the floor area, significant cooling consumption reductions and cost savings are predicted in all of the climate regions shown above. There are even larger reductions in lighting electricity consumption and costs. (There is a modest heating increase due to from replacement of electric light by sunlight of lower heat content.) The potential benefits of daylighting suggest that it Even if installed lighting capacities substantially smaller than those assumed in this assessment are practical in the near future, should be one of the highest priority research areas in the national passive program. Even if installed lighting capacities substantially smaller than those assumed in this assessment are practical in the near future.

B. EVAPORATIVE COOLING

FINDING: Results of the assessment for the two types of realistic evaporative cooling systems simulated showed modest savings in all climates. (Ideal potential would be much greater.)

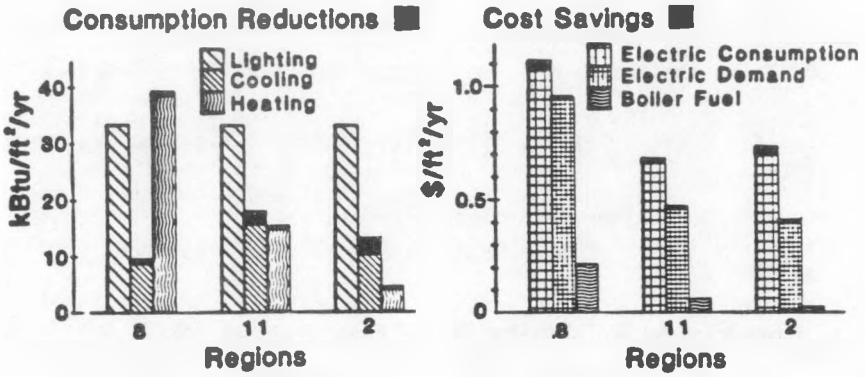

Only two of the many possible evaporative cooling/hybrid systems were analyzed for the assessment; this limited analysis did not adequately ascertain the potential of this strategy but did point to a number of possibilities for further research. The two systems evaluated were direct and direct/indirect. Results for the direct/indirect system show a greater potential. These figures show cooling electricity savings in many climates and the wide variation between climates; the greatest energy savings occurs in the drier climates of the Southwest as expected. Cost savings patterns across climates are somewhat different than the energy savings patterns due to variations in utility rate structures. The small heating reductions shown are believed to be an artifact of the simulation rather than a real effect.

RECOMMENDATION: Extend analysis of evaporative cooling to include performance of thermodynamically ideal, innovative, and combination/hybrid systems to better define the potential of this concept.

RECOMMENDATION: Extend analysis to promising concepts to determine cost effectiveness and penetration potential in all climates.

C. VENTILATION

FINDING: Simulation results for a thermodynamically ideal night ventilation system in a thermally massive building showed significant performance improvements in most of the climates investigated.

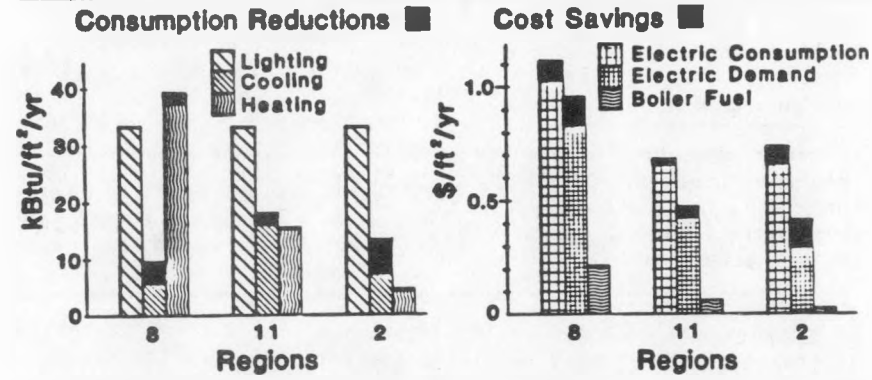

The addition of thermal mass in the building simulated is primarily responsible for substantial reduction in cooling demand and modest reductions in heating consumption. It is believed that using mass in the building would also result in equipment downsizing benefits that were not evaluated in this assessment.

Ventilating at night to cool the building mass was shown to be effective in reducing electric cooling consumption even though these results are based on state-of-the-art convection coefficients, which recent research has indicated may be low. Night ventilation also avoids certain comfort and system interaction issues because of daytime occupancy of office buildings. There is a strong possibility that this strategy could be combined with other strategies such as day ventilation

RECOMMENDATION: Continue fundamental convection research.

RECOMMENDATION: Develop innovative concepts for incorporation of night ventilation strategies into new and existing buildings.

RECOMMENDATION: Perform parametric analyses of night ventilation concept alternatives, with emphasis on the effects of thermal mass.

FINDING: Simulation of an idealized daytime ventilation system (for non-massive buildings) showed results similar to night ventilation (with mass) in reducing total electricity consumption and costs.

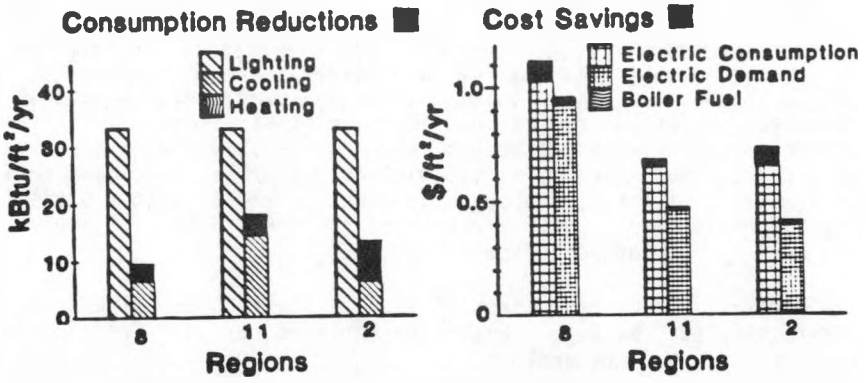

Ventilating the occupied space of the one-story building directly with outside air when possible produced substantial reductions in space cooling loads; these in turn produced savings in cooling energy and total electricity consumption and demand. This system has greater potential than conventional economizers because cooling load in the space is offset directly, and the savings shown are in addition to those achieved from the economizer. Heating performance was not determined due to limitations of the simulation program. Total energy cost savings patterns across climates do not correlate in a simple manner with the energy savings patterns; the relationship between energy cost savings and energy consumption savings across climates do not correlate with building size.

RECOMMENDATION: Improve simulation tool algorithm to allow investigation of more realistic day ventilation systems.

RECOMMENDATION: Extend assessment to examine integration of day ventilation with other building systems.

RECOMMENDATION: Conduct system analyses of day ventilation combined with other systems.

D. DEHUMIDIFICATION

FINDING: Dehumidification as a cooling strategy shows only limited potential for office buildings.

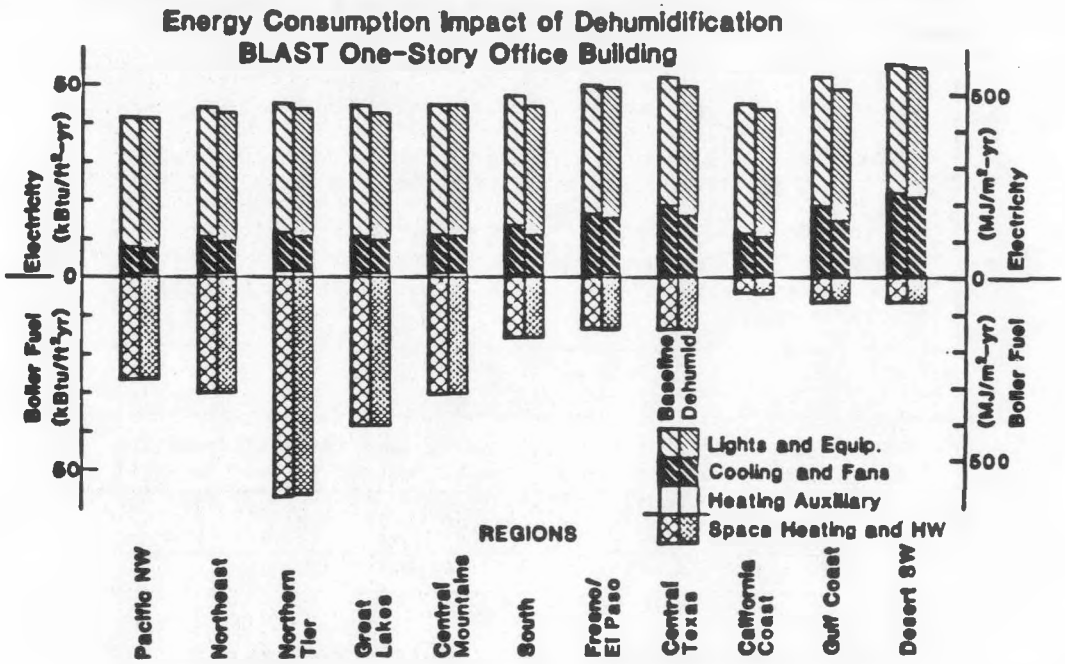

Performance improvement from utilization of this strategy is small in most of the climate regions analyzed, and only modest in those few regions where the best improvement was seen. No greater potential can be expected because the ideal system that was analyzed utilized the most favorable assumptions possible to characterize performance of the technology. Moreover, there is little possibility that more than a small fraction of the ideal potential could be achieved by real dehumidification systems.

However, the energy potential of the ideal system simulated is underestimated because benefits achieved by modified comfort requirements were not explored.

RECOMMENDATION: Only limited subsequent evaluative efforts should be continued for office buildings.

RECOMMENDATION: Extend analysis to other building types, occupancy patterns, and comfort criteria.

E. RADIATIVE COOLING

This technology was not analyzed as part of the assessment because of resource limitations and scheduling difficulties. It is anticipated that a level of analysis will be completed in the near future that will be comparable to the technologies that were studied. Owing to the lack of quantitative analysis results for this technology. Only one research recommendation is included herein.

RECOMMENDATION: A technology assessment of the scope included in this document should be performed for this technology.

F. GROUND COUPLING

This technology was not analyzed as part of the assessment because of resource limitations and scheduling difficulties. It is anticipated that a level of analysis will be completed in the near future that will be comparable to the technologies that were studied. Owing to the lack of quantitative analysis results for this technology. Only one research recommendation is included herein.

> RECOMMENDATION: A technology assessment of the scope included in this document should be performed for this technology.

V. NATIONAL IMPACT

A. TOTAL NATIONAL IMPACT

> FINDING: The four passive cooling technolgies studied to date display significantly different potentials for reducing national energy consumption in office buildings.

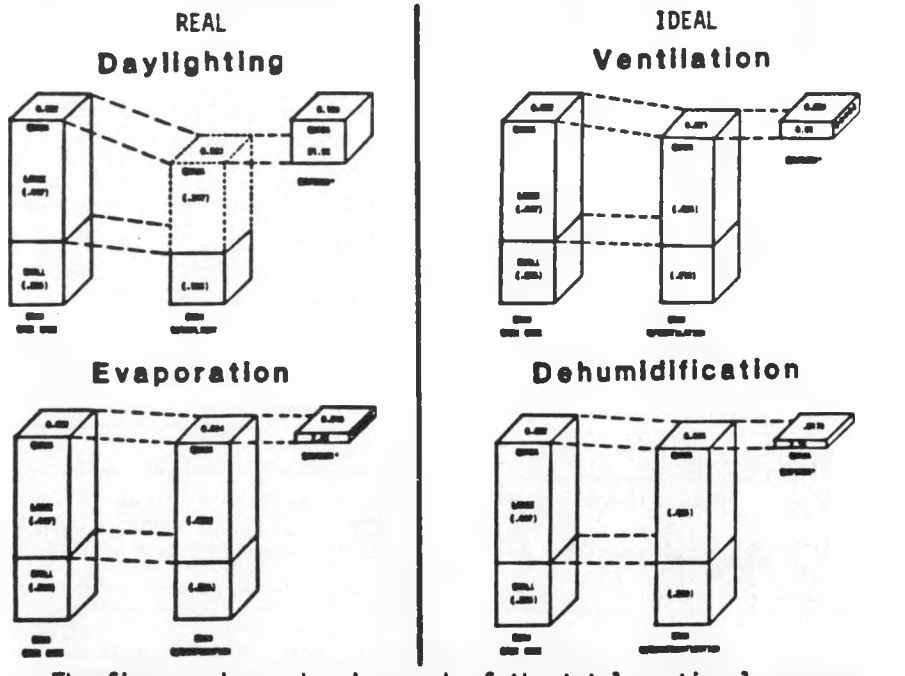

The figures above show how much of the total national consumption of energy in office buildings could be reduced by each technology which passive cooling could achieve by assuming 100% penetration in the total building stock by the year 2000. Actual penetration is likely to be considerably less, as will be discussed on the following pages. Estimates of potential savings from daylighting are based only on the one-story case and are extrapolated to large office buildings (dashed box). Potential savings for the evaporation and daylighting systems are for real systems and whould be increased for thermodynamically ideal systems. Potential savings for ventilation and dehumidification are for thermodynamically ideal systems.

B. POTENTIAL PENETRATION

FINDING: Actual estimates of the penetration of passive cooling strategies into the building stock are highly uncertain. However, ignoring issues of penetration overstates the potential aggregate impact of passive cooling technologies on national energy consumption.

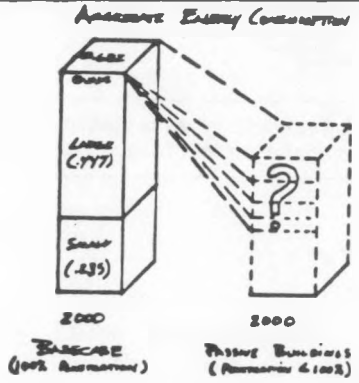

In-depth analysis of potential penetration was not possible as part of this preliminary assessment. While total stock (new and existing) at any given time represents the ultimate potential for penetration, actual penetration, especially during early years of strategy implementation, will be substantially lower. Based on the history of other building innovations, penetration will likely be faster for new than for existing buildings. In addition, penetration will probably vary significantly among passive cooling technologies due to economics, suitability, and other situation-specific characteristics. National impact projections are very sensitive to assumptions about possible penetration rates, timing of introduction, growth of building stock, and retrofit potential.

RECOMMENDATION: Devote a portion of R&D resources to development of better estimates of penetration (large vs. small, buildings in design vs. existing buildings, cost vs. benefit, etc.) so that assessment results can be translated to meet needs of policy makers.

C. ECONOMIC ANALYSIS

FINDING: The economic attractiveness of passive cooling strategies will have a substantial effect on their penetration, and thus will strongly affect their ultimate impact.

A preliminary cash flow analysis was performed for this assessment that indicates how much money an investor could afford to pay as increased first cost for the implementation of a passive strategy. The results of this preliminary effort indicated that the amounts were strongly dependent on ownership perspective, including the state and federal tax environment, and on other economic and financial conditions. Also, without any direct cost estimates for the actual implementation of the strategies, it is not presently possible to ascertain their economic attractiveness, or their ultimate penetration potential.

RECOMMENDATION: Perform detailed economic analyses based on life-cycle costing methods over a range of ownership characteristics.

RECOMMENDATION: For promising technologies, proceed to specify more realistic first-cost estimates.

PROJECT SUMMARY

PROJECT TITLE: Validation of Building Energy Analysis Simulation Programs with Detailed Empirical Data

PRINCIPAL INVESTIGATOR: Ronald D. Judkoff

ORGANIZATION: Solar Energy Research Institute

PROJECT GOALS:

1). Develop an overall validation methodology.

2). Develop performance monitoring criteria to meet the specific data needs for validation of building energy analysis simulations.

3). Construct and monitor a Class A data acquisition facility.

4). Use the validation methodology on the DOE-2.1, BLAST-3.0, and SERIRES computer programs.

PROJECT STATUS: This is the second year of a five year project. Goals #1 and 2 have been completed and are documented in a 300 page SERI technical report entitled "Validation of Building Energy Analysis Simulations" by R. Judkoff, D. Wortman, J. Burch, and B. O'Doherty. Goal #3 is on schedule. A 1,000 sq. ft. test residence and a 120 sq. ft. two-zone test-cell have been constructed and instrumented with approximately 500 sensors at the SERI field site. Both the test residence and the test-cell have been monitored for several experimental configurations during the spring and summer of 1982. Site handbooks have been prepared describing these facilities and data tapes are being reduced for archiving at Los Alamos National Laboratory. Goal #4 is on schedule. Input files describing the house and the cell have been prepared for the DOE-2.1, BLAST-3.0, and SERIRES computer programs. Validation runs will be made in time to appear in the annual project report due in November of 1982.

CONTRACT #: SERI

CONTRACT PERIOD: Sept. 1981 through Nov. 1982 (for this fiscal year)

FUNDING LEVEL: 300K

FUNDING SOURCE: U. S. DOE

EMPIRICAL VALIDATION OF BUILDING ENERGY ANALYSIS SIMULATION PROGRAMS: A STATUS REPORT

Ronald Judkoff
Solar Energy Research Institute
1617 Cole Blvd.
Golden, CO 80401

ABSTRACT

Under the auspices of the DOE Passive/Hybrid Solar Division Class A Monitoring and Validation Program, SERI has engaged in several areas of research in fiscal year 1982. This research has included: (A) development of a validation methodology, (B) development of a performance monitoring methodology designed to meet the specific data needs for validation of analysis/design tools, (C) construction and monitoring of a 1,000-ft^2 multizone skin-load-dominated test facility, (D) construction and monitoring of a two-zone test cell, and (E) sample validation studies using the DOE-2.1, BLAST-3.0, and SERIRES-1.0 computer programs. This paper reports on the status of these activities and briefly describes the validation methodology and the Class A data acquisition capabilities at SERI.

INTRODUCTION

The Class A, B, and C performance monitoring programs were initiated in 1979 because of the demand from researchers and industry for passive and hybrid building performance data at various levels of detail [1]. Class A monitoring was defined to provide detailed data (on the order of 200 channels per building) under controlled conditions at a few sites for algorithm development and validation of building energy analysis simulation programs. Class B was to provide limited detail (about 20 channels per building) in approximately 100-200 occupied buildings for field testing of passive/hybrid designs and statistical evaluation of simplified design tools. Class C was to provide utility bill data and a survey of occupant reactions.

SERI's involvement in the validation of building energy analysis simulations (BEAS) resulted from two comparative studies conducted in 1980 and 1981 [2,3]. These studies showed significant disagreement between four state-of-the-art simulations: DOE-2.1, BLAST-3.0, DEROB-4.0, and SUNCAT-2.4 when given equivalent input for a simple, direct-gain building with a high and low mass parametric option (Fig. 1). These studies indicated the need for high quality controlled validation data and a validation methodology. SERI assumed responsibility for defining the data acquisition criteria for validation, developing a validation methodology, and constructing a Class A data collection facility. Los Alamos National Laboratory was assigned the role of coordinating the Class A Program which included SERI, the National Bureau of Standards, several universities, and several subcontractors.

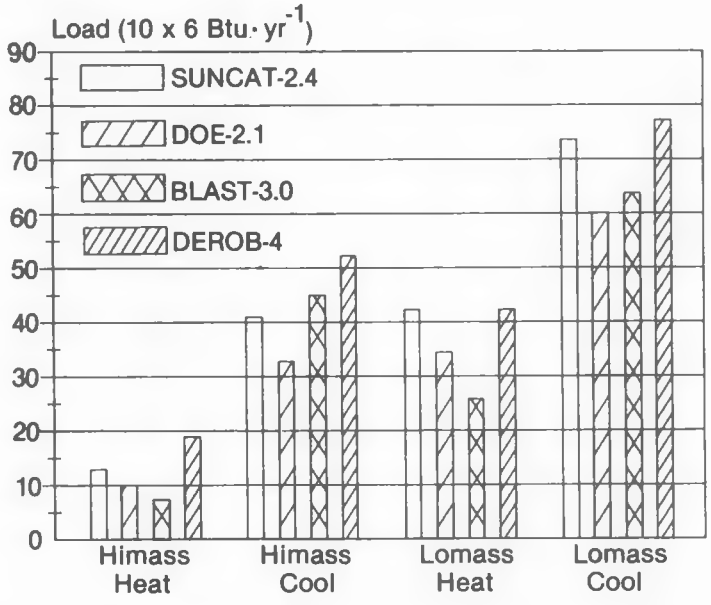

Figure 1. Phase II Comparative Study: Albuquerque

VALIDATION METHODOLOGY

The overall validation methodology uses three different kinds of tests: (1) Analytical Verification, (2) Empirical Validation, and (3) Code-to-Code comparisons. The advantages and disadvantages of these three techniques are shown in Table 1.

The need for these three tests has been described in detail elsewhere [4,5] and only a brief discussion will be possible here.

Each comparison between measured and calculated performance represents a single data point in an immense N-dimensional parameter space. We are constrained to establishing a very few data points within this space. Yet we must somehow be assured that the results at these points are not coincidental and are representative of the validity of the simulation elsewhere in the parameter space. The analytical and comparative techniques are used to minimize the uncertainty of the extrapolations we must make around the limited number of Class A empirical data points it is possible to sample. These extrapolations are classified in Table 2.

Table 1. Validation Techniques

Technique	Advantages	Disadvantages
A. Comparative Relative test of model and solution process	• No input uncertainty • Any level of complexity • Inexpensive • Quick: Many comparisons possible	• No truth standard
B. Analytical Test of numerical solution	• No input uncertainty • Exact truth standard given the simplicity of the model • Inexpensive	• No test of model • Limited to cases for which analytical solutions can be derived
C. Empirical Test of model and solution process	• Approximate truth standard within accuracy of data acquisition system • Any level of complexity	• Measurement involves some degree of input uncertainty • Detailed measurements of high quality are expensive and time consuming • A limited number of data sites are economically practical

Table 2. Types of Extrapolation

Obtainable Data Points	Extrapolation
1. A few climates	Many climates
2. Short-term (e.g., monthly) total energy usage	Long-term (e.g., yearly) total energy usage
3. Short-term (hourly) temperatures and/or flux	Long-term (yearly) total energy usage
4. A few buildings representing a few sets of variable mixes	Many buildings representing many sets of variable mixes
5. Small-scale, simple test cells and buildings	Large-scale complex buildings

Figure 2 shows the process by which we use the analytical empirical and comparative techniques together. The first step is to run the code against the analytical test cases. This checks the numerical solution of major heat transfer models in the code. If a discrepancy occurs, the source of the difference must be corrected before any further validation is done. The next step is to run the code against Class A empirical validation data and to correct discrepancies. A quantified definition of these discrepancies has been proposed by LANL [6]. SERI and several other Class A sites are currently collecting these data. The data along with site handbooks will be archived at LANL. The third step involves checking the code against several prevalidated building energy analysis simulations (BEAS) in a number of comparative studies. If the code passes all three steps, it can be considered validated for the range of climates and building types represented by these studies. The prevalidated BEAS will have successfully passed steps one and two and will have shown substantial agreement for all the comparative study cases. These comparative study cases will, to the extent possible, use Class B data. SERI is currently prevalidating the DOE, BLAST, and SERIRES programs as part of its Class A empirical validation project.

DATA COLLECTION METHODOLOGY

There are many levels of validation depending on the degree of control exercised over the possible sources of error in a simulation. These error sources consist of seven types, divided into two groups:

External Error Types

1. Differences between the actual weather surrounding the building and the statistical weather input used with the BEAS.
2. Differences between the actual effect of occupant behavior and those effects assumed by the user.
3. User error in deriving building input files.

4. Differences between the actual thermal and physical properties of the building and those input by the user (generally from ASHRAE handbook values).

Internal Error Types

5. Differences between the actual thermal transfer mechanisms taking place in the "real building" and the simplified model of those mechanisms in the simulation.
6. Errors or inaccuracies in the numerical solution of the models.
7. Coding errors.

At the most basic level, the actual long-term energy usage of a building is compared to that calculated by the computer program with no attempt to eliminate sources of discrepancy. This level is similar to how the BEAS would actually be used in practice and is therefore favored by many representatives of the building industry. However, it is difficult to interpret the results of this kind of validation exercise because all possible error sources are simultaneously operative. Even if good agreement is obtained between measured and calculated performance, the possibility of offsetting errors prevents drawing conclusions about the accuracy of the method of calculation. More informative levels of validation are achieved by controlling or eliminating various combinations of error types. At the most detailed level, all known sources of error are controlled to identify and quantify unknown error sources. This is the approach taken in Class A data acquisition for validation.

Table 3. Energy Transport Mechanisms

I. CONDUCTION: Measure Temperatures and Conduction Fluxes
A. Structural elements
1. Skin and interzonal opaque walls
2. Glazings
B. Ground coupling
II. CONVECTION: Tracer Gas, Special Experiments
A. Film coefficients
1. Inside surfaces: free convection
2. Outside surfaces: forced convection
B. Air motion
1. Infiltration
2. Zone to zone
a. Natural convection through doorways
b. Natural convection through cracks
3. Stratification
III. RADIATION: Measure Radiant Fluxes
A. Infrared surface coupling
1. Internal surfaces
2. External surfaces (sky temperature)
B. Solar
1. External absorption
2. Glazing transmission and absorption
3. Internal absorption

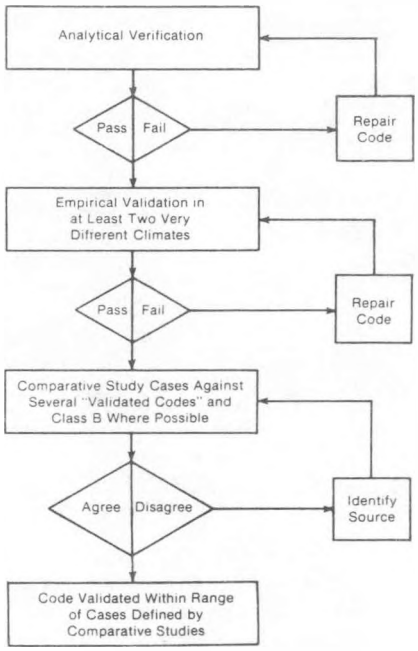

Figure 2. Validation Method

Detailed meteorological and microclimate measurements are taken at the site to eliminate error type #1. The buildings are kept unoccupied to eliminate error type #2. Input files are derived independently by several experienced users and then cross-checked until collective agreement is reached to control error #3. Thermophysical properties are directly measured through destructive and non-destructive testing to control error #4. Once all external error types have been controlled, it is possible to isolate internal errors.

To validate the key thermodynamic models which comprise error types 5 and 6, data of two different kinds need to be acquired. First, data must be taken to define the overall building energy performance. This overall system level includes zone air and globe temperature data and (if temperature controlled) auxiliary energy measurements. These data summarize building energy performance. Energy transport mechanisms are summarized in Table 3. Where this is not possible due to limitations in the state of the art of measurement, or where no acceptable models exist for a mechanism, the mechanism may be physically suppressed as was done in our test cell for ground coupling. This two-level approach allows the identification of those mechanism inaccuracies that lead to system level errors.

To ensure that all major transport mechanisms are monitored, we provide for internal consistency

checks. Failure to achieve closure on the measured heat balance $Q_{in} = Q_{out} + Q_{stored}$ can be attributed only to faulty data or to important mechanisms not represented in the measurements.

SERI CLASS A DATA FACILITY

The SERI Class A validation facility consists of two structures: a 1,000-ft^2 residence and a 120-ft^2 two-zone test cell. These two structures are instrumented with approximately 500 sensors to achieve the degree of experimental control discussed in the previous section. The sensors include type J thermocouples, heat flux transducers, hall effect watt-hour meters, Kip & Zonen and Eppley pyranometers, and an Eppley pyrheliometer. Wind speed, direction, and humidity are also measured.

Details of the house and the test cell are provided in two handbooks [7,8]. Figures 3a and 3b show the plan and south elevation of the house. The cell and the house were designed to be complementary to each other and to other Class A facilities. The approach in the cell was to supress all difficult mechanisms. These included ground coupling, interzonal and cavity convection, stratification, and infiltration. The house was operated in a more realistic fashion, and attempts were made to measure such difficult transport paths as ground coupling via a crawlspace and multizone infiltration. The crawlspace configuration was chosen to complement the floor slab configuration at NBS. For multizone infiltration, a project was initiated to develop an apparatus capable of continuous multizone infiltration monitoring [9]. A prototype of this apparatus was produced and has been collecting data since April 1982. Table 4 shows the measurement approach taken for various mechanisms in the house and the cell.

Both the house and the cell were monitored through a number of configurational changes in the Winter and Spring of 1982. In the case of the house this consisted of a number of conservation and solar retrofits including: (A) insulation blown into walls and attic, (B) batt insulation on foundation walls in crawlspace, (C) storm windows, (D) caulking and weatherstripping, (E) orientation of largest glazed areas to south, and (F) addition of thermal mass to south-facing rooms. These retrofits reduced the effective crack area as measured by a blower door from approximately 200 to 50 in.^{2} (see Fig. 4).

Data from the house and the cell are currently being reduced and analyzed. Results from this work will appear in our annual report, which is scheduled for completion in December 1982.

VALIDATION STUDIES

Figure 5 shows preliminary results from the validation study. Temperatures measured in the northwest (kitchen) zone of the SERI test house have been plotted along with the temperatures calculated by the BLAST-3.0 and SERIRES-1.0 computer programs for the period from April 21 to April 26. The two computer programs agree closely with each other but show a considerable absolute difference from the measured data. However, the shape of the measured and calculated curves are quite similar, with the calculated temperatures being about 9°F (5°C) warmer than the measured curves.

The differences may be explained mainly by the fact that these runs were made prior to reduction of the data for internal heat generation from equipment. Manufacturers' specifications were used to estimate internal heat generation in Zone 1 at 1 kW (3,143 Btuh). Data that became available too late for inclusion in this publication indicated actual internal heat closer to 0.6 kW (1885 Btuh). Thus, approximately 0.4 kW (1,200 Btuh) less energy was actually introduced into the zone than was assumed in the computer simulatons. This would, of course, cause the calculated temperatures to be higher than the measured temperatures.

Subsequent runs will be made using measured data for internal heat generation, infiltration, and thermophysical properties of the building for all four zones. We expect that the discrepancies will diminish when this is done and that remaining differences will reflect true differences between the models and the experiment. Additionally, predicted versus measured auxiliary energy usage will be analyzed. The results from this work will appear in our annual report scheduled for completion by December 1982.

CONCLUSIONS

1. A methodology has been developed by which any building energy analysis simulation may be systematically validated.
2. Class A data acquisition criteria have been defined to meet validation needs for skin-load-dominated buildings.
3. The SERI and NBS Class A data sites are in place and ready to produce archivable validation data in FY 1983.

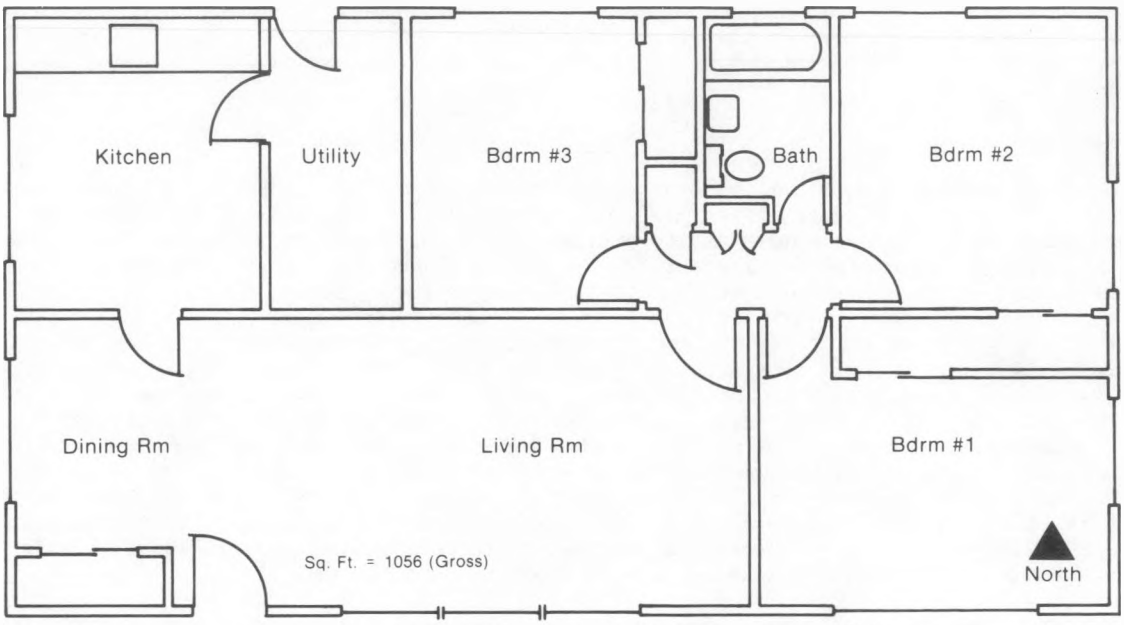

Figure 3a. Validation Test Residence: Floor Plan

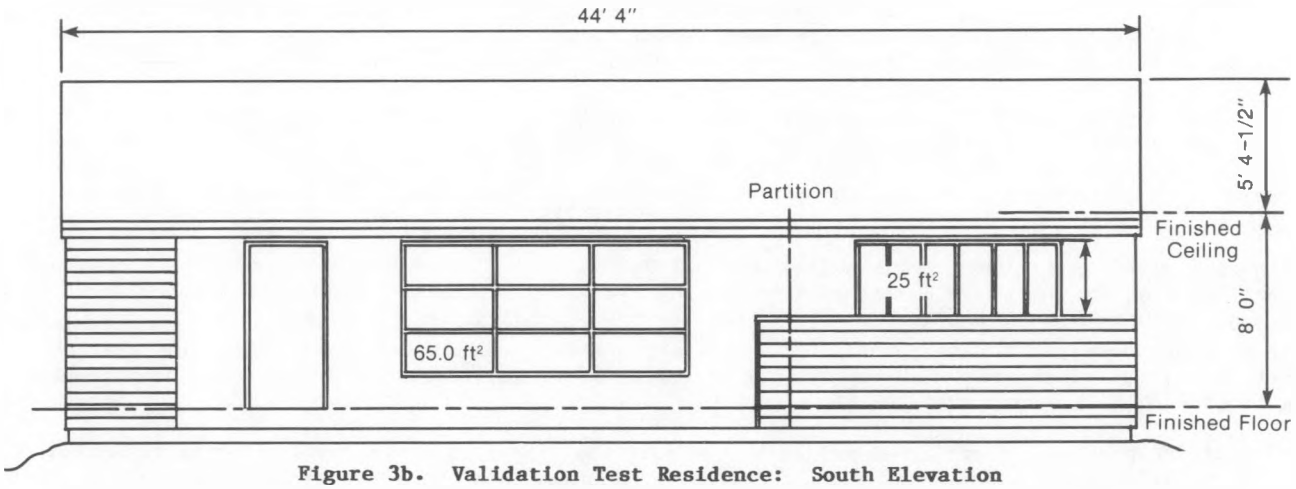

Figure 3b. Validation Test Residence: South Elevation

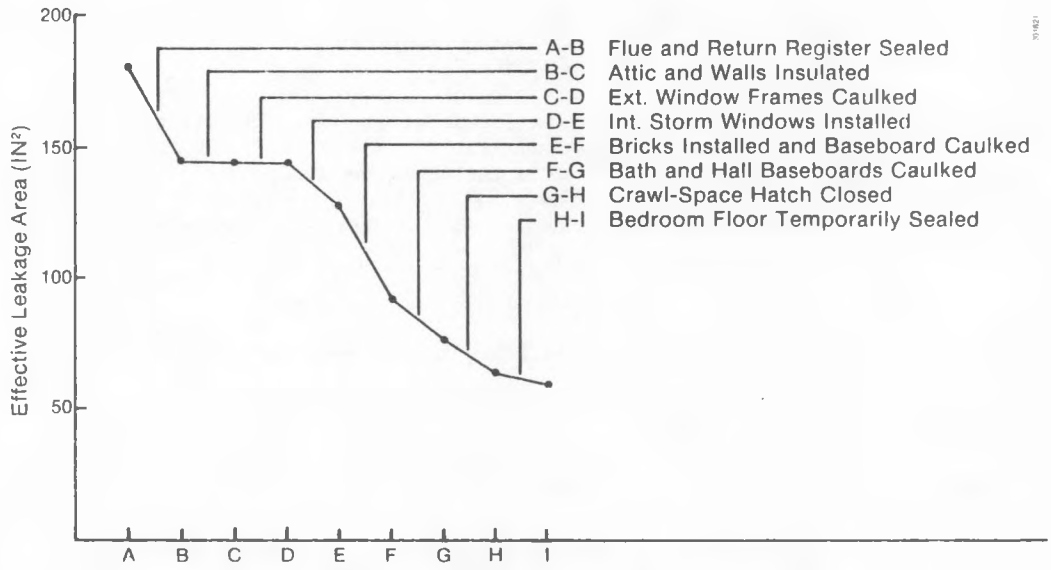

Figure 4. Blower-Door Results for SERI Retrofit House

Table 4. Measurement Approaches

Mechanism	Code Approach	Measurement Approach: Test Cell	Measurement Approach: House
Building-Related Processes			
1. Wall Conduction			
a. Basic assumption	a. One-dimensional flow	a. Insulate edges where possible to ensure one-dimensional flow	a. One-dimensional flow assumed
b. Wall conductivities	b. Inputs, constants	b. Measurements to directly determine U_{wall}, U_{layer}	b. Same as cell
c. Mass storage	c. Not directly available; can be computed from	c. Compute from temperature data, ~10 rakes in mass.	c. Compute from temperature data, ~2 locations per zone
d. Ground coupling	d. One-dimensional flow to ground temperature, neglecting edge effects	d. Eliminate entirely	d. Study in detail, flux and temperature at ~10 locations
2. Boundary Conditions			
a. Interior surfaces	a. Varied approaches from h_{tot} = const. (e.g., SANCAT) to explicit IR + convection correlations (e.g., DEROB)	a. Measure h_{conv} separately; define effective interior temperature, and compute infrared flux (Q_{IR})	a. Measure films only on glazing, same techniques as for cell
b. Exterior surfaces	b. Varied approaches, from constant (SUNCAT) or wind-driven only or wind and sky infrared.	b. Measure $\dot{Q}_{IR}^{sky}$ T_{ground}; deduce h_{conv} on average.	b. Same as cell
3. Zone-Related Effects			
a. Zone mixing	a. Always isothermal	a. Destratify to force zone to be isothermal	a. Destratify continually (FY 1982); study destratification in FY 1983.
b. Interzonal advection and conduction	b. Uncertain, approximate algorithms for advection; wall conduction included	b. Measure conduction directly; advection minimized by careful caulking	b. Measure conduction; closed doors between cells (FY 1982). Study natural advection in FY 1983.
c. Occupancy effects	c. Schedules input, major uncertainty	c. None	c. None
d. Furnishings	d. Neglected or approximate	d. None	d. Unfurnished
e. Internal humidity	e. Latent heat usually included	e. Not measured	e. Not measured
4. System Effects			
a. Heating systems	a. Set points; ramp	a. Measure $\dot{Q}_{heater}$ with electrical inputs of known efficiency, η = 1.0; small deadband	a. Electric heaters, to be computer-controlled for night setback at night.
b. Night ventilation	b. Schedule or constraint for $\dot{V}_{night}$; volume flow $\dot{V}$ is input	b. None	b. Measure $\dot{V}_{once}$ by tracer decay.
Environment-Related Processes			
1. Solar Radiation			
a. Descriptive inputs	a. Need I_{beam}, G_H	a. Measure I_{beam}, G_H directly	a. Same as cell
b. Tilted surface irradiance	b. Various models, mostly isotropic or anisotropic	b. Exterior: measure south irradiance broken into south sky and ground diffuse components Internal: floor, north wall, east wall	b. External: same as cell Internal: measure vertical transmitted, each orientation; and floor and mid-wall irradiance in living room
c. Glazing transmissions	c. Beam transmission calculated from input index of refraction and extinction coefficient diffuse transmission = some input or default constant	c. Measure beam and diffuse transmission directly; extract best fit index of refraction and extinction coefficient from data. Done only occasionally.	c. Same as cell, for the south glass only, before and after storm glazings.
d. Ground reflections	d. Input α_{GR}	d. Measure α_{GR} continuously; $\alpha_{GR}^{Eff.}$ once	d. α_{GR} is some as for cell, use cell data
e. Solar glazing back losses	e. Calculatable from various models, or input constant (SUNCAT)	e. Measure cell albedo directly for clear, cloudy conditions	e. No albedo measurements
2. Wind	a. Input velocity, direction; assume same value for film calculation and infiltration model, very uncertain	a. Measure at two heights at ~100 yards from cell; uncertain microscale problems - Average $h_{convection}$ to be calculated. - Reduce effects by tight construction	a. Same as cell
3. Other: humidity, pressure	a. Inputs used for air heat capacity, latent loads	a. Adequate direct measure	a. Same as cell
4. Precipitation	a. No impact on thermal models	a. Field site observation, plus α_{GR} data effects	a. Same as cell

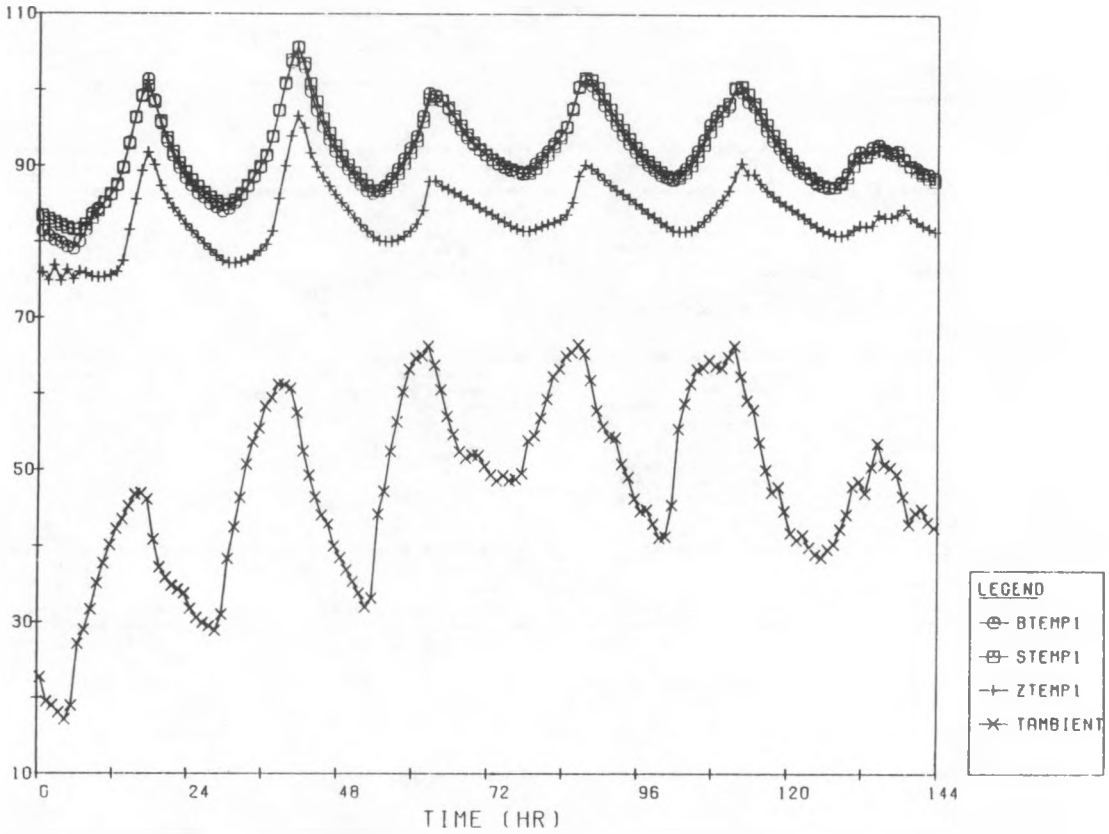

Figure 5. Zone 1 Temperature from Apr. 21 to Apr. 26, 1982

4. The data bank and methodology should be expanded to include mechanical systems so that commercial buildings can be included in the validation activity.

5. The Class A program should continue as a coordinated multilab effort for at least three more years. Only in this way will industry gain confidence in innovative building design options and associated analysis/design tools.

REFERENCES

1. M. Holtz, Program Area Plan for Performance Evaluation of Passive/Hybrid Solar Heating and Cooling Systems. SERI/PR-721-788, Solar Energy Research Institute, Oct. 1980.

2. R. Judkoff et al., A Comparative Study of Four Building Energy Simulations: DOE, BLAST, SUNCAT-2.4, DEROB-III. SERI/TP-721-837, Solar Energy Research Institute, Oct. 1980.

3. R. Judkoff et al., A Comparative Study of Four Building Energy Simulations, Phase II: DOE-2.1, BLAST-3.0, SUNCAT-2.4, and DEROB-4. SERI/TP-721-1326, Solar Energy Research Institute, July 1981.

4. D. Wortman et al., The Implementation of an Analytical Verification Technique on Three Building Energy Analysis Codes: SUNCAT-2.4, DOE-2.1, and DEROB-III. SERI/TP-721-1008, Solar Energy Research Institute, Jan. 1981.

5. R. Judkoff et al., Validation of Building Energy Simulations, SERI Report to be published.

6. Hunn et al., Validation of Passive Solar Analysis/Design Tools Using Class A Performance Evaluation Data. LA-UR-82-1732, Los Alamos National Laboratory, Aug. 1982.

7. J. Burch et al., Site Handbook for the SERI Validation Test Residence. SERI Report to be published.

8. J. Burch et al., Site Handbook for the SERI Two-Zone Validation Test Cell. SERI Report to be published.

9. Wortman et al., A Multizone Infiltration Monitoring System. SERI/TP-254-1638, Solar Energy Research Institute, June 1982.

PROJECT SUMMARY

Project Title: The DOE Passive Solar Class A Performance Evaluation Program

Principal Investigator: B. D. Hunn

Organization: Los Alamos National Laboratory
Solar Energy Group
Los Alamos, NM 87545

Project Goals: To collect, analyze, and archive detailed test data for the rigorous validation of analysis/design tools used for passive solar research and design.

Project Status: Test data needs, for both component/algorithm and full-program validation, have been matched with available or needed test facilities. Five heating and four cooling facilities are in operation. Standard data collection and reporting formats have been developed.

A general validation methodology, including both analytical and empirical tests, has been developed. It is being tested by comparing empirical data sets, taken at the Class A test facilities, against predicted space air temperatures and auxiliary energy use from five building energy analysis computer programs. A quantitative definition of validation has been developed as part of this methodology.

Empirical data sets have been collected from the National Bureau of Standards Direct-Gain Test Cell and the Lo-Cal House. These data have been analyzed and tested; some will be of high enough quality to be archived. Site handbooks have been written for these two facilities. Data sets have also been collected from the Two-Zone Test Cell and the Retrofit facility at the Solar Energy Research Institute; these data sets have not yet been analyzed. Data for component/algorithm validation have been collected from the four cooling test facilities but these data have not yet been analyzed.

Contract Number: W-7405-ENG-36

Contract Period: October 1, 1981 through September 30, 1982

Funding Level: $125K

Funding Source: US Department of Energy, Passive and Hybrid Systems Division

THE DOE PASSIVE SOLAR CLASS A PERFORMANCE EVALUATION PROGRAM: PRELIMINARY RESULTS*

by

B. D. Hunn, W. V. Turk, and W. O. Wray
Los Alamos National Laboratory
Solar Energy Group
Los Alamos, New Mexico 87545

ABSTRACT

The major objective of the DOE Passive Solar Class A Performance Evaluation Program is to collect, analyze, and archive detailed test data for the rigorous validation of analysis/design tools used for passive solar research and design. The Los Alamos National Laboratory, working closely with the Solar Energy Research Institute, has recently become the coordinator of this effort.

This paper describes elements of the plan for Class A validation. A proposed validation methodology, including both analytical and empirical tests, a quantitative definition of validation, minimum data requirements, and a standard reporting format, is outlined. The preliminary testing of this methodology using hourly data from two Class A test facilities is presented. Finally, the collection, analysis, and documentation of preliminary data sets is discussed.

INTRODUCTION

In the fall of 1981, the Los Alamos National Laboratory assumed responsibility for coordinating and executing the Class A performance evaluation activities of the DOE Passive and Hybrid Solar Energy Program. Under the Class A program, detailed hourly data are being collected, analyzed, and archived for the dual purposes of (1) rigorous validation of analysis and design tools (both component models and complete tools) and (2) for performance evaluation of passive solar systems; only the first of these purposes will be addressed here.

The program is outlined in a Solar Energy Research Institute (SERI) report;[1] SERI and the National Bureau of Standards (NBS) have been actively involved in the program since its beginning in late 1979. Although the initial thrust involves test cells, small unoccupied test buildings, and a residence, the program is expected to be expanded later to include commercial buildings and other test facilities.

The Class A plan for validation and performance evaluation is being updated, based on the identified data needs of a variety of researchers and tool users. The elements of that plan are described in this paper. Minimum data requirements and a standard reporting format for archived Class A data sets have been developed. A validation methodology that includes both analytical and empirical elements and a quantitative definition of validation are under development. This methodology is undergoing testing through the validation of several analysis/design tools using hourly data from Class A test facilities. Preliminary results of that testing are reported here.

THE CLASS A PLAN

A preliminary outline of the plan for Class A validation of passive solar analysis/design tools is given in Ref. 1. This plan is being updated and expanded at Los Alamos and includes the following four elements (see Fig. 1).

(1) Data-needs definition and matching with available or needed test facilities;

(2) Development and testing of a general validation methodology;

(3) Collection, analysis, and archiving of Class A test data for

- full-program validation,
- component/algorithm validation,
- performance evaluation; and

(4) Program management.

*Work sponsored by the US Department of Energy, Office of Solar Heat Technologies.
This work is reported, in essentially the same form as here, in the Proceedings of the Seventh National Passive Solar Conference held August 1982 in Knoxville, Tennessee.

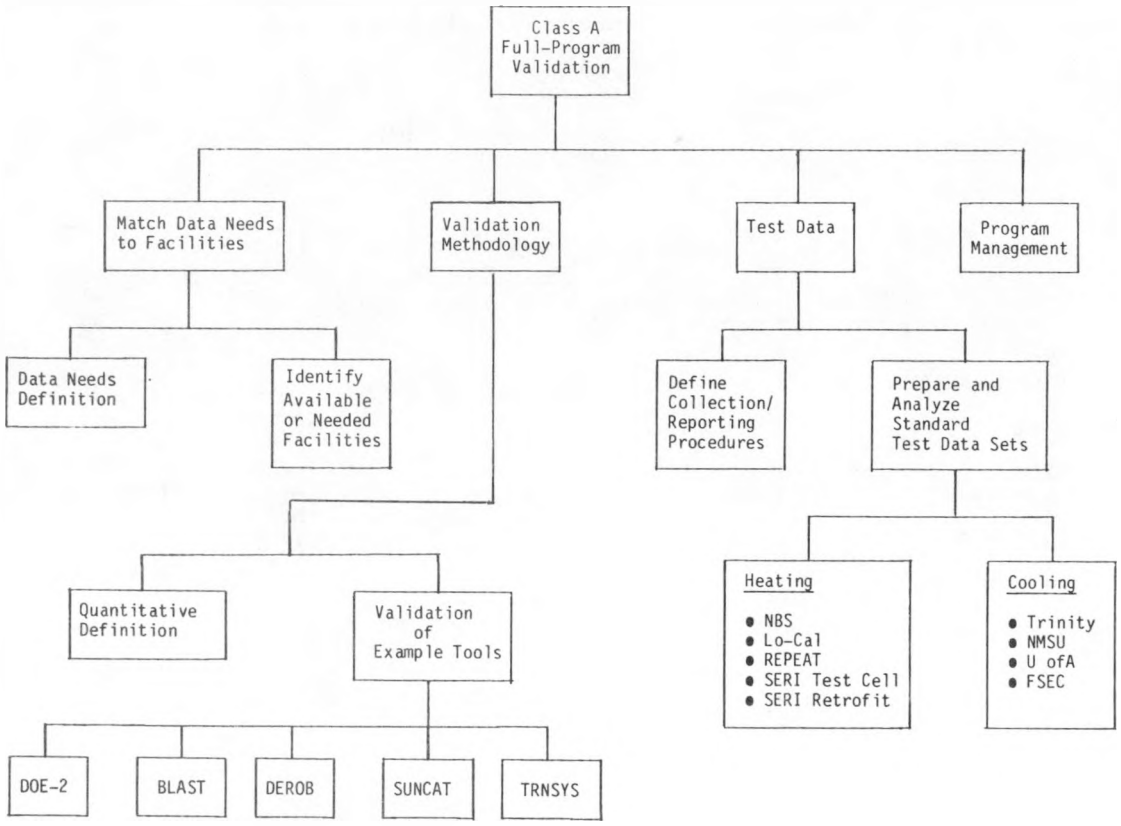

The first three of these elements are addressed in detail below. Management of the program can be summarized in the following comments. Los Alamos is the technical manager for the Class A program and has responsibility for its direction and execution; the Memphremagog Group of Newport, Vermont, is assisting in general management tasks. Several organizations, principally SERI, NBS, and Lawrence Berkeley Laboratory, are participating in the program. Los Alamos is responsible for assuring that a standard validation methodology and standard data collection/reporting procedures are established and maintained. Los Alamos will serve as the archive of Class A data, including site handbooks and data tapes with documentation.

DATA NEEDS AND TEST FACILITIES

Data-Needs Definition

The data needs for Class A validaton fall into two categories:

(1) Data for full-program analysis/design tool validation, and

(2) Data for component or algorithm validation.

Data collection in both of these categories is necessary for comprehensive validation of analysis/design tools. At present, emphasis in the Class A program is on gathering high-quality data for full-program validation.

The Class A test facilities are equipped for acquisition of hourly data sufficient to allow all terms of an energy balance on the building envelope to be determined. This requires hourly solar and weather data, and in most cases indoor dry-bulb temperature and humidity, vent discharge temperature and flow rate, average inside-to-outside temperatures (or heat fluxes) on each surface exposed to ambient conditions, internal heat sources, auxiliary heating and cooling energy, infiltration, and surface and internal temperatures (or surface heat flux) on primary thermal storage elements. Thermophysical property data of the soil and of building materials are usually measured directly; in some cases the building overall loss coefficient and heating/cooling plant efficiency are measured in coheating experiments.

Available and Needed Facilities

At present, nine test facilities or buildings are in the Class A network. Class A level data are being taken at several other facilties, both within and outside of DOE sponsorship. Data from these other

facilities are being reviewed and compared with the data needs for a balanced program; those facilities found to be appropriate will later be included in an expanded Class A network. Table 1 summarizes the types of facilities presently in the network; no commercial buildings are yet included.

TABLE 1
FULL-PROGRAM VALIDATION TEST FACILITIES
SUMMARY OF FACILITY TYPES

	TEST CELLS	DEDICATED FULL SCALE TEST FACILITIES	MONITORED BUILDINGS RESIDENTIAL		MONITORED BUILDINGS COMMERCIAL	
			OCCUPIED	UNOCCUPIED	OCCUPIED	UNOCCUPIED
(1) NBS (RECONFIGURABLE)		●				
(2) LO-CAL			●	●		
(3) REPEAT (RECONFIGURABLE)		●				
(4) SERI TEST CELL	●					
(5) SERI RETROFIT				●		
(6) TRINITY UNIV.		●				
(7) NMSU		●				
(8) U OF A		●				
(9) FSEC (RECONFIGURABLE)		●				

The passive heating test facilities are

(1) NBS Passive Test Facility, Gaithersburg, Maryland;

(2) Lo-Cal House, Small Homes Council, University of Illinois, Champaign, Illinois;

(3) REPEAT Facility, Colorado State University (CSU), Ft. Collins, Colorado;

(4) SERI Two-Zone Passive Test Cell, Golden, Colorado; and

(5) SERI Retrofit Test House, Golden, Colorado.

The passive cooling test facilities are

(1) Trinity Cooling Test Facility, Trinity University, San Antonio, Texas;

(2) New Mexico State University (NMSU) Roof Pond Test House, Las Cruces, New Mexico;

(3) University of Arizona (U of A) Passive Cooling Experimental Facility, Tucson, Arizona; and

(4) Florida Solar Energy Center (FSEC) Passive Cooling Laboratory, Cape Canaveral, Florida.

The heating facilities and the Trinity and FSEC cooling facilities will be used for full-program validation; all four cooling test facilities will be used for component/algorithm validation as well as for performance evaluation and component testing.

It is highly desirable that the full-program validation facilities cover the range of passive heating and cooling technologies. The summary in Table 2 shows that only a few more facilities need to be identified to attain complete coverage.

TABLE 2

FULL-PROGRAM VALIDATION TEST FACILITIES
SUMMARY OF TECHNOLOGIES INCLUDED

● = PRESENT TESTING MODE
O = POTENTIAL FUTURE TESTING MODE

	HEATING					COOLING						LIGHTING
	DIRECT GAIN (HIGH MASS)	DIRECT GAIN (LOW MASS)	THERMAL STORAGE WALL	THERMAL STORAGE ROOF	SUN-SPACE	VENTI-LATIVE	EVAPO-RATIVE	RADI-ATIVE	GROUND COUPLING	HIGH MASS	DESIC-CANT	DAY-LIGHTING
(1) NBS	●		●									O
(2) LO-CAL		●										
(3) REPEAT	●	●	●		●							O
(4) SERI TEST CELL	●											
(5) SERI RETROFIT	●	●										O
(6) TRINITY UNIV.	O			●			●	●				O
(7) NMSU				●			●	●		O		
(8) U OF A						●	●	●	●	●		O
(9) FSEC						●	●	●		●		

VALIDATION METHODOLOGY

Development of Methodology

A proposed methodology for full-program validation[2] is the basis of the Class A validation methodology. It includes methods for analytical and empirical validation, and concentrates initially on the energy processes at the building envelope. The analytical tests involve the determination of closed-form analytical solutions of several simple cases for single-zone buildings.[3]

In the empirical tests, modeling errors, input uncertainties, and user-effect uncertainties are addressed; the methodology initially concentrates on the first two of these. The approach is to compare predicted space air temperatures or auxiliary energy use with values measured in the test facilities. The test facilities have been selected to include a range of controlled conditions. The greatest control is obtained in the SERI Test Cell where ground coupling, infiltration, and internal gains essentially have been eliminated. These effects are included in the SERI Retrofit facility, the REPEAT facility, and the NBS facility. The Lo-Cal house is an occupied residence, which has been monitored in occupied and unoccupied modes. In this situation, the test is more realistic, but significant uncertainty exists for input parameters and the energy mechanisms cannot be isolated.

A series of standard, high-quality data sets, for continuous one- to two-week periods, is being developed at each site. Data are being archived for periods of floating and fixed space temperatures for at least a heating (or cooling) season and a swing season.

Testing of Methodology

The analytical tests have been checked for appropriateness by being applied to three building energy analysis computer programs.[3] The quality of the empirical data coming from the Class A test facilities is being assured by testing them against simulations using five building energy analysis computer programs: DOE-2, BLAST, DEROB, SUNCAT and TRNSYS (see Collection and Analysis of Test Data section below). In this manner, problems with the data sets are being resolved and additional data needs are being identified.

Quantitative Definition of Validation

The purpose of the quantitative definition of validation is to provide an objective basis for evaluating passive solar simulation programs in terms of their accuracy as analysis/design tools. Although the quantitative definition may reveal the presence of errors in a simulation model, our primary purpose is not to provide a debugging procedure, but to quantify predictive capability..

The procedure will employ Monte Carlo methods to quantify the uncertainty in output performance variables resulting from input parameter uncertainty and possible systematic errors introduced by the modeling procedure. There are four basic steps in our method:

(1) Test building characterization,

(2) Performance monitoring of the test building,

(3) Simulation of test building performance, and

(4) Comparisons of predicted and measured performance variables.

The test building should be unoccupied and extremely well characterized. Each descriptive parameter should be carefully measured and estimates of the random uncertainty associated with the measurement obtained. The descriptive parameters of interest include all physical properties, dimensions, and other characteristics input to simulation models. The random variations of measured input quantities are assumed to be normally distributed. Each input parameter is characterized by its mean value and its standard deviation, σ; one can expect 95% of the measured values to lie within limits of $\pm 2\sigma$.

The performance of the test building should be monitored for a period of about two weeks. Estimates of the random variations in the measurement of all initial conditions, weather variables, and performance variables are obtained as described above. The performance variables of primary interest are the space temperature and auxiliary energy use.

Next, simulations are performed on the test building using input parameters randomly selected from the normal distributions obtained in steps (1) and (2). This set of performance calculations yields corresponding sets of output variables. If N performance calculations are performed, a set of N normally distributed values will be obtained for each performance variable at each hour during the test period.

The final step in the procedure is to compare the calculated values of the performance variable (actually a distribution of the output variable) with the measured values. This can be done in terms of the error observed in a selected performance variable, say the heating power, P, that is a measure of the auxiliary energy use. The fractional error in P is defined as

$$P^* = \frac{PM - PC}{\overline{PM}} \quad , \tag{1}$$

where PM is the power measured at a particular hour, PC is the calculated power at the same hour and $\overline{PM}$ is the average measured heating power for the full test period. A set of N values of P* can be obtained for each hour of the test period.

$$P^*_n = \frac{PM_n - PC_n}{\overline{PM}} \quad , n = 1,2, \ldots N \quad . \tag{2}$$

Now, if we combine all hourly sets of N fractional heating power errors, we have a family of N·H values where H is the number of hours in the test period:

$$P^*_{nh} = \frac{PM_{nh} - PC_{nh}}{\overline{PM}} \quad , \begin{matrix} n = 1,2, \ldots N \\ h = 1,2, \ldots H \end{matrix} \quad . \tag{3}$$

The estimated mean value of this distribution at a particular hour, h, is given by

$$\bar{P}^*_h = \frac{\sum_{n=1}^{N} P^*_{nh}}{N} \quad .$$

The accuracy of this estimate depends on the value of $(\sigma_h)_m$, the standard error of the hourly mean. The quantity $(\sigma_h)_m$ is related to σ_h, the standard deviation of the relative error at hour h, as follows:

$$(\sigma_h)_m = \frac{\sigma_h}{\sqrt{N}} \quad . \tag{5}$$

Thus, we see that one must perform 16 simulations to obtain a standard error for the hourly mean that is one-fourth the standard deviation of the hourly distribution. An estimate of the deviation of the hourly distribution is given by

$$\sigma_h = \left[\frac{1}{N-1} \sum_{n=1}^{N} \left(P^*_{nh} - \bar{P}^*_n \right)^2 \right]^{1/2} \quad . \tag{6}$$

Now, the most probable value of the mean fractional error over the entire test period is obtained from the weighted average of the hourly mean values as follows:

$$\bar{P}^* = \frac{\sum_{h=1}^{H} \bar{P}^*_h / (\sigma_h)^2_m}{\sum_{h=1}^{H} 1/(\sigma_h)^2_m} \quad . \tag{7}$$

The quantity $\bar{P}^*$ is a measure of the systematic error present in a simulation model. The systematic error could be caused by systematic errors in the input parameters, but careful measurement techniques should all but eliminate this source. More likely, it is the result of the inevitable approximations made in modeling complex physical phenomena. Random variations in the fractional heating power are caused entirely by random variations in the input parameters. Examples are being prepared that will test and illustrate this definition.

COLLECTION AND ANALYSIS OF TEST DATA

Full-Program Validation Data

Experimental data have been collected from two (NBS and Lo-Cal) of the five heating test facilities listed above. These data are preliminary because they were taken during shakedown of the two facilities involved. Nonetheless, they have been carefully analyzed and are representative of typical Class A data sets that will be archived. Additional sets of data have been taken at these facilities, but analysis is not yet complete. Data have also been taken at both of the SERI facilities, but tapes of reduced data have not yet been produced. The data acquisition system is being installed in the REPEAT test facility; data taking will begin in the fall 1982. Extensive data have been taken at the Trinity University and NMSU facilities and preliminary data have been taken at the U of A and at the FSEC Passive Cooling Laboratory. However, these data have not yet been analyzed.

A data tape from the NBS test facility for a 25-day period in October 1981, has been analyzed. The data are from the 330 ft^2 slab-on-grade direct-gain test cell; the cell temperature was allowed to float during this period. Solar gain is provided by south-facing patio door units and a clerestory window. (The clerestory was blocked off for this test run.) Thermal mass is contained in the floor slab and in an 8-in.-thick solid core concrete block thermal storage mass on the north wall.

Measured space air temperatures from the cell were compared with DOE-2 predicted data (Fig. 2) as a means of identifying problems with the data and to test its usability for validation. Infiltration was measured hourly using a tracer-gas monitor. The agreement between the DOE-2 predictions and the measured test-cell air temperatures is quite good on clear days; however, the agreement is not as good on days with low insolation. Careful analysis revealed that the low intensity solar radiation measurements are not reliable. Therefore, measurement of the fall-period data at NBS is to be repeated in 1982. Also, most of the material property data used in the DOE-2 input were taken from tabulated values. However, core samples are being taken of the floor slab and soil property measurements are being made; these measured values will be used in subsequent runs.

A data tape for an unoccupied, cloudy 2-day period during September 1981 at the Lo-Cal House has also been analyzed. These data are from the 1700 ft^2, single-family residence for a period when the space temperature was floating and hourly infiltration measurements were made. The sun-tempered house uses moderate south glazing for direct gain, but contains no extra thermal mass. A comparison between measured space air temperatures and those predicted by DOE-2, assuming the house to be a single zone, is shown in

Fig. 3. Despite the fact that these data were taken during the shakedown period and are, therefore, preliminary, the agreement is quite good. Similar results were obtained by LBL in a comparison with BLAST 3.0 predictions.[4]

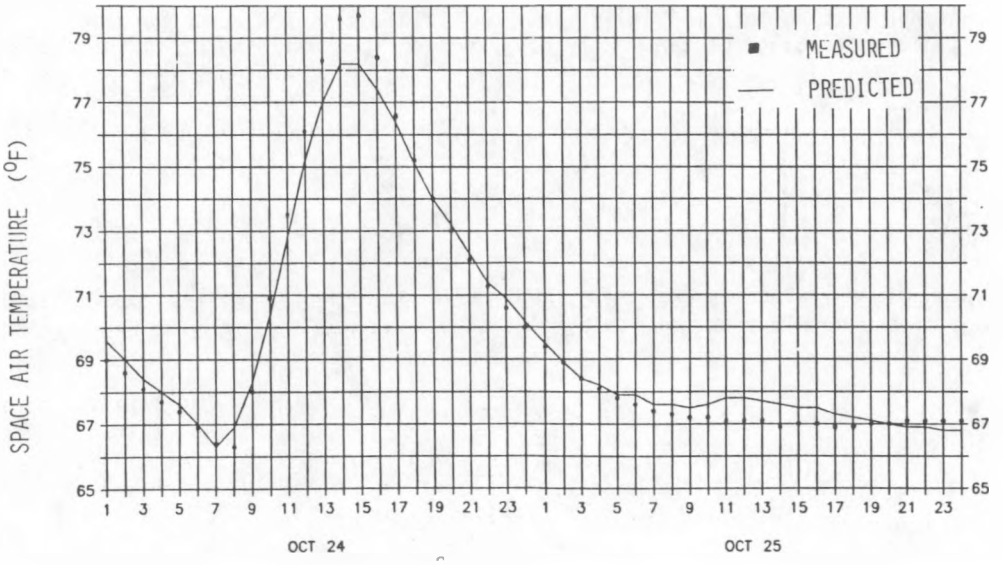

Fig. 2. Measured and predicted space air temperatures for the October 1981 NBS direct-gain test cell data.

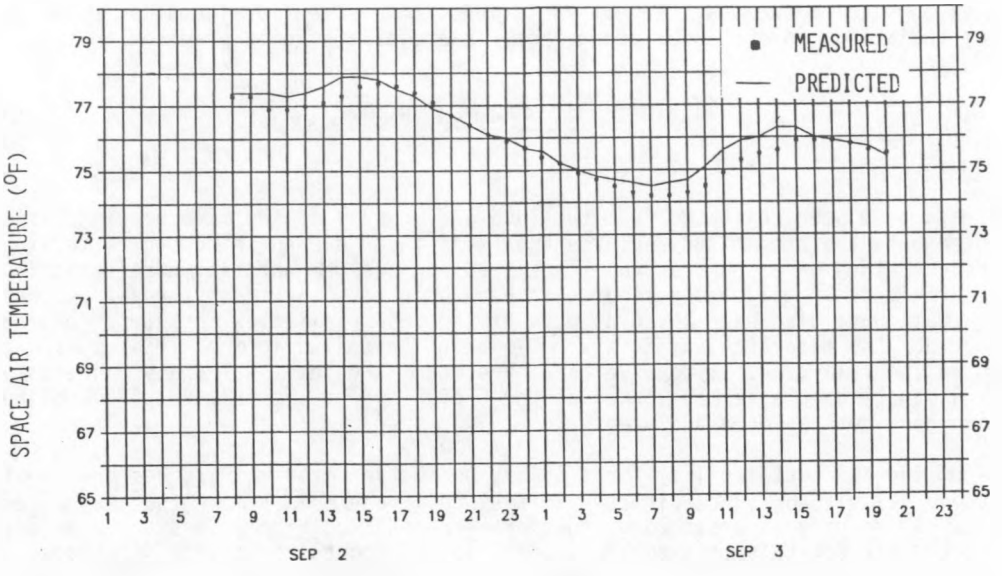

Fig. 3. Measured and predicted space air temperatures for the September 1981 Lo-Cal House test data.

Documentation of Data Sets

Site handbooks have been prepared for the NBS and Lo-Cal facilities. These contain a detailed description of construction, instrumentation, and material properties.

Component/Algorithm Validation

The four cooling test facilities will be used primarily for component and algorithm validation. These units will be supplemented by other test facilities already in existence or to be built later. Data have been taken at all four sites, but have not yet been analyzed for inclusion in the Class A validation data base.

CONCLUSIONS

Through our Class A progress to date, we have concluded the following.

(1) The data needs for detailed validation of hour-by-hour passive analysis/design tools are fairly well characterized,

(2) A comprehensive program and management structure has been developed for this validation effort, and

(3) Although considerable progress has been made, continuation of this program for at least three more years is necessary.

REFERENCES

1. "Program Area Plan for Performance Evaluation of Passive/Hybrid Solar Heating and Cooling Systems," Solar Energy Research Institute report SERI/PR-721-788 (October 1980).

2. R. Judkoff, D. Wortman, J. Burch, and B. O'Doherty, "Validation of Building Energy Simulations," Solar Energy Research Institute report to be published.

3. D. Wortman, B. O'Doherty, and R. Judkoff, "The Implementation of an Analytical Verification Technique on Three Building Energy Analysis Codes: SUNCAT 2.4, DOE-2.1, and DEROB III," Solar Engineering-1981, Proc. of the ASME Solar Energy Division Third Annual Conference on Systems Simulation, Economic Analysis/Solar Heating and Cooling Operational Results, April-May 1981, Reno, Nevada (American Society of Mechanical Engineers, New York, New York, 1981), pp. 268-276.

4. F. Bauman, "Preliminary Verification of BLAST by Comparison with Lo-Cal House Data," Technical Note No. 31, Passive Solar Analysis Group, Lawrence Berkeley Laboratory, May 12, 1981.

Project Title: Passive Cooling by Natural Ventilation

Principal Investigators: Subrato Chandra, Philip W. Fairey, III

Organization: Florida Solar Energy Center (FSEC), Cape Canaveral, Fl 32920

Project Goals: Develop data to permit analysis of naturally ventilated buildings and prepare a ventilation design handbook.

Project Description and Status:

Predicting the thermal performance of ventilated buildings requires estimation of airflow through the building zones and average convective room surface coefficients. Airflow estimation requires knowledge of building pressure distribution at apertures (windows) and their discharge coefficients. Pressure distributions on many buildings have been obtained in boundary layer wind tunnels. To determine the applicability of such sealed building data for ventilation calculations, wind tunnel tests on solid and porous buildings are being performed under subcontract by Dr. B. J. Vickery of the University of Western Ontario (UWO). In addition, the subcontract will analyze existing data and catalog them as average surface pressure coefficients. This pressure data when combined with discharge coefficient data and wind speed and terrain data available in the literature will permit accurate estimation of natural ventilation airflow rates for cross ventilated buildings where turbulence induced ventilation has only a small effect.

The estimation of average convective heat transfer coefficients (h_c) is quite difficult. Under another subcontract, Dr. J. E. Cermak of Colorado State University (CSU) is developing data on aperture boundary conditions and interior flow speed and direction by testing three simple cross ventilated rectangular models. This data will be forwarded to Lawrence Berkeley Labs (LBL) for validating the LBL convection code developed by Dr. A. Gadgil. This code can generate h_c data for a variety of building geometrics for which the aperture boundary conditions are known. Under another subcontract, H. Sobin is analyzing data from hundreds of naturally ventilated scale model wind tunnel tests he conducted in a boundary layer wind tunnel during 1963-1966 in London. The purpose of these tests were to measure the effects of a variety of window shapes and sizes on the average room air velocity.

At FSEC, thermal experiments are being performed on a full size 12x18x8 ft. room of the FSEC Passive Cooling Laboratory (PCL) which is either turbulence or mean pressure ventilated depending on wind direction. Measurements of temperature drops and airchange rates are being made. This data will be used to empirically generate a set of h_c data. Two to three day-long experiments in the FSEC PV House where the house is unoccupied will also be accomplished. These experiments will include permanent and night only natural ventilation as well as forced night ventilation tests.

To establish the validity of wind tunnel testing, a series of experiments were conducted at CSU in 1981 using a 1:25 scale model of the FSEC-PCL. The wind tunnel data has been compared with full scale data with good correlations when the flow is mean pressure driven. For turbulence driven conditions, the comparisons are not so good.

For those without access to a good boundary layer wind tunnel, a new test method has been proposed. This consists of testing a small scale model in the natural wind. This method has been validated by testing the CSU built FSEC-PCL model in the natural wind at FSEC and comparing the data to full scale results. The correlations for mean pressure driven and turbulence dominated ventilation are both excellent.

The final series of tests at FSEC will compare scale models of two innovative windowless ventilator designs with a well ventilated conventional residence. Flow visualizations with a laser have already been completed and recorded. Thermal tests where heated metal blocks will be placed in all models being naturally ventilated and temperature decays recorded will be accomplished next.

In the design area, a preliminary design handbook will be issued by September 30, 1982. This is based primarily on the comprehensive literature review completed by FSEC in 1981 and results to date. A revised design handbook containing all results will be completed by the end of February 1983.

Contract No: DE-AC03-SF11510.

Contract Period: September 30, 1980 through February 28, 1983.

Funding Level: $405,274.

Funding Source: U.S. Department of Energy, San Francisco Operations Office.

PROJECT SUMMARY

Project Title: Earth Contact Systems

Principal Investigator: George D. Meixel Jr.; Co-Principal Investigator: Thomas P. Bligh, MIT

Organization: Underground Space Center
University of Minnesota
Minneapolis, Minnesota 55455

Project Goals: Develop a detailed numerical model for predicting earth contact heat transfer from buildings. Design and implement an experimental plan for validating the detailed model with data from real buildings. Develop earth contact subroutines for inclusion in the response factor type of building thermal analysis programs such as DOE-2 or BLAST. Utilize the experimentally validated computer programs to carry out parametric studies of the performance of earth contact building components. Incorporate the results of the parametric studies into preliminary design guidelines.

Project Status: The detailed models of earth contact heat transfer and the earth contact subroutines for inclusion in DOE-2/BLAST have been written. Experimental data from several earth contact buildings in different climates is being obtained, processed and utilized in the validation of the computer codes. As the validation of each numerical model nears completion, these computer codes are introduced into the ongoing investigation of the thermal performance of earth contact components to generate predictions for use in the development of preliminary design guidelines.

Both implicit finite difference and finite element computer codes have been utilized in modelling the conduction heat transfer from earth contact buildings. Appropriate definition of the boundary conditions, e.g. radiation, conduction, convection, and evapotranspiration at the ground-atmosphere interface, and attention to the details of the spatial domain, e.g. increased computational detail near corners and insulation boundaries, have been included for both solution techniques. For the detailed studies of coupled heat and moisture transport in soils, our initial work has extended the implicit finite difference conduction code to include moisture transport. Creation of earth contact subroutines for interfacing with DOE-2/BLAST, has been accomplished by calculating two-dimensional response factors from the finite element data structure.

Experimental measurements are being performed on an earth-sheltered residence to determine the temporal and spatial variations in soil temperature, soil thermal conductivity, building wall heat flux and building interior temperatures associated with building operating conditions and weather. New methods for measuring soil thermal conductivity and calibrating heat flux meters have been developed. Surface heat flux profiles and contour plots of soil isotherms have been generated from the experimental data to facilitate an understanding of the thermal behavior of this earth contact building and to validate the detailed computer models.

Preliminary design guidelines are being prepared for the basic earth contact components: walls, floors and roofs. These guidelines present information on thermal performance to enable engineers, architects and builders to compare design strategies.

Contract Number: DE-AC03-80SF11508

Contract Period: October 1, 1980 through December 31, 1982

Funding Source: U.S. Department of Energy through the San Francisco Operations Office

EARTH CONTACT SYSTEMS: DETAILED MODEL DEVELOPMENT, RESPONSE FACTOR SUBROUTINES AND PRELIMINARY DESIGN GUIDELINES

George D. Meixel, Jr.
Lester S. Shen
John C. Carmody
Underground Space Center
University of Minnesota
Minneapolis, MN 55455

Zulfikar O. Cumali
Paul K. Davis
James C. Bull
CCB/Cumali Associates
1221 Broadway, Suite 330
Oakland, CA 94612

ABSTRACT

A detailed numerical model predicting earth contact heat transfer due to conduction has been completed and is currently being validated. This model incorporates appropriate definition of surface boundary conditions and building details. Creation of the earth contact subroutines have utilized discretization processes and boundary conditions similar to the detailed model to generate response factors. Extension of the detailed model to include moisture transport and the associated validation experiments are discussed. The process for preparing preliminary design guidelines for basic earth contact components--walls, floors and roofs--are presented.

INTRODUCTION

Passive and hybrid cooling systems for buildings have the potential to reduce the total energy requirements as well as the peak load demands. Earth contact systems, one means of passive cooling, offer aesthetic appeal, potential environmental benefits and a new dimension for land use planning.

The overall aim of this project is to produce the analytic capability to assess the thermal performance of the earth contact facets of buildings. Computer-based analyses are being validated by carefully planned experimental studies on actual earth-sheltered buildings. Computer subroutines have been developed and interfaced with the response factor energy analysis program DOE-2.1. Both the detailed models and DOE-2.1 enhanced by the earth contact subroutine are being utilized to perform sensitivity studies on earth contact building configurations to develop design guidelines.

Progress on the following goals are discussed in this proceedings:

-Develop a detailed numerical model for predicting earth contact heat transfer from buildings.

-Design and implement an experimental plan for validating the detailed model with data from real buildings.

-Develop earth contact subroutines for inclusion in the response factor type of building thermal analysis program such as DOE-2 or BLAST.

-Utilize the experimentally validated computer programs to carry out parametric studies of the performance of earth contact building components.

-Incorporate the results of the parametric studies into preliminary design guidelines.

Details of the experimental process for defining the earth contact heat transfer from an occupied earth-sheltered building are found in the companion paper "Earth Contact Systems: Soil Temperature and Thermal Conductivity Data, Heat Flux Data and Meter Calibration" by T. P. Bligh, B. H. Knoth, E. A. Smith and D. M. Apthorp; the other goals are discussed in this paper.

1.DETAILED MODELS OF EARTH CONTACT HEAT TRANSFER

For many earth contact configurations numerical solution of the heat diffusion equation

$$C \frac{\partial T}{\partial t} = \vec{\nabla} \cdot (\lambda \vec{\nabla} T) \qquad (1.1)$$

to determine the soil temperature T for constant soil volumetric heat capacity C and apparent thermal conductivity λ (subject to the appropriate boundary conditions at the ground-atmosphere surface, the building interior and deep in the ground) gives reasonable accuracy in the prediction of building earth contact heat transfer. A comprehensive review of relevant methods has been prepared as a deliverable for

this contract [1], and determination of the parameters that influence the accuracy of these models is part of the ongoing validation process discussed later in this paper.

For situations in which the soil apparent thermal conductivity undergoes spatial and temporal changes, a set of coupled equations for heat and moisture flow must be solved simultaneously. Heat is both conducted through the solid soil matrix and convected in the soil pores due to moisture flow. Futhermore, latent effects of the soil moisture play a role in the soil heat flow. The objectives of the current work in model development are to utilize a two-dimensional numerical method to simulate the thermal performance of an earth-sheltered structure and to assess and develop methods for obtaining the soil thermal and moisture properties that are required for the implementation of the numerical method.

Soil Heat and Moisture Transport Model

In the study of soil heat and moisture transport, two principle macroscopic models have been used. These are the mechanistic model of Philip and deVries [2] which applied the transport laws to coupled heat and water flow and the phenomenological model of Taylor and Cary [3] which is based on irreversible thermodynamic theory. When these models are extended to analyze the thermal performance of earth-sheltered buildings, some severe limitations are encountered. This type of problem can be characterized by a heterogeneous domain with both saturated and unsaturated moisture flow and transient boundary conditions. The Taylor and Cary model can not handle transient problems. The Philip and deVries model, with its moisture content-based flow equations, is incapable of describing either saturated moisture flow or a heterogeneous domain. Consequently, a third macroscopic model, proposed by Sophocleous [4], and rederived by Milly [5] are being considered.

The Sophocleous model is a mechanistic model. The principal advantage of this model over the Philip and deVries model is that the moisture flow equation is now based on the soil matric potential rather than the volumetric moisture content. This enables all the problem specifications described above to be treated. The transient flow equations of the Sophocleous model are given by:

$$F\frac{\partial \psi}{\partial t} = \vec{\nabla}\cdot\left(K_\psi \vec{\nabla}\psi\right) + \vec{\nabla}\cdot\left(D_T \vec{\nabla}T\right) - \frac{\partial K}{\partial z} \tag{1.2}$$

and

$$C\frac{\partial T}{\partial t} = \vec{\nabla}\cdot\left(\lambda \vec{\nabla}T\right) + \rho L' \vec{\nabla}\cdot\left(K_{\psi,v} \vec{\nabla}\psi\right) - c_\ell \vec{q}_w \cdot \vec{\nabla}T \tag{1.3}$$

where: ψ is the matric potential,

T is the temperature,

t is the time,

F is the generalized storage coefficient,

K_ψ is the total water hydraulic conductivity,

D_T is the thermal water diffusivity,

C is the volumetric heat capacity of a moist porous medium,

K is the liquid hydraulic conductivity,

λ is the apparent thermal conductivity,

ρ is the liquid water density,

L' is the latent heat of vaporization of water,

$K_{\psi,v}$ is the vapor hydraulic conductivity,

c_ℓ is the specific heat of liquid water,

q_w is the total water flux density.

The generalized storage coefficient is given by:

$$F = \frac{\partial \theta}{\partial \psi} + \frac{\theta}{\phi} S_s$$

where ϕ is the porosity of the soil and S_s is specific storage. The volumetric heat capacity is given by:

$$C = C_{mm} \chi_{mm} + C_o \chi_o + \theta$$

where C_{mm} and C_o are the specific heats of the mineral and organic matter in the soil, respectively, χ_{mm} and χ_o are the volumetric fractions of the mineral and organic matter, and θ is the volumetric moisture content.

From equation (1.2), the flow of soil moisture is a function of the matric potential, the temperature gradient, and gravity. The moisture transport coefficients are given by:

$$K_{\psi,v} = f D_a \nu \left(\frac{Mg}{RT}\right)^2 P_v^s h$$

$$K_{\psi,l} = K$$

$$D_{T,v} = S f D_a \nu \left(\frac{Mg}{RT}\right) h \frac{dP_v^s}{dT}$$

$$K_\psi = K_{\psi,v} + K$$

$$D_T = D_{T,v} + D_{T,l}$$

While such parameters as the molecular diffusion coefficient of water vapor into air, D_a and the humidity, h, can be readily obtained, the pore geometry factor f, the mass flow factor ν, and the ratio of the average temperature gradient in air-filled pores to the overall temperature gradient S must be determined for the particular soil type.

Heat flow in the soil is dependent upon the soil apparent thermal conductivity, the flow of vapor, and the total water flux. The apparent conductivity is a function of soil composition and moisture content. The total water flux is given by:

$$\vec{q}_w = -\rho \left[K_\psi \vec{\nabla}\psi + D_T \vec{\nabla} T + K \hat{e}_3\right]$$

Thus, from the above expressions, the transport and storage coefficients of the two flow equations are functions of temperature and moisture content. Not only are the governing equations coupled and consequently must be solved simultaneously, but they can also be highly non-linear. Analytical solution of these equations is not possible and numerical techniques are required. Because of the non-linear, coupled nature of the problem, instabilities in the numerical approach can cause convergence problems.

Sophocleous formulated his model in an attempt to describe heat and moisture flow under field conditions. In validating his model, a one-dimensional problem was studied with transport coefficients and soil properties being obtained experimentally for two different field soil types. An objective of this study is to extend the application of the Sophocleous model to a transient, two-dimensional problem with boundary conditions similiar to those encountered in the study of earth-sheltered buildings. Model validation is being performed with a two-dimensional axi-symmetric laboratory experiment.

Application of Transport Model to Earth-Sheltered Construction

In order to extend this model to the study of earth-sheltered buildings, a two-dimensional problem must be handled. A sample domain showing a basement case is given in Fig. 1, where q_w is a given moisture flux and q_h is a given heat flux. This is a typical calculation domain which must be properly handled when examining an earth-sheltered construction.

Numerical Method

The solution of the coupled governing equations must be performed numerically. The numerical method used is the Patankar-Spalding finite difference method. This method is an integrated, fully implicit finite difference method developed and implemented by Dr. Suhas V. Patankar here at the University of Minnesota. Because of the complicated numerical problem of the coupled, non-linear equations, this method is particularly well suited for the soil heat and moisture problem. The method has been successfully applied to solution of fluid flow problems governed by the non-linear Navier-Stokes equations. A wide range of convective heat flow problems have also been solved with this method. The numerical scheme is also capable of handling either Cartesian or cylindrical coordinates without major changes in the code.

Experimental Apparatus

An axisymmetric, two-dimensional problem is being used for experimental validation of the calculations. The experiments selected permit the numerical work to be compared to measured temperature and moisture profiles. The configuration is fully defined and has boundary conditions consistent with those that occur in the soil surrounding buildings.

The two-dimensional, axisymmetric experiment involves a cylinder filled with a Mississippi River sand. The choice of sand is based on the relative speed at which the sand will reach steady state. The sand will be sieved such that grain sizes will range between .1 and 2 millimeters. This will be done to minimize the effect of hysteresis on the sorption-desorption curves of the soil. Thus, hysteresis effects will be minimized for the numerical model. The cylinder is adiabatic and impermeable along the side walls. (This boundary is consistent with the far field boundary that exists around a building.) Saturated conditions are held at the bottom of the soil column with temperatures being fixed at both ends. (The saturated constant temperature boundary condition is similar to that below many buildings.) Down the middle of the apparatus there is a tube through which warm water is circulated. This provides a zero moisture flow, constant temperature boundary condition down the center of the cylinder. (This is similar to the condition along the building wall.) The axisymmetric problem is, thus, shown by Fig. 2.

The soil column is allowed to reach steady state with insulation placed in the center tube. This case should be essentially a one-dimensional problem. After steady state is reached, the insulation is removed and warm water circulated through the tube. This then gives a transient two-dimensional axisymmetric problem.

The soil column is one meter tall and approximately 76 cm in diameter. The size is large enough to allow local measurements to be made yet small enough to provide reasonable response times. The isothermal, one-dimensional steady state moisture profile in the appartus is a linear relationship of the form shown in Fig. 3. At the saturated boundary at the bottom of the soil column, $z=0$, the matric potential, ψ is zero while at the upper boundary where z = 1 meter, ψ = -.1 bars. However, if evaporation is permitted at the upper boundary, the soil can dry out to as low as -15 bars. Therefore, the range of matric potentials in the soil will be between zero and -15 bars. Two types of moisture probes are being used: tensiometers and thermocouple psychrometers. Each probe can read matric potentials in the following ranges: tensiometers 0 to -.6 bars and thermocouple psychrometers -0.5 to -30 bars. The tensiometers have been built using porous caps and plastic tubing. Matric potentials are read using manometers. Temperatures are monitored using thermocouples. A Fluke datalogger is being used to record the outputs of the thermocouples. The pychrometers are read by a Wescor psychrometer logger.

For dredged Mississippi River Sand, the moisture characteristic curve has been experimentally determined as shown in Fig. 4. To insure that the moisture profile in the experimental apparatus extends over a wide range of moisture contents, a coarser sand is used below the main soil column to enhance drainage. A tensiometer near the bottom of the soil column is used to help specify a given matric potential for the lower boundary condition. The bottom of the apparatus is set-up as shown in Fig. 5.

Evaluation of the Soil Thermal and Moisture Properties

To reproduce the results obtained from the laboratory experiment by using the numerical model, several soil properties of the sand must be determined experimentally. These are the water characteristic curve, the saturated hydraulic conductivity, the unsaturated hydraulic conductivity, the density and porosity, the apparent thermal conductivity, and the heat capacity of the soil.

The moisture characteristic curve is evaluated using three techniques to obtain data points along the full range of the matric potentials. For matric potentials of -.1 bars to zero, a hanging water column experimental apparatus has been constructed and measurements have been performed. For tensions of -.1 to -15 bars, pressure chambers with ceramic porous plates provided by the Agricultural Engineering Department of the University of Minnesota were used.

The saturated hydraulic conductivity can be obtained by following the level of soil saturation as water drains from a column of soil. The saturated hydraulic conductivity is given by:

$$K_s = \left[\pi R^2 \ln\left(\frac{y_1}{y_2}\right)\right] / \left[s\,(t_2 - t_1)\right]$$

where: R is the radius of the column,

y_1 is the distance from the water table to the water level in the column at time t_1,

y_2 is the distance from the water table to the water level in the column at time t_2,

and S is the shape factor with dimensions of length

The shape factor depends on the geometry of the intake of the column.

The unsaturated hydraulic conductivity can be obtained using the Campbell equation where

$$K = K_s \left(\frac{\theta}{\theta_s} \right)^{2b+3}$$

where K_s is the saturated hydraulic conductivity, θ and θ_s are the moisture content and saturated moisture content, respectively, and b is an empirical constant that can be derived from the moisture characteristic curve.

The porosity of the soil is given by:

$$\phi = 1 - \left(\frac{\rho_b}{\rho_s} \right)$$

where ρ_b is the bulk density, and ρ_s is the particle density. It is acceptable to assume a constant value for the bulk density while the particle density must be obtained experimentally. As with the above parameters, the particle density will be determined using procedures and equipment currently available at the University of Minnesota.

The thermal conductivity of the soil is being determined using an apparatus built by Mostaghimi for previous research at the University of Minnesota. Additionally, the thermal conductivity can be obtained from the theory of deVries [6].

The soil heat capacity is found from the relation:

$$C = C_{mm} \chi_{mm} + C_o \chi_o + \theta$$

where from deVries, C_{mm} is taken as 0.46 cal/cm^3 °C and C_o is given by 0.60 cal/cm^3 °C. The volumetric fraction of the mineral matter, χ_{mm} and the volumetric fraction of organic matter, will be obtained from soil analysis by the Soil Science Lab of the University of Minnesota. With the evaluation of these parameters, the various transport and storage coefficients can be evaluated for the soil being used and the numerical model can be used to simulate the soil column experiment.

Field and Building Verification Studies

Application of the numerical scheme to field studies requires an understanding of the thermal and moisture fluxes present at the earth surface. Such processes as evapotranspiration, rain infiltration, and solar fluxes must be handled in modelling an earth sheltered construction. Work has begun in identifying the important surface moisture and thermal fluxes. An undisturbed field on the St. Paul campus of the University of Minnesota has been instrumented by the Soil Science Department for the purpose of studying the interactions taking place at the soil-plant-atmosphere interface.

In addition to these experiments, field work is being be done at the Massachusetts Institute of Technology around the earth sheltered building constructed there. Temperature, heat flux and moisture measurements are being performed for use in applying the numerical model described above to real world boundary conditions and run for a building geometry. The soil environment around the building has been instrumented with temperature and heat flux probes as well as specially constructed thermal needles to measure thermal conductivity.

2. RESPONSE FACTOR SUBROUTINE FOR EARTH CONTACT ANALYSIS

If one is to adequately define energy conservation measures or develop innovative energy efficient building design, accurate analytical models of the heat transfer processes in residences and commercial structures are required. Various energy analysis computer simulation programs are presently available for use in the public sector. Amoung these, DOE-2.1a and BLAST represent the state of the art in determining building thermal loads and energy useage. However, these programs do not rigorously analyze earth contact heat transfer. For single family residences, below grade or basement heat losses may represent upwards of

20% of the annual heating load. For buildings that have extensive earth contact, heat exchange may be dominated by the earth-sheltered surfaces. Thus, it is apparent that adequate mathematical models must be developed to properly define such phenomena.

The thermal load in an earth contact structure is a function of the local climate, ground, wall and floor properties and the geometry and the environmental conditions maintained in the structure itself. The problem is to establish a method or methods whereby the energy required to maintain a space environment can be estimated. Heat conduction to the ground is in principle a three dimensional problem. The shape of the space and its relationship to the ground need to be considered. The construction of the walls and floors may be multilayered and insulated to different depths. The ground itself is multilayered and some layers are subject to freezing and thawing. Water content of the ground changes by season. In addition, the ground surface is subjected to daily and annual fluctuations in temperature, solar radiation, wind and ground cover such as vegetation, snow, etc. The internal environment is also subject to change which further complicates the problem.

However, certain simplifications can be made to allow a description of the fundamental processes. The exterior environment can be described by determining a ground surface temperature as the driving function. This accounts for the air temperature, solar radiation, ground absorptivity and the surface heat transfer coefficient. It can also be modified to account for snow cover and evapotranspiration. Therefore, the primary exterior influences can be obtained in terms of a single variable. Further simplifications result by assuming time independent ground, wall and floor properties, and geometry such that one can ignore the third dimension.

With these constraints it is feasible to construct solutions to this problem for most of the common earth contact configurations encountered in buildings. The solutions can be obtained in a manner that is fast and well within the needed range of accuracy. When the time dependance of material properties are introduced, the problem is considerably more complicated. Although we have not dealt with time dependent properties in this study, work done has considered its implications and the techniques and computer codes developed have taken this eventuality into account.

Work completed in the development of response factor subroutines for earth contact analysis can be summarized under the following headings:

1. Identification of earth contact structure classifications.
2. Identification and development of the heat transfer model and accompanying input/output variables.
3. Development of a detailed program outline for the interation between this model and DOE-2.
4. Execution and testing of the program outline.
5. Documentation.
6. Installation.

The successful completion of this work has resulted in an algorithm that captures the essence of an expensive detailed finite element computation of earth contact heat transfer through an inexpensive response factor formulation without sacrificing accuracy in predicting building heat transfer. Remaining paragraphs in this section present the response factor concept as it applies to the earth contact subroutines.

Thermal Response Factors

Quite often complex conduction heat transfer problems cannot be solved analytically. By discretizing the problem using nodal points, the problem can be expressed in terms of first order differential equations. This set of equations can be solved at each time step for all the nodes. Frequently, only the heat fluxes and temperatures at the boundaries are required and not at interior points in the calculation domain. For example, consider a one dimensional slab (e.g. a wall section) shown in Fig. 2.1, where the T's are the temperatures (subscripts refer to o-outside, r-room and s-surface), L is the slab thickness and q is the surface heat flux. One can express the problem in terms of the response factor series X, Y, Z as follows:

$$q_o(t) = \sum_{i=1}^{\infty} X_i T_{so}(t-i) - \sum_{i=1}^{\infty} Y_i T_{sr}(t-i) = h_o (T_o - T_{so}) \qquad (2.1)$$

$$q_r(t) = \sum_{i=1}^{\infty} Y_i T_{so}(t-i) - \sum_{i=1}^{\infty} Z_i T_{sr}(t-i) = h_i (T_{sr} - T_r) \qquad (2.2)$$

Physically the response factors correspond to the time history of the heat flux resulting from the application of a unit temperature pulse at time t=0 at a surface either at that surface (X for surface so, Z for surface sr) or at the opposite surface (Y for surface so to surface sr) for all succeeding times t. As these are the results for unit pulses, arbitrary functions of time T(t) can be accommodated as multiples of the unit pulse. For a two dimensional situation such as that found in the below-grade portion of a building, Fig. 2.2, one can develop response factors for each surface as well as from one surface to another. In the case shown in Fig. 2.2 there are four sets of response factors for each surface, e.g. at the ground surface there are the response factors X_g, Y_{gw}, Y_{gf}, Y_{gd} (note that the subscript g designates the ground-atmosphere surface, w-wall surface, d-deep ground, f-floor surface). The net flux at the wall can be described as:

$$q_w(t) = \sum_{i=1}^{\infty} \left[T_g(t-i) Y_{gw}(i) + T_d(t-i) Y_{dw}(i) + T_r(t-i) Y_{fw}(i) - T_r(t-i) X_w(i) \right] \qquad (2.3)$$

Note that we have defined the response factor in this case from the ground surface to room air thus including the surface film coefficient rather than to the wall surfaces in the room. Response factors can be generated in a variety of ways. References 7, 8, 9, provide further descriptions of the various methods. The method of obtaining the ground response factors is discussed in the following section.

Ground Response Factor Generation

Ground thermal response factors are obtained by setting up a finite element model to represent the configuration of the ground layers, walls and floors relative to each other, specifying their respective thermal properties and surface boundary conditions and solving the resulting equations using the method of Ceylan and Myers. [10]

The finite element method applied to heat transfer problems is described in the report completed as part of Task 1.2 of this contract [1]. The Ceylan and Myers method is documented in detail in Ceylan's Ph.D. Thesis [11] and reference [10]. Only the governing equations and results will be described here.

The process for calculating the weekly response factors that describe the heat flow through the ground can be divided into two portions. These are: (1) the construction of the finite element model (or models), and (2) the solution of the model to obtain response factors.

The method employed by Ceylan and Myers uses an exact solution of the governing transient heat conduction equation to obtain the response factors. By dividing the calculation domain into regions, the governing differential equation is discretized for each element. This results in matrices that correspond to the set of finite element discretization equations. The coefficients of these equations are calculated by the method defined by Wang [12]. The analytical solution of this matrix can be obtained by employing Duhamel's theorem. Determination of the exact solution to the matrix avoids the lengthy simulation techniques of finite difference or finite element methods. Solution of the coefficient matrices generates the necessary response factors.

The construction of the model can be seen as the transformation of the data from the input form to the matrices which describe the model. We have used the DOE-2 input routines to scan the language structure, supply default values and provide the input data in numeric form in an organized, compact set of arrays. We selected the matrix data structure from the finite element program by Wang. Some routines from Wang's program have been used to calculate some of the matrix components. The response factors are solved from the finite element model by the method of Ceylan and Myers, with some modifications.

In the following sections we describe the solution method first and then the model generation.

A. Solution Method for Ground Response Factors

In matrix form the heat diffusion equation is the equation to be solved is:

$$[C]\,[\dot{T}] + [S]\,[T] = [P]\,[s] \tag{2.4}$$

This is supplemented by

$$[u] = [U]\,[T] \tag{2.5}$$

The terms in the above equations are as follows:

The capacitance matrix, [C]: This is a diagonal matrix. The values are the thermal capacitance per unit width associated with each node of the model.

The conductance matrix, [S]: This is a banded symmetric matrix. The values are the thermal conductances per unit width between nodes and, for diagonal values corresponding to nodes of an external boundary, the convective transfer coefficient per unit width.

The driving function matrix, [P]: This is rectangular. The values are the convective transfer coefficient per unit width between a given driving function and a given node.

The resultant flux matrix, [U]: This is rectangular. The values are conductances per unit width which would be used in calculating resultant heat fluxes. There is a resultant heat flux for each driving function.

[T] is the time varying temperature vector with the dot over T indicating the time derivative.

[s] is the vector of driving functions. The driving functions are the ground surface temperature, deep ground temperature and air temperature.

[u] is the heat flux vector. Typically we will be interested only at fluxes at boundary nodes.

Ceylan and Myers demonstrate a solution for the response factors, which they notate as a matrix $[A_i]$ with i being the number of time steps delay, of the form:

$$A_0 = [u][X][\Lambda]^{-1}[X]^T[P] - [u][X][\Lambda]^{-1}\left(\frac{[I] - e^{-[\Lambda]N_h}}{N_h}\right)[\Lambda]^{-1}[X]^T[P] \tag{2.6}$$

$$A_i = [u][X]\left(e^{-[\Lambda]N_h}\right)^{i-1}[\Lambda]^{-1}\left(\frac{[I] - e^{-[\Lambda]N_h}}{N_h}\right)^2[\Lambda]^{-1}[X][P] \tag{2.7}$$

in which N_h is the time step size (168 hours in the present implementation) and $[\Lambda]$ and [X] are the solutions of:

$$[S]\,[X] = [C]\,[X]\,[\Lambda] \tag{2.8}$$

$$[X]^T[C]\,[X] = [I] \tag{2.9}$$

Here the [X]'s are the eigenvectors, $[\Lambda]$ is the diagonal matrix representing the eigenvalues of the above set of equations. [I] is the identity matrix. A further simplification is accomplished by defining

$$[H] \equiv [C]^{-1/2}[S]\,[C]^{-1/2} \tag{2.10}$$

$$[Z] \equiv [C]^{1/2}[X] \tag{2.11}$$

Since [C] has no zero's on the diagonal we can transform the equations to be solved (2.8, 2.9) to standard form:

$$[H]\,[Z] = [Z]\,[\Lambda] \tag{2.12}$$

$$[Z]^T[Z] = [I] \tag{2.13}$$

After solving equations (2.12) and (2.13) [ ] is known and from equation (2.1) the vector [X] is obtained. Substitution of [Λ] and [X] into equations (2.6) and (2.7) produces the response factors.

Details of this process are currently in draft form as a deliverable for Task 1.7 of this contract.

3. VALIDATION PROCESS FOR EARTH CONTACT COMPUTER MODELS

The computer code validation plan is composed of a series of studies that progress from a focus on the elements of the computer analysis to the validation of the comprehensive multi-dimensional model of earth contact heat transfer necessary to represent the most complex aspects of the thermal performance of earth contact buildings. Separate examination of the various analytical elements--e.g., ground surface boundary condition, phase change due to freezing and thawing, or three dimensional effects at building corners--facilitates comparison with experimental data to specifically validate each aspect of the model. Once confidence in the representations for each component are established, integration of these components into more sophisticated analytical tools will generate the capability to compare numerical predictions with experimental data from more complex building configurations. Because the DOE-2/BLAST subroutine is derived from the detailed analytical model, once consistency with the detailed model is established, successful validation of the detailed model simultaneously establishes confidence in the subroutine. In addition, because the DOE-2/BLAST earth contact subroutine has been incorporated into a dynamic building energy analysis computer program, this capability to predict energy performance can be utilized to further verify the earth contact models by comparisons with data on building energy use.

Data for detailed model and earth contact subroutine validation and verification is being obtained from a variety of sources. The most comprehensive heat transfer and energy performance data from a real world, occupied earth contact building is being generated at the MIT earth sheltered residence. Data on earth contact heat transfer in a predominantly cooling environment is being collected at the Environmental Research Center at the University of Arizona. Detailed laboratory data describing coupled heat and moisture transfer is being recorded and analyzed at the University of Minnesota. In addition to the preceding data acquisitions which are primarily funded by the Department of Energy, the Owens-Corning Fiberglass Technical Center in Granville, Ohio, has agreed to share extensive data on the thermal response in and around basements, and the University of Minnesota Agricultural Research Station is furnishing comprehensive data on both the energy balance at the surface of a sod covered field and the temperature response beneath it.

Primary Variables for Validation

Comparisons between measured and computed temperatures and heat fluxes comprise the majority of the initial validation efforts. Because computer predictions and experimental measurements of moisture movement and ground thermal conductivity are complex, modeling of these quantities in the vicinity of the earth sheltered building will be intensely pursued only after the initial studies are completed.

As shown in Fig. 3.1, ground temperature profiles beneath the surface of a uniform sod covered field clearly show the thermal state of the soil and are readily compared with computer predictions. Similarly, a two dimensional description of the thermal relationship between a building and the ground can be clearly represented by mapping the temperature field in the earth surrounding the building. The process for obtaining this data is described in chapter 4 of the experimental plan developed in Task 1.5 for this contract. Examples of computer predictions of the isotherms in the ground between two earth contact buildings are shown in Fig. 2. Comparison of the experimentally measured temperature field with such computer predictions readily show areas of agreement or discrepancy.

The most sensitive measure of the earth contact heat transfer process, both analytically and experimentally, are local values of heat flux. Measurements of this variable are being made on the building earth contact surfaces. Figure 3.3 shows plots of the computer predicted heat flux profile for an underground wall during February and July. Even a cursory examination of Fig. 3.3 reveals changes in heat flux due to insulation placement and due to multi-dimensional heat flow at the corners.

Earth contact surface heat flux is directly related to the HVAC load. The spatial integral of the heat flux over the inside of the building envelope is the instantaneous HVAC load; the time integral of the instantaneous HVAC load is the HVAC energy required to condition the living space. Thus measurements and predictions of heat flux are of primary importance to the building performance studies. A discussion of experimental building energy balance is presented in chapter 6 of the Task 1.5 experimental plan.

Determination of moisture movement in soils and definition of the heat transfer at the boundaries of the building or at the ground surface require additional measurements that have been discussed under the heading "1. Detailed Models of Earth Contact Heating Transfer" of this paper.

Elements of the Validation Process

The purpose of this section is to provide a cursory delineation of most elements in the validation process. As comparisons between experimental data and computer predictions continue to be made, it is expected that additional elements requiring inclusion in the validation process will be identified.

The list of topics is organized in general order of increasing complexity and sophistication and, therefore, is in approximate chronological order.

One dimensional Detailed Model

The one dimensional detailed model of earth contact heat transfer has formed the basis for all future increases in modeling complexity. Because only one spatial dimension is involved, evaluation of the level of agreement is particularly straightforward. Specific attention is being given to validating the computer models ability to describe:

(1) the ground surface boundary energy balance,

(2) phase change due to freezing and thawing of the soil, and

(3) seasonal changes in soil thermal conductivity.

The comprehensive data necessary to perform this validation is being recorded at the experimental field site at the University of Minnesota. In addition to soil temperature and moisture profiles, the requisite experimental measurements for performing an energy balance at the ground surface are being made. Incoming and outgoing long and shortwave radiation, evaporation rate, and air relative humidity, temperature and wind speed, are continually monitored. To check the numerical model for a different set of climatic conditions, additional one dimensional data is avaliable from the University of Arizona experimental site.

Once the detailed one dimensional model is validated against field data it can be applied immediately to the analysis of the earth covered roof at the MIT earth sheltered residence. Study of this situation will also verify the analytical model of the inside surface convection coefficient on the ceiling.

Two Dimensional Detailed Model

Extension of the detailed model to a two dimensional spatial analysis results in the potential to predict earth contact heat transfer from the walls and the floor in situations where a two dimensional representation is valid. For example, such an analysis appears to be appropriate along the axis of symmetry of an earth contact building. One important aspect of the response of earth contact buildings which can be estimated with this level of detail concerns the time period necessary for the building to reach an equilibrium condition, or a time dependent steady state, with the ground. Preliminary analysis has indicated that this initial period of ground warm-up may vary from several months to more than one year. To meet both the need to validate the detailed model during the initial transient period and the necessity of determining valid long term earth contact heat transfer rates, data from several experimental locations are being gathered.

The MIT earth sheltered residence and the University of Arizona earth contact building will furnish data on ground temperatures and earth contact heat fluxes. Because these buildings will have been operational for less than a year, they will serve to document the initial interactions of an earth contact building with the ground. Although it is expected that these buildings will approach time dependent steady state in the ground, to establish the detailed computer models capability to accurately predict the long term response of an earth contact building, comprehensive long term data is required. At the Owens-Corning Fiberglass Technical Center (OCF) in Granville, Ohio, three basements have been in the ground for many years. For the past year and one-half, detailed data has been obtained to document the thermal response in the soil surrounding these basements. In cooperation with OCF, this basement data will be used to determine the long term accuracy of the detailed model.

Three Dimensional Detailed Model

Although it is probable that many aspects of earth contact heat transfer can be accurately predicted with the two dimensional model, certain characteristics vital to the evaluation of the passive cooling performance of earth contact facets of buildings require a full three dimensional representation for accurate modeling. Because: 1) the potential of the ground to act as a heat sink may be strongly influenced by the volume of earth available to store heat, and 2) the precise definition of that volume requires three dimensional specifications, the full three dimensional model is necessary for the validation process and the basic parametric studies. Once the parametric dependencies on three dimensionalality are

defined, through the use of a validated three dimensional numerical model, it is probable that correction factors can be developed for the detailed two dimensional model.

Another three dimensional aspect of earth contact heat transfer that is significant for both heating and cooling season thermal performance concerns the multi-dimensional heat flow at building corners. Because a corner may be characterized by two dimensional heat transfer--e.g., the intersection of the floor and one wall--or by three dimensional heat flow where three surfaces intersect--e.g., two walls and the floor--resulting in increased heat exchange with the ground at these locations, the resulting magnitude of the nonuniforminity in heat flux must be determined to accurately predict energy consumption.

To experimentally document the three dimensional response of the MIT earth sheltered residence, considerable effort has been directed at developing a comprehensive plan for measuring the three dimensional variations in earth contact heat flux and soil temperatures. The details of the experimental plan are presented in the Task 5 experimental plan. Predictions of variations in surface heat flux and soil temperatures as generated by the three dimensional detailed computer model will be compared with this experimental data.

Earth Contact Subroutine for DOE-2/BLAST

Validation of the earth contact subroutine occurs both implicitly, since it is based on the validated detailed models, and explicitly, as the computer predictions of energy use at the MIT earth sheltered house are compared with experimental data. To insure that the process for distilling the constant property two dimensional detailed model into a response factor representation suitable for interfacing with both DOE-2 and BLAST has maintained the sensitivity of the analysis to the key parameters--e.g., building configuration, insulation placement, and ground thermal properties--a series of consistency checks between the subroutine and the detailed models is being performed. The subroutine will be tested for the basic building configurations as outlined in the final report for Task 7.

Energy Performance

The bottom line for evaluation of the development of the analytic capability to assess the thermal performance of the earth contact facets of buildings is the accuracy of the predictions of available energy savings and improvements in comfort. A thorough experimental analysis of the energy balance of the MIT earth sheltered residence is being performed to define the thermal performance of this structure. Similarly, a thorough computer analysis of this structure will be performed utilizing both the detailed models of earth contact heat transfer and the earth contact subroutine as implemented in DOE-2. Comparisons of the experimental measurements and the computer predictions will provide guidance for the interpretation of the computer predicted energy savings available with earth contact passive cooling techniques.

4. DEVELOPMENT OF PRELIMINARY DESIGN GUIDELINES

A basic purpose of the current research of earth contact structures is to develop tools to accurately analyze their energy-related behavior, particularly with regard to passive cooling. These tools can then be used to assess cost-effectiveness and provide comparisons between different energy-efficient strategies for small structures. They can also be used to optimize designs of earth contact buildings depending on local conditions and individual priorities. In many cases earth contact structures are built for a variety of reasons aside from energy conservation in cooling or heating. It is therefore important to optimize the design of earth contact buildings so that energy-related benefits can be realized while the effect of potential drawbacks can be diminished. The design guidelines portion of the current research project is intended to provide a useful explanation of the thermal behavior of earth contact structures. When appropriate, definite guidelines concerning optimal design will be stated.

Relationship of Earth Contact Structures to Energy-Efficiency in Housing

Since the primary focus of the current research is on the energy-efficient potential of small earth contact structures (mainly housing), it is useful to examine how earth contact buildings are related to overall energy use in housing. Diagram 1 indicates the wide range of energy uses that can be attributed to the development, construction and operation of housing. Also indicated are several areas in which earth contact structures can have a direct effect on energy use. In addition to the benefits associated with space heating and cooling, there are various benefits associated with the unique ability to build earth contact housing at reasonably high densities on steeply sloping land that is normally considered unbuildable with conventional structures. Also, earth contact buildings can be built adjacent to uses that are normally considered incompatible or undesirable for housing (i.e., noisy freeways, airports, industry). These diverse advantages of earth contact structures underline the need for adequate tools of energy analysis.

Decisions in Planning and Design of Housing That Affect Energy Use

In examining relatively detailed problems such as the effect of roof, wall and floor components on space cooling and heating, it is useful to consider the numerous interrelated decisions made at various scales which affect energy use in housing. In diagram 2, decisions are grouped into three categories: (1) the community or development scale, (2) the site design and building form scale, and (3) the scale of individual building systems and details. The current research and resulting design guidelines for earth contact structures focus mainly on the latter category emphasizing thermal behavior of roof, wall, and floor components. There are also guidelines to be determined in the more general second category particularly concerning the optimal configuration of the building and its relationship to the earth. Although some of the most significant energy-related decisions are made at the community scale, they are not within the scope of the current project. The project has been defined as the analysis of single, detached structures. Some of the community scale decisions, such as the use of sloping topography have an important relationship to the feasibility and density of earth contact structures.

In examining diagram 2, it is important to recognize that determining energy-efficient development and construction patterns does not occur in a hierarchial manner. Nor does the planning and design process in general proceed directly from large scale to small scale decisions. There is an interaction between the different scales to determine the optimal solutions. For example, heat transfer through walls must be understood to determine optimal building shape or the impact of attached vs. detached units. Each issue area in diagram 2 implies that a decision must be made between various alternatives. It will be of great use to place the results of future research into this overall context so that energy-efficient patterns can occur at all scales and their relative impact assessed.

Basic Decisions Concerning Guidelines

The concept of presenting data on energy use for earth contact structures and developing guidelines from this data appears to be direct and simple. There are a number of complex and interrelated decisions that must be made, however, to ensure that the information is usable and that the guidelines are, in fact, valid conclusions based on the data that is generated.

The following is a list of the major decisions that must be made concerning the content and form of the guidelines:

1. SELECTION OF CASES TO BE ANALYZED
   (includes variations in roof, walls, floor, and overall building configuration)

2. SELCTION OF CLIMATES
   (locations representing predominantly cold and hot as well as temperate climates)

3. DETERMINATION OF TYPE OF DATA
   (appropriate use of annual energy use data, heating season data, cooling season data, monthly energy use data, and peak loads)

4. DETERMINATION OF COST EFFECTIVENESS
   (establishing appropriate ranges for energy costs and construction costs associated with various strategies)

5. PRESENTATION OF MATERIAL
   (determination of clearest and most efficient form of presentation using graphs, charts and summarizing basic guidelines)

As a means of illustrating the factors involved in developing design guidelines for earth contact structures, the wall component has been selected as an example. For simple variations in insulation placement and thickness on an earth contact wall to be meaningful, a number of priorities and characteristics must first be defined. These factors are indicated in diagram 3. Following diagram 3 is a series of illustrations showing some of the extensive variations that can be analyzed in order to develop design guidelines.

ACKNOWLEDGEMENTS

The cooperative nature of the Earth Contact Systems work among researchers at the University of Minnesota, CCB/Cumali Assoicates, MIT, Honeywell and Architectural Alliance has characterized this project. Researchers at MIT directed by Professor Thomas P. Bligh have made significant contributions to the work discussed in this paper. We also thank Professor Donald Slack from the Department of Agriculture Engineering at the University of Minnesota for his continuing guidance in the studies of coupled heat and moisture transport.

The author acknowledges the financial support for this project from the Department of Energy San Francisco Operations Office. Also noted are the contributions of moisture sensing equipment from the Control Data Corporation and the Department of Agricultural Engineering at the University of Minnesota. Computer time has been furnished by the Department of Civil and Mineral Engineering at the University of Minnesota.

REFERENCES

1. MacArthur, J. Ward, Earth Contact Systems contract DE-AC03-80SF11508 Task 1.2 deliverable: "Analytical Methods for Predicing Heat Flow in Earth Contact Systems," June 1981.

2. Philip, J.R. and deVries, D.A., "Moisture Movement in Porous Materials Under Temperature Gradients," Transactions, AGU, 38, 222-232, 1957.

3. Taylor, S.A. and Cary, J.W., "Analysis of the Simultaneous Flow of Water and Heat or Electricity with the Thermodynamics of Irreverisble Processes," Trans. Int. Congr. Soil Sci. 7th, I, 80-90, 1960.

4. Sophocleous, M., "Analysis of Water and Heat Flow in Unsaturated Porous Media," Water Resources Research, 15, 1195-1206, 1979.

5. Milly, P.C.D., "Moisture and Heat Transfer in Hysteretic, Inhomogeneous Porous Media: A Matric Head Based Formulation and a Numerical Model," Water Resource Research, 18, 489-498, 1982.

6. deVries, D.A., "Thermal Properties of Soils" in Physics of Plant Env., ed. R.W. van Rijk, 210-235, North Holland, Amsterdam, 1963.

7. CCB/Cumali Associates, Interim Report - Passive Solar Calculation Methods, DOE Contract Number EM 78-C-01-5221, April 15, 1979.

8. Mitalas, G.P. and Stephenson, D.G., "Cooling Load Calculations by Thermal Response Factor Method," ASHRAE Transactions, Vol. 73, Part 1, 1967.

9. Mitalas, G.P. and Stephenson, D.G., "Room Thermal Response Factors," ASHRAE Transactions, Vo. 33, Part 1, 1967.

10. Ceyland, H.T. and Myers, G.E., "Long-Time Solutions to Heat Conduction Transients with Time-Dependent Inputs," Journal of Heat Transfer, Vol. 102, 115, 1980.

11. Ceylan, H.T., Long-Time Solution to Heat Conduction Transients with Time-Dependent Inputs, Ph.D. Thesis, University of Wisconsin, Madison, 1979.

12. Wang, F.S., User's Manual for the Finite Element Heat Conduction Computer Program, Unpublished Draft, Styrofoam Brand Products, Granville, Ohio, 1979.

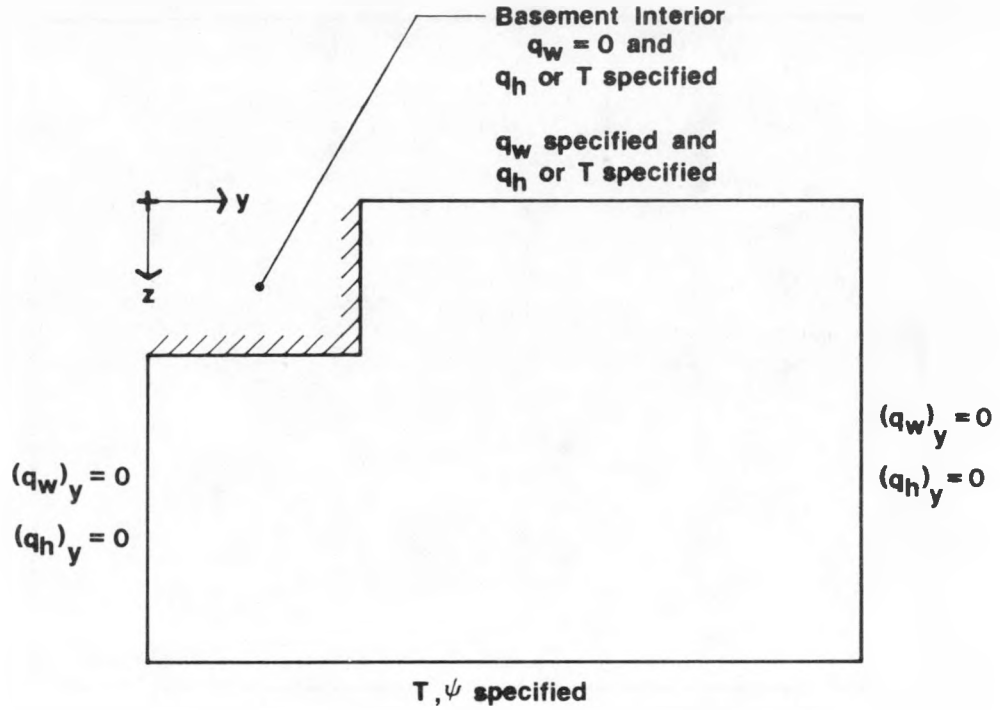

Figure 1. Sample Calculation Domain for Earth Contact Portion of Basement Wall. In the designation of the boundary conditions q_w is the moisture flux, q_h is the heat flux, Ψ is the matric potential, T is the temperature and $(\ )_y$ indicates the y or horizontal component.

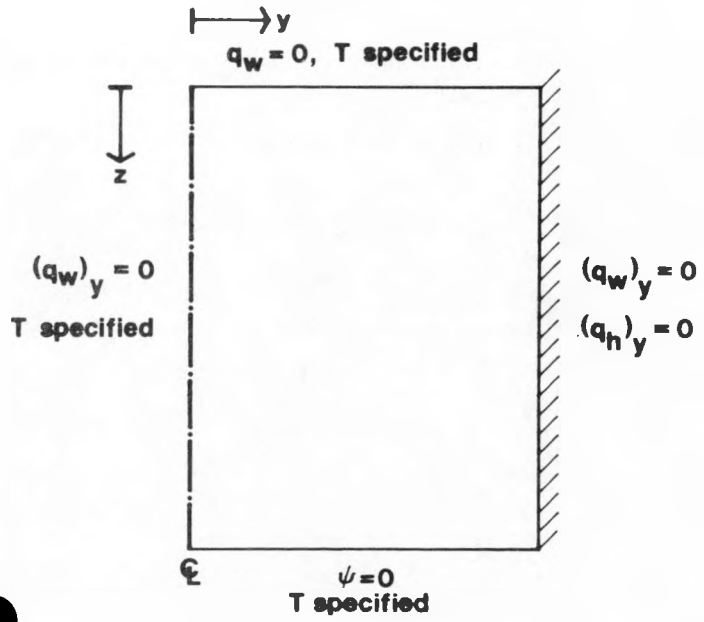

Figure 2. Axisymmetric Calculation Domain for Laboratory Experiments.

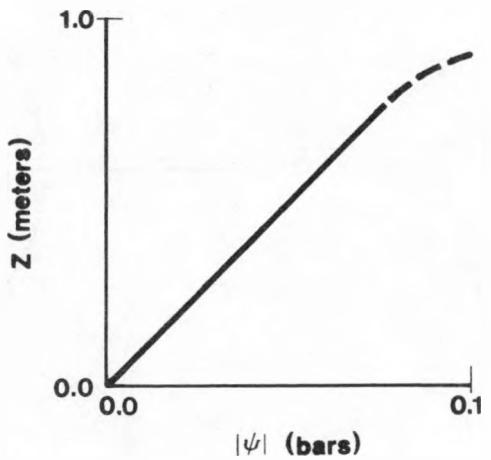

Figure 3. Sketch of General Form for Vertical Moisture Profile in Experimental Apparatus at Steady State.

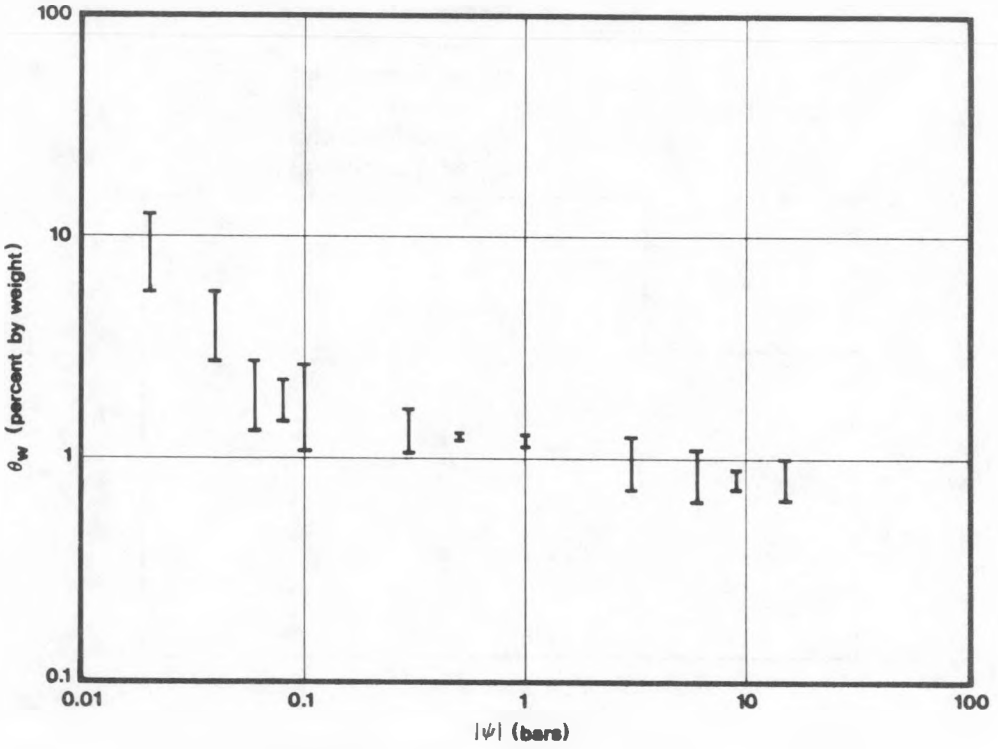

Figure 4. Soil Moisture Characteristic for dredged Mississippi River Sand.

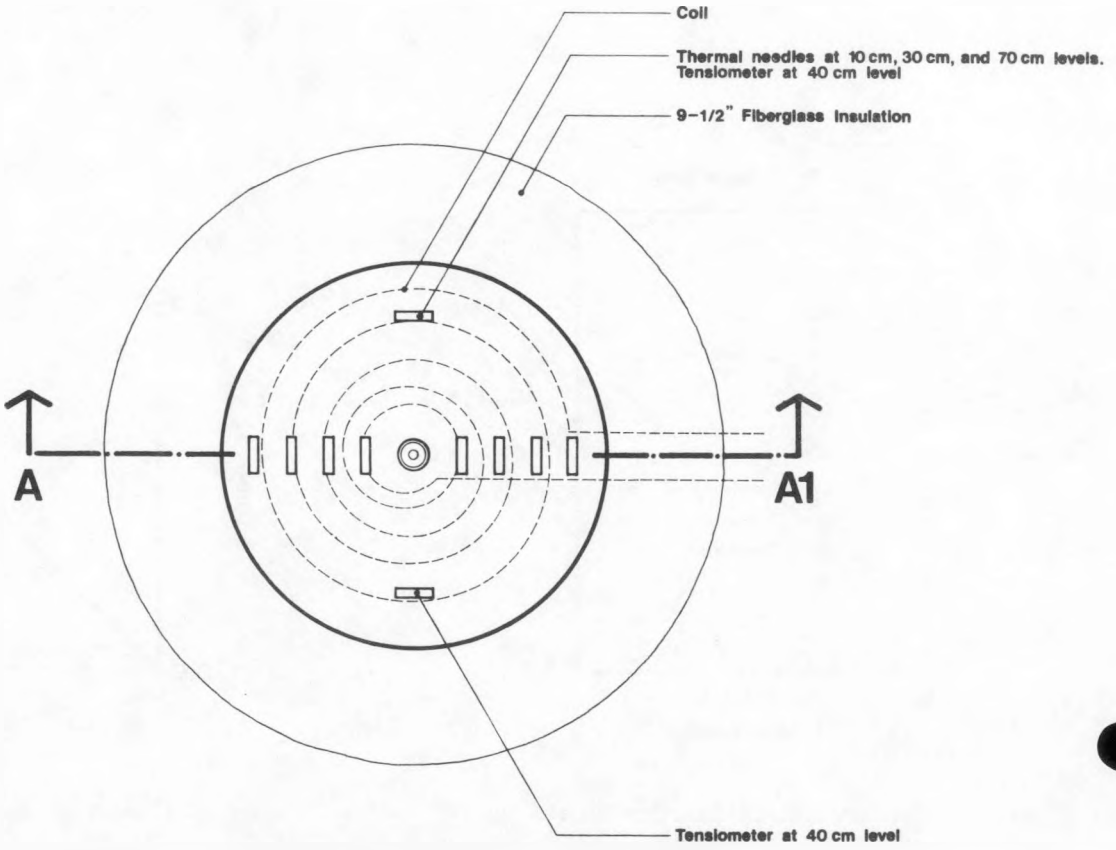

Figure 5a. Plan View of Axisymmetric Experimental Apparatus for Coupled Heat and Moisture Transport Studies.

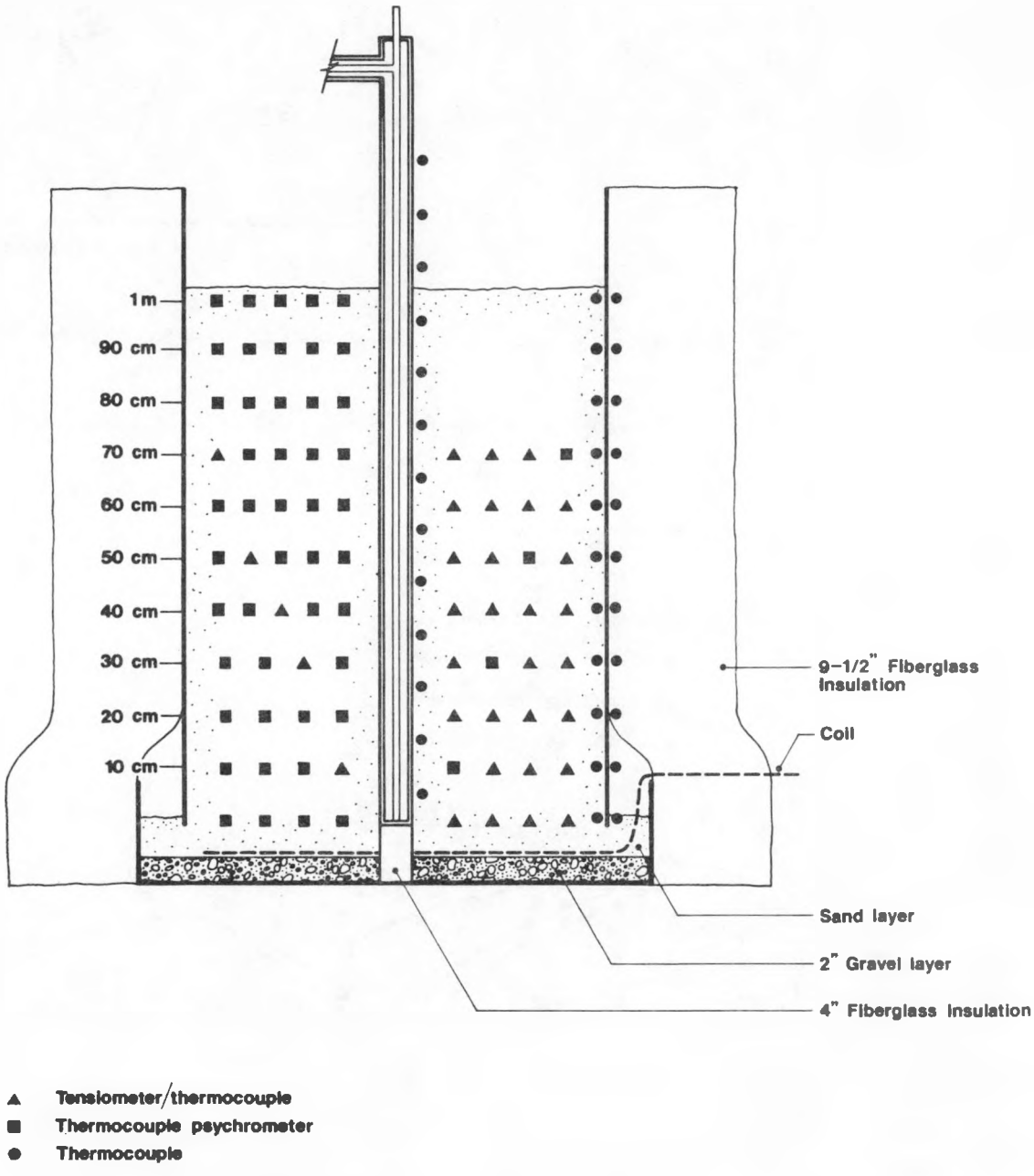

Figure 5b. Section View of Axisymmetric Experimental Apparatus for Coupled Heat and Moisture Transport Studies.

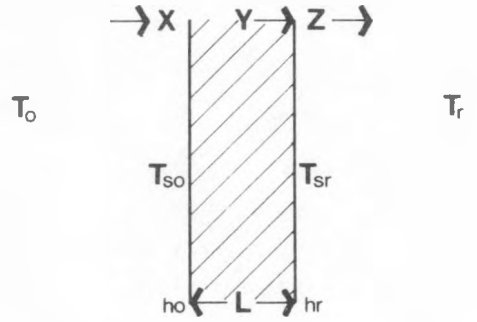

Figure 2.1. Wall Section Showing Coordinate System for Response Factors.

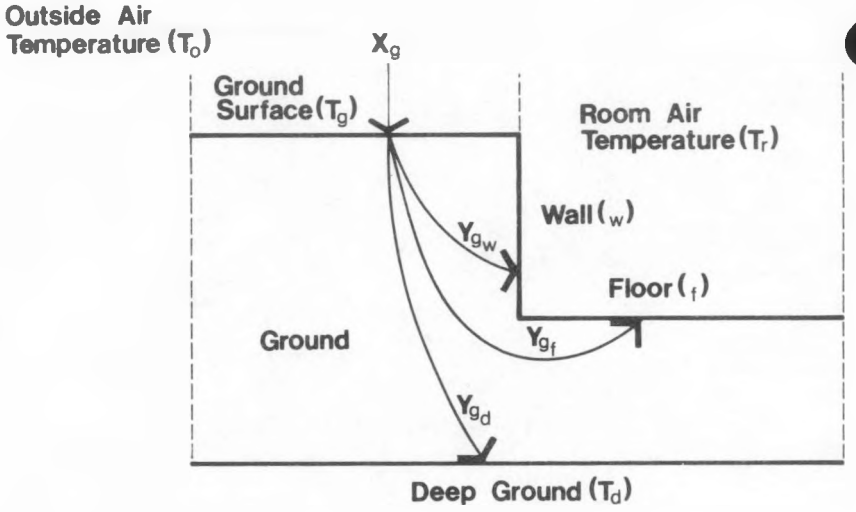

Figure 2.2. Schematic for Response Factor Representation of Earth Contact Heat Transfer.

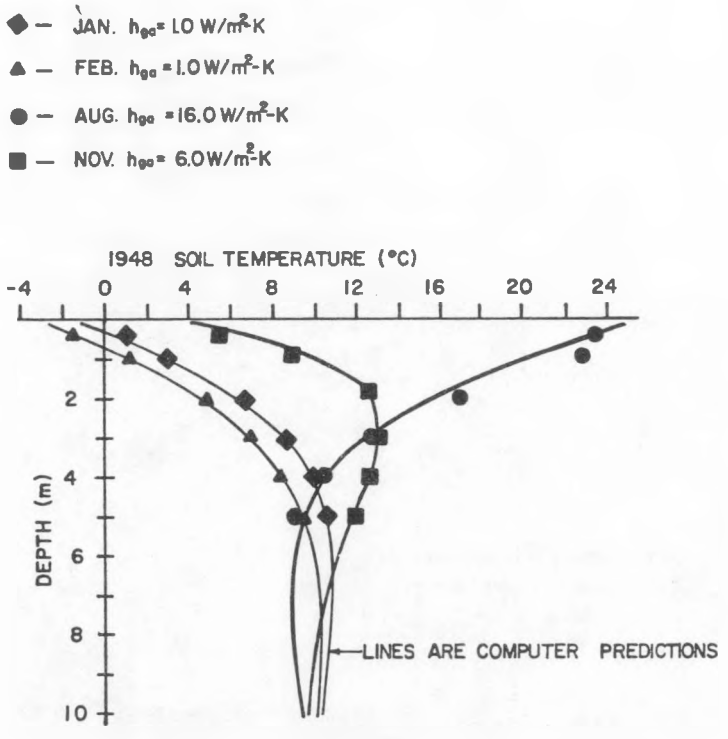

Figure 3.1. A comparison of Numerically Predicted Soil Temperatures (Solid Lines) with Measured Values (Symbols) taken by Algren in 1948 in Edina, Minnesota.

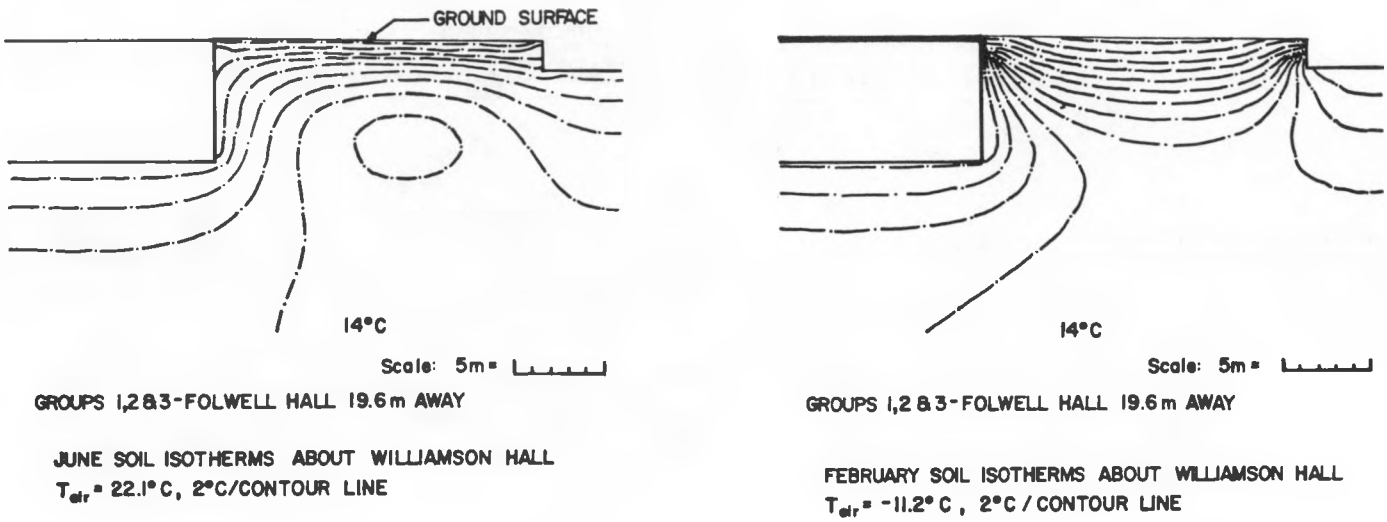

Figure 3.2. Computer Predicted Earth Temperatures.

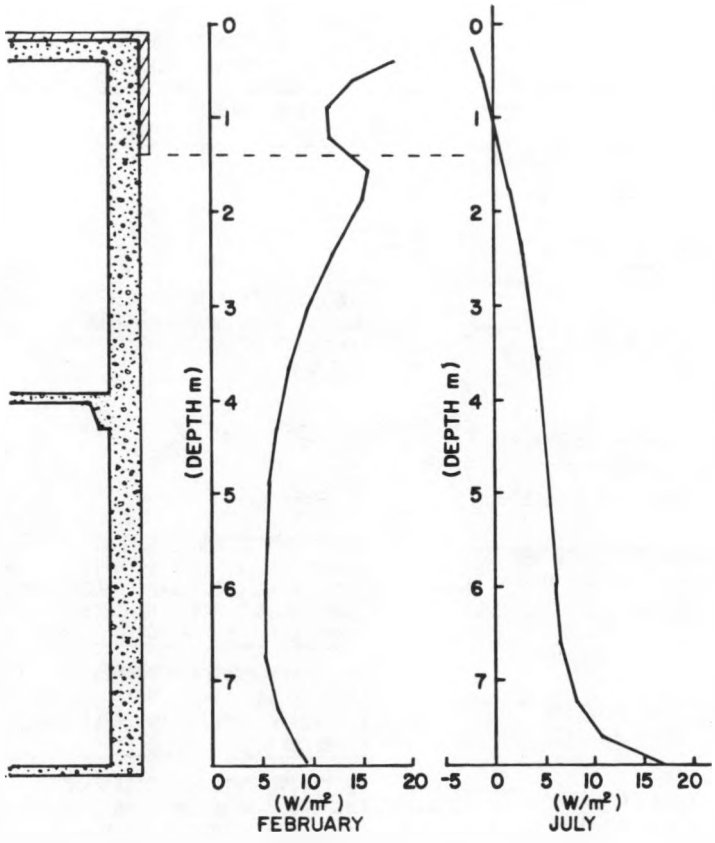

Figure 3.3. Inside Surface Wall Heat Flux for Williamson Hall.

DIAGRAM 1

ENERGY-EFFICIENCY IN HOUSING AND THE RELATIONSHIP TO EARTH CONTACT STRUCTURES

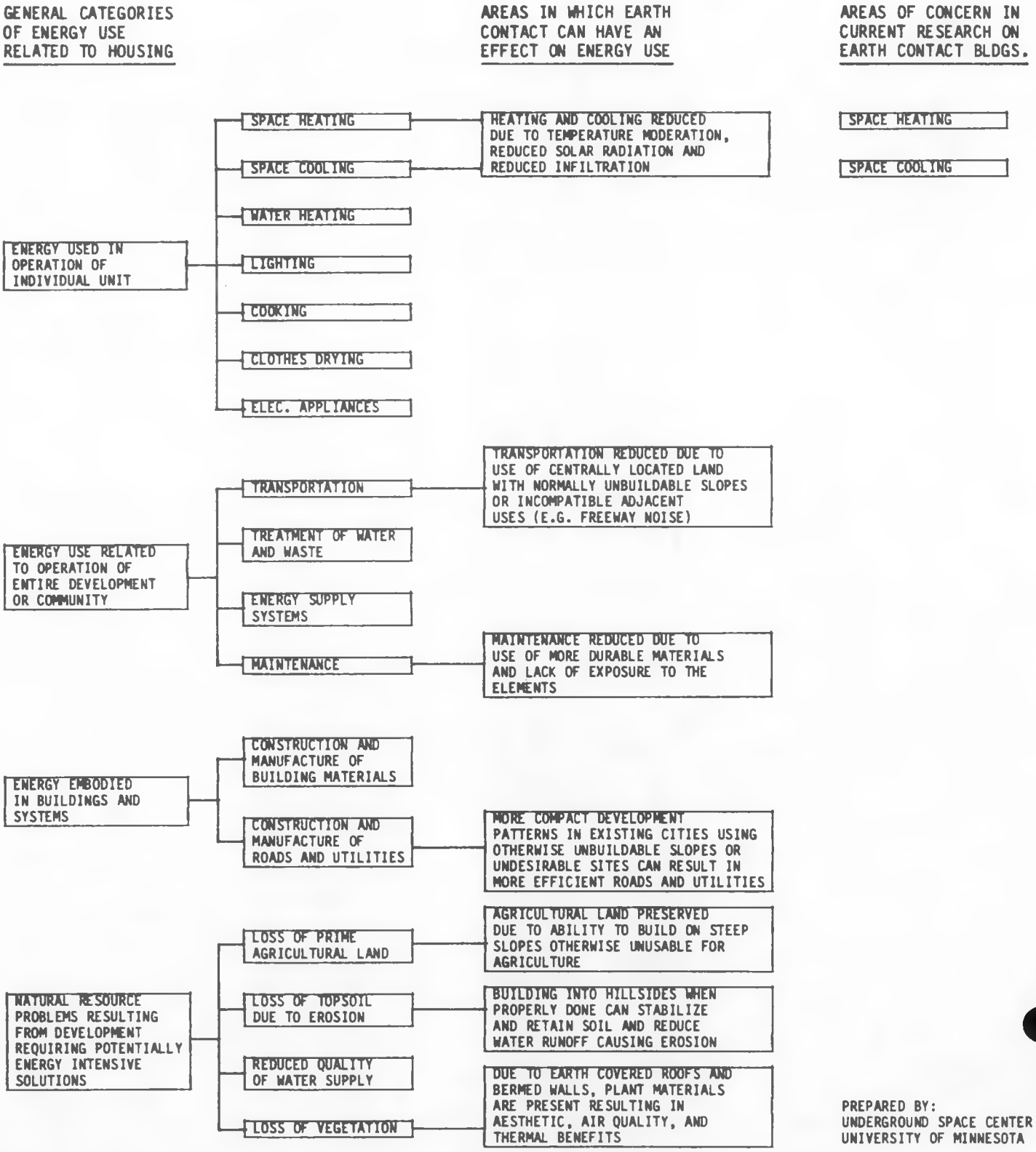

PREPARED BY:
UNDERGROUND SPACE CENTER
UNIVERSITY OF MINNESOTA

DIAGRAM 2

DECISIONS IN PLANNING AND DESIGN OF HOUSING WHICH AFFECT ENERGY USE

COMMUNITY SCALE

DENSITY OF DEVELOPMENT
- MEDIUM TO HIGH (COMPACT)
- LOW (SPREAD OUT)

LAND USE PATTERNS
- HOUSING SEPARATE FROM OTHER USES
- HOUSING INTERMIXED WITH COMMERCIAL AND WORKPLACES

TYPE OF HOUSING UNIT
- ATTACHED
- DETACHED

TOPOGRAPHY AND ORIENTATION OF LAND
- FLAT
- SOUTH-FACING SLOPES
- EAST/WEST-FACING SLOPES
- NORTH-FACING SLOPES

ENERGY SUPPLY SYSTEMS
- CONVENTIONAL SYSTEMS
- DISTRICT SCALE SYSTEMS

WASTE DISPOSAL SYSTEMS
- CONVENTIONAL DISPOSAL
- RECYCLING AND/OR USE OF WASTE AS FUEL

SITE DESIGN AND BUILDING FORM SCALE

RELATION TO SUN
- MAXIMUM EXPOSURE FOR HEAT GAIN IN WINTER
- MINIMUM EXPOSURE TO REDUCE HEAT IN SUMMER
- COMBINATION OF STRATEGIES

RELATION TO WIND
- MAXIMUM PROTECTION FROM WINTER WINDS
- MAXIMUM EXPOSURE TO SUMMER BREEZES
- COMBINATION OF STRATEGIES

RELATION TO VEGETATION
- MINIMIZE SHADING AND PROTECT FROM WINDS IN WINTER
- MAXIMIZE SHADING AND PROMOTE VENTILATION IN SUMMER
- COMBINATION OF STRATEGIES

RELATION TO EARTH
- MAXIMIZE EARTH CONTACT TO REDUCE HEAT GAIN AND MODERATE TEMPERATURES IN SUMMER
- MAXIMIZE EARTH CONTACT TO REDUCE INFILTRATION AND MODERATE TEMPERATURES IN WINTER
- LIMIT EARTH CONTACT TO PURSUE STRATEGIES REQUIRING ABOVE GRADE EXPOSURE: SOLAR, NATURAL VENTILATION AND SUPERINSULATION
- COMBINATION OF STRATEGIES

SHAPE OF BUILDING
- COMPACT SHAPE MINIMIZING SURFACE TO VOLUME RATIO RESULTING IN REDUCED HEAT LOSS AND GAIN THROUGH THE BUILDING ENVELOPE
- EXTENDED CONFIGURATION MAXIMIZING SURFACE TO VOLUME RATIO RESULTING IN GREATER OPPORTUNITIES FOR SOLAR EXPOSURE, NATURAL VENTILATION AND EARTH CONTACT COOLING
- COMBINATION OF STRATEGIES

SCALE OF INDIVIDUAL BUILDING SYSTEMS AND DETAILS

ROOF COMPONENT
- MATERIALS
- AMOUNT AND PLACEMENT OF INSULATION
- AMOUNT AND PLACEMENT OF EARTH
- RELATION TO OTHER SYSTEMS, I.E. STORAGE MASS FOR SOLAR

WALL COMPONENT
- MATERIALS
- AMOUNT AND PLACEMENT OF INSULATION
- AMOUNT AND PLACEMENT OF EARTH
- RELATION TO OTHER SYSTEMS

FLOOR COMPONENT
- MATERIALS
- AMOUNT AND PLACEMENT OF INSULATION
- CONTACT WITH EARTH
- RELATION TO OTHER SYSTEMS

OPENINGS
- SIZE AND ORIENTATION OF WINDOWS AND SKYLIGHTS IN RELATION TO SOLAR GAIN
- SIZE AND LOCATION OF OPENINGS IN RELATION TO NATURAL VENTILATION
- USE OF SHADES AND THERMAL SHUTTERS
- LOCATION AND DESIGN OF DOOR OPENINGS TO REDUCE HEAT EXCHANGE

SYSTEMS AND EQUIPMENT
- SPACE HEATING (CONVENTIONAL FURNACE, FIREPLACE, SOLAR)
- SPACE COOLING (AIR CONDITIONING, FANS)
- MECHANICAL VENTILATION (HEAT EXCHANGER)
- WATER HEATING (CONVENTIONAL FUEL SOURCES, SOLAR)
- ELECTRICAL APPLIANCES (CONVENTIONAL SOURCES, WIND, PHOTOVOLTAICS)

PREPARED BY:
UNDERGROUND SPACE CENTER
UNIVERSITY OF MINNESOTA

DIAGRAM 3

FACTORS INVOLVED IN THE ANALYSIS AND DEVELOPMENT OF DESIGN GUIDELINES FOR EARTH CONTACT WALLS

GOALS AND PRIORITIES TO BE DEFINED AFFECTING ENERGY ANALYSIS OF WALL COMPONENT

BASIC ASSUMPTIONS
- GOAL IS TO SELECT OPTIMAL WALL CONFIGURATION WHETHER OR NOT IT EMPLOYS EARTH CONTACT
- EARTH CONTACT IS ASSUMED FOR A VARIETY OF REASONS, GOAL IS TO SELECT OPTIMAL WALL CONFIGURATION FROM EARTH CONTACT VARIATIONS

HEATING/COOLING PRIORITIES
- OPTIMIZE FOR HEATING SEASON
- OPTIMIZE FOR COOLING SEASON
- COMBINATION OF STRATEGIES

COMFORT ZONE LIMITATIONS
- NARROWLY DEFINED (72°)
- MODERATELY DEFINED (68-78°)
- BROADLY DEFINED (65-80° OR MORE) (RELATION TO MEAN RADIANT TEMP. MUST BE ANALYZED)

RELATION TO OTHER SYSTEMS
- USE OF WALL AS A STORAGE MASS FOR INTERMITTENT HEAT SOURCES (PASSIVE SOLAR, FIREPLACE)
- RELATIVE SIGNIFICANCE OF HEAT TRANSFER THROUGH WALLS COMPARED WITH TOTAL BUILDING LOADS

GENERAL CHARACTERISTICS TO BE DEFINED FOR ANALYSIS OF SPECIFIC CASES

WALL HEIGHT
- ONE STORY
- TWO STORY

RELATION TO GRADE
- ABOVE GRADE
- PARTIALLY BERMED
- FULLY BERMED WITH CONVENTIONAL ROOF (SAME AS BASEMENT)
- FULLY BERMED WITH EARTH COVERED ROOF

SOIL AND GROUND COVER
- SOIL TYPE
- SOIL MOSITURE CONTENT
- AMOUNT AND DURATION OF SNOW COVER
- TYPE OF GROUND COVER

TYPE OF WALL MATERIAL
- CONCRETE
- MASONRY
- WOOD FRAME

VARIATIONS IN INSULATION DETAILS TO BE ANALYZED

INSULATION CONFIGURATION
- OUTSIDE WALL
- INSIDE WALL
- WITHIN EARTH MASS
- COVERING ENTIRE WALL
- COVERING UPPER HALF OF WALL ONLY
- TAPERING INSULATION WITH THICKER LAYERS ON UPPER HALF AND THINNER LAYERS BELOW

INSULATION AMOUNT
- R=0
- R=10
- R=20
- R=30
- R=40
- VARIOUS COMBINATIONS ON HALF-BERMED WALLS
- VARIOUS COMBINATIONS IF INSULATION IS TAPERED

PREPARED BY:
UNDERGROUND SPACE CENTER
UNIVERSITY OF MINNESOTA

EARTH CONTACT SYSTEMS: SOIL TEMPERATURE AND THERMAL CONDUCTIVITY DATA, HEAT FLUX DATA AND METER CALIBRATION

T. P. Bligh
B. H. Knoth
E. A. Smith
D. M. Apthorp
Massachusetts Institute of Technology
77 Massachusets Avenue, Room 3-445
Cambridge, MA 02129

ABSTRACT

This paper presents thermal data from laboratory experiments and in-situ measurements from an earth sheltered house; soil temperature, wall heat flux and apparent soil thermal conductivity data are presented and discussed. The data shows some of the characteristics of the thermal behavior of the house and soil. Thermal conductivity probe design is included. Soil temperatures are presented in the form of isotherms for various times of the year, examples of heat flux data for one day, and soil thermal conductivity data for several days duration are plotted. Discussions of soil temperature measurements, heat flux meter calibrations are presented.

INTRODUCTION

An earth sheltered house, illustrated in Fig. 1, was instrumented to monitor soil and structure temperatures, heat flow into the earth contacting envelope, energy use, and the interior air and meteorological conditions. This house features an unique insulation arrangement; 15 cm of styrofoam TM insulation cover the concrete roof slab and extend out into the soil, in reduced thicknesses, parallel to the berm surface. There is no insulation in direct contact with the walls, for the extended roof insulation cuts the direct heat flow path from the walls to the ground surface. Leaving the soil in direct contact with the walls improves the summer cooling (Bligh, Shipp, and Meixel, 1980) by preventing heat gain from warm surface soil and keeping a direct path for heat loss to the cool soil at depth.

The laboratory and field data will lead to a better physical understanding of the thermal properties of soil, and the heat and mass transfer around an earth contact system as well as the overall energy characterization of an earth sheltered house. In addition, the data will be used to validate computer codes describing the heat and moisture transfer.

IN-SITU SOIL TEMPERATURE MEASUREMENTS

Temperatures in the soil surrounding an earth sheltered house can vary in one, two, or three dimensions depending on location. In the roof soil, which is generally shallow compared to its width, temperature variation will be one dimensional. Two dimensional distributions can be found in cross sections through the berms sufficiently far from the house corners, where the temperatures are influenced by the ground surface and deep earth conditions as well as the vertical wall. Three dimensional effects are produced at and near the house corners. Instrumentation has been installed in these three regions of an earth sheltered house to measure temperatures. The resulting temperature data is described here.

Sensor Locations

Two vertical thermocouple rakes each measure temperatures in the one dimensional field of the roof soil and insulation as shown in Fig. 2. These rakes are located well away from the roof's edge to avoid errors due to edge losses which produce two dimensional effects. Figure 2 also shows the five grids of sensors located in the berm. Three full grids (A, B, and C) contain 45 thermocouples each. Grid C, located at the east wall midline, is in a two dimensional temperature field. Grids A and B, extending from the north-east corner, are in a three dimensional field. Two partial grids, D and E, contain 10 thermocouples each. Grid D, which is intended for comparison with grid B, also extends from the corner, and grid E, located on the north wall 3 meters from the corner is for comparison with grid C. Sensor manufacture and installation will be described in a later paper.

Sources of Error

There are three possible sources of error in the temperature data: imprecision in the thermocouples and measuring equipment, heat conduction along the PVC tubes and thermocouple wires, and inaccuracies in the thermocouple positions.

Inaccuracy in the thermocouple wire is minimized by using wire conforming to the "special limits of error" (ANSI MC-96.1) which requires that the wire accuracy be sufficient to give temperature readings to better than + 0.5°C. The accuracy of the wire, however, is not as important as the precision of the wire. The precision of a group of thermocouples is a measure of the consistency with which each measures a given temperature; thermocouple accuracy is a measure of how closely the thermocouple output represents the true temperature being measured. A group of thermocouples may be very precise but have poor accuracy if

they all misrepresent the temperature equally. If thermocouples are used to determine the temperature difference between two locations, the accuracy of the wire is not important but the precision is; if both thermocouples have the same error they still produce an accurate value for the temperature difference.

Error due to the imprecision in the thermocouples was minimized by making all the sensors from one single batch of thermocouple wire, and the precision of sample thermocouples taken at regular intervals from the batch was tested. The tests indicated an imprecision of $\pm$ 0.015°C for the combination of thermocouples and measuring equipment. Therefore, when looking at the difference between two temperatures in the soil, the indicated difference will be within $\pm$ 0.03°C of the true value.

Conduction along the PVC tubes holding the thermocouple wires should have a negligibly small effect. It can be shown that the tubes and filler will not contribute any significant error, however conduction along the wires may contribute an error of up to $\pm$ 0.03°C (Shipp, 1982).

Inaccuracy in the spatial positioning of the thermocouple junctions will also contribute to the error, this contribution has been calculated to be up to $\pm$ 0.03°C. Thus, the maximum total error from these sources is $\pm$ 0.09°C.

Data Analysis and Presentation

The one dimensional roof data is presented in plots of temperature against depth for various times during one day. In the two and three dimensional cases the data is presented as isotherms in two dimensional cross sections taken from the two and three dimensional temperature fields for one day each month.

The variation in roof soil temperatures in a twenty four hour period is shown in Fig. 3. This data, is plotted in two hour intervals for mid May when the grass cover was sparse, and demonstrates that roof soil buffers the house from daily changes in outside temperatures. Although the soil surface temperature variation has an amplitude of about 15°C, the top of the slab roof changes less than 1°C and the house has a small heat loss all day, as shown by the direction of the temperature gradient in the insulation. This heat loss is also confirmed by heat flux measurements, from the same location which will be reported in a later paper.

The data for this figure was interpolated using a computer routine (Akima, 1972) which is designed to provide curves that appear natural, without the undulations produced by routines which assume a functional form for the whole curve. In subsequent figures, the two dimensional data field from each grid was interpolated using an algorithm (Akima, 1978) which operates in a similar way on two dimensional data fields.

The data from thermocouple grids is given in two groups. The first group, Figs. 4 and 5, show how the soil isotherms vary with time for the two dimensional field, Grid C, for a day in alternating moths from November, 1981 to May, 1982. The second group, Fig. 6, shows the two and three dimensional effects for March 10, 1982.

Figure 4 shows isotherms generated from Grid C for winter together with the positions of the house and insulation. Some of the data used to generate the isotherms is shown to demonstrate that the isotherms pass through the appropriate data points. All 45 data points corresponding to each of the small circles shown were used to compute the isotherms.

Changes in the soil near the building occur slowly and can be considered quasi-steady state, thus heat flow will be orthogonal to the isotherms, and the magnitude of the heat flux is roughly proportional to the temperature gradient, or distance between the isotherms. Comparison of temperature fields for different months shows how the heat flow patterns change. The winter months, November to March, show heat flowing away from the house and towards the cold berm surface, with some heat flowing down from the lower house corner. The isotherms near the house are packed more closely in January and March than in November, indicating greater heat loss in the late winter.

In may, heat is flowing into the ground away from the warm surface, and the isotherms are far apart indicating a low heat flux. Notice the flux from the entire wall now travels down into the cool deep earth, providing the summer passive cooling.

Figures 5 and 6 compare isotherms, on March 10, 1982, from three cross-sections of the berm. Figure 5 top shows isotherms from the two dimensional field, Grid C, while Fig. 6 is taken from the three dimensional field at the corner. The data from Grid A shows a stronger influence of the berm surface and soil on heat flow than at locations B or C. Here, almost all isotherms tilt toward the surface, but at the other locations the lower regions show some heat flow towards the deep ground. In particular, the temperature near the building is almost 2°C cooler in the three dimensionally affected Grids A and B. The stronger influence is expected because the corner is in communication with a larger surface area and larger soil volume in contact with the deep colder soil.

HEAT FLUX MEASUREMENTS

Heat flux data for the building envelope is required for validating earth contact computer models and for completing of an energy balance on the building. Heat flow through the earth contacting structure is measured with commercially manufactured heat flux meters. These meters distort the heat flow and will produce erroneous data unless, as discussed in the following sections, the meters are installed carefully, calibrated correctly and the data is corrected for the distortions in the heat flow.

Heat Flow Distortion

When a heat flux meter is mounted in a material it does not measure the true undisturbed heat flux (unless its conductivity is identical to that of its surroundings). For example, if the meter has a low conductivity it will reduce the local heat conduction and so underestimate the original true value. This effect can be broken into two factors, the first is due to a change in the thermal resistance in the heat flux path which is dependant on the thickness and conductivity of the meter and surroundings; the second is caused by the local distribution of the heat flow lines around the meter which is a function of the two conductivities and the thickness of the meter.

The three-dimensional distortion effect is strongest around the edges of the meter and can be greatly reduced by surrounding the meter with a guard frame made of the same material as the meter, thus making a larger meter of the same thickness, with the distortion effects removed from the heat flux sensing area in its center. If large guard frames are used, the three-dimensional effects are removed from the meter and only the first effect need be considered.

Both these effects have been studied by many investigators (e.g. Portman, 1958, Philip, 1960, Schwerdtfeger, 1970) but until now all studies have been two-dimensional, whereas the effect is inherently three-dimensional for all but circular meters.

A three-dimensional steady state finite difference computer model has been written at M.I.T. which predicts the ratio of heat flux through the meter to true heat flux, for rectangular cross section meters, as a functioin of the ratio of the conductivity of the meter to the conductivity of the surrounding material, meter geometry, guard frame size and the thickness of the surrounding materials. Both the one and three-dimensional effects are included in Fig. 7, which was generated by the computer model. It shows that the heat flux ratio is a strong function of conductivity ratio. For example, a typical meter mounted in concrete, giving a conductivity ratio of 0.1, will give a flux reading only 0.37 times the true value; clearly an accurate curve of the type in Fig. 7 is vital for any measurement of heat flux.

Once the curve is known, it will have two uses. First it will enable the calibration of meters by mounting a single meter in a material of known conductivity and passing a known flux through the whole apparatus. As long as the meter conductivity is known, and at present the manufacturers do not publish this data, a curve such as Fig. 7 can be used to find the heat flow through the meter, so that the calibration factor of the meter (heat flow through the meter divided by the meter's output voltage) can be calculated. Second, given this calibration factor a curve such as Fig. 7 will allow the calculation of the true heat flux from the meter output when it is mounted in any material of known conductivity.

At present the computer model is limited to homogeneous meters, with or without guard frames, in uniform conductivity surroundings. It is currently being expanded to model meters with metal cover plates (many commercially available meters have these) and to model meters mounted on the interface of two surfaces of different conductivities (for example, concrete/soil).

As yet the model has not been validated by experiment, although this validation will be completed at M.I.T. in the next few months. Until it is validated the model should be used with extreme caution.

Meter Calibration

There are three currently used methods of calibrating heat flux meters--the radiation enclosure method, the guarded hot plate method and the M.I.T. method. The radiation enclosure method, currently used by our main supplier of heat flux meters, has the disadvantages of using a very high flux level (two orders of magnitude higher than typical building fluxes), and of requiring a large amount of complex, expensive equipment. The guarded hot plate method can operate at low flux levels but also requires expensive equipment to be used accurately. The M.I.T. method, however, is inexpensive and simple. It generates a steady, one-dimensional heat flux through 4 meters, which are guarded radially by 12 others. The flux is produced by two resevoirs, each held at a constant temperature by the phase change of a pure substance, one melting n-Octadecane (28°C) and the other ice water (0°C). The flux can be varied by changing the number of polystyrene layers and is measured by measuring the temperature drop across a precalibrated layer of Dow "Styrofoam™" which has been sealed to prevent outgrassing and moisture absorption. The low cost and inherent accuracy of this method makes it widely suitable. The apparatus and procedure will be discussed in a future paper.

At present, the main disadvantage of this method is that it requires 16 meters; however once the M.I.T. computer model is validated it will enable meters to be calibrated singly, with no need for any guarding. The validation will be done by mounting precalibrated meters in different materials of known conductivity in the calibration apparatus, and comparing the change in effective calibration factor, (actual heat flux through the material divided by the meter output) to that predicted by the computer model.

When the calibration factors from the M.I.T. tests were compared with the manufacturer's quoted values large discrepancies were found. Figure 8, the results from 39 meters calibrated at M.I.T., shows errors of up to 25% in the manufacturer's values. These may be due either to errors in the manufacturer's calibration process or to nonlinearity in the meter response over two orders of magnitude in flux from building fluxes (2 to 10 W/m^2) to the manufacturer's calibration flux (1600 W/m^2). These errors mean that one cannot use the manufacturer's calibration factor at building fluxes and that all meters must therefore be recalibrated, at the correct flux level, by either the M.I.T. or guarded hot plate methods.

It should be noted that all these calibration methods give a steady state calibration factor, which may not be applicable when the heat flux is time varying.

Heat Flux Meter Installation

Heat flux meters were installed in the earth sheltered house at the locations shown in Fig. 9. The locations were chosen so that heat flux profiles near a corner, as well as the centerline, of a wall can be determined.

The meters have been installed in a way which minimizes errors due to disturbances in the conduction, convection, and radiation heat transfer at the meter's location. An installed meter is depicted in Fig. 10. The meters are tightly fitted into frames constructed of the same materials as the meters. These guard frames remove the three-dimensional edge effects from the vicinity of the meter, thus improving the accuracy of the measurements. The assemblies are mounted in depressions cut into the concrete wall and bonded to the wall with a high thermal conductivity grease to minimize contact resistance (note that plaster is first used to fill the depressions in the rough cut concrete surface). The assemblies are finally plastered flush with the wall. Since the wall is smooth at the meter's locations, the boundary layer is not disturbed and there is no change in the convection heat transfer. Also, the entire wall has the same surface finish so that the radiation heat transfer is not affected by the meters.

Heat Flux Data

Heat flux data from two locations on the wall is presented in Figs. 11 and 12. The data shows that heat flux at the wall surface is not steady state but has fluctuations that vary in duration from minutes to hours and the magnitude of the indicated heat flux may change by a factor of six or more during these transients. Unfortunately, the dynamics of heat flux measurements are not known; although the meters have been calibrated for use in steady temperature fields they have not been tested in fluctuating heat flows, so the relation of the measured heat flux to the actual heat flux is unclear at this time. The data suggests that the heat flux into the concrete walls fluctuates over a wide range, but analysis and experimentation are required to determine how the actual flux varies.

The shapes of the two plots are the same, although the magnitudes differ, and data from all other meters show the same trends. The similarity between plots suggests that the fluctuations are not a local transient condition but are governed by a significant heat input. Heat flux is presumably influenced by the living habits of the residents and the daily and yearly changes in climate, but an in-depth investigation of the heat flux data and its relation to other parameters has not yet been undertaken.

Figure 12 also shows the variation in wall temperature at the heat flux meter's location; the temperature data is plotted on an enlarged scale so that the shape of the graph is apparent. The wall temperature plot has the same shape as the heat flux plot, but wall temperature only changes by 0.7°C while the flux varies by a factor of five.

THERMAL CHARACTERISTICS OF SOIL

The experimental validation of the earth contact systems computer model requires soil thermal property data in addition to soil temperature and building heat flux measurements. These measurements have been discussed in Bligh, et al. (1982b), in which it was found that transient measurements of thermal conductivity using a thermal conductivity probe would be best suited for the field and laboratory program.

Variation of Thermal Properties with Soil Moisture

The thermal properties of soil are strongly influenced by the amount of water in the soil. Thus, to completely observe the behavior of earth contact systems which can change the amount of water in the soil, it is important to directly measure the soil thermal properties.

For liquid water, Fig. 13 shows how the apparent thermal conductivity (see later), volumetric heat capacity and apparent thermal diffusivity, all normalized to 0% moisture content, vary with the volumetric moisture content of a soil. Given an 18% increase in volumetric water content, these properties increase by factors of nearly 7, 2 and 4 times their dry values, respectively.

Water and ice can be present in moist soils when the temperature is below approximately 0°C (Lunardini, 1981). Ice can have a significant effect on soil thermal properties and hence heat flow. Bligh, Pfender and Eckert (1980) measured a sudden increase in apparent thermal conductivity of moist soils as the temperature dropped below 0°C.

Apparent Thermal Conductivity

In general, apparent thermal conductivity of soil will be defined as a constant expressing a linear relation between heat flux and a temperature gradient accounting for simultaneous heat transport by conduction, convection and radiation by soil particles, liquid water, water vapor and air. This is in contrast to thermal conductivity which is defined for pure conduction only. The apparent thermal conductivity characterizes the thermal response of soil for the duration and magnitude of the temperature difference under which it was measured. The apparent thermal conductivity as measured in soil will depend on the measurement technique used, since the heat transport now depends on temperature gradients and the time taken for the measurement. Thus, apparent thermal conductivity is not a property in the thermodynamic sense. For example, significant differences in apparent thermal conductivity were observed when steady state and transient thermal conductivity measurements were used for tests of moist soils by Eckert, Pfender, and Bligh (1976).

THERMAL CONDUCTIVITY PROBES

In a thermal conductivity measurement less time is required to perform a transient than a steady state measurement which must wait until all transient effects have damped out. Because of the shorter time required, transient techniques add less energy to the soil and properties such as temperature and moisture content are disturbed to a lesser extent. As the time and temperature gradient are reduced, the apparent thermal conductivity should approach the pure-conduction thermal conductivity. A number of measurement methods were evaluated (Bligh et al, 1982b) and, for the following reasons, thermal conductivity probes were used in the experimental program:

1) Only thermal conductivity probes can be placed in soil around the earth-sheltered building to measure the "in-situ" apparent thermal conductivity.

2) The transient thermal conductivity probe method minimizes moisture migration since small temperature gradients of short duration are used during a test.

3) Thermal conductivity probes can be installed in the field with a minimum of physical disturbance to the soil.

4) Thermal conductivity probes are easily constructed.

5) Operation of a thermal conductivity probe is relatively simple.

The thermal conductivity probe or line heat source method can be used in the field or laboratory. The apparatus consists of a cylindrical heat source embedded in an "infinite" soil sample. A typical probe consists of a resistance wire and a device for temperature measurement inside a long hollow tube. When the soil sample is at a uniform temperature, a clock is started and DC current is supplied to the resistance wire which, midway along the tube, produces one dimensional radial heat flow. A record of the probe temperature rise with time is made. The apparent thermal conductivity is derived from the time dependent temperature rise and the power dissipated in the wire. The theory describing a transient cylindrical heat source simplifies if the diameter of the heat source approaches zero. In practice, it was found that, the M.I.T. thermal conductivity probe is a close physical representation of a line heat source.

The M.I.T. Probe

The M.I.T. probe design was derived from the test results of Wechsler (1966), Fritton (1974) and our own laboratory experience, and consists of a folded enamelled chromel heater wire inserted into a stainless steel sheath. The dimensions are given in Fig. 14 and result in a length to diameter ratio of 52. Midway from the end of the sheath a polystyrene coated cooper-constantan thermocouple senses temperature changes. A high conductivity thermal grease compound fills the airspace left within the sheath. At the top the heater and thermocouple wires are welded to lead wires. The lead wire connections are reinforced and scaled with heat shrink tubing inside a plastic sleeve filled with epoxy cement.

It is worth noting special features in the M.I.T. design. The enamelled coated heater wire and polystyrene coated thermocouple are electrically insulated from the sheath. Both of the wires used have

small cross sections to reduce axial heat leaks from the probe. To improve thermal contact between the heater wire, thermocouple and steel sheath, a thermal grease compound was used.

Probe Measurements of Thermal Conductivity

A computer data acquisition system, DC power supply and digital voltmeter/ohmeter are the equipment used in a probe measurement. The computer data acquisition system is not necessary, but it automates the probe thermocouple measurements and performs data reduction. The power supply applies a constant voltage to the resistance wire of the probe. The voltmeter/ohmeter measures the voltage supplied and probe resistance, so that the power dissipation can be calculated.

Line heat source theory predicts the temperature rise of the probe to be a straight line when plotted against the logarithm of time. A least squares method is used to find a straight line through the data points in the form of $T = m * \ln(t) + b$ where;

T is the temperature rise, (°C).
m is the slope of the straight line, (°C).
b is the T intercept at t = 1 min., (°C).
t is the time (min).

A sample plot of the temperature rise during heat-up against time is shown in Fig. 15. An apparent thermal conductivity is calculated as: (Bligh, et al, 1982b):

$$\lambda = \frac{V^2/RL}{4\pi m}$$

λ is an apparent thermal conductivity, (W/mK).
V is the voltage across the probe resistance, (V).
R is the probe resistance, (Ω).
L is the probe length, (m).
m is the slope of the straight line between 0.2 and 2 minutes, (°C).

Apparent thermal conductivity measurements of probes in a dry quartz sand (20-30 Ottawa Sand) were evaluated for accuracy and precision. Three groups of probe measurements compared well to a steady state measurement performed in a heat flux meter apparatus (ASTM C518-76) under the same conditions (Dynatech, 1982). These results have been tabulated in Table 1. In group 1, a mean apparent thermal conductivity of 0.349 W/mK was obtained in tests of 32 probes. In groups 2 and 3 mean apparent thermal conductivities of 0.356 and 0.344 W/mK were obtained from 20 repeated tests of 2 probes. These results are within +2% of the apparent thermal conductivity obtained by the steady state measurement. The precision of the probe measurements as measured by the standard deviation is within +4% of the means.

The consistency of thermal conductivity measurements using one probe demonstrates that the test procedure is repeatable. Also, since 32 probes give values within ± 2% of each other, variations in the probe construction do not contribute significant error. The agreement between the probe tests and the steady state test indicates that the probes measure the apparent thermal conductivity of dry soils accurately.

TABLE I. Results of Apparent Thermal Conductivity Measurements of a Dry 20-30 Ottawa Sand

Group	T (°C)	Bulk Density (g/cm^3)	Mean (W/mK)	Standard Deviation (W/mK)
1. 1 measurement each by 32 probes	26.4	1.80	0.349 + 0.002	0.0128 (3.7%)
2. 20 measurements by probe No. 76	23.1	1.80	0.356 + 0.003	0.0124 (3.5%)
3. 20 measurements by probe No. 78	23.3	1.80	0.344 + 0.003	0.0132 (3.8%)
4. 1 measurement by steady state heat flux meter apparatus, ASTM C-518-76 (Dynatech, 1982)	24	1.76	0.350	--

Field Measurements

Forty-two thermal conductivity probes, of the M.I.T. design, were constructed and buried at the bermed earth sheltered building site. All probes are oriented horizontally and parallel to the building walls and were buried during backfill operations.

The locations of the thermal conductivity probes in the northeast berm at the earth sheltered house are shown in plan in Fig. 16. There are two probe groups in the berm, grids F and G. They extend 3 m from the wall and are 3.6 m deep. Grid E contains 32 probes (Fig. 17) and Grid F contains 10 probes. There are also 2 probes each below the floor and above the roof.

The results of measurements from a day in May and August are shown in Fig. 17a & b respectively. At this time, the behavior of soil apparent thermal conductivity is difficult to explain in terms of soil moisture. Between May 23rd and August 14, 1982 the apparent thermal conductivity generally increased throughout the berm, presumably from summer precipitation. Note, however, that apparent thermal conductivities are higher near the house wall, which is contrary to the expectation that horizontal heat flux from the house would cause moisture to migrate away from the walls. The high conductivity near the wall may be caused by the concrete walls drying or poor drainage.

Apparent thermal conductivity measurements are made once every nine hours. The variation of apparent thermal conductivities over a twenty day period, 0.6 m and 2.4 m from the house wall are plotted in Fig. 18a & b respectively. Each figure contains data from 5 probes in the soil at various depths measured from the top of the roof slab. Surprisingly, the apparent thermal conductivities measured by probes 0.6 m from the wall are generally greater and fluctuate more than those for probes 2.4 m from the wall.

ACKNOWLEDGEMENTS:

DOE Solar Passive Division for supporting this research. Philip and Karen Dunkelbarger, for graciously allowing us to monitor their earth sheltered home and to the following for donations: Hewlett-Packard for several data acquisition components, Massachusetts Electric Company for two watt-hour meters and Ralph Drinkwater Construction for the use of a front end loader for a day.

REFERENCES

1. Akima, H., Interpolation and Smooth Curve Fitting Based on Local Procedures, Comm of ACM, 15, 914:918, 1972.

2. Akima, H., Bivariate and Smooth Surface Fitting for Irregularly Distributed Data Points, ACM Trans on Mathematical Software, 4, 160:164, 1978.

3. Bligh, T.P., Shipp, P. and Meixel, G., Energy Comparisons and Where to Insulate Earth-Sheltered Buildings and Basements, Energy, 5, 451:465, 1980.

4. Bligh, T.P., and Roslansky, W.F., Reducing heat gain in buildings through shading with plants, D.O.E. Solar Passive Division report published under contract #DC-AC03-80SF 11508, 1982a.

5. Bligh, T.P., Knoth, E.A., Smith, S.P., Cole and Meixel, G., An experimental plan for an earth contact system: Techniques for monitoring soil temperature, building heat flux, soil thermal properties and soil moisture content, D.O.E. Solar Passive Division report published under contract #DC-AC03-80SF 11508, 1982b.

6. Dynatech R/D Company, The apparent thermal conductivity and thermal resistance of a dry and water saturated specimen of Ottawa Sand, Dynatech report number MIT-15, 1982.

7. Eckert, E.R.G., Pfender, E., and Bligh, T.P., Energy conservation by subsurface construction - heat transfer studies in a large underground building, First Annual Report, NSF (RANN) Contract SLA-75-03481, University of Minnesota, 1976.

8. Eckert, E.R.G., Pfender, E., and Bligh, T.P., Energy Conservation by Subsurface Construction, Heat Transfer Studies in a Large Underground Building, Final Report, NSF (RANN) contract SIA-75-03481, University of Minnesota, 1980.

9. Fritton, D.D., Inexpensive but durable thermal conductivity probe for field use, Soil Science Society of America Proceedings, 38: 854-855, 1974.

10. Lunardini, V.J., Heat Transfer in Cold CLimates, Van Nostrand Reinhold Co., Inc., New York, NY, 1981.

11. Magnusson, J.H., Sources of heat flux meter errors, Unpublished S.B. Thesis, M.I.T., 1982.

12. Meixel, G.D., Shipp, P.H., and Bligh, T.P., The Impact of Insulation Placement on the SEasonal Heat Loss through Basement and Earth Sheltered Walls, Underground Space, 5, 41:47, 1980.

13. Phillip, J.R., The theory of heat-flux meters, J. Geophys. Res. 66:571-579, 1961.

14. Portman, D.J., Conductivity and length relationships in heat-flow transducer performance, Trans. A. Geophys. Union 39, 1089-1094, 1958.

15. Schwerdtfeger, P., The Measurement of heat flow in the ground and the theory of heat flux meters, Tech. Report 232, Corps of Engineers, U.S. Army, Cold Regions Research and Engineering Laboratory, New Hampshire, 1970.

16. Shipp, P.H., Personal Communication, 1982.

17. Wechsler, A.E., Development of thermal conductivity probes for soils and insulations, CRREL Technical Publication TR-182, Cold Regions Research and Engineering Laboratory, Hanover, New Hampshire, 1966.

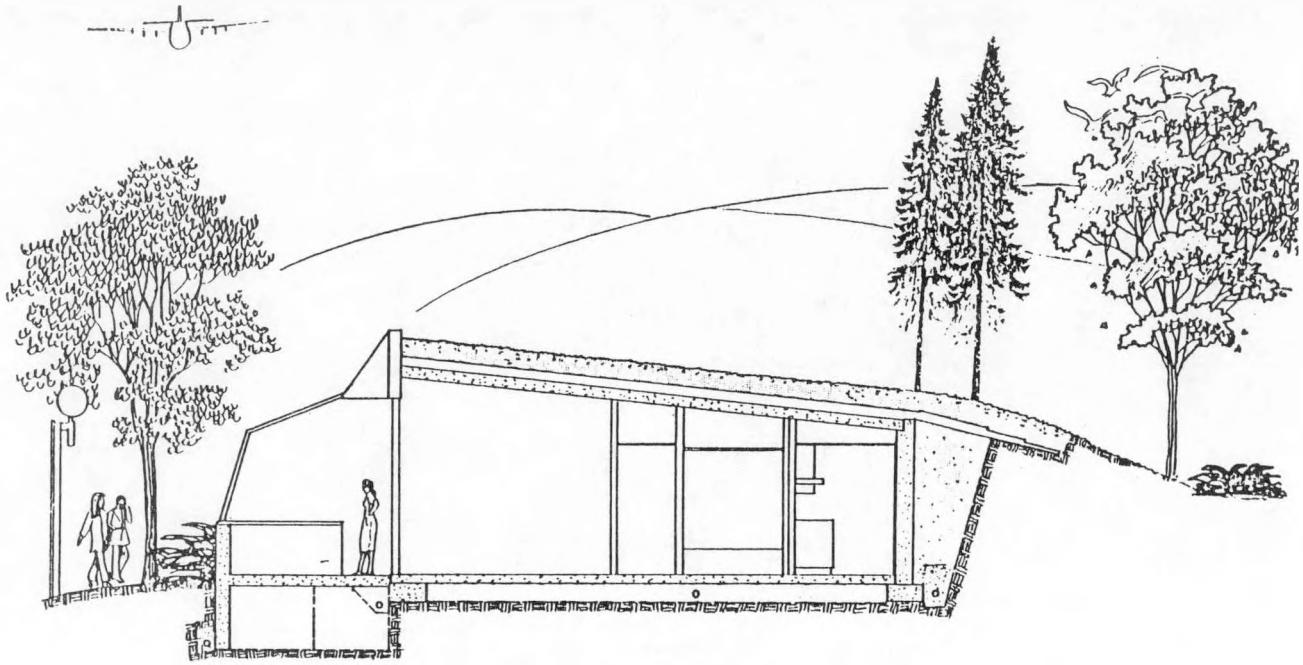

Fig. 1. Section of Bermed Earth Sheltered House.
P. Dunklebarger, Boston, MA.

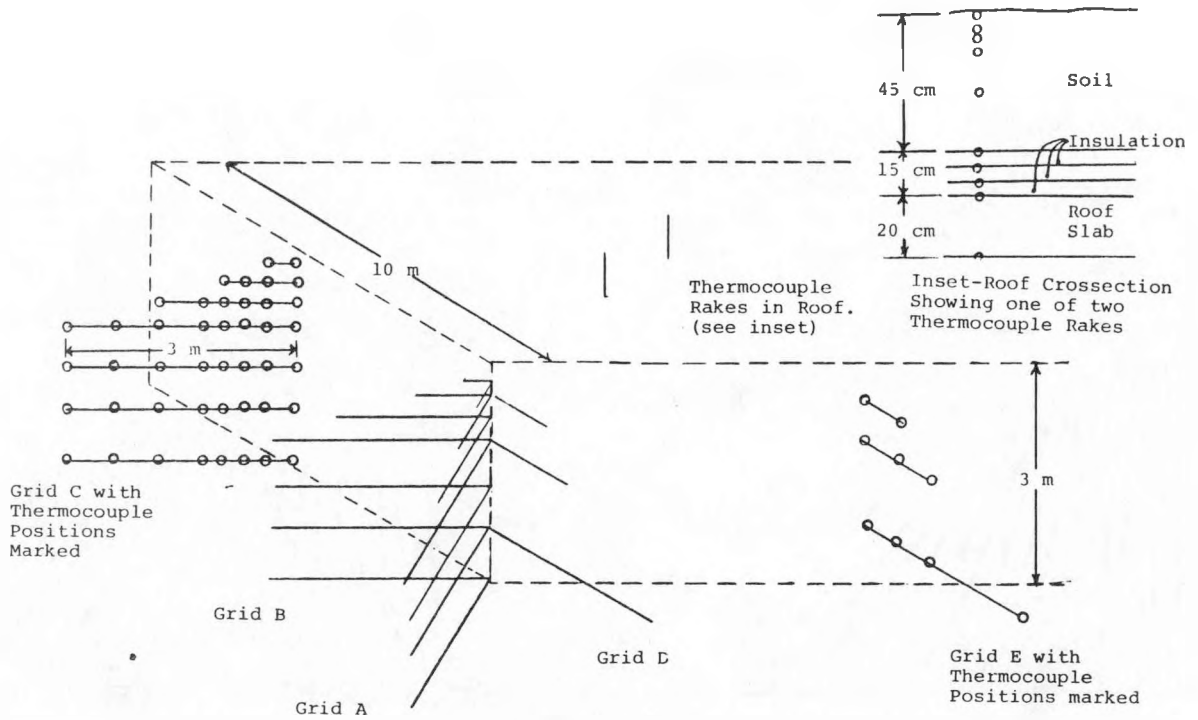

Fig. 2. Earth Sheltered House with Soil and Insulation Removed Exposing Thermocouple Grids (Viewed from the North).

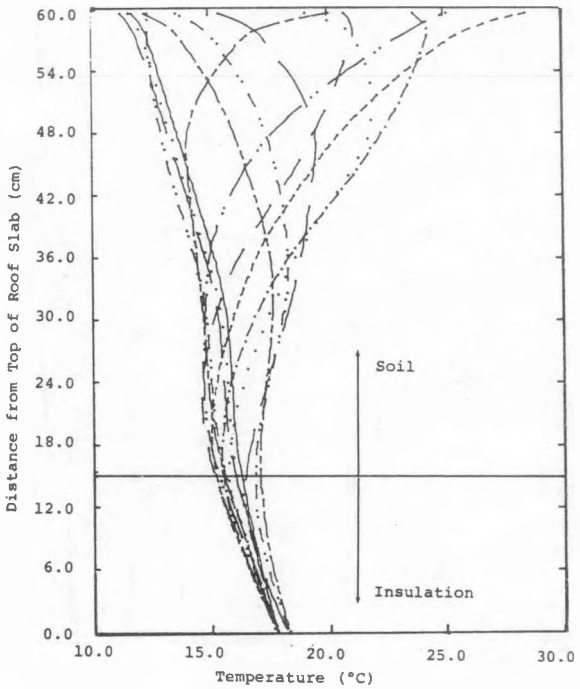

Fig. 3. Roof Temperatures on May 24, 1982.

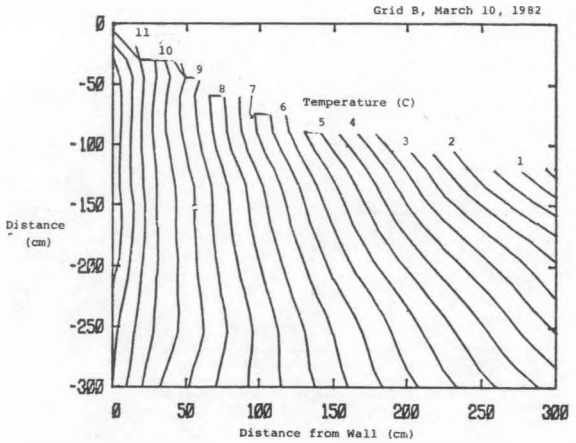

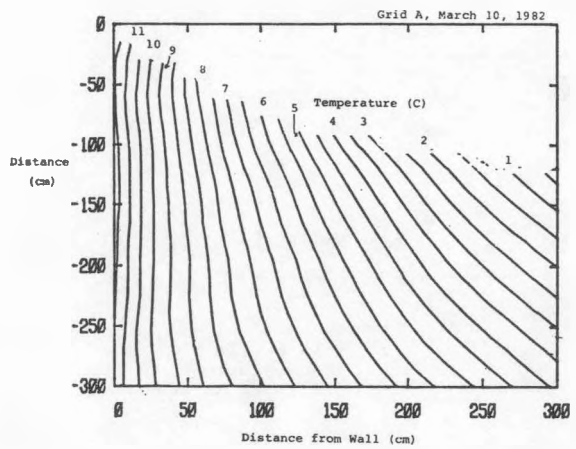

Figure 4.

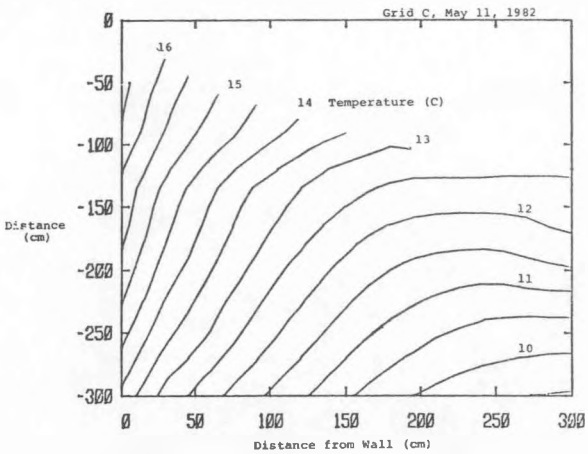

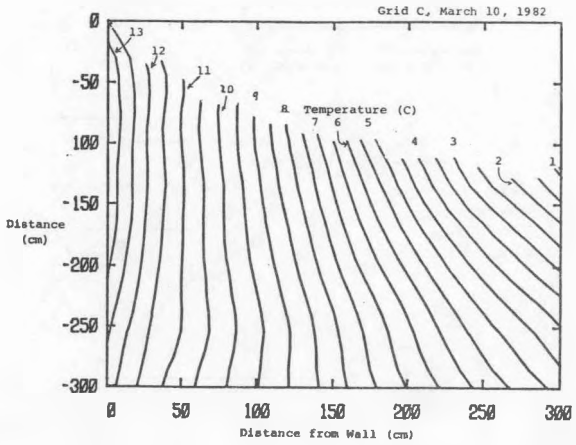

Figure 5.

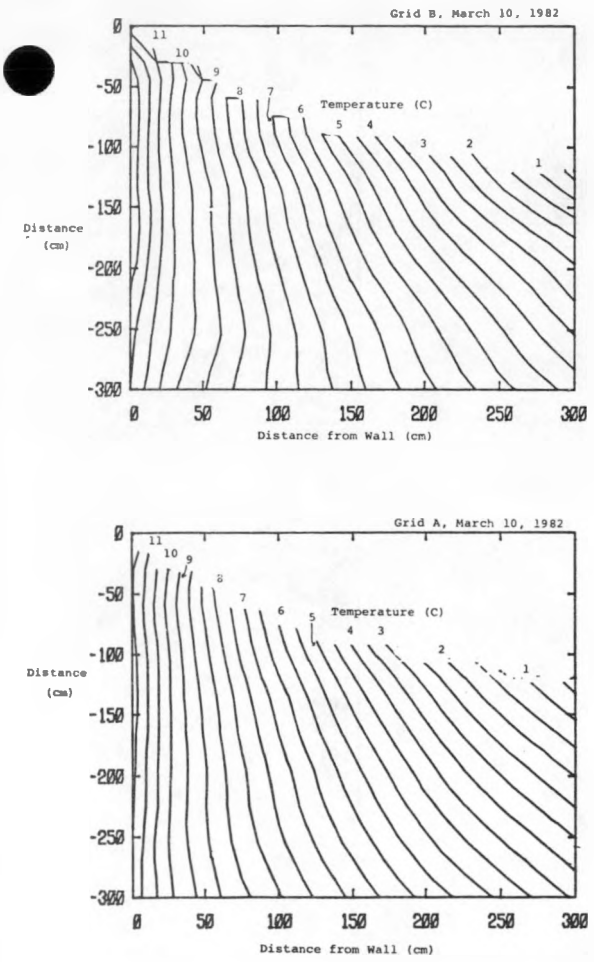

Figure 6.

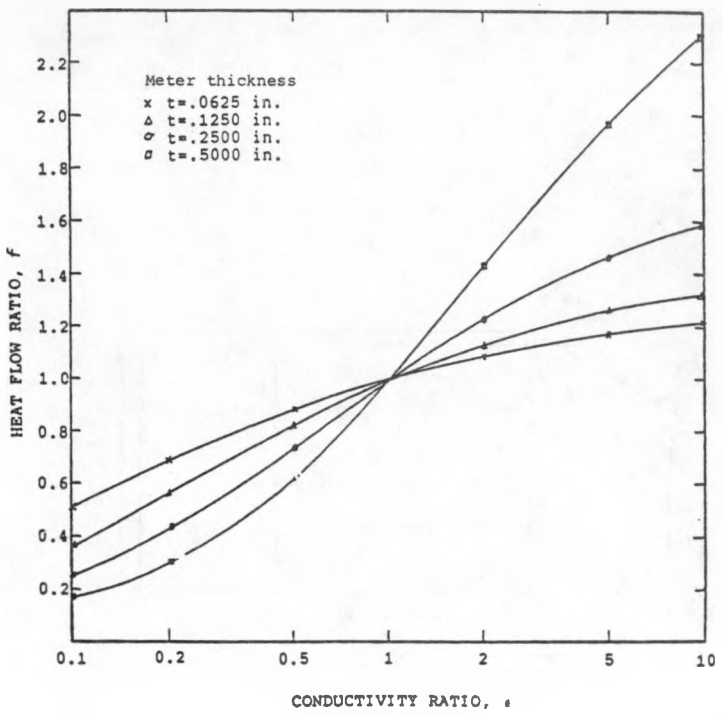

Fig. 7. Graph of the Heat Flow Ratio, f, versus the conductivity ratio, ϵ, for a 50.8x50.8x3.2 mm In 1" of surrounding material

From Magnusson (1982)

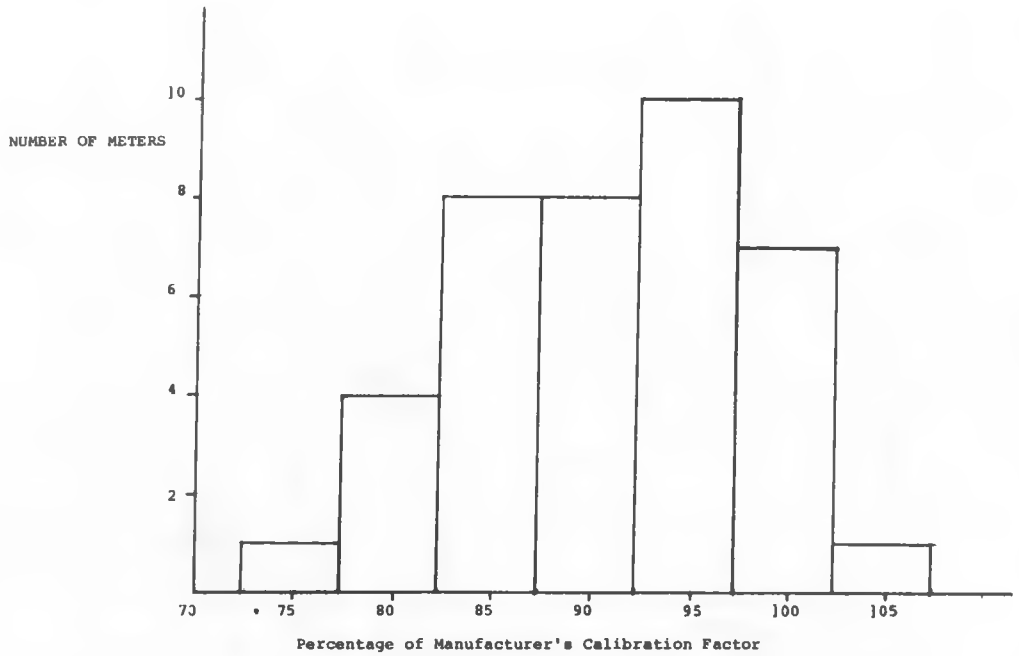

Fig. 8. Distribution of Experimentally Determined Heat Flux Meter Calibration Factors Expressed as a Percentage of the Manufacturer's Value.

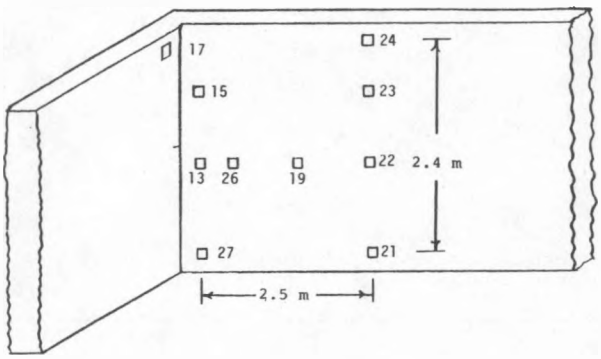

Fig. 9. Interior View of a Portion of the Northeast Wall Showing Heat Flux Meter Locations.

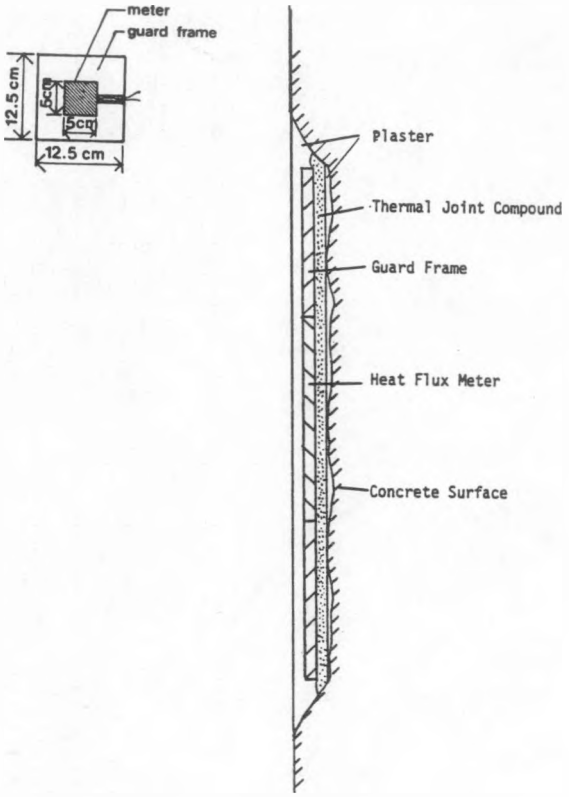

Fig. 10. Cross Section of a Heat Flux Meter Installation.

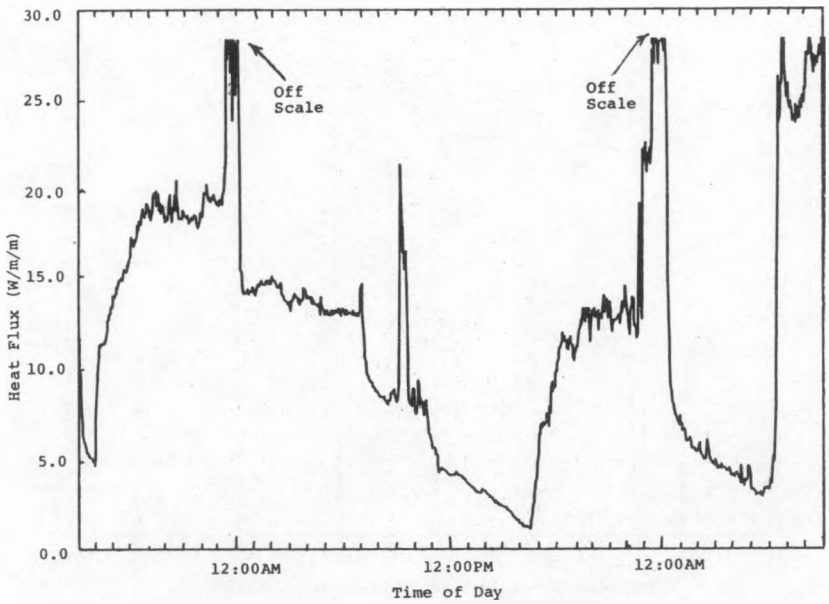

Fig. 11. Heat Flux at Location 24 Starting on January 6, 1982.

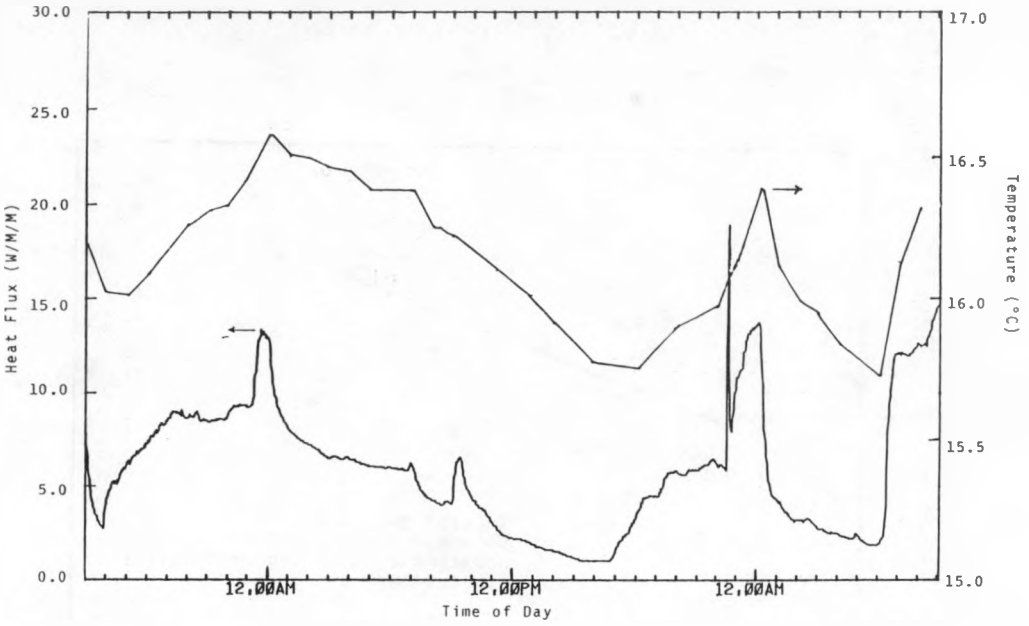

Fig. 12. Heat Flux and Wall Temperature at Location 23 Beginning on January 6, 1982.

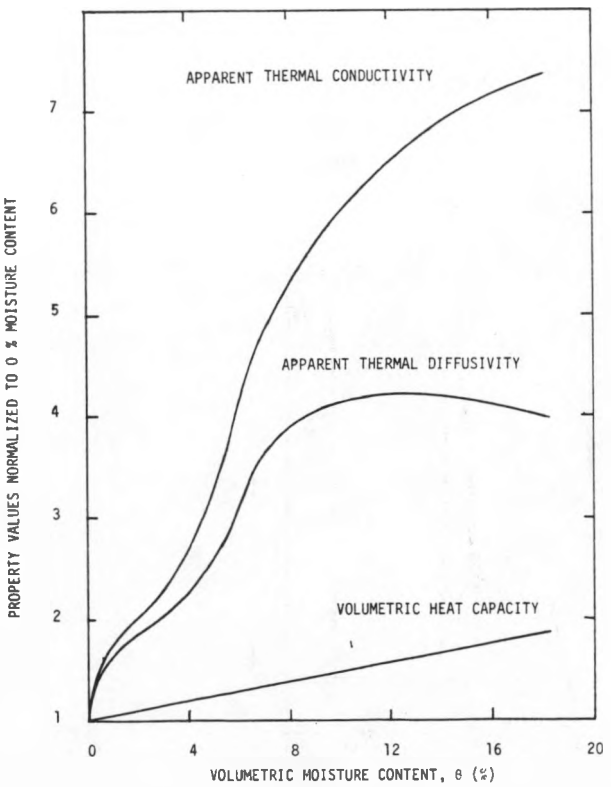

Fig. 13. The Effect of Moisture Content on the Thermal Properties of a Silt Loam. Thermal Conductivity Data Adapted from Bligh, Pfender and Eckert, (1980). T = 20°C, Porosity = 0.43.

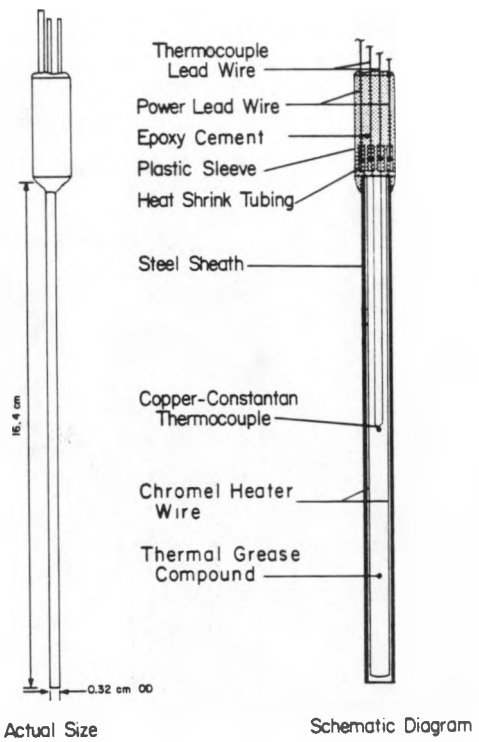

Fig. 14. M.I.T. Thermal Conductivity Probe.

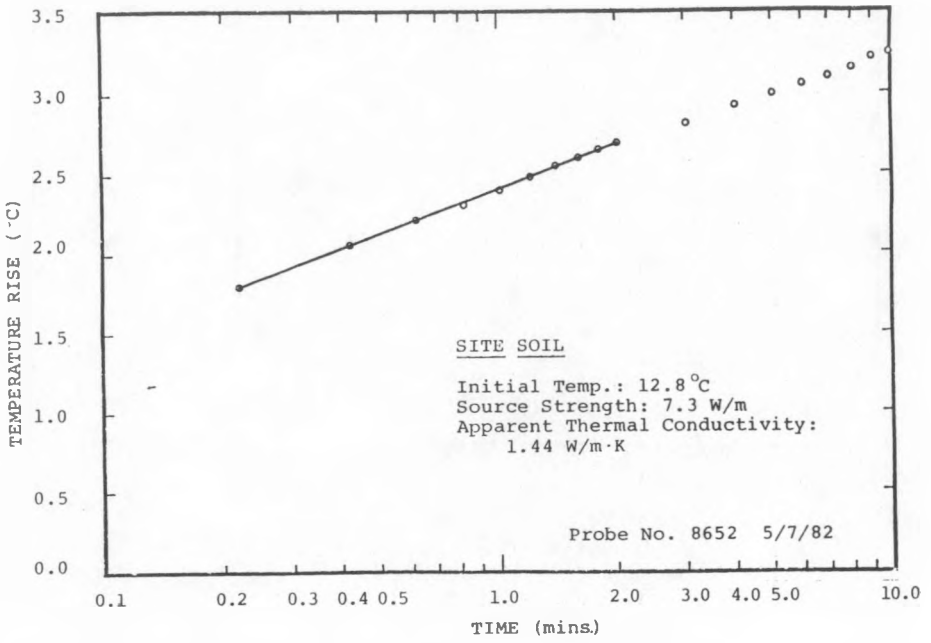

Fig. 15. Typical Output of a Thermal Conductivity Probe Measurement.

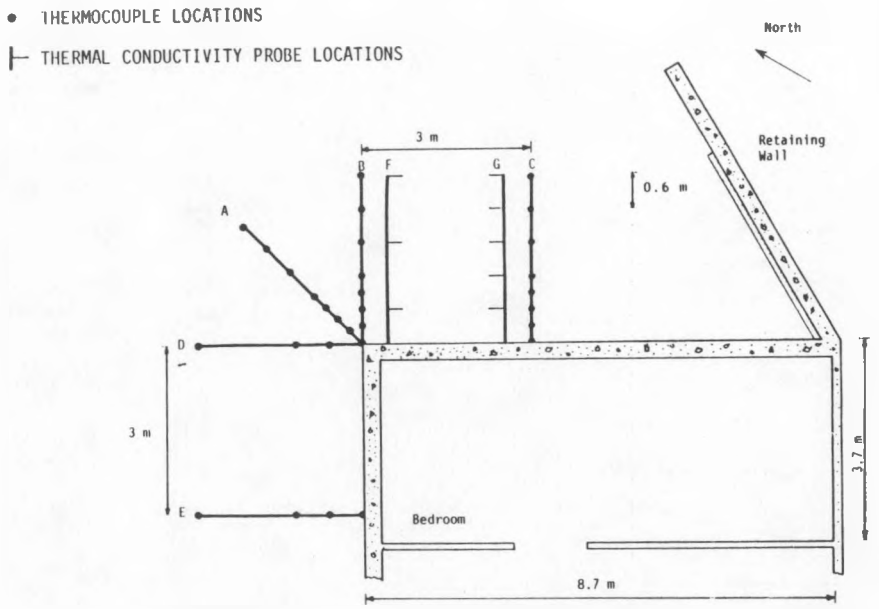

Fig. 16. Plan View of Soil Instrumentation Grid Locations for the Earth Sheltered House. Roof and Floor Instruments are not shown.

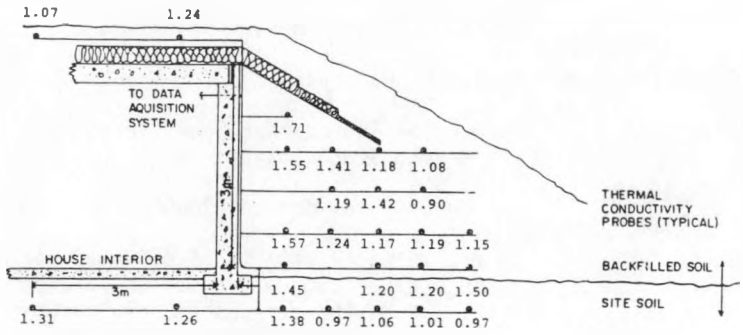

(a) May 23 and 24, 1982

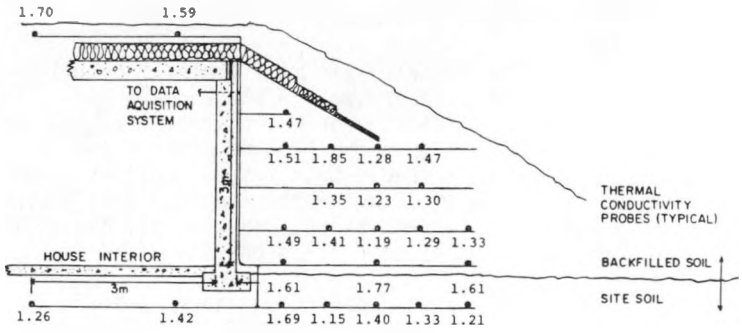

(b) August 14 and 15, 1982.

Fig. 17a and 17b. Soil Apparent Thermal Conductivity as Measured by Thermal Conductivity Probes in Grid G. Numbers are in (W/m K).

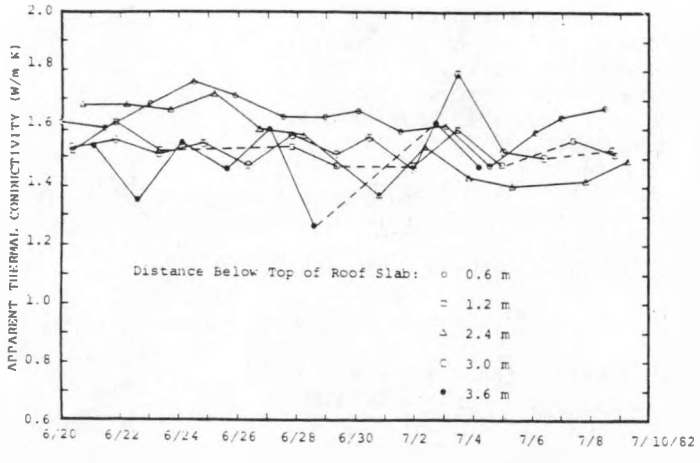

(a) Thermal Conductivity Probes 0.6 m from the House Wall

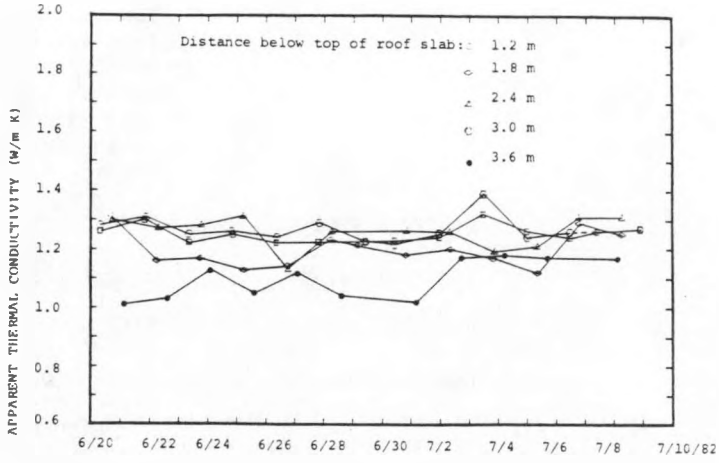

(b) Thermal Conductivity Probes 2.4 m from the House Wall.

Fig. 18a and 18b. Apparent Thermal Conductivities Measured by Thermal Conductivity Probes Over a 20 Day Period.

PROJECT SUMMARY

Project Title:	The New Mexico State University Passive Skytherm™ Solar House Evaluation
Principal Investigator:	Thomas R. Mancini
Organization:	Mechanical Engineering Department New Mexico State University P. O. Box 3450 Las Cruces, New Mexico 88003
Project Goals:	To evaluate the effects of deflated air cells, water depth, evaporative cooling and panel operation on the performance of the Skytherm™ system in the cooling mode of operation.
Project Status:	The experimental testing has been completed and the data for the summer of 1982 is presently being evaluated. The deflated air cell inhibits both the loss and the gain of heat in the cooling mode of operation. Because of the advantage of the inflated air cell in the heating mode of operation, it is most probable that the air cell is a net energy saver for the system and should be employed in all systems except for possibly those involving evaporative cooling only. The water depth effect appears to be consistent with the additional thermal mass which is added to the structure. That is, the addition of 26% additional thermal mass resulted in reduction of about 20% in the magnitude of the temperature fluctuations of the water bags. Evaporative cooling is by far the greatest contributor to the heat rejection from this system. The evaporative cooling accounts for about an order of magnitude greater heat loss from the system than do radiation and convection alone. The opening and closing of the movable insulation panels does not appear to greatly affect the performance of the system in the cooling mode of operation. However, it is most important to have the water bags exposed to the ambient conditions during the late morning hours prior to dawn.
Contract Number:	DE-AC03-80CS30228
Contract Period:	June 1, 1980 to December 1, 1982
Funding Level:	$165,800
Funding Source:	U. S. Department of Energy through the San Francisco Operations Office, Passive Cooling Division

The New Mexico State University Passive Solar House

Thomas R. Mancini
Mechanical Engineering Department
New Mexico State University
Las Cruces, New Mexico 88003

ABSTRACT

The New Mexico State University Passive Solar House is of the Skytherm™ type in which roof ponds and movable insulation are used to control the collection and rejection of energy for the heating and cooling of the interior space. In this paper some of the results of the 1981 and 1982 cooling season tests are presented. These include the effects of deflated air cells, a change of water pond depth from 7.5 to 15 cm, and the effects of evaporative cooling and panel control on the performance of the system.

INTRODUCTION

The Skytherm™ system for heating and cooling has been discussed by a number of investigators including its inventor Mr. Harold Hay (1,2,3,4,5, 6,7); therefore, only a brief discussion will be offered here. Figure 1 is a schematic diagram depicting the operation of the Skytherm™ system. When the system is in the summer cooling mode of operation, the movable insulating panels are removed at night and closed over the water bags during the daylight hours. In this way the energy absorbed by the water from the house is rejected through the heat transfer mechanisms of convection and radiation to the clear night sky. One of the attractive features of this particular cooling system is that it can also be used for heating the house in winter by simply reversing the panel opening and closing sequence. This dual use of the system, for both heating and cooling, is an important consideration from a cost/benefit point of view and in terms of the potential commercialization.

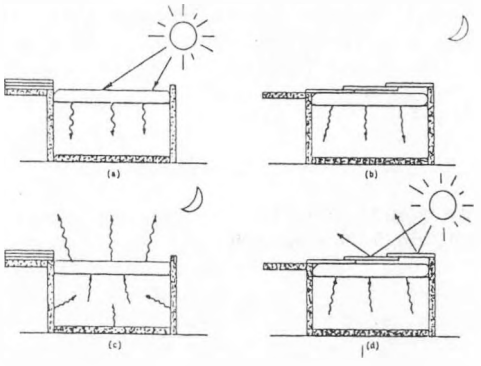

Figure 1. Schematic diagram of the operation of the Skytherm system. (a) and (b) represent the winter operation and (c) and (d) the summer operation.

The purpose of the New Mexico State University Passive Solar House Project is to evaluate the Skytherm™ concept in the hot, arid climate of southern New Mexico. The specific objectives of this study are to evaluate the effects of the deflated air cells, water depth, evaporative enhancement, and panel operating procedures on the perfromance of the system.

BACKGROUND

The climate of New Mexico varies greatly across the state with the terrain ranging from high mountain valleys to arid desert. The Passive Solar House is located in Las Cruces in the upper Chihuahuan Desert. Las Cruces' climate is classified as arid with an average rainfall of 21.1 cm, an average annual temperature of 15.6 C, 80% of the total possible sunshine, and a low relative humidity (8,9). The four months of June, July, August, and September are the hottest of the year averaging 24.4 C, 26.1 C, 25.0 C, and 21.7 C, respectively. The average high temperatures during these months are: June 34.4 C, July 33.9 C, August 33.3 C, and September 30.6 C. Daily high temperatures in excess of 43 C are not uncommon during late June and early July. More than half of the rainfall occurs during the months of July, August, and September. The relative humidity generally ranges from 60% in the early morning hours to 30% in the late afternoon.

To design the house we used an extensive computer code developed at New Mexico State University (10,11,12). The results of the simulations indicated that the Skytherm™ system would operate very well in the arid Southwest. Furthermore, the results predicted that the system performance in the cooling mode of operation is most sensitive to the internal loads, panel control strategy, infiltration rate, and water pond depth.

Using the results of the computer simulation, we designed and built in 1977 and 1978 an energy efficient house of traditional spanish-southwestern architecture. Energy efficiency is achieved through the use of double-paned windows, insulated doors, and the location of a large thermal mass interior to the building insulation envelope. Figure 2 is the floor plan for the house. All of the exterior walls and the three load bearing interior walls are constructed from precast concrete 15 cm thick. This is a standard method of construction for commercial buildings but it has not been widely applied to residential

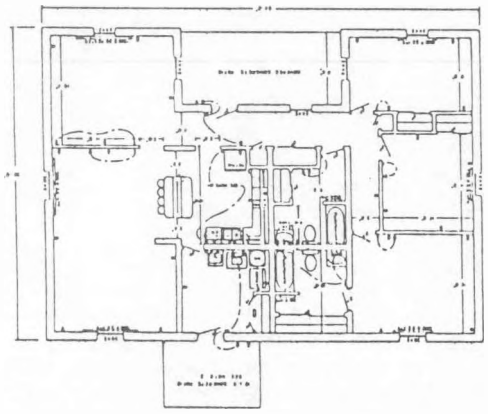

Figure 2. Floor plan of the NMSU Passive Solar House.

structures. The panels were fabricated at the plant and then trucked to the building site and assembled. The roof-ceiling of the house is a metal deck covered with concrete to a depth of 7.5 cm and coated with a black rubberized coating. The massive walls, slab and the roof contain 130,000 kg of concrete. Once the walls were installed, they were insulated externally with 5 cm of air-sprayed urethane foam, U = 2.1 W $M^{-2}K^{-1}$. Metal lath was then attached to the insulation and a conventional stucco finish applied.

The roof-pond and movable insulation systems for the house were designed to use off-the-shelf components wherever possible. Thus, conventional garage door tracks and wheels were selected for the movable panels. Two types of panels have been used on the house. The first was a prefabricated panel made of a wood frame, epoxy-impregnated paper honeycomb filled with cellulose and covered with aluminum skin on the top and bottom. These panels worked well for about a year and a half until they began to lose thermal efficiency and sag due the added weight from rain water being absorbed by the cellulose. They were then replaced with urethane foam panels which have an aluminum skin on the bottom. The roof pond system was designed to match the floor plan of the house with five bays located in a north-south orientation. The two outermost bays are longer than the three inner ones and there is a total of 121 M^2 of the roof covered with water bags. The water bags are made from 8 mil thick Monsanto 602. The roof presently contains some water bags that have an insulating air cell which, although it is deflated during the summer, does represent an additional insulating layer of polyethylene.

Preliminary testing and some data analysis were done on the system during the winter of 1978 and 1979 and the summer of 1979 (13,14,15).

TESTING PROGRAM

The main objectives of the testing program for the summer of 1981 were to evaluate the effects of water depth and the additional layer of polyethylene on the performance of the system. The principal mechanisms for heat transfer are radiation to the clear night sky and convection to the air. It is not possible to eliminate some elements of evaporative cooling as well when it rains, however. Consequently, information regarding the times when it rained as well as other events which occurred during the period reported in this paper are noted in Table I.

Table I
Daily Log of Events at the NMSU Passive Solar House

Day No.	Date	Event
1	28 May	Testing Begins with 7.5 cm of water in the water bags
7	3 June	Power outage
8	4 June	Power outage
12	8 June	Datalogger misprogrammed
18	12 June	Occupants began ventilat
23	19 June	Datalogger malfunction repaired
28	24 June	Rain - Panels not opened
30	26 June	Water depth changed
33-48	29 Jun to 14 July	Datalogger sent out
50	16 July	Rain
52	18 July	Rain

Day 1 is 28 May 1981 and the following days are numbered consecutively from there.

During this period the panels were opened at 10:00 P. M. and closed at 5:00 A. M. MST. These times were determined from the results of simulations (10,11,12). There is some sensitivity of the system performance to opening and closing times, but these times represent "the best" performance for a fixed schedule. The house is occupied which presents some problems with regard to the energy balances and evaluation. However, it is felt that this is necessary to have a truly representative test as would occur in an actual residence. During part of the testing season, the occupants did not cool through ventilation. After June 12 there was forced ventilation done by the occupants, this was monitored and dumped on the data tape.

During the summer of 1982, the house was unoccupied; bay B was sprayed with water for 15 seconds four times each hour when the panels were opened. In addition the opening schedule for the movable panels was varied by one hour each week from 9:00 to 10:00 and 11:00 in rotation throughout the summer.

DATA ACQUISITION AND INSTRUMENTATION

The data acquisition system for the house is an Acurex Autodata 10. Ninety-one channels of data are collected and dumped onto magnetic tape each hour of the day. A variable which can change rapidly, such as solar radiation, is sampled every 15 seconds and the hourly average value is dumped. Other variables are sampled at rates of once each minute or each hour depending on how quickly they might vary. The measurements which are made are temperatures, solar radiation, infrared radiation, relative humidity, wind speed and direction, and

heat fluxes through the walls, ceiling and floor. The accuracies of these measurements are shown in Table II below.

Table II.
The Accuracies of the Instrumentation

Instrument	Accuracy	Manufacturer
Thermocouples (T)	± .5 C	Omega (cal.)*
Relative Humidity	± 5 %	Texas Elect. (Manufact.)
Solar Radiation	± 1.5 %	Eppley PSP (Manufact.)
Infrared Radiation	± 1.5 %	Eppley PIR (Manufact.)
Heat-Flux Sensor	± 2.0 %	Hy Cal Bi 6 (Manufact.)

* Refers to the source of the reported accuracy.

It should be noted that the accuracies listed in Table II do not necessarily reflect the accuracy of the actual measurement. In particular the relative humidity is probably in question whenever it is below 10 to 15 %, and the heat-flux measurements depend very strongly on the method of application of the sensor to the surface. The heat-flux measurement is one of the more critical variables in the thermal analysis. At this time, no reliable in-place calibration method for these thermopile devices exists. Our approach to the problem has been to use mounting procedures which yield repeatable, consistent results. Even with care, there are still cases in which we cannot use the heat-flux measurements to close the energy balances.

RESULTS AND DISCUSSION

During the summer of 1981, the testing at the NMSU Passive Solar House was directed at determining the effects of the deflated air cell versus no air cell and the water depth on the ability of the roof ponds to reject heat. Detailed descriptions of the data and its analysis are presented in references 16 and 17. Shown in Figure 3 are two water bag temperatures for bags with and without air cells. Bay B has bags with deflated air cells and thus, an additional 8 mils of polyethylene

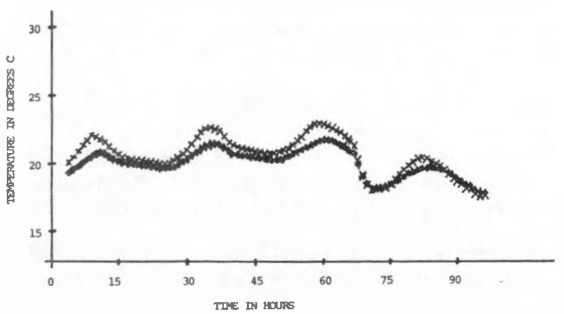

Figure 3. Temperatures of water bags over a three day period. The diamonds are bay B with a deflated air cell and the exes are bay D without an extra layer of polyethylene.

over the water while Bay D has a single layer of insulating plastic. Bay B does not experience either the high or the low temperatures which Bay D does. This is because the additional layer of Monsanto 602 not only reduces the energy which the water bag can reject by radiation and/or convection but also reduces the heat gains during the day. The overall heat-transfer coupling coefficient between the bag and the ambient when the panels are closed is 5.4 W $M^{-2}K^{-1}$ for the bags which have no air cell and 4.8 W $M^{-2}K^{-1}$ for the bags with the deflated air cell. The ability of the roof to reject heat solely through radiation and part of the time through convection (convection results in heat gain to the bags during part of the time when the panels are open) ranges from 31 to 69 W M^{-2}. The convective effects range ± 10 W M^{-2}.

In Figure 4 are shown the maximum (Δ), average (✱) and minimum (+) temperatures of the water bag in Bay A over the course of the summer's testing. The zeros on the horizontal axis correspond to days when the data acquisition system malfunctioned. As can be seen in this figure when the water depth was changed on day 30 from 7.5 to 15 cm, the difference between the maximum and minimum temperatures was reduced. The temperature swing was reduced about 20% with the addition of about 23% to the total thermal mass of the house. This is consistent with what should be expected since not all of the thermal mass (roof, walls, and slab) are in immediate thermal communication with the water ponds.

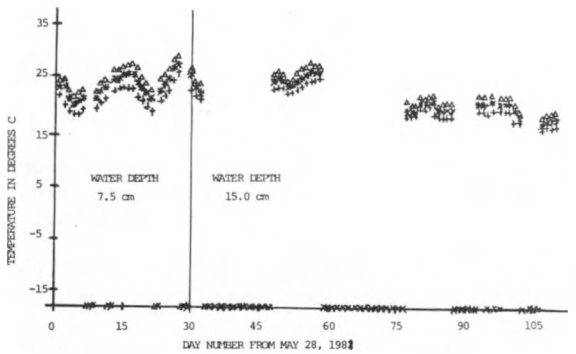

Figure 4. Daily Average (*), Maximum (Δ), and Minimum (+) temperatures of the water in bay A.

The testing during the summer of 1982 has been directed at evaluating the effects of evaporation and panel operating strategy on the heat rejection from the water bags. The data have not yet been evaluated in detail but some of the preliminary results can be presented. Shown in Figure 5 are the ambient temperature and water bag temperatures for two bays one of which is sprayed with water four times each hour when the panels are open. The bay which is sprayed, bay B, ranges from 4.5 to 5.6 C lower temperature than bay A which is not cooled by evaporation. This is typical and evaporation is an order of magnitude more effective in rejecting heat than are radiation and convection.

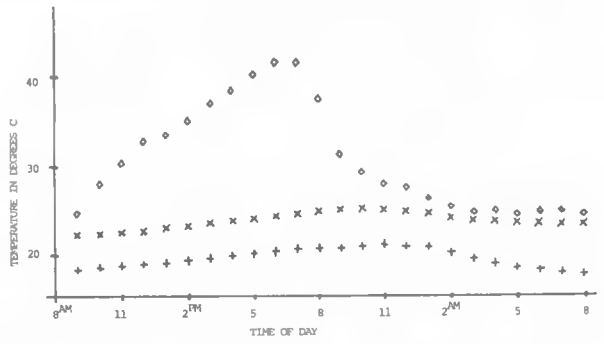

Figure 5. Transient ambient temperature (diamonds), water bag without evaporative cooling (exes), and water bag with evaporative cooling (plus signs).

Evaluation of the data for the panel control strategy indicates that the heat rejection from the water bags is not greatly affected by varying the opening time of the insulating panels from 9:00 to 11:00 P.M. This is most likely due to the fact that convection is serving as a net heat gain to the bags during the late evening hours. One could logically expect a similar two hour change in the closing time, i.e. from 6:00 to 4:00 A.M., to result in a decrease in the energy rejected from the bags because it is during the early morning hours that the heat rejection by both convection and radiation is greatest.

ACKNOWLEDGEMENTS

We should like to acknowledge the support of the New Mexico Energy and Minerals Department for the construction of the house and the United States Department of Energy under contracts EG-77-c-03-1606 and DE-AC03-80CS30228 for the support to run the experiments and evaluate the data.

REFERENCES

1. Hay, H. R. and Yellott, J. I., 1969a, "Natural Air Conditioning with Roof Ponds and Movable Insulation," ASHRAE Transactions, Vol. 75, Part 1, pp. 165-177.

2. Hay, H. R. and Yellott, J. I., 1969b, "International Aspects of Air Conditioning with Movable Insulation," Solar Energy, Vol. 12, pp. 427-438.

3. Hay, H. R., 1972, "Energy, Technology and Solar Architecture," Paper No. 72-WA/Sol-11, ASME Proceedings.

4. Yellott, J. I. and Hay, H. R. , 1969, "Thermal Analysis of a Building with Natural Air Conditioning," ASHRAE Transactions, Vol. 75, Part 1, pp. 178-189.

5. Haggard, K. L. et. al., "Research Evaluation of a System of Natural Air Conditioning," National Technical Information Center, Report No . PB-243 498, Washington D. C.

6. Niles, P. W. , 1976, "Thermal Evaluation of a House Using a Movable-Insulation Heating and Cooling System," Solar Energy, Vol. 18, pp. 413-419.

7. Niles, P. W. , Haggard, K. L., and Hay, H. R., 1976, "Nocturnal Cooling and Solar Heating with Water Ponds and Movable Insulation," ASHRAE Transactions, Vol. 82, Part 1, pp. 793-801.

8. Houghton, F. E., 1972, "Climatic Guide, New Mexico State University, Las Cruces, New Mexico, 1851-1971," Agricultural Experiment Station Research Report 230, New Mexico State University, Las Cruces, New Mexico.

9. Tuan, Y., et. al., 1973, "The Climate of New Mexico-Revised Edition," State Planning Office Santa Fe, New Mexico.

10. Miller, W. C., and Mancini, T. R., 1977, "Numerical Simulation of a Solar Heated and Cooled House Using Roof Ponds and Movable Insulation," Proceedings of the Solar World Conference, AS/ISES, Orlando, Florida.

11. Miller, W. C. and Mancini, T. R., 1978, "The Effects of Selected Parameters on the Heating and Cooling Performance of a Passive Solar House," 2nd Annual Passive Conference, Philadelphia, Pennsylvania.

12. Miller, W. C. , 1977, "Numerical Modeling of a Passive Solar House," M. S. Thesis, Mechanical Engineering, New Mexico State University, Las Cruces, New Mexico.

13. Fate, R. E. and Mancini, T. R., 1979,"The Performance of a Roof Pond Solar House," The Proceedings of the 4th National Passive Solar Conference, Vol. 4, pp. 728-732.

14. Mancini, T. R. and Fate, R. E., 1979, "Evaluation of a Roof-Pond Solar House," final report submitted to the United States Department of Energy.

15. Fate, R. E., 1980, "Analysis of the New Mexico State University Passive Solar House," M. S. Thesis, Mechanical Engineering Department, New Mexico State University, Las Cruces, New Mexico.

16. Mancini, T. R., Suter, K. J., and Price, D. M., "The New Mexico State University Skytherm™ Solar House: Summer Cooling Data 1981", Proceedings of the ASME Solar Division Conference, Albuquerque, New Mexico, 1982.

17. Suter, K. J., 1982, "Thermal Performance Evaluation of the New Mexico State University Passive Skytherm Solar House, Summer 1981", M. S. Thesis, Mechanical Engineering, New Mexico State University, Las Cruces, New Mexico.

PROJECT SUMMARY

Project Title:	Radiative Cooling of Buildings
Principal Investigators:	Marlo R. Martin, Ronald C. Kammerud
Organization:	Lawrence Berkeley Laboratory University of California Berkeley, California 94720
Project Goals:	Determine the resource for radiative cooling, including the spectral and angular components of thermal infrared sky radiation. Develop and evaluate conceptual designs for radiative cooling systems. Develop new materials which permit systems to more closely approach theoretical performance.
Project Status:	Spectral and angular sky radiance measurements in six U.S. cities and analysis of the data have been completed. Data summaries are being issued which describe the characteristics of the extensive data set. Based on the collected data, several useful estimation procedures have been developed. The global total sky emissivity (equivalent to a knowledge of the "sky temperature") can be estimated based on surface dewpoint temperature, for clear skies. An approximate method for correcting for the presence of clouds has been suggested. A method has been developed which yields statistical estimates of the angular and spectral components of sky radiation based solely on the global, total emissivity and the air temperature. The performance of simple radiative cooling panels with existing radiator surfaces (white paint, polyvinyl fluoride) has been tested and documented. The performance of advanced selective radiators is currently being measured.
Contract Number:	DE-AC03-76SF00098
Contract Period:	March 1977 to the present
Funding Level:	$175,000 in FY 1982
Funding Source:	Office of Solar Heat Technologies, Passive and Hybrid Solar Energy Division, U.S. Department of Energy

SUMMARY OF RESULTS OF SPECTRAL AND ANGULAR SKY RADIATION MEASUREMENT PROGRAM*

Marlo Martin and Paul Berdahl
Lawrence Berkeley Laboratory
University of California
Berkeley, CA 94720

Abstract

Results are analyzed and plotted for a series of more than 50 thousand spectral infrared sky radiation measurements made in 6 U.S. cities. An empirical equation is developed to disaggregate the total sky emissivity into its spectral and angular components. This information is of special relevance to the performance of radiative cooling systems.

1. Introduction

Infrared transfer between the building envelope and the environment is typically treated in a very approximate manner in calculations of building thermal performance. Corrections to the skin temperature of building walls and windows due to this phenomenon are required since half the field of view "seen" by these surfaces is at the "sky temperature." Reductions in the skin temperature of roof surfaces can be more significant since roofs are completely exposed to the radiatively cooler sky dome. It is desirable to be able to estimate these effects accurately in order to properly model the thermal performance of buildings. It has also been demonstrated that with a roof system designed to take advantage of infrared heat rejection to the sky, it is possible to achieve cooling rates of the same order of magnitude as the cooling loads for single story buildings. The degree to which this can be done depends on the effectiveness of the radiative and convective coupling of the radiator surface to the sky and to the interior space being cooled. It also depends on the amount of downward infrared radiation received from the sky dome.

Previous studies have concentrated on measurements and evaluation of the total downward radiative flux, which is usually expressed in terms of an effective "sky temperature," or a total sky emissivity [1]. It now appears, however, that the development of spectrally selective radiator and glazing materials could permit increased cooling rates to be achieved, thus requiring knowledge of spectral sky radiation properties.

A blackbody emitter radiates according to the relationship

$$R_r = \varepsilon_r \sigma T_r^4 \qquad (1)$$

where ε_r is a constant emissivity having a value near unity for radiator surfaces ($\varepsilon_{r=1}$ for a true black body emitter); $\sigma = 5.67 \times 10^{-8}$ Wm^{-2} K^{-4}, and T_r is the radiator temperature in degrees Kelvin. For a spectrally selective radiator the surface material is chosen to make the emissivity large in one portion of the infrared spectrum and small over the remainder.

The calculated spectral and angular behavior of typical midlatitude clear sky radiance is shown in Figure 1. The plotted curves are most sensitive to variations in the moisture content and temperature profile of the atmosphere, and especially to the presence of cloud cover. The region between approximately 8 and 14 micrometers is the part of the infrared spectrum through which most heat can be rejected to the sky, since the incident radiation from the sky is at a low level. This region is often referred to as the infrared "atmospheric window". A selective radiator would be designed to emit and receive radiation strongly only within this window region. The measurements presented here are the result of a multiyear program to investigate the specular and angular sky radiation properties over a range of climates in the southern continental United States.

Detailed spectral measurements of the sky radiation are reported for six U.S. locations; Tucson, AZ, San Antonio, TX, St. Louis, MO, Gaithersburg, MD, West Palm Beach, FL, and Boulder City, NV. The radiometers used in this study were developed at Lawrence Berkeley Laboratory to measure the incident sky radiation through a 2^o field of view at five zenith angles (0^o, 20^o, 40^o, 60^o, 80^o). At each angular position, the incident radiation was recorded through seven infrared filters for which the transmission characteristics are presented in Figure 2. The "no filter" channel actually represents the spectral radiation passing through a coated germanium lens. The remaining six channels will be referred to in terms of their central wavelengths or their pass bands; 8.8 μm, 9.6 μm, 11 μm, 8-14 μm, 15 μm, and 17-22 μm.

During the course of approximately 1 1/2 years of measurements readings were taken at half hour intervals. Analysis of the resulting data base yielded a total of 57 months of good data from among the six locations. Radiation measurements were averaged over each month for all seven filter channels and for each

*This work was supported by the Assistant Secretary for Conservation and Renewable Energy, Office of Solar Heat Technologies, Passive and Hybrid Solar Energy Division of the U.S. Department of Energy under Contract No. DE-AC03-76 SF00098.

f the five zenith angles. The data for no filter and the 8-14 micrometer filter is plotted as a function of the total sky emissivity in a series of graphs presented in section 7.

2. Apparent Sky Emissivity

Sky radiation data can be expressed in a number of ways which are essentially equivalent, but differ in their ease of interpretation. The sky radiance $R_s(\lambda, \theta)$ which is a function of wavelength λ and zenith angle θ is the quantity most directly related to the net radiative heat flux at any time. This quantity is not expressed by means of an equation similar to Eq.(1) because the sky does not radiate as a blackbody, as can be seen from the typical radiation profiles of Figure 1. An effective "sky temperature" T_s can be defined as being the temperature of a blackbody for which the emitted radiative flux is the same as for the sky:

$$R_s = \sigma T_s^4 \tag{2}$$

where R_s is the measured incident flux containing all thermal wavelengths at all angles from the sky. The objections to using an effective sky temperature are twofold; first, the concept of temperature refers to a body in thermal equilibrium in a well defined state, whereas the atmosphere consists of a gradation of layers at different temperatures, whose spectral emissivity changes as a function of altitude. Due to the partial transparency of the air layers, the observer in reality "sees" a weighted average of temperatures from each layer which is a function of the wavelength. The second objection is more pragmatic in nature. The "sky temperature" as defined in Equation 2 fluctuates strongly with the ambient air temperature T_a throughout the day [1]. The changes in apparent emissivity of the sky can thus be masked to a great extent by ambient air temperature changes. In this report we choose to express the sky radiation data in terms of the spectral and angular sky emissivity $\varepsilon_s(\lambda,\theta)$ which is defined to yield the spectral sky radiance:

$$R_s(\lambda,\theta) = \varepsilon_s(\lambda,\theta) B_a(\lambda). \tag{3}$$

Here $B_a(\lambda)$ is the Planck function evaluated with the ambient air temperature T_a (^oK). The temperature T_a is to be measured in the conventional meteorological fashion at a height of 1 to 2 meters above the ground. The Planck function is given explicitly by

$$B_a(\lambda) = 2hc^2\lambda^{-5}\left[\exp\left(\frac{hc}{\lambda k_B T_a}\right)-1\right]^{-1}, \tag{4}$$

where h is Planck's constant (6.626×10^{-34} Js), k_B is Boltzmann's constant (1.381×10^{-23} J K^{-1}), and c is the speed of light (2.998×10^8 m s^{-1}).

Under clear sky conditions, the value $\varepsilon_s(\lambda,\theta)$ remains practically constant throughout the day. Multiplication by the Planck function allows the incident radiance to be calculated readily, since air temperatures are available for most locations. The total incident sky radiation received by a horizontal surface is obtained by integration of equation (3) over all wavelengths and zenith angles.

$$R_s = 2\pi\int_0^\infty d\lambda B_a(\lambda)\int_0^1 \cos\theta \; d\cos\theta \varepsilon_s(\lambda,\theta). \tag{5}$$

The total sky emissivity ε_s may be defined by

$$R_s = \varepsilon_s \sigma T_a^4, \tag{6}$$

analogous to Eq.(3). Equations (5) and (6) can be used to express the total sky emissivity in the form

$$\varepsilon_s = \int_0^\infty d\lambda B_a(\lambda)\int_0^1 \cos\theta \; d\cos\theta \varepsilon_s(\lambda,\theta)\left[\int_0^\infty d\lambda B_a(\lambda)\int_0^1 \cos\theta \; d\cos\theta\right]^{-1} \tag{7}$$

which shows that ε_s is a weighted average of $\varepsilon_s(\lambda,\theta)$.

3. The Sky Radiance Equation

An empirical equation has been developed to describe the spectral sky emissivity $\varepsilon_s(\lambda, \theta)$ as a function of zenith angle θ and total sky emissivity ε_s. The spectral emissivity of the sky can be written in terms of the apparent sky transmissivity:

$$\varepsilon_s(\lambda,\theta) = 1 - \tau(\lambda,\theta) \tag{8}$$

We make the assumption that the wavelength and angular dependences can be separated, and that the angle enters in the form

$$\varepsilon_s(\lambda,\theta) = 1 - A t(\lambda) e^{-b/\cos\theta} \tag{9}$$

where $1/\cos\theta$ is the air mass. The constant A can be determined by the condition that $\varepsilon_s(\lambda, \theta)$ averaged over all wavelengths and over the angles 0 to 90^o corresponding to the sky dome must equal the total sky emissivity ε_s (Eq.7):

$$\varepsilon_s = 1 - 2A\bar{t}\int_0^1 e^{-b/\cos\theta}\cos\theta \; d\cos\theta \tag{10}$$

$$\text{where} \quad \bar{t} = \int_0^\infty d\lambda t(\lambda)\, B_a(\lambda) / \int_0^\infty d\lambda B_a(\lambda),$$

The integral over $d\cos\theta$ in Equation (10) is equal to twice the third exponential integral [2], $2E_3(b)$, which can be well approximated over the range of interest ($0 <= b <= 0.6$) by the exponential function $e^{-1.7b}$. We can thus write Equation (10) as:

$$\varepsilon_s = 1 - \bar{t}\, A\, e^{-1.7b}$$

which yields an expression for A,

$$A = (1 - \varepsilon_s)\, e^{1.7b} / \bar{t}$$

Substitution in Equation (9) results in the sky radiance equation:

$$\varepsilon_s(\lambda,\theta) = 1 - (1 - \varepsilon_s)\left[t(\lambda)/\bar{t}\right] e^{b(1.7 - 1/\cos\theta)} \tag{11}$$

The expressions $t(\lambda)/\bar{t}$ and b implicitly contain a dependence on the total sky emissivity ε_s, which will be determined by analysis of the experimental data. The following Sections 4 and 5 document how these dependences were obtained, and Section 6 presents methods for users of Eq. (11) to estimate ε_s.

4. Determination of Total Sky Emissivity

The spectral radiometer used to make the sky radiation measurements was considered to be a more accurate instrument than the pyrgeometer. After each set of measurements (every half hour) the sensor was directed into a blackbody reference cavity of known temperature. Once a day the cavity was caused to pass through a fixed temperature range allowing an absolute calibration of the radiometer to be carried out. The pyrgeometer cannot be calibrated as readily, and is thus considered to be less accurate. Furthermore, the radiometer readings are not affected by the sun, whereas a correction must be applied to pyrgeometer readings due to heating of the silicon dome by shortwave solar radiation.

For these reasons, a quantity called the "pseudo pyrgeometer" was derived from the recorded data. The emissivities measured at each zenith angle with the "no filter" channel are weighted by the solid angle subtended by them in the sky dome, and by the cosine of the zenith angle to account for their projection onto a horizontal surface. The quantity thus constructed behaves like a pyrgeometer reading, if the pyrgeometer is averaged over a sufficient interval to smooth out fluctuations due to cloud asymmetry. A plot showing the pseudo pyrgeometer as a function of dewpoint temperature is presented in Figure 3. The straight line in the figure is a least square fit to the 57 monthly average pseudo pyrgeometer values:

$$\varepsilon_{ps} = 0.00831\ T_{dp} + 0.6033, \tag{12}$$

where T_{dp} is the dewpoint temperature in degrees Celsius. Each of the measured average monthly spectral sky emissivities $\varepsilon_s(\lambda,\theta)$ can be plotted against the pseudo pyrgeometer reading, where ε_{ps} replaces ε_s in Equation (11). The advantage of doing so is that this equation provides a good fit to the data points taken under all sky conditions, as well as under the clear sky conditions used to empirically establish the constants in the equation. However, since the pseudo pyrgeometer is not a readily available instrument, it is more desirable to express the equation in terms of the true total sky emissivity as would be measured by a properly calibrated pyrgeometer.

A relationship can be derived between the pseudo pyrgeometer (Equation 12) and the pyrgeometer reading based on the correlation developed by Berdahl and Fromberg [1], which can be expressed as

$$\varepsilon_s = 0.00614\ T_{dp} + 0.734. \tag{13}$$

This equation was originally developed by analyzing 11 months of clear sky data, and applying correction factors to account for daytime solar heating of the pyrgeometer and small calibration corrections. In applying this equation to the data based on 57 months of clear sky data it was found necessary to adjust the relationship given in Equation (13) to read

$$\varepsilon_s = 0.00696\ T_{dp} + 0.709 \tag{14}$$

The reason for this adjustment is that the mean clear sky conditions for the original 11 month data set were systematically (if slightly) different from conditions for the full 57 month data set. The full data set indicates slightly lower emissivities for a given dewpoint temperature. To maintain consistency in our analysis we require a relationship between ε_s and T_{dp} based on the entire 57 month data set. The adjustment of Equation 13 to produce Equation 14 was determined by evaluating the difference between the two data sets using the pseudo pyrgeometer and then using the approximate relation

$$\Delta\varepsilon_s \approx 0.84\ \Delta\varepsilon_{ps}$$

to determine the adjustment required. In principle Equation 14 is an improvement over Equation 13 because it is based on more data. However, the difference is small, especially at dewpoint temperatures above 0°C, and the current derivation is somewhat indirect. The utility of Equation 14 in the present context is that it is consistent with Equation 12, especially since it is based on the same data set. Eliminating the dewpoint temperature between equations (12) and (14), one arrives at the desired expression for total sky emissivity ε_s as a function of the pseudo pyrgeometer value ε_{ps}. .

$$\varepsilon_s = 0.838\varepsilon_{ps} + 0.204 \qquad (15)$$

This relationship is plotted in Figure 4, along with the data points which display measured pseudo pyrgeometer values versus the measured pyrgeometer values for clear skies. The small systematic difference between the derived line and the data is due to the effect of sunlight on the pyrgeometer. If it were possible to correct the pyrgeometer observations for this error, agreement would be better. The same relationship is presented in Figure 5, which shows the corresponding plot for all sky conditions. For the purposes of this paper the pyrgeometer values ε_s are always obtained from measured pseudo pyrgeometer values by the use of Equation 15.

5. Determination of Parameters in the Sky Emissivity Equation

Equation (11) is of a form suggested by the physical phenomena taking place within the atmosphere. However, it is not a rigorously derived equation, and the primary purpose for introducing it at this time is to provide a concise analytical expression which adequately embodies the results of tens of thousands of individual spectral sky emissivity measurements. The nature of the transmissivity function $t(\lambda)$ has as yet been left undefined, except to state that it is related to the atmospheric spectral transmissivity (in the zenith direction). It is expected to be a function dependent on the total sky emissivity ε_s.

In order to fit the experimental data measured through seven infrared filters at five zenith angles, we consider the quantities $t(\lambda)/\bar{t}$ and b to be linear function of ε_s. In all four filter regions included in the atmospheric window (8-14 micrometers), and for the "no filter" case, the parameter b is a well defined linear function of ε_s. In the 15 micrometer channel there is only a slight dependence of either parameter on the total emissivity, since the atmosphere is optically dense at this wavelength. In other words, due to the fact that most 15 micrometer radiation reaching the detector originates within a few tens of meters from the instrument, the angular dependence described by the air mass term ($1/\cos\theta$) is no longer of relevance. This is borne out by the fact that the average value of the parameter $t(\lambda)/\bar{t}$ approaches zero (approx 0.02), and each spectral emissivity, as well as the total emissivity approaches unity.

The other anomalous channel is the 17-22 micrometer region. Here the clear sky data can be used to determine a least squares fit for the b-parameter, but a large amount of scatter exists. Again, as in the 15 micrometer case, the value of $t(\lambda)/\bar{t}$ is small (≤ 0.2 for $\varepsilon_s > 0.7$) indicating a situation where all emissivities approach unity. The unique feature in this spectral region is that a secondary "window" begins to open at low values of ε_s (low dewpoint temperatures).

The results of performing least squares fits for the two parameters b and $t(\lambda)/\bar{t}$ to straight lines as a function of the total sky emissivity ε_s are presented in Table (2).

Table 2

Values of least squares fit parameters for use in Equation 11 to predict spectral sky emissivity.

	$b = A\varepsilon_s + B$		$t(\lambda)/\bar{t} = C\varepsilon_s + D$	
	A	B	C	D
"no filter"	1.4929	-0.8668	1.1243	0.5997
8-14μm	1.7915	-1.1127	1.8068	1.0340
8.8μm	1.2809	-0.7710	5.1191	-1.1922
9.6μm	1.3046	-0.7153	5.3211	-1.6090
11.0um	1.7784	-1.1592	3.1744	0.4515
15.0μm	-5.7780	5.2576	0.0410	-0.0066
17-22μm	-0.6914	1.6528	-1.5486	1.2975

These values are substituted into the sky radiance equation (Equation 11) in order to produce the curved lines through the data points in the graphs presented in section 4 (Figures 6-9). Clear sky data has been used to generate the parameters in Table 2, which have not been altered for presentation of the data from all sky conditions. In obtaining the values for these parameters, the b-coefficient is determined by fitting the data points at the zenith and 60° angles. Measurements at a zenith angle of 80° were judged to be of less practical importance for radiative cooling purposes due to the small projected area of a horizontal surface in that direction (cosine effect).

6. Estimation of Total Sky Emissivity

The most straightforward way to obtain a value for the total sky emissivity ε_s for use in Eq.(11) is to measure it directly with a pyrgeometer. A correction to the reading is required to account for heating of the silicon dome whenever the instrument is located in direct sunlight. Unfortunately, pyrgeometers are not common instruments, and little data from them is available on a long term basis. Even weather stations operated by the National Oceanic and Atmospheric Administration (NOAA) do not use such an instrument for routine measurements.

A correlation has been documented by Berdahl and Fromberg [1] for the total emissivity as a function of dewpoint temperature (^oC). This correlation has been developed from clear sky pyrgeometer data which was subjected to corrections to account for solar heating of the instrument. Berdahl and Fromberg report two linear relationships for this function; one is a nighttime correlation; and the other is valid during the daytime:

$$\text{daytime} \quad \varepsilon_s = 0.0060\ T_{dp} + 0.727; \quad \text{nighttime} \quad \varepsilon_s = 0.0062\ T_{dp} + 0.741 \tag{16a, 16b}$$

A third relationship, valid for 24 hour average emissivities, can be obtained by simply averaging the coefficients of these two equations, and has been given as Equation 13.

Use of the linear fit which best describes the day/night conditions of interest in a given situation will yield total sky emissivities nearly as accurate as pyrgeometer readings if the clear sky condition is satisfied.

When clouds are present, a number of complexities are introduced into the estimation of the total sky emissivity. The temperature of the cloud base as well as its zenith angle and angular extent must properly be taken into consideration to produce accurate results. In practice this detailed an analysis is not usually feasible. One must be content with estimating the fraction of the sky vault covered by clouds, and the cloud base temperature must be roughly inferred from its altitude and the atmospheric lapse rate. The assumption is made that over a period of time the angular distribution of clouds as seen by an observer is uniform over the sky dome.

The method recommended here is that in the presence of clouds, the total sky emissivity be assigned a value [3]:

$$\varepsilon_s = \varepsilon_s^{clear}\,(1-\Gamma n) + \Gamma n, \tag{17}$$

where ε_s^{clear} is the clear sky emissivity calculated from Equation 13 or 16, n is the estimated fraction of sky covered by clouds, and Γ is a parameter which depends on the cloud height and type. Values for Γ range over 0.16 for cirrus clouds (height 12.2 km), 0.66 for altocumulus clouds (height 3.7 km), and 0.88 for stratocumulus clouds (height 1.2 km). Measurements in Atlanta, GA [4] and San Antonio, TX [5] indicate that a value of Γ = 0.55 to 0.6 can be used as an average for opaque clouds at these locations. Further information is available in the Mongraphs by Sellers [6] and Kondratyev [7].

Once the total sky emissivity has been determined by the above means, it can be used directly in the sky radiance equation, or one can use it to find the desired spectral emissivity from one of the graphs presented in section 4.

7. Discussion of Results

A total of 12 graphs are used to plot the spectral sky emissivities as a function of the total sky emissivity for each measurement channel. Half of these graphs are used to plot monthly averaged emissivities over clear sky conditions only, and the other half plot the same quantities using data from all sky conditions. Each set of graphs represents measurements made through six zenith angles (actually five angles and one composite channel referred to as the "global" measurement).

Due to the importance of blackbody emitters and radiators which emit strongly between 8 and 14 micrometers, we present detailed results for these two cases in Figures 6-9.

Both the clear sky conditions and all sky conditions are well described by equation (11) using the parameters provided in Table (2). At a zenith angle of 80° (10° above the horizon) the equation consistently predicts larger emissivity values than are observed. In all cases it will be noted that the angular-weighted global measurement closely approximates the emissivity at a zenith angle of 50°. For smaller zenith angles the sky emissivity varies only slightly achieving its lowest value in the overhead direction. As one approaches within 30° of the horizon all the measured emissivities increase rapidly, confirming the known fact that a cooling surface should be in radiative contact with the upper portion of the sky dome. However, little is to be gained by focusing a radiator sharply toward the zenith, since the emissivity values do not begin to increase rapidly until within 30° of the horizon.

The potential advantage of using a selective radiator which is highly emissive only within the 8-14 micrometer region is shown by an examination of the 8-14 micrometer global results (Figs 8,9). The maximum

temperature depression (below air temperature) which can be produced by a non-selective (blackbody) radiator is roughly proportional to $(1 - \epsilon_s)$, the deviation of the total sky emissivity from unity. The maximum temperature depression which can be produced by an 8-14 micrometer selective radiator is proportional to the deviation of the corresponding emissivity from 1, with approximately the same constant of proportionality. Since the slope of the curve in Figure 8a is greater than 2, the maximum temperature depression achievable with an 8-14 micrometer selective surface is more than twice the value achievable with an ordinary blackbody radiator. This can be particularly beneficial under overheated conditions where the dewpoint temperature, and hence the total sky emissivity ϵ_s, is relatively high.

8. Acknowledgment

The authors gratefully achknowledge the conscientious participation of Charlotte Standish and Cecelia Webster in the preparation of several revisions of this paper under deadline pressures.

9. References

1. P. Berdahl and R. Fromberg, "The Thermal Radiance of Clear Skies," to be published in Solar Energy, 1982.

2. M. Abramowitz and I. Stegun, eds., Handbook of Mathematical Functions, National Bureau of Standards Applied Mathematics Series, published by the U.S. Gov't. Printing Office, p.228, formula 5.1.4 (1964).

3. P. Berdahl and R. Fromberg, "An Empirical Method for Estimating the Thermal Radiance of Clear Skies," Lawrence Berkeley Laboratory Report LBL-12720, (May 1981). This report is a sightly more comprehensive version of Ref.1.

4. 4. K.G. Picha and J. Villanueva, "Noctunal radiation measurements," Atlanta, Georgia, Solar Energy 6, 151 (1962).

5. G. Clark and C.P. Allen, "The estimation of atmospheric radiation for clear and cloudy skies," Proceedings Second National Passive Solar Conference, Vol. 2, p.676, Philadelphia (1978).

6. W. Sellers, Physical Climatology, p.58, Univ. of Chicago Press, Chicago (1965).

7. K. Kondratyev, Radiation in the Atmosphere p.576, Academic Press, New York (1969).

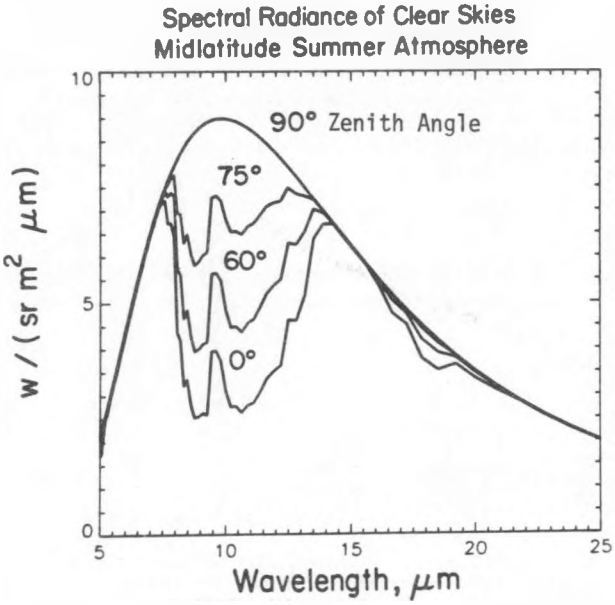

FIGURE 1

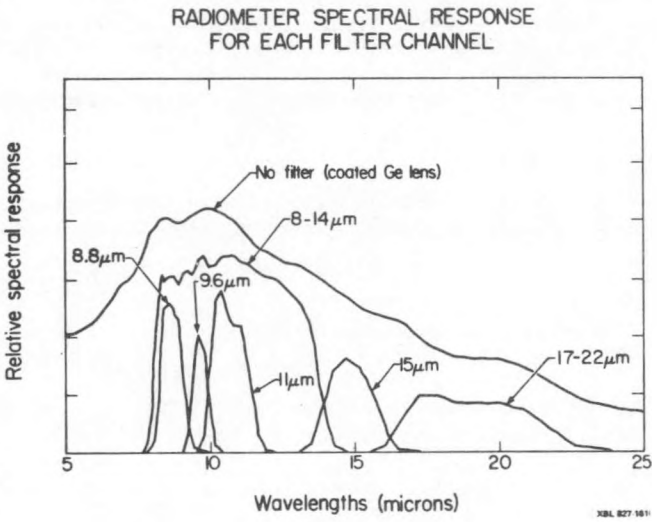

FIGURE 2

NOTATION: In all the subsequent graphs each letter symbol represents a full month of averaged data from one of the six U.S. cities at which radiometer measurements were taken. The key to interpreting these symbols is:

A = San Antonio, TX
B = Boulder City, NV
G = Gaithersburg, MD
L = St. Louis, MO
T = Tucson, AZ
W = West Palm Beach, FL

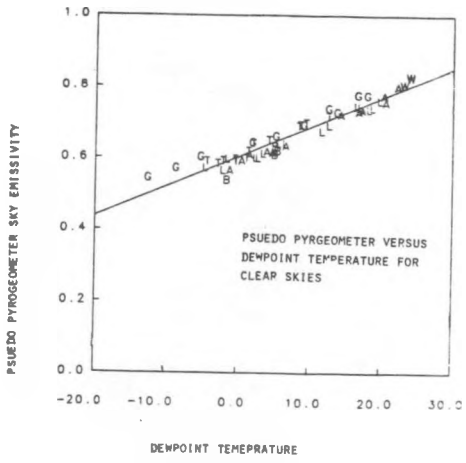

FIGURE 3

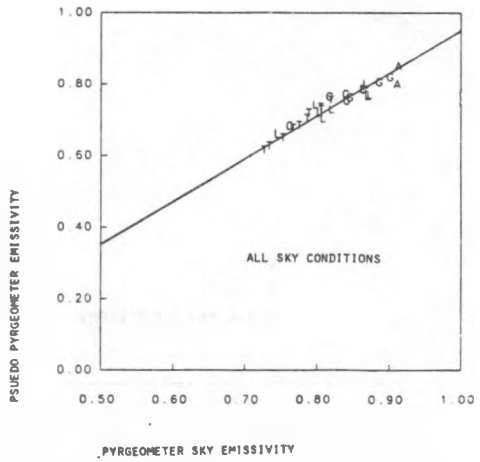

FIGURE 5

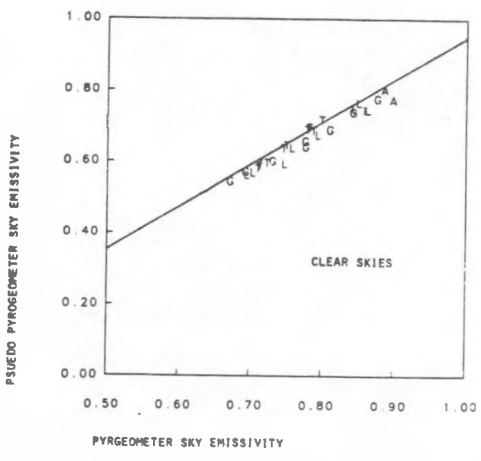

FIGURE 4

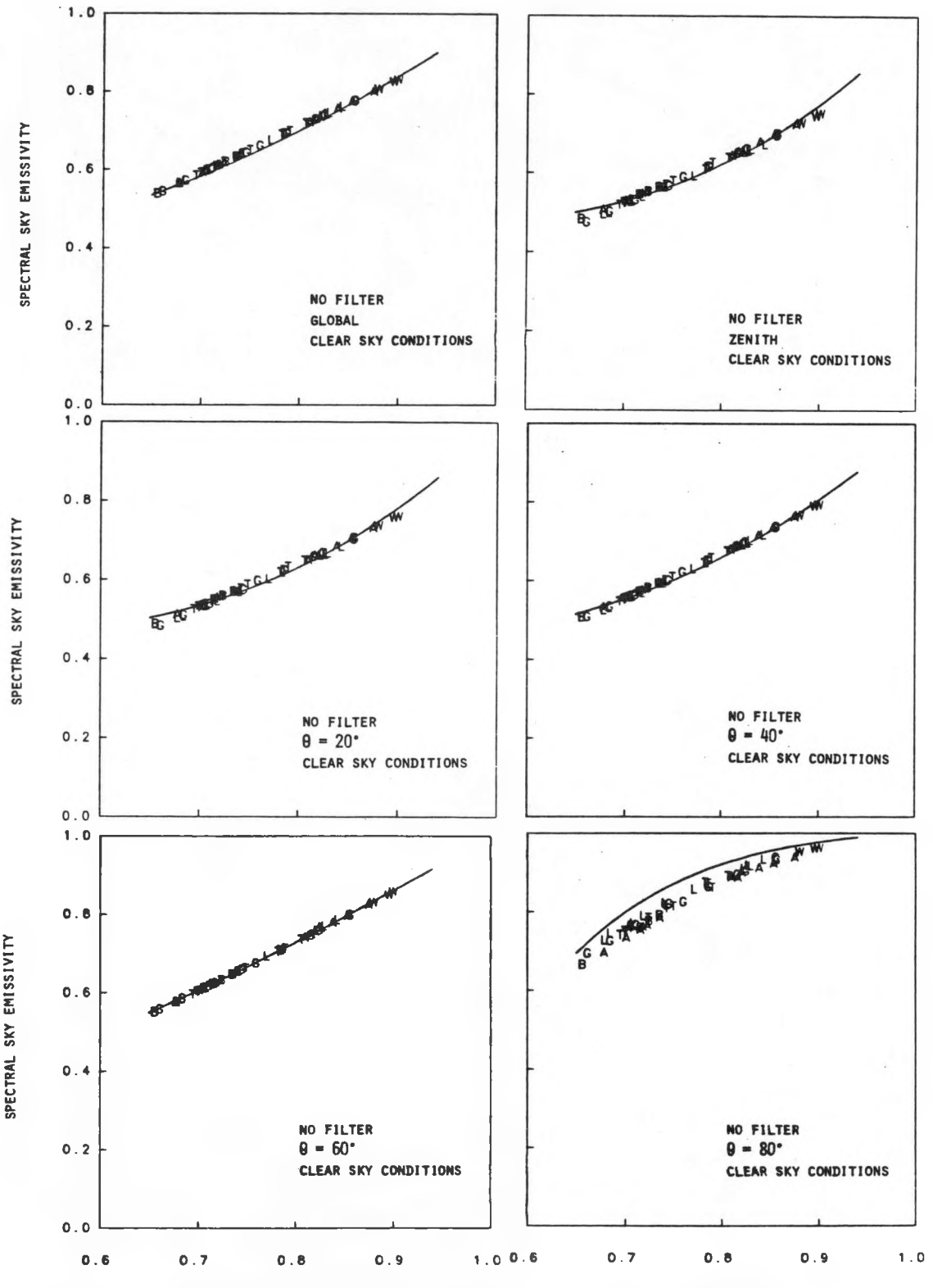

Figure 6

Solid curves are based on Eq. (11) and Table 2.

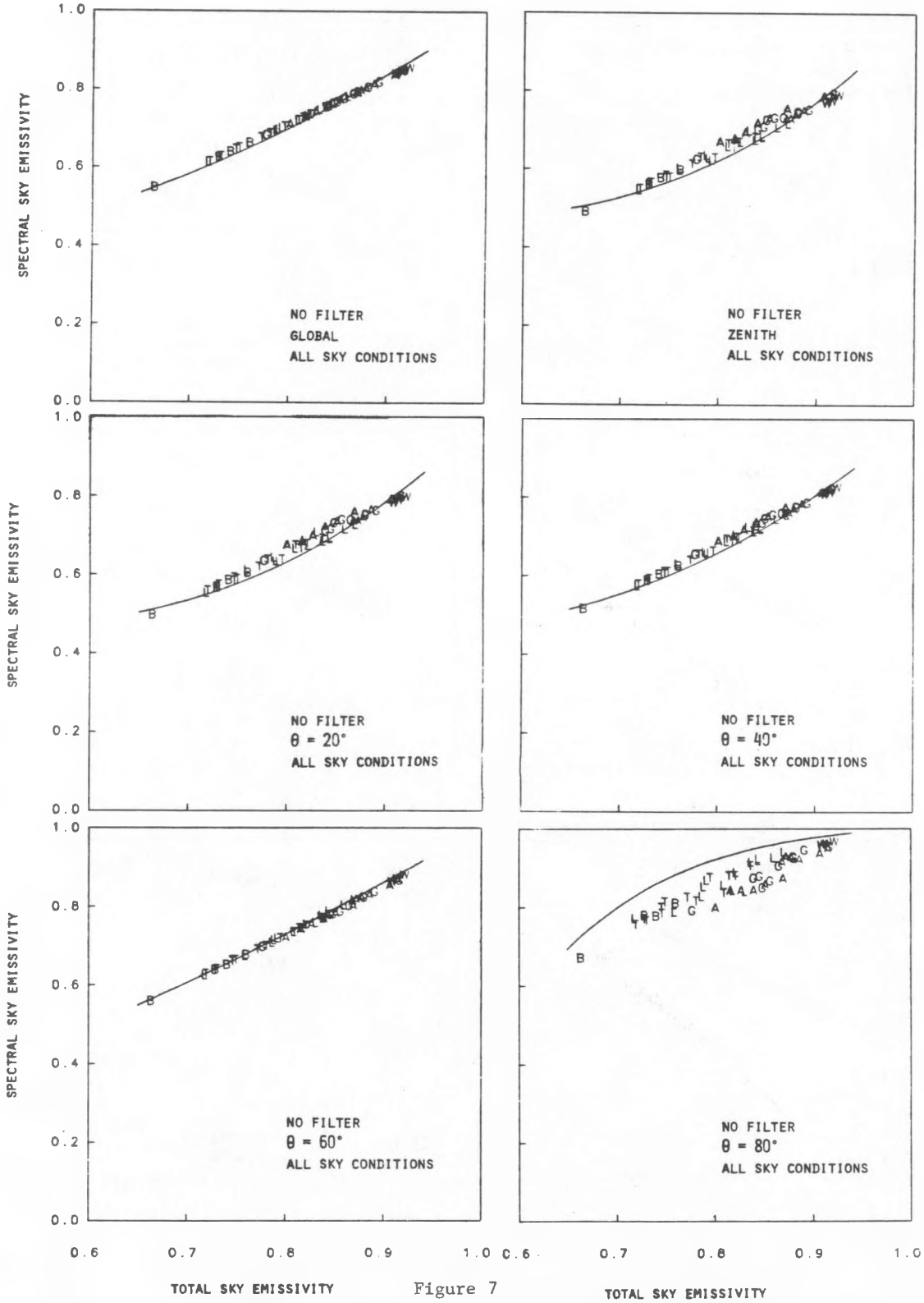

Figure 7

Solid curves are based on Eq. (11) and Table 2.

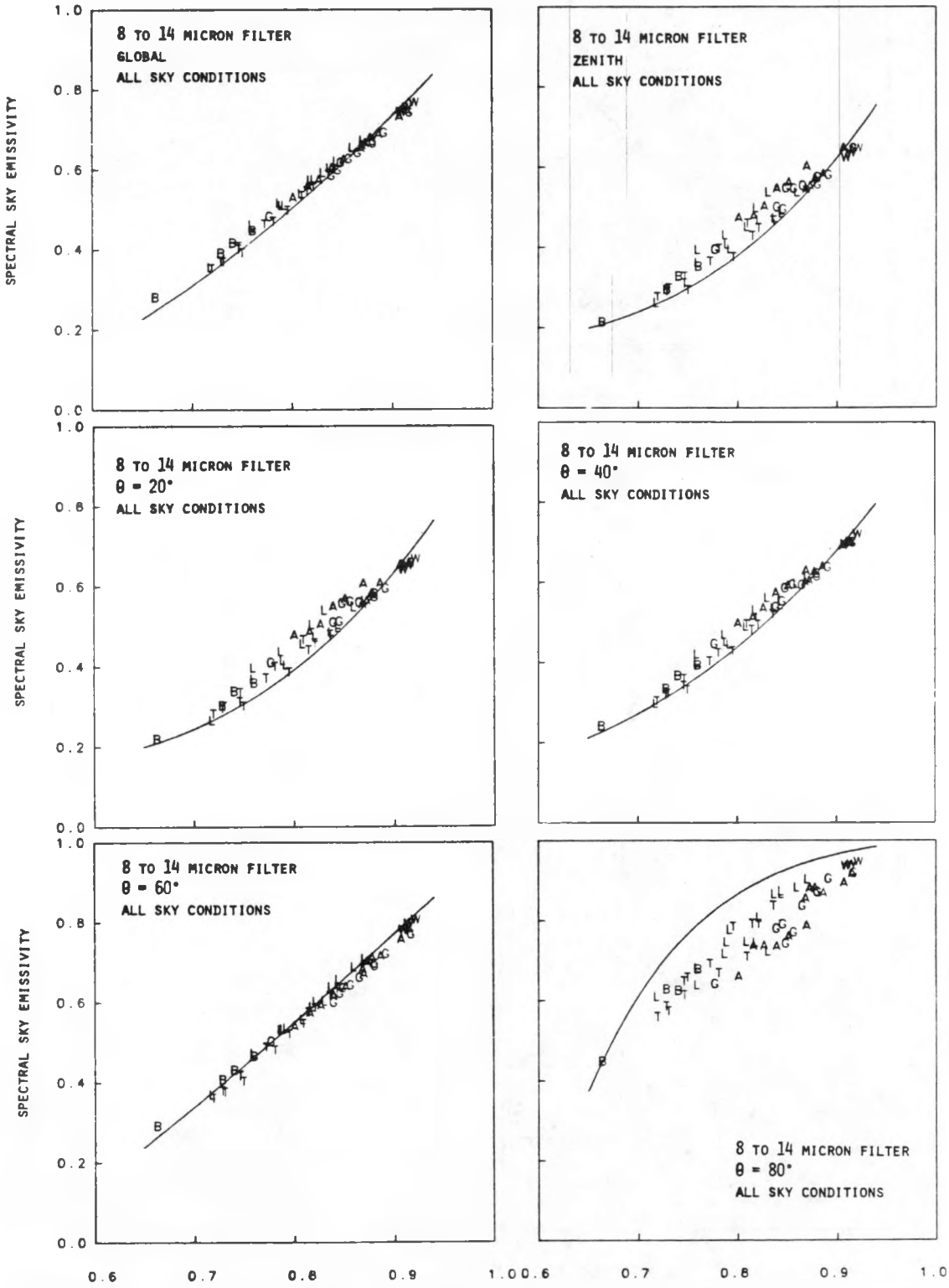

Figure 9
Solid curves are based on Eq. (11) and Table 2.

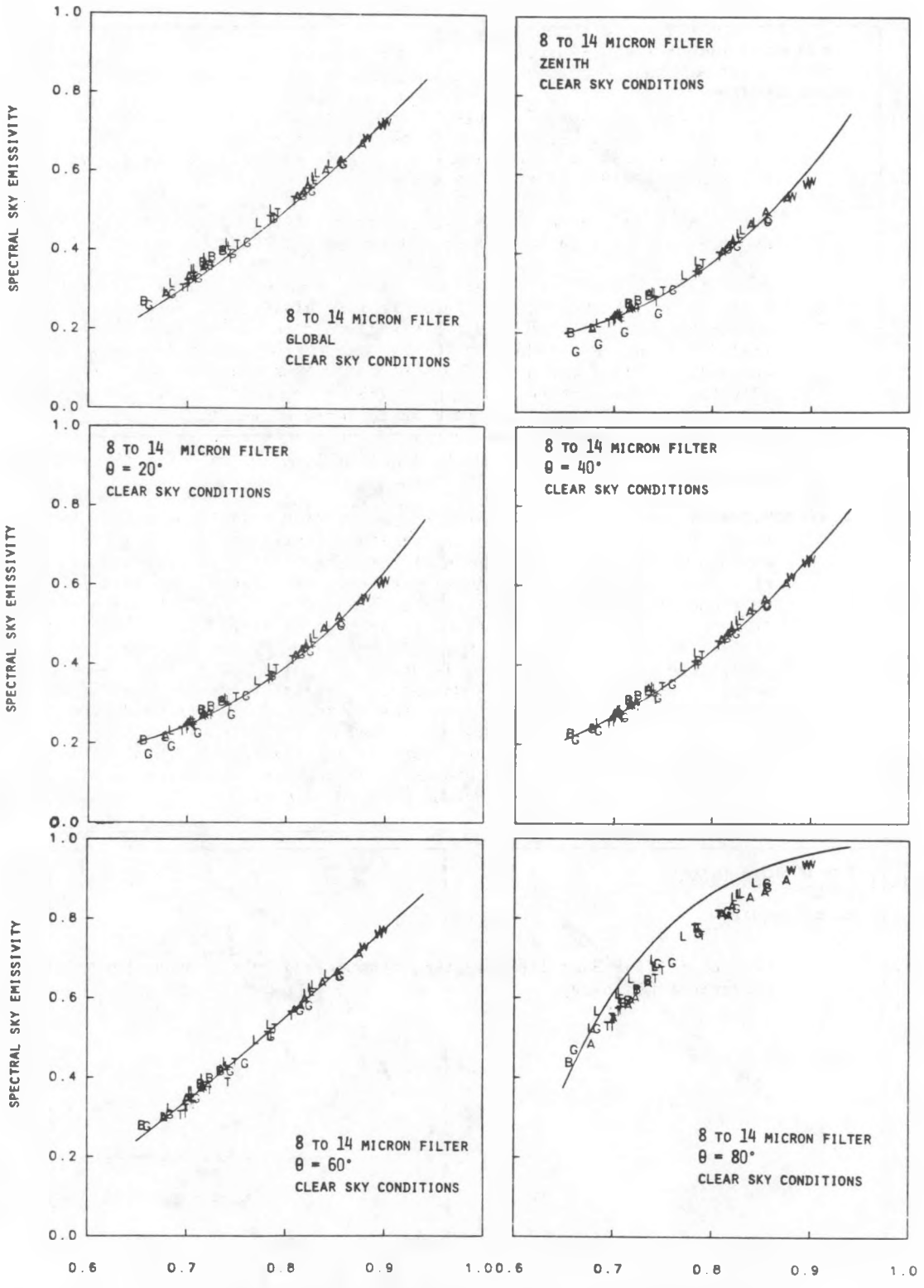

Figure 8
Solid curves are based on Eq.(11) and Table 2.

PROJECT SUMMARY

Project Title: Natural Convection in Buildings

Principal Investigator: Ronald C. Kammerud

Organization: Lawrence Berkeley Laboratory
University of California
Berkeley, California 94720

Project Goals: To develop techniques for calculating convective heat transfer rates in buildings. The calculation methods are to be based on experimental or analytic examinations (as appropriate) of convection processes in enclosures, and are intended for use by the energy analyst or building designer.

Project Status: The project is continuing; a status report will be presented for the ongoing work at Lawrence Berkeley Laboratory and at the Solar Energy Research Institute.

Convection is the least understood of the fundamental heat transfer processes which take place in buildings. Yet they play significant roles in passively heated or cooled structures. For example, the convection coefficient represents the thermal resistance at a window or other high thermal conductance portion of a building envelope; it is a key determinant of the thermal load of a building, and therefore affects passive system sizing. The convection coefficients also influence the effectiveness of thermal storage mass, again affecting sizing. Other convection processes of importance are zone coupling by natural convection, and natural ventilation and infiltration. The current focus of this project is quantifying surface convection coefficients.

Existing calculation techniques for convection coefficients are based on experiments which were not representative of typical building geometries. Recent experiments and analyses have given heat transfer rates substantially different from those the standard techniques predict. The present research project consists of development of a data base for heat transfer in enclosures representative of buildings, and from that data base, extraction of simplified correlations relating the convection coefficients to the enclosure geometry and surface temperature boundary conditions. The data base is obtained from a few detailed heat transfer experiments and a large number of numerical simulations of convection in situations not included in the experimental data base. Results to date have produced a relatively simple correlation applicable to a class of building situations wherein a room has cold and warm surfaces on opposite vertical walls. Comparisons of predictions using this correlation with standard calculation techniques clearly demonstrate the superiority of the present calculation technique.

Contract Number: DE-AC03-76SF00098

Contract Period: Continuing

Funding Level: $75,000

Funding Source: Office of Solar Heat Technologies, Passive and Hybrid Solar Energy Division, U.S. Department of Energy

CONVECTION COEFFICIENTS AT BUILDING SURFACES*

Ronald C. Kammerud, Emmanuel Altmayer, Fred Bauman,
and Ashok Gadgil
Passive Research and Development Group
Lawrence Berkeley Laboratory
University of California
Berkeley, California 94720

Mark Bohn
Solar Energy Research Institute
Golden, Colorado 80401

ABSTRACT

Correlations relating the rate of heat transfer from the surfaces of rooms to the enclosed air are being developed, based on empirical and analytic examinations of convection in enclosures. The correlations express the heat transfer rate in terms of boundary conditions relating to room geometry and surface temperatures. Work to date indicates that simple convection coefficient calculation techniques can be developed, which significantly improve accuracy of heat transfer predictions in comparison with the standard calculations recommended by ASHRAE.

INTRODUCTION

Among the fundamental heat transfer processes, convection is the least understood. In contrast to conduction and radiation, the equations governing convective heat and mass transfer in fluids, the Navier-Stokes equations, typically do not have closed solutions even under steady-state conditions. As a result, convection research has been largely limited to experimental work which is difficult to generalize.

The influence of convective heat transfer processes on the energy performance of buildings can be described in terms of three mechanisms: (1) coupling between room air and the surfaces to which it is exposed, (2) distribution of thermal energy within and between zones due to air circulation, and (3) coupling of the interior air to the external environment through ventilation or infiltration. These processes are all significant and are the subjects of ongoing research. The work summarized here consists of analyses and experiments under way at Lawrence Berkeley Laboratory and the Solar Energy Research Institute; it is directed at understanding the coupling between room air and the room surfaces. The objective is to develop simple, accurate, and highly generalized correlations for the surface convection coefficients in enclosures typical of rooms in buildings.

The LBL research consists in developing numerical analysis capabilities for convection in enclosures, and execution of small-scale laboratory experiments which produce data used to validate and guide the development of the analysis. The numerical analysis is then used to perform "numerical experiments," i.e., to produce a numerically-generated data base of heat transfer information from the surfaces of an enclosure for a variety of temperature and geometry boundary conditions. The LBL experimental research has concentrated on two-dimensional heat transfer in enclosures, which are long enough that the end walls have no effect on the internal convection process. The SERI research consists of small-scale laboratory experiments where the effect of the third dimension of the enclosure is explicitly examined. Heat transfer data and flow visualizations are produced in order to develop a detailed data base from which heat transfer correlations can be developed, and which can be used to validate the analysis.

The experimental effort is limited in the number of configurations that can be examined, but provides a frame of reference for the analysis and is the ultimate test for the analysis. The "numerical experiments," on the other hand, are far more rapidly performed than their physical counterparts. Assuming that carefully selected validation experiments are performed in conjunction with the analysis, the "numerical experiments" provide a larger amount of accurate data on velocity, fluid temperature, and heat transfer than the best experiments reported in the literature. The two research efforts are highly complementary; the experimental work provides depth to the research, while the analysis provides breadth.

---

*This work was supported by the Assistant Secretary for Conservation and Renewable Energy, Office of Solar Heat Technologies, Passive and Hybrid Solar Energy Division, of the U.S. Department of Energy under Contract No. DE-AC03-76SF00098 and EG-77-C-01-4042.

BACKGROUND

Heat transfer between the surfaces of a room and the enclosed air can be characterized in terms of a surface convection coefficient which describes the thermal conductance between the air and the surface. In comparison to the conductance of a normally insulated building envelope element, the convection coefficient is large and has little influence on the overall thermal resistance of the wall. At windows and other highly conductive envelope elements, however, the convection coefficient can represent a significant portion of the total resistance; uncertainty in the coefficient leads to potentially large errors in the calculation of conductive gains and losses, i.e., in the thermal load calculation [1]. For this reason, accurate values for the surface convection coefficients are necessary, for example, to properly determine the size of the passive heating or cooling system and the capacity of the mechanical system.

Heat transfer between room air and exposed surfaces is normally modeled using the convection coefficients documented by ASHRAE [2,3]. These coefficients are based on experimental research conducted 40 to 50 years ago [2,3 and references cited therein] using vertical free-standing flat-plate geometries rather than boundaries of enclosures which have configurations typical of buildings. As a result, the applicability of the reported convection coefficients to building heat transfer calculations is questionable. While these pioneering experiments appear to have been carefully conducted, the temperature dependence of the reported data (e.g., [4]) disagrees with more recent experimental results [5].

More recently there has been extensive research in natural convection in enclosures. Although much of this work has dealt with geometries atypical of rooms in buildings [6,7], there has also been renewed interest in convective heat transfer processes in buildings (see [1] for a recent bibliography). Though much of the recent research does not focus directly on the evaluation of convection coefficients, the research methodology and analysis tools are sufficiently well developed to reconsider past estimates of the importance of convective heat transfer processes in buildings. In one of the recent studies [1] by the present authors, it was shown that the convection coefficients typically used in building energy calculations [2] are in substantial disagreement with the coefficients calculated by existing numerical techniques. It was further shown that the dynamic variability of convection coefficients can lead to substantial errors in the calculation of thermal loads in buildings. Finally, for an example enclosure configuration, it was shown that the most commonly used convection coefficients (ASHRAE constants) are in disagreement by at least 50% with both the laminar and turbulent temperature dependent correlations also recommended by ASHRAE, and differed by about 80% from a preliminary correlation developed at LBL from experimental results (Table 1).

TABLE 1. Convection Coefficient Research Background

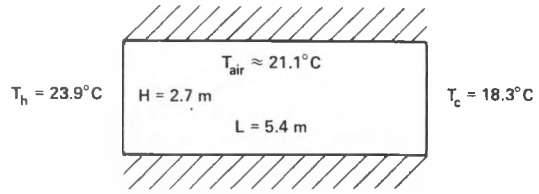

CALCULATION METHOD	HOT WALL, W/m²
ASHRAE - CONSTANT	23.3
- TURBULENT	14.0
- LAMINAR	10.8
EXPERIMENTAL CORRELATION	13.0

XBL 829-11607

The examples cited above clearly demonstrate the need for improved correlations for convection coefficients. Because of the complexity of the recirculating natural convection flow of room air, which is influenced by the temperature distribution on all the room surfaces, we do not expect that a single set of correlations can be obtained which will accurately predict the convection coefficients for all possible configurations of surface and air temperatures. The experimental and numerical simulation techniques used at LBL

and SERI to investigate convection coefficients are described in the following section.

TECHNICAL APPROACH

Experiment

The LBL and SERI natural convection experiments utilize apparatuses scaled down by factors of approximately ten and twenty, respectively, from typical rooms. The experiments utilize water as the working fluid in order to suppress radiative exchange within the enclosure and obtain Rayleigh numbers* typical of buildings under enclosure surface temperature boundary conditions that are not so far from ambient that significant heat losses occur from the apparatus. Because the Prandtl** number for air is significantly different from that for water at the temperatures of interest, these are not similitude experiments and the measured heat transfer rates at a given Rayleigh number are not identical to those obtained in a full-scale, air-filled enclosure. The measured heat transfer rates in the LBL experiment are approximately 10% higher than for the full-scale room [1]. For the data from the two experiments used to validate the numerical analysis, the lack of perfect similitude is not a serious disadvantage, because the analysis includes the Prandtl number as a variable. However, the experimental data itself cannot be applied directly to building situations without corrections. The magnitude of the correction is not well understood and will be examined in detail in the near future.

Both experiments allow measurement of enclosure surface temperatures, surface heat fluxes, and temperature distributions within the working fluid for a variety of surface temperature boundary conditions. Both experiments also allow flow visualizations, which are critical to the understanding of the characteristics of the convection process, in particular to determining the conditions under which turbulence sets in.

The LBL apparatus is 15.2 cm x 30.5 cm in vertical cross section with a plan depth of 83.8 cm. The depth was selected to ensure that the end walls would not affect the convection process in the central region of the enclosure; the measurements therefore correspond to two-dimensional convection processes. One vertical wall of the enclosure can be heated and the opposite wall is cooled; all other surfaces are heavily insulated and approximately adiabatic.

The SERI experiment [8] is cubical with edge dimensions of 30.5 cm. The geometry was intentionally selected to investigate the effects of the third dimension of the enclosure on the heat transfer rates from individual surfaces. Furthermore, the apparatus allows the temperature of four of the six surfaces of the enclosure to be controlled so that the effect of the third dimension in real enclosures or rooms can be thoroughly explored for the cubical geometry. This is a largely unexplored area that will require considerable research before the understanding of convection in buildings is placed on equal footing with radiation and conduction.

Numerical Analysis

Computer programs which solve the full Navier-Stokes equations of motion for air flow in buildings have been developed [9-11]. These programs are based on the finite difference method in which the physical volume of interest is divided into a large number of subvolumes, and time is divided into discrete steps. The time-dependent differential equations are then integrated over the finite number of subvolumes and over each time step to obtain a large number of simultaneous algebraic equations, which are solved by matrix inversion. Solutions are obtained for a large number of successive time steps until steady-state flow fields are obtained. The program methodology is described in detail in [11].

The program developed at LBL [11] is suitable for modeling both natural and forced convection in two and three dimensions, for internal and external flows. In addition, the program can model obstacles (internal partitions, furniture), heat sources and sinks (space heating and cooling), and velocity sources and sinks (fans, windows). The program can, in principle, simulate both laminar and turbulent flow. The laminar flow calculations have been verified against analysis and detailed experiments performed at LBL and elsewhere [12-14]. The turbulence modeling capability has recently been added and is presently undergoing testing. This capability is particularly appropriate for the study of wind and fan-driven ventilation and other forced convection phenomena.

In order to use this program, it is necessary to define the problem by specifying the geometric configuration, thermal and velocity boundary conditions, and fluid properties. For example, to obtain the solution of natural convection of air driven by different wall temperatures in a room, one must specify the room geometry, the temperatures of all room surfaces, and the thermophysical properties of air. The air velocity

---

*$Ra = GrPr = g\beta \cdot \Delta T H^3 Pr/\nu^2$, where Gr = Grashof number, g = acceleration due to gravity, β = coefficient of thermal expansion, ΔT = characteristic temperature difference, H = height of enclosure, Pr = Prandtl number, and ν = kinematic viscosity.

**Prandtl number: $Pr = \nu/\alpha$, where ν = kinematic viscosity and α = thermal diffusivity.

(or its derivatives) must also be specified on all bounding surfaces of the enclosure, such as at obstacles and internal surfaces where the velocity is zero, and at fan outlets where it is specified by the fan parameters. The computer simulation predicts the velocities and temperatures throughout the volume of interest and also predicts convective heat fluxes on all the surfaces, allowing the calculation of the heat transfer coefficients as a function of position on all the surfaces of the room.

CORRELATION METHODOLOGY

The goal of this activity is to develop technically sound and usable expressions for the convection coefficient or heat flux at each interior surface of an enclosure. There is not a known functional form for the convection coefficients or even assurances that an appropriate expression can be developed. Hence this method consists of (1) generation of a heat transfer data base from physical and numerical experiments and (2) analysis of the data base to extract functional dependencies of the surface heat fluxes on the variables which are expected to influence them. This approach assumes that the sensitivity of the heat flux to all important variables has been examined; if not, the correlation will not be generally applicable.

It is known that the convective heat flux at any given surface in an enclosure will depend on the temperature of that surface and temperature of the air adjacent to the surface:

$$q_i = h_i (T_i - T_{adj}) \qquad (1)$$

where h_i, q_i, and T_i are the convection coefficient, heat flux, and temperature, respectively, for surface i, and T_{adj} is the adjacent air temperature. The adjacent air temperature will in turn depend somehow on the temperatures of all surfaces in the enclosure and on the enclosure geometry and on internal heat sources or sinks; these variables determine the velocity and temperature distributions throughout the volume, in particular the air temperature adjacent to the surface in question. The correlation problem is therefore equivalent to developing a method for calculating T_{adj}. In most building energy calculations, the adjacent air temperature is assumed to be the mean room air temperature.

The experimental portions of the heat transfer data base developed at LBL and SERI during the past year include two configurations; this is insufficient to allow extraction of the geometric sensitivity of the convection coefficient. The correlations from the experiments therefore explore the sensitivity of the heat flux (typically expressed by the Nusselt number*) to the magnitude of the characteristic temperature difference in the enclosure (typically expressed by the Rayleigh number). Caution must be used when applying these correlations to other geometries. It is noted that the geometry variable is the most difficult to access experimentally, since it requires several experimental apparatuses or a highly reconfigurable model.

In order to supplement the experimental data base, the numerical analysis computer program has been used to perform sensitivity studies, especially in regard to geometric sensitivity. This portion of the heat transfer data base includes explicit dependence on the areas of subsurfaces for a particular two-dimensional enclosure. The data base has been analyzed to determine the sensitivity of the heat flux at the enclosure surfaces to both geometry and surface temperatures.

The parametric sensitivity studies were conducted for a two-dimensional room with a height of 2.44 m and a length of 3.66 m, and each of its four major surfaces have been divided into three subsurfaces (described in detail in [15]). The room is shown schematically in Fig. 1; the individual subsurfaces are identified numerically in this figure. The enclosure volume was discretized with an unevenly spaced 20 x 30 grid with a high density of grid lines near the surfaces for good resolution of the boundary layers.

For the first boundary condition configuration selected, the hottest and coldest surfaces are located on opposite vertical walls. Nine simulations were performed to study natural convection under the different temperature boundary conditions displayed in Table 2. The results from these nine simulations have been used to develop simplified correlations for convection coefficients for this particular configuration, as described in detail in reference [16] and briefly summarized here.

It was found that subsurfaces 1, 2, 7, and 8 contribute, in most cases, a very large portion of the total heat transfer into or out of the room air, typically on the order of 90%. The data interpretation has focused on these four subsurfaces, which have been labeled "active" subsurfaces. Successful development of correlations for predicting the heat transfer from the active subsurfaces would account for about 90% of the total heat transfer for this particular configuration. The remaining subsurfaces, which together contribute only about 10% of the total heat transfer between the bounding surfaces on the enclosed air, have not been considered in developing correlations; they have been labeled "inactive" subsurfaces.

When the convection coefficients for the various subsurfaces were calculated with reference to the mean

---

*Nusselt number: $Nu = q \cdot H / \Delta T \cdot k$, where q = surface heat flux, H = height of enclosure, ΔT = characteristic temperature difference, and k = thermal conductivity.

TABLE 2. Parametric Run Description

Run #	T_2		T_8	
	(°C)	(°F)	(°C)	(°F)
1	-6.67	20	21.11	70
2	-6.67	20	29.45	85
3	-6.67	20	37.78	100
4	4.45	40	21.11	70
5	4.45	40	29.45	85
6	4.45	40	37.78	100
7	15.56	60	21.11	70
8	15.56	60	29.45	85
9	15.56	60	37.78	100

For all runs: $T_1 = T_3 = T_4 = T_5 = T_6 = T_7 = T_8 = T_{10} = T_{11} = T_{12} = 20°C$ (68°F)

FIG. 1

PARAMETRIC STUDY

ENCLOSURE DESCRIPTION

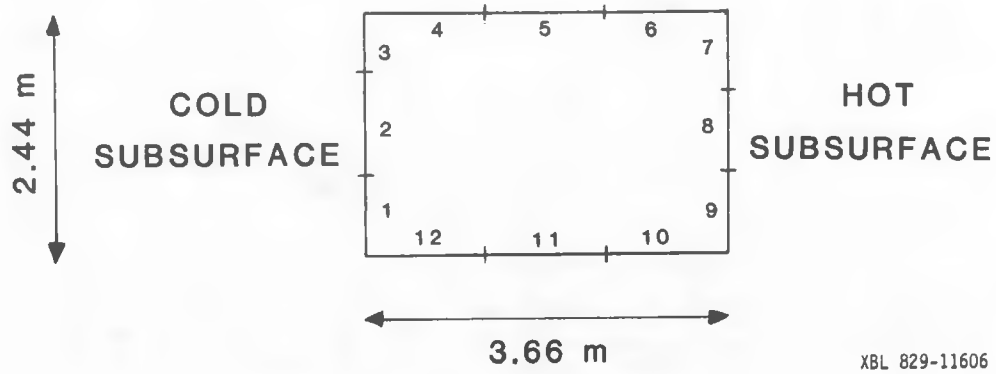

air temperature in the enclosure, large variations were observed, particularly for subsurfaces other than 2 and 8. Even for these two subsurfaces the convection coefficients vary by nearly 50-60%. This variability results from the fact that the temperature of air immediately adjacent to a subsurface (T_{adj}) is often quite different from the mean room air temperature. The convection coefficients calculated with reference to the mean air temperature lacked an observable pattern, and would therefore be difficult to predict using a simple equation. Furthermore, convection coefficients calculated with reference to the mean air temperature can have nonphysical negative values. For example, the updraft of warm air leaving subsurface 8 will deposit heat into the cooler subsurface 7 in spite of the fact that the mean room air temperature is less than the temperature of subsurface 7.

When the convection coefficients were calculated with reference to the adjacent air temperature predicted by the numerical analysis, far more consistent results were obtained. For this reason the correlation efforts focused on attempts to obtain an expression for calculating T_i, the air temperature adjacent to subsurface i. The first attempt at obtaining such an expression is described below.

The analysis determined that the adjacent air temperature for all of the active subsurfaces could be calculated from

$$T_i' = K_1\left(T_H \frac{A_H}{A}\right) + K_2\left(T_C \frac{A_C}{A}\right) + K_3\left(T_I \frac{A_I}{A}\right) + K_4 T_H + K_5 T_C \quad (2)$$

where K_1, K_2, K_3, K_4, and K_5 are constants, T and A are subsurface temperatures and areas, and subscripts H, C, and I refer to the hot, cold, and inactive subsurfaces, respectively. The values of the constants were determined by examining the individual dependence of the calculated adjacent temperature on each of the terms in the above equation. The preliminary results are shown in Table 3.

TABLE 3. Correlation Constants

Subsurface Number	K_1	K_2	K_3	K_4	K_5
2	1.49	1.38	0.89	0	0
8	1.49	1.38	0.89	0	0
1	0.76	0.70	0.45	0	0.49
7	0.76	0.70	0.45	0.49	0

The convective heat flux (q_i') for each active subsurface can be calculated from

$$q_i' = 2.42\ (T_i' - T_i) \quad . \quad (3)*$$

RESULTS

Experiment

Data from the LBL experiments have been published elsewhere [12,17] and are not repeated here. Portions of the data have been used to validate the convection analysis computer program [12].

The more recent SERI results [8] have included both flow visualizations and heat transfer measurements for Rayleigh numbers between 0.3×10^{10} and 6.0×10^{10}. Flow visualizations have revealed the persistence of a relatively inactive central region of the enclosure for four combinations of heated and cooled vertical walls (the horizontal walls are adiabatic), which is qualitatively similar to the observations made in previous two-dimensional enclosure experiments. Fluid temperature measurements indicated that linear stratification profiles extended through the core region with deviations from linearity near the upper and lower surfaces where hot (top) or cold (bottom) fluid flowed in boundary layer type flows between the hot and cold vertical surfaces. These horizontal boundary layers dominate the heat transfer mechanisms between the temperature controlled surfaces; the core region plays only a small role at the Rayleigh numbers and boundary conditions explored to date. Finally, the beginnings of transition to turbulence in the boundary layers were observed at a Ra number of 3.6×10^{10}. These observations, too, are very consistent with those made previously for two-dimensional flow.

The heat transfer data from the SERI experiment has been analyzed and a correlation developed. Regression analysis of several hundred data points, representing all four hot and cold wall combinations, yielded an expression:

$$Nu = 0.620(Ra)^{0.250} \quad (4)\#$$

for Rayleigh numbers between 0.3×10^{10} and 6.0×10^{10} for a water filled enclosure. Experimental, numerical, and analytic results from various researchers for two-dimensional enclosure flows are compared with this correlation in Fig. 2. For comparison purposes, all the Nu values in Fig. 2 are based on the hot-to-cold wall temperature difference. Considering the differences between the SERI three-dimensional experiment and previous two-dimensional experiments, there is excellent agreement among the data. This is one extremely important result in that it lends credibility to the applicability of the past two-dimensional experiments and analyses to three-dimensional situations, but it is emphasized that considerably more three-dimensional work is necessary in order to fully understand this relationship.

---

*2.42 (W/m^2-°C) represents the heat flow weighted average of the convection coefficients on subsurfaces 2 and 8, calculated using the temperature difference between the mean room air and the subsurface for the nine simulations shown in Table 2.

#Nu in Eq. (4) is based on the difference between the bulk fluid temperature and the surface temperature.

FIG. 2

COMPILATION OF TWO-DIMENSIONAL HIGH RAYLEIGH NUMBER DATA AND COMPARISON WITH PRESENT RESULTS

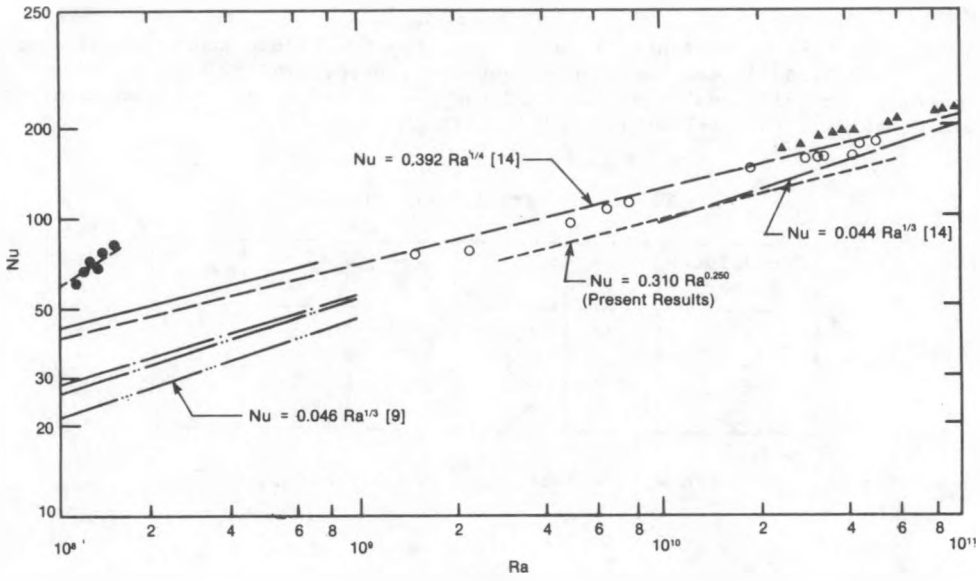

(This figure taken in its entirety from [8], including reference numbers in the figure and the key.)

KEY

- Raithby laminar b. l. theory [14], A=.5, Pr=3.5
- Raithby turbulent b. l. theory [14], A=.5, Pr=3.5
- Gadgil numerical analysis [26], A=1, Pr=.7
- Gadgil numerical analysis [21], A=.2, Pr=1
- Gadgil numerical analysis [21], A=.1, Pr=1
- MacGregor and Emery [9]
- ○ Bauman, et al. [18], A=1, Pr=.7
- ▲ Nansteel and Greif [25], A=.5, Pr=3.5
- ● Burnay, et al. [18], A=1, Pr=.7

Analysis

The heat flux predictions for all four "active" subsurfaces calculated from Eq. (3) are compared against the results of the numerical simulations in Fig. 3. The solid 45° line represents the line of perfect agreement between the two calculation techniques. Calculations based on the present correlation are seen from this figure to compare well with the numerical predictions of the convection program for all four "active" subsurfaces. The points plotted on Fig. 3 have a root mean square deviation from the 45° line of only 2.5 W/m^2. The relative errors in heat flux predictions are observed to be large only in cases when the temperature differences between "inactive" and "active" subsurfaces are small.

Two methods* of calculating convective heat flux recommended by ASHRAE are compared with the numerically obtained results, in Figs. 4 and 5. Both methods relate the convection coefficient to ΔT_{as}, the difference in the mean enclosure air temperature and surface temperature. The convective heat fluxes in Fig. 4 are calculated using the ASHRAE constant convection coefficients according to the following equation:

$$q_{A1} = h \cdot \Delta T_{as} \qquad (5)$$

where h = 3.08 (W/m^2-°C) for vertical surfaces

*The ASHRAE constant convection coefficient for a vertical surface is derived from Table 1, page 23.12, 1981 Handbook of Fundamentals, by subtracting out the radiative component of the total surface heat transfer coefficient. The radiative component is based on a 5.6°C (10°F) surface-to-surroundings temperature difference, which is not always typical for real buildings. In addition, it is extremely surprising to notice that the constant convection coefficient is representative of a 13°C (23°F) surface-to-air temperature difference in order to be consistent with the ASHRAE temperature dependent convection coefficient for turbulent flow. The ASHRAE temperature dependent convection coefficient for turbulent flow is recommended for use with large plates (typical for buildings) and is taken from Table 5, page 2.12, 1981 Handbook of Fundamentals.

FIG. 3

LBL HEAT FLUX CORRELATION

Comparison with Numerical Calculations

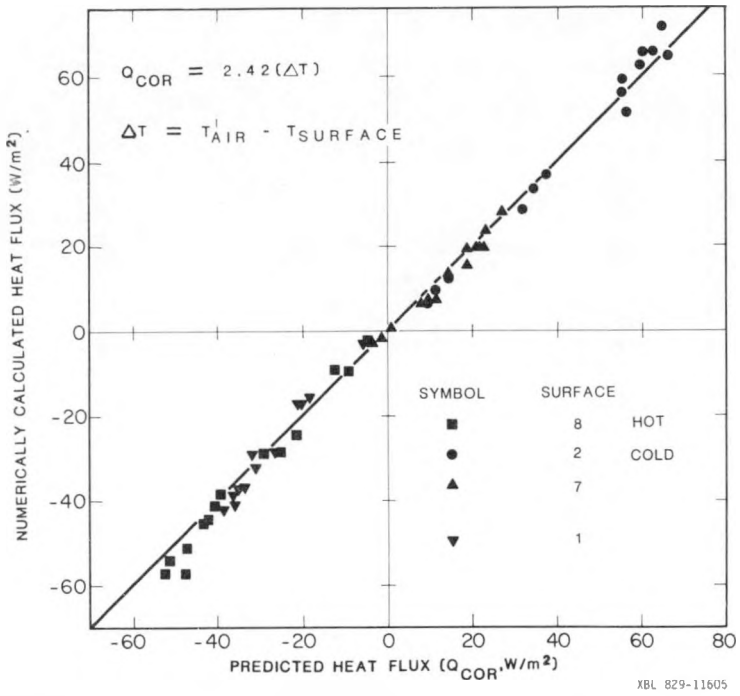

= 4.04 (W/m^2-^oC) for horizontal surfaces with heat flow upwards

= 0.95 (W/m^2-^oC) for horizontal surfaces with heat flow downwards.

The convective heat fluxes in Fig. 5 are calculated using the ASHRAE correlations for turbulent convection coefficients according to the following equation:

$$q_{A2} = h \cdot \Delta T_{as}$$

where $h = (1.31)(\Delta T_{as})^{0.33}$ for vertical surfaces

$= (1.52)(\Delta T_{as})^{0.33}$ for horizontal surfaces with heat flow upwards.

For horizontal surfaces with heat flow downwards, no expression for h is given for turbulent convection. The laminar correlation given by ASHRAE is used herein:

$$h = 0.51 \frac{\Delta T_{as}}{L}^{0.25}$$

where L is the characteristic length of the surface. Both of the ASHRAE correlations roughly approximate the heat flow to the room air from the cold and hot subsurfaces, 2 and 8, and have large errors for the other two active subsurfaces, 1 and 7. The ASHRAE correlations, in fact, often predict the wrong direction of heat flow for subsurface 7. The root mean square (RMS) deviations of the points in Figs. 4 and 5, from the 45° line are 13.3 W/m^2 and 15.8 W/m^2 respectively. These numbers are of the same order of magnitude as the heat fluxes on most subsurfaces. By comparing Figs. 3, 4 and 5, it is clear that the predictions from Eq. (3) show substantially better agreement than do the ASHRAE calculations.

For one of the nine numerical analyses the net imbalance in total convective flux from all surfaces has been calculated for each of the two ASHRAE recommendations for the correlations. Using Eq. (3), an imbalance of approximately 2% was observed. The two ASHRAE methods produced imbalances of -11% and +50% for the constant and temperature-dependent coefficients, respectively.

FIG. 4

ASHRAE CONSTANT COEFFICIENT CORRELATION
COMPARISON WITH NUMERICAL CALCULATIONS

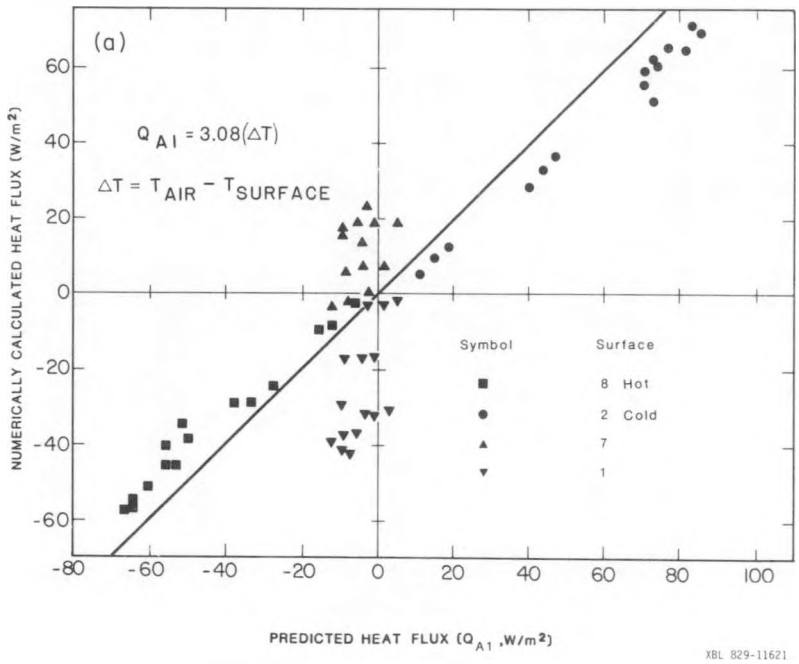

XBL 829-11621

FIG. 5

ASHRAE TURBULENT CORRELATION
COMPARISON WITH NUMERICAL CALCULATIONS

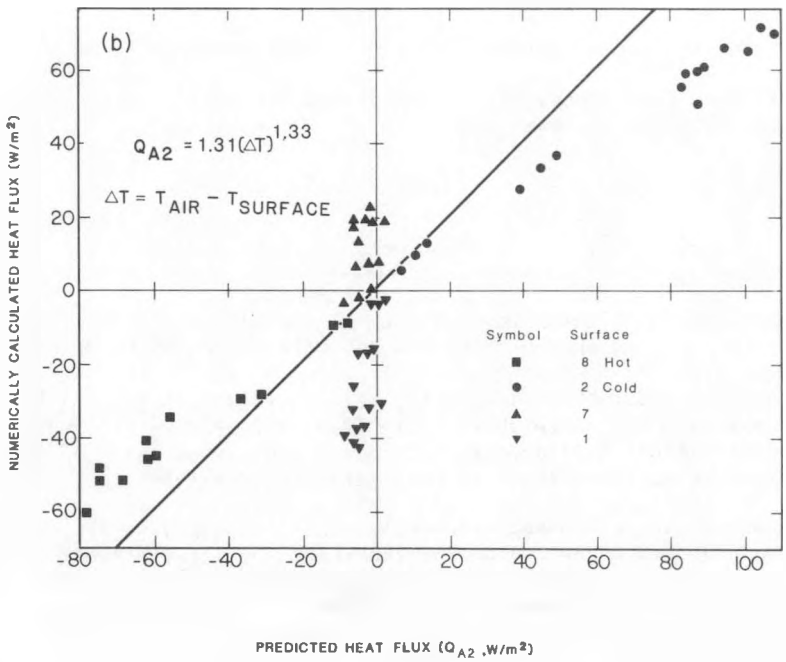

XBL 828 – 1085A

CORRELATION SENSITIVITY

A number of additional simulations have been performed in order to test the generality of the correlation by examining its ability to properly predict convection coefficients for configurations other than those on which it is based. For each sensitivity configuration the "active" subsurface heat fluxes were recalculated using the correlations and then compared with the results computed by the convection program. The parameters varied in the sensitivity studies were:

- Area of hot subsurface, A_8.
- Area of cold subsurface, A_2.
- Temperature of "inactive" subsurfaces, T_I.

If the accuracy of the correlation is strongly affected by any of the above parameters, then caution must be exercised in extrapolating the present correlations to parameter values beyond the range of this study. Results from each of these sensitivity studies are presented below.

Figure 6 presents "active" subsurface heat fluxes for three different areas of the hot subsurface. The hot subsurface area was varied from 41% (1.01 m^2) of the total vertical wall area to 100% (2.44 m^2) of the total vertical wall area. The area and location of the hot subsurface for each sensitivity run is shown in the accompanying diagrams. Despite the wide range of hot subsurface areas, the results of the present correlation all agree quite well with the numerical predictions of the convection program. The root mean square (RMS) error for the correlation results shown in Fig. 6 was calculated to be only 2.30 (W/m^2).

FIG. 6

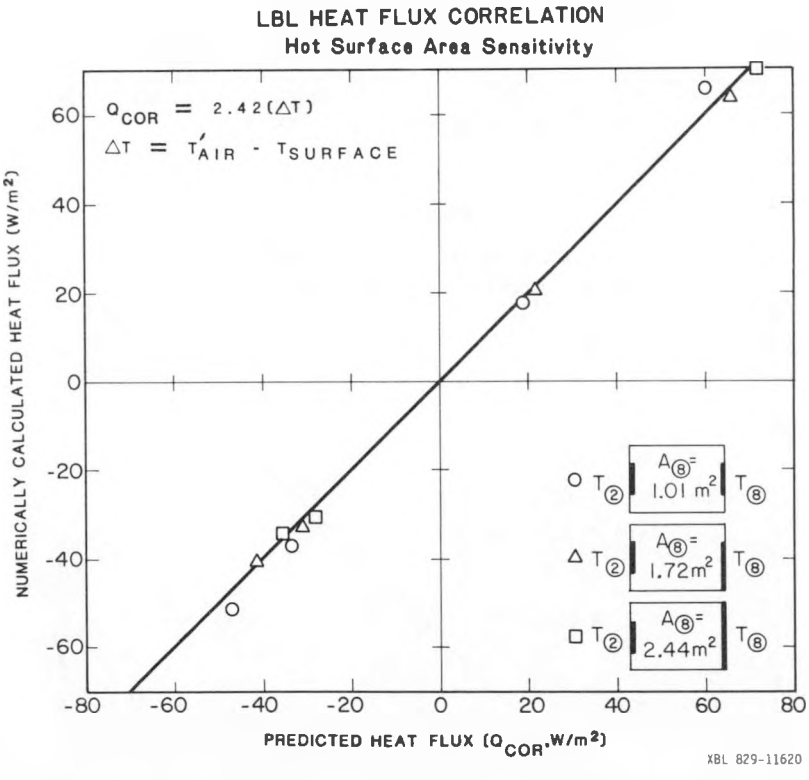

Figure 7 presents "active" subsurface heat fluxes for three different areas of the cold subsurface, shown in the accompanying diagrams. For these sensitivity runs, the area of the cold subsurface was varied from 52% (1.26 m^2) of the total vertical wall area to 100% (2.44 m^2) of the total vertical wall area. Again the correlation results are reasonably insensitive to this parameter with the RMS error being 3.22 (W/m^2).

In Figure 8 the results are shown for three different values of "inactive" surface temperatures: the reference value of 20°C, and plus and minus 2.8°C from the reference value (22.8°C and 17.2°C). The accuracy of the present correlations over this range of "inactive" surface temperatures is seen to be of the same order as the other sensitivity runs, with the RMS error being 3.82 W/m^2. Part of this insensitivity may be due to the small magnitude of the "inactive" subsurface temperature variations (5.6°C) relative to the maximum temperature difference in the room (44.4°C).

The results for all three of the above sensitivity runs indicate that the present correlations can

FIG. 7

LBL HEAT FLUX CORRELATION
Cold Surface Area Sensitivity

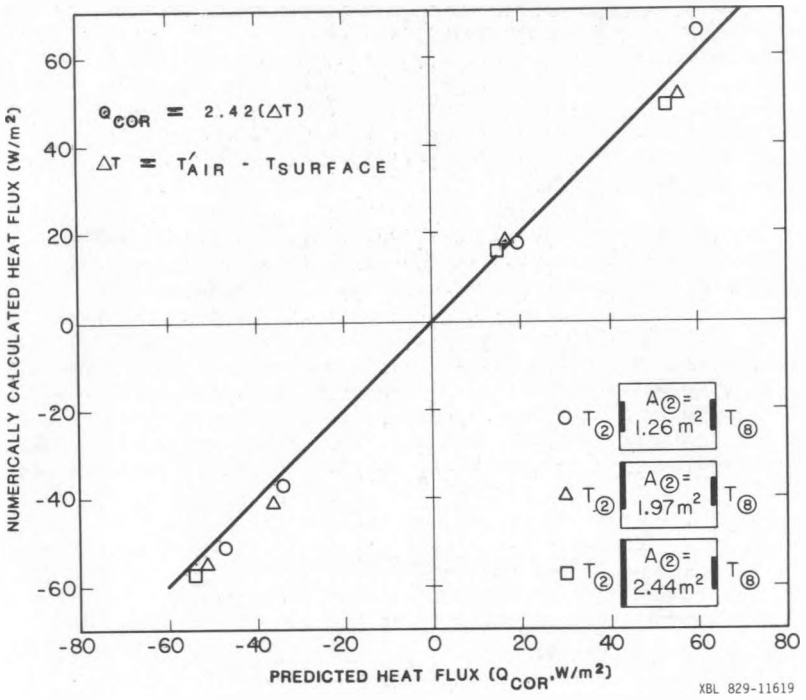

FIG. 8

LBL HEAT FLUX CORRELATION
Inactive Surface Temperature Sensitivity

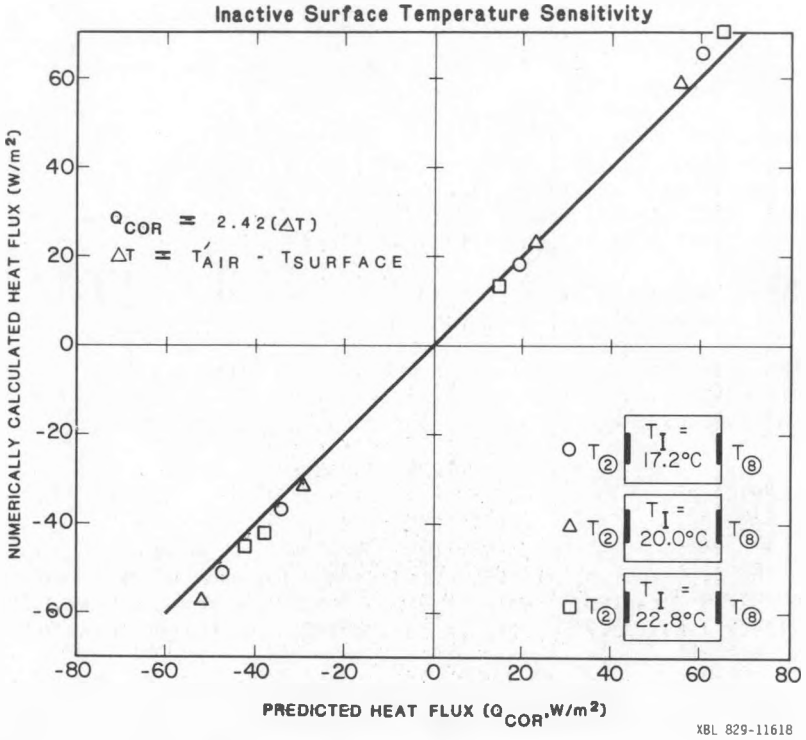

provide the same level of accuracy (10–15%) over a wider range of configurations than the particular one for which the correlation was originally developed. Future sensitivity analyses will concentrate on other parameters and configurations.

CONCLUSIONS

Convection coefficient correlations have been obtained by analyzing results from numerical simulations of the natural convection process in an enclosure described by a two-dimensional configuration with the hottest and coldest surfaces on opposite vertical walls. The correlations allow prediction of the dominant convective heat fluxes in configurations approximating the one that has been analyzed. The correlations presented apply for a variety of subsurface temperatures and areas. The correlations are a significant improvement over the standard techniques for calculating convective heat fluxes from room surfaces for this particular configuration. Of course, the validity of the present correlations is limited to the particular configuration for which the numerical simulations were performed. However, the methodology presented in this report is quite general and can be applied to other configurations of hot and cold surface positions, as well as to three-dimensional situations. The correlations obtained for other configurations may not be identical in form to those presented here.

An area needing careful consideration in the future is the prescription for identifying a given real situation with the single most appropriate configuration from the complete set of configurations for which correlations will be published. It is evident that in each and every case, one may not be able to identify one hottest and one coldest subsurface; all the subsurfaces may have temperatures close to one another. In this case, all the different applicable correlations will predict similar results. In other words, the correlations, if properly formulated, should (and must) give predictions that continuously and smoothly vary over all the possible variations of subsurface temperatures, even as one ranges from one configuration to another.

The numerical analysis technique used in this study has been compared with experimentally obtained flow patterns, temperature fields, and heat flows at the walls for enclosure geometries similar to the one considered in this report. These comparisons have shown agreement usually within a few percent, giving one confidence in using the computer program as a fast device for performing "numerical experiments" for a variety of conditions within the domain of this configuration. It would be desirable, in proceeding to obtain correlations for significantly different configurations, to reconfirm the validity of the computer program in each case, using experimental data for that configuration.

Several cautions are in order relating to the use of the preliminary correlation reported here. In particular, it should be pointed out that experimental evidence exists showing steady, laminar flow in enclosures for the present configuration, even at the high Ra number values that we have considered. However, almost all the experiments in this regard have used fluids in the Pr range of 2.5 and higher. Since it is known that the Ra number for the onset of turbulence is decreased for lower Pr number fluids (Pr of air at room temperature is 0.71), the assumption of steady laminar flow needs to be carefully examined experimentally. Similarly, the Ra number for the onset of turbulence is influenced by the configuration (i.e., the temperature distribution on the subsurfaces), and this again needs careful experimentation. The computer program is unable to determine the Ra number for the onset of turbulence, and this information must be experimentally obtained for each configuration.

The importance of the three dimensionality of the flow must be determined. This effect is known to exist, but has not been sufficiently studied and quantified in the literature to assert that the present correlations, obtained from two-dimensional simulations, are satisfactory approximations to the three-dimensional conditions that almost always exist in real buildings. Experimental results obtained to date imply that the two-dimensional results are valid in that the primary features of the convection process in enclosures at Rayleigh numbers of interest herein are consistent between two and three dimensions. This similarity persists for (1) the inactivity of the core region, (2) dominance of boundary layer flow in the heat transfer process, and (3) transition to turbulence.

The results presented in this report indicate that the problem of predicting convective heat transfer in rooms using simple correlations is not a hopeless task. The success achieved for the one case considered is encouraging, and leads one to expect that a similar approach will yield successful predictions in other cases as well.

REFERENCES

1. F. Bauman, A. Gadgil, and R. Kammerud, with E. Altmayer and M. Nansteel, "Convective Heat Transfer in Buildings: Recent Research Results," submitted for presentation at the ASHRAE Society Meeting in Atlantic City, N.J., 23-27 January 1983. Lawrence Berkeley Laboratory Report LBL-13883, to be published.

2. Handbook of Fundamentals, American Society of Heating, Refrigerating, and Air Conditioning Engineers, New York, 1981.

3. M. Lokmanhekim, ed., Procedure for Determining Heating and Cooling Loads for Computerized Energy Calculations, ASHRAE, New York, 1976.

4. G.B. Wilkes and C.M.F. Peterson, "Radiation and Convection from Surfaces in Various Positions," ASHVE Trans. 44, 513 (1938).

5. J.P. Holman, Heat Transfer, McGraw-Hill, 1976, p. 255.

6. S. Ostrach, "Natural Convection in Enclosures," in Advances in Heat Transfer, 8, 1972.

7. I. Catton, "Natural Convection in Enclosures," in Proceedings, Sixth Int. Heat Transfer Conference, Toronto (1978).

8. M.S. Bohn, D.A. Olson, and A.T. Kirkpatrick, "Natural Convection in a Cubical Enclosure," submitted for presentation at the ASME-JSME Thermal Engineering Joint Conference, March 20-24, 1983, Honolulu.

9. N.C. Markatos and M.R. Malin, "Mathematical Modeling of Buoyancy-Induced Smoke Flow in Enclosures," Int. J. Heat & Mass Transf. 25(1), 63-75 (1982).

10. A.D. Gosman, P.V. Nielsen, A. Restivo, and J.H. Whitelaw, "The Flow Properties of Rooms with Small Ventilation Openings," Trans. ASME, J. Fluids Engrg. 102, 316-323 (Sept. 1980).

11. A. Gadgil, "On Convective Heat Transfer in Building Energy Analysis," Ph.D. Thesis, Department of Physics, UC Berkeley (1979). Lawrence Berkeley Laboratory Report LBL-10900 (1980).

12. F. Bauman, A. Gadgil, R. Kammerud, and R. Greif, "Buoyancy Driven Convection in Rectangular Enclosures: Experimental Results and Numerical Calculations," ASME Paper No. 80-HT-66, presented at the 19th National Heat Transfer Conference, 27-30 July 1980, Orlando, Florida. Lawrence Berkeley Laboratory Report LBL-10257 (1980).

13. G. Shiralkar, A. Gadgil, and C.L. Tien, "High Rayleigh Number Convection in Shallow Enclosures with Different End Temperatures," Int. J. Heat & Mass Transf. 24(10), 1621-1629 (1981).

14. J. Tichy and A. Gadgil, "High Rayleigh Number Laminar Convection in Low Aspect Ratio Enclosures with Adiabatic Horizontal Walls and Differentially Heated Vertical Walls," Trans. ASME, J. Heat Transfer, 104, 103-110 (1982).

15. A. Gadgil, F. Bauman, and R. Kammerud, "Natural Convection in Passive Solar Buildings: Experiments, Analysis and Results," Passive Solar Journal, 1(1), (1982). Lawrence Berkeley Laboratory Report LBL-9297.

16. E. Altmayer, A. Gadgil, F. Bauman, and R. Kammerud, "Correlations for Convective Heat Transfer from Room Surfaces," Lawrence Berkeley Laboratory Report LBL-14893, to be published.

17. M. Nansteel and R. Greif, "Natural Convection in Undivided and Partially Divided Rectangular Enclosures," Trans. ASME, J. Heat Transf. 103, 623-629 (Nov. 1981).

PROJECT SUMMARY

Project Title: Total Energy Analysis of Daylit Commercial Buildings

Principal Investigators: Wayne Place and Ron Kammerud

Organization: Lawrence Berkeley Laboratory
University of California
Berkeley, California 94720

Project Goals: To characterize the heating, cooling , and lighting energy behavior of prototypical commercial buildings outfitted with solar apertures and electric controls which reduce power to the lights in response to the presence of sunlight in the occupied space. This information will allow the cost-benefit optimization of various features of the solar apertures and the electric lighting controls.

Project Status: An experimental facility has been established for gathering illumination data from scale models in a form which is useful as an input to the building energy analysis computer program BLAST. Both internal and external illumination and radiation data are taken with photometers and pyronometers. The capability exists to scan fifty sensors five times, calculate a mean and standard deviation for each sensor, and flag defective data, within a fraction of a second. This allows the accumulation of large amounts of highly reliable data for a wide range of conditions. Experimentally derived illumination algorithms have been used as input to BLAST which is used to determine the lighting electricity reductions and heating and cooling impacts of various alterations of the solar aperture, the electric lighting system, and other features of the building. To date, efforts have been focused on a single-story prototypical office building fitted with south-facing, tilted roof monitors. Future studies will deal with different orientations of glazing, multi-story structures, and other building types.

Contract Number: DE-AC03-76SF00098

Contract Period: March 1977 to present

Funding Level: $185,000 for FY 1982

Funding Source: Office of Solar Heat Technologies, Passive and Hybrid Solar Energy Division, U. S. Department of Energy

DAYLIGHT STRATEGIES*

Wayne Place, Marc Fontoynont, Craig Conner, Ron Kammerud,
Brandt Andersson, Fred Bauman, William Carroll, T.C. Howard,
Atila Mertol, and Tom Webster#
Passive Research and Development Group
Lawrence Berkeley Laboratory
University of California
Berkeley, California 94720

ABSTRACT

An investigation has been made of potential lighting electricity reductions and associated thermal impacts of replacing electric light with sunlight admitted through rooftop glazing on a single-story, prototypical office building. Experimental scale models have been used to determine the fraction of the solar radiation entering the aperture which reaches the work plane as useful illumination. This information is used in a developmental version of the building energy analysis computer program BLAST-3.0$ to predict reductions in lighting electricity and the impacts on energy consumption for heating and cooling the building. It is found in general that the lighting electricity reductions are more significant than the heating and cooling impacts in a properly designed system. In an improperly designed daylighting system, where reduction of lighting electricity is the only design criterion, deleterious thermal impacts can negate the lighting electricity benefits. The design implications of the results are discussed and future directions for the work are outlined.

INTRODUCTION

Providing illumination in buildings using sunlight as a substitute for electric light is attractive for several reasons:

- The amount of energy used for lighting is significant; lighting accounts for about one quarter of the total primary energy use in the existing American commercial building stock [1] and the fraction is closer to one-half for office buildings constructed with current practice thermal envelope integrity and HVAC efficiency [2].
- The solar illumination resource is substantial; during most working hours, the solar illumination incident on a building is several times greater than that required to illuminate the building interior, indicating that it should be possible to design solar apertures that provide enough illumination to offset most of the lighting electricity consumption.
- The luminous efficacy of natural light is generally higher than that of commercially available electric lamps, which means that sunlight has the potential for reducing cooling loads by replacing electric light of higher heat content.
- Reductions in site electricity (for both cooling and lighting) result in substantially larger savings in primary energy, owing to utility generating inefficiencies and network losses.
- Sunlight is plentiful during the hot, clear summer periods when many utilities experience their peak demand, suggesting that there is potential for reducing demand for both cooling and lighting electricity, with consequent demand charge savings for the building owners and the potential for reduced capacity requirements for the utility.
- Well designed daylighting systems can be aesthetically pleasing to building occupants, thereby increasing the value of the building.

---

*This work was supported by the Assistant Secretary for Conservation and Renewable Energy, Office of Solar Heat Technologies, Passive and Hybrid Solar Energy Division, of the U.S. Department of Energy under Contract No. DE-AC03-76SF00098.

#The authors express their appreciation to Michael Wahlig, Stephen Selkowitz, Frederick Winkelmann, and Francis Rubenstein for serving as technical advisors and to Carolyn Mangeng for the energy cost calculations.

$BLAST (Building Loads Analysis and System Thermodynamics) is trademarked by the Construction Engineering Research Laboratory, U.S. Department of the Army, Champaign, Illinois.

PROBLEM APPROACH

The purpose of this study is to make a preliminary assessment of the maximum potential for reducing energy consumption in a commercial building using simple daylighting apertures constructed with current technology. Although daylight can be admitted through any aperture in the building, achieving the most efficient and effective interior illumination with sunlight requires care in the placement and design of the illumination glazing. To achieve the maximum potential energy savings without reducing illumination effectiveness, the following requirements must be satisfied:

(1) The illumination aperture should be oriented to collect sunlight effectively throughout the diurnal and seasonal cycles. In general, an attempt should be made to maximize the solar intensity on the illumination glazing, in order to minimize the required area of glazing, thereby minimizing both the capital cost of the glazing and the deleterious thermal effects of conductive gains and losses through the building envelope.

(2) The sunlight admitted through the apertures must be delivered to the task surface in an efficient and effective manner. In the case of the office building under study, this means delivering as much of the admitted sunlight as possible, as uniformly as possible, to the plane of the desk tops.

(3) The room must be free of glare which diminishes the effectiveness of the illumination system.

Glazing Orientation

Figures 1 and 2 illustrate the effect of glazing orientation relative to the sun. Figure 1 shows the light transmitted by double-pane glass in Atlanta during the month of June, while Fig. 2 shows the corresponding data for the month of December. Each of the squares contains data for a particular azimuthal orientation and tilt of the window, which can be identified from the legend in the figure. The square at the center of the array corresponds to horizontal glazing. The eight outer squares correspond to vertical glazings facing in the four cardinal directions (north, east, south, and west--with north at the upper center) and the four intermediate directions (northeast, southeast, southwest, and northwest--with northeast at the upper right). The eight squares surrounding the center square have the same azimuthal orientations as the corresponding outer squares, but are tilted 60 degrees up from horizontal. For each square, the vertical axis indicates transmitted light in units of 1000 lumens/square meter (KLux). The hours of the day are listed along the horizontal axis, with midday in the middle. The width of each black area indicates the frequency of occurrence of the particular level of transmitted light for the hour and month in question. Hours during which the light transmission is essentially zero have not been indicated. Two continuous lines are drawn through the data: the dashed lower line indicates the average beam sunlight transmitted during the hour indicated and the solid upper line represents the average total sunlight (beam plus diffuse) transmitted during the hour indicated. Typical Meteorological Year (TMY)* weather tapes were used in preparing these statistical summaries. In converting radiation data on the TMY tapes to sunlight data for the graphics of Figs. 1 and 2, the following constant luminous efficacies were assumed: 105 lumens/watt for beam radiation and 120 lumens/watt for diffuse radiation. Diffuse radiation and diffuse sunlight were both assumed to be uniformly distributed over the sky vault. Ground reflected radiation was not included in the graphic summary. Double-pane, clear glazing without shading was assumed.

The December data (Fig. 2) indicates that low levels of transmitted daylight make the following orientations seem unpromising: vertical glazing facing northwest, north, or northeast and tilted glazing facing northwest, north, or northeast. Also, low levels of transmitted light during parts of the work day limit the attractiveness of the following orientations: vertical glazing facing west or east and tilted glazing facing west or east. However, combinations of vertical glazings facing west and east and tilted glazings facing west and east look attractive because the potentially high uniformity of collection throughout the day. The approach of using multiple glazing orientations to collect solar illumination is in marked contrast to most conventional solar thermal systems. For solar thermal systems with diurnal storage, the collection surface should be oriented in the single direction which provides the maximum day-long collection. In contrast, the daylighting system should have highly uniform day-long collection, particularly during the cooling season, since there is no storage; periods of low collection fail to provide the needed illumination and periods of high collection can aggravate the building cooling loads. For the daylighting system, some sacrifice in total light collection and building envelop thermal resistance can be justified for the sake of greater uniformity of light collection. A comparison of June and December data indicates that substantially more sun is collected during the summer than during the winter for the following glazing orientations: vertical facing west, tilted facing west, horizontal, tilted facing east, and vertical facing east. The thermal disadvantages of collecting more solar radiation during the summer than during the winter diminish the attractiveness of these orientations and combinations of these orientations. Tilted glazing facing southwest or southeast is also limited by poor light collection during parts of the day. However, combinations of these two orientations look extremely attractive, because of the transmitted sunlight for each orientation is highly uniform throughout the year (with slightly higher transmission during the winter) and because the combination of orientations has the potential for highly uniform collection throughout the day.

*"Typical Meteorological Year User's Manual: Hourly Solar Radiation - Surface Meteorological Observations," TD-9734, National Climatic Center, April, 1981.

Vertical glazing facing southeast, south, or southwest tends to collect inefficiently during the summer time. Of the glazing orientations shown, the best single orientation from a point of view of high transmitted light levels and low seasonal variation is tilted south-facing. The major disadvantage of tilted, south-facing glazing is the large diurnal variation in the transmitted light. In order to simplify the current study, this single orientation was chosen for investigation. Future studies will examine promising combinations of orientations which together reduce the diurnal variations.

Light Distribution within the Building

The use of south-facing glazing tilted 60 degrees up from the horizontal satisfies requirement (1), that the aperture be oriented to effectively collect sunlight. Both requirements (2) and (3) can be addressed by careful selection of:

- the aperture position relative to the occupied space;
- the configuration and surface treatment of materials around the aperture; and
- the properties of the glazing material.

The importance of avoiding glare cannot be overestimated. There are actually situations where admitting sunlight can increase the electric lighting illumination levels required to achieve a satisfactory luminous environment. Such an effect is likely to be created in any situation where beam sunlight is allowed to slash through the work plane, thereby creating extreme contrast in the immediate field of view of the person engaged in the primary work task. A common response to this kind of glare is to close any drapes that are available or to turn up the lights in order to even out the illumination and reduce the contrast. In fact, with beam sunlight on the work plane, the level of electric lighting necessary to reduce the contrast to acceptable levels may be much higher than the level required to produce an acceptable illumination intensity in a situation where the high contrast does not exist. Because of the glare, it is difficult to quantify the illumination benefit of unfiltered, direct-beam sunlight incident on the work plane. For the tilted, south-facing aperture under consideration, the use of diffusing glazing or reflective surfaces is essential in order to prevent the penetration of beam sunlight to the work plane. For simplicity, diffusing illumination glazing is assumed in this study.

In order to avoid discomfort glare in the prototype building under study, a clear distinction has been drawn between view glazing and illumination glazing. View glazing is by definition something through which the building occupants are expected to look. In order to avoid visual discomfort, it is desirable that light admitted by the view glazing not be very intense. If the view glazing is bright enough to provide illumination, then there is a significant likelihood it will cause discomfort when viewed. Another problem with trying to use view glazing for illumination purposes is the fact that view glazing is normally set low in the wall where the light admitted through the glazing impinges on most parts of the work plane at an unfavorably low angle. Finally, view glazing must be optically clear, which means that beam sunlight admitted through the view glazing can cause glare. By contrast, an illumination aperture should admit intense light in order to maximize the illumination benefits per area of glazing, should disperse light to avoid high contrast in the space, and should provide light from a sufficient height that reasonably intense and uniform illumination can be achieved on most of the work plane.

Requirements (2) and (3) can be satisfied in a single-story building (or on the top floor of a multistory building) by:

- using highly diffusing, closely spaced, illumination apertures in the roof, thereby producing uniform illumination on the work plane and minimizing visual discomfort by keeping the light sources above the normal field of view of the building occupants (see Fig. 3);
- using reflective view glazing in the walls, thereby eliminating a bright source in the field of view of the occupants;
- using light-colored interior surfaces, thereby increasing the amount of light reaching the work plane from the apertures and reducing contrasts between the light sources and opaque surfaces within the space.

This roof aperture system has light quality equal to the electric lighting system which it is replacing, so that all the design criteria which apply to the electric lighting system (e.g., required intensity and uniformity of light in the work plane) are equally applicable to the daylighting system. Consequently, there are no qualitative deficiencies of the daylighting system which would require that we discount its quantitative illumination contribution when making comparisons to the electric lighting system.

This paper presents BLAST predictions of the lighting electricity reductions and heating and cooling energy impacts of daylighting in a single-story office building designed according to the rules outlined above. Future papers will deal with the energy implications of daylighting schemes in multistory buildings

BUILDING DESCRIPTION

The floor plan of the building chosen for analysis is shown in Fig. 4. For simulation purposes, the square, 10,000 ft^2 building is divided into five thermal zones: four perimeter zones and one larger core zone. The 12-ft high external walls contain 15% transmittance, double-pane, view glazing 3.5 ft high, extending the full length of each wall. A more complete description of the building's thermal envelope, internal loads, operating schedules, and HVAC system can be found in Ref. [2].

The daylighting system consists of roof monitors fitted with south-facing, double-pane glass tilted 60 degrees up from the horizontal and extending the full width of the building. Figure 3 shows the roof aperture configuration, the roof structural elements, and the arrangement of ducts and electric light fixtures. The illumination glazing consists of two panes of .25-inch thick glass with a combined normal solar transmissivity of 0.624. The inner glass pane is assumed to be an excellent diffuser. Simulations were performed for a range of aperture ratios from 1.25% to 10.0%. (Aperture ratio is defined here as the ratio of the total illumination glazing area to the total building floor area.) Both experiments and analysis have been used to estimate the appropriate spacing between roof monitors for achieving satisfactory uniformity of the illumination on the work plane. A future report will describe the experimental model and present the illumination measurements.

The electric lighting system consists of standard, cool-white, fluorescent lamps in diffusing luminaires mounted at ceiling level between the roof monitors. The Illumination Engineering Society (IES) room cavity calculation [3] was used to determine the number and spacing of lamps and fixtures required to supply the design illumination level of 50 footcandles on the work plane. From this calculation, a power level of about 2.5 W/ft^2 for the lights was deduced. (Future studies will examine the impact of a more efficient electric lighting system on the energy savings potential of the daylighting system.) The lighting hardware and the daily 12-hour operating schedule were chosen to be representative of current practice rather than the current state of the art. Controls are provided to adjust the electric lighting power level in response to the presence of sunlight, thereby expending no more electric power than necessary to maintain 500 lux on the work plane.

ANALYTIC METHOD

For each hour and thermal zone, BLAST-3.0 calculates: thermal exchanges between the environment and external surfaces of the building; solar radiation absorbed on external surfaces; conductive gains and losses through opaque elements of the building structure (using response factors to account for mass effects); radiant exchanges between interior surfaces; convective exchanges between the zone air and the associated interior surfaces; radiant heat transferred to interior surfaces from internal heat sources (lights, equipment, and people); convective heat transferred to the zone air from internal heat sources; and solar gains through all glazing. These calculations are based on detailed descriptions of the building elements and weather contained on TMY weather tapes.

In the BLAST daylighting simulation, it is assumed that:

(1) Power to the electric lights is reduced linearly in response to the usable amount of sunlight entering the illumination glazing each hour.

(2) Electric lighting illumination on the work plane is directly proportional to the power supplied to the electric lights.

(3) Power to the lights is adjusted to maintain the combined illumination (solar plus electric) at a constant level of fifty footcandles on the work plane (unless constrained by assumption (4) below).

(4) Power to the lights cannot be reduced below 20% of full power. (This assumption is based on current limitations of the technology for continuous control of fluorescent bulbs. Further power reductions could be achieved by combinations of continuous controllers and on-off switches, but that topic is not treated in this paper.)

Each hour BLAST keeps track of the lighting electricity savings associated with reductions in power to the lights. At the same time, BLAST also accounts for the heating and cooling impacts of solar gains and conductive losses associated with the illumination glazing and reduced lamp heat output. To perform a BLAST daylighting analysis, the user must specify the following two parameters of the daylighting and electric lighting systems:

(1) The luminous efficacy of the radiation: a ratio of light content to energy content. The BLAST simulations described in this paper assume the luminous efficacy of both beam and diffuse sunlight transmitted through the illumination glazing to be 100 lumens/watt. The luminous efficacy of light from the cool white fluorescent lamps was assumed to be 62 lumens/watt [3].

The fraction of the radiation from the emitting surface which reaches the workplane, expressed as a dimensionless quantity called the coefficient of utilization (CU). Based on both small-scale experiments and analytic information, a CU of 0.72 was selected for the light emitted from the interior surface of the illumination glazing. (These experimental and analytical results will be presented in a future paper.) The CU for light emitted from the surface of the fluorescent bulbs is 0.61 [3]. In

this case, the predominant reason for the superior CU of the solar system is that much of the light emitted by the interior surface of the illumination glazing can go directly to the work plane; this is in contrast to the electric lighting system which has a cover plate on the luminaire.

Using the luminous efficacies of sunlight and electric light and the coefficients of utilization for the daylighting and the electric lighting systems, BLAST calculates the reduction in electric lighting power as a function of the solar power admitted through the illumination glazing.

RESULTS

A number of annual and design day BLAST simulations of the prototype building were performed with TMY weather data from New York, Atlanta, and Los Angeles. The results from some of these simulations are presented below. Figure 5 shows the hourly variations in lighting requirements in Atlanta on July 10th for two design conditions: one clear day (maximum normal beam = 877 W/m^2, maximum horizontal diffuse = 118 W/m^2) and one overcast day (maximum normal beam = 15 W/m^2, maximum horizontal diffuse = 120 W/m^2). An aperture ratio of 2.5% was used for both simulations. The plots indicate that the illumination apertures work much better near midday than in the morning and afternoon--a result of diurnal variations of solar radiation direction and intensity, reinforced by the directional selectivity of the illumination glazing. The diurnal variation in the direction of beam sunlight could be addressed by using glazing of more than one aperture orientation.

The annual energy consumption for lighting electricity (at the site) is plotted in Fig. 6 as a function of the aperture ratio. (The consumption of primary energy by the utility to generate power would be on the order of three to four times higher than the consumption at the site, owing to generating inefficiencies and utility network losses.) For small aperture ratios (0 to 2.5%), the electric consumption goes down rapidly with each additional increment of aperture area. At larger aperture ratios (above 2.5%), the electric consumption goes down less rapidly with each additional increment of aperture area, indicating the diminishing number of hours during which additional sunlight can have a beneficial impact. The curve approaches asymptotically toward a lower limit which is imposed by the 20% lower limit on electric lighting power and by the daily 12-hour lighting schedule, which includes many hours when there is little or no sunlight available. The reductions in lighting electricity were greater in Atlanta than New York, because the lower latitude of Atlanta results in more availability of sunlight, particularly during the winter months when short days and cloudy conditions seriously limit the effectiveness of daylighting in New York. The greatest reductions in lighting electricity were observed in Los Angeles, which has almost exactly the same latitude as Atlanta, but clearer weather.

The annual energy consumption for cooling electricity at the site (fans plus DX cooling unit) is plotted vs. aperture ratio in Fig. 7. For small aperture ratios, cooling electricity consumption decreases with increasing aperture ratio for all three locations. At small aperture ratios all of the admitted sunlight is effective in displacing electric light of higher heat content, thereby reducing cooling loads. For larger aperture ratios, the excess solar gains outweigh the cooling benefits associated with the higher luminous efficacy of the sunlight, and the cooling loads increase with increasing aperture ratio.

The annual energy consumption in boiler fuel is plotted versus aperture ratio in Fig. 8. For small aperture ratios, boiler fuel consumption increases with increasing aperture ratio, resulting from the replacement of electric light with sunlight of lower heat content. This apparently negative effect is of little consequence, since the effect is small and boiler fuel is a much cheaper and more efficient source of heat than dissipating electric power in lamps. For large aperture ratios, the excess solar gains dominate the effect of the sunlight's higher luminous efficacy, and the boiler fuel consumption decreases with increasing aperture ratio. In all three locations, and at large aperture areas, boiler fuel consumption is less sensitive than cooling electricity consumption to the aperture ratio, since the net heat gain through the glazing is lower during the winter. Figures 6, 7, and 8 suggest that movable insulation could produce significant reductions in energy consumption for lighting and cooling, and some reductions in energy consumption for heating, if the insulation were controlled (1) to limit summer gains to the level needed for illumination and (2) to maximize winter gains when heating is required and the glazing is a net gainer.

Figure 9 shows the annual operating costs which have been computed for each location using local billing policies for gas and electricity, including peak demand charges.* In all three locations, costs decrease rapidly with increasing glazing area, up to an aperture ratio between 2% and 3%. Reductions in both lighting and cooling electricity consumption contribute to these utility cost decreases (see Figs. 6 and 7). Beyond an aperture ratio of 3%, increases in cooling electricity dominate decreases in lighting electricity, and the costs increase gradually with aperture area. The shapes of the energy cost curves in Fig. 9 were influenced by two important assumptions in the study:

*The rate schedules for the utilities serving each of the three cities were obtained from the Johnson Environmental and Energy Center at the University of Alabama. No demand ratchet was used in the cost calculation.

(1) The COP of the cooling system may have been somewhat higher than appropriate when compared to the general quality of the other energy systems in the building. (Unlike the electric lighting system, no account was taken of cooling system performance degradation over time.)

(2) The thermal control in the building was based strictly on air temperature, which by itself is not a sufficient indicator of occupant comfort.

If the simulations were rerun with a lower COP for the cooling system, the cooling consumption curves would rise more rapidly for large aperture ratios. Furthermore, the peak-power demand charges, which are highly sensitive to cooling loads [2], would also rise rapidly at large aperture ratios. Both effects would tend to make the cost curves in Fig. 9 rise more rapidly than indicated after the minimum cost point. The assumption of strict air temperature control of the building thermal conditions also tends to underestimate the rate of rise of the cost curves for aperture ratios beyond the minimum. In a real situation, the larger aperture ratios would produce higher mean radiant temperatures in the building and would also cause more solar radiation to impinge directly on the occupants of the illuminated space. The likely effect would be that the occupants of a building with a large aperture ratio would want a lower air temperature to compensate for the warmer radiant environment. Lower air temperatures would result in higher cooling loads and higher costs than indicated by the results presented. It is likely that the minimum energy cost would still occur between 2% and 3% aperture ratio, but the shape of the curve would change in a manner to make the minimum more pronounced.

CONCLUSIONS

(1) A large fraction of the electricity consumed for lighting a single-story office building can be displaced using modest amounts of glazing to admit sunlight through the roof.

(2) Both cooling and heating energy consumption reductions are possible from a daylighting system, but they are much smaller than the potential lighting electricity reductions.

(3) Potentially deleterious thermal effects cannot be ignored in the proper design of a daylighting system.

(4) For south-facing, tilted illumination glazing, the total annual energy cost to operate the prototype building in each climate decreases rapidly with increasing glazing area, up to an aperture ratio between 2% and 3%, beyond which the cost increases gradually.

(5) Movable insulation or external shades, which properly control the solar gains and/or thermal transfer through the illumination glazing, could enable the daylighting system to eliminate most of the lighting electricity consumption while significantly reducing the cooling electricity consumption.

(6) In contrast to typical solar thermal systems having diurnal storage capacity, a single orientation of collection surface may not be the preferred configuration for daylighting systems.

REFERENCES

1. J. McMahon, C. Conner, R. Kammerud, and W. Place, "A Review and Analysis of Commercial Building Energy Consumption Studies," LBL Report LBL-10620 (to be published).

2. W.L. Carroll et al., "Passive Cooling Strategies for Nonresidential Buildings: An Impact Assessment," LBL Report LBL-14558 (to be published).

3. IES Lighting Handbook, edited by J.E. Kaufman, Illumination Engineering Society of North America, New York, 1981.

Double-Pane Glass Atlanta, GA June

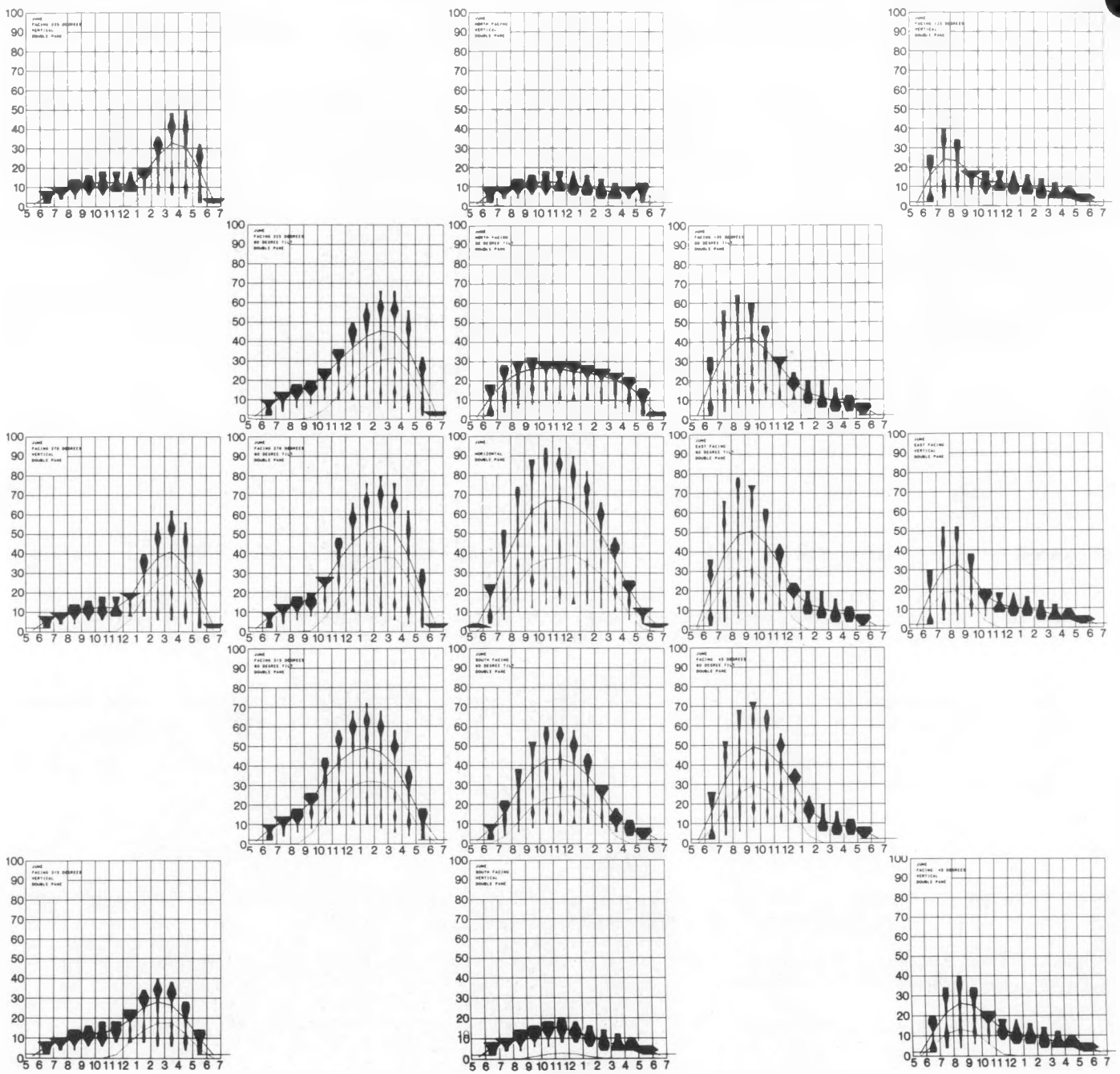

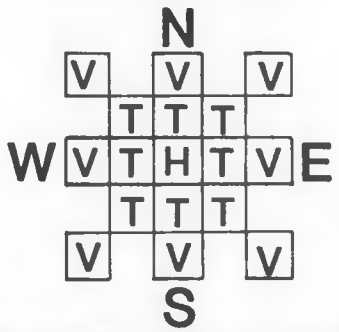

FIG. 1.

THE EFFECT OF GLAZING ORIENTATION ON THE COLLECTION OF BEAM AND DIFFUSE SUNLIGHT

Double-Pane Glass Atlanta, GA December

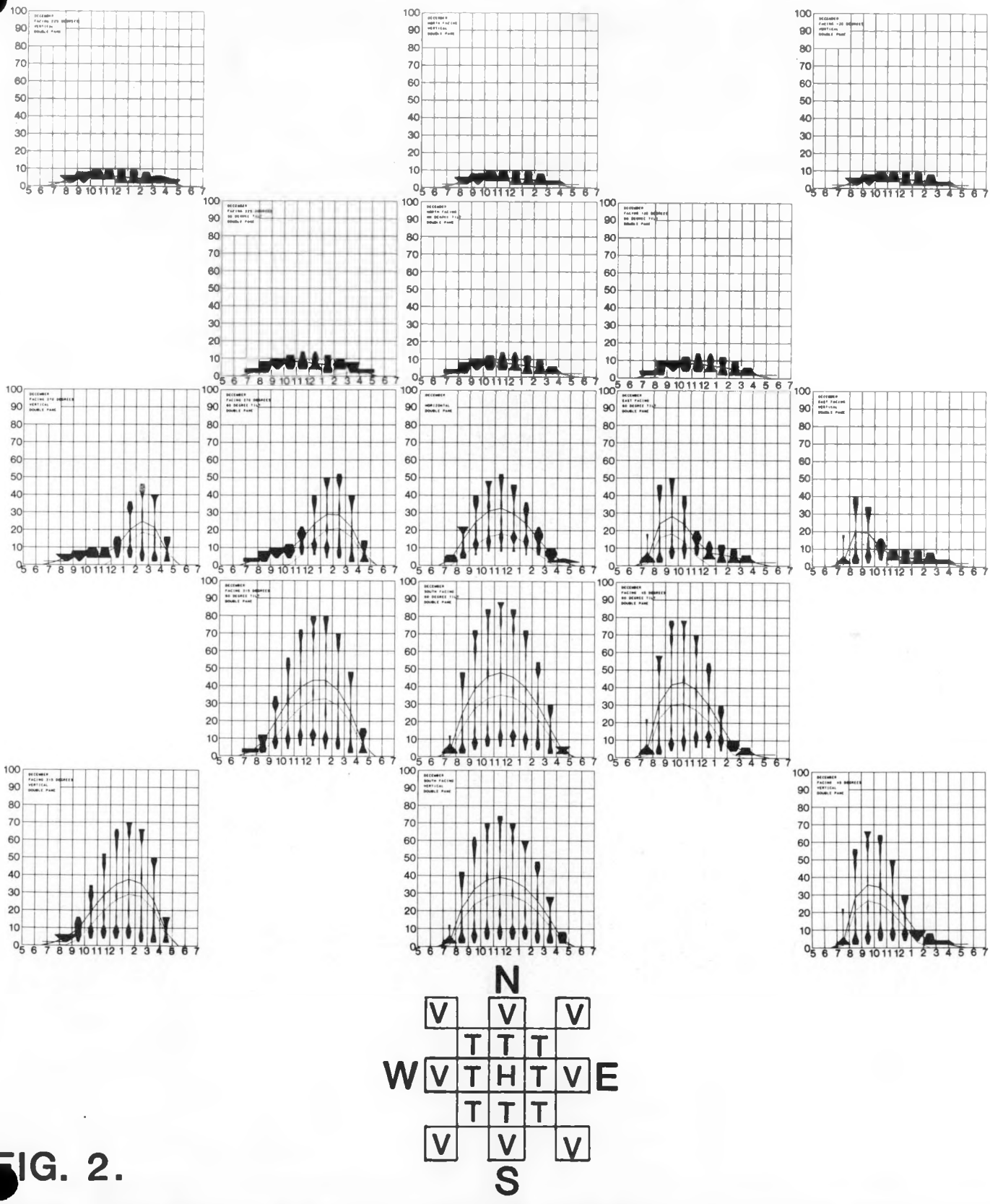

FIG. 2.

THE EFFECT OF GLAZING ORIENTATION ON THE COLLECTION OF BEAM AND DIFFUSE SUNLIGHT

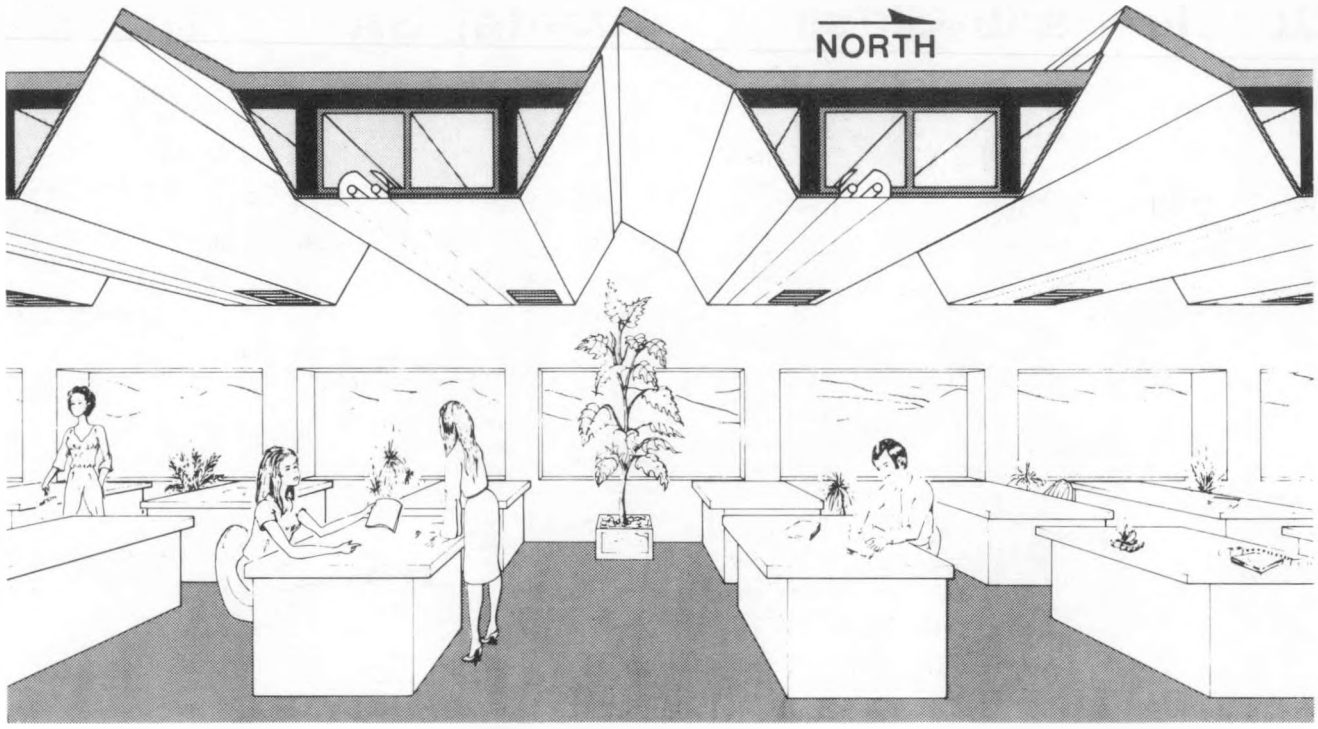

XBL 825-10228

FIG. 3. PERSPECTIVE SECTION OF PROTOTYPE COMMERCIAL BUILDING.

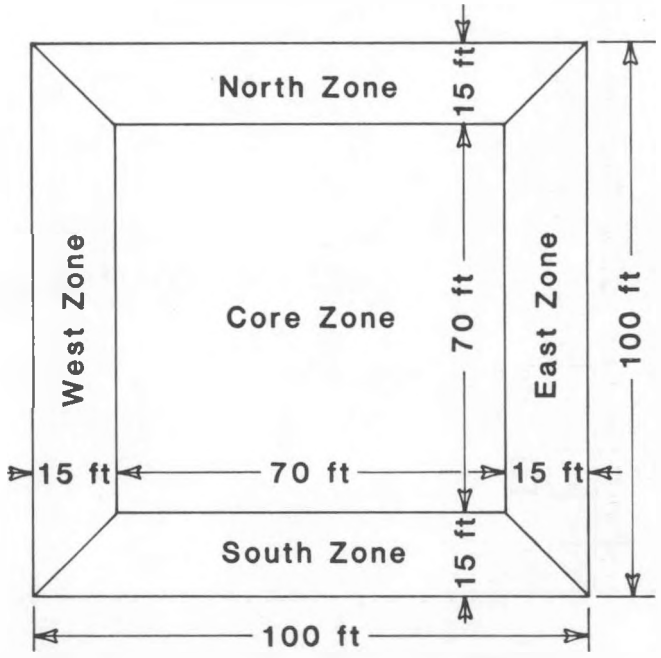

FIG. 4. SCHEMATIC FLOOR PLAN PROTOTYPE COMMERCIAL BUILDING.

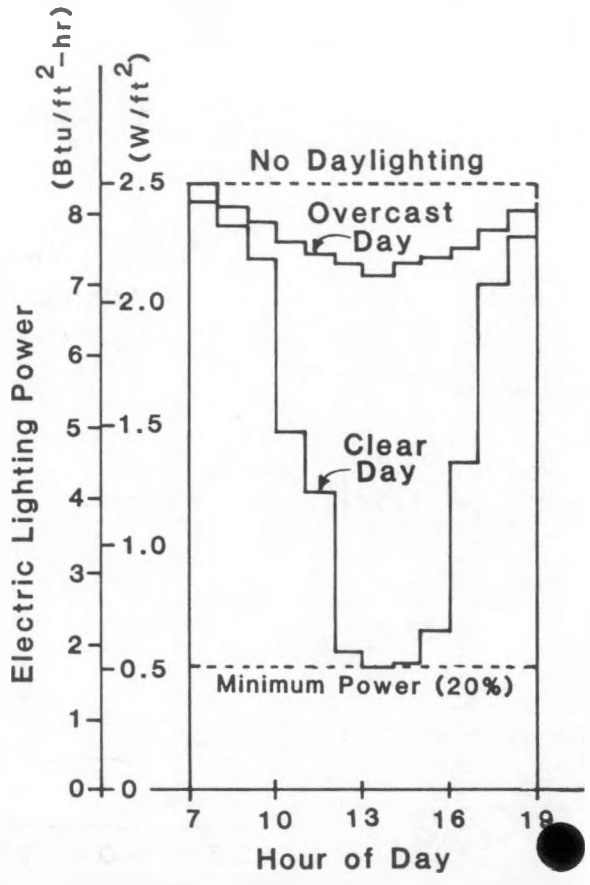

FIG. 5. HOURLY VARIATIONS OF ELECTRIC LIGHTING POWER.

XBL 829-11544

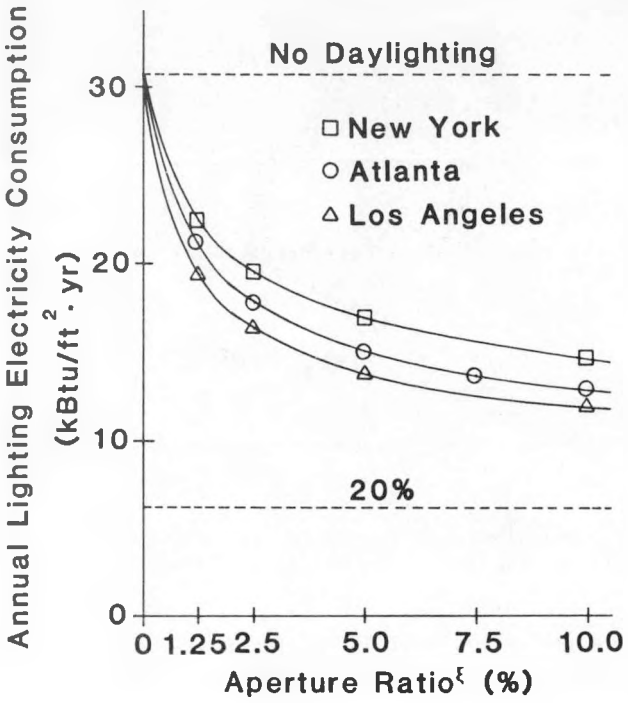

FIG. 6. ANNUAL LIGHTING ELECTRICITY.

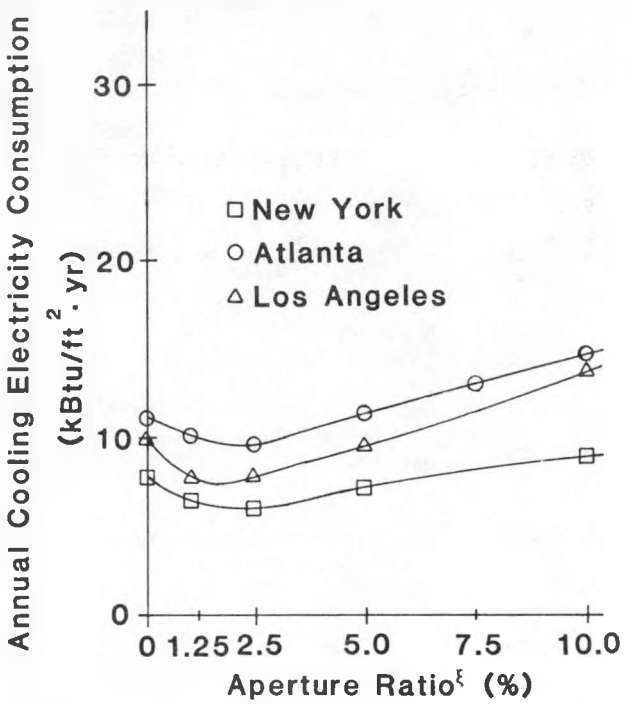

FIG. 7. ANNUAL COOLING ELECTRICITY.

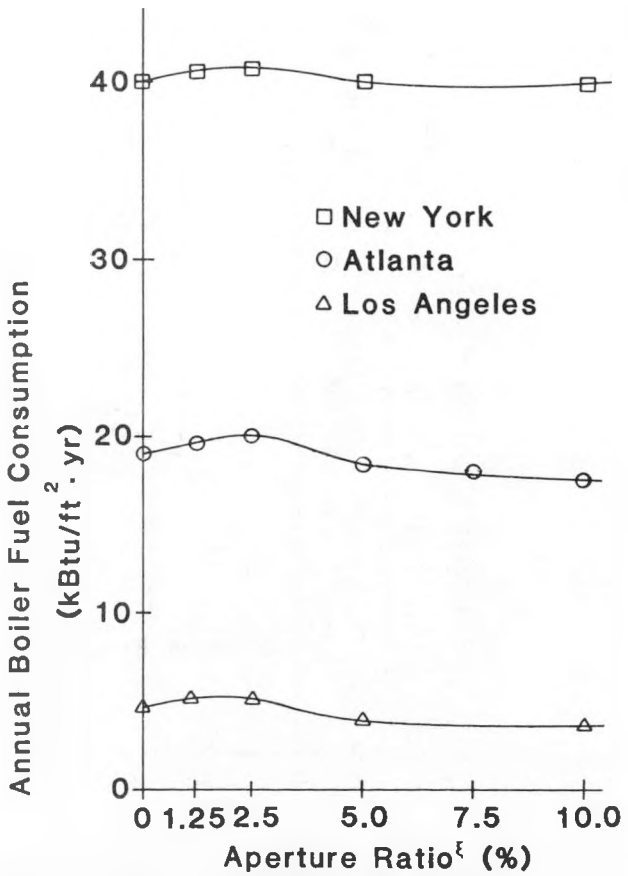

FIG. 8. ANNUAL BOILER FUEL.

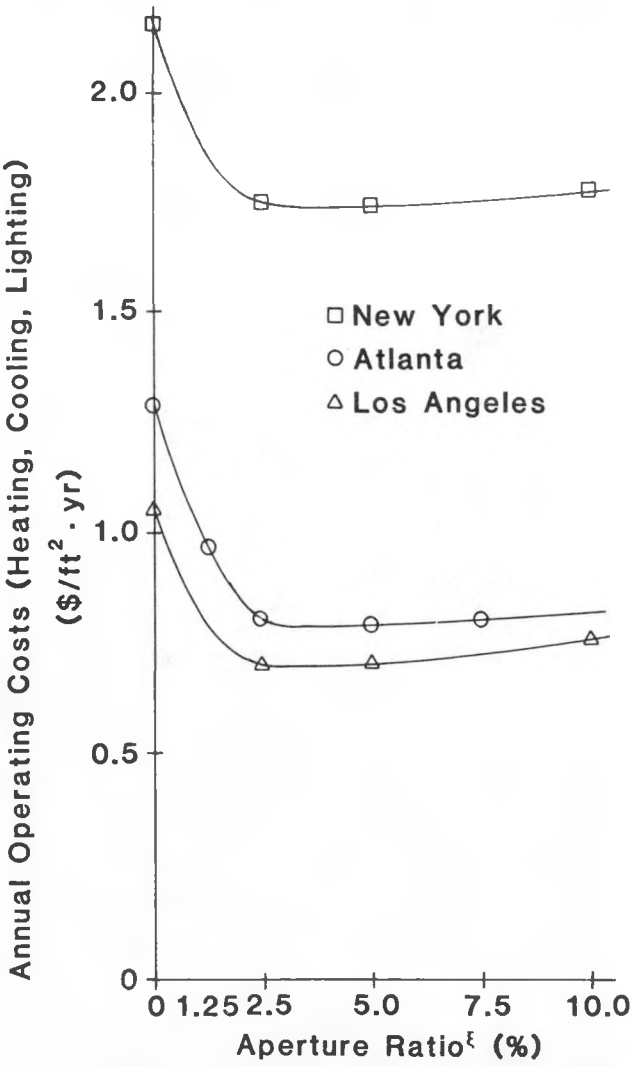

FIG. 9. ANNUAL OPERATING COSTS.

[ξ]Aperture Ratio Equals Ratio of Illumination Glazing Area to Building Floor Area

PROJECT SUMMARY

Project Title: The DOE Passive Solar Commercial Buildings Program: Technical Support Services

Project Manager: Harry T. Gordon

Organization: Burt Hill Kosar Rittelmann Associates
440 First Street N.W., Suite 500
Washington, D.C. 20001

Project Goals: Provide technical planning, monitoring and analysis services for the construction and performance evaluation phases of the DOE Passive Solar Commercial Buildings Program.

Project Status: The project is in progress with all services to be provided by the end of FY 83. Burt Hill Kosar Rittelmann is providing services jointly with Booz-Allen & Hamilton, Sizemore/Floyd, William I. Whiddon, and Benjamin H. Evans. This team is assisting DOE in planning and monitoring the activities of the 23 building projects in the Program. After completing construction, all building projects are required to collect data on thermal performance and on occupancy for the period of a year. The technical services project team has developed performance evaluation manuals, data reporting forms, and reporting procedures to be used in the evaluation process. The objective of the performance evaluation process is to determine how the buildings perform thermally in relation to conventional buildings and how occupants react to them.

Members of the project team are visiting the 23 building projects to inspect their instrumentation systems and review data collection procedures. Data on thermal performance and occupancy is being reported in a uniform manner and analyzed. Performance evaluation to date indicates that the 450,000 sq. ft. of passive commercial space involved in this program are expected to use about 50% less energy than conventional alternative buildings. This savings will be achieved at a 5-10% increase in construction cost.

Contract Number: DE-AC02-81CS30632.A000

Contract Period: September 28, 1981 through September 30, 1983

Funding Level: $902,944

Funding Source: U.S. Department of Energy, Chicago Operations Office

THE DOE PASSIVE SOLAR COMMERCIAL BUILDINGS PROGRAM: PERFORMANCE EVALUATION

Harry T. Gordon, AIA
William J. Fisher
BURT HILL KOSAR RITTELMANN ASSOCIATES
440 First Street N.W., Washington, DC 20001

ABSTRACT

Performance evaluation is the final part of a three-phase DOE Commercial Building Program which is assisting in the design, construction, and analysis of 23 exemplary passive solar commercial buildings. The passive solar features are being measured to determine the effects on occupant performance and actual building energy consumption.

Three hypotheses are being tested in the DOE Commercial Buildings evaluation effort:

- o the use of passive solar features reduces auxiliary fuel requirements for heating, cooling and lighting
- o the actions of the occupants of the building can help to reduce building energy requirements; and
- o the inclusion of passive solar features may enhance the ability of the building occupants to perform their job responsibilities.

Although it is unlikely that the 23 buildings currently in the program will be able to provide definitive answers to these hypotheses, the data base should be sufficient to give useful evaluation of passive solar thermal and occupant performance.

I. INTRODUCTION

In previous technical papers published at the 5th National Passive Conference (1, 2, 3) and the 6th National Passive Conference (4, 5, 6) several aspects of the predicted performance of buildings funded by the DOE Passive Solar Commercial Buildings Program have been discussed. The projects in this program (which began in late 1979) have been involved in three phases: Phase I - Design Assistance; Phase II - Construction Assistance; and Phase III - Performance Evaluation. Currently, all projects have completed the design phase activities and 21 of the 23 projects have begun construction; of these, approximately one half have completed construction and are now occupied. Two projects are waiting for favorable construction financing before beginning construction.

The purposes of this paper are to provide details of the results of design phase activities and to explain the Performance Evaluation activities which each constructed project will undertake. This performance evaluation effort is intended to provide information concerning three basic hypotheses:

- o the use of passive solar features reduces auxiliary fuel requirements for heating, cooling and lighting
- o the actions of the occupants of the building can help to reduce building energy requirements; and
- o the inclusion of passive solar features may enhance the ability of the building occupants to perform their job responsibilities.

Although it is unlikely that the 23 buildings currently in the program will be able to provide definitive answers to these hypotheses, the data base should be sufficient to at least give clear indications of the likely answers and to aid in formulating hypothetical questions to be tested by subsequent research.

II. BASIS FOR PERFORMANCE PREDICTION

In order to define both increased first cost and decreased energy consumption over conventional buildings, the architectural/design teams had to define a "reasonable" conventional building--one that owners would have been likely to build had they not chose a solar alternative. The conventional alternative is called the "base case." This can be a controversial exercise. The base building is, by definition, theoretical. At best, it may be a building somewhat like the proposed new building or it could be the last building that the owner built. Usually, however, it is not a real building. The base case does not get built and instrumented, so estimated "savings" can never be proven precisely.

Projects in the program were required to make their best efforts in defining a base case against which a solar alternative could be compared. The process was monitored by DOE technical experts who had to judge the reasonableness of the proposed base cases based on the best current information available. Based on our experience in this program we believe that it is possible, within technical and ethical limits of the profession, to produce such a base case and to use it as an effective yard stick

against which solar buildings can be measured. Whether this is the best method for judging either cost or performances of new passive solar technology is a matter to be discussed in coming months by the passive solar community and other interested groups responsible for telling the world at large and building owners in particular whether or not passive solar energy is a viable alternative for commercial buildings.

Another point of particular interest is that all energy predictions done in the program are based on design tools and simulation models currently in use. It has never been the purpose of this program to verify design tools. Nevertheless, DOE will be extremely interested to see at least the range of accuracy possible with the given set of tools used. Figure 1 lists the tools used in the program. They range from simple nomograph and energy graphic techniques to full computer simulations like DOE-2 and BLAST. Figure 2 shows the estimated energy savings for each energy end use in the solar building and the estimated cost of including the passive solar features. Both the estimated energy savings and the estimated costs are calculated by comparing the anticipated results of the solar building to that of a non-solar "base case" building.

III. PERFORMANCE EVALUATION

Each of the projects which receives construction assistance will also participate in the performance evaluation phase of this program. Once buildings are in place and have been "de-bugged," participants are required to provide a year's worth of performance data on both thermal and occupant behavior.

As shown in Figure 3, the basic question being asked in the performance evaluation phase is, "How well do the buildings work?" There are two components to the question: (1) Do the buildings save auxiliary energy compared to non-solar buildings, and (2) do the buildings function as well as non-solar alternatives?

To gather information regarding auxiliary energy savings, each project will use data recording equipment or sub-meters to measure the purchased energy requirement for heating, cooling, lighting and other end uses. These measurements will be compared to the design phase energy prediction discussed previously. If a substantial difference exists between predicted and measured energy use, a series of steps will be undertaken in an attempt to identify the probable cause. Several potential reasons for such a difference are shown in Figure 3.

We believe that it is also important to know how these buildings function to support their intended use. Even substantial energy savings will not offset a small loss in productivity of the personnel using the building. Conversely, if the building provides an environment which is conducive to the intended use, that alone may be sufficient reason to incorporate passive solar features. Accordingly, we are using survey techniques to record information concerning maintenance requirements, comfort levels and personal responses which indicate the degree of users' satisfaction in these buildings. Collectively, this information will help to indicate whether the buildings function as well as their non-solar counterparts.

In preparing the Performance Evaluation Manuals for this program, considerable research was done to examine the possibility of using performance monitoring approaches developed for the Passive Residential Program (Class A, B, C) or for the Active Solar Program (currently managed by VITRO Laboratories Division of Automation Industries Inc.). While both of these preceding efforts provided useful information regarding building energy performance evaluation, they were not directly usable for thermodynamically more complex passive commercial buildings. This performance evaluation approach differs from its predecessors in two principal ways: (1) it does not attempt to identify a solar fraction; instead it allows a designer or owner to compare measured energy use data with alternatives of their own selection. This more closely relates to the typical architectural/-engineering practice; (2) the substantial influence which building users have on energy use in passive buildings, and the effect which the passive building has on its users, indicates the importance of collecting data from people as well as from instruments.

IV. CONCLUSIONS

Preliminary results are currently being compiled with detailed analysis expected by Fall 1983. However, the primary conclusions which can be drawn from the DOE Passive Solar Commercial Buildings Program are:

1) The 450,000 sq ft of passive commercial space involved in this program are expected to use about 50% less energy than conventional alternatives. This benefit was achieved at a cost increase of 5-10% compared to conventional buildings.

2) Performance evaluation methods have been developed which will enable the energy use and occupant response to these buildings to be compared to conventional alternatives.

V. REFERENCES

1. Harry T. Gordon, AIA; W.I. Whiddon; Strategies for the Use of Passive Solar Approaches in Commercial Buildings, 5th National Passive Solar Conference, Amherst, MA, October 1980.

2. Ted L. Kurkowski; Steven E. Ternoey, AIA; The Design of Passive Commercial Buildings, 5th National Passive Solar Conference, Amherst, MA, October, 1980.

3. W.I. Whiddon; Harry T. Gordon, AIA; Process Issues in the Design of Passive Solar Commercial Buildings, 5th National Passive Solar Conference, Amherst, MA, October 1980.

4. William J. Fisher, Robert G. Shibley, Passive Solar Opportunities in Commercial Buildings: Technical Insights and a Model for Professional Development, 6th National Passive Solar Conference, Portland, OR, September 1981.

5. Kimball Hart, Harry T. Gordon, W.I. Whiddon, Scott I. McIsaac, Economic Analysis of Selected Passive Solar Commercial Buildings, 6th National Passive Solar Conference, Portland, OR, September 1981.

6. Ted L. Kurkowski; Steven E. Ternoey, AIA; An Overview of Designs from the DOE Passive Commercial Buildings Program, 6th National Passive Solar Conference, Portland, OR, September 1981.

DESIGN TOOLS MATRIX

BUILDING TYPE & LOCATION	THERMAL	DAYLIGHTING
1 SCHOOL - FAIRBANKS, AK	TRNSYS	N/A
2 SCHOOL - BESSEMER, AL	TEANET, TRACE	model, TRACE
3 SCHOOL - IRVINE, CA	Energy Graphics, TEANET, DOE-2	model
4 COLLEGE BUILDING - GLENWOOD SPRINGS, CO	ASHRAE calculations, BLAST	model
5 AIRPORT TERMINAL - GRAND JUNCTION, CO	P-chart, SLR, Quikee model	LUMEN II program
6 AIRPORT TERMINAL - GUNNISON, CO	PASSLR	N/A
7 SENIOR CITIZENS CENTER - BALTIMORE, MD	ASHRAE calculations, Bin method, TETD	N/A
8 BANK - WELLS, MN	ASHRAE, Energy Graphics, SLR	model
9 CHURCH ADDITION - COLUMBIA, MO	PASOLE	N/A
10 LIBRARY - MT. AIRY, NC	SLR, ECAL	models
11 OFFICE - PRINCETON, NJ	ASHRAE, Energy Graphics, SLR, proprietary program	model, simulation
12 COLLEGE BUILDING - PRINCETON, NJ	IMPSLR, ASHRAE, Energy Graphics, SKYKING	SKYKING
13 VISITOR CENTER - TROY, NY	ASHRAE, SLR, proprietary program	model, simulation
14 MEETING HALL - DEADWOOD, OR	Rules-of-thumb, TEANET	model
15 NURSING HOME - ALBANY, OR	unavailable	unavailable
16 AUTO FACILITIES - PHILADELPHIA, PA	ASHRAE calculations, BLAST	model
17 RECREATION CENTER - PHILADELPHIA, PA	TRNSYS	model
18 GREENHOUSE - MEMPHIS, TN	ASHRAE calculations	model
19 COMMUNITY CENTER - MISSOURI CITY, TX	proprietary program, DOE 2.0a	N/A
20 WORKSHOP - NEW BRAUNFELS, TX	ASHRAE calculations, Bin method, TEANET	measurements
21 OFFICE - SALT LAKE CITY, UT	Equinox proprietary program	model
22 GYMNASIUM - ALEXANDRIA, VA	Rules-of-thumb, IMPSLR, PEGFLOAT, PEGFIX, SUPERFIX	N/A
23 STORE/OFFICE - WAUSAU, WI	ASHRAE calculations, Energy Graphics	N/A

Figure 1. Thermal and daylighting design tools for projects in Passive Solar Commercial Buildings Program

BUILDING TYPE & LOCATION	ESTIMATED ENERGY SAVINGS (Btu/Sq.Ft./Yr)						ESTIMATED PASSIVE COSTS ($/Sq.Ft.)
	HEATING	COOLING	LIGHTING	DHW	OTHER	TOTAL	
1 SCHOOL - FAIRBANKS, AK	39,900	--	289,400	--	--	329,300	5.56
2 SCHOOL - BESSEMER, AL	UNAVAILABLE					11,120	4.71
3 SCHOOL - IRVINE, CA	3,105	26,085	18,132	241	95	47,658	13.13
4 COLLEGE BUILDING - GLENWOOD SPRINGS, CO	50,100	8,240	8,670	1,280	-610	67,680	6.27
5 AIRPORT TERMINAL - GRAND JUNCTION, CO	6,552	--	8,126	--	105	14,783	3.29
6 AIRPORT TERMINAL - GUNNISON, CO	18,117	--	8,352	--	--	26,469	5.35
7 SENIOR CITIZENS CENTER - BALTIMORE, MD	16,000	17,500	9,200	3,000	--	45,700	5.74
8 BANK - WELLS, MN	24,510	9,710	20,520	80	1,780	56,600	13.19
9 CHURCH ADDITION - COLUMBIA, MO	102,980	390	1,940	--	420	105,730	11.71
10 LIBRARY - MT. AIRY, NC	2,912	3,100	29,343	707	2,315	38,378	15.98
11 OFFICE - PRINCETON, NJ	30,137	14,000	16,620	927	197	61,880	8.04
12 COLLEGE BUILDING - PRINCETON, NJ	63,200	--	20,300	--	--	83,500	5.30
13 VISITOR CENTER - TROY, NY	23,300	3,980	10,410	530	-2,990	35,230	18.97
14 MEETING HALL - DEADWOOD, OR	UNAVAILABLE						18.76
15 NURSING HOME - ALBANY, OR	UNAVAILABLE						
16 AUTO FACILITIES - PHILADELPHIA, PA	157,200	--	3,700	1,100	--	162,000	2.63
17 RECREATION CENTER - PHILADELPHIA, PA	10,300	300	8,700	3,100	--	22,400	9.83
18 GREENHOUSE - MEMPHIS, TN	28,750	3,564	--	178	1,657	34,146	1.20
19 COMMUNITY CENTER - MISSOURI CITY, TX	270	4,330	5,350	2,180	--	12,130	12.09
20 WORKSHOP - NEW BRAUNFELS, TX	8,100	7,850	5,600	1,250	-800	22,000	2.61
21 OFFICE - SALT LAKE CITY, UT	13,600	-530	10,600	--	--	23,700	10.02
22 GYMNASIUM - ALEXANDRIA, VA	36,500	-1,010	15,200	--	-140	50,550	9.00
23 STORE/OFFICE - WAUSAU, WI	10,625	2,140	5,100	--	--	17,865	15.16

Figure 2. Cost and energy savings data for projects in the Passive Solar Commercial Buildings Program

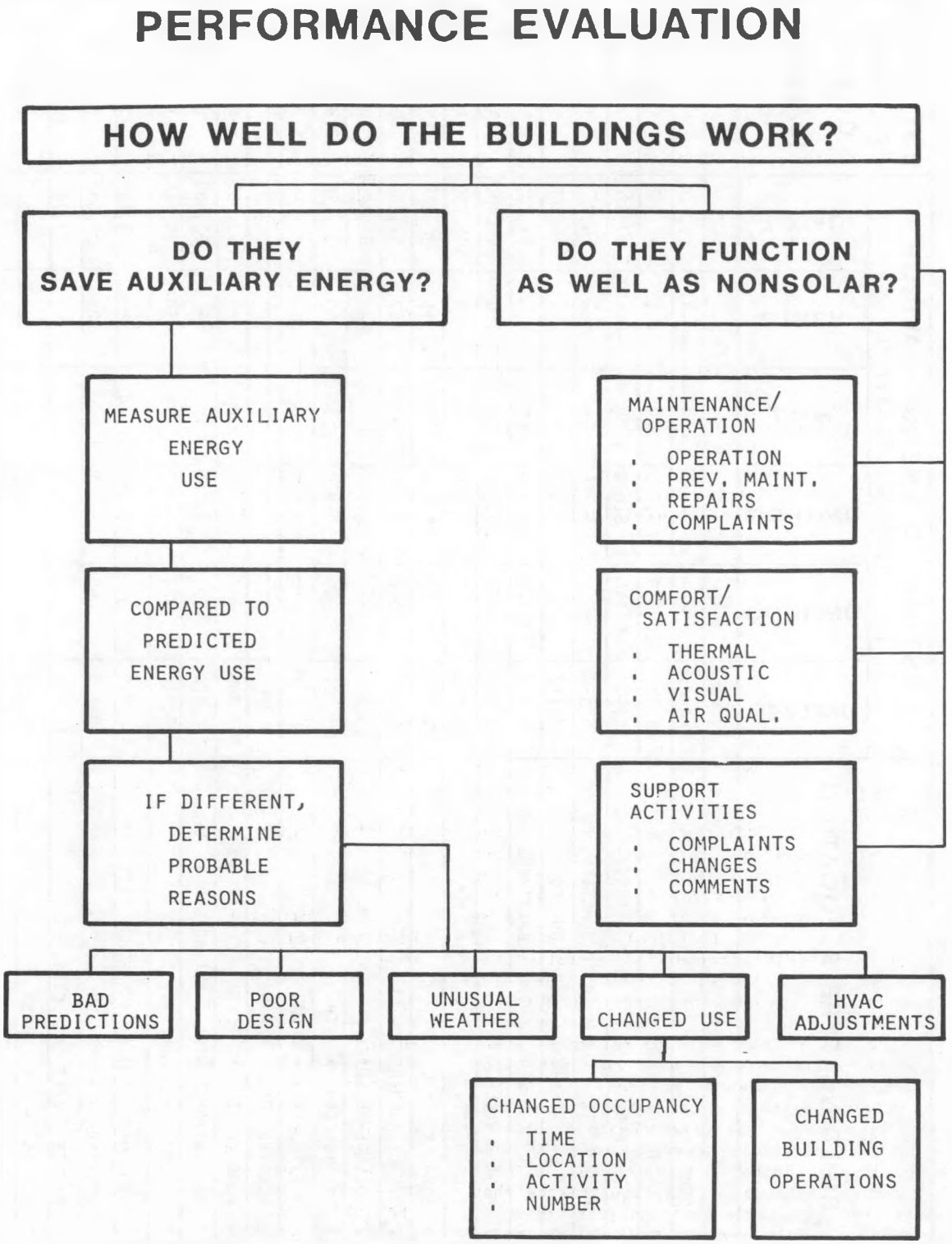

Figure 3. The performance evaluation process in the Passive Solar Commercial Buildings Program

DESIGN, CONSTRUCTION AND INITIAL MONITORING

John R. Schade
Johnson Controls, Inc.
Milwaukee, Wisconsin

INTRODUCTION

The passive design process and the resulting building described in this paper demonstrate how technical, economic, and organizational objectives intermingle to affect the final building. A clear conclusion that can be drawn at this point in the project is that the design and construction program of a large, profit-oriented corporation can effectively incorporate passive solar measures in small branch offices; but that passive design -- even if cost effective -- is secondary to the goals and operating characteristics of the organization -- including its design approach, its management priorities, and its employee work environment. Many of us working in the energy and buildings field -- with the best of intentions -- tend to underestimate the importance of these institutional factors, while focusing closely on the technology and economy of energy issues. An important lesson of this project is that unless organizational and institutional design issues are given high priority during the design development process, new and innovative solutions will probably not be achieved in a practical way, and will certainly not be accepted by the market at large.

ORGANIZATIONAL AND PROGRAM OBJECTIVES

Johnson Controls, Inc., designs, produces, and services building environment controls systems. To accomplish this, it has a network of 120 branch offices throughout the U.S. The company's new branch in Salt Lake City, Utah, is one of 23 buildings included in the U.S. Department of Energy Passive Solar Commercial Buildings Program. The objectives of that program are to design, build, test, and evaluate practical passive solar buildings, and by doing so, determine their technical and economic potential in the U.S. commercial construction market. The project began with a successful application to DOE by Johnson Control's Marketing Department in July of 1979. Johnson Control's objectives for the project were to determine what, if any, passive solar measures were successful for use in other U.S. branch offices. Johnson Control's primary criteria for success included: 1) cost effectiveness - the relationship of benefit to costs for any particular measure over the life of the building. Corporate investment criteria proved to be more rigorous in its requirements than typical long term life cycle cost analysis criteria, and established a simple payback goal of five years for any package of additional passive measures; 2) construction cost - irrespective of payback, the building had to achieve a reasonable overall cost when compared to other Corporate branch offices, that overall cost level was $45-$55/sq. ft.; 3) employee comfort and productivity - branch office management determined that a reasonable comfort range was 72°F setpoint for cooling, and a 68°F for heating; 4) employee and management acceptance - a management organization made up of experienced controls engineers stressed comfort control, reasonable lighting levels, comfortable ventilation levels, and aesthetic quality; 5) reliability - branch management stressed maintainability, maintenance frequency and practicality and 6) design time - time requirements for passive design must be reasonable since the Corporate Facilities Planning Office is responsible for design of 3 to 5 branches per year, plus other Corporate Facilities. All of these criteria were important to determine the usability of passive measures in other U.S. branch offices.

DOE program objectives stressed cost effectiveness, as well as the potential for successful technical and economic evaluation, demonstration and market acceptance. The project was a joint cooperative agreement, cost shared by DOE to a major extent, and managed by Johnson Controls Facilities Planning Office.

PROGRAMMING AND DESIGN

There were four major incentives for Johnson Controls, Inc., to enter the program: 1) programing/design support for the passive portions of the design; 2) support for increased construction costs of the passive design; 3) performance testing and evaluation of an experimental branch building using passive components and Johnson products; and 4) the potential for market recognition.

The initial step of energy programming and design was crucial. It provided an impetus of time, money, and the inspirational expertise of nationally prominent outside consultants in the passive field. The Corporate Architect's office was aware of various passive and conservation design measures, and had evolved a cost effective design solution to energy efficient branch offices. However, the production schedule demands of the Corporate building program did not allow for the extensive level of energy analysis required to justify the cost of innovative passive designs to a profit conscious Branch Manager and Board of Directors. Programming and design activities went through several schematic and design xevelopment iterations, each involving increasingly more detailed energy/cost simulations. Energy design and analysis was completed jointly by the Corporate Architect, Doug Drake, and Don Watson, the team leader for the passive design team. In addition, Fred Dubin advised on HVAC, Bill Lam on daylighting, Bob Busch on energy and cost design evaluation, and

Robert Frew on computerized energy performance simulation.

ROLE OF INTERNAL REVIEW

Schematic, design development and construction document work was reviewed internally by Johnson Controls management at several levels, including Field Engineering, Corporate Facilities Planning, Corporate Sales, Salt Lake Branch Management and Controls Engineers, and the Office of the Coporate Secretary, which oversees Corporate facilities, design, planning, and construction. In hindsight, the management review by Johnson Controls was crucial to the success of the Project. It provided a rigorous in-house technical, financial, and practical kind of scrutiny -- primarily from the perspective of Johnson line and corporate management, most of whom are professional controls engineers. The combination of practicality and vested interest provided by Johnson management served as the key in screening out most experimental, unworkable, or unproven concepts, and generating a "lean" design which helped to result in a constructive budget below original cost estimates; and which, from initial monitoring results, is saving more energy than originally projected.

BASE CASE VS. PROPOSED PASSIVE DESIGN

The base case design is similar to the design by the Corporate Facilities Planning Staff for the Branch Office in Wyoming, Michigan. It is a design that was already energy efficient and includes features such as earth berms, low wattage lighting, proper glass orientation, and good levels of insulation. The energy efficiency of the base case provided a difficult standard for justifying additional passive and energy conserving measures. Figure 2 illustrates the annual energy use of the base case. Based on the analysis of the base case, the proposed design included the following primary strategies, as described by Don Watson:[1]

1) Utilize daylighting and winter solar gain more effectively;
2) Utilize thermal mass;
3) Utilize winter solar gain for warm air supply; and
4) Increase insulation levels.

Figure 3 illustrates the annual energy use of the proposed design. Figure 4 illustrates how key architectural and mechanical measures are integrated into the proposed design.

ROLE OF PASSIVE DESIGN SUPPORT

Energy design and evaluation costs were significant. Typical industry design costs for a small owner-occupied office/warehouse space might range from 6% to 8% of project costs, or from $54,000 - $72,000 for this $900,000 project. However, Johnson Controls, Inc., costs for branch design are typically well under this range, since Corporate Facilities Planning Staff have evolved standard design approaches for branch offices. Consequently, the Phase I energy design and reporting costs of $49,000 represented a high power injection of energy sensitivity into the Corporate design/building procedur The costs required to do this supported not only energy design and evaluation, but also education and orientation of Johnson staff and management in the areas of energy design development and construction detailing.

CONSTRUCTION

Construction documents were completed in August 1981; bidding occurred in September, 1981, construction began in October 1981, and was completed for occupancy in March, 1982. The passive portion of the project caused no significant delays in construction. Initial cost estimates for the project were $825,000 or about $55/sq. ft. The successful bid was $784,000 or approximately $50/sq. ft. The difference between estimated and actual construction is attributable to economic conditions in the Salt Lake construction industry at the time of bidding. Bid and actual passive component construction costs are shown in Figure 5.

With the exception of moveable night insulation costs were very consistent with bid estimates. Air handing equipment including dampers, air handlers, and fans exceeded bid cost by about 20% ($4,900). However, this excess was made up by a $6,300 reduction in the cost of passive architectural components. The major exception to controlling project passive costs is the moveable night shade insulation system. Although initial installation costs were less than anticipated, major changes in framing, motor mounts, materials and controls have increased the cost of this component from an initial estimated cost of $13,200 to an estimated final cost of $28,700. Since the night insulation system was found to be the most marginal aspect of the passive design in terms of payback at its original estimated cost level, it clearly will not be cost effective when completed.

INITIAL PERFORMANCE

The word "initial" must be stressed. Occupancy occurred in early March, 1982, and since that time building operation and control, as well as monitoring, have undergone continual adjustment. Early results, however, are quite promising, and reflect the consistently conservative approach in projecting savings during the design analysis phase of the project. Figures 6 and 7 compare predicted to actual energy use for April and May, 1982. April consumption is substantially below (58% - 95%) predicted predicted levels for all energy and use categories except heating, which is 82% above predicted levels. Total energy use is 11% below the level projected for April. A similar trend exists in May, with a higher discrepancy (153% of predicted) in the heating category and an overall budget which is only 4% below that predicted Higher heating energy use can be explained in pa by a 25% above average degree day heating load in Salt Lake for these periods in 1982, and by excess run time for the fans and heating system during low occupancy and unoccupied periods. Savings for

lighting, which constitutes about 21% of total energy use and 42% of projected annual energy costs, are expected to increase. This is because the daylighting system is not affecting interior lighting zone ambient light at all during late spring and summer, and is less effective now than during fall and winter months in the perimeter zones. During construction completion in late winter, no general lighting was required of any of the three lighting zones. Thus we expect annual lighting energy use will be well below levels we are now experiencing for late spring and summer.

In summary, initial results interpreted conservatively indicate an overall energy use trend that is from 5% to 10% below predicted levels. These results are cause for optimism, but are not conclusive, since 5% to 10% is well within the accuracy range of our design prediction tools and methods. The combined factors of assured additional savings in heating due to reduced operating schedules, more typical heating seasonal loads and additional savings from reduced lighting and cooling loads in winter and swing seasons, indicate a high probability that total energy use will be substantially below originally predicted levels. The savings thus far have been achieved without the use of night insulation, which indicates that the major passive/conservation components are more cost effective than originally estimated.

COMFORT/PRODUCTIVITY

Occupancy evaluation reports were completed by Salt Lake Office employees. Seventy-five percent of the full time occupants were "highly satisfied" with the space, none were "disatisfied," and six "loved it." Of the twenty respondents, four indicated a desire for more individual control of lighting and temperature.

CORPORATE RESPONSE

Perhaps the most significant outcome of the project in terms of long term objectives of both the Department of Energy and Johnson Controls, Inc., is that the promising passive and energy conserving measures have been introduced into the Branch Office design process. As a result of conclusions arrived at from design, analysis and construction of the Salt Lake Building -- but prior to detailed evaluation of monitored performance -- the Denver, Seattle, and Charlotte, S.C., branches incorporated many of the passive measures used in the Salt Lake design. The favorable energy and economic performance of the Salt Lake design and positive acceptance by branch personnel are likely to reinforce this trend.

PROJECT TEAM

Doug Drake, Corporate Facilities Architect
Johnson Controls., Inc., Milwaukee, Wisconsin

Donald Watson, FAIA, Architectural Consultant, Guilford, Ct.

Fred S. Dubin, P.E., Consulting Engineer, Dubin-Bloome Associates, New York, HY.

William Lam, Lighting Consultant, Cambridge, Mass.

Ken Kammeraad, Secretary of the Corporation
Johnson Controls, Inc., Milwaukee, Wis.

Bob Busch, Technical Monitor, AREA, Inc., Albuquerque, NM.

John Schade, Project Director, Office of the Corporate Secretary, Johnson Controls, Inc., Milwaukee, Wis. (Currently at Conservation Division, California Energy Commission, Sacramento)

REFERENCES

1. See "Johnson Controls Branch Office Building, Salt Lake City, UT, Passive Solar Energy Analysis, and Design," by Donald Watson, FAIA

FIGURE 1

	% HEAT improvement	% COOL improvement	% TOTAL improvement	solar fraction	Btu/SF/DD SF=14,884 DD = 6280
00 BASE CASE 68-75F setpoints	0	0	0	5	7.7
01 BASE CASE 68-80F setpoints	1	53	8	9	
02 BASE CASE 00 w/ 50% south glass	1	-3	1	9	
03 CASE 02 SOUTH GLASS w/ sunshading	1	3	1	8	
04 CASE 02 SOUTH GLASS w/ night-shades	2	3	2	8	
05 BASE CASE 00 w/ clerestory	5	-9	3	15	
06 CASE 05 CLERESTORY w/ sunshading	5	-7	4	14	
07 CASE 06 CLERESTORY w/ night-shades	6	-7	5	14	
08 BASE CASE 00 w/ earth-berms	3	10	4	8	
09 BASE CASE 00 w/ R 15.8 walls	3	13	5	8	
10 BASE CASE 00 w/ R 28 roof	3	29	26	11	
C1 PROPOSED DESIGN 68-75F setpoints	51	-15	37	21	5.6
C3 PROPOSED DESIGN w/ night-shades	53	-15	39	21	5.5

Pre-Design and Proposed Design Options Salt Lake City Climatic Data Test Year: 1952
Equinox Competer Program (ARGA Associates, New Haven, CT)

FIGURE 2

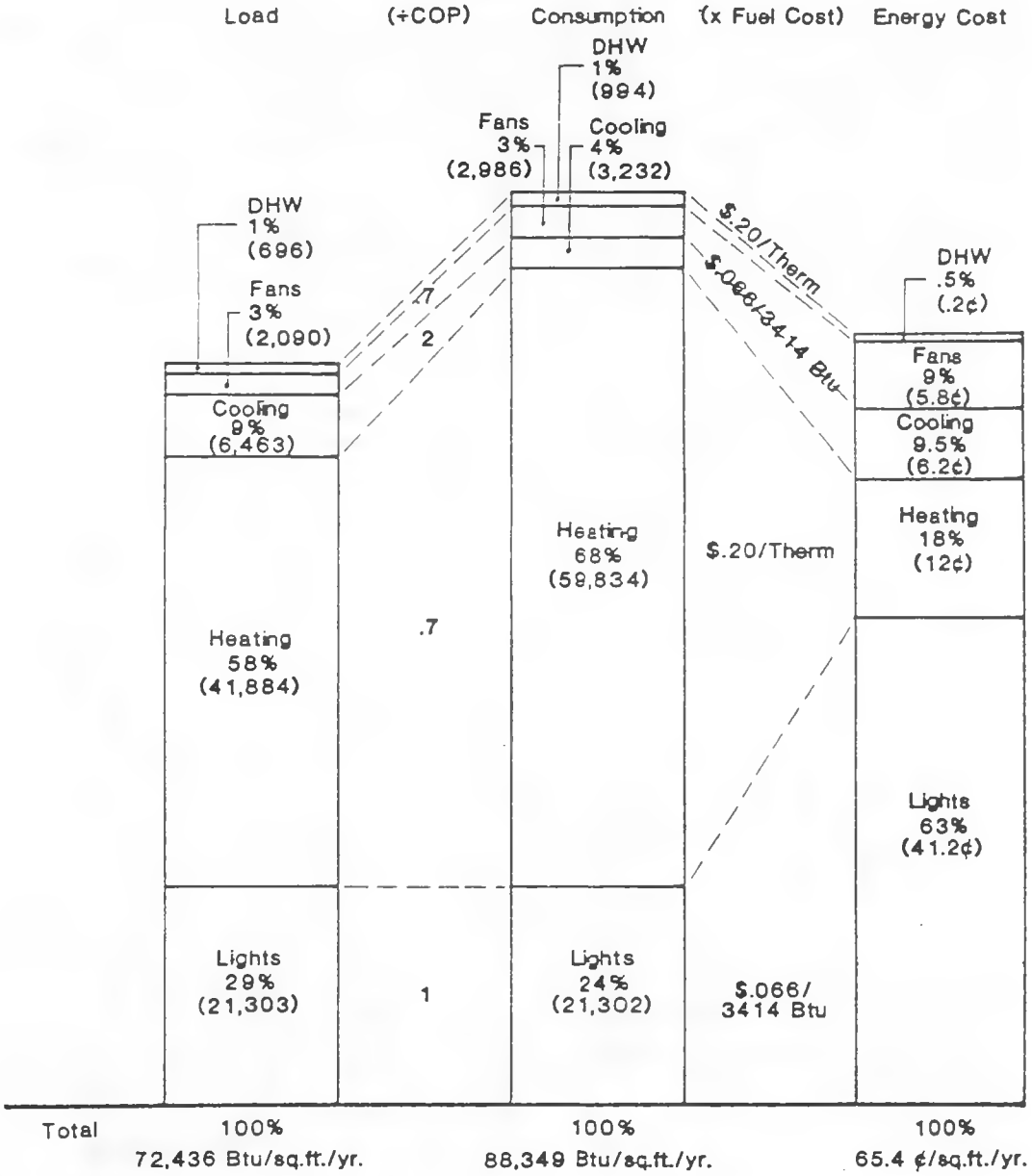

Annual Energy Use Summary: Load, Metered and Purchased: BASE CASE

FIGURE 3

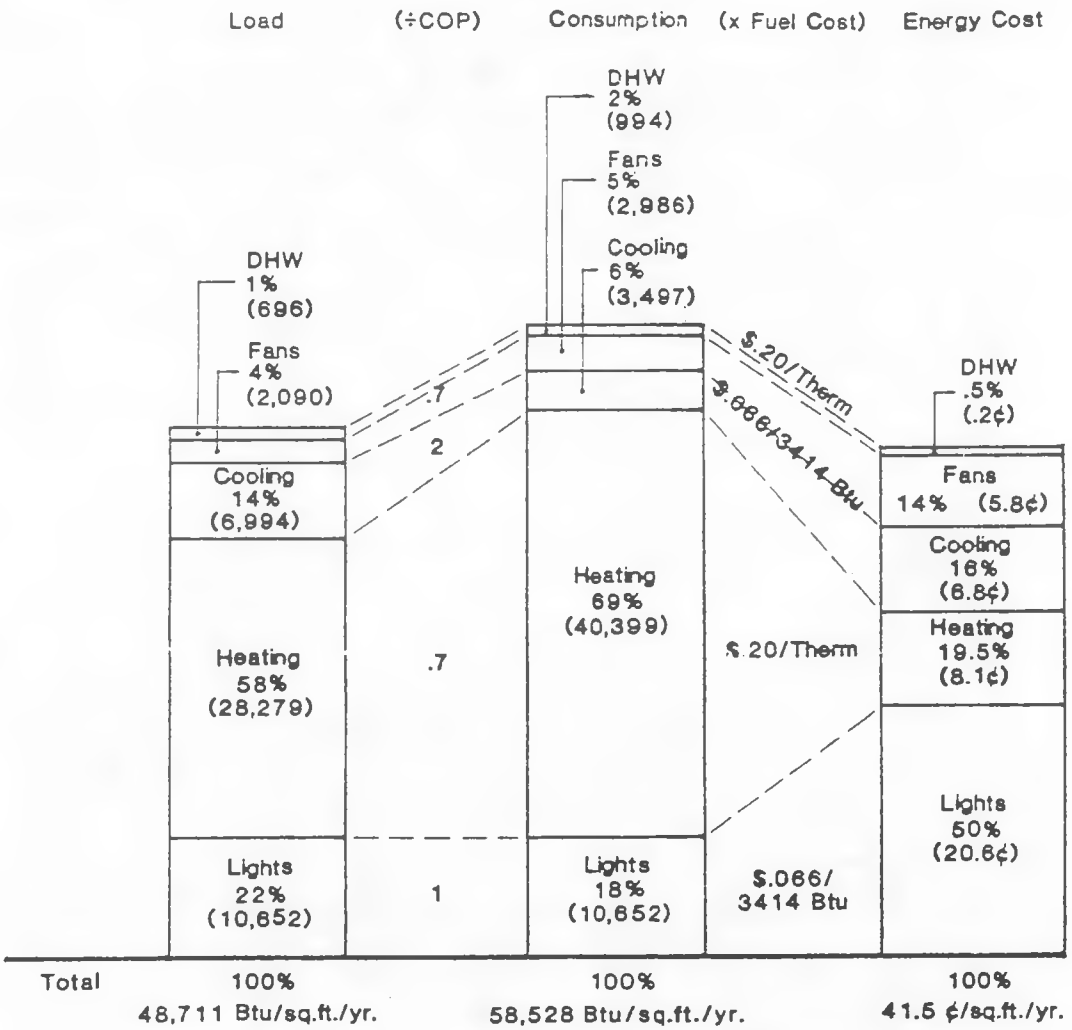

C2 PROPOSED DESIGN
w/ lighting 1.5W/SF

Annual Energy Use Summary: Load, Metered and Purchased: PROPOSED DESIGN

FIGURE 4

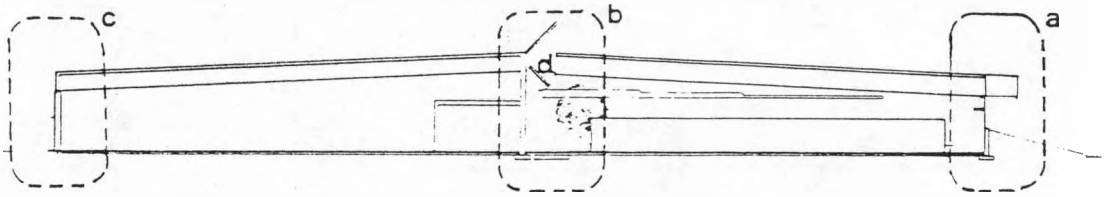

PLAN LAYOUT	Airlocks at all entries Office on south for view and solar utilization Warehouse on north for buffer Entries on south for sunspace effect Solar court on south for outdoor lunch & conferences Interior spaces grouped according to schedule
ENVELOPE	**a** Southwall used for daylight and winter solar gain Insulating/Sunshade at south for balance **b** Skylite at center for daylight and winter solar gain **c** Earthberms all sides for insulation and heat sink Increased insulation on walls and roof Insulation on outside of masonry walls for heat sink Reduced infiltration/exfiltration due to above factors
STRUCTURAL	Coordinated with mechanical, lighting, and architectural requirements for building system efficiency
MECHANICAL	VAV air supply and return system for load-following, economizer cycle, nite venting, and evaporative cooling efficiency. **d** High return placed in Skylite for destratification and heat recovery. Operating controls on temperature and scheduling for maximum energy economy.
LIGHTING	Daylighting utilization to replace ambient lighting electrical load, with block switching. Task lighting all work stations. Energy efficient illuminaires specific to each task and occupancy area.

Summary of Design Development Recommendations

FIGURE 5

As-Built Construction Costs - Passive Premium Only

	Original Estimate	Actual Contractor Cost	Difference
General Construction			
1. light shelf	$ 8,300	$ 13,791	
2. clerestory windows	15,735	15,735	
3. insulated shade	19,150	13,192*	
4. earth berms	3,900	3,900	
5. roof overhang	6,600	6,600	
6. wall insulation	26,500	20,674	
7. roof insulation	22,500	22,500	
Subtotal	$102,685	$ 96,392	- $ 6,303
HVAC			
1. air handlers	2,355	5,423	
2. night vent			
a) two dampers	302	1,000	
b) three fans	2,541	3,675	
3. auto. temp. controls	22,043	22,043	
Subtotal	$ 27,241	$ 32,141	+ $ 4,900
Electrical			
1. panel & wiring	1,300	1,300	
2. insulated shade	2,300	2,300	
3. ATC for shades, fans, lighting	15,615	15,615	
Subtotal	$ 19,215	$ 19,215	0
TOTAL	$149,141	$147,748	- $ 1,403

*incomplete - remaining work by JCI

FIGURE 6

PREDICTED VERSUS ACTUAL ENERGY USAGE PER SQUARE FOOT - APRIL, 1982

	PREDICTED BTU	ACTUAL BTU	DELTA BTU	DELTA %
HEATING	1414.07	2577.79	+1163.72	+82%
COOLING	146	0	- 146.00	0
DOMESTIC HOT WATER	66.66	27.59	- 39.07	-58%
BLOWERS AND HVAC	266.66	64.41	-202.25	-76%
OFFICE MACHINES	416.66	120.01	-296.65	-71%
LIGHTING	888.83	44.88	-843.95	-95%
TOTAL	3198.88	2833.00	-366.00	-11%

FIGURE 7

PREDICTED VERSUS ACTUAL ENERGY USAGE PER SQUARE FOOT - MAY, 1982

	PREDICTED BTU	ACTUAL BTU	DELTA BTU	DELTA %
HEATING	342.4	865.54	+523.14	+153%
COOLING	1064.6	146.43	-918.17	- 86%
DOMESTIC HOT WATER	66.66	25.02	- 41.64	- 63%
BLOWERS AND HVAC	266.66	103.97	-162.69	- 61%
OFFICE MACHINES	416.66	123.81	-292.83	- 70%
LIGHTING	888.83	186.25	-702.58	- 79%
TOTAL	2480.23	2387.73	- 92.50	- 4%

PROJECT SUMMARY

ENERGY PERFORMANCE OF A PASSIVE SOLAR BANK BUILDING IN MINNESOTA

John Weidt
John Weidt Associates, Inc.
Chaska, Minnesota

PROJECT GOALS:	Design, construct, and monitor a passive solar commercial building.
PROJECT STATUS:	Construction was completed December, 1982. Energy performance has been monitored for five months, January, February, April, June and July, 1982.
CONTRACT NUMBER:	DE-FC02-80CS30353
CONTRACT PERIOD:	October 1, 1979 through 30 June, 1983
FUNDING LEVEL:	$175,385.00
FUNDING SOURCE:	U.S. Department of Energy, Chicago Operations Office.

ENERGY PERFORMANCE OF A PASSIVE SOLAR BANK BUILDING IN MINNESOTA

JOHN WEIDT ASSOCIATES, INC.
401 LAKE VILLAGE CENTER
CHASKA, MINNESOTA 55318

This paper serves as an interim report on the performance of the first 5 months of submetered data on the Security State Bank of Wells, Minnesota and concentrates on the comparison of actual vs. estimated performance of the facility.

A number of caveats should precede the body of the paper:

1. The period described is one of building shakedown, and the energy performance of the facility is expected to improve substantially over time.

2. The automated data collection system has undergone a period of installation, trial and debugging and thus, only partial submetered data is available for the 5 month period.

3. A number of assumptions regarding building systems, occupancy and operation made during the design phase do not match the actual building and operation. Changes to either the predictions or conditions should be made to analyze the accuracy of the prediction techniques.

EXECUTIVE SUMMARY

Based on analysis of the 5 months of submetered data, the following conclusions are offered for consideration:

- Excess gas ue of 97,690 MBTU, at a cost of $400, appears due to problems in outside air controls and thermostat setback. These problems have been corrected.

- Excess electrical energy use for lighting of 13,893 MBTU at a cost of $226 appears due to erratic operation of the lighting systems and extended hours of occupancy.

- Excess energy use for DHW appears to be +- 1900 MBTU at a cost of +- $31 due to excess standby losses or indicative of a sensor problem.

- Excess energy use for Miscellaneous of 11,434 MBTU at a cost of $186 appears due to increased equipment operating hours and increased connected equipment load.

Lights, heating, cooling, fans and DHW are currently operating at +- 3,645 BTU/SF/MO, or 43,740 BTU/SF/YR. The base building used as reference would have an energy use of 80,427, 86% greater than the current bank use, before accounting for extra energy used in increased occupancy hours, cooling to 70 Deg F, etc. This equates to $.33/SF/Yr. Correction of controls for DHW and high volume fan system, operation of the lighting system as anticipated and care in use and occupancy of the building can lead to future energy consumption within predicted values.

COMPARISON OF ACTUAL VS. PREDICTED PERFORMANCE

1. Fuel for Heating

The sensor for monitoring natural gas usage was not installed and operational until July 10, 1982. All usage numbers are directly from the gas meter.

	Predicted MBTU	Metered MBTU	Diff. MBTU	
January	45,170	116,400	- 71,230	
February	32,710	45,400	- 12,690	
April	6,230	19,900	- 13,670	
June	-0-	100	- 100	
July	1,770	4,191		- 2,421
Total	9,900	23,793		-13,893

During the 5 months of submetered data, the lighting system consumed 2.4 times predicted electrical energy.

2a. Calculations

a. The calculation techniques used to predict daylight illumination appear to be reasonably accurate. Further evaluation will be undertaken.

The assumptions used for the calculation of daylight contribution vary from the building's construction and operation in a number of ways.

- Connected Wattage by Zone Varied from Prediction:

Zone	Estimated MBTU	Actual MBTU	% Change
Dalite	6,070	7,948	31%
Misc	1,160	1,074	- 7%
Bsmt	5,150	2,587	- 50%
Total	12,380	11,609	- 6%

Any estimate of lighting energy consumption must be varied by these factors on a zone-by-zone basis. New light fixtures have been added in the basement for computer room usage which were not in the assumptions.

- Hours of building occupancy used in the predictions were far lower than those indicated by the submetered data. Based on employee working hours of 8:00 AM through 4:30 PM four days per week and extended hours through 7:00 PM on Friday nights, the average occupied hours could be 45 hours per week, an average of 198 hours per month for the 5 months with submeterd data. Judging by the on/off status of the 3 major lighting zones, the building was occupied (all or part of the lights were on) an average of 282 hours per month, 43% more than predicted.

- Light levels used as minimums for task and ambient lighting may not match desired levels in the building, judging from operation of the lights in the daylight zone. More observations in this area will be made.

2b. Function

The lights appear to function well as designed, in fact, little use is made of task lights due to the quality of ambient light available. This may, however, account for some of the excess energy use of the ambient system. It may be set to switch on at the task rather than the ambient condition and thus be on for longer hours.

2c. Operation

The lighting system is definitely not operated as assumed.

- Basement Lights: The basement lights appear to be turned on and left on during the day in both the occupied and unoccupied areaas; double the hours of use predicted.

- Miscellaneous Lights: 80% of the lights in the miscellaneous service areas and auto tellers areas appear to be turned on and left on throughout the day. Since much of this area is partial use, and some of it serviced by daylight, the use of lights in this area was assumed to be far less than actual.

- Daylight Zone Lights: Except for random weeks, the ambient lights in the daylight zone are on for most of the daylight hours, contrary to assumptions. Several reasons for this are possible:

a. Insufficient daylight light is available to perform the tasks in the area due to:

1) outside light availability
2) daylight distribution performance

The outside light level sensors have proved erratic in operation and do not indicate past light availability reliably. Judging by on-site light meter readings made on clear and cloudy days, the daylight factor predictions made for the space appear reasonably accurate. Further, several on-site observations have indicated that the light systems are switched on and left on even during periods of adequate daylight.

b. Automatic sensors are overridden and lights remain on even during periods of adequate daylight. The light sensor relays can be manually overridden. The switches have been observed in the manu on position during some site visits. A review of submetered data indicates relatively consiste patterns of the entire daylight zone switched on shortly before 8:00 AM and left on all, or a majority, of the day. A detailed review of hourly data for several July weeks indicates that on certain days or series of days, the lights are on when more than minimal task or ambient light levels are available at the tellers and bookkeeping areas. On other days, the artificial light

system is off during equivalent light availability, indicating manual override during the day-long lights-on situations.

c. Automatic sensors are set to switch on the ambient lighting system at task, rather than ambient levels, thus lengthening the operating hours of the system.
The time of automatic on/off was observed during the debuggin trips of July 10 and 16 and appeared to be set at ambient light levels used during prediction runs.

3. Electricity Used for Energy Distribution

The electricity used for energy distribution is 12% less than predictions.

	Predicted MBTU	Actual MBTU	Diff.
January	2,560	4,131	- 1,571
February	2,300	2,877	- 577
April	2,590	2,436	154
June	4,540	3,469	1,071
July	6,390	3,280	3,110
Total	18,380	16,193	2,187

The extra energy used during the winter months appears due to a combination of factors:

- Connected fan horsepower is 28% higher than anticipated.

- The fans run longer than anticipated due to lack of night setback and increasing the minimum outdoor air control above maximum.

- Use of the high-velocity fan during periods of overheating on sunny days.

The energy use for distribution is lower than anticipated during the summer months. The high-volume, high-velocity fan system was anticipated to use a considerable amount of power during this period, however, it appears to have been stepped down so that the motor is loaded only slightly. This may lead to an insignificant cooling contribution on the part of the fan with attendnt increased chiller load.

4. Electricity Used for DHW

Less than 20 days of submetered data are available for analysis. Based on this data, however, the DHW unit appears to be using triple the predicted load. A review of the hourly data indicates that there is a base (standby) consumption of 2X the actual use. This data indicates either a sensor calibration problem or excess standby losses that require attention.

5. Electricity Used for Chilling

Less than 14 days of submetered data are available for analysis. This data indicates operation of the chiller system at or modestly above prediction.

6. Miscellaneous

The miscellaneous sector has used 124% more energy than originally predicted.

	Predicted MBTU	Actual MBTU
January	4,260	8,084
February	3,830	5,234
April	4,320	10,296
June	4,320	11,311
July	4,260	12,175
Total	20,990	47,100

The extra energy use for miscellaneous may be due to a variety of factors:

- Building occupied hours are higher than anticipated; an increase in miscellaneous energy may be expected.

- Miscellaneous energy includes DHW and cooling energy use except for part of July. This can account for 2565 MBTU in DHW load (based on July DHW energy use) and 11,275 MBTU cooling load (based on predictions for April, June and July), leaving 33,260 miscellaneous energy use.
- More miscellaneous equipment is connected to the building than anticipated. Predictions were based on 6220 watts of connected miscellaneous equipment. Unanticipated added equipment includes a Digital microcomputer with hard disks, high speed printer and four terminals.

Project Summary

Project Title:	A Case Study of Two Passive Solar Commercial Buildings
Principle Investigator:	Tom Hartman
Organization:	ESG, Inc. 2231 Perimeter Park Suite 11 Atlanta, Georgia 30341
Project Goals:	Develop an in-depth analysis and case study on the performance of two passive solar commercial buildings: the Johnson Controls Branch Office, Salt Lake City; and the Security State Bank Building, Wells, Minnesota.
Project Status:	Initial efforts are underway in computer modeling, daylighting, analysis, and selection of instrumentation. The goals will be accomplished through three inter-related efforts: Computer modeling will be used to provide normalized performance of the building. The computer model will be calibrated using measured performance data. Once an accurate model is obtained, the effects of parametric variation (glazing areas, etc.) can be studied, along with the suitability of the design solution to other climates. The buildings will be monitored in the field to very intense levels for brief periods of time in order to provide the data necessary for the model calibration. In addition, this field data will allow a deeper understanding of the current building operation. Daylighting is expected to provide a significant portion of the building's energy savings. This will be investigated using both computer and architectural models in conjunction with the field performance measurement.
Contract Number:	DE-AC02-82CE-30742
Contract Period:	July 20, 1982 - June 30, 1983
Funding Level:	$156,414
Funding Source:	U. S. Department of Energy through Chicago Operations Office

DOE/CE/30742-1

ADVANCED PERFORMANCE MONITORING & ANALYSIS FOR THE JOHNSON CONTROLS BRANCH OFFICE AND SECURITY STATE BANK

Tom Hartman
ESG, Inc.
2231 Perimeter Park
Suite 11
Atlanta, Georgia 30341

Abstract

Initial work has started on a project to conduct performance monitoring and analysis on two passive solar commercial buildings: the Johnson Controls Branch Office, Salt Lake City, Utah and the Security State Bank, Wells, Minnesota. This project will use intensive performance monitoring (over limited time spans), computer modelling, and daylighting analysis to generate extensive quantitative information. This includes the current performance of these buildings versus the design predictions; suitability of the design solutions to other climates and operating conditions; and the impact on performance if new materials and components are utilized. The paper describes the philosophy of the project, how the work is to be carried out and integrated, and describes the types of results that are expected.

Introduction

With few exceptions it has been widely accepted that performance monitoring is a desirable feature. Rarely, however, is the question asked "Why?" Normally the answer to this question is that we desire to know if the building is meeting the design expectations and to provide documented performance data for future designs. The problem is that normal performance monitoring does not answer these questions. Conventional performance monitoring will indicate what the building's performance was on a particular date, or during a particular period of time. It will also tell us if the building is not being operated in the designed manner. The information that we really want is, given "normal" weather or conditions, how will the building work; and how will the building work if operated as intended.

The U. S. Department of Energy's Chicago Operations Office has contracted with ESG, Inc. to conduct a project to study the performance of two passive solar commercial buildings: the Johnson Controls Branch Office in Salt Lake City, Utah; and the Security State Bank Building in Wells, Minnesota. The key questions to be addressed are: Is the building meeting the design goals? Is this design solution appropriate for other climates? How would the availability of new components and materials change the performance? In order to answer these questions, a three fold approach involving computer modelling, performance monitoring, and daylighting analysis is being used (Figure 1).

Computer Modelling

A major component of the project is the computer modelling effort. The subject buildings will be modelled using BLAST 3.0 as currently implemented at Lawrence Berkeley Laboratory (LBL). BLAST 3.0 was chosen due to its analytic rigor and availability of support from LBL. An initial BLAST model is being developed to provide information on expected building performance. In addition, this model will provide information necessary for selection of sensor locations for the field monitoring. Input data for the model comes from the building working drawings, final design reports, and the initial daylighting model.

Upon completion of the first round of field monitoring, the BLAST model will be "calibrated". The computer model will be adjusted so that the model performance matches the measured building performance. This may involve some minor code modifications, but principally will involve changing schedules, internal loads, and equipment characteristics to match the actual conditions at the site.

Using this modified model, a preliminary sensitivity analysis will be conducted. This preliminary analysis will be used to identify sensitivity studies to be conducted in the field. The selected studies can be readily implemented yet produce measurable changes in the building performance. An example would be changes in the glazing transmittance such as temporary application of a film.

Once the field sensitivity studies are accomplished, the BLAST models will be recalibrated to demonstrate the same performance sensitivity. This final model will give the same predicted performance as the measured building performance, and, as closely as possible, exhibit the same sensitivity to parameter variation. With the computer model, however, we can readily make changes in materials, operating schedules, or even location simply and so inexpensively. Parametric

studies using this model can answer the questions that we started with.

Field Monitoring

The necessary close interaction between the computer modelling and the field measurement makes for some interesting constraints and opportunities in field measurements. Sensor selection and data point selection are critical. Typically, a building is monitored for a long period of time in order to ensure that the entire range of climatic and operating variables are encountered. In this project, the buildings will be monitored for a brief period of time. This will be long enough, however, to obtain the necessary data to calibrate the computer model. This means that the absolute accuracy of the sensors will be critical. The sensors used will be relatively sophisticated.

Field performance measurement for each building will be conducted in two phases. The first phase will provide data for the initial model calibration. This phase, lasting for approximately five days, will provide the baseline performance data on the building. In addition to acquiring measured performance, such necessary data as occupancy profiles, equipment nameplate data, etc. will be gathered.

The second phase of the field monitoring efforts consists of a number of short sensitivity studies. This will involve modifying the building, monitoring it for a short period of time (3 days), then restoring the building, modifying another feature, etc. This second phase will take approximately two weeks per building.

Daylighting Analysis

Both buildings derive a significant amount of their projected energy savings from the use of daylight to offset artifical lighting. Unfortunately, daylighting analysis tools are not at the same advanced state of development as building heat transfer models. For example, daylighting analysis in BLAST consists of a "percent replaceable" parameter. Therefore the daylighting analysis results are actually a required input to the computer model. This required input is determined through a four step process involving field measurements and architectural models. First, the lighting levels resulting from electric lighting on the various workplanes is calculated using standard techniques. Accurate architectural models are then used to determine the lighting levels on the various workplanes resulting from diffuse solar radiation alone, and then from total solar radiation under a clear sky. Concurrently a larger scale model of the glazing system would be used to measure the total solar radiation exterior to, and admitted by, the glazing. This second step is repeated for each hour of the day, for several seasons (probably the solstices and equinoxes). If the results show that daylighting is strongly affected by time of year, then more intermediate dates may be required. Finally, based upon the daylighting levels and incoming solar radiation measurements, the usable fraction of beam and diffuse radiation are determined. The fraction of electric lighting that is replaced is then a straightforward calculation, depending upon the efficiency of the lighting. By the use of these two techniques, the daylighting inputs can be modelled and manipulated in the same manner as the computer models.

Results

The foregoing process will develop very accurate computer models of the buildings under study. The results of this project, however, will be achieved through application of this model. It will be determined whether or not the building performance meets the design expectations; if the design solution is suitable to other climates and operating conditions; and what impact will new and improved materials and components have on the performance.

The building performance estimates that currently exist are based upon a number of design tools and assumptions. The computer models allow us to generate performance estimates based upon actual operating conditions, but using standard weather data for reference purposes. In addition, comparison of the design assumptions with the actual building operating conditions will allow analysis as to how critical these assumptions are, and as to the adequacy of the design tools used.

The computer model also allows us to develop a deeper understanding of the building process through parametric analysis. The computer model allows us to charge operating schedules, equipment sizes and performance, aperture areas, insulation levels, thermostat schedules, and even building location in a rapid, straightforward, and inexpensive manner. From such analysis the suitability of the design for other applications, or locations, can rapidly be inferred.

Finally, the models will be useful tools for the development of new materials and components. Not only will the analysis indicate areas where performance improvements can be made, but a means of simulating the effect of new components in an actual building will exist.

Acknowledgements

The work described above is a team effort. This team involves not only ESG, Inc. staff but the designers of the building (principally John Schade and John Weidt), Lawrence Berkely Laboratories (Ron Kammerud), Burt Hill Kosar Rittleman (Harry Gordon), Mueller Associates (Jeff Sningleton) and U.S. DOE.

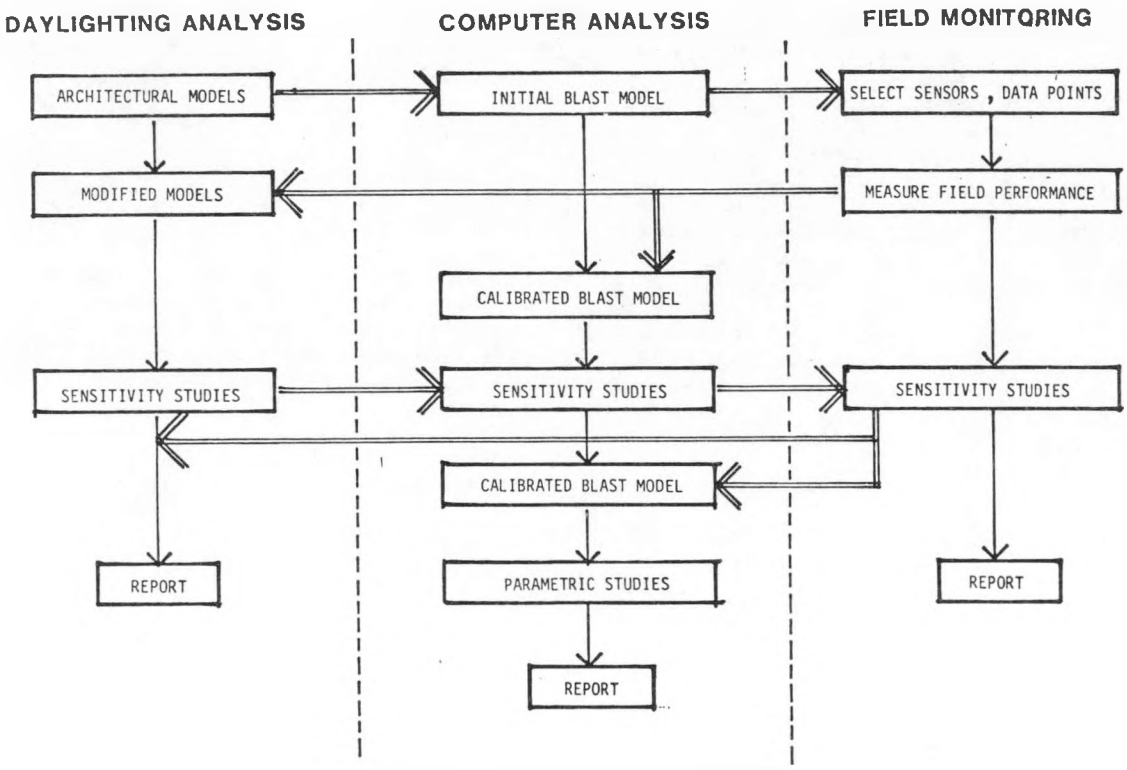

FIGURE 1 - PROJECT FLOW CHART

September 9, 1982

PROJECT SUMMARY

Project Title: Design guideline for commercial buildings: Design process design tools by building type

Program Manager: Robert N. Floyd

Organization: Tennessee Valley Authority
Commercial and Industrial Passive Solar Buildings
350 Credit Union Building
Chattanooga, Tennessee 37401

Principal Goals: To develop guidelines and tools for private architects, engineers, developers, planners, and investors to design energy-efficient buildings, to optimize energy-conscious investments, and to enhance the possible evaluation of a less energy-demanding commercial and industrial building stock.

Project Status: Design guideline for schools will be completed by January 1983. Work on the guidelines for four other building types has started and is expected to be completed in 1983.

Funding Level: Tennessee Valley Authority

DESIGN GUIDELINES FOR COMMERCIAL BUILDINGS: DESIGN PROCESS DESIGN TOOLS BY BUILDING TYPE

Robert N. Floyd
350 Credit Union Building
Chattanooga, Tennessee
37401 USA

ABSTRACT

The Tennessee Valley Authority and its architectural, engineering, and other professional consultants are now developing Design Guidelines for commercial and industrial buildings. Design Guidelines for twenty building types are scheduled for development over the next few years with five Design Guidelines being produced at this time. This paper describes the structure and content of the Design Guidelines and addresses a few key issues surrounding the development and use of these essentially resource oriented design process design tools.

1. INTRODUCTION

The Design Guidelines contain individual and summarized end-use energy data for each building type. The unique economic conditions of each building type are discussed and a graphic tool for optimizing solar and energy conservation investments is presented. Energy planning rationale and energy programming graphic tools are included and discussed. An analysis method for selecting the appropriate design direction(s) is described and energy saving design strategies are listed, analyzed, documented, ranked and discussed. Designs generated by TVA and its consultants using the Design Guidelines are included as examples.

The Design Guidelines are intended to facilitate design professionals in their conscious efforts to design energy efficient buildings, to optimize energy conscious investments, and to enhance the possible evolution of a less energy demanding commercial and industrial building stock.

2. OUTLINE OF DESIGN GUIDELINES

2.1 Section 1. Introduction

This section discusses the scope and intent of the manual in the context of organizational structure, and the contents of the manual. The audience for whom the manuals are written and their essential qualities are described.

2.2 Section 2. Preface

In this section the line is drawn when the question is asked, "What is different about energy-conscious design?" The answer composes the next twelve pages of the manual encompassing the key elements of energy planning, which include: an essential cognizance of the relevance of energy as a design element, understanding the shortcomings and organizational constraints of the old "Design Team" approach and the blurred lines of responsibility within the "New Energy-Conscious Design Team." Energy is discussed as the fifth and additionally complicating element of William Pena's now complete design determinants: FORM, FUNCTION, ECONOMY, TIME AND ENERGY. The issues of better information and useable design tools are contrasted to "Energy Performance Standards" and arbitrary but legislatable "Energy Budgets." Conventional architect, engineer and client roles are reviewed and the primary elements of Energy-Conscious Design are graphically delineated and supported with illustrations and photographs.

2.3 Section 3. End-Use Energy

This section gives definition to the building type. Drawing from thousands of energy audits, performed over the past few years by TVA and its contractors, end-use energy data is presented in both a summarized format showing the aggregate energy use characteristics of a building type and the areas of obvious sensitivity and in a matrix format identifying specific physical and operational characteristics of a large number of individual representative buildings selected to illustrate apparent significant sensitivities of the given building type.

This energy end-use data base allows the architect, engineer and building owner an historical empirical foundation on which to base initial discussions regarding their project. The data base simply gives context and information about the energy characteristics of a building type. As the energy end-use data base gives historical empirical information on consumption and demand, it also gives valuable information on energy costs and trends.

2.4 Section 4. Economics

This section begins by describing the general economic and financial nature of each building type. Energy design costs, operating costs, motivation, organizational constraints for making additional investments and programming economic values are addressed and some regularly overlooked energy costs issues such as demand charges and rate structures are discussed.

In addition to putting energy cost issues in the context of the building type, an innovative approach to analyzing energy-related design decisions is presented, consisting primarily of a graphic tool for optimizing solar and energy conservation investments. The graphic tool is the key element in the design process used in the Design Guidelines. It is composed of a set of interchangeable economic nomographs which allow the building owner to input his/her assumptions. The output of the nomographs establishes a threshold in time by which the value of any energy strategy can be assessed on the merits of the owner's assumptions, eliminating arbitrary payback periods and the need for dubious base case comparisons. Based on the economic assumptions and the investment threshold an entry is made into a final set of nomographs whose output describes the net cash flow. The tool can be operated in reverse to determine or observe potential adjustments to the initial economic assumptions.

2.5 Section 5. Process

The following topics are discussed: Energy-Conscious Design Team Selection, E.C.D.T. Work Plan, Energy Planning, Architectural Programming, Energy Programming, Energy Program Analysis, Energy Problem Statement, Energy Opportunity Statement, Economic Analysis of Energy Opportunities, Design Directions, Energy Strategy Development, Economic Analysis of Energy Strategies, Energy Strategies Selected, Design, Design Analysis, etc.

Most are graphically presented in such a way as to provide the user with fill-in-the-blank formats and a sequential order intended to emphasize an appropriate order of pursuit occasionally leading the user back through the process.

Programming forms, analysis procedures, graphic tools, basic background information, identified resources and lists of energy strategies analyzed and documented allow the user to adopt the energy-conscious approach to design without the enormous research expense and with an enormously enhanced potential for success.

2.6 Section 6. Strategies

A master list of over 250 energy-saving strategies has been developed and concept pages addressing the characteristics of each strategy and comments on their relative values are discussed with respect to the building type. Each strategy or group of strategies having been analyzed is grouped with other complimentary or categorically similar strategies and listed as energy conserving or climate-adapted.

Energy strategies or groups of energy strategies especially appropriate for consideration with respect to a given building type are identified as such in the concluding statement. Conversely, strategies that are inappropriate for consideration are identified and the excluding characteristic is noted.

2.7 Section 7. Examples

Noteworthy examples of existing energy efficient projects will be listed as appropriate case studies. In instances where the use of the Design Guidelines and the associated reseach indicates an opportunity to present advanced design solutions, the designs generated will be included as case studies as well.

2.8 Section 8. Reference

- o Economics
- o Calculation Procedures
- o Glossary
- o Bibliography
- o Index

Reference material per building type.

3.0 CONCLUSIONS

The emphasis of the Commercial and Industrial Passive Solar Buildings Program of the Tennessee Valley Authority is and has been (since its inception in January 1980) on the development of process design tools and the development and documentation of the necessary relevant information for use in conjunction with these design tools.

The building type approach is intended to generate a product directly in response and complementary to the needs and efforts of design professionals and building owners.

It is our belief that the best way to save energy in the commercial and industrial building sector is by assisting those who make programmatic and design decisions affecting the energy requirements of commercial buildings as an element of an ordinary day's business.

PROJECT SUMMARY

Project Title: Commercial Industrial Passive Solar Buildings Project

Project Manager: Kaihan D. Strain

Organization: Tennessee Valley Authority
Commercial and Industrial Passive Solar Buildings
350 Credit Union Building
Chattanooga, Tennessee 37401

Principal Goals: To significantly influence the development of more energy-efficient commercial and industrial building stock, to reduce energy consumption in 2,000 new buildings/year and 93,000 existing buildings in the Tennessee Valley region.

Methodology:
1) Technical and design assistance program to private sector architect, engineer, planner, developer, investor, etc.
2) Demonstration and monitoring
3) Design guidelines
4) Educational program

Project Status: As of August 31, 1982
1) Significant assistance given to 136 Commercial and Industrial projects.
2) Design of 1 demonstration greenhouse is completed, 7 others will start soon. Five buildings are in different stages of being monitored.
3) One design guideline will be completed by January 1983, and 4 others are being worked on.
4) A number of seminars and training courses for E/A's, Tennessee Valley Authority staff, and university students have been conducted.

Funding Level: Tennessee Valley Authority

SLIDE PRESENTATION ON COMMERCIAL INDUSTRIAL PASSIVE SOLAR BUILDINGS PROJECT

Kaihan Strain
Tennessee Valley Authority
Commercial and Industrial Passive Solar Buildings
350 Credit Union Building
Chattanooga, Tennessee 37401

PROGRAM PURPOSE AND APPROACH

The intent of the Commercial and Industrial Passive Buildings Program is to significantly influence the development of a more energy efficient commercial and industrial (C&I) buildings stock. This program seeks to influence the design of as many as possible of the 2,000 new C&I buildings constructed annually within the TVA region. The program also attempts to influence as many as possible of the 93,000 existing buildings which in 1979 constituted just under one billion square feet of C&I buildings. The goal of the program is to assist owners and designers of C&I buildings in their efforts to manage and design buildings that require less energy. The ultimate result will be buildings with manageable energy demands that will prove mutually advantageous to the building owner and the energy suppliers.

The methodology which we intend to employ to achieve these goals is composed of three primary components: Technical Assistance and Design Assistance, Design Guidelines, and Demonstration and Monitoring. Through these three component approaches and with the cumulative experience, knowledge, and established cooperation of many TVA employees we hope to significantly influence energy utilization in C&I buildings. Total energy savings of 40 to 65 percent have been achieved through the incorporation of passive design in C&I buildings. The three C&I Passive Building Program components, described in the following papers, should be sufficient to encourage, expedite, and facilitate similar results throughout the TVA region in the near future.

PROGRAM COMPONENTS

Technical Assistance and Design Assistance

Technical and design assistance was first delivered to private sector building owners and designers in late 1978. The Architectural Design Branch was the office that responded to technical and design questions from the private sector at that time. In January of 1980 the Solar Applications Branch assumed responsibility for managing these efforts and is coordinating this function in cooperation with the Architectural Design Branch and C&I engineers in the district offices.

The assistance being delivered is composed of a wide variety of technical, design, and financial advice and services. Technical questions and answers are often addressed to issues such as computer modeling of the energy dynamics of existing buildings or new designs. Design questions generally revolve around proper site selection, landscape design, building form or configuration, glazing area sizing, shading design, system selection, and a proper understanding of the nature of energy and how it is associated with the design and function of any building. Financial questions are primarily related to cost effectiveness of various solar designs and solutions.

To date (August 1982) 275 formal requests for assistance have been received and processed. Of these, 136 have received significant assistance from TVA.

Numerous benefits are being gained through the technical and design assistance component. By helping individuals throughout the TVA region who have the personal initiative to seek out assistance on their own projects, TVA is helping to ensure that fewer mistakes are made as innovations in design are attempted. TVA staff and private sector designers who cooperate in these assistance efforts are gaining valuable knowledge and experience on a variety of applications which can be shared with other designers. The interaction between TVA staff and private sector C&I building owners and designers is essential in gathering pertinent data and information about a wide variety of C&I building types. This information can be used to assess the impacts of energy-efficient design for the consumer and power system and is also necessary for the development of the other two components of this program. The financial and technical information generated by this component may be very helpful in dissolving many of the myths that surround solar energy at this time and may be valuable in efforts to remove institutional barriers that are presently hindering the development of renewable energy systems applications.

The discussion to this point has centered on the one-on-one interaction between TVA staff members and individual private sector C&I building owners and designers. However, another important aspect of the Technical Assistance and Design Assistance Program is the educational and training activities that are being carried out by the staff members involved in delivering assistance. The Solar Applications Branch and the Architectural Design Branch of TVA have conducted several in-house capabilities, a series of seminars for A/E's, and have taught the students of fifth-year design at the University of Tennessee at Knoxville. Also, two joint seminars, co-sponsored by TVA and the Solar Energy Research Institute (SERI), have been conducted at an intermediate training level for private sector architects, engineers, and district C&I solar specialists.

Design Guidelines

Whereas the technical and design assistance portion of the program provides direct and individual attention to the specific problems of a project, the limits to the amount of individual assistance that can be delivered to the private sector will always fall short of the need. For this reason, the second component of the C&I Passive Buildings Program is designed to have a broad based application.

The Design Guidelines component of our program takes into account the fact that there are thousands of professional designers and thousands of C&I projects initiated annually within the TVA region. If these projects are to be influenced toward energy efficiency, the most feasible route appears to be to facilitate the designers of these projects by placing in their hands the necessary tools required to do the job rather than to attempt to assist all these projects on an individual basis. The design guidelines are these tools and, once developed, would be useable by private sector architects, engineers, planners, developers, and investors as well as TVA's design and planning staffs for designing more energy-efficient buildings. Although developed specifically for use within the TVA region, their use could easily be adapted for use throughout the nation by some simple adjustments to the weather data portions of the document.

The guidelines will be assembled to help designers and decision makers ask the appropriate questions at the appropriate time in the design process and will assist in making the right choice as to which design direction should be taken or which system should be selected. They will consist of information about weather, building types, financial characteristics, load profiles, and system concepts and methodologies which pertain to energy use and availability. This information will be provided in a manner that can be easily used by anyone involved in the design of a commercial or industrial facility.

Demonstration and Monitoring

The third component of the program is demonstration and monitoring. This component is designed to accomplish two basic objectives: (1) to ensure that necessary data is available to validate energy assumptions used in the technical and design assistance and design guideline components of the program and (2) to ensure that examples of cost-effective and innovative passive solar energy solutions are pursued and given adequate exposure so as to encourage the adoption of these concepts by others.

These objectives can be achieved in several ways. Some passive solar and energy-efficient design projects are being undertaken in the private sector as a result of the technical and design assistance which has been provided. Monitoring efforts are presently underway on five projects which received technical and design assistance. As more projects are completed that have received technical and design assistance and that show special potential for achieving a high level of energy savings, they will be monitored to verify and define the limits of their performance. Monitoring activities will also be required in some cases to generate profile data on building types that are to be covered by the design guidelines.

Demonstrations requiring some financial assistance may be desirable in instances where the project has a high potential for public exposure and replicability. Numerous requests were received from school officials and teachers asking that we assist them in demonstrating to their students alternative ways of supplying and using energy. They recommended involving their students in the design, fabrication, construction, and maintenance of passive solar systems. These systems will be retrofitted to their existing school buildings and be highly visible to the public. We therefore initiated a limited demonstration program consisting of the retrofit to schools of 7 passive solar greenhouses supported by TVA. One demonstration passive solar retrofit greenhouse will be completed in each of the 7 districts within the TVA region. These retrofits will be comparable to the type of retrofit that would be applicable to a single family residence.

SUMMARY

These 3 components constitute the major activities planned for addressing the many questions that surround the complex issue of energy use in C&I buildings. The technical assistance and design assistance component provides needed one-on-one assistance to those designers and owners who are ready to incorporate passive solar features into their buildings. The design guidelines component seeks to address the problem on a broader basis by providing tools for determining appropriate energy solutions for the major C&I building types. The third component, demonstration and monitoring, is needed to validate and generate data for the first 2 program components and to ensure that cost-effective and innovative passive solar solutions are pursued. Although no single one of these components could satisfactorily address the C&I buildings problem, together the components provide a sound, comprehensive approach toward incorporating energy-efficient passive solar techniques into the design of new structures and the modification of existing structures.

PROJECT SUMMARY

Project Title:	Passive Solar Commercial Buildings Program Gunnison County Airport Terminal
Principal Investigators:	Dr. Jan F. Kreider Leon H. Waller
Organization:	Gunnison County Board of County Commissioners 200 E. Virginia Ave. Gunnison, Colorado 81230
Project Goals:	- With the project being located at an elevation of 7664 feet in the central Rocky Mountains of Colorado, the primary concern was to design for the extreme heating loads while the cooling loads were not of any significance. - The owner desired a solar system that utilized a minimum of mechanization so as to decrease the level of technical expertise required to operate and maintain the building. - With the building serving as a gateway to a recreation oriented market, the exposed elements of the solar system had to be designed in an aesthetically pleasing manner. - Design an energy conscious shell so as to minimize the total energy loads. - Integrate the solar system with the back-up, conventional mechanical system. - Economic evaluation of the solar system as to both initial cost and life cycle cost compared to conventional construction.
Project Status:	The project was substantially constructed and occupied in a November of 1980. After a de-bugging period, instrumentation was installed in order to monitor the building's overall energy consumption. Data collection will continue until September of 1982, after which time a final report will be prepared which will cover the following topics: - Comparisions of the end use energy consumption to the initial design assumptions - Analysis of climatic occupant and other variables as to their effects on the data - Recommendations to the owner as to how to improve the building's energy performance through operations and/or design modifications.
Contract Number:	DE-FC02-80CS30339
Contract Period:	October 1, 1979 through December 30, 1982
Funding Level:	$96,091
Funding Source:	U.S. Department of Energy

PASSIVE SOLAR COMMERCIAL BUILDINGS PROGRAM

GUNNISON COUNTY AIRPORT TERMINAL

Dr. Jan F. Kreider
Jan F. Kreider & Associates
1455 Oak Circle
Boulder, CO 80302

Leon H. Waller
Associated Architects of Crested Butte
P.O. Box 1209
Crested Butte, CO 81224

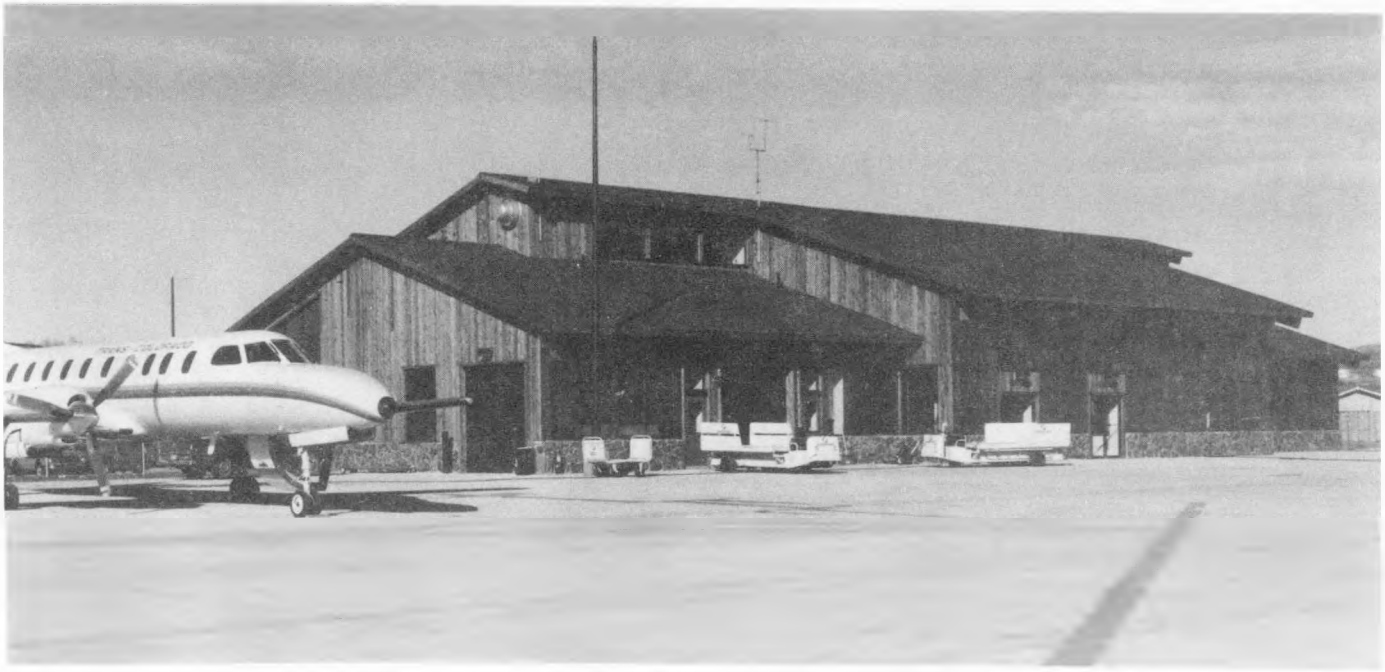

I. INTRODUCTION & SUMMARY

It is the purpose of this report to present the preliminary results of solar system performance studies carried out on the final construction of a passive space heating system for the Gunnison County Airport Terminal. The principal topic of this report is the economic performance of the system with supporting material on thermal performance and system design.

II. BUILDING AND SOLAR SYSTEM DESCRIPTION & THERMAL DEMANDS

The building is approximately 70' x 140' with the long axis east-west to favor high solar gain on the south wall. (See Figure 1)

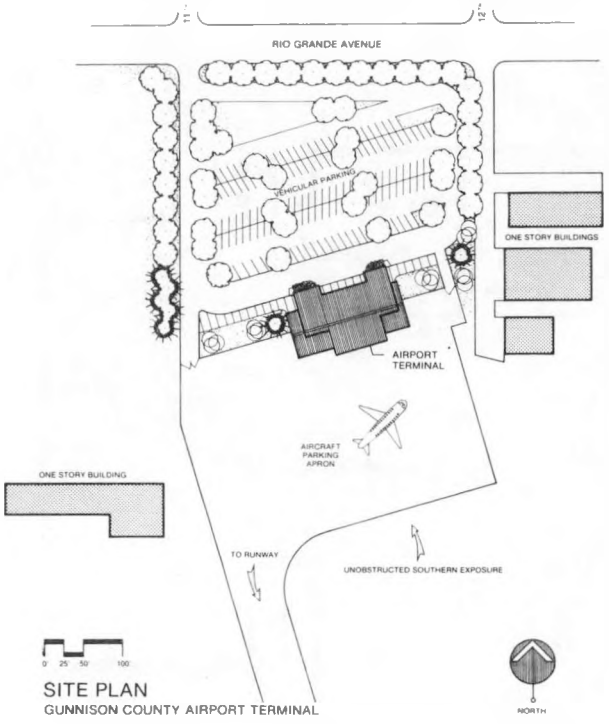

(Figure 1)

the airport is not operating.

In response to the extremely cold climate of the Gunnison site, high insulation levels have been used. The roof assembly is insulated at R-33 and the wall assembly at R-21. Double glazing is used throughout the night insulation at R-10. To control infiltration losses at the entry/exits, air locks are specified. Slab perimeter insulation is used to reduce floor heat losses.

The peak heat load on the building is 314,000 Btu/hr for a design interior, night temperature of 55°F. During the operating day (8 hrs) with 65°F interior temperature, the peak heat load based on design -17°F outdoor temperature is 355,000 Btu/hr. Stated another way, the heat load is 7 Btu/ft^2/degree day - a rather low value reflecting the high levels of wall and window insulation and tight construction used. Heat loads were provided by Winzer-Ottmer Consulting Engineers.

Internal heat sources tending to reduce the heat load including lighting at an average of 1.5 W/ft^2 and people at 250 W/person if not clothed heavily. In addition, non-public areas such as garage spaces have a lower design temperature to lessen energy demand. Expected annual heating energy consumption is shown in Table 1 based on the preceding loads. The annual demand for heating is seen to be 305.9 MMBtu/yr on the average. The degree day method has been used with the effect of 55°F night setback accounted for by using degree days to base 55°F instead of the usual 65°F for those hours of the day when the airport is not operating.

Table 1. Monthly Heating Requirements for the Gunnison Airport

Month	Load (MMBtu/mo)
Jan.	63.2
Feb.	49.1
March	40.8
April	22.8
May	15.4
June	3.6
July	0
August	.1
Sept.	3.8
Oct.	16.5
Nov.	34.4
Dec.	56.2
Annual	305.9

Based on night set back to 55°F

Heating design data are given below in Table 2.

Table 2. Heating Design Data

Median of Extremes	-21°F
0.2% (18 hrs/yr)	-22°F or below
0.6% (53 hrs/yr)	-17°F or below
Coincident Wind	Very light, 57 mph
Average Barometric Pressure	22.4 in. HG
Latitude	38° 33' NORTH
Longitude	106° 56'
Elevation	7664 ft. msl.

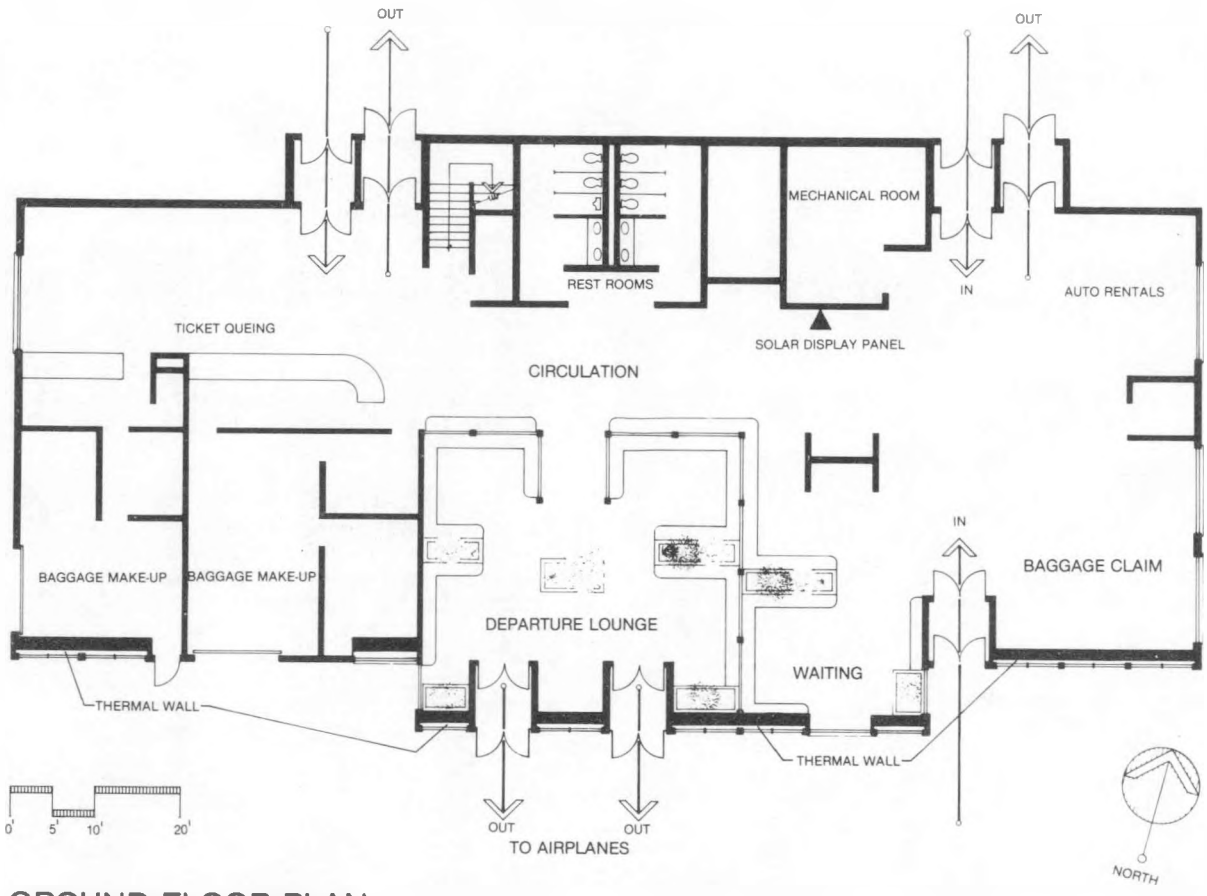

GROUND FLOOR PLAN

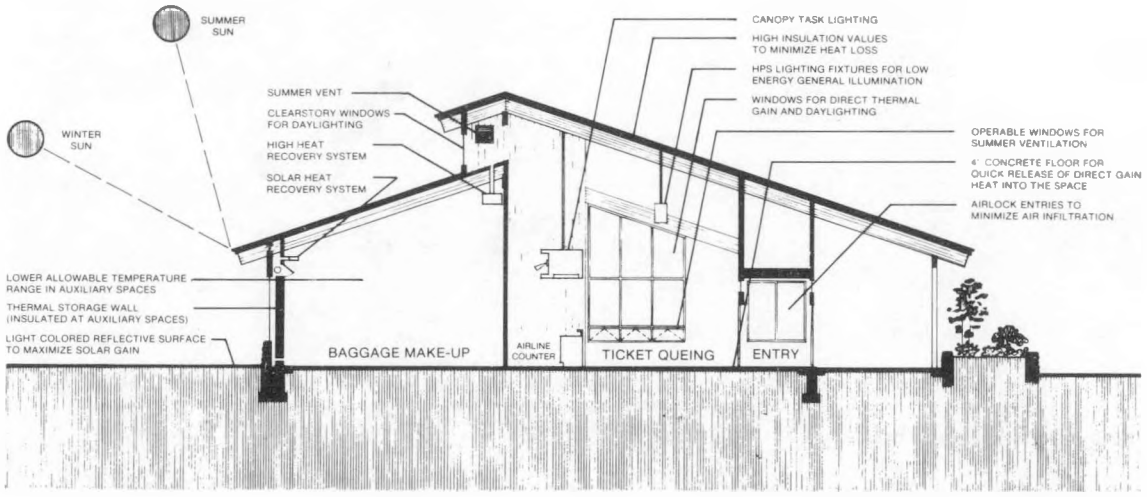

BUILDING SECTION

OTHER ENERGY CONSERVING FEATURES

- MINIMAL GLAZING WITH NORTHERN EXPOSURE
- PROPER ROOF OVERHANG AT THE SOUTH TO SHADE THE FACADE IN THE SUMMER AND TO ALLOW MAXIMUM SOLAR EXPOSURE IN THE WINTER
- HEATING SYSTEM INTERLOCK TO TURN OFF BACK-UP HEATING WHEN GARAGE DOORS ARE OPEN
- STRIP VINYL CURTAINS AT BAGGAGE CLAIM DOORS TO MINIMIZE AIR INFILTRATION
- TEN DEGREE NIGHT SET BACK FOR THE BACK-UP HEATING SYSTEM
- NO MECHANICAL COOLING IS NECESSARY FOR THE MILD CLIMATE. NATURAL VENTILATION IS SUFFICIENT

The architect and solar engineer concluded that a masonry, thermal storage wall (TSW) was the appropriate passive system for the Gunnison Terminal. A moderate amount of direct gain is present resulting from runway viewing requirements. A south facing clerestory of 160 ft^2 (net) provides both light and heat (via the high heat return duct) to the building.

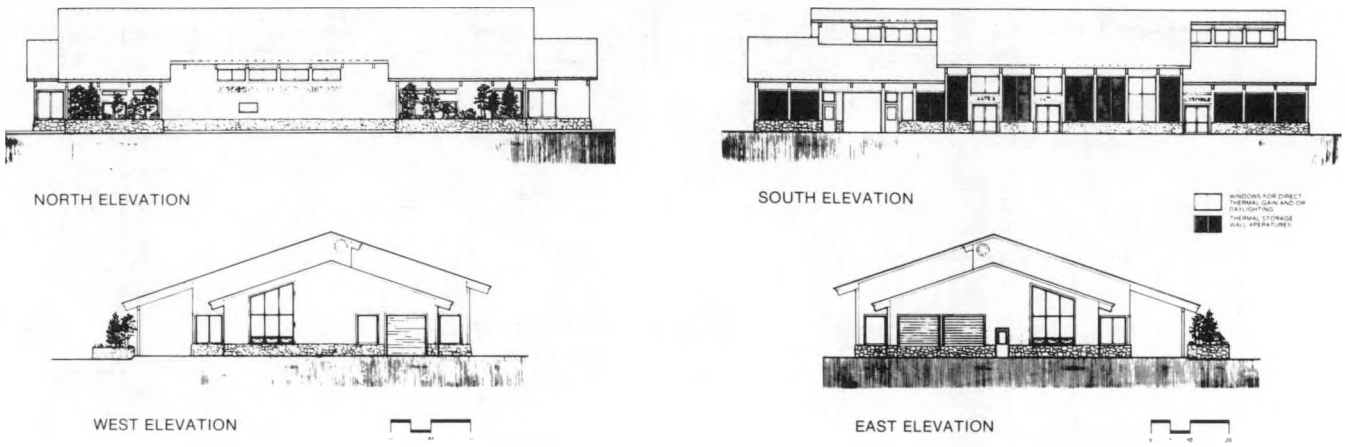

(Figure 4)

Energy collection for heating occurs by absorption of solar radiation and its conversion to heat on the south-facing surface of the TSW. The poured, concrete wall is stained dark earth-brown and absorbs about 90% of the sunlight passing through the south-facing, double-glazed aperture. The heat produced at the wall surface is split into two roughly equal parts. The first slowly passing through the wall to its north side for space heating after sunset for the south zones of the building. The north side is kept clear of furniture, vending machines, etc. to insure good heat transfer.

The remaining heat produced at the wall passes into the air space between the glazing and the wall. The simple airflow diagram (Figure 5) shows the control sequence, If heat is required to a given zone, the low temperature contact on the zone dual-point thermostat will close turning on one of the blowers. Heated air from the south wall enclosure will then be distributed to the zonal load. In this way the passive wall heat can be used throughout the building, not just in the south zones. TSW's at garage spaces are insulated at R-30 in order to maximize heat transfer to the northern zones.

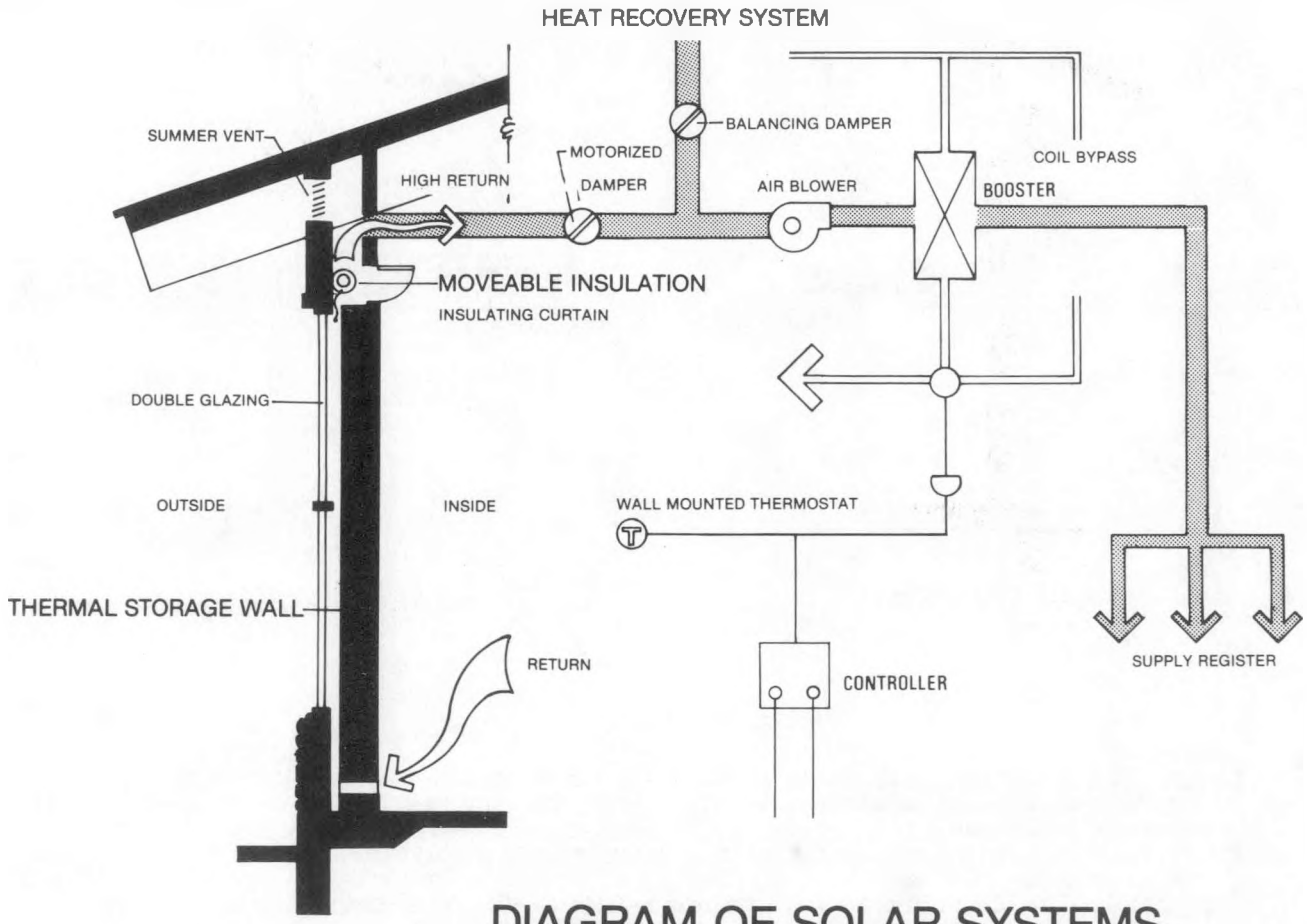

DIAGRAM OF SOLAR SYSTEMS

(Figure 5)

During periods of solar outage, the south facing passive wall will be insulated from the environment by means of insulating "shades" manufactured by Thermal Technology Corporation as shown in the passive wall section in Figure 6. These devices consist of four stagnant air layers separated by aluminized Mylar ™. A typical R-value is R-9 to R-10. The shades run in vertical tracks to block inflow around the edges and the bottom. These shades fully expand to fill the TSW - to glazing gap at night so the usual backdraft dampers for reverse flow control are not needed:

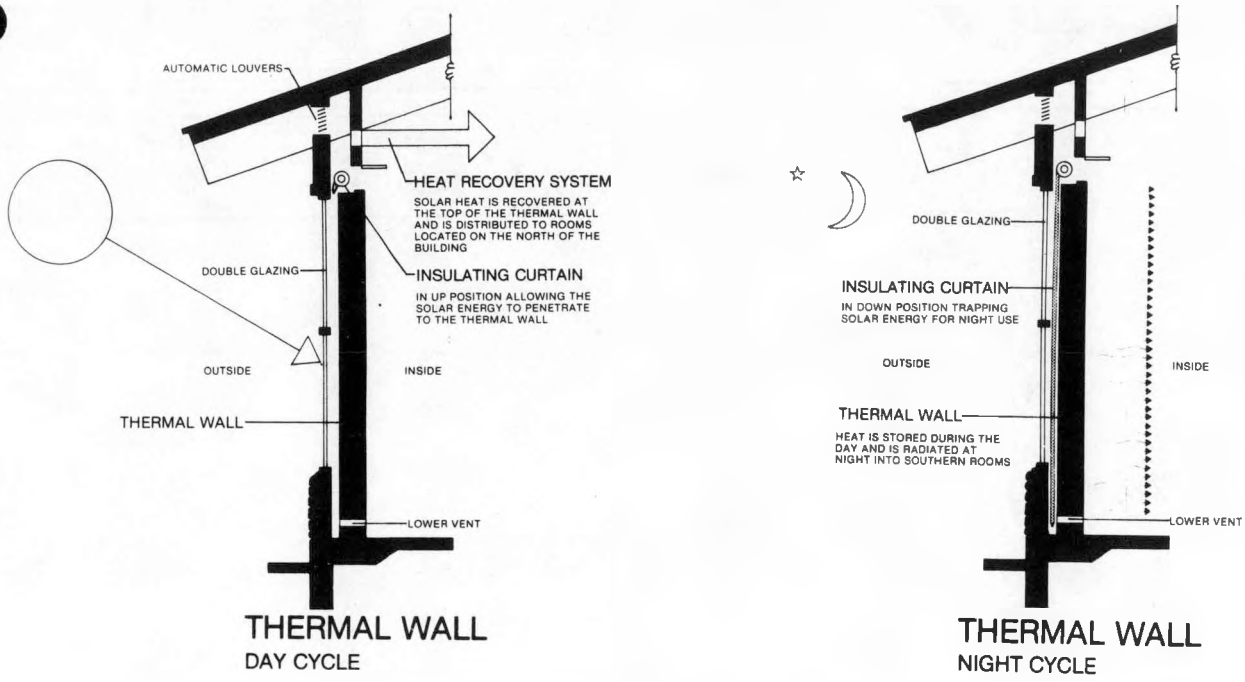

(Figure 6)

The decision as to whether the insulation is open or closed is made by a single, central controller with sensor located as shown in the wall section on the south facade in an area clearly exposed to the sun but concealed from tampering. A manual override is used for manual operation and to reverse the shade operation in summer. In summer, the shade may be closed during the day to block the solar gain and open at night for wall cooling using ambient air.

Storage of heat occurs in the TSW elements constructed on concrete. The specific heat of this material is 0.21 BTU/lb^{o}F and the density is 144 lb/ft^{3}. This results in a sotrage of 30 Btu/ft^{2} glass^{o}F, the optimal amount for a masonry TSW. The transport properties of concrete are such that they provide heat to the space after sunset. To reduce loss from the perimeter of the TSW elements, they are insulated. Nocturnal losses from the south storage surface are controlled by use of the movable insulation described above. A large space at the top of the storage wall permits easy access, through removable panels, to the insulation motor assembly for adjustments and maintenance as needed.

Storage for direct gain heating is provided in the 4" thick concrete floor slab which is directly illuminated by direct gain sunlight. Most of the direct gain serves the purpose of rapid morning heat pickup to warm the building from its 55^{o}F overnight temperature. As a result, storage need not store as large a fraction of the absorbed solar heat as for the TSW. Hence, the use of a thinner floor slab to encourage less storage and quicker release to the space.

III. SOLAR SYSTEM MODELING & THERMAL PERFORMANCE

The expected performance of the passive system has been calculated using the PASSLR computer model developed by Dr. Jan F. Kreider, P.E. It is based on the SLR method developed at the Los Alamos Scientific Laboratory (LASL) from the hourly PASOLE computer model. The night-insulated TSW mode of the model is used.

Table 3 summarizes the solar environment expected for Gunnison. Since no solar data for Gunnison exist, data for Grand Junction, 85 miles away, have been used as a conservative basis for design.

Table 4 summarizes the important physical characteristics of the Gunnison Airport Passive System used in the computer modeling study. The effective passive aperature (TSW plus direct gain aperature) of 1154 ft^{2} represents the maximum available area for this facility.

Table 3. Gunnison, Colorado Solar Climatic Data Summary

Month	Horizontal[1] Insolation (Btu/ft^2 day)	Vertical[2] Insolation (Btu/ft^2 day)	Average Temperature (^{o}F)	Heating Degree Days (Base 65^{o}F)
Jan.	837	1488	11	1686
Feb.	1195	1600	16	1397
Mar.	1600	1441	26	1246
April	2013	1134	40	789
May	2268	899	48	533
June	2610	839	57	282
July	2492	877	62	103
Aug.	2194	1058	61	169
Sept.	1895	1447	53	384
Oct.	1375	1668	43	704
Nov.	959	1625	28	1110
Dec.	782	1542	16	1538
Annual	1681	1302	39	9941

[1]Data for Grand Junction

[2]Calculated based on 20% foreground reflectance; will be higher in winter owing to snow cover

Table 4. Passive System Components

Component	
Net aperture area	1154 ft^2
Wall angle	Vertical (90^o)
Wall azimuth	About SE 15^o
Number of glazings	2
Insulation - night	R-10
Collection type	Dark, Masonry thermal storage
Thermal storage	Masonry; 30 Btu/ft^2 ^{o}F
Air Flow Rate	1 SCFM/ft^2
System location	Gunnison, Colorado

IV. ECONOMIC SUMMARY

Computer performance predictions using the PASSLR model are given in the previous section and a summary of economic assumptions and TSW economic performance are given in Table 5.

Table 5. Gunnison Airport Passive TSW System Economic Summary

Economic Criterion	
Inputs	
Discount Rate	0.0%*
Annual Inflation Rate	10%
Fuel Inflation Rate (DOE Solar Handbook)	16%
Property Taxes	0.0%
Federal Taxes	0.0%
Maintenance of Solar System	1/2 of Initial Cost per year
Life Cycle Term	20-40 yr.
Total Extra Solar System Cost (see breakdown below +)	$45,480
Energy Cost (Electricity)	$7.74/MMBtu
PASSLR Economic Outputs	
Cost of Heating without Solar (20 yr)	$390,860
Cost of Heating with Solar (20 yr)	$291,000
Net Saving with Solar (20 yr)	$100,000
Payback Period	13 yr.

* Airport funding is from FAA grants and explanement revenue. No monies are borrowed. The airport is exempt from local and Federal taxes.

+ Passive wall costs were estimated by the architect and solar engineer and actually installed according to the following figures:

	Actual	Estimated
Concrete	$8,590	$4,100
Concrete Stain	$540	$500
Insulating Curtains	$11,190	$4,950
Curtain Tracks	$1,000	$500
Curtain Access Panel & Hardware	$1,430	$1,840
Thermal Wall Glazing	$9,840	$16,500
Clerestory Glazing	$2,360	$2,400
Fittings	$3,000	$2,200
Heat Recovery Ducts	$5,000	$5,500
Instruments	$1,890	$450
Perimeter TSW Insulation	$640	$700

V. BUILDING CONSTRUCTION, PROBLEM AREAS AND COST ANALYSIS

Actual construction of the building resulted in only minor deviations from the original design concepts. Due to an unavailability of the specified form ties, the contractor modified the TSW detail resulting in 14" thick TSW masses rather than the 12" called for in the drawings. This results in increased thermal storage at no additional cost to the owner. The solar system status panel, which had originally been located in the mechanical room, was upgraded in appearance and moved to the public circulation space. Graphics describing the solar functioning of the building have been placed adjacent to this panel under Phase III of the D.O.E. Solar Cooperative Agreement in order to provide the public a mechanism for self-education when viewing these materials.

Some problem areas occurred during the installation and initial operation of the solar components. Four of the eleven motors operating the movable insulation shades burned out upon initial start-up. Improperly adjusted limit switches and uneven vertical tracts causing the shades to bind were found to be the cause. Cycling of the various mechanical equipment in the different seasonal modes also required extensive review and adjustment. Thorough testing and balancing, adjusting of thermostats and revising of some of the control system circuitry resulted in the described sequencing of the mechanical systems. Inadequate inflation of the insulating shades has been traced to the omission of motorized dampers in the ducts leading from the TSW's to air handler units. Installation of these dampers should allow us to realize the full anticipated R-value for the shades.

Eight change orders were issued during the construction process affecting both the solar system costs and the overall building budget. The solar costs were projected at $39,640 (5.6% of the initial total budget) and at completion were at $45,480 (5.9% of the final budget). A detailed breakdown of cost increases due to solar components appear in Table 5.

Subsequent to the occupancy of the building and the monitoring of the building's energy performance, several other problem areas were discovered. A completely new occupant group took over the facility and they were not instructed on the performance features of the building. They moved their offices into an area not intended for long term use and also brought in heat generating equipment (computers). These new occupants then began modifying building features and operating the building controls in ways detrimental to thermal efficiency. Through analysis of our sub-metered data and user questionaires, we discovered that even though daylighting features of the building often provided adequate illumination, there was no realization of energy savings for lighting. Part of the problem lies in the fact that there is not enough user control at each space, but to a large degree controls are not used when they are available.

After interviewing the building's Operations Supervisor and the Mechanical System Control Engineer, we found several energy related variables. From a design standpoint, the major change was that the night setback control only affected a portion of the back-up heating system. As a result of this the building is heated ten degrees warmer than desired at night. From an operations standpoint the building's energy performance improved due to such owner actions as turning off the make-up air unit in winter and the back-up heating system from May to November. All of these variables must be taken into account in order to produce a valid analysis of the building's actual energy performance.

VI. CONCLUSIONS

The preliminary conclusions of this study, using the methods of computer modeling and life-cycle economics (not analysis of monitored data) are:

1. The final design passive solar heating system with night insulation will provide, on the average, 41% of the annual heating load for the terminal.

2. The passive system will result in a saving of 125 million Btu per year or, equivalently, 36,625 kWh per year.

3. Over a 40-year period the system is expected to save approximately 3 million dollars in heating energy costs after the solar system investment has been paid off. Over the first 20-year period the net savings are approximately $100,000. The simple payback period is 13 years.

PROJECT SUMMARY

PROJECT TITLE: CUMC School: The First Year

PRINCIPAL INVESTIGATOR: Nicholas Peckham AIA

ORGANIZATION: Peckham & Wright Architects, Inc.
1104 E. Broadway
Columbia, Missouri 65201
(314) 449-2683

PROJECT GOALS:

1. Meeting expanded programmatic needs of Community United Methodist Church.
2. Design school to use minimum energy.
3. Maximize use of natural energy sources.

PROJECT STATUS: The School Building has been in operation for one year.

Starting on September 1, 1981, and continuing for one year, natural gas and electrical energy use has been monitored on the new solar school wing and on four other portions of the church complex (i.e. the sanctuary, old house, old educational wing and fellowship hall). The energy use in the School has been very close to the calculated consumption included in the Final Design Report:

	PREDICTED	ACTUAL	DIFFERENCE
Gas	70.1 MBTU	76.7 MBTU	+ 8.6%
Electricity	17.2 MBTU	11.2 MBTU	-53.6%
Total	87.3 MBTU	87.9 MBTU	+ 0.7%

The building has one year of fine tuning where owners, users and consultants have worked toward minimizing energy consumption while maximizing comfort.

The CUMC School has had several secondary effects on the City of Columbia. It has been the site of many public meetings including two solar conferences, and the school's Total Energy Index of 15,798 BTU/SF/YEAR has been discussed in public meetings concerning citywide energy consumption.

CONTRACT NUMBER: 02-80CS-30334.000

CONTRACT PERIOD: 1/2/81 through 6/30/83

FUNDING LEVEL: $124,142

FUNDING SOURCE: U.S. Department of Energy

CUMC SCHOOL: THE FIRST YEAR

Nicholas Peckham AIA

The growth and resulting iconography of Community United Methodist Church is similar to many churches in Columbia, Missouri. In 1956 a house was purchased to serve all the needs of the new church. The congregation grew and in 1960 a new fellowship hall was built to serve as both sanctuary and meeting space. Four years later the classroom wing was built, and in 1970 the new sanctuary was completed.

All this construction took place with little regard to either energy consumption in the buildings - or natural energy utilization.

In 1979 the Church had decided to build a school building to meet the growing needs of both church and community groups. The DOE PON for Passive Solar Commercial Buildings was published at about this time - which caused the Church to abandon their plans to build a pre-engineered steel building with (again) little regard for energy.

The non-solar pre-engineered steel building had a total energy budget of 407 MBTUs per year. During schematic design of the solar building, this was reduced to 145 MBTU per year - while the final design reduced this further to 87.3 MBTU per year.

During the first twelve months of operation the actual energy use was 87.9 MBTU- or 7/10 of one percent more than predicted. So this 5,500 square feet School used 15,982 BTU per square foot for the first year - about 1/3 of BEPS standards for schools in Columbia, Missouri. I should point out that last winter was 270 degree days colder than normal.

The "Natural Gas Usage" and "Electrical Usage" charts reveal two interesting outcomes of operating a 66,000 cubic foot building containing 139 tons of thermal mass.

During the first winter - in an effort to minimize energy use - the janitor turned the thermostat down to 50^{o} except when the building was actually in use. This caused two problems. First, the thermal mass cooled off; and second, it did just what it is supposed to: act as thermal inertia. On some occasions the building would cool to 60 degrees or less. An hour before scheduled use the thermostat would be turned up to 68^{o} but the furnace had neither the time nor the capacity to warm all the mass in the building.

After realizing this backup heat/thermal mass relationship was critical, we set the thermostat at 63^{o} - or 5^{o} less than the desired temperature. During the first heating season, the CUMC School used 6.6 MBTU more gas than predicted. With last year's experience behind us we expect next winter to do as well or better.

Cooling the building has produced some particularly encouraging data. During the first year no air conditioning has been used. Cooling has been accomplished by using the 6,000 CFM exhaust fan for about six hours each night - unless there is no scheduled use the next day. As can be seen on the Daily Monitoring Chart, the average day to night delta T is about 20 degrees. Running the fan overnight reduces the building temperature by about 10 degrees.

The exhaust fan is performing well for night sky cooling. If it were less noisy it could also work as a normal exhaust fan for evening meetings of 100 people who add both heat and smoke to the environment. We are currently costing out moving the fan further from the wall of the central space - or adding more sound alternatives, and replacing the motor with a 2 speed unit so this fan can also serve as a typical exhaust fan.

Daylight is working as well as expected by the designers - and better than expected by the users. We now regret economizing by eliminating the roof monitor skylights over the Narthex. The sunspace is so bright that the Narthex must have some lights on whenever it is in use - unless that use is viewing slides.

In hindsight, several conclusions can be drawn:

1) The overall design process including the architects, engineers, and DOE consultants produced a better building than any one of these would have done alone.

2) Siting the School against the glass north wall of the existing Fellowship Hall resulted in energy savings not seen in the School's Total Energy Index.

3) This building has about 50 pounds of thermal mass per square foot of floor area. On an annual basis, this appears to be OK - and has been very good this summer. Winter operation will have to be automated more than last year.

4) Superinsulation works very well in skin load dominated buildings.

5) Daylight works better than the users expected.

6) This School is having a positive effect on the energy consciousness of Columbia.

COMMUNITY UNITED METHODIST CHURCH

NATURAL GAS USAGE

September 1, 1981 to September 1, 1982

	Fellowship Hall		House		Old Educational		Solar		Sanctuary	
	Therms	$	Therms	$	Therms	$	Therms	$	Therms	$
Sept.	8	4	17	21	0	0	4	2	0	0
Oct.	26	9	76	28	45	16	4	2	36	13
Nov.	62	25	168	66	101	40	15	5	76	30
Dec.	165	67	381	156	239	98	107	44	347	142
Jan.	285	90	499	115	362	116	289	93	492	157
Feb.	138	49	338	121	225	81	204	74	359	129
Mar.	125	34	233	65	141	39	81	23	176	48
Apr.	59	22	138	54	81	31	43	17	107	42
May	11	5	24	12	12	6	8	4	6	3
Jun.	4	3	4	3	0	0	4	3	5	4
Jul.	3	3	4	4	0	0	4	4	3	3
Aug.	3	3	5	5	0	0	4	4	5	5
Totals:										
Therms	889		1882		1216		767		1612	
$		$314		$636		$427		$273		$574

SOLAR BUILDING USAGE: Actual 767 Therms or 76.7 MBTU
Predicted 701 Therms or 70.1 MBTU

ELECTRICAL USAGE

September 1, 1981 to September 1, 1982

	Fellowship Hall		House		Old Educational		Solar		Sanctuary	
	KWH	$	KWH	$	KWH	$	KWH	$	KWH	$
Sept.	361	23	519	14	280	17	284	18	459	27
Oct.	282	20	406	28	219	15	222	15	359	25
Nov.	294	18	424	26	262	16	281	17	499	30
Dec.	277	18	609	40	309	20	272	18	773	51
Jan.	339	18	666	35	379	20	454	24	1090	57
Feb.	310	20	650	41	296	19	325	21	915	58
Mar.	247	14	601	35	312	18	326	19	722	42
Apr.	296	19	529	33	293	18	274	17	640	40
May	208	13	356	23	209	14	171	11	320	21
Jun.	222	13	308	18	250	15	205	12	519	31
Jul.	225	13	319	19	270	16	168	10	1370	82
Aug.	290	17	304	18	248	15	313	19	845	51
Totals:										
KWH	3351		5691		3327		3295		8511	
$		$206		$330		$203		$201		$515

SOLAR BUILDING USAGE: Actual 3295 KWH or 11.2 MBTU
Predicted 5039 KWH or 17.2 MBTU

COMMUNITY UNITED METHODIST CHURCH

DAILY MONITORING - COOLING SEASON

AUGUST 19-26, 1982

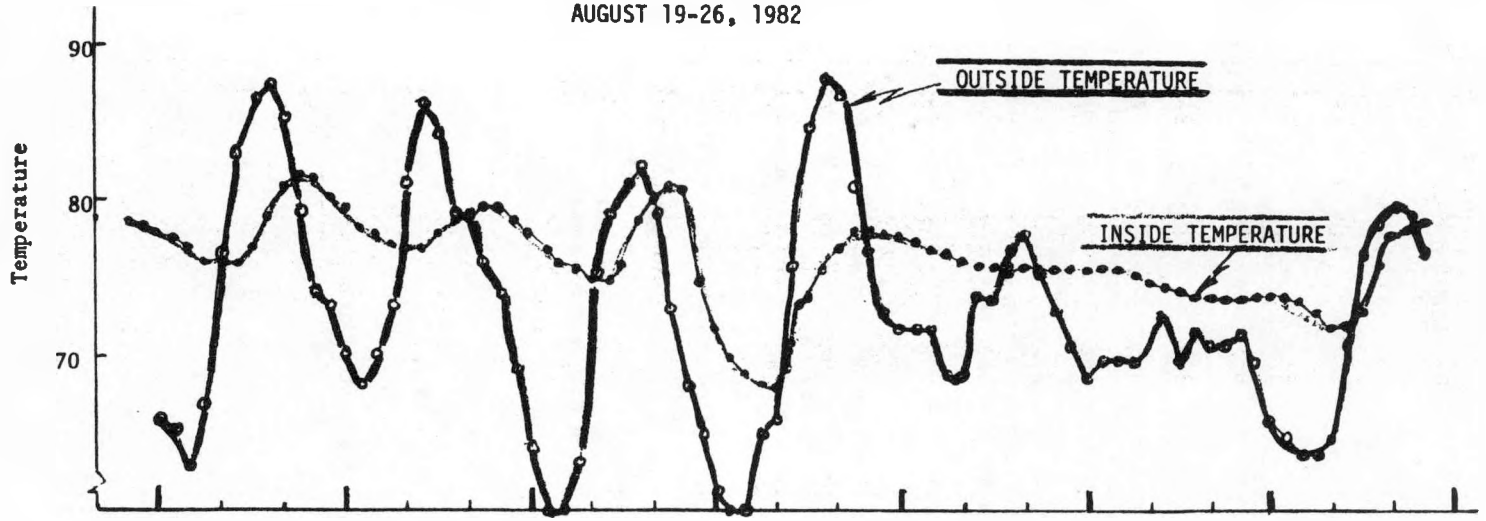

DATE	August	19	20	21	22	23	24	25
ENERGY (kWh)	Lights	4	2	3	11	2	1	0
	Paddle Fan	1	1	0	0	0	0	0
	Exh. Fan	0	0	5	6	0	0	0
	A/C	0	0	0	0	0	0	0

Exhaust Fan On

Occupancy

100+ people

PROJECT SUMMARY

Project Title:	The Performance of a Retrofit Office/Store in Wausau, Wisconsin
Principal Investigator:	Bruce D. Kieffer
Organization:	North Design A/E/P Madison, WI 53705
Project Goals:	Design, construct, evaluate and promote the utilization of passive solar technologies in a prototypical, older commercial building in a northern climate.
Project Status:	PHASE I: Analysis and design has been completed. PHASE II: Construction has been completed as modified. PHASE III: Performance monitoring and documentation, along with promotional and information dessemination activities, are currently on-going and partially completed. The monitoring system has been in place and operational since Oct. 1, 1981. Data is being taken and analysed on a continuing basis. Completion of twelve months of data acquisition will occur at the end of September. Final analysis of that data, along with a project report, will be completed shortly thereafter. Recorded performance to date has varied significantly from that originally predicted. Daylighting performance has been better than expected, while space heating has been poorer than predicted. Following a detailed analysis of October through May data, the reason for these discrepancies has been identified. Information dissemination and promotional activities have been somewhat delayed. It was felt that promotion of the concept should await the collection and analysis of actual building performance data. Now that this data is available, informational activities have begun in earnest and include the development of professional promotional materials for all program contractors being prepared by a media specialist.
Contract Number:	DE-FC02-80CS30343
Contract Period:	September 30, 1979 through January 30, 1983.
Funding Level:	$59,135 (PHASE II & PHASE III).
Funding Source:	U.S. DEPT. OF ENERGY CHICAGO OPERATIONS & REGIONAL OFFICE ARGONNE, IL

THE PERFORMANCE OF A RETROFIT OFFICE/STORE IN WAUSAU, WISCONSIN

BRUCE D. KIEFFER
NORTH DESIGN A/E/P
MADISON, WISCONSIN

ABSTRACT

A prototypical passive solar commercial building addition has been designed and constructed in Wausau, WI. The project is currently in Phase III of the program with its performance being monitored and evaluated. As of this writing, ten months of data has been accumulated. The performance of the building has been evaluated through the end of May. Performance through Fall, Winter, and Spring has been documented and analysed. Significant variations between projected and actual energy use were observed. A detailed analysis of the data indicated the reasons for these variations and are noted in the paper.

INTRODUCTION

The final project design involved the retrofitting of a passive solar sun space onto an older, reinsulated 2-story, wood frame structure, providing for winter heating and induced summer ventilation. The wall between the sun space and the existing building was also retrofitted with a light shelf and three feet of glazing above it to assist in lighting the existing lower level of the building. The original design scheme also included two roof monitors for daylighting of the upper level which has not yet been completed.

The design solution was low cost and the existing building is quite typical of many existing commercial structures. It is thought to have potentially wide scale replication. The basic design scheme is illustrated in the plan and section below (figures 1 and 2).

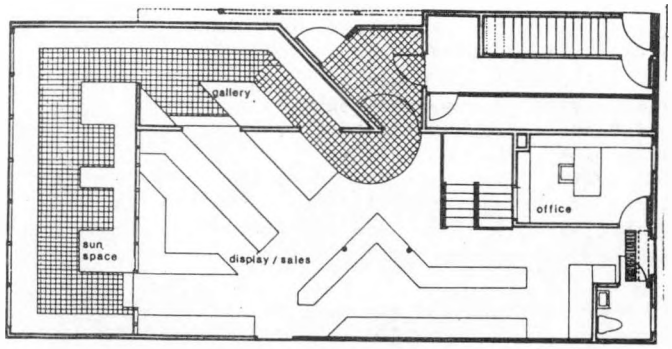

Fig. 1. Lower-level Plan

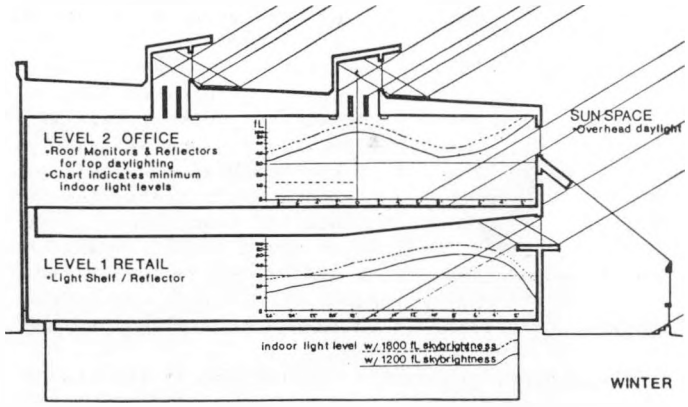

Fig. 2. Section

The lower level retail space was completed and occupied in June of 1981. A monitoring system was installed and became operational in September of 1981. Data on the actual performance of the building has been continuously accumulated since October 1, 1981. The data has been analysed through the end of May, 1982 (including the entire heating season). The measured performance of the building is the subject of the balance of this paper.

PREDICTED vs. ACTUAL ENERGY USE

The method of energy use analysis, prediction and comparison was an amalgamation of several techniques and design tools gradually refined through the various stages of design. Daylighting assessments were analytical (not measured) and used IES methods (standard daylighting configurations) combined with our own analysis of statistical skybrightness on a seasonal/daily basis. Energy use due to space conditioning criteria was assessed through a straightforward application of the Energy Graphics technique. This tool, along with application of the Solar Savings Fraction (SSP), was also used in the evaluation of actual building performance.

The original energy use analyses were done for the building as a whole. Due to code problems encountered with the upper level (office), only the design elements involving the lower level retail space were completed at the beginning of the monitoring activities. Thus, prior to proceeding with the analysis, it was first necessary to separate the energy use attributable to the retail space only. In addition, energy use had to be monitored on a monthly basis, while the Energy Graphics method is calculated and extrapolated on a seasonal basis.

To separate out energy use of only the retail space, the entire building was reanalysed as two separate zones (lower level retail and upper level office). The energy use of these two zones was then summarized and compared with the original calculation. The two zone calculation was within 2% of the original estimate.

To arrive at monthly, rather than seasonal energy use figures, the Energy Graphics technique was modified for use on a monthly basis. Similarly, seasonal skybrightness characteristics were translated through straight extrapolation into monthly data for daylighting analysis.

As noted in the abstract, significant variations between actual and predicted energy use were recorded. Energy required for lighting was less than expected, while energy required for space heating was substantially higher than anticipated.

We were aware of certain factors contributing to the variation in energy use while the data was being tabulated. However, these factors could not account for all the differences, nor did they become apparent until a more detailed analysis was performed.

Our first thoughts were that perhaps the analytical methods were not accurate. However, a detailed examination of the data and reports indicated the causes were due to changed operating conditions and variations in performance assumptions. The original calculation of energy consumption assumed the following:

1. Weather conditions would be close to historical patterns.
2. Occupancy would be a "typical" retail tenant.
3. Building operation would be as scheduled.

In actual operation these three assumptions were substantially changed:

1. Weather conditions (temperature, solar availability and wind) were more severe than expedted.
2. The use of the building as a horticultural shop prooved to be far from a "typical" retail occupancy; primarily, in terms of excessive latent heat loss due to very moist internal air conditions.
3. Certain major operational problems occurred. First, although installed, the night insulation system was not operational for most of the winter. Second, the actual infiltration rates were elevated due to weather stripping problems on some of the windows which was not recognized until well into the winter heating season.

In order to identify the effect of these factors and as a check on the accuracy of the Energy Graphics design tool, a series of additional annual performance predictions for the project were run and compared with actual performance data. Having completed these re-evaluations, we are again reasonably confident in the further use of our originally chosen analytical tools. Certain exceptions are implicit in this statement and discussed in the description of performance and the conclusion which follows.

PERFORMANCE EVALUATION
SPACE HEATING

The greatest variations between actual and predicted energy use were noted in the space heating component.The following series of graphs illustrates four sets of energy use scenarios performed to identify, test and compare energy use based on the revised operating conditions.

Group A represents the performance based on original operational assumptions and historical weather conditions. They compare the originally calculated energy use of the entire building done during Phase I of the project (A1), with the building calculated as the sum of two separate zones on a seasonal basis (A2=A2.1 + A2.2 or the two zone total equals the lower level plus the upper level). Seasonal data is averaged into monthly figures. Actual monthly calculations were also generated and are illustrated in the graph of A3.1 (lower level zone). (See following page, Fig. 3.)

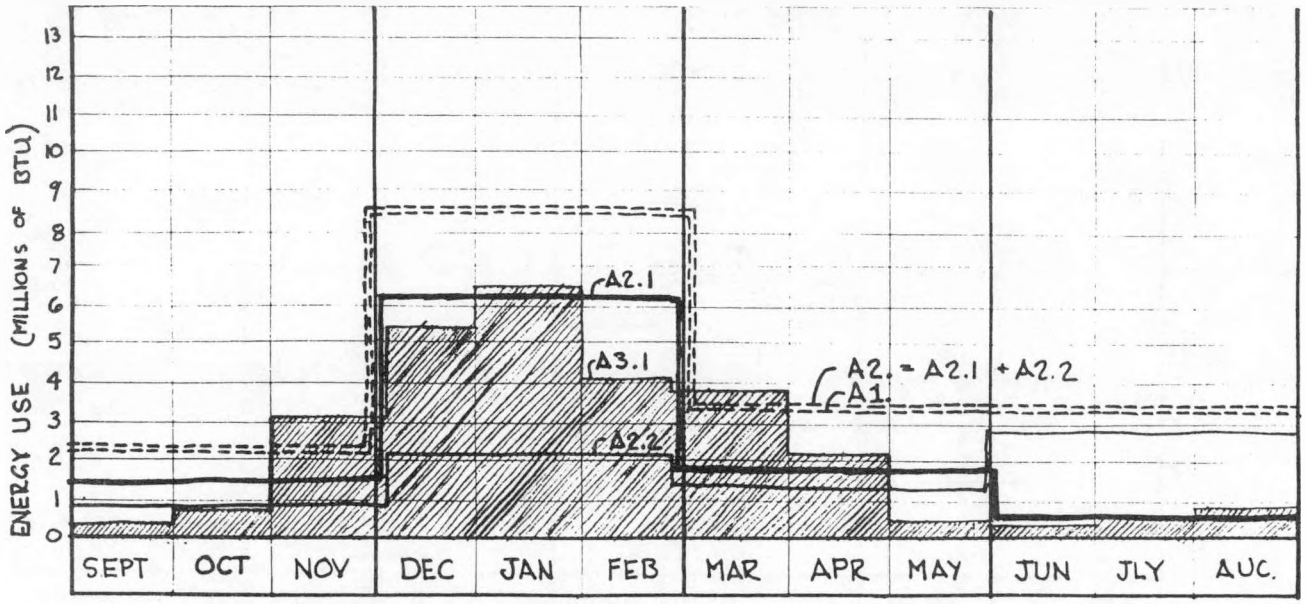

Fig. 3. Group A Graphs

Group B graphs the predicted (or actual) performance of the building (lower level only) operating under actual documented conditions. B1.1 is the performance of the retail zone predicted by the Energy Graphics method. B2.1 is performance predicted through application of SSF method. B3.1 is a graph of actual recorded performance.

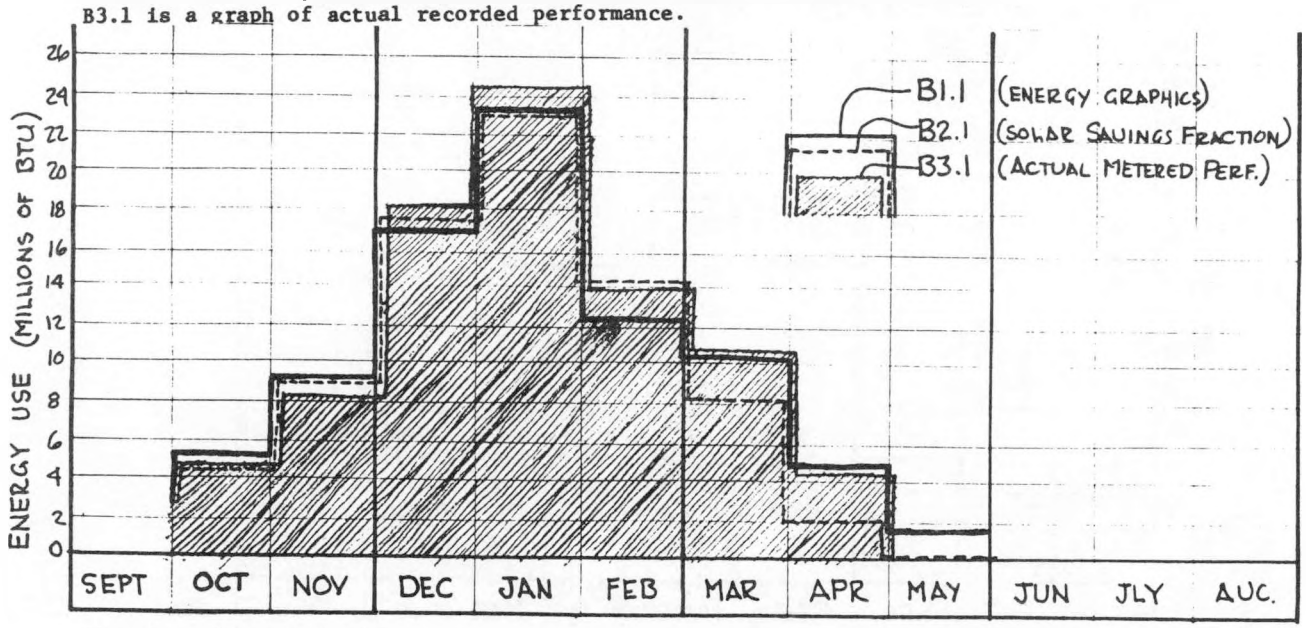

Fig. 4. Group B Graphs

Group C curves are monthly performance graphs of energy use which utilize actual "in use" conditions and historical weather data. They are actually intended to replace the performance data generated in in Phase I for the solar building case (occupied by a horticultural shop rather than a more typical retail tenant).

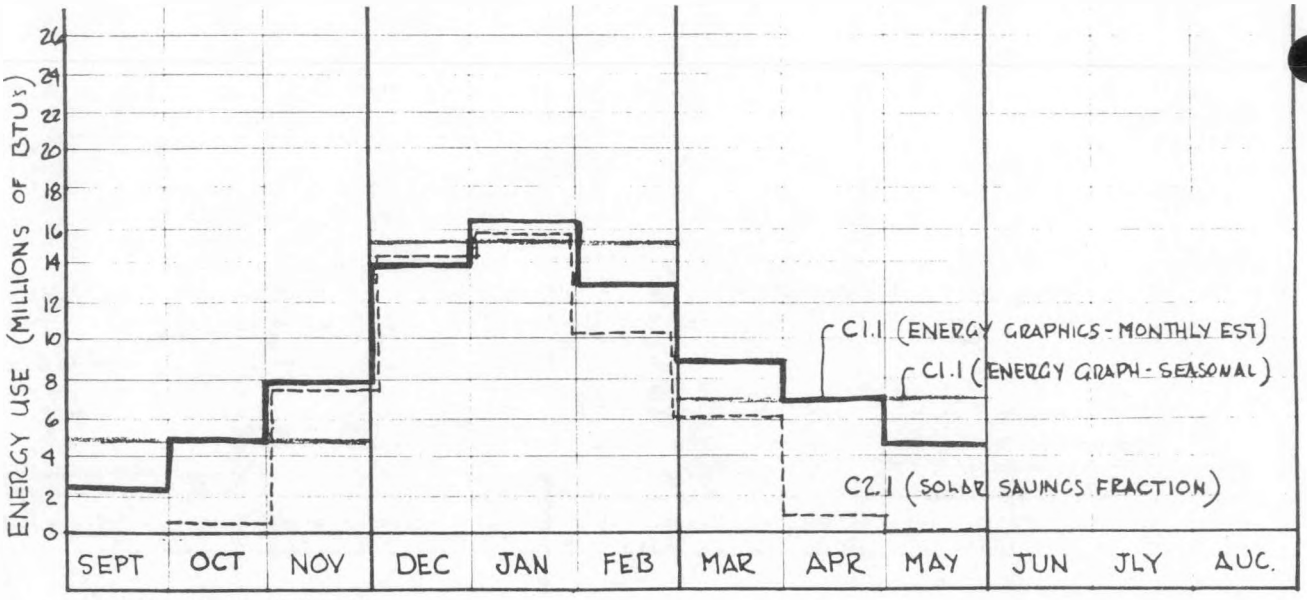

Fig. 5. Group C Graphs

Group D curves are intended to serve as a revised "base case" situation. These graphs illustrate the performance which could be expected from a traditional or non-solar solution to the design of a "horticultural shop" (not a traditional retail tenant).

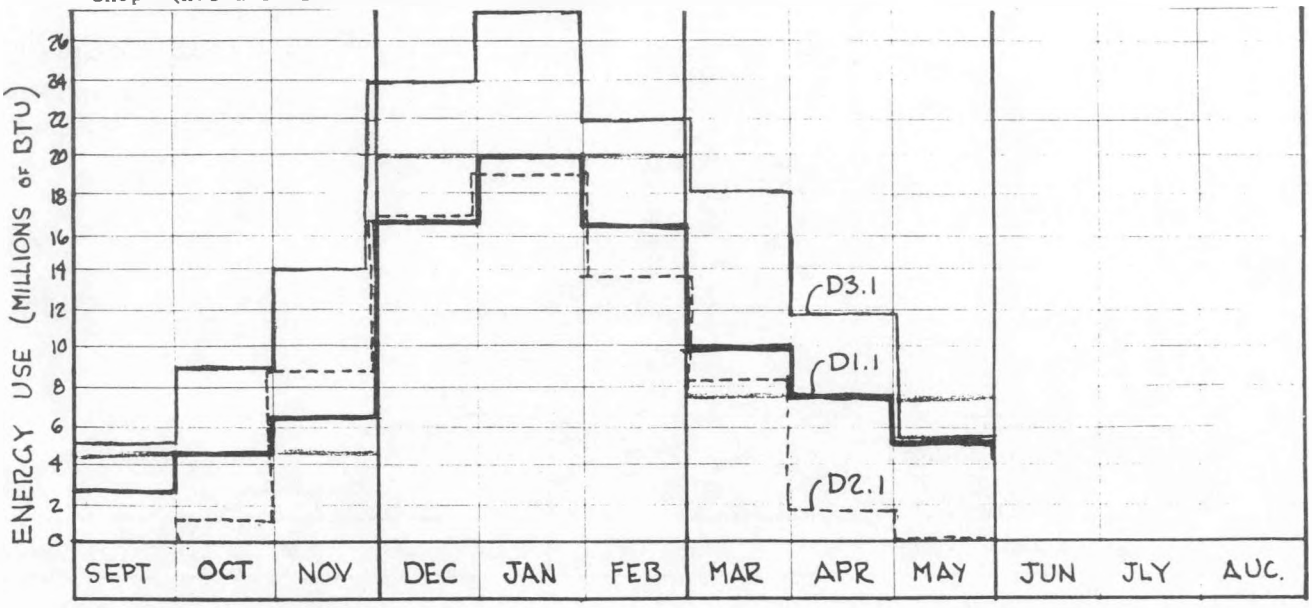

Fig. 6. Group D Graphs

Actual data regarding cooling performance, as of the date of this writing, had not yet been evaluated in detail. Preliminary qualitative assessments during non-summer, but potentially overheated periods in October and May, indicates reasonably sufficient performance. The induction ventilation and shading system during these periods keeps interior sun space temperatures at about 4-5 F. above exterior ambient conditions. An 80% shading fabric, according to the users, appears to reduce the intensity of the radient environment to within the comfort range.

PERFORMANCE EVALUATION
LIGHTING

Although actual space conditioning energy use has been much poorer than originally predicted (due to reasons previously cited), daylighting performance has been better than predicted. The original energy use projection in Phase I equaled 4,844 BTU/SF as an average for the entire building. Adjusted figures for the lower level only equaled 6,150 BTU/SF. Actual sub-metered performance of the lower level lighting averaged 4,022 BTU/SF for the period from October 1981 through May 1982. This is a 35% reduction. The primary reason for this reduced consumption appears to be the user/tenant's acceptance of lower than assumed interior lighting levels. In our original calculations a minimum of 30 fc of general illumination was assumed. The tenant has found a threshold of 22-25 fc to be entirely acceptable. Although this has led to an additional discrepancy in the data, it bodes well for the acceptability of both the quality of daylighting and reduced levels of general illumination.

COMPARISONS

The following graphs are intended to show overall building performance in relation to that originally predicted and in relation to a revised 'base case' undergoing similarly altered operating conditions. It was performed in order to make a reasonable and fair comparison with the 'solar case'. The first set of bar graphs (Fig. 7a and 7b) illustrate actual energy use on a BTU/SF basis. The second set of graphs (Fig. 8a and 8b) illustrate energy use on a cost/SF basis.

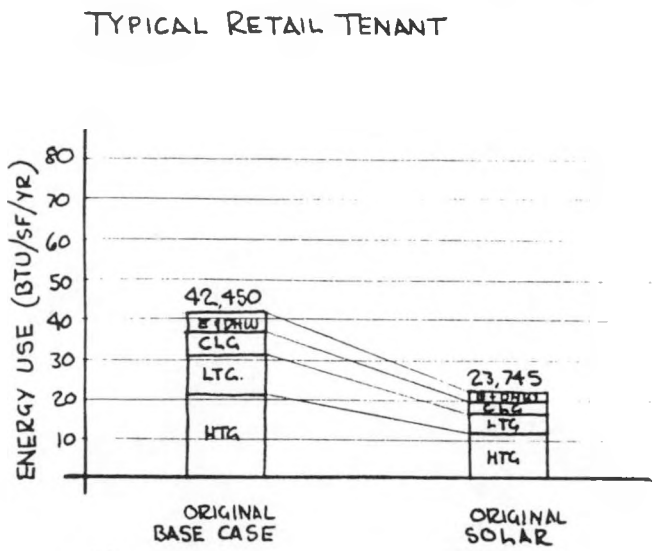

Fig. 7a

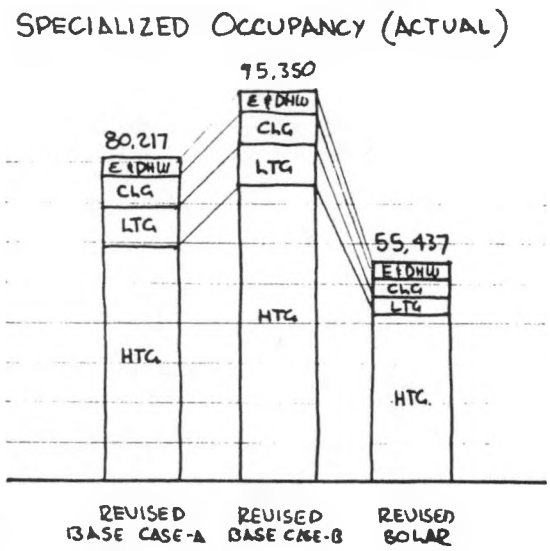

Fig. 7b

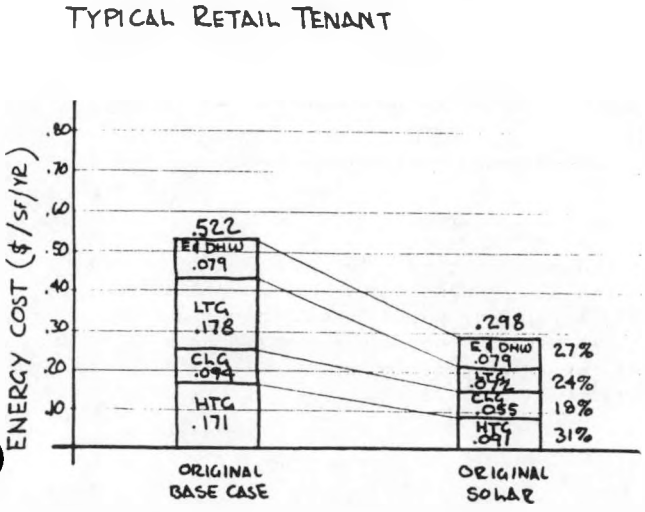

Fig. 8a

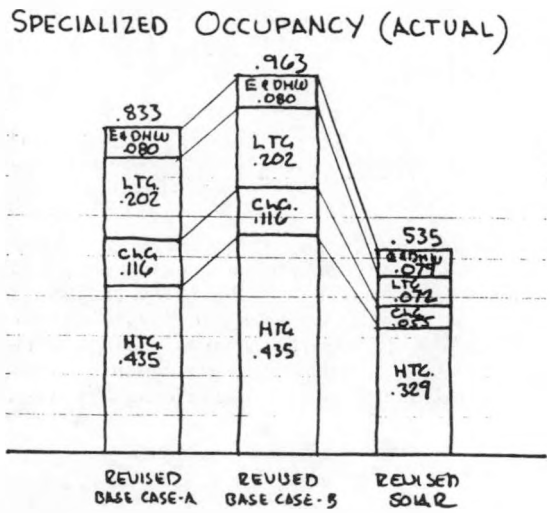

Fig. 8b

CONCLUSIONS

Although significant variations between predicted and actual energy use have been encountered dur during the monitoring of this project, we feel reasonably confident in having identified the sources of these discrepancies. Thus, we are also confident in the continuing use of our design tools, once a thorough analysis and assessment has been made of what the actual 'in use' conditions of the building operations will be.

PROJECT SUMMARY

Project Title:	"Energy in Architecture," The AIA Energy Professional Development Program
Organization:	The American Institute of Architects 1735 New York Avenue NW Washington, DC 20006
Organizational Contact:	Ms. Brenda Henderson 202/626-7353
Project Goal:	The "Energy in Architecture" Professional Development Program is a comprehensive, incremental program designed to provide energy professionals with the knowledge and skills necessary to incorporate energy considerations into the design process.
Project Status:	As of August 27, 1982, approximately 1800 design professionals had attended the "Energy in Architecture" workshops series. The attendence distribution is as follows: Level 2 Workshop 1368 Level 3 Workshop 356 Level 3b Workshop 76 1800 Workshop Attendees
Project Cost:	
Private Sector Contribution:	The AIA's contribution - over $1.5 million for program development expenses -
Government Funding:	
Contract Number:	B-D2-163-A-4
Contract Period:	August 18, 1982 - September 30, 1983
Funding Level:	$149,177
Funding Source:	U.S. Department of Energy through Battelle Memorial Institute, Pacific Northwest Laboratory

"Energy in Architecture"
The AIA Energy Professional Development Program

The American Institute of Architects
1735 New York Avenue, NW
Washington, DC 20006

MISSION

The "Energy in Architecture" Professional Development Program is a comprehensive, incremental program designed to provide energy professional with the knowledge and skills necessary to incorporate energy considerations into the design process.

Evolving from the Institute's commitment to energy efficiency in the built environment, "Energy in Architecture" is the most comprehensive program of its kind ever developed by the AIA. Divided into levels of increasing proficiency, the program is targeted toward the energy-concerned design professional. It promises to show participants how they can substantially reduce energy consumption in buildings through careful design, based on knowledge of energy principles and analyses of alternative strategies.

AUDIENCE

Design professionals in the disiplines of architecture, engineering, system design, facility development, and related professions.

SKILL LEVELS

Level 1: Energy in Design: An Overview, is a 56-page, full color book, Energy in Architecture. Written as a general informational tool, Energy in Architecture outlines the basic principles of energy-conscious design. As an overview, Energy in Architecture will also be of interest to the general public. It is not to be considered an integral part of professional preparation, but it is an attractive introductory summary of energy-conscious design principles. (Order #4N910 through Publications Fulfillment Division, AIA; $9.95; $7.00 for AIA members and other design professional association members; bulk orders of 10 copy minimum at $5.00 per copy.)

Level 2 and 3 of the program consist of two-day workshops sponsored by Institute components at locations nationwide. Workshop registration is limited to 50 persons and requires a minimum of 10 persons.

Level 2: Energy in Design: Techniques, is the entry-level experience for design professionals. It is a two day (14 hour) workshop focusing on design fundamentals, techniques and options as they relate to energy use. Using a 200-page workbook, recommended reading material and case studies, professionals who are experts in the field will guide participants in examining energy design principles, concepts, and tools. The objective is to gain a sound understanding of the concepts, options, and strategies needed to incorporate energy considerations into the design process.

A typical Level 2 workshop includes:

- o Introduction
- o Fundamentals: basic thermodynamics, fundamentals of solar design, introduction of the analysis/design process, introduction of the analytical tools used in the workshop.
- o External factors: methods of defining the impact of the climate on design; defining human comfort using the Bio-climatic and Psychometric charting methods
- o Internal Factors: building use as a determinor of design; delineation of factors involved; developed of an energy profile
- o Form and Envelope: historic and contempory approaches; shape and orientation; S/V, aspect ratios daylighting and energy transfer consideration.
- o Energy analysis: discussion of the various tools and their uses; introduction of the Buehrer analysis technique; case studies.
- o Systems: block load diagrams; energy sources; system types and management; energy management.
- o Economic analysis: introduction to the basic process of life-cycle costing

course fee: $175. per registrant includes 14 hours of instruction and all course materials; does not include meals or accommondations.

Level 3a: Energy in Design: Process, has been formulated to guide participants in the application of design techniques, building on the foundation established in Level 2. Participants will select appropriate techniques for the design process and evaluate the results using the Workbook and regional case studies. Opportunities for energy-conscious design will be keyed to the climatic region where the individual workshops are held.

A typical Level 3a workshop includes:

- o Definition of climate completed; climatic problems identified and tactics developed.
- o Design strategies: Level 2 reviewed; discussions of fans, atrias, sunspaces, natural ventilation, zoning, control systems, solar, etc.
- o Concept analysis: introduction of the Nomographic (G-SEET) analysis technique.
- o Daylighting analysis: light quality vs. quantity; data qualifiers; concept summary; azimuth and altitude; sample problem.
- o Energy analysis -- completed
- o Economic analysis -- completed
- o Short design problem

Level 3B: Energy in Design: Practice, allows participants to solve an actual design problem keyed to the climatic region. Participant teams will examine various environmental conditions confronting the designer, and will then work through a detailed design problem establishing the building's energy performance and the design strategies that can be employed to achieve it. Participants may bring a building plan of their own to the workshop, or work on a problem designed for the course by the faculty. This experience provides the participants with the opportunity to insure that they fully understand the energy design process, and to return to their offices with a thorough understanding of the techniques involved in developing truly energy-efficient building plans.

course fee: $280. (3a and 3b) per registrant including 14 hours of instruction and all course materials; does not include meals or accommodations.

REGISTRATION

Contact Ms. Brenda Henderson, Workshop Coordinator at 202/626-7353, or write to her at: The American Institute of Architects, 1735 New York Avenue NW, Washington, DC 20006.

PASSIVE SOLAR MANUFACTURED BUILDINGS DEVELOPMENT AND ANALYSIS

Robert deKieffer
Robert Taylor
Steven Brant
David Simms
Solar Energy Research Institute
1617 Cole Boulevard
Golden, CO 80401

ABSTRACT

Manufactured buildings are quickly becoming the most cost-effective residential and light commercial buildings in the American marketplace. Over the past three years the Solar Energy Research Institute (SERI) and the Department of Energy (DOE) have worked with building manufacturers to design, develop, and build passive solar manufactured buildings. This development process has lead to extremely valuable information in design development and design options, cost analysis, and estimated and monitored thermal performance on all types of manufactured buildings. Because of the tight cost/marketing restrictions in this industry, the lessons learned in this program are beneficial to all sections of the design and building community. This paper describes the scope and content of this data by using a case study developed for the program.

1. INTRODUCTION

SERI and DOE developed the Manufactured Buildings Program to work with industry in determining the applicability of passive solar systems to factory-produced buildings. Throughout the program, individual manufacturers have worked with solar consultants to integrate passive solar techniques into their product line. The results appear to give cost-effective, marketable, and easily constructed passive solar buildings. Of the 22 original participants, all have completed numerous designs, which include detailed costs, design considerations, and estimated thermal performance. This revision process provides invaluable insight into the tradeoffs that result in technically and economically acceptable designs.

SERI is producing two types of documentation on the program. The first is a selection of case studies; the second is a series of reports that provide a comparative analysis of the designs and system types.

The case studies are divided into four sections. The first is an Executive Summary that provides an overview of the important aspects of passive design, the increased costs involved in incorporating passive solar systems, and estimated solar system performance. The other three sections detail the design development that supports the Executive Summary. Section 2 discusses the solar options that were considered in selecting a particular system type and describes the final solution. Sections 3 and 4 describe the thermal performance and costs of the building. The costs not only consider the total and incremental costs but the relative cost-effectiveness and savings. A computer model (SERI-RES) estimates thermal performance by comparing the solar model with a manufacturer's present product and with a U.S. Housing and Urban Development Minimum Thermal Requirements (HUD/MTR) prototype. In addition to estimated data, SERI has monitored the thermal performance on the constructed prototypes.

Through this program SERI has developed an invaluable data base on design and performance of passive solar systems. This allows SERI to review and analyze the important variables, such as the effects of air infiltration on measured performance, system types, cost-effectiveness of thermal mass, and innovative solar controls. These topics will be covered in individual reports that will be available in addition to the case studies.

This paper describes the three technical sections of the case studies using the case study prepared by Dynamic Homes Inc. as an example.

2. DESIGN DEVELOPMENT

Each solar design in the Passive Solar Manufactured Building Program was developed through an interactive design process. We documented the design process, highlighting the solar design options that were considered and the rationale for eliminating or retaining those options. This process comprises the cost, thermal performance, and marketability or perceived acceptance of proposed designs.

Manufacturers took different approaches to designing the solar model. Many manufacturers started with an entirely new design using solar concepts and production criteria. Other manufacturers took existing popular designs and incorporated solar concepts. This valuable experience can provide other manufacturers with a good foundation for designing solar models.

The design development process that Dynamic Homes went through was typical for a majority of the manufacturers in this program. Dynamic Homes' design team, which included the architectural firm of Ritter, Suppas, and Plautz, aggressively investigated a wide range of solar designs and strategies during the preliminary design process. Four basic housing types were studied in the beginning: a rambler, split entry, split level, and two story. After reviewing the initial studies of these four generic house types, the design team chose the split-entry and the split-level models to develop based on their market appeal.

Dynamic Homes developed plans for the solar split-entry home and the solar, split-level home, so they could market them as basic passive solar homes that could accept a variety of additional solar options. Figure 1 shows some of the solar options, including a roof monitor, a solar domestic hot water system, and an attached greenhouse. The ability to offer varying options to the base house was very well received, but the cost for the total package of $110,000 was considered too high for most of Dynamic Homes' market.

After reviewing these plans and reassessing their market, Dynamic Homes decided that the most logical unit to develop initially would be the split-entry unit with variations so they could market passive solar houses with a selling price from $60,000 to $90,000 including lot and interior finishing.

Each case study provides a detailed review of the solar elements and the final design, which not only points out the functional elements of the design but also the alterations made to their typical construction practices. The review focuses on particular solar construction details and particularly interesting design development patterns.

Dynamic's solar prototype has been built and is being tested in Fargo, ND, which has 9270 heating degree days and 472 cooling degree days. Fargo has severe winters with bitter arctic winds from the northwest. This 167 m^2 (1800 ft^2) solar split-entry home [7 x 10 m (24 x 36 ft)] includes four bedrooms, two baths, and large living and family rooms. Energy conserving measures include 2 x 6 R-22 walls with a 6-mil continuous vapor barrier on all ceilings and walls, R-50 attic insulation, magnetic-sealed insulated doors, air-lock entry, triple-glazed east and north windows, and a fully insulated wood foundation.

Dynamic's final design (Figs. 2 and 3) has 13 m^2 (140 ft^2) of direct gain collection area on the south side with minimal amounts on the east and north. No glass faces the west. The majority of the south glass is shaded from high summer sun by fixed overhangs. R-5 movable insulation covers all south windows, reducing heat loss at night. In addition to the heat capacity of the interior wall surfaces [with 1.3-cm (1/2-in.) gypsum board], thermal storage is provided by PCM (phase change materials—Texor heat cells) in cans located in the living/dining room area and a brick fireplace hearth in the lower-level family room.

3. THERMAL PERFORMANCE

As required by the program, each manufacturer's design team prepared at least three preliminary designs, supported with estimates of thermal performance. At the final design review, the teams presented a refined product. SERI took this final design and analyzed it using the residential energy simulator (SERI-RES), a multizone, computer simulation tool that estimates the building energy use.

Using SERI-RES, we compared buildings constructed to (1) HUD/FHA minimum thermal requirements (HUD/MTR house); (2) the manufacturers' standard levels of thermal protection (present product); and (3) the solar model. We used the HUD/MTR version as a point of reference for each manufacturer's climate. Dynamic's present product line incorporates HUD/MTR levels of insulation and window quality. Dynamic's standard construction practices include the use of a continuous polyethylene vapor barrier and extensive

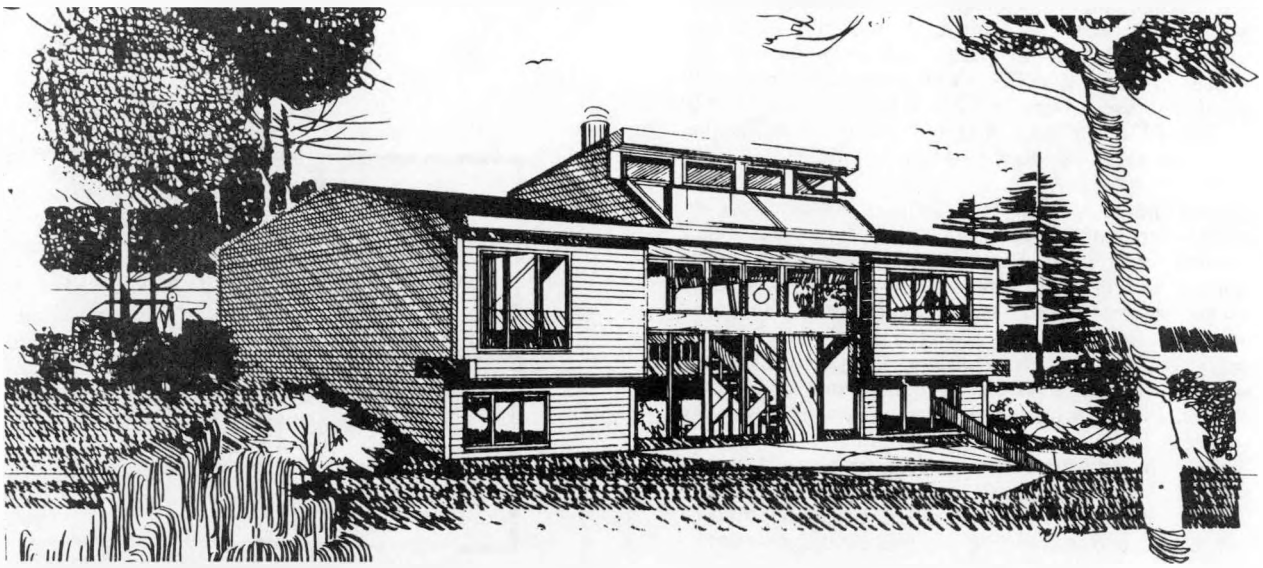

Figure 1. Preliminary Design

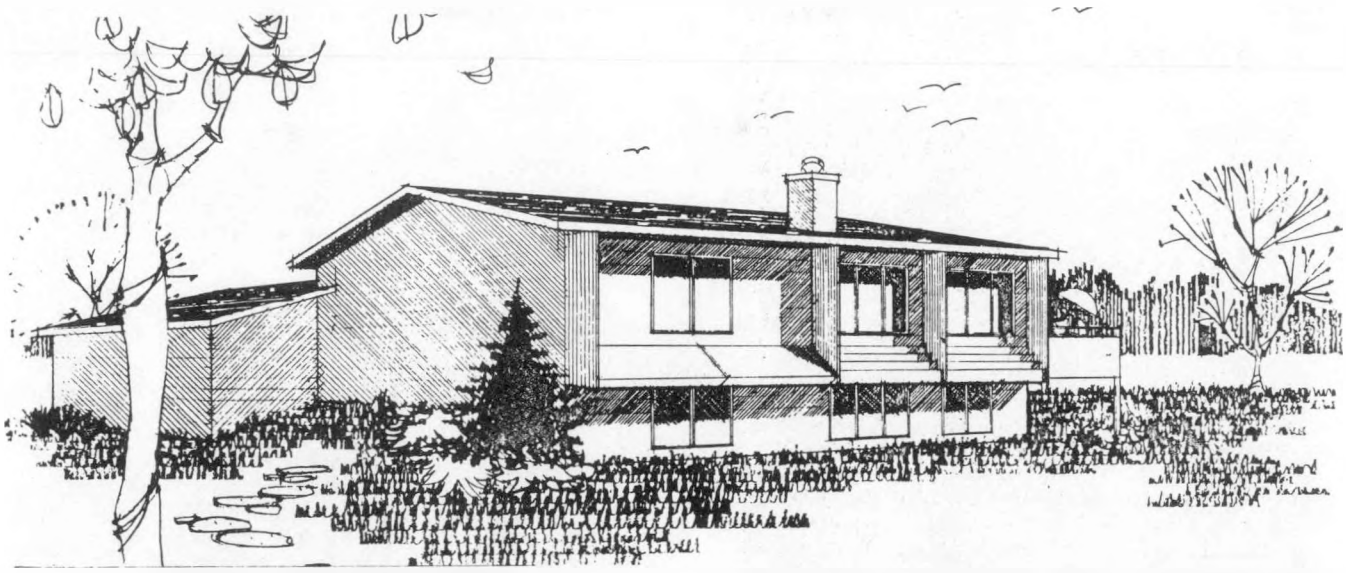

Figure 2. As Built Final Design

caulking to reduce air infiltration. Thus, 0.5 air changes per hour (ACH) were assumed for the present product in the analysis rather than the 0.8 ACH for the HUD/MTR house. Figure 4 shows the results of the SERI-RES analyses with the major parameters given. The solar prototype is predicted to conserve up to 36% of the auxiliary fuel use of Dynamic's present model and 47% of the HUD/MTR building's auxiliary heating load. The small reduction in the load of the present product attributable to solar concepts assumes a south orientation for that unit as opposed to a random orientation for the HUD/MTR house. We also assumed a south orientation on the solar model. Figure 5 gives the estimated monthly heating loads for the solar prototype. The solar contribution was derived by analyzing the solar prototype as built and then substituting the present product glazing areas and levels of thermal mass.

We are also using SERI-RES to analyze the thermal benefits from major components of the manufacturers' final design. Because the movable window insulation on the Dynamic Homes' solar model was the largest single cost item of the design, an analysis was done to determine its effect. With the window insulation in place regularly during the winter months, the SERI-RES computer simulation predicted the annual auxiliary heating load would be 38 kJ (36 MMBtu). Without the movable insulation, the load increased to 41 kJ (39 MMBtu).

Actual monitoring of the thermal performance of each solar model built under the program is being carried out using Class B data acquisition systems. Thermal data relevant to building energy usage is collected continuously and archived hourly. For Dynamic Homes' solar model, solar radiation, indoor and outdoor temperatures, and auxiliary electric heating requirements are monitored. Figure 6 shows plots representing a six-day segment in February for the Dynamic Homes' solar home. In addition, we are calculating daily and monthly functions such as solar, auxiliary, and internal contributions to the total heating load of the house and measuring overall heat-loss coefficients, furnace efficiency, and air infiltration rates for each building. A Dynamic Homes' heating test showed an overall heat-loss coefficient of 58.43 W/°C (291 Btu/h °F) at an average wind speed of 10 km/h (6 mph) and average difference between indoor and outdoor temperature of 26°C (79°F). The SERI-RES computer tool is now correlating this actual data and the predicted performance data.

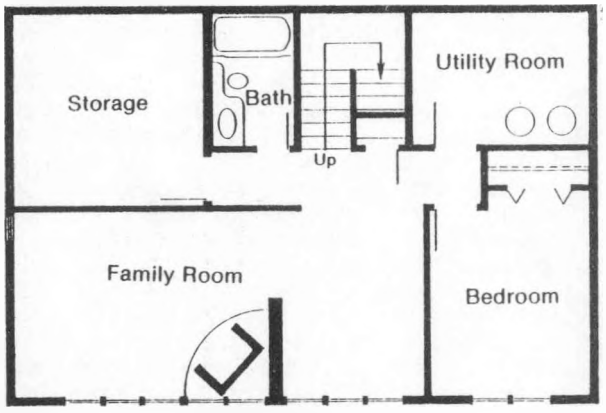

Figure 3. Upper/Lower Floor Plans

4. MARKETING AND COSTS

The overall costs of producing passive solar housing determines, to a great extent, the marketability of the end product. The cost/marketing portion of each case study compares the present home to the new solar model looking at cost range, target market, and available options. In addition, construction costs are compared, reviewing a cost summary of present homes and the solar model, both in total cost and cost/m^2 (ft^2).

Dynamic Homes' split entry sells for $50,000 to $75,000 depending on how the lower level is finished. The solar prototype was sold for $74,000 including a completely finished lower level and a solar domestic hot water heating system. Some market resistance and buyer qualification problems could be expected if the costs of subsequent solar homes are not streamlined. As Fig. 7 shows, the cost to build the solar prototype was approximately $401 m^2 ($37/ft^2) (contractor's cost). This model will probably sell for $70,000, avoiding many of the prototypical costs. A comparable Dynamic Homes' split entry was estimated to cost $18.30/$m^2$ ($1.70/$ft^2$) less or $382.50/$m^2$ ($35.50/$ft^2$). (Neither cost includes solar DHW since it was optional on both homes.) The airlock entry and cantilevered upper floor on the solar model increased the floor area to 167 m^2 (1800 ft^2) so the total incremental costs reflect a more dramatic increase of $5,618. The standard energy conservation features that Dynamic Homes incorporates is so close to the new HUD/MTR requirements for the Fargo climate that there is very little difference in the estimated costs.

Figure 8 breaks down the costs for Dynamic Homes' recent product line compared to a house meeting HUD/MRT standards and the as-built solar prototype. Dynamic estimated that the extra attention to reducing air infiltration in their present product added only $228. On the other hand, they made substantial investments in both energy conserving measures and passive solar applications in the solar prototype. Upgrading the insulation levels in the attic and subgrade walls added very little cost compared to adding the airlock entryway and movable insulation system, which together constituted 52% of the additional expenditures for the solar prototype. Of the 13 m^2 (140 ft^2) of south glazing, only 3 m^2 (32 ft^2) were considered extra because Dynamic's solar design strategy included shifting most of the glazing from the north to the south side of the house.

Figure 4. Thermal Performance Comparison

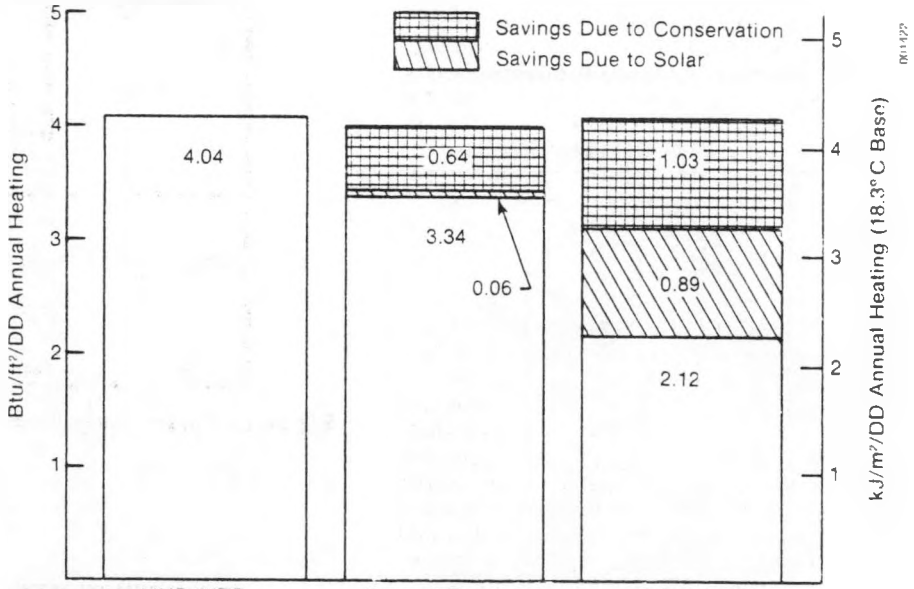

	HUD/MTR House	Present Product Line	Solar Model
Floor Area	1728 ft² (160 m²)	1728 ft² (160 m²)	1800 ft² (167 m²)
Insulation Levels:			
Walls	R-20	R-20	R-20
Ceiling	R-38	R038	R-50
Foundation Walls	R-11	R-11	R-20
Glazing Area:	Southeast: 64 ft² (6 m²) Total: 139 ft² (13 m²)	South: 64 ft² (6 m²) Total: 139 ft² (13 m²)	South: 139 ft² (13 m²) Total: 171 ft² (16 m²)
Thermal Storage:	(Only mass inherent in light construction such as gypboard. etc.)		Brick P.C.M.
Air Infiltration Rate:	0.8 ACH	0.5 ACH	0.5 ACH

(SI) Please note all measurements in parenthesis are SI units

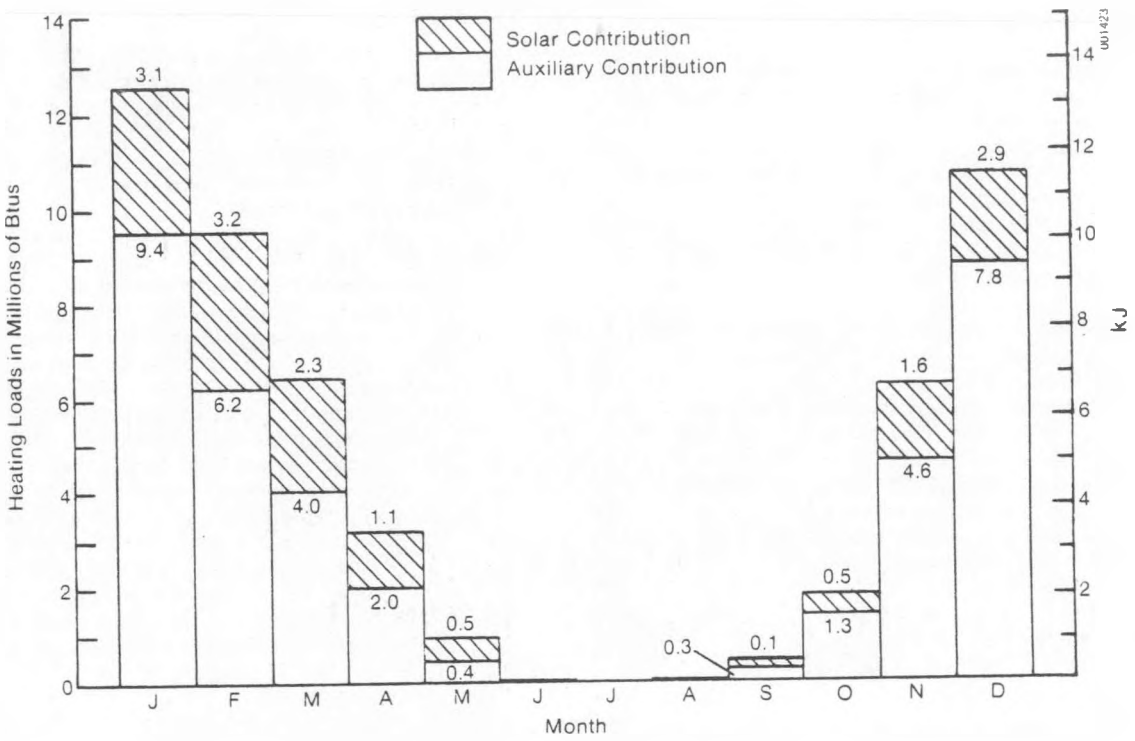

Thermal Performance Summary

A. Predicted Data

Figure 5. Thermal Performance Summary

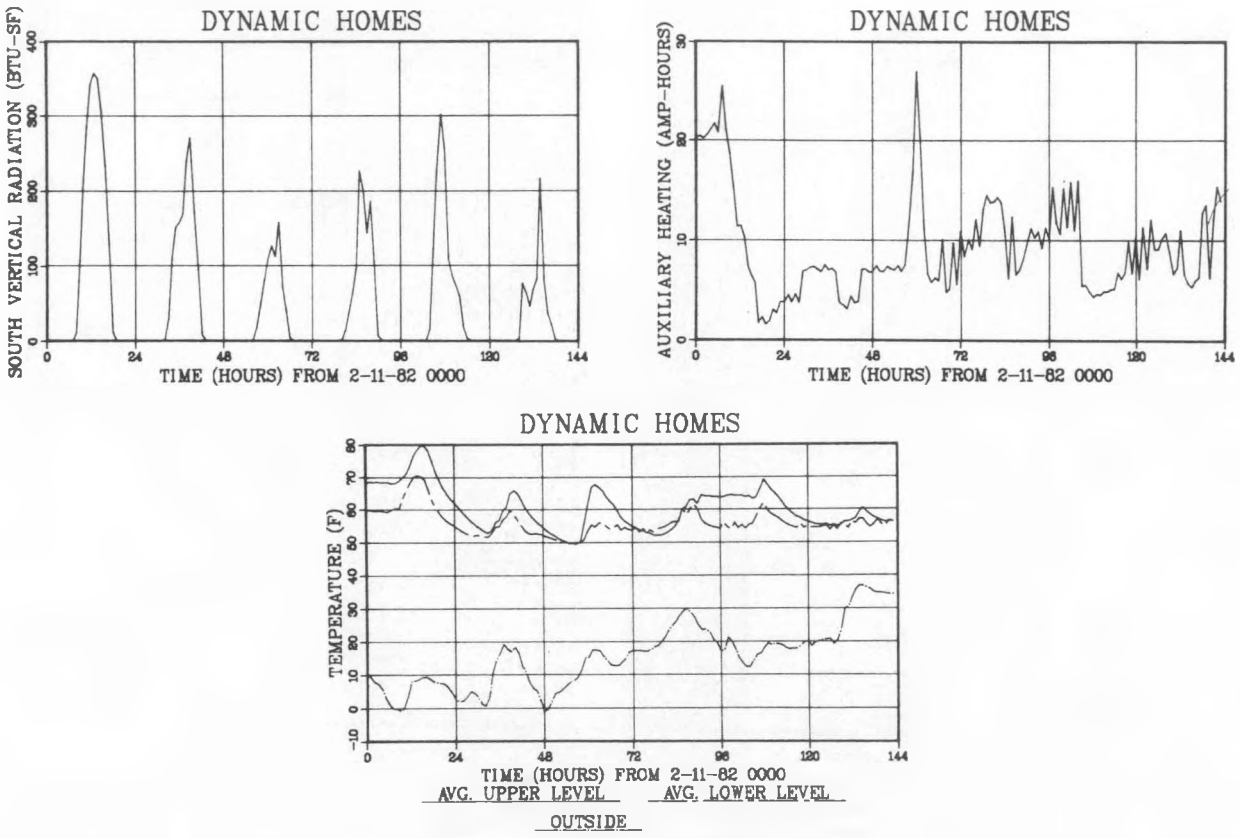

Figure 6. Monitored Performance Data

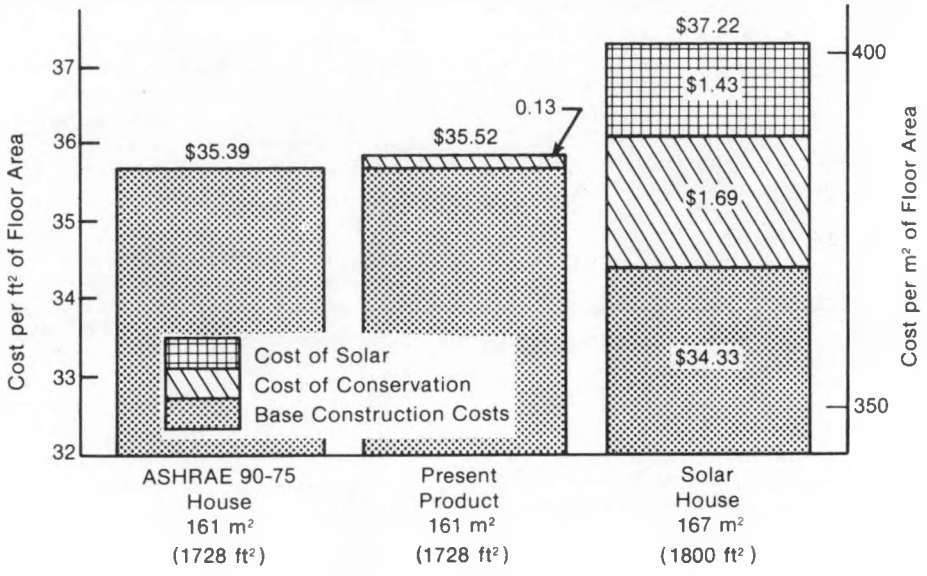

Figure 7. Cost Summary

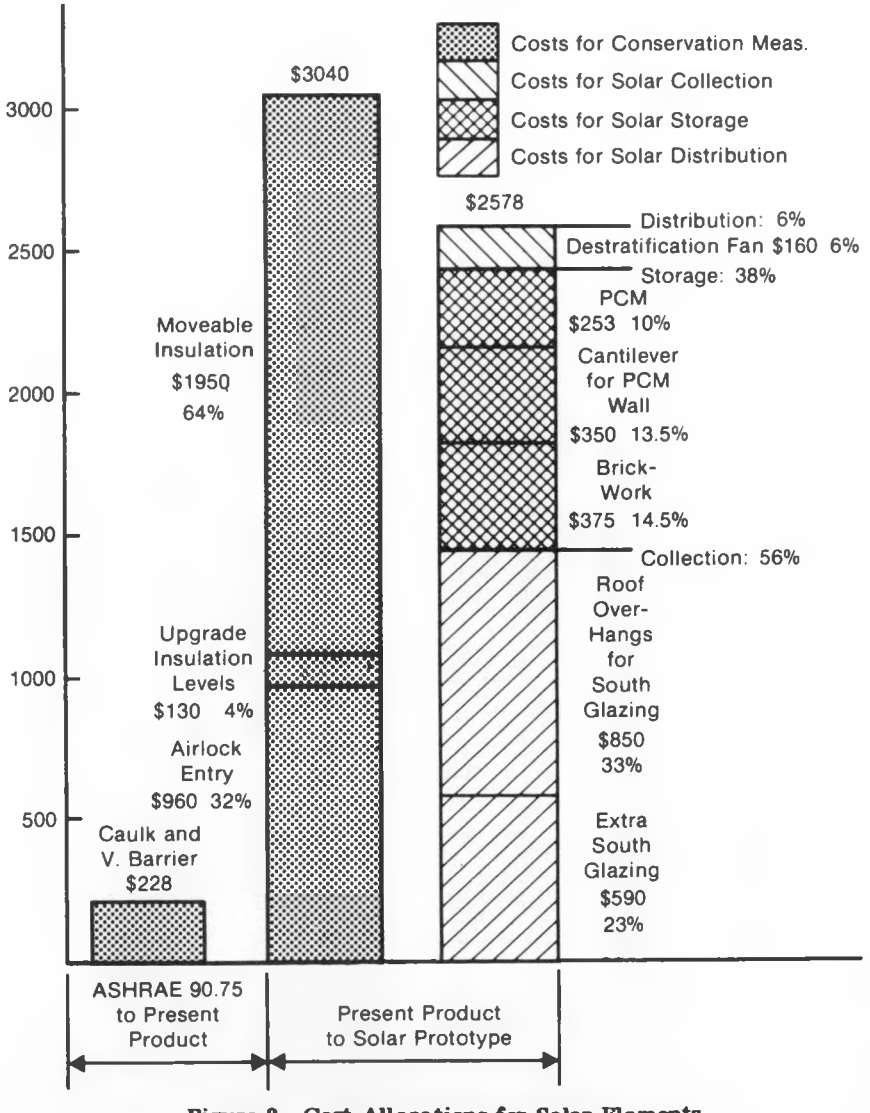

Figure 8. Cost Allocations for Solar Elements

The thermal storage systems for Dynamic's solar model included phase change materials (PCM) on the upper level and a brick enclosure around a wood-burning stove in the lower level. For this analysis we assumed that one-half the brick was incorporated solely for solar direct gain mass backing. Building the cantilevered upper floor section and installing the PCMs cost approximately $600.

5. COST SAVINGS

Northern States Power provides the heating fuel for Dynamic's solar prototype in Fargo. The average 1981-1982 heating season cost was $0.04/kWh or $11.72/MMBtu.

Figure 9 shows the predicted fuel bill savings for the Dynamic Homes' present product and solar model using electrical resistance baseboard auxiliary heating. The $122/yr savings due to conservation measures in Dynamic's present product represents the effect of changing the air infiltration rate from 0.8 ACH in the HUD/MRT house to 0.5 ACH in the present product. The additional $10/yr savings is due solely to orienting the axis of the house east-west and exposing a major portion of the house's window area to the south. The HUD/MRT house had the same amount of window area, but was analyzed with this glazing 45 degrees east of true south. The total savings of $132 represents a 17% reduction in the predicted fuel bills of the HUD/MRT version.

The solar model incorporated more insulation in the roof and subgrade walls than the present model, which helped reduce the fuel bill. The small savings in this area indicate the diminishing returns of adding more and more insulation. The small savings due to conservation efforts is a result of the air infiltration rate being held constant between Dynamic's present product and their solar model in our analysis.

The fuel cost savings due to solar designs resulted from the increased glazing area on the south side of the building and the addition of massive elements for storage. The movable night-time insulation for the south glazing was included in the solar savings. Analysis showed that the movable insulation with a R-value of approximately 2.3 over the windows with regular noninsulating curtains saved about 3 MMBtu/yr, which calculates to about a $35/yr fuel bill savings.

The overall predicted fuel bill of the solar model is 36% less than Dynamic's present model and 47% less than a comparably-sized house built to HUD/MRT standards for the Fargo climate.

The predicted thermal performance of Dynamic's prototype showed a 15.9 MMBtu/yr savings over Dynamic's present product line. The costs associated with achieving these deducted savings amounted to $5,618. Therefore, the cost/MMBtu saved in the first year is estimated to be $5,618/15.9 MMBtu = $374.

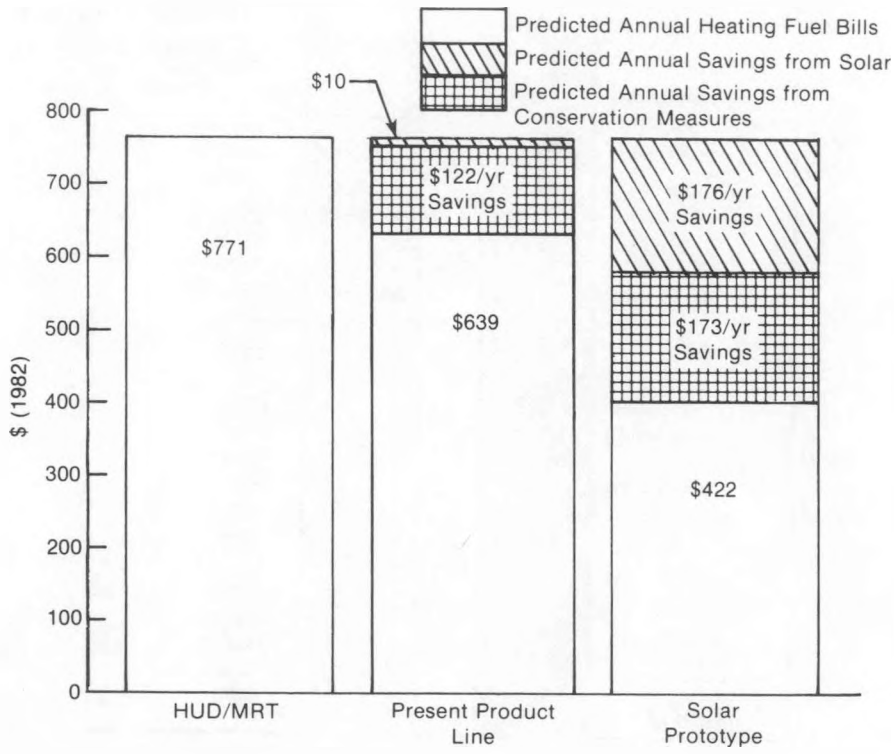

Figure 9. Predicted Fuel Savings

6. CONCLUSION

The reports being produced under this DOE program provide important data for the building, design, and research communities. As mentioned in the example case study using the work of Dynamic Homes, several valuable conclusions resulted: (1) the as-built prototype in Fargo, N.D., is slightly overglazed for the existing level of thermal storage mass provided, causing localized overheating in south facing rooms; (2) the P.C.M. thermal storage used in this prototype is expensive with little effect on human comfort or total auxilary heating; (3) being a very energy conserving building, the solar elements appear to have a small impact of the overall building energy use, but in context saves a considerable amount of fuel over Dynamic Homes' present product line (36%) and much more than the HUD minimum standards (47%); (4) the movable insulation scheme used was the highest cost element of the passive system and did not prove cost- or thermally-effective. Similar detailed information is being prepared for the 23 participating manufacturers, and we will include them in soon-to-be-released case studies.

7. ACKNOWLEDGMENTS

The work described in this paper was funded by the Systems Research and Development Branch, Passive and Hybrid Solar Heat Technologies Division of the Department of Energy, with direction from Ron Lutha at the Chicago Operations, Regional Office.

The authors would like to thank the Dynamic Home's design staff for providing detailed cost and marketing information. Special thanks for the development of the SERI-RES computer tool by Larry Palmiter and Terry Wheeling of the Ecotope Group under contract by SERI.

PROJECT SUMMARY

Project Title: The Passive Solar Manufactured Residential Building in Richmond, Virginia.

Principal Investigator: J. Durwood Usry

Organization: Usry, Inc.
1415 Chamberlayne Avenue
P. O. Box 27463
Richmond, Virginia 23261

Project Goal: The objectives of this project concerned the integration of energy conserving and passive and hybrid solar technologies into the existing construction/mass production processes of modular housing. To this end, the USRY DESIGN TEAM was also committed to the application of passive solar and energy conscious design techniques as a vehicle for improving the "market quality" of modular housing. Already far ahead of typical site-built wood frame construction in terms of structural integrity and tightness of seal, modular construction could greatly benefit from improved design concerning unit relationship to site; openness and interrelationship of interior spaces; improved, "more permanent" quality of interior finishes; variations in interior spatial experiences (to overcome the nature of smallness), and interior spaces that can open to link to exterior living spaces. From the USRY DESIGN TEAM'S assessment, it was felt that these qualities were easily associated with passive solar and energy-conscious system design. The team was determined to emphasize both low cost and improved design, with these alternate energy technologies as the catalyst for their development. In this way, the team felt it possible to develop a vastly improved, energy self-sufficient alternative to the low cost modular house and a new kind of modular house. This new house would be one which, although modular, could compete with, and supercede the stick-built of its variety, in terms of quality of design, cost, time, and energy efficiency.

Project Status: Two modular passive solar homes have been erected and completed. Both are located in Richmond, Virginia, on the Usry sales center. The first home, the "Solarium", with its 1500 square feet was completed in April of 1982. It will be featured in the October issue of "Better Homes & Gardens". The second home, the "Direct Gain", 1100 square feet, was completed August, 1982. Both homes are being monitored by the Solar Energy Research Institute with the Aoleian Kinetics PDL 24 microprocessor. Monitoring will continue until September, 1983, in order to determine heating and cooling loads.

Very little data is available at this time so no conclusions have been reached.

Contract Number: DE-FC02-80CS30385

Contract Period: November 1, 1979, through September 30, 1983

Funding Level: $136,690.00

Funding Source: U. S. Department of Energy, Chicago Operations Office

PASSIVE & HYBRID SOLAR HEATING FOR MANUFACTURED HOUSING

J. DURWOOD USRY
USRY, INC.
1415 CHAMBERLAYNE AVENUE
RICHMOND, VIRGINIA 23261

OBJECTIVE

The goal of this project is to create widespread production and sales of energy conserving passive solar heated and cooled manufactured homes. All completed buildings will be built in a factory utilizing wood construction and integrating applied and accepted on-site construction techniques. The Usry design team has evaluated many processes of construction and has determined that environmentally controlled manufactured systems are much more cost efficient as well as quality coordinated. Utilizing certain preliminary market assessments in the Richmond metropolitan area, it was determined that a typical home consisting of 1000 to 1600 square feet would be most favorable.

CONCEPT & BACKGROUND

The first step in this project's development involved visits to the factory where the modular units would be constructed. The team investigated current processes of construction, factory organization, design development, and scheduling procedures. Costs of production and conditions normally associated with prototype production were discussed as well as how prototype design and fabrication evolves into factory-efficient mass production. Current factory uses of materials and the costs associated with these uses were analyzed.

A study was then made of the typical modular housing units now produced by the factory. The analysis centered around those standard characteristics of space layout, construction technique, and aesthetic appeal that stimulated the market and minimized construction costs. Characteristics of flexibility/adaptability, inherent in most units through the use of space planning and material options were analyzed, also.

The team then determined the problems and opportunities inherent in factory processes, field construction techniques, and the popular designs as they relate to the building and design characteristics associated with passive solar design. It was decided by the design team that a great deal of flexibility must be incorporated in the prototype's design in order to provide a potential buyer with a range of choices. Options to be considered were: space planning - basement or crawl space, storage closet or master half bath; auxilliary heating system - furnace, heat pump, baseboard, wood stove; and siting orientation - north or south entries.

With this criteria in mind, the design team took three generic passive system-types consisting of Direct Gain, Trombe, and Solarium, and began to study what implications each of these systems had on existing modular plans. For each generic type, the team developed low and moderate cost units (to relate and identify the possibilities inherent in the system's adaptation to both the 1000 square feet and the 1600 square feet models), each with north and south entry options. Development of these concepts led to simultaneous study of thermal storage and how to best achieve it. Due to the limitations of weight, which regulate the transport of the modular units, it was determined that thermal storage incorporation should maximize site built operations and particularly, those operations associated with current USRY site construction techniques. In this way, costs could be minimized due to the standard nature of the construction, and the fact that it will already be occuring on site.

Water mass was considered and rejected by the design team after much study because it doesn't use existing Usry site construction expertise to its optimum.

Precast concrete panels (Fig. 1) were studied and found to require special handling equipment with high initial costs. Custom prefabrication was also a problem.

Site built poured-in-place concrete requires factory built form work which would be integral with modular wall construction and overall framing structure. This technique presented problems with interior finishing of the units on site rather than the usual completion of interiors in the factory. This change in practice would require more on site building inspections which lengthen critical construction time. The technique also increased the complexity of both factory and field operations, adding unnecessary costs to the unit's construction. (Fig. 2)

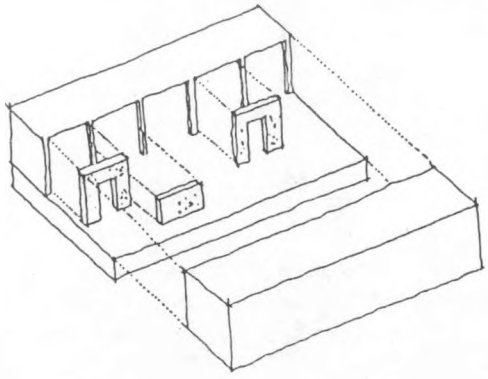

Fig. 1. Precast concrete mass wall construction.

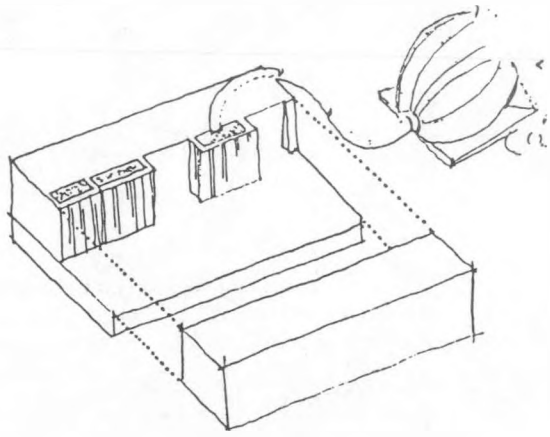

Fig. 2. Site-built poured-in-place mass wall construction.

Site built masonry (Fig. 3) was assessed by the team as having the most potential in that this material and construction procedure is already a part of the normal construction process. It was determined that this alternative would be the most feasible technique from the first cost standpoint, in terms of optimizing Usry, Inc.'s existing site construction capabilities.

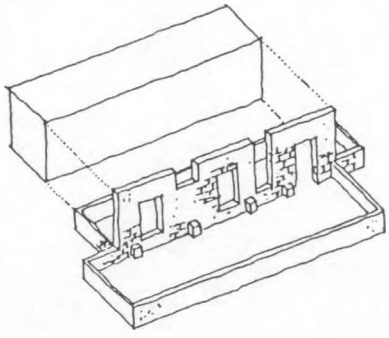

Fig. 3. Site-built concrete block mass wall.

Climatic analysis of Richmond, Virginia, was done based on twenty year data obtained from the National Climatic Center in Asheville, North Carolina. From this data, it was determined that the passive system's performance in heating should attempt to reach 70-75 percent due to the temperate winter weather conditions occuring in this area. Study also indicated that strong ventilation in summer was an absolute necessity in order to offset not only high temperatures, but extremely high humidity conditions as well.

DESIGN DEVELOPMENT

After much study of construction techniques, design concepts, site construction, and factory processes, along with costing, the design team identified the Direct Gain concept and the Solarium concept as being the most promising of the three developed. This was due to the ease associated with placing site built masonry walls between modular units in a typical double wide arrangement. In this type of configuration, the mass wall could effectively serve to tie the two (or three) modular units together, with the foundation wall for this central masonry wall easily constructed as part of the foundation wall construction that supports the typical double wide arrangement. The Trombe concept was eliminated as a viable condition for development at this point, due to the difficulty of integrating site built masonry with a finished factory built unit, particularly with regard to the attachment and seal of outside glazing. The construction staff felt that the extra costs and site liabilities involved in such a system outweighed its benefits at this time.

Direct Gain. This system centers around the construction of a solid concrete masonry wall which runs east-west between two modular units, and the exposure of this wall to a maximum amount of direct solar radiation. (Fig. 4) This maximum exposure was achieved by the location of high glazing on the southern modular, which offered direct gain heating and the daylighting to bedroom and kitchen areas (lower conventional windows in these spaces provided views, privacy and ventilation control).

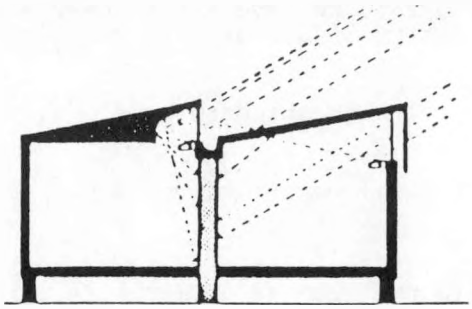

Fig. 4. Direct Gain - light entering south facing glass and clerestories. Mass wall is heated from both sides.

Solar exposure to the mass wall was also provided by a linear clerestory aperture on the south face of the northern modular, which reflects light back to the mass wall, provides daylighting, and offers high space in the unusually dark and tight modular corridor. This clerestory also preheats domestic hot water in a series of coils that are located on the cornice table just under the aperture glazing. The living room has a trombe wall which consists of a continuation of the site built masonry mass wall with field installed sliding doors. This trombe can be expanded to a greenhouse and will be considered as a design option for this housing model. The aperture (except for the area where the domestic hot water preheat is located), and southern high glazing are shaded in summer. The house is designed for cross ventilation with an inducement from the vented trombe in summer.

Solarium Concept. This system involves a solarium space which is located centrally on the south side of the house. Three modular units (one on the north and two on the south) join around a central masonry site built wall which is integral with the foundation wall construction for the modular units. The floor, roof, and side walls of the solarium space will be finished in the factory. The glazing wall, defining the solarium, will be site installed. In winter, solar radiation will directly hit the mass wall from the solarium for storage and re-radiation to the spaces in the northern module. A ceiling plenum will allow convection of heat built up in the solarium space for supply to the spaces in the northern modular. This plenum will act to exhaust in summer. When temperature in the occupied space on the northern sides become warmer than necessary for heating or uncomfortable for cooling, a fan will divert heat to the crawl space for either extended storage and return to the solarium, or, in summer, for exhaust through foundation wall venting. (Fig. 5) An aluminized curtain in the solarium space (separating the solarium space from the corridor), will provide night insulation and summer shading. In conjunction with the passive exhaust of heat through the roof vents, low openings in the solarium glazing will allow an induced ventilation action to occur, venting the solarium space, and drawing cool air through the house. The fan action will serve to augment this cycle.

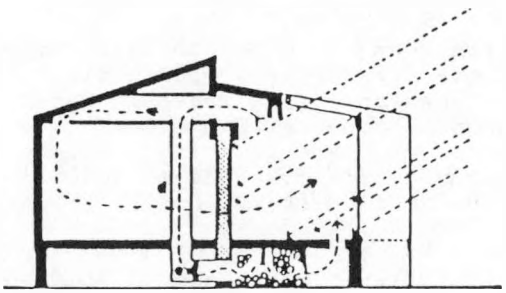

Fig. 5. Solarium Model - sun energy enters through greenhouse glazing and absorbed in mass wall and tile floors. Excess heat is moved via fan to rockbins under living room and bedroom.

SUMMARY

The Usry team along with its design arm, Archetype, have concluded with the aid of many marketing tests that the need for such housing in and around the state of Virginia is very strong. Thus far, we see the home buying market is well educated in the field of alternative energy as well as willing to support. All that is needed is the solution. We feel that through our efforts to research design and cost in coming up with a marketable product, we have further educated more of the populus in the southeast region. It appears that more and more families are striving to become independent of the utility companies out of necessity. With the cost of non-renewable resources escalating at the rate of 25 to 50 percent per year, the need for alternative energy such as solar is becoming more and more a reality.

Over the past year while working under our grant, we have experienced a number of breakthroughs. For the manufactured housing industry we see several technical accomplishments:

Introduction of the mass wall concept integral with standard type construction of modular homes. (Fig. 4 and Fig. 5)

Integration of passive solar options into typical construction of manufactured buildings.

A change in design concepts associated with manufactured structures; cost effective alternatives in design are much more prominent in the process of manufacturer's thinking.

Direct Gain Model

Low cost passive heating water system.
Use of aperture in corridor of home for the purpose of getting direct gain heat to both sides of mass wall.
Development of simple cost effective direct gain system which space heats as well as naturally ventilates.
Highly efficient and very affordable home appealing to moderate income group.

Solarium Model

Low cost rock storage system.
Low cost greenhouse space which can be integrated into typical modular construction.
Use of return air duct adjacent to solarium space to achieve high level of temperature control.
Integration of typical modular roof construction (tilt up roof system) as plenum space for supply of passive heat to living spaces.
Integration of passive techniques (solarium space) to achieve open daylit spaces in typical modular construction.
Use of solarium space to achieve induced ventilation throughout entire house.
Use of standard window shade technologies to perform as night insulation as well as shading for solarium.

FUTURE ACTIVITIES

Project Activities

With the sale of each passive solar home will be an owners' manual which will describe each function of the house. It will tell the homeowner exactly how to operate movable insulation, windows, vents, exhausts, and other mechanical devices. It will illustrate each item in clear detail. This manual will be a part of the phase two program of this grant.

During the first phase of this grant the design team, in order to test certain assumptions about the prototypes, produced in exhibit (renderings, plans, diagrams, and models) of the two proposed concepts. This presentation was taken in March and June 1980, to the Richmond Home Show and the Richmond Chamber of Commerce Energy Forum. At this time, public surveys were made to document and identify reactions to the Solarium and Direct Gain concepts, their appearance, and costs as an appealing, average priced housing alternative in the typical Richmond market. Public reactions were exceedingly favorable and encouraging.

Public reaction at these presentations, particularly at the Richmond Home Show and events following, also reinforced the team's assumption that the Direct Gain concept could viably compete (in terms of appearance and cost) with the standard modular unit. As a result of these assessments, the design team proceeded with the development of both the low cost Direct Gain unit, and the moderate (up-market) Solarium model.

Market assessments indicate that the Solarium model will be viable in the middle/upper housing market in Richmond, with a one acre or more site. The deck design as it relates to the use of the solarium space has a market potential for its expansion to relate to specific site topography when appropriate. To capitalize on this potential, Usry plans to offer site planning services, and design revisions/adaptations as options with the sale of this home.

Monitoring

Now that the prototypes are completed, testing has begun. The on-going monitoring program will now validate the thermal calculations which have previously been performed by the design team. Results of these studies will be published often for the benefit of those interested parties following the program.

System monitoring for both units is being implemented through the Solar Energy Research Institute (SERI). Under the direction of Rob DeKeiffer and Steve Brandt (SERI), a 24 channel microcomputer has been installed in each prototype. The totally integrated data acquisition system, the PDL-24 Programmable Data Logger, is produced by Aeolian Kinetics. The PDL-24 automatically calibrates and linerarizes sensor readings to engineering units. The Usry team will collect the data, and will work with the SERI team to evaluate the results. This information will act as a feedback to generate future design revisions. A print out unit, part of the microcomputer package, has been installed in each unit (prototype) in order to input variable conditions (number of people in the building and prevailing conditions), and to demonstrate to the public various system outputs. Performance will address climate (what was it?), construction (how does it operate?), and energy savings (what was last month's energy bill?).

PROJECT SUMMARY

Project Title:	Passive Solar Manufactured Residential Panelized Buildings: Phase III of the Independence Project.
Principal Investigator:	Art Milliken, Jon Slote
Organization:	Acorn Structures, Inc. P.O. Box 250 Concord, MA 01742
Project Goals:	This paper summarizes the third phase of the Independence Project, whose principal activities were the marketing of the homes designed in phase I and the performance analysis of a home constructed in phase II.
Project Status:	PROMOTIONAL ACTIVITIES: Open houses have been held at the Independence III in Boulder, CO., and the Independence IV in Butler, MD. Thousands of promotional brochures and technical bulletins describing various facets of the Independence designs have been circulated. Articles in the May 1982 issue of Solar Age and the October 1982 Better Homes and Garden feature the Independence IV to an audience of over 8 million. The Butler Independence IV home received an order of merit from the recently conducted National Passive Solar Design Competition, which had over 400 entries. By virtue of the award the home will be published in Progressive Architecture, Solar Age, The Passive Solar Journal, and be shown at the Seventh National Passive Solar Conference held in conjunction with the World's Fair in Knoxville, TN. SALES: To date 14 Independence Series homes or their design derivations have been sold. They are distributed over nine states in climates ranging from 4200 to 7500 degree days. Two-thirds of the homes have been Independence IV models, which employ an isolated gain sunspace coupled to a remote thermal storage slab to achieve the highest solar performance in the series. A strong consumer preference for larger homes has been noted, as demonstrated by the appeal of the Indy IV (the largest home in the series) and the fact that virtually every customer has chosen to expand the standard house plan. PERFORMANCE: The Independence III home in Boulder has been monitored as a part of the SERI Class B Passive Solar Data Acquisition Program. Results for the 1981-82 heating season show that auxiliary space heating energy consumption was 2.4 BTU/($ft.^2$xDD), higher than the original prediction of 1.4. The seasonal solar heating fraction was .68, matching the Acorn prediction exactly but falling short of the Berkeley Solar Group's .81. The biggest surprise was the low efficiency of the electric forced-air heating system, which was measured at .66. When the performance indices are re-calculated using the measured heating system efficiency, the predictions and the actual performance are in fair agreement.
Contract Number:	DE-FC02-80CS30363
Contract Period:	March 9, 1981 - September 30, 1982
Funding Level:	Phases II and III: $72,000
Funding Source:	U.S. Department of Energy

INDEPENDENCE PROJECT: MARKETING AND PERFORMANCE ANALYSIS OF PANELIZED PASSIVE SOLAR HOMES

Arthur N. Milliken Jonathan A. Slote
Acorn Structures Inc.
Box 250
Concord, MA 01742

OBJECTIVE

This paper summarizes the combined second and third phases of the Independence Project, whose principal activities were the marketing of the homes designed in Phase I and the performance analysis of a home constructed in the beginning of phase II.

BACKGROUND

The Independence Series consists of four similar floor plans in sizes ranging from 1400 to 1900 square feet. The designs were completed by the end of 1979 and promotional and descriptive literature was released in October, 1980. A model of the Independence III was constructed in Boulder, Colorado and finished in May, 1981. It has been visited by thousands of interested consumers and professionals during the last 18 months and during the last year considerable performance data has been gathered by monitoring devices and record keeping. Meanwhile along the eastern seaboard, which is Acorn's prime market area, a number of Independence houses have been built.

MARKETING AND SALES

Promotional activities have run the gamut from newspaper and magazine articles to open houses. Needless to say the various public relations and merchandizing efforts work hand in hand and their effectiveness is finally measured by sales results. In this section the activity and results to date are reviewed and further directions are outlined.

The initial thrust of promotion surrounded the SERI-NAHB sponsored Denver Metro Passive Solar Tour of Homes in February and March of 1981. Several thousand potential buyers visited the Acorn and other solar houses in the Denver area and a good deal of valuable educating of the public was accomplished. Acorn and Acorn builders have sponsored open houses for Independence models in Boulder, Colorado; Philadelphia, Penn.; and Butlter, Maryland, a suburb of Baltimore. In each case the open house was promoted by a combination of news articles, advertising and direct mail. Turnout has been good, but poor market conditions have meant that we have done a lot better job of increasing awareness of the practicality of solar than producing signed contracts.

Catalogue material has been prepared to describe each of the four designs and to highlight the functional, aesthetic and technical aspects of the product line as a whole. The former tells about the house plans and the latter discusses performance and the living environment. These brochures, put in the hands of the visitors to the open house, have a continuing educating value and selling role to play. Additionally, a more general use has been made of the Independence catalogue sheets. In February, 1981, we announced the series to a mailing list of 33,000 names and since then the brochure pages have been included in our complete design kit.

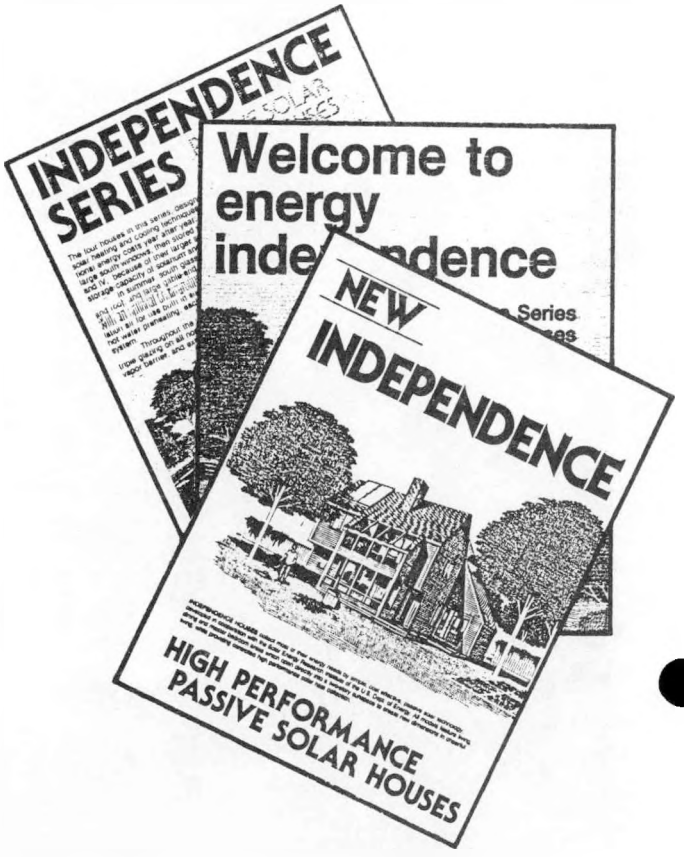

The public relations program which was so effectively aided by SERI for the Denver Passive Solar Tour has continued. For example, House Beautiful's Spring 1982 Building Manual featured the Independence III; a May, 1982 article in Solar Age described in detail the remote storage of Independence IV and currently the October issue of Better Homes and Gardens includes a four color feature on the Butler, Maryland Independence IV.

A TOP-OF-THE-LINE TWO-STORY

Although the generous amount of south glass tells you immediately that this house is solar-heated, absolutely nothing indicates that it's manufactured. The 2,100-square-foot house, located on a hilltop in Butler, Maryland, has its own little heat factory—a two-story solarium—that collects a whopping 80 percent of the heat the house needs.

Whenever warmth builds up in the solarium, fans pull the heat into a large duct that runs across the attic floor and down the inside of the north wall to a channeled concrete slab below the basement floor. The warm air gives up its heat as it travels south through the channels in the concrete and eventually returns to the solarium through a duct in the south wall, completing the convective cycle. When the house cools down in the evening, the concrete slab floor radiates its stored warmth, and the heat rises to all the living spaces.

To help cool the house in summer, air is drawn into an underground cooling duct (which is buried six feet below the earth) and is tempered by the soil to about 55 degrees F. The tempered air

This same house recently received an Award of Merit from the 1982 National Passive Solar Design Competition. By virtue of being singled out from among 400 entries, the Independence IV will be published in Progressive Architecture, Solar Age, and the Passive Solar Journal. Exposure at the recent Passive Solar Conference in Knoxville increased the impact of the award, particularly in the profession.

In the last two years 14 Independence houses or custom designed derivatives have been sold. Does this make the Independence Series and all the costs and efforts that have gone into design and promotion worthwhile and a commercial success? At this point in time the answer has to be, not yet. The following discussion may provide helpful insight.

1. Designing to the mainstream of American housing as suggested by DOE/SERI was probably an error. Particularly given poor market conditions the houses and individual spaces should have been larger and positioned for the custom buyer.

2. The Independence Series as a way of opening new markets for Acorn has not so far been successful. We attribute this in large part to the sorry state of the housing business during the last two seasons. This has not been a period where buyers take risks.

3. Most Independence Series sales have been made in established geographical areas and to buyers well aware of Acorn's 35 years of experience and quality reputation, further reinforced by word of mouth referral. The combination of design aesthetics and passive technology, offering a new product choice, has resulted in sales which would not otherwise have been made.

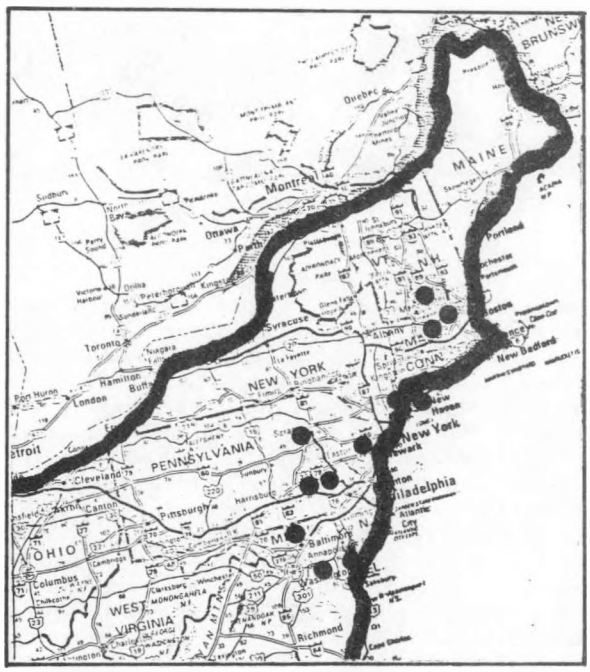

4. The association with DOE/SERI has been a useful and effective selling tool.

5. The technical data developed and the resulting increased solar expertise have helped in overall product development. Future products will be more energy efficient.

In short it's too early to make a final assessment of the DOE/SERI program which jointly with Acorn brought about the Independence Series.

The breakdown of sales of the 14 Independence houses has indicated the direction the product should take. First, most houses are considerably larger than the standard models which were the starting point. Second, there is a clear preference for the maximum degree of solar performance judging from the delivery of nine Independence IV houses with isolated gain space and remote storage. Among these, one of the more successful has a 60-foot two-story isolated gain solarium with more than 5500 square feet of living space. Others have doubled the sizes of the basic models. Cost is obviously not the prime consideration among discretionary buyers in a down market, but value, uniqueness, and performance appear to be key goals.

SALES	
INDY I	1
INDY II	1
INDY III	3
INDY IV	9
TOTAL	14

As we ponder what comes next in housing, we hope for a return of the middle priced market for which the Independence Series was designed, but we plan to meet the needs of the sophisticated and demanding upscale buyer with new Independence designs incorporating larger 2000 - 2400 square foot living spaces and eye catching architectural forms and details.

We doubt that solar and energy efficiency alone can be main selling features of a housing product line. Acorn is putting renewed emphasis on good architecture, design flexibility and courting the custom house buyer. At the same time energy related technology is here to stay. Demanding customers want to know how a house will perform as well as how it will look. Leadership and growth requires more service to the buyer and builder, a quality product and continued research and development.

PERFORMANCE MONITORING

Energy research activities at Acorn typically focus on three principal goals: documenting the energy efficiency of built structures validating the simulation tools used in the design process, and refining the designs and details to improve the performance. Fortunately, the Independence Project has yielded results in all three areas.

A variety of techniques have been used to gather data on the performance of the Independence homes, including the installation of automated data loggers, site visits by Acorn engineers to take one-time measurements, and records of fuel use from utility bills or homeowners themselves.

INDEPENDENCE IV RESULTS

This latter method has produced useful results from an Independence IV in Allenwood, N.J. The "thermal index" for this house, the BTU's of auxiliary space heating energy required divided by the product of the heated square footage and the degree days, was

ACORN INDEPENDENCE IV
ALLENWOOD, NJ

AUXILIARY FUEL CONSUMPTION
1981-82 HEATING SEASON

UNITS: BTU/(FT^2 X DD)

MONTH	DEGREE DAYS	FUEL USE
OCT	420	0.0
NOV	618	1.6
DEC	962	4.1*
JAN	1305	1.5
FEB	891	1.3
MAR	779	1.5
APR	490	2.3
MAY	127	0.0
SEASON	5592	1.9
(W/O DEC)	(4630)	(1.4)

*CHANGE IN OCCUPANCY

1.9 for the 1981-82 heating season. This compares favorably with the thermal index of 2.5 projected for so-called "BEPS" homes in this climate by Lawrence Berkeley Labs as reported in SERI's New Prosperity report.[1]

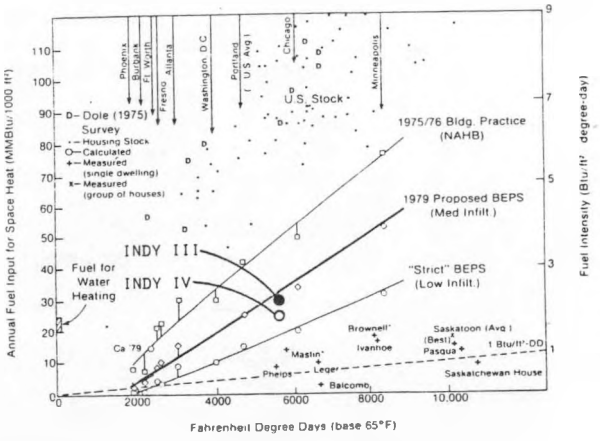

Several observations about the design and use of this particular house which affect its thermal index rating should be pointed out. First, the larger size of the house (5762 ft.^{2}) biases the index downward, since the smaller surface-area-to-volume ratio reduces relative building heat loss. On the other hand, the thermal curtains planned for the home have not yet been installed, indicating that this year's index is abnormally high. Space heat consumption was also increased nearly 35% when the owner's mother visited in December, as noted on the accompanying table. The row of parenthesized numbers at the bottom of the table shows how much lower the home's auxiliary consumption was when December usage was excluded from the calculation. Nonetheless, auxiliary fuel consumption is sufficiently low that, by comparison, the internal gains from appliances are significant. In this house the electric appliances and lighting use added about one BTU for every two supplied by the gas furnace, a figure which is not counted in the "Fuel Use" column of the table.

INDEPENDENCE III RESULTS

The Boulder Independence III, which was monitored both by Acorn and SERI, yielded results which initially surprised us. The thermal index was over 50% higher than predicted -- 2.3 BTU/(ft.^{2} x DD) versus Acorn's 1.5 and the Berkeley Solar Group's 1.4 -- but the solar fraction exactly matched the .68 predicted by Acorn. In discussions with SERI we discovered that the efficiency of the electric forced-air heating system had been measured at an abysmal 66%.

ORIGINAL HEATING SYSTEM EFFICIENCY CALCULATION:

$$\frac{\text{BUILDING LOAD - COHEATING TEST}}{\text{ENERGY PRODUCED BY FURNACE}} = \frac{238{,}700 \text{ BTU}}{364{,}600 \text{ BTU}} = .66$$

The SERI Class B Passive Solar Data Acquisition Program technique for estimating heating system efficiency relies on a comparison between two measured heat loads -- the first is measured as the house is "coheated" by electric space heaters dispersed throughout, and the second is measured while the furnace system does the same job. The difference between the two is assumed to be due to non-recoverable system losses through the ducts and furnace, which in this case represents a total of 125,900 BTU's over the course of a 12-hour furnace test. When these system losses were carefully calculated, (using some techniques which ASHRAE has updated since the house was designed)[2], we found that the losses were larger than we expected but smaller than the reported difference between the two tests.

FOR A 12-HR. TEST CONDUCTED 12/28/82:

	BTU OVER 12-HR. TEST	% OF FURNACE OUTPUT
ENERGY PRODUCED BY FURNACE:	364,600 BTU	100.0%
BUILDING LOAD FROM COHEATING TEST:	238,700 BTU	65.5%
ENERGY REMAINING:	125,900 BTU	34.5%

NON-RECOVERABLE SYSTEM LOSSES:

	BTU OVER 12-HR. TEST	% OF FURNACE OUTPUT
SLAB EDGE	39,600 BTU	10.9%
RETURN DUCT IN ATTIC	8,700 BTU	2.4%
SUPPLY DUCT IN UTILITY ROOM	7,800 BTU	2.1%
INFILTRATION THROUGH DUCTS	7,300 BTU	2.1%
SUPPLY DUCT TO BEDROOM	5,300 BTU	1.5%
RETURN DUCT IN UTILITY ROOM	4,700 BTU	1.3%
FURNACE JACKET	1,100 BTU	0.3%
TOTAL	74,500 BTU	20.4%

	BTU OVER 12-HR. TEST	% OF FURNACE OUTPUT
ENERGY REMAINING:	125,900 BTU	34.5%
SYSTEM LOSSES:	−74,500 BTU	20.4%
ENERGY ABSORBED BY MASS:	51,400 BTU	14.1%

We theorized that the remaining 51,400 BTU's were spent raising the temperature of the home's mass an average of 1.2°F. SERI confirmed that the average indoor air temperature had risen 3°F during the furnace test, which suggested that the furnace was in fact producing more energy than the building needed to maintain steady-state conditions. This led to a recalculation of the heating system efficiency, yielding 76%.

$$\frac{\text{ENERGY ABSORBED BY THERMAL MASS}}{\text{HEAT CAPACITY OF THERMAL MASS}} = \frac{51{,}400 \text{ BTU}}{42{,}000 \text{ BTU/°F}} = 1.2°\text{F RISE IN MASS TEMP.}$$

NOTE: A 3°F AVERAGE INDOOR AIR TEMPERATURE RISE WAS REPORTED DURING THE TEST.

REVISED HEATING SYSTEM EFFICIENCY CALCULATION

$$\frac{\text{(BUILDING LOAD FROM COHEATING TEST)}}{\text{(BUILDING LOAD FROM COHEATING TEST)} + \text{(NON-RECOVERABLE SYSTEM LOSSES)}} = \frac{(238{,}200)}{(238{,}700) + (74{,}500)} = .76$$

The new furnace efficiency value was fed into Acorn's SLR-based simulation program (along with corrected numbers on the night insulation R-value and the occupancy schedule) and the simulation was re-run. The table below compares the new simulation to the original, as well as to the actual energy consumption derived from daily electric meter readings and the SERI Class B Monitoring effort.

ACORN INDEPENDENCE III BOULDER, CO

AUXILIARY FUEL CONSUMPTION FOR SPACE HEATING
1981 - 82 HEATING SEASON

UNITS: BTU/(FT^2 X DD)

MONTH	ORIG. SLR PREDICTION	METER READINGS	SERI CLASS B MONITORING	NEW SLR SIMULATION
SEP	0	0.5	NA	0
OCT	0.4	3.2	NA	0.5
NOV	1.9	1.7	0.7	2.2
DEC	2.6	3.6	2.6	2.9
JAN	2.6	3.8	3.0	2.9
FEB	2.2	3.7	3.1	2.5
MAR	2.0	2.7	2.1	2.4
APR	1.4	2.6	1.8	1.6
MAY	0.3	1.9	1.2	0.4
SEASON	1.9	3.1	2.3	2.2

The 2.3 thermal index reported by SERI is less than the 2.7 projected for a BEPS home in this climate as described in the New Prosperity report.

A similar comparison is drawn for the solar heating fractions shown in the following table. Here, the SERI data is modified by using the higher heating system efficiency value, resulting in closer agreement with the new simulation. Since the solar fractions are computed by subtracting the auxiliary and internal heat contributions from the load computed in the coheating test, numerically increasing the furnace efficiency while holding the other terms constant has the apparently paradoxical effect of reducing the solar fractions.

ACORN INDEPENDENCE III BOULDER, CO

SOLAR HEATING FRACTION
1981 - 82 HEATING SEASON

MONTH	SERI MONITORING ORIG.	SERI MONITORING ADJ.	NEW SLR SIMULATION
SEP	NA	NA	1.00
OCT	NA	NA	.89
NOV	.81	.78	.57
DEC	.66	.60	.45
JAN	.60	.54	.45
FEB	.59	.52	.51
MAR	.73	.68	.54
APR	.69	.65	.65
MAY	.74	.70	.88
SEASON	.68	.62	.55

APPLICATION OF THE DATA

The importance of these findings is not that we can measure the performance of homes better but that we can design and build them better. Data from the Boulder home tells us that duct losses are greater than we anticipated, especially at the slab edge which apparently leaked over 10% of the furnace's output. For this reason, Acorn is beefing up its heated slab edge insulation detail with extra insulation in the three places shown in the drawing. R-values at the slab edge will now total 12.5, while an R-20 barrier will protect the duct from the cold.

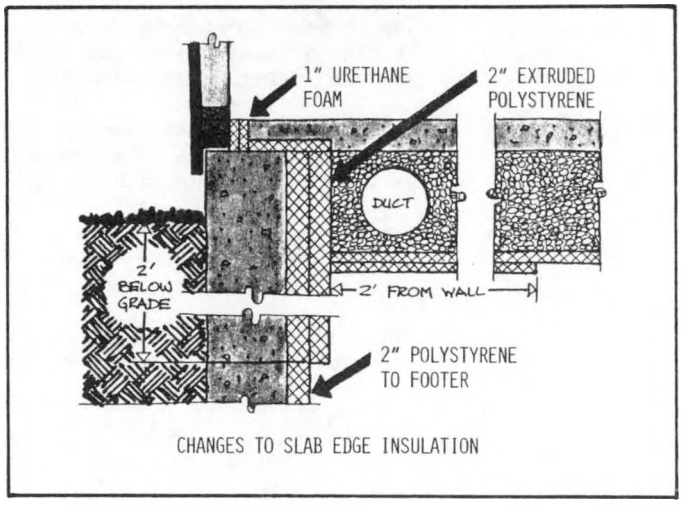

CHANGES TO SLAB EDGE INSULATION

The architect Mies Van der Rohe said, "God is in the details." As we seek more and more energy-efficient housing, details such as slab edge insulation become more important to house performance. Getting these details right demands an unusual level of commitment and skill from a builder. We at Acorn have been fortunate to have worked with such builders in the Independence Project. The performance results we are seeing are clear testament to the zeal and pride in workmanship they bring to the job.

In summary, designs intended to penetrate the broad housing market must be not only thermally effective but buildable right down to the details. Our experience tells us that superior performance results from both designer and builder taking pains to respect each other's crafts while perfecting their own.

FOOTNOTES

[1] A New Prosperity, Building a Sustainable Energy Future (United States: Solar Energy Research Institute, 1981), pp. 24 - 26.

[2] ASHRAE Handbook of Fundamentals (Atlanta: American Society of Heating, Refrigerating, and Air-Conditioning Engineers, Inc., 1981), pp. 25.8 - 25.9.

PROJECT SUMMARY

Project Title: National Solar Data Network (NSDN) Program

Project Manager: Sharon M. Rossi

Organization: Vitro Laboratories Division
Energy Systems Department
Silver Spring, Maryland 20910

Project Goals: Assist in the development of solar technologies for buildings by providing data and information on the effectiveness of specific systems, the effectiveness of particular solar technologies, and the areas for potential improvement.

Project Status: Three years of performance data has been collected and analyzed on passive structures throughout the United States. Performance information has disseminated via solar reports, public media and technical conferences.

The NSDN is the primary vehicle for the Federal Government to monitor the performance of many solar space heating systems selected for demonstration and research purposes.

During the contract period, nineteen passive structures were monitored. These systems included direct gain, direct gain with water wall, sunspace with mass wall and a double envelope site.

The season performance of these sites show that:

- No particular type of passive solar system is superior. With good design practices and conservation measures, each system provided excellent performance.
- Automated movable insulation yielded the maximum system performance.
- Conservation measures proved to be more important than any other single parameter.
- Proper site selection and passive collector orientation are necessary for good performance.

Contract Number: DE-AC-01-79CS30227

Contract Period: October 1, 1979 through December 31, 1982 for the NSDN Program, which includes active and passive sites.

Funding Level: $13.5 Million

Funding Source: U. S. Department of Energy

NSDN PASSIVE PROGRAM

VITRO LABORATORIES DIVISION, AUTOMATION INDUSTRIES, INC.
14000 GEORGIA AVENUE, SILVER SPRING, MARYLAND 20910

DE-AC01-79CS30027

EDWARD O. POLLOCK

OBJECTIVE

The objective of the National Solar Data Network (NSDN) is to evaluate the performance of a large variety of solar systems in both residential and commercial buildings dispersed throughout the United States. The purpose is to obtain operational data from solar systems in actual applications rather than from systems operating under carefully controlled test conditions. Eleven of the solar systems monitored by the NSDN during the past year were passive.

BACKGROUND

The National Solar Data Network (NSDN) has been continuously monitoring the performance of a number of passive solar buildings located throughout the country. The length of the monitoring period ranges from one to three years. Each passive site has been instrumented with an average of 90 sensors which measure environmental data; interior temperatures and relative humidity; fossil and electrical energy consumption; operation of windows, doors, vents and movable insulation; and surface and gradient temperatures of all thermal storage masses. Thermal evaluation of the structures using these data includes determination of the total building heat loss, equipment heating load, and solar energy collection and utilization (1).

SUMMARY

Performance of eleven passive space heating systems, eight residential and three commercial, was evaluated during the past heating season. System types included low mass direct gain, high mass direct gain, Trombe wall, sunspace and double envelope designs. Seasonal performance reports for each of the systems have been prepared.

SYSTEM DESCRIPTIONS

1. Residential Systems

The residential systems ranged in size from 1360 ft^2 to 2600 ft^2.

1.1 Gill Harrop

The collector aperture of this 1360 ft^2 single-story residence, located near Corning, NY, consists of the entire south wall (305 ft^2) and a clerestory (98 ft^2) which admits solar energy into the north half of the structure. Most of the glazing is fixed double-walled fiberglass but both glazed areas include operable glass windows to permit venting. The south wall is provided with R-3.4 insulating curtains. Walls of the structure are insulated to R-19 and the roof is insulated to R-38. Solar energy is stored in the six inch concrete floor and eight inch concrete walls.

1.2 Rymark I

This two-story residence, in Frederick, MD, is a standard architectural design which has been sited with the back of the house facing south. The windows are double glazed with 84 ft^2 on the south side. Walls of the structure have R-14 insulation and the roof has R-30. The house has 800 ft^2 of floor area on each floor. Although the structure is slab on grade, the first floor is carpeted so the floor mass does not participate much in solar storage. No other storage mass has been added.

1.3 Rymark II

Rymark II is located beside Rymark I. The floor plan of this house is the same as Rymark I, however, the amount of south glazing has been increased to 160 ft^2. All windows are triple glazed and equipped with R-3.4 insulating curtains. No other design changes were made.

1.4 Rymark III

Also located on the same street as the other two Rymark homes, this house incorporates the MIT phase change ceiling system. The 227 ft^2 triple glazed south windows are equipped with special venetian blinds which reflect the sun onto the ceiling.

1.5 Lo-Cal

This low mass house in Champaign, IL has 1848 ft^2 of floor area. Two hundred square feet of double glazed windows admit solar energy into the house. The heat ducts run through the crawl space which is insulated around the perimeter to R-20, but had to be vented to meet local building codes. Walls of the house are insulated to R-24 and the roof to R-33.

1.6 Roberts Home

One of the National Concrete Masonry Associations homes, this three-story building in Reston,

VA features a two-story Trombe wall with 663 ft^2 of single glazing and a sunspace located on the third floor with 99 ft^2 of double glazing. The house has a total of 2600 ft^2 floor area and 264,000 lbs. of solar storage mass in the 12-inch Trombe wall, the hollow core north wall, and two centrally located fireplaces. Four fans draw air from the space between the Trombe wall and the glazing through the north wall. Three R-12 Thermal Technology curtains reduce nighttime losses from the Trombe wall. The house walls are insulated to R-24 and the roof to R-32. A combination of heat avoidance and earth tube cooling is used to provide summer cooling.

1.7 Environmental Partnership

Located in Cream Ridge, NJ, this 2050 ft^2 has 344 ft^2 of Trombe wall and 168 ft^2 of sunspace. Both systems are double glazed. Solar storage is in the 50,000 lbs. of concrete block in the Trombe wall and 32 Thermal 81 phase change rods. The walls of the house are insulated to R-20 and the roof to R-40.

1.8 Arno Kahn

This 2500 ft^2 three story double envelope house is located in Duluth, MN. Solar energy is collected by 442 ft^2 of double glazed sunspace and 100 ft^2 of direct gain windows. Thermal Technology insulating curtains were added to the sunspace this past year. The mass wall in the sunspace provides 68,000 lbs. of storage mass. The outside shell of the house is insulated to R-19 in the walls and the roof to R-38.

2. Commercial Systems

2.1 Taos State Office

Located in Taos, NM, this 12000 ft^2 single story office building utilizes both daylight and passive solar space heating to conserve energy. The solar system consists of 2700 ft^2 of clerestory configured in 11 sawtooth rows, 300 ft^2 of south window and 109 ft^2 of window scoops on the east and west sides of the building. The clerestory windows have pneumatically controlled shutters which regulate the amount of solar energy and light admitted to the building and reduce heat losses at night. Solar storage is in the floor slab and in 14000 gal. of water in containers suspended in the clerestories.

2.2 Contemporary Systems, Inc.

This 3700 ft^2 system located in Walpole, NH, used both passive and active systems for space heating. This single story office and manufacturing facility has 190 ft^2 of double glazed direct gain windows and 320 ft^2 of double glazed sunspace. The direct gain windows are equipped with R-3.4 window curtains.

2.3 Telluride School

The retrofit of this 43000 ft^2 school in Telluride, CO with a Trombe wall and sunspace cost only $230,000. A vented Trombe wall was added to the gym by attaching 1478 ft^2 of glazing to an existing brick wall. Solar energy for the classroom wing is provided by a 1400 ft^2 sunspace.

PERFORMANCE DATA

Table 1 summarizes the performance of the 11 systems. The table lists performance over the entire monitored period and for the month of February. Data for the one month period is presented to permit comparison of the systems since the monitoring period varied from three to eight months. The average insolation listed in the table represents the solar available at the surface of the passive collector glazing. The equipment heating load (EHL) is the building envelope losses less the internal gains. The building envelope losses were determined by use of ASHRAE procedures to calculate a loss rate and actual measured temperature differences across the wall sections including losses through the south glazing. These values were confirmed by comparing them with auxiliary energy usage during periods of no solar gain and stable storage temperatures.

The last column of Table 1, Building Performance Index (BPI), shows a ratio which can be used to compare relative performance of the systems. This ratio is based on the amount of non-solar energy used per square foot of floor area. As can be seen from the BPI values, all of the residential systems demonstrated good performance. The systems, in general, were of good design with the proper balance between aperature size, storage mass and load. The commercial systems had a wider range of BPI values. Contemporary Systems had the best BPI value, even including the active solar energy as auxiliary energy. The Telluride School BPI value was quite high compared to the other buildings. It is a masonry building which is not well insulated and has a collector to floor ratio of only 0.07 sc the high BPI value is no surprise.

Even discounting the effect of variations in the available insolation, it was observed that there is an inverse relationship between the collector to floor area ratios and the BPI values. A way was sought to compare building performance which would account for the variation in insolation available and collector size. This led to the development of an Index of Relative Value (IRV) which is derived by using performance data from each of the systems to model performance of a reference building. The following factors were used in the model.

1. Floor area of 1000 ft^2 for residences and 10,000 ft^2 for the commercial buildings.

2. The same design parameters as each of the actual systems, i.e., the same type of system with identical collector to floor and mass to collector ratios.

3. Actual construction cost data for most of the systems was not available. Since the structures were built at various times and parts of the U. S. A., use of actual costs would not have permitted meaningful comparisons anyway.

TABLE 1. PERFORMANCE DATA

MONITORING PERIOD	INSOLATION (BTU/FT^2-DAY)	AVE. AMB. TEMP. ^oF	AVE. BLDG. TEMP. ^oF	HDD BASE 65^oF	ΔTDD[a]	INTERNAL GAINS MBTU	AUX. ENERGY (MBTU)	EQUIPMENT HEAT LOAD (MBTU)	BLDG. PERFORMANCE INDEX[b] (BTU/FT^2/^{o}F-DAY)
RESIDENTIAL SYSTEMS									
GIL HARROP[c]									
9/81-4/82	701	37	58	6776	5160	8.76	12.63	37.34	3.05
2/82	888	25	57	1088	896	1.57	3.11	6.53	3.84
RYMARK I									
10/81-3/82	857	37	62	4893	4454	10.61	27.19	33.13	5.30
2/82	952	34	59	821	700	1.97	4.58	5.46	5.85
RYMARK II[d]									
10/81-3/82	857	37	66	4893	4714	4.42	32.13	39.48	4.85
2/82	952	34	67	821	924	0.70	6.74	8.41	5.03
RYMARK III[e]									
10/81-3/82	857	37	65	4893	4308	3.51	30.79	39.46	4.98
2/82	952	34	58	821	672	0.74	3.74	4.52	4.17
LO CAL									
1/82-4/82	1073	31	71	3975	4729	14.68	25.77	36.39	4.63
2/82	1375	23	71	1152	1344	4.20	5.13	9.53	3.76
ROBERTS HOME									
2/82-5/82	588	50	66	1818	2206	12.70	3.58	21.45	2.84
2/82	678	38	62	729	672	3.64	2.43	7.54	3.47
ENVIRONMENTAL PARTNERSHIP									
10/81-3/82	671	40	65	4521	4570	8.92	27.27	41.27	3.86
2/82	599	35	66	814	868	1.34	4.98	7.68	3.55
ARNO KAHN									
9/81-4/82	908	30	65	9546	8472	21.33	61.24	103.09	3.90
2/82	1090	18	63	1312	1260	2.39	12.39	16.27	4.69
COMMERCIAL SYSTEMS									
TAOS STATE OFFICE									
9/81-3/82	1436	39	74	5336	7529	122.01	223.71	527.40	3.83
2/82	1384	28	74	978	1288	18.48	45.20	88.23	4.12
CONTEMPORARY SYSTEMS									
10/81-4/82	1083	30	65	7450	7417	19.26	64.97[f]	103.61	3.07
2/82	1219	22	62	1219	1120	2.27	10.03[g]	15.30	2.97
TELLURIDE SCHOOL									
2/82-4/82	939	30	70	2942	3516	402.00[g]	647.00	-	6.94
2/82	931	23	71	1120	1344	122.00[g]	232.00	-	6.13

a. Heating degree days based on temperature difference between the measured inside and outside temperatures.

b. Building non-solar energy usage per square foot of floor area per ^{o}F measured daily average difference between inside and outside of the building.

c. Building unoccupied until January 1982.

d. Building unoccupied over the entire period.

e. Building unoccupied until March 1982.

f. Active solar energy used. No fossil fuel used to heat the building.

g. Estimated internal gains.

Therefore, the following assumptions about costs were made.

(a) System costs were assumed to be proportional to the collector area and were priced at \$30/ft^2. Since most non-solar houses will have some south glazing, it was assumed that Rymark I is typical of the non-solar house and the costs of the first 50 ft^2 of collector deducted from the system costs in each case.
(b) Movable insulation costs are assumed to be above the general system costs and were priced at \$6.00/ft^2 for insulated curtains, \$8.00/ft^2 for the Thermal Technology curtains and reflective Venetian blinds and \$15.00/ft^2 for the Taos shutters.

4. If a system was equipped with movable insulation but it was not used because the structure was unoccupied, as in the case of Gill Harrop and Rymark II, the costs are estimated as if the movable insulation were not there.

5. A 30 year life expectancy of the system was used.

6. Energy costs were based on the cost of electricity at 5.66¢/kWh.

Figure 1 shows the IRV values for the eight residential buildings and Figure 2 shows the values for the commercial buildings. The index has been plotted for heating degree day values of 4000 HDD, 6000 HDD and 8000 HDD when 1000 BTU/ft^2-day average insolation is available. These values were selected since they represent much of the USA. From Figure 1, it can be seen that there is not a very wide range in the IRV values. The low mass houses with smaller collector to floor area ratios appear to have the best value. The model used assumed that fuel costs will increase at a rate equal to inflation. If fuel costs should increase at a rate much greater than inflation as they have in the past decade, then the systems which had a larger aperture and higher solar fraction will be more cost

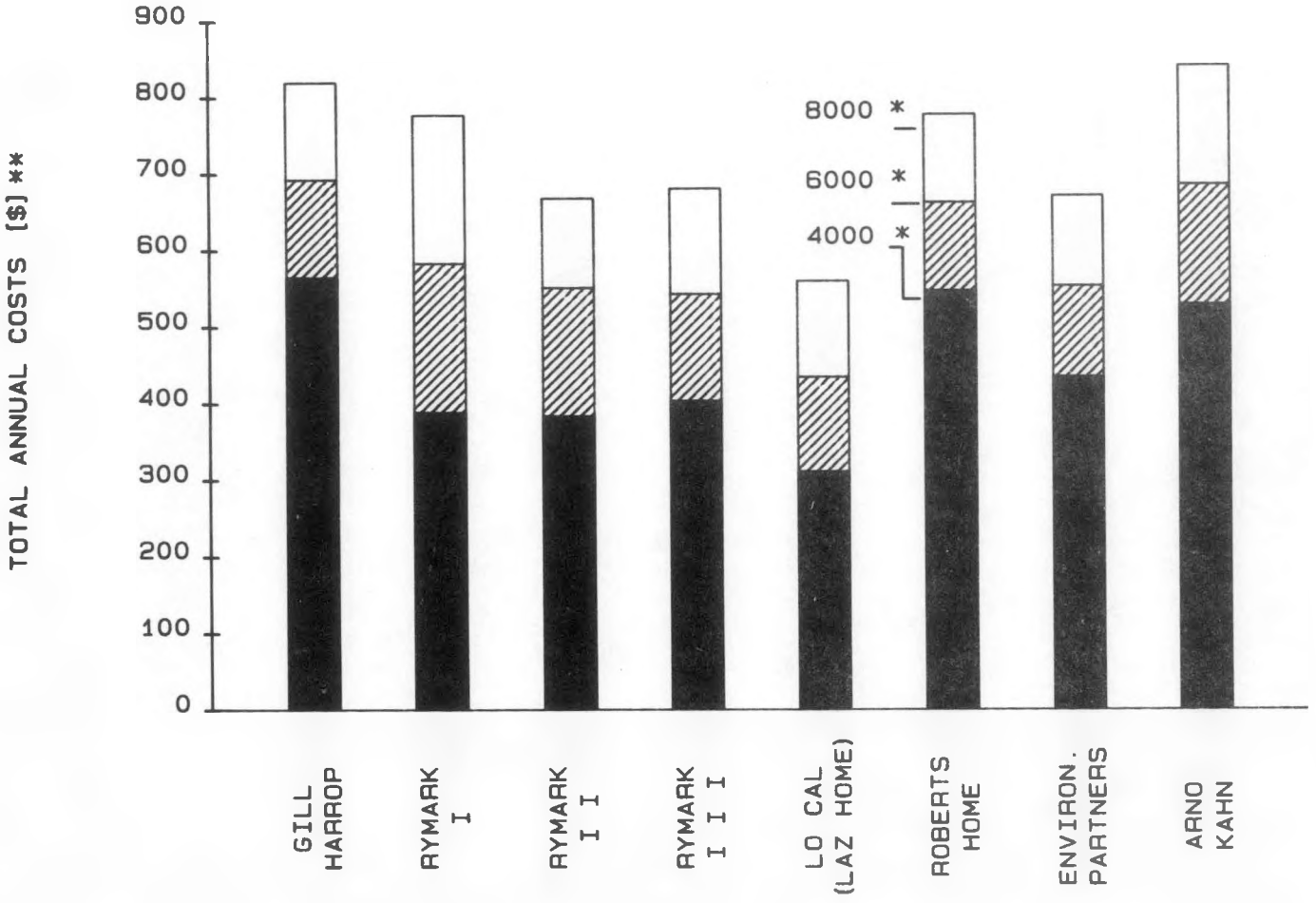

* Incremental increase in total annual costs for 4000, 6000, and 8000 heating degree days zones (base 65°F)

** Total annual costs including solar system procurement costs amoritized over a 30 year period plus annual non-solar space heating costs (including internal gains) modeled for 1000 BTU/ft^2-day insolation and 4000, 6000, and 8000 heating degree days (base 65°F)

Figure 1. Residential Systems - Index of Relative Value

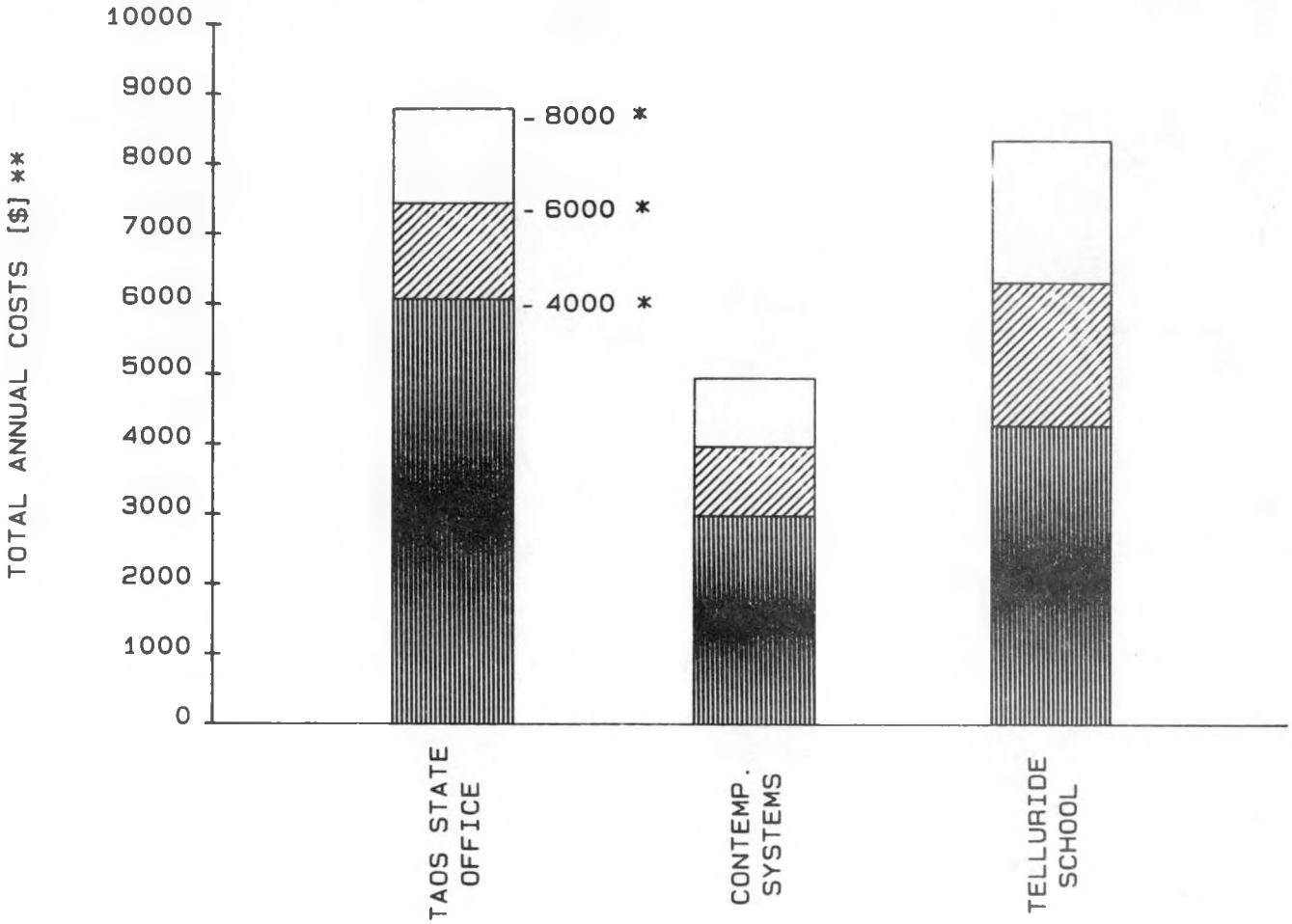

* Incremental increase in total annual costs for 4000, 6000 and 8000 heating degree day zones (base 65°F)

** Total annual costs including solar system procurement costs amoritized over a 30 year period plus annual non-solar space heating costs (including internal gains) modeled for 1000 BTU/ft^2-day insolation and 4000, 6000 and 8000 heating degree days (base 65°F)

Figure 2. Commercial Systems - Index of Relative Value

effective. It should be noted that the model does not factor in the cost of insulation for the building shell. Since all of the residences are insulated to about the same level, this is not significant when comparing these systems, but it would be if this approach is used to compare systems where the insulation values varied.

SUMMARY AND CONCLUSIONS

No particular type of solar system appears to be superior in performance.

Cost analysis indicates the direct gain, low mass systems may be the most cost effective for most environmental conditions.

The impact of occupants on passive system performance is significant. Systems should be user proof. In the more severe climates where movable insulation is required, it should be automated.

With the exception of Telluride School, all of the buildings are well insulated. This increased use of conservation measures appears to be a good strategy.

PUBLICATIONS/REPORTS

Publications

The following reports are available through the U. S. Department of Energy, Technical Information Center, P. O. Box 62, Oakridge, Tennessee 32930.

1. Solar Energy Systems Performance Evaluation Gill Harrop,, 10/81-4/82, SOLAR/1096-82/14, Vitro Laboratories, Silver Spring, Maryland.

2. Solar Energy Systems Performance Evaluation Rymark I, II and III, 5/81-3/82, SOLAR/1106-82/14, 1111-82/14, and 1107082/14, Vitro Laboratories, Silver Spring, Maryland.

3. Solar Energy Systems Performance Evaluation Lo Cal, 1/82-4/82, SOLAR/1109-82/14, Vitro Laboratories, Silver Spring, Maryland.

4. Solar Performance Bulletin, Roberts Home, 2/82-7/82, SOLAR/1122-82/16, Vitro Laboratories, Silver Spring, Maryland.

5. Solar Energy Systems Performance Evaluation Environmental Partnership, 10/81-3/82, SOLAR/1027-82/14, Vitro Laboratories, Silver Spring, Maryland.

6. Solar Energy Systems Performance Evaluation Arno Kahn, 9/80-4/82, SOLAR/1103-82/14, Vitro Laboratories, Silver Spring, Maryland.

7. Solar Energy Systems Performance Evaluation Taos State Office Building, 6/81-3/82, SOLAR/2080-82/14, Vitro Laboratories, Silver Spring, Maryland.

8. Solar Energy Systems Performance Evaluation Contemporary Systems Inc., 10/81-4/82, SOLAR/2116-82/14, Vitro Laboratories, Silver Spring, Maryland.

9. Solar Energy Systems Performance Evaluation Telluride School, 2/82-4/82, SOLAR/2118-82/14, Vitro Laboratories, Silver Spring, Maryland.

10. Comparative Report: Performance of Passive Space Heating Systems, 1980-1981 Heating Season, SOLAR/0022-82/39, Vitro Laboratories, Silver Spring, Maryland.

Reports

1. E. O. Pollock, "Comparison of Monitored Passive Building," Proceedings of the AS/ISES Sixth Passive Solar Conference, Portland, Oregon, September 1981.

2. B. D. Howard, "Net Solar Radiation: Passive Systems Performance with Movable Insulation", Proceedings of the 9th Energy Technology Conference, Washington, DC, February 1982.

3. B. D. Howard & E. O. Pollock, "Insolation vs. Insulation: Comparison of Monitored System Performance", Proceedings of the Seventh Passive Solar Conference, Knoxville, Tennessee, September 1982.

4. J. W. Spears, "Side by Side Testing of Three Production Type Passive Solar Homes", Proceedings of AS/ISES Solar Conference, Houston, Texas, June 1982.

5. J. W. Spears, "Monitored Performance of a Passive Phase Change Storage System", Proceedings of the Seventh Passive Solar Conference, Knoxville, Tennessee, September 1982.

THE CONSUMER PERSPECTIVE

CarolAnn Shindelar
Associate Building Editor
Better Homes and Gardens
1716 Locust Street
Des Moines, IA 50336

It's not easy being a consumer today. Deciding what to buy and when to buy it has never been more difficult. An unpredictable economy, a depressed marketplace, and a confusing array of new goods and services have turned the market topsy turvy. And amidst this clamor the passive solar industry, still in relative infancy, must struggle to identify itself as a movement of worth, as a technology whose time has come.

One of the many roles of Better Homes and Gardens magazine over the last five years has been to translate that technology into understandable language and provide tangible evidence that passive solar works. Better Homes and Gardens is the largest consumer service magazine in the country, with a circulation of 8 million and a readership of 37 million. When our readers talk, we listen! Over the past few years they've shared their views with us on solar energy through letters, phone calls, surveys--and by simply telling us (via readership studies) what they like in our magazine.

The overall feeling we sense from consumers is confusion. As in all new technologies, a time lag of several years must go by before information and products about solar is filtered to all segments of society. And the process involved in disseminating knowledge about passive solar has been doubly difficult because of the confusing array of solar devices and techniques available. Back in the Fifties a tv was a tv; today a solar house is not just another solar house. In March of 1980 a Better Homes and Gardens survey asked a representative sampling of readers (who are better educated and have slightly higher incomes than the general populace) whether they felt they knew enough about solar energy designs and products to make a decision on whether or not to purchase them. 88 percent of the respondents answered No; only 10 percent answered Yes.

The editors of Better Homes and Gardens use this research data to help determine the kinds of articles to publish. And it also helps us get a real feel for what is happening in middle America. Our consensus is that the role of all passive solar designers, manufacturers, and believers has never been more important; the honeymoon is over, the novelty has worn off. Now it's time to get to work.

THE CONSUMER PERSPECTIVE

CarolAnn Shindelar
Better Homes and Gardens
1716 Locust Street
Des Moines, Iowa 50336

It's not easy being a consumer today. Deciding what to buy and when to buy it has never been more difficult. An unpredictable economy, a depressed marketplace, and a confusing array of new goods and services have turned the market topsy turvy. And amidst this clamor the passive solar industry, still in relative infancy, must struggle to identify itself as a movement of worth, as a technology whose time has come.

One of the many roles of Better Homes and Gardens magazine over the last five years has been to translate that technology into understandable language and provide tangible evidence that passive solar works. Better Homes and Gardens is the largest consumer service magazine in the country, with a circulation of eight million and a readership of 37 million each month. When our readers talk, we listen! Over the past few years they've shared their views with us on solar energy through letters, phone calls, surveys--and by simply telling us (via readership studies) what they liked in our magazine.

The overall feeling we sense from consumers is confusion. As in all new technologies, a time lag of several years must go by before solar products and information are filtered to all segments of society. And the process involved in disseminating knowledge about passive solar has been doubly difficult because of the confusing array of solar devices and techniques available. Back in the Fifties a TV was a TV; today a solar house is not just another solar house.

Back in 1978, Better Homes and Gardens conducted a survey to discover consumer attitudes regarding solar energy. The survey was nationally distributed to 500 members of the Better Homes and Gardens Panel; panel members, who are a representative group of Better Homes readers, respond to several questionnaires each year. Because incentives are provided, the response is always high. We asked our readers to indicate the importance of various factors in making a decision to purchase a solar heating system. Their responses are tallied in Table 1. As you can see, cost was the primary factor. The availability of service, the

TABLE 1

Listed below are a number of factors that you might want to know about before you make a decision to purchase a solar heating system. Please indicate how important each of these factors would be to you.

	Very Important	Somewhat Important	Neither Important nor Unimportant	Somewhat Unimportant	Very Unimportant	No Answer
Cost (installed)	79.1%	5.8%	1.2%	--	.3%	13.6%
How available service is	73.3	11.4	1.5	--	--	13.8
How system works	73.5	11.9	1.7	--	--	12.9
How much money is saved each year	72.1	12.1	2.2	.2%	--	13.4
Whether the system is warranteed and for how long	72.6	11.4	2.2	.5	--	13.3
Protection against rising energy costs	65.3	18.9	1.9	.5	--	13.4
Whether it will work on cloudy days	64.3	17.7	4.1	.3	.5	13.1
How the system is installed	50.0	29.4	6.1	.5	.5	13.5
That it will add value to my house	49.3	26.2	10.0	1.0	.4	13.1
That return on my investment is tax free	34.2	30.3	18.2	2.0	.7	14.6
Ability to get government credits	29.9	35.9	15.8	2.7	2.2	13.5

way the system works, the amount of money saved each year, and whether or not the system is warranteed are factors that followed close behind.

Better Homes and Gardens has long been the magazine of choice of middle America. To give you an idea of demographics of our readers so that the Consumer Panel respondents can be put into perspective, the median age of the Better Homes and Gardens reader is 40 years old; his/her household income is just less than $24,000, and 75 percent of the households consist of two to four persons. Over 75 percent of the readers own their own homes, 72 percent are married, and over 42 percent attended or graduated from college.

The same 1978 Consumer Panel survey also asked panel members to respond to a set of reasons for not installing a solar heating system. The two primary responses, based on mean scores, were that technology will advance and systems will become more reliable, and that prices will come down in the future. A summary of the responses is shown in Table 2. Prices for solar systems have come down a bit since 1978, but consumers who expected a dramatic drop have been disappointed. Solar heating systems simply won't become the pocket calculators of the Eighties. The reasons are obvious; passive solar heating is directly tied to the new housing and construction industries, and we all know the state those industries are in. Costs for passive solar systems in new homes are not easily separated from the cost of the home itself; thus, the state of the building industry is the state of the passive solar industry. And chances are, construction costs won't come down, even if mortgage interest rates do.

TABLE 2

Following are a number of reasons why you might not want to install a solar heating system at this time. Please indicate how important each of these reasons would be for not installing a solar heating system.

	Very Important	Somewhat Important	Neither Important nor Unimportant	Somewhat Unimportant	Very Unimportant	No Answer
Technology will advance; system will be more reliable	62.4%	18.2%	4.4%	.7%	.2%	14.1%
Prices will come down in the future	51.7	21.1	9.0	.7	2.4	15.1
Larger, well-known companies will begin to manufacture reliable systems	34.0	29.6	17.2	2.2	1.7	15.3
Government will provide tax incentives and loans	21.9	29.1	26.7	3.4	2.9	16.0
Until electricity, oil and natural gas prices increase, you can't save that much money	18.0	27.2	26.0	5.3	4.4	19.1
Solar heating systems decrease the value of a home and make it harder to sell	10.9	12.9	31.1	10.7	17.0	17.4

Prices for the hardware systems--active solar components, photovoltaics, passive domestic water heaters and air panels--stand a better chance of coming down as technology advances. But only in the photovoltaic industry can we expect to see a "breakthrough" comparable to the microchip of the Seventies, which may result in plummenting prices.

It's a tough time in our country's history, so it's no wonder that consumers are confused and uncertain about the energy situation in general, and solar in particular. There are still those who insist that the energy crisis is a hoax trumped up by big oil companies at the consumer's expense. And just recently I've heard others say that because the price of gasoline has come down, the energy problem must be over. (Since when did we start heating our homes with gasoline?)

What's obviously needed is education. Better Homes and Gardens has been trying very hard over the last five years to provide insight and information on solar energy, but the press can't--and shouldn't--do it alone. Texaco, Phillips 66, Shell, and a host of others have gone to consumers with advertising that tells their story. But I don't see the solar industry marching forward to tell their side. Granted, Fortune 500 companies have many more dollars to spend on advertising, but money alone doesn't get the job done. I'd like to see more grass-roots support for solar eduation and more advertising for solar homes and products pitched in terms of costs and fuel savings, with basic information on how the system or

product works. Passive solar has too much of a trendy, glamorous aura--it's wonderful, it's healthy, it uses the sun instead of dirty, nasty fuels--but the facts are that solar technology is hard-hitting, reliable, and cost-effective. Consumers will not buy what they don't understand and will generally speak negatively of anything that mystifies them.

A 1980 Consumer Panel survey demonstrates how hungry consumers are for educational information.

Which of the following types of information do you feel is the most important in deciding to buy a solar product such as a passive solar home or a solar hot water heater?

Price of product	15.5%
Pictorial layouts (to better understand the product or design	8.0
Energy and dollar savings calculations	47.1
Reliability	36.0
Lists of dependable contractors	3.6
Reputation of the product manufacturers or home builder	9.4
Other	.8
No answer	1.7

You can see a shift away from an emphasis on installer servicing and warranties as indicated in the 1978 Consumer Panel (see Table 1).

The same 1980 Consumer Panel was also asked the following question:

Do you presently feel that you know enough about solar energy designs and products to make a decision on whether or not to purchase them?

Yes	9.5%
No	87.7
No answer	2.8

I would expect that very high negative response to have dropped some in the last two years, but I'm sure you'll agree that it will still be significantly higher than the positive response. Another factor that has delayed the mainstreaming of solar energy into our society is the infighting among various factions of the solar industry. Instead of fighting each other we should be fighting the wasteful use of hydrocarbon fuels and the ill-advised direction of our national energy policy. Better Homes and Gardens has long been a staunch supporter of passive solar, yet most of our readers in a Consumer Panel Inquiry on home remodeling/home maintenance in 1980 did not know the difference between active and passive solar.

Do you know the difference between passive solar and active solar energy?

Yes	29.2%
No	66.4
No answer	4.4

We fervently hope that many more would answer "Yes" now, two years later. But we pacifists must accept the fact that passive systems do need an active boost now and then, from fans, controllers, and the like. And in some regions of the country active systems--especially domestic hot water--do make sense.

In a way, it's unfortunate that cost and payback are always the bottom line in a solar energy decision. Do we buy our cars, remodel our kitchens, or send our kids to college based on the number of years it takes to recoup our investment? Hardly. If it were true, I doubt if some of us would ever buy a new car again. The 1980 Consumer Panel inquiry posed this question regarding payback:

Would you consider including active/passive solar energy saving features in your remodeling plans if you could be satisfied that these features would pay for themselves in 7 years or less?

Yes	59.3%
No	34.5
No answer	6.2

The Energy Project at the Harvard Business School corroborates the Consumer Panel findings. In the 1977 study, three key points emerged: solar heating is very attractive; people are poorly informed about how systems work; and an average, five-year payback is necessary to attract serious considerations. In 1982 the idea of solar heating is still very attractive, people are somewhat better informed, and a good payback is still a necessary requirement.

Solar energy does have a certain attraction, and certainly has far more consumer support than its arch-enemy, nuclear energy. The nationally-reknowned research firm, Yankelovitch, Skelly, and White in the 1982 Monitor Study asked these questions:

How much do you approve/disapprove of these technologies/scientific innovations?

	Monitor			
	1979	1980	1981	1982
Solar Energy				
Strongly approve	64%	67%	68%	72%
Moderately approve	30	28	28	25
Disapprove	6	5	4	3
Nuclear Reactors for Energy				
Strongly approve	18	17	18	17
Moderately approve	57	48	51	47
Disapprove	25	35	31	36

Apparently there are still a bunch of fence-sitters who aren't quite sure that nuclear is the answer. Solar has a very high approval rate, but a not-high-enough purchase rate.

In the late Seventies, solar was trendy; it was "in". Now it's accepted by most of society, but it certainly hasn't been mainstreamed. We've all learned to live with the rising costs of food, clothing, and shelter, so we're not surprised or angered by escalating energy costs. But energy prices are something consumers can fight. The reasons the 1980 Consumer Panel gave for wanting to purchase a solar energy design or product are shown in Table 3. Saving money was far and away the most important reason.

TABLE 3

The following are a number of reasons why you might want to use solar energy designs and products in your present or future home. Please indicate how important each of these would be to you in your purchasing decision.

	Very Important	Somewhat Important	Neither Important nor Unimportant	Somewhat Unimportant	Very Unimportant	No Answer
Can save money on my energy bills	86.0%	7.6%	.7%	--	.2%	5.5%
Can help the country be less dependent on foreign oil	64.5	23.0	6.2	.7%	.9	4.7
They can add to the value of my house	58.5	24.9	6.6	1.4	1.0	7.6
Government is providing tax credits and incentives	32.0	40.0	14.0	3.8	2.8	7.4
They can create more attractive living space for entertaining and family recreation	20.4	40.0	19.2	6.2	4.0	10.2
Can grow plants and vegetables year round	21.8	29.4	23.9	7.6	7.6	9.7
Just want to	13.5	15.9	25.1	5.0	18.0	22.5
Can be a leader in my neighborhood on how to use alternative energy sources such as solar	4.5	9.2	42.2	9.5	24.4	10.2

But we mustn't forget that energy isn't the only factor in buying a house. The 1980 Consumer Panel respondents placed a great deal of importance on the traditional reasons, too, as shown in Table 4. People are not going to buy or accept something that's ugly, and unfortunately, ugly is what comes to many people's minds when they envision solar homes. We must reach a point where south-facing glass and increased thermal mass are simply accepted architecture and everything else is unusual. We must reach a point where solar collectors are no longer traffic stoppers, and where homes that aren't energy-efficient (and preferably solar-heated) won't sell.

TABLE 4

If you were to build your own home, how important would the following be to you?

	Very Important	Somewhat Important	Neither Important nor Unimportant	Somewhat Unimportant	Very Unimportant	No Answer
Floor plan	90.3%	4.3%	.2%	.2%	--	5.0%
Heating and cooling system	84.6	10.7	.2	--	--	4.5
Energy conserving features	82.5	11.6	.5	.2	--	5.2
Size (total square feet)	72.0	19.9	2.8	.5	--	4.8
Number of rooms	68.5	22.7	3.1	.2	--	5.5
Exterior appearance	65.4	28.7	.7	.2	--	5.0
Uses solar designs and products	34.4	35.3	15.9	7.1	.7%	6.6

How much money people are willing to spend to get solar features has always been a question. Of course, most of us know that passive solar needn't cost a penny more, especially if solar features (such as attached sunspace) are simply part of the living space--and a very nice part at that. The 1980 Consumer Panel asked this question:

> If your desired solar features were to add to the cost of your home improvement project or new home purchase, how much would you be willing to spend?

Nothing	2.8%
Less than 10%	22.2
10% - 15%	41.8
16% - 20%	11.9
As much as it will take	17.5
No answer	3.8

As you can see, people are willing to shell out a bit more for their new home or retrofit if it means saving dollars in the long run.

There are many methods, products, and ideas these days for bringing down the costs of housing and energy. Many are DOE-supported, and we laud the department's efforts. Others are in the areas of wide land use, more efficient building methods, creative financing, and do-it-yourselfism. People are smart when it comes to spending money; they'll do what's inexpensive and cost-effective first, but think twice about anything else. Fortunately, that's also the wisest way to approach energy-saving; conserve first, solarize second. The 1980 Consumer Panel asked respondents who were considering energy-conserving designs and products this question:

> Which of the following designs and products are you considering:

Sunspace addition	14.3%
Insulated windows	54.6
Brick, masonry or tiles for storing heat	9.2
Insulated window shades	28.6
Insulated curtains	40.3
Insulated wood shutters	11.8
Solar domestic hot water system	7.6
Solar space heating and cooling system	5.0
Other	26.9
No answer	.8

You can clearly see where Better Homes and Gardens readers are putting their money. This testimoney is expanded by a question in the Yankelovitch 1982 Monitor. As shown in Table 5, the Monitor study asked for opinions on a broad-ranging field of subjects. According to the nation-wide study, only 11% of the people in this country are installing or considering installing solar. That's not as high a percentage as we'd all like to see, especially when you note that it's only risen one point since 1979--which certainly indicates that the solar movement hasn't made much progress over the last three years.

TABLE 5

ADAPTING TO THE PROSPECT OF SHORTAGES

	Bench-mark	Monitor 1979	1980	1981	1982
Now Doing or Seriously Considering Doing					
Energy/Resources					
Keeping thermostats at a lower temperature	67%	63%	64%	67%	59%
Buying a car which consumes less gasoline	45	41	39	43	42
Installing better insulation in home to conserve heat	44	35	30	31	29
Installing wood or coal burning stove		13	17	13	12
Using fireplace heat circulator		12	14	12	13
Installing solar heating		10	9	12	11
Changing home heating system			32	28	27
Buying home furnishings with energy saving in mind--e.g., heat retaining fabrics, dark colors, etc.				12	12
Using wind power as an energy source				6	4
Installing my own generator				3	4

But in general, the future for solar energy looks good. The passive solar industry is in a transitional period, evolving from a grass-roots movement on the fringes of society to a solidly-established, legitimate technology. We seem to have lost the urgency of the Seventies, however, partly because the movers and shakers have gone on to something else, partly because the technology has been stonewalled by lethargic government bureaucracy, and partly because some of the early designs, products, and producers have not lived up to the standards of a scrutinizing public. But we can't give up now! Now's the time to stand firm and push hard, because once the economy loosens up, passive solar must be ready to leap forward. This incubating phase is a golden opportunity to research and develop, to analyze the marketplace, and to make plans for the future.

The year 2000 is a bench-mark the industry has long been looking forward to. And everyone has an opinion on what percentage of our country's energy needs will then be filled by solar. The Energy Project at the Harvard Business School predicts that we can expect anywhere from seven to 23 percent, depending on many factors and figures. When the question was put to the 1978 Better Homes and Gardens Consumer Panel, here's how they responded:

In your opinion, by the year 2000, what percentage of our energy needs will be fulfilled by solar energy?

None	.7%
1% - 9%	13.8
10% - 24%	36.9
25% - 49%	20.7
50%	16.0
More than 50%	7.9
No answer	4.0

You can see that back in 1978, middle America was pretty optimistic about solar energy. Much has changed since then, of course, but by and large, Americans have always been and always will be an optimistic bunch. And as far as solar is concerned, optimistic is a pretty good place to be.

PROJECT SUMMARY

Project Title:	EPRI Passive Solar Energy Study
Principal Investigator:	Peter F. DeDuck
Organization:	JBF Scientific Corporation 2 Jewel Drive Wilmington, MA 01887
Project Goals:	Evaluate the potential impact of passive solar and energy conserving housing on the electric utility industry.
Project Status:	The first two phases of the project have been completed. The final report and executive summary are in preparation. Thermal performance analyses have been completed for houses located in the service territories of seven utilities across the country. These are Boston Edison Co. at Boston, Pennsylvania Power and Light Co. at Harrisburg, Alabama Power Co. at Montgomery, Public Service Co. of New Mexico at Albuquerque, Salt River Project at Phoenix, Pacific Gas and Electric Co. at Fresno, and Pacific Power and Light Co. at Medford, Oregon and Casper, Wyoming. Complete utility impacts analyses have been conducted for Pennsylvania Power and Light Co., Alabama Power, Co., Pacific Gas and Electric Co., and Public Service Co. of New Mexico. Documentation for the economic and diversity computer models is currently in preparation.
Funding Source:	Electric Power Research Institute

EVALUATING HOW PASSIVE SOLAR HOUSES AFFECT ELECTRIC UTILITIES

Robert A. Wood, Peter F. DeDuck, Michael D. Siegel
JBF Scientific Corporation
2 Jewel Drive
Wilmington, Massachusetts
01887 U.S.A.

ABSTRACT

Methodology and results are presented for the Electric Power Research Institute's Passive Solar Energy Study. Results are presented for 2 utilities: Public Service Company of New Mexico (PNM) and Alabama Power Company (APCo). A comparison is made between conventional, energy conservation, and passive solar housing types. Preferred housing types are discussed that minimize the total of homeowner equipment costs, and utility energy and demand costs.

I. INTRODUCTION

Interest in passive solar systems has increased significantly in the United States in recent years as one response to higher energy prices and as the widespread popularity of virtually all solar technologies has increased. Yet, while a large number of new houses and other buildings incorporating passive solar design have been constructed, little work of a rigorous nature has been done to determine what impact these buildings have on electric utilities and what economic benefits, if any, they might offer.

This study assesses this impact and these benefits from a utility perspective for the residential sector - specifically for single-family, detached houses.

The study has two primary objectives. First, to establish requirements by which a preferred passive solar design[1] could be determined for a given utility system. And second, to establish and apply a methodology for projecting and evaluating the potential impact of large numbers of passive solar houses on utility systems.

Seven utilities participated in the study and eight analyses sites were established within their service regions. These included Boston Edison at Boston, Pennsylvania Power and Light at Harrisburg, Alabama Power Co. at Montgomery, Public Service Co. of New Mexico at Albuquerque, Salt River Project at Phoenix, Pacific Gas and Electric Co. at Fresno, and Pacific Power and Light Co. at Medford, Oregon and Casper, Wyoming.

Data used in the study included projections of load growth and generation mix, and of the number, size, and type of houses expected to be built within the service territories through to the year 1995. This included information on the type of heating these houses would use, and on the number of air conditioners, heat pumps, and evaporative coolers that were expected. These projections were made in consultation with the respective electric utilities.

II. METHODOLOGY

Establishing Building Characteristics

In the first step, three types of buildings, all with the same floor plan, were defined and compared. The first building is of a "conventional" design, representative of houses which were constructed several years ago. The second building, called the "energy conserving" design, has significantly lower heat loss (e.g., an energy conserving design might include more insulation or triple-pane windows). The third building is the "passive" design. The passive design is insulated to the same levels as the energy conserving design but has additional south window area or a mass wall.

Two levels of simulations were run. The first is a one-month comparison of the house designs using weather data for July and January (important cooling and heating months). The second level was a one-year simulation. The one-month simulations were used to help determine the preferred passive design and show the sensitivity of this design to various design parameters. The list of the parameters varied is given in Table 1. In some instances, not all these parameters were examined (e.g., where cooling is insignificant, parametric analysis of the cooling load was not done).

---

[1] Preferred is defined as the one design among the wide range of potential house designs that provides maximum economic benefit to both the utility and the individual homeowner.

TABLE 1. PARAMETRIC INVESTIGATIONS

South Glazing Area	Building Insulation
Direct Gain	Infiltration
Thermal Storage Walls	Thermostat Setting
Internal Mass	Fan-Forced Ventilation
Greenhouses	Heat Pump
Nighttime Insulation	Evaporative Cooler
Summer Shading	

From this preliminary, first-level analysis and discussions with the architect, final designs were developed for the conventional, energy conserving, and passive solar houses. The regional housing market was examined to determine the expected penetration of passive solar houses.

The second level, one-year simulations were run for the conventional, energy conserving, preferred passive, and sometimes one additional passive design.

The thermal simulations were done using the EMPSS 2.0[2] hourly building simulation program. The output of the simulation is estimated hourly electrical usage by a house's HVAC system.

Utility Production Cost and Reliability Analysis

The hourly electrical demands from the one-year simulations are diversified to account for noncoincidence of individual demand peaks by using a diversity equation, developed by Aerospace Corporation[3]. These diversified, one-year, hourly demands are used to modify the given one-year, hourly utility load shape. This modified utility load shape is input to SYSGEN[4].

SYSGEN is used to compute variable and fixed cost savings to the utility associated with a conglomerate of house designs. The production costs include operation and maintenance, generation start-up and fuel costs. As the system load decreases, different fuels are saved. The sum of these savings make up the total fuel cost saving.

Improvements in generation reliability will usually occur when energy conserving or passive houses are substituted for conventional houses. These improvements in reliability reduce the utility's need for additional capacity. In general, a generation capacity credit is taken from a generating unit planned to come on line near the year of analysis. The amount of capacity credit and the type of generation deferred will depend on the generation mix and the impact of the alternate home designs.

Economic Analysis

In the economic analysis of renewable energy projects, electric rates are normally used to establish the cost of utility-supplied backup energy. Electric rates are often based on average costs and may be an imperfect measure of real costs. This methodology uses the utilities' production costs (primarily fuel costs) and the changes in generation capacity to establish these costs. Homeowner equipment costs incurred directly by the homeowner (maintenance, taxes, insurance, and increased mortgage payments on additional equipment) are treated by calculating a uniform annual cost which recovers the present value of these costs.

III. RESULTS

The passive solar and energy conserving houses modeled significantly outperformed the conventional house in both sites served by Public Service Company of New Mexico (PNM) and Alabama Power Company (APCo) in the following areas: kWh use, utility fuel savings, generation capacity demand, and generation reliability. The best passive solar house performs better than the energy conservation house in the heating-load dominated PNM climate. In the cooling-load dominated climate, APCo, the best passive house performs roughly equivalent to the energy conservation house.

---

[2] EMPSS 2.0: Computer Program for Residential Building Energy Analysis, Electric Power Research Institute, Prepared by Arthur D. Little, EPRI 1830 (1982).

[3] SHACOB: Requirements Definition and Impact Analysis, Electric Power Research Institute, Prepared by Aerospace Corporation, EPRI ER-808, Vol. 2 (1979).

[4] SYSGEN: A Utility Production Cost and Reliability Model, Prepared by the MIT Energy Laboratory (1979).

Alabama Power Company

The APCo direct gain passive home required slightly more cooling energy and slightly less heating energy than the energy conservation home; see Fig. 1B. The large areas of south glazing caused higher cooling loads because they allowed proportionately larger amounts of diffuse sunlight and conductively transferred more heat into the homes during the summer months. Summertime direct sunlight was prevented from entering the home by properly designed overhangs. Appropriate manipulation of drapes helped reduce summertime heat gain due to diffuse and reflected sunlight. The net result was reduced passive cooling loads with no significant effect on heating performance.

The cooling problem, however, was severe enough in the APCo climate to minimize the amount of south glazing designed into the passive home. This had the attendant effect of reducing heating season performance.

Fig. 2B shows the utility fuel savings which would result if energy conserving or passive solar houses were built instead of conventional houses. The fuel savings for APCo were derived from displacement of 100% coal-fired generation. The energy conserving design saved slightly more fuel than did the passive solar design.

Percentage improvements in generation reliability resulting from this substitution of energy conservation and passive houses for conventional houses are listed in Table 2. These improvements indicate that this substitution of houses reduces the utility's need for capacity. The improvement in reliability for APCo is equivalent to a capacity savings of 1.2 kW for each passive house.

TABLE 2. GENERATION RELIABILITY IMPROVEMENT

Utility	Conventional	Energy Conservation	Direct Gain Passive
Public Service of New Mexico	100%	140%	150%
Alabama Power Company	100%	115%	113%

The homeowner equipment costs of Fig. 3B show that homeowner investment is greatest for passive solar and least for the conventional house. Expenses for conservation and backup equipment are equal between the energy conserving and passive solar homes. The differences between total ownership costs of the passive and energy conserving designs is the cost of passive equipment. For the direct gain passive case these equipment costs are for additional south window area.

Referring to Fig. 4B, both the energy conserving and the direct gain passive designs are preferred over the conventional design, and the energy conserving design is preferred, although not greatly preferred, over the passive solar design.

Public Service Company of New Mexico

Referring to Fig. 1A, the PNM passive house results in a large reduction in total kWhs over the conventional home and a moderate reduction in total kWhs over the energy conserving house.

The PNM climate is dry enough during the summer to allow use of an evaporative cooler. The evaporative cooler reduces cooling energy to an insignificant amount. These results suggest that use of an evaporative cooler might allow larger south window areas without incurring significantly higher cooling costs.

The passive solar house with mass walls was also modeled for PNM. Heating savings in reference to the energy conservation buildings increased from 35% to 57%.

There are fuel savings for PNM, as shown in Fig. 2A, over the conventional design for the energy conserving and both passive designs. Fuel savings were greater for the passive with mass wall and direct gain passive solar design. All fuel savings for PNM were derived from displacement of 100% coal-fired generation. Houses with an evaporative cooler saved more utility fuel than those with a vapor compression air conditioner.

The percentage improvements in generation reliability listed in Table 2 show that the direct gain passive design outperforms the energy conserving and especially the conventional design. The biggest improvement in reliability was achieved when a passive solar mass wall was combined with an evaporative cooler. It was taken that this house would replace a conventional house with vapor compression air conditioning. In this event, the resulting capacity savings was 3.66 kW per house over the conventional design; see Table 3 for comparison. If this house had replaced an energy conserving house with an evaporative cooler, the ca- pacity savings would have been 1.04 kW per house.

TABLE 3. DIVERSIFIED DEMAND PER HOUSE

Utility	Conventional	Energy Conservation	Direct Gain Passive
Public Service of New Mexico	4.1 kW	2.1 kW	1.3 kW
Alabama Power Company	4.1 kW	2.6 kW	2.9 kW

The homeowner equipment costs of Fig. 3A show that homeowner investment is again greatest for passive solar and least for the conventional house. Expenses for backup equipment are again equal between the energy conservation and passive solar homes. The differences between total ownership costs of the passive and energy conserving designs is the cost of passive equipment. For the mass wall passive case, the additional costs are for both south window area and the mass wall. For the direct gain design, additional equipment ownership costs are for south glazing area only.

Referring to Fig. 4A, the preferred house for PNM site is the direct gain design. The passive design with mass wall has very low utility costs, but these are overshadowed by high equipment costs. The direct gain passive design offers the best balance between homeowner and utility costs.

Annualized homeowner and utility cost totals are more often higher for the houses at the PNM site due primarily to the larger house size. The PNM houses have 1515 square feet of floor area as opposed to only 1230 square feet for the APCo houses.

IV. CONCLUSION

Passive solar houses can significantly reduce homeowner and utility costs over conventional house designs, and can moderately reduce these costs over energy conserving designs in some climates. Passive solar houses perform better in cool, dry climates than in warm, humid climates; but, even in the warm and humid Alabama climate, the passive solar design reduced costs almost as much as the energy conserving design.

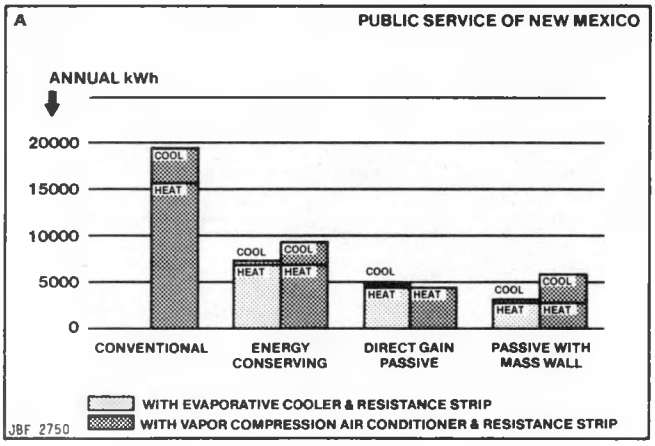

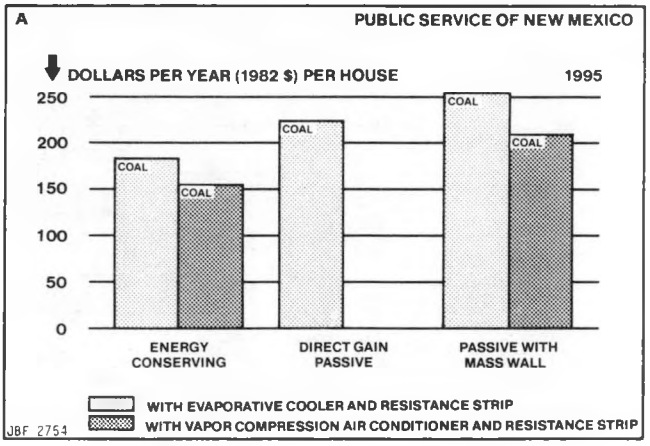

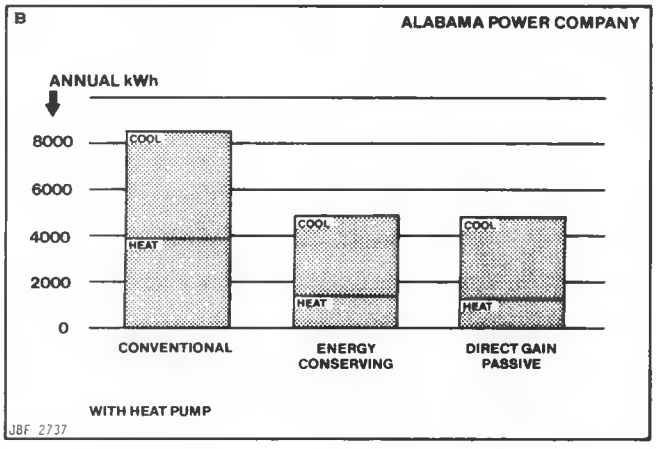

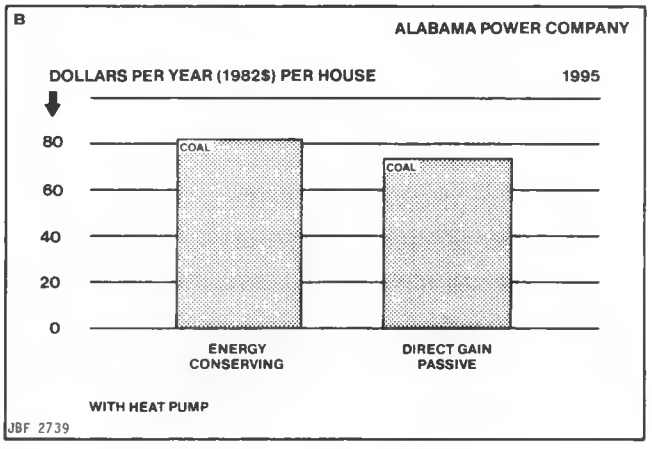

Fig. 1. Annual kWh Use

Fig. 2. Utility Fuel Savings

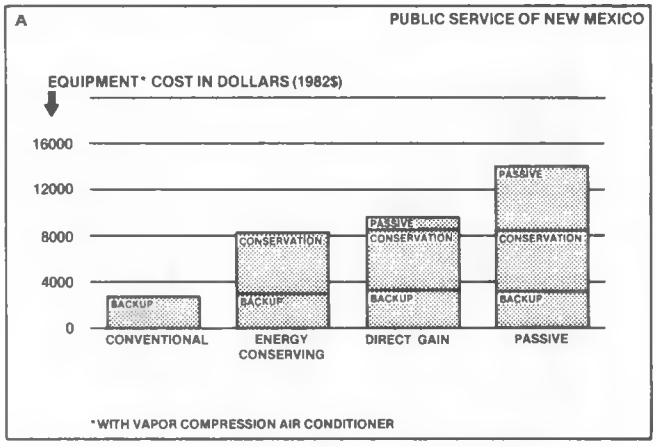

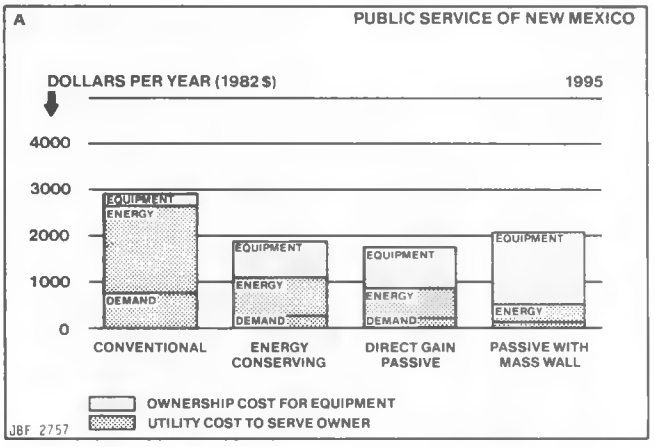

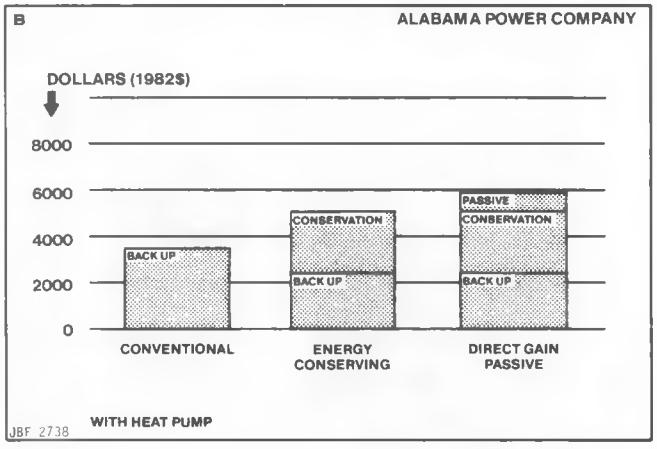

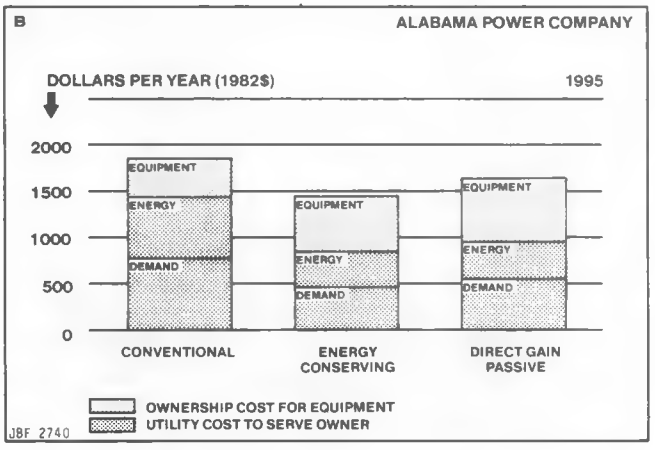

Fig. 3. Homeowner Equipment Costs

Fig. 4. Annualized Homeowner and Utility Costs

PROJECT SUMMARY

Project Title:	Materials Research for Passive Systems
Principal Investigator:	David K. Benson
Organization:	Solar Energy Research Institute Golden, Colorado
Project Goals:	Evaluate the feasibility of using solid-state phase change materials for thermal storage in passive solar applications. Evaluate the feasibility of using in situ Fourier Transform Infrared (FT-IR) spectroscopy to study the mechanisms of polymer photodegradation under simulated solar irradiation.
Project Status:	The project is ongoing. The feasibility of in situ FT-IR spectroscopy for photodegradation studies has been demonstrated; and will be used in subsequent projects. The feasibility of using solid-state phase change materials for passive thermal storage is still under study. A range of materials based on the polyols homologous to pentaerythritol, $C(-CH_2OH)_4$, have been characterized thermophysically and found to be promising for passive thermal energy storage. Systems analyses have been initiated to determine the probable performance of solid-state phase change thermal storage in typical passive applications. Parametric studies are being used to identify optimum material parameters (such as transition temperature, thermal conductivity, and degree of supercooling). These optima will be used to guide efforts to improve the phase change material characteristics through modification of composition and through design of composites. Preliminary results of systems analyses indicate that the solid-state phase change materials can out perform sensible heat storage alternatives such as water walls or concrete Trombe walls. Their light weight (per unit energy storage) suggest applications in retrofit or in modular home construction.
Contract Number:	SERI EG-77-C-01-4042 (WPA 02-304-82)
Contract Period:	Ongoing
Funding Level:	$150,000
Funding Source:	U.S. Department of Energy, Passive and Hybrid Solar Energy Division

MATERIALS RESEARCH FOR PASSIVE SYSTEMS - SOLID-STATE PHASE CHANGE MATERIALS AND POLYMER PHOTODEGRADATION

D.K. Benson, J.D. Webb, R. Burrows, J.O. McFadden, and C. Christensen
Solar Energy Research Institute
Golden, Colorado

ABSTRACT

A set of solid-state phase change materials is being evaluated for possible use in passive solar thermal energy storage systems. The most promising materials are organic solid solutions of pentaerythritol ($C_5H_{12}O_4$), pentaglycerine ($C_5H_{12}O_3$) and neopentyl glycol ($C_5H_{12}O_2$). Solid solution mixtures of these compounds can be tailored so that they exhibit solid-to-solid phase transformations at any desired temperature within the range from less than 25°C to 188°C, and with latent heats of transformation between 20 and 70 calories/gram. The transformation temperature, specific heats and latent heats of transformation have been measured for a number of these materials. Limited cyclic experiments suggest that the solid-solutions are stable. These phase change materials exhibit large amounts of super cooling; however, the addition of certain nucleating agents as particulate dispersions in the solid, phase change material greatly reduces this effect.

Computer simulations suggest that the use of an optimized solid-state phase change material in a Trombe wall could provide better performance than a plain concrete Trombe wall.

A novel technique for studying the photodegradation of polymers was also explored as a small part of this research. It was shown that Fourier Transform Infrared (FTIR) spectroscopy could be used to measure chemical changes as they occur in polymer films during simulated solar irradiation. In polymers such as polycarbonates which undergo rapid solar degradation, measurable changes could be observed by FTIR spectroscopy in a few minutes. In polymers such as polymethyl methacrylate, chemical changes could be measured only if the irradiation wavelength was extended down to about 270 nm. The FTIR spectroscopy appears to be a powerful tool for studying polymer photodegradation.

BACKGROUND

The organic, solid-state phase change materials which we are now studying for possible passive solar applications were first considered for use in the passive temperature control of earth satellites. Under NASA sponsorship, a large number of such solid-state phase change materials were evaluated ten years ago (1). At SERI, we have extended the earlier NASA research and discovered a set of organic solid-solutions which lower the useful temperature range of solid-state phase change materials into the realm of possible interest to passive solar system designers.

This paper reports progress in this ongoing exploratory research project.

OBJECTIVES

The principal objective of this research is to evaluate the feasibility of using organic, solid-state phase change materials (S-S PCM's) for thermal energy storage in passive solar systems. The evaluation involves the measurement of thermal properties of the S-S PCM's, the modeling of their probable performance in typical passive systems and their cost/benefit comparison with more conventional thermal energy storage. Other important issues, such as the acceptability of such materials for long term exposure in buildings are not yet being addressed.

A secondary objective of this task is unrelated to thermal energy storage. It is to test the feasibility of using a novel experiment to measure the photodegradation in polymer glazing materials. Only a very small fraction of the task effort was applied to this objective.

MATERIALS

The S-S PCM's included in this study are simple organic compounds which are used in large quantities as chemical feedstocks in the resins and munitions industries. Table 1 lists some of the characteristics of the three compounds which are the focus of this work. All three are closely related members of an homologous series of polyols. They all have a central carbon atom with four attached carbons forming a tetrahedron.

Either 4,3, or 2 hydroxyl (-OH) groups are attached to the four corners of the tetrahedral molecule. The archetypical member of this series, pentaerythritol, has the largest latent heat of solid-state transformation of any known material. It is comparable to the latent heat of fusion for water/ice. The latent heat of transformation of the other two compounds are much lower. These compounds appear to be infinitely

soluble in each other and to form stable solid solutions which exhibit solid-state transformations with intermediate latent heats.

Reagent grade chemicals were used in the experiments reported here; however, similar measurements were also made on the technical grade chemicals with only insignificant differences being detected.

SOLID-STATE PHASE CHANGE MATERIAL PROPERTIES

	SOLID-STATE TRANSITION (^oC)	MELTING TEMPERATURE (^oC)	LATENT HEAT OF TRANSFORMATION (KJ/KG)	HEAT CAPACITY* (KJ/KG-^oC)	COST ($/KG)
Pentaerythritol $C-(CH_2OH)_4$	187	269	269	2.9	1.57
Pentaglycerine $CH_2-C-(CH_2OH)_3$	82	197	174	2.8	1.30
Neopentyl Glycol $(CH_2)_2-C-(CH_2OH)_2$	48	126	139	2.8	1.30

*Just above the transition temperature

TABLE 1

RESULTS

Thermal Analysis of Solid-State Phase Change Materials. Several methods of thermal analysis are being used to characterize the S-S PCM's. Differential scanning calorimetry (DSC) is being used to measure the latent heats of transformation, the temperatures of transformation, and the specific heats as functions of temperature. Apparatus has been set up and experiments designed to measure thermal expansion and mechanical strength as a function of temperature by use of thermo-mechanical analysis (TMA); and to measure vapor pressure as a function of temperature by thermogravimetric analysis (TGA). In addition, a SERI designed heat flux calorimeter will be used to measure the thermal conductivity of selected S-S PCM's. Only the results from the DSC experiments are complete enough to be reported here. A Perkin Elmer DSC 2 with digital processing unit (TADS) was used throughout these experiments.

Figure 1 shows a typical recording obtained by DSC. The inset drawing shows schematically how a sample and a reference material are held in sealed metal pans inside of separately heated and controlled furnaces. The reference chamber is heated at a linear rate (typically 20°C/minute or less), and the power required to maintain the sample chamber at the same temperature is recorded in millicalories per second. The recording shows the solid-state transformation peaking at about 313 K (40°C) and the melting transformation starting at about 380K (107°C). The sample is a 50%-50% (Molar) solid solution of neopentyl-glycol in pentaglycerine. The integrals under the transformation peaks indicate that the latent heat of solid-state transformation in this sample is 20.9 calories per gram and the latent heat of melting is 5.79 calories per gram.

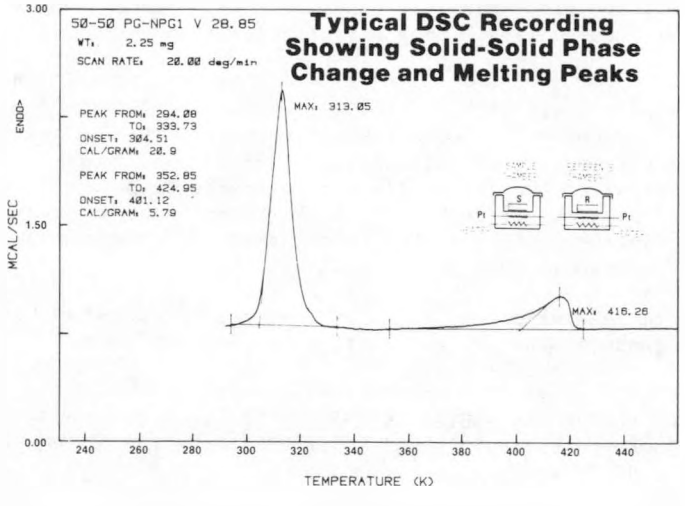

Figure 1. Differential Scanning Calorimetry (DSC) Recording During Heating of a 2.25 mg Sample of 50 Molar Percent Neopentyl Glycol in Pentaglycerine.

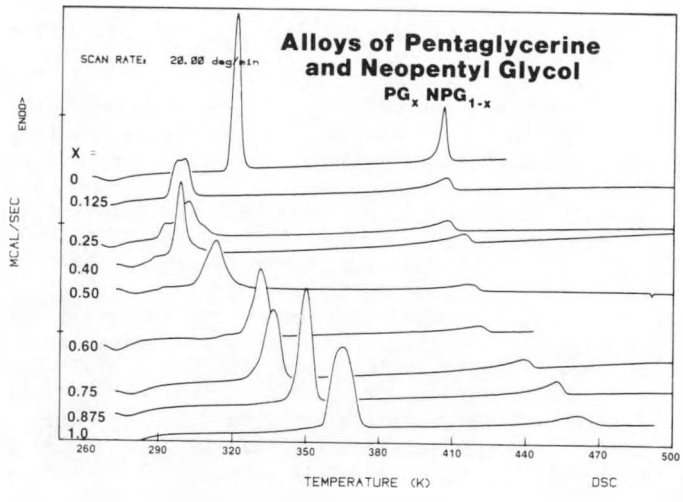

Figure 2. A Series of DSC Recordings for Solid-Solution Mixtures of Neopentyl Glycol and Pentaglycerine. X is the Molar Fraction of Pentaglycerine.

Figure 2 shows a series of DSC recordings for different solid-solution mixtures of pentaglycerine and neopentyl glycol. Notice that the solid-state transformations occur at lower temperatures in the solid-solutions than in either of the pure components and that some of these mixtures exhibit solid-state transformations near 300K (27°C). Such mixtures may be particularly suitable for thermal energy storage in passive solar systems. Table 2 summarizes the measured characteristics of some of these selected solid-solution mixtures.

The specific heats of the S-S PCM's have also been measured as functions of temperature with the DSC. For such measurements a reference material such as Al_2O_3 (National Bureau of Standards Reference Material) is compared against the S-S PCM. Except in the vicinity of the phase transformations of the PCM, the DSC signal is proportional to the specific heat of the sample. Since the specific heat of the reference material is known accurately, the specific heat of the PCM can be calculated from the ratio of the recording amplitudes, the respective sample weights and the known Al_2O_3 specific heat. Specific heats have been measured from room temperature to above the melting points in 26 different solid solution mixtures of the S-S PCM's. Representative values are given in Table 2.

SOLID-STATE PHASE CHANGE MATERIALS
SELECTED SOLID SOLUTIONS

SUMMARY OF CHARACTERISTICS

COMPOSITION (MOLAR %)	SOLID-STATE TRANSITION (°C)	MELTING TEMPERATURE (°C)	LATENT HEAT OF TRANSFORMATION (KJ/KG)	HEAT CAPACITY* (KJ/KG-°C)
Pentaglycerine-Neopentyl Glycol				
(87.5 - 12.5)	77	170	133	3.0
(75 - 25)	62	155	105	3.0
(60 - 40)	47	138	103	2.5
(40 - 60)	26	124	76	2.6
Pentaerythritol Neopentyl Glycol				
(25 - 75)	119	152	50	3.2
(12.5 - 87.5)	39	192	83	3.2

*Just above the transition temperature

TABLE 2

One of the concerns with the use of PCM's for thermal energy storage is the stability of the material and its retention of full, reversible latent heat of transformation after a large number of thermal cycles. The solid-state phase change process is quite different from the salt hydrate solid-liquid PCM's and is not expected to suffer any changes during cycling because there is so little migration of material in the solid, even above the transformation temperature. Nevertheless, a cyclic stability experiment was conducted on a typical solid-solution mixture using the automatic cycling capability of the differential scanning calorimeter.

Figure 3 shows the solid-state transformation peaks recorded after 13, 327, and 732 thermal cycles (heating through the transformation and immediately cooling back through the reverse transformation). The changes in the shape of the transformation peak are not significant, nor is the slight variation in peak temperatures (2°K variation). Both of these variations are typical of the stochastic nature of the transformation process when measured in small samples (2.28 mg in this case) and at relatively high thermal scanning rates (20°C/min). The most important result of this cycling experiment is that the latent heat of transformation did not change significantly, remaining at 28-29 calories/gram throughout 732 cycles.

Further cyclic experiments should be conducted under more realistic conditions of larger samples and slower heating/cooling rates; but this preliminary experiment supports the contention that the S-S PCM's are basically stable to thermal cycling.

Another common problem with PCM's is undercooling. When the PCM is cooled back down, the reverse transformation which liberates the stored heat occurs at a lower temperature than the forward transformation. This super cooling effect is particularly large in the S-S PCM's.

Figure 4 shows tracings of DSC recordings for pentaglycerine at different heating/cooling rates. The temperature difference between the heating and cooling transformation peaks is a strong function of the heating/cooling rate. In a typical passive, thermal energy storage application, the heating/cooling rate would be very low; but even at rates as low as 0.1°C/min., the super cooling is about 16°C in this sample.

The kinetics of the transformation can be changed by the addition of a nucleating agent which lowers the activation energy for the nucleation of the phase transformation. A number of additions were tested. In Figure 4, the 0.1% amorphous carbon addition did not reduce the super cooling of pentaglycerine; but in Figure 5 we show the effect of adding 0.1% fine graphite powder to the pentaglycerine. The graph shows the super cooling as a function of heating/cooling rate for pure pentaglycerine and with the added graphite. In spite of the considerable scatter in the super cooling, it is clear that the nucleating agent has reduced the extent of super cooling, particularly at low heating/cooling rates. These fine particulate nucleating agents are dispersed throughout the solid PCM and cannot segregate as some nucleating agents have done in salt hydrate solid-liquid PCM's.

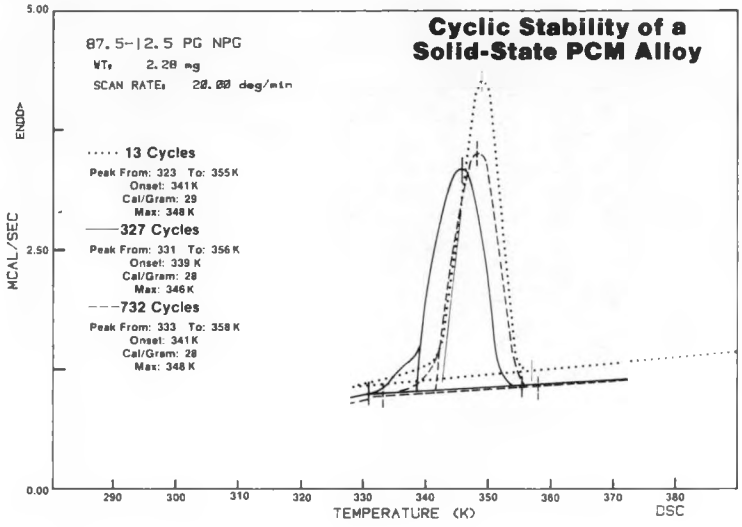

Figure 3. Three Representative Solid-State Transformation Peaks Recorded During the Heating Portions of a Thermal Cycling Experiment. The Three Peaks Were Recorded on the 13th, 327th, and 732nd Cycle. The Sample is a 12.5 Molar Percent Solid Solution of Neopentyl Glycol in Pentaglycerine.

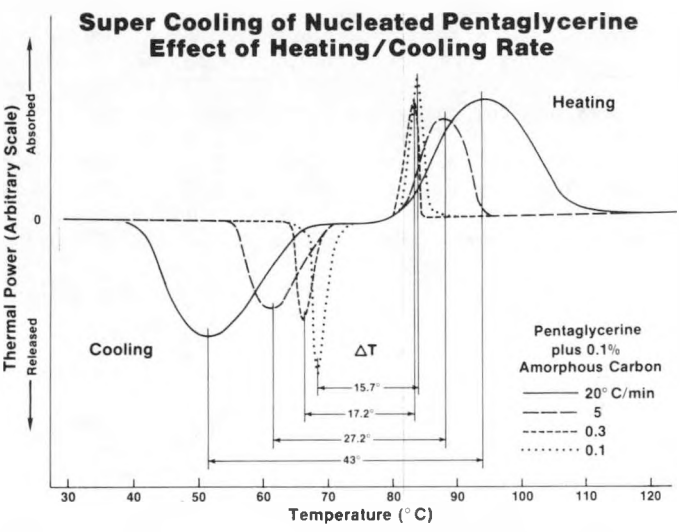

Figure 4. Three Representative Solid-State Transformation Peaks Recorded During Both Heating and Cooling Portions of a Thermal Cycling Experiment. The Three Recordings Were Obtained at Three Different Heating/Cooling Rates and Show Different Degrees of Super Cooling.

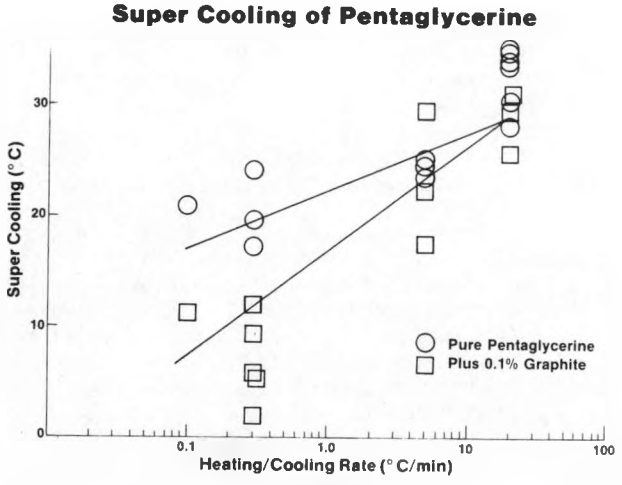

Figure 5. Super Cooling of Pentaglycerine (With and Without an Effective Nucleating Agent) as a Function of Heating/Cooling Rate. The Scatter in Supercooling is Typical for Small Samples Such are Required in DSC Experiments.

Further work may identify a better nucleating agent for the S-S PCM's or may show that such agents are not needed in some passive solar applications.

Systems Analysis of S-S PCM Use in Trombe Walls. The purpose of these analyses is to guide the experimental research by determining optimum parameters for the S-S PCM's in typical passive solar applications. The first set of analyses focused on S-S PCM use in a Trombe wall. In these preliminary analyses, super cooling of S-S PCM was not included.

A thermal network model was developed for the Trombe wall; and this model was incorporated into a thermal simulation code for residential buildings. A SERI experimental house which has been subjected to extensive Class A monitoring was modeled using the SERIRES* computer code. The performance simulation is performed using forward finite differencing with time steps of one hour or less.

Table 3 lists the characteristics of the modeled house. A base building annual heating load of 11.07 million BTU was determined from a SERIRES assuming an adiabatic south facing wall (for the purpose of calculating solar savings fraction). The assumed characteristics of the Trombe wall are listed in Table 4. Thermal storage was modeled with multiple thermal nodes in order to account for the effect of thermal conductivity and the resulting temperature gradients in the wall. For the PCM's, this multi-node modeling was accomplished with the SERIRES code by inputting multiple single-node PCM layers, each with a specific thermal conductivity. Simulation results were examined in terms of hourly Trombe wall surface temperatures and heat fluxes on selected days. Annual solar savings fraction were based on annual simulations with and without the Trombe wall. As a check, the predicted performance of a concrete Trombe wall was compared to the performance predicted by a Los Alamos solar load ratio method. The two predictions agreed well.

BUILDING CHARACTERISTICS/ASSUMPTIONS

Retrofit Test House at SERI -- Denver, CO
(modelled as a single thermal zone)

Floor area	= 1080 sq. ft.
Windows	= double glazed
Ceiling	= R36
Walls	= R11
Crawl space walls	= R19
Infiltration	= 0.5 air changes per hour
Internal Gains	= 53,000 BTU/day
Heating setpoint	= 60°F
Venting setpoint	= 76°F
Cooling setpoint	= 78°F

TABLE 3

TROMBE WALL CHARACTERISTICS/ASSUMPTIONS

Area	= 200 ft^2
Glazing	= double
Overhang	= 2.25 ft, 1.0 ft. above top of glazing
Vent area	= 3%

Concrete: (modelled with a thermal node every 2 inches)

Thermal conductivity, k	= .7576 BTU/ft -°F-h
Density, ρ	= 140 lbs/ft^3
Specific heat, C	= .2 BTU/lb-°F

NPG: (modelled without supercooling, with six thermal nodes)

Thermal conductivity, k	= .1156 BTU/ft-°F-h
Density, ρ	= 66.55 lbs/ft^3
Specific heat, C	= .5996 BTU/lb-°F
Heat of transformation, Q_t	= 52.03 BTU/lb
Transformation temperature, T_t	= 118.4°F

TABLE 4

Figure 6 shows the results of a series of simulations with solid-state phase change temperature as a parameter. Under the assumption of no super cooling, the optimum phase change temperature is about 29°C (84°F). The inclusion of a super cooling effect of several degrees would be likely to raise this optimum temperature. However, simulations including a super cooling effect have not yet been done. Figure 6 also shows the incremental benefit of increasing the thermal conductivity of the PCM by a factor of five when the transition temperature is near optimum. Such an increase could be achieved by adding a material with a high thermal conductivity to the PCM. For example, an addition of 2% by weight of graphite powder would

*SERIRES was developed by Ecotope Group as a major extension of SUNCAT 2.4.

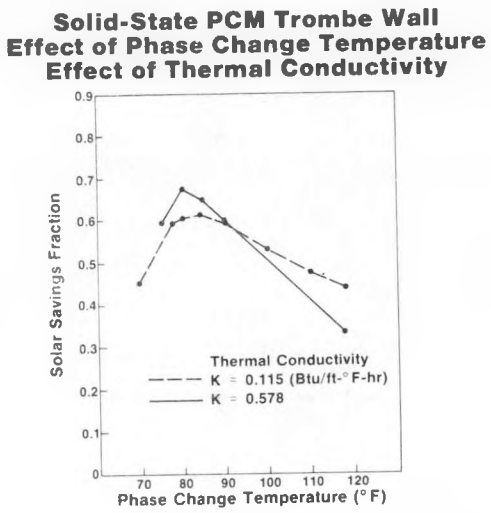

Figure 6. The Solar Savings Fraction Provided by a Solid-State Phase Change Material Wall as a Function of the Phase Change Transformation Temperature and for Two Different Values of the PCM Thermal Conductivity.

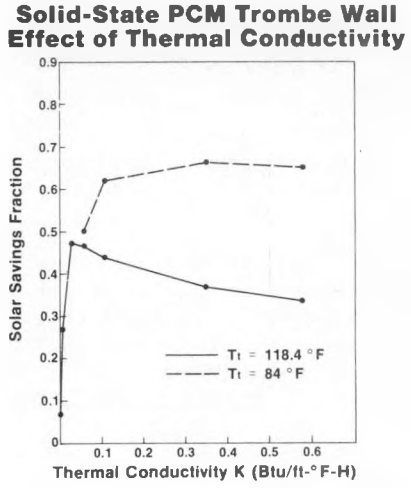

Figure 7. The Solar Savings Fraction Provided by a Solid-State Phase Change Material Wall as a Function of the PCM Thermal Conductivity and for Two Different Phase Change Temperature.

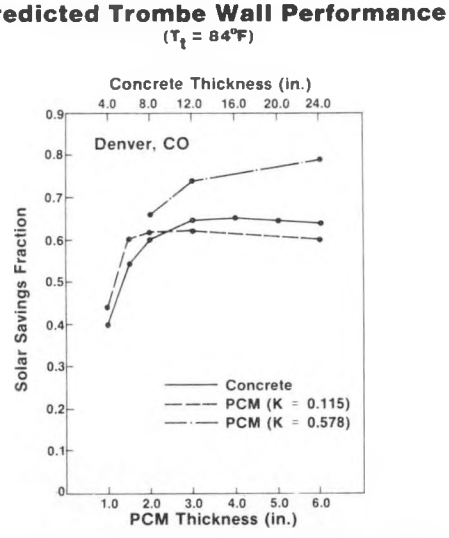

Figure 8. A Comparison of the Solar Savings Fraction Provided by a Solid-State Phase Change Wall and a Concrete Wall as a Function of the Wall Thicknesses and for Two Different Values of the PCM Thermal Conductivity.

raise the thermal conductivity of pentaglycerine by a factor of approximately five. Figure 7 further explores the effect of thermal conductivity on the predicted performance of a S-S PCM Trombe wall.

Finally, the performance of the simplified (no super cooling, 84°F Transition) S-S PCM wall was compared to a more conventional, concrete Trombe wall. Figure 8 shows that a PCM wall might perform about as well as a much thicker concrete wall. If the thermal conductivity were increased the PCM wall might perform significantly better than the concrete wall.

A S-S PCM wall two inches thick and 200 ft.^{2} in area would weigh about one ton and cost about $1,300 for the raw materials, whereas an eight inch thick concrete wall of 200 ft.^{2} would weigh 9 1/3 tons and cost about $300 for materials (excluding foundation).

Photodegradation of Polymers. A technique has been developed for the in-situ study of polymer photochemical degradation (2). The technique uses a controlled environmental chamber in a Fourier Transform Infrared

(FTIR) spectrophotometer. The chamber permits exposure of the polymer sample to controlled, simulated solar radiation, gas mixtures and temperatures while infrared reflection-absorbance measurements are being made.

The Nicolet 7199 FTIR spectrophotometer used for these experiments includes fast digital data acquisition, processing and storage capabilities as well as a very high sensitivity, liquid nitrogen cooled mercury cadmium telluride detector. Large numbers of rapidly acquired spectra can be digitally summed to enhance the signal to noise ratios. A specially designed optics system provides for highly efficient IR beam throughout.

The polymer sample is cast as a thin film on a gold surface. The IR beam strikes the film at an angle of 77.5°, penetrates, reflects from the gold substrate, and passes through the film again as it exits. This geometry, while optically efficient, required development of optical models for the dependence of the spectra upon changes in the complex refractive index and methods for measuring the index as a function of IR frequency. The technique for estimating the concentration of reaction products or functional groups in the polymer from the IR spectra was shown to be accurate by independent measurements using ultraviolet spectroscopy.

The infrared spectroscopy in conjunction with untra-violet spectroscopy and gel permeation chromatography (to determine changes in polymer molecular weight changes) was used to determine the critical photodegradation pathways to Bisphenol-A polycarbonate. The major mechanisms were found to be first and second photo-Fries rearrangement at the carbonyl group, and chain scission, also at the carbonyl group. The buildup of degradation products could be accurately determined after as little as 30 minutes exposure to the simulated solar radiation.

The same experimental procedure was used on thin films of polymethyl methacrylate with less success. The PMMA absorbs significantly only in the shortest wavelength portion of the solar spectrum; and while solar radiation below 290 nm may be the cause of photodegradation in PMMA and other polymers (3), it is not sufficiently available in well controlled, simulated solar radiation to produce detectable changes in reasonably short experiments.

CONCLUSIONS

Solid-State Phase Change Materials. The solid-state phase change materials based on pentaerythritol and its homologs can be mixed as binary solid solutions to produce phase transformation temperatures of any desired value from below room temperature up to up to 188°C. Latent heats of transformation for these mixtures are generally in the range of 20-70 calories per gram. Limited experiments suggest that the solid solution mixtures are stable and provide reproducible transformation characteristics for at least several hundred cycles.

The solid state phase change materials exhibit large degrees of super cooling - the degree depending upon the exact composition and the heating/cooling rates used. The addition of a dispersion of particulate nucleating agents in the solid PCM has been shown to decrease the amount of super cooling to $\sim$ 10°C or less. The most effective nucleating agent identified so far is a finely powered graphite.

Computer simulations of a building's performance with an idealized (zero super cooling), solid-state phase change material Trombe wall suggests that the PCM wall could outperform a more conventional, concrete Trombe wall even if the concrete wall were four times thicker and nine times heavier. Parametric studies showed an optimum transformation temperature for the PCM wall was 29°C (84°F) and that improving performance resulted from increased PCM thermal conductivity (when zero super cooling is assumed).

Photodegradation of Polymers. The in-situ study of the photochemical degradation of transparent polymer films via collection of infrared reflection-absorbance spectra was demonstrated to be a powerful method of analysis, particularly when performed in conjunction with other analytical techniques. Using this technique in combination with gel permeation chromatography and ultra-violet reflection-absorbance spectroscopy enabled elucidation of the primary photodegradation mechanisms in bisphenol-A polycarbonate films on metallic substrates. Photoinduced chain scission is evidently initiated at the carbonyl group in the polycarbonate liberating CO_2 and reducing the molecular weight of the polymer rapidly at the surface where the effective radiation (wavelengths below 320 nm) is strongly absorbed.

On the other hand, the practicality of in-situ measurements under simulated solar radiation may be limited to those polymers which absorb significantly in the solar spectrum. Polymethyl methacrylate (PMMA) undergoes photodegradation under irradiation at wavelengths below 270 nm (not normally considered part of the solar terrestrial spectrum) and does not show readily detectable changes by the technique in reasonably short experiments.

A proposed addition of a timeable, pulsed, UV LASER to the apparatus would provide the ability to study the photochemical processes more incisively, extend the range of utility to polymers such as PMMA and facilitate time-resolved measurements of intermediate species in the degradation processes.

REFERENCES

1. Hale, D.V., Hoover, M.J., and O'Neill, M.J., "Phase-Change Materials Handbook," NASA Report B-72-10464, August, 1972.

2. Webb, J.D., "An Experimental Approach to Evaluating Environmental Degradation Mechanisms in Bisphenol-A Polycarbonate Films on Metallic Substrates," Masters Dissertation, University of Denver, Denver, Colorado.

3. Barker, R.E., "The Availability of Solar Radiation Below 290 nm at Its Importance in Photomodificatio of Polymers," Photochemistry and Photobiology, 1, pp. 275-295 (1968).

HIGH PERFORMANCE WINDOWS FOR PASSIVE SOLAR

THE SOUTHWALL CORPORATION
Palo Alto, California

Steven B. Brown
Director of Commercial Marketing Programs

INTRODUCTION

The Southwall Corporation continued this past year leading the way to a new level of high performance glazing for both passive solar and energy conservation designs. From our early work as Suntek Research Associates, which was a small partnership largely funded by the Department of Energy, we have grown to a viable commercial company with multimillion dollar private capitalization and a product, Heat Mirror™ transparent insulation, that is quite literally leading the way to "high performance glazing" in the North American and European markets.

This paper will serve as both an update to the many solar enthusiasts that have watched us grow up and also as a means to communicate the latest developments in our work.

WHAT IS HEAT MIRROR™

Heat Mirror™ is the result of almost a decade of research and development by a group of innovative scientists and engineers. With funding from the Department of Energy they have been able to take their dream of a transparent insulation from an idea all the way to a commercial reality.

Heat Mirror™ quite simply is a wavelength filter. The Suntek scientists developed a coating that was selective by wavelength. Recognizing that the wavelengths of solar radiation are much shorter than the infrared wavelengths given off by room temperature objects, they reasoned that a coating that was transparent to short wavelengths but reflective of longer wavelengths would significantly enhance the efficiency of windows for direct gain passive solar applications. In other words, maintain a high transparency to solar radiation while significantly boosting the insulation value of the glass against the loss of heat.

After the concept had been developed and even after much of the technical work had been completed, a decision had to be made about how and where to place the Heat Mirror™ coating in a window. The obvious two candidates for substrate were film and glass. The various advantages and disadvantages of the two materials were considered. The two key areas of consideration were performance and price. If you ask yourself what configuration of two pieces of glass and one coating will yield the highest R value, the answer will be use the coating to split the air space into two air spaces. This choice will typically yield 50 to 60% higher R values than placing the coating on one of the glass surfaces.

The second key consideration was cost. This type of sputtered thin film coating must be done in a vacuum. Glass is inherently a difficult, bulky material to feed through a vacuum chamber. In contrast, a mile long roll of film can literally be processed with one loading of the vacuum chamber. This yields significant economies for the film choice.

These factors led Southwall to set up production of Heat Mirror™ as a coated polyester film for use mounted midway in the air space of insulating glass. This means that today, clear insulating glass units with R values in excess of 4.3 are available for use in both passive and conservation applications.

AVAILABILITY OF HEAT MIRROR™ EQUIPPED WINDOWS

For some the long debut of Heat Mirror™ has been so long that it is hard to believe it is here. On March 20, 1981 The Southwall Corporation announced the commercial availability of Heat Mirror™.

It has taken time for window companies to integrate the use of Heat Mirror™ into their product lines. Today, I am pleased to be able to say, Heat Mirror™ equipped windows are available in over 40 states from over 350 window dealers. The Heat Mirror™ dream that was nurtured for so many years by dedicated scientists and funded through so many steps by our good friends in the Department of Energy is a reality today in over 600,000 square feet of windows in the United States and Europe. As this number grows, the resulting reduction in the consumption of non-renewable energy sources is indeed exciting.

NEW DEVELOPMENTS AT SOUTHWALL

Heat Mirror™ was designed to be a high transparency transparent insulation for direct gain passive solar glazings and other applications where the sun's energy

is welcome inside the building. It has, however, become obvious that one version of Heat Mirror™ cannot be all things to all windows. East and west elevations are often ideally designed with lower transmission windows. Also, southern climates where air conditioning is more of a problem than heating demand a lower transmission transparent insulation. Ideally, such lower transmission windows would reduce the relative heat gain from the sun by reflecting the invisible near infrared while still transmitting relatively large amounts of the visible solar radiation in order to benefit from the natural lighting.

In response to these various requirements, The Southwall Corporation has just announced the availability of three versions of Heat Mirror™ transparent insulation. Heat Mirror™ has expanded into a family of transparent insulations to satisfy the varying performance demands placed on windows.

- Heat Mirror™88 - Southwall's original transparent insulation is now the worldwide standard for high performance windows. It is colorless and transparent and is ideal for colder climates or buildings with large heating loads.
- Heat Mirror™77 - This transparent insulation is visually almost indistinguishable from Heat Mirror™88, but reflects more solar infrared. It is ideal for warmer climates or applications where cooling loads and natural daylighting are important.
- Heat Mirror™55 - This insulation is ideal for buildings with large cooling loads. It rejects even more solar near infrared and slightly surpasses the outstanding insulating properties of Heat Mirror™88 and Heat Mirror™77.

Technical Specifications of Heat Mirror™

Product	Emissivity [1] Coated Side	Transmittance [2] % Visible	% Total Solar
Heat Mirror™ 88	.15	86	71
Heat Mirror™ 77	.09	81	61
Heat Mirror™ 55	.05	57	36

[1] ±.01 [2] ±2%

Transmission Characteristics of Heat Mirror™ Insulations

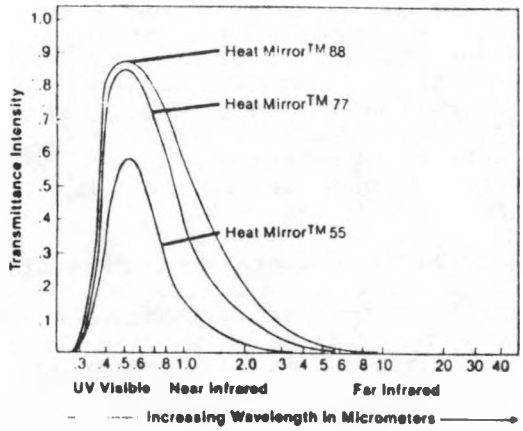

BENEFITS OF HEAT MIRROR™ EQUIPPED GLASS

The benefits of equipping windows with the various Heat Mirror™ transparent insulations can be broken into three primary categories:

1. Reduced First Costs
   - Reduced HVAC costs
   - Additions without new HVAC systems
   - Elimination of perimeter draft heaters
   - Reduced structural support over triple glazing

- Reduced HVAC Costs

  Low performance windows increase construction costs by requiring large initial outlays for heating, ventilating and cooling (HVAC) systems. As much as 25% of a typical high rise office building's cost may be for HVAC systems. For example, Heat Mirror™55, with its low U-value, reduces heating system peak loads; its low shading coefficient and low U-value reduce air conditioning peak loads. The result is significant reductions in HVAC system size, often resulting in first cost savings exceeding the cost of Heat Mirror™ equipped windows.

Which Wavelengths Should Windows Transmit?

Building Energy Requirements	Solar Radiation UV	Visible	Infrared	Far Infrared (Heat)	Product
Maximum Heating	Block	Transmit	Transmit	Reflect	Heat Mirror™ 88
Balanced Shading and Lighting	Block	Transmit	Partially Reflect	Reflect	Heat Mirror™ 77
Maximum Cooling	Block	Transmit	Reflect	Reflect	Heat Mirror™ 55

- Additions Without New HVAC Systems

  When adding to an existing structure, Heat Mirror™ equipped windows may allow the addition to be heated or cooled with existing HVAC equipment. This is even more likely if old low performance windows are replaced, a move that could not only reduce first costs for the new construction, but also reduce operating costs.

- Elimination of Perimeter Draft Heaters

  Another first cost savings occurs in the elimination of perimeter draft heaters. In the winter, the inside surface of low performance window glass is cold, and this reduces the temperature of adjacent air. Since cold air is heavy, it drops away from the window, creating a chilly draft. Perimeter draft heaters are commonly used to warm the air near cold windows. With higher inside glass temperatures, Heat Mirror™ equipped windows eliminate cold drafts and the expense, energy consumption, and wasted space of draft heaters. The following table compares glass surface temperatures.

Interior Surface Temperatures [1]

Window	Interior Temperature °F	°C
Monolithic Glass	16	– 9
Double Glass	46	8
Triple Glass	54	12
Heat Mirror™ 88 Equipped Double Glass	57	14
Heat Mirror™ 77 Equipped Double Glass	58	14
Heat Mirror™ 55 Equipped Double Glass	58	15

[1] 0°F (– 18°C) outside temperature, 15 mph wind (6.7 m/sec) and 70°F (21°C) interior room temperature. No interior wind, two 1/2" (12.7mm) airspaces, 1/4" (6mm) clear glass.

Eliminating draft heaters can increase usable and therefore rentable space, thereby improving the economics of new construction or remodeling. When combined with lower HVAC costs, the savings can be significant.

First Costs – Air-Conditioning System plus Draft Heaters[1]

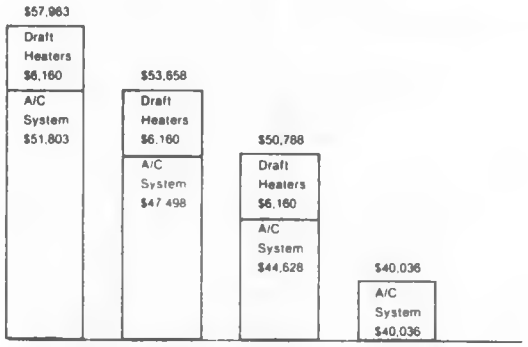

[1] Light commercial building, 21,000 sq. ft., Dallas, Texas 1760 sq. ft. (169m²) of windows, 2 floors, CALPAS computer simulation.

- Reduced Structural Support Over Triple Glazing

  A further first cost savings results when Heat Mirror™ equipped windows are selected rather than triple glazed windows. Triple glazed windows are extremely heavy, adding to structural support costs as well as installation costs. Heat Mirror™ equipped windows significantly outperform triple glazed windows, but weigh no more than conventional double glazed windows (the weight of Heat Mirror™ insulation is negligible). Thus, expensive extra support is not required, resulting in lower construction costs while achieving superior window performance.

2. Lower Operating Costs

   - Low U-values means air conditioning and heating savings
   - High daylight transmission provides cool, natural lighting
   - Warmer glass surface substantially eliminates condensation

- Lower U-Values Mean Air Conditioning and Heating Savings

  A window's insulating ability is measured by its U-value. Heat flows from warm to cold. In winter, heat flows from a warm interior, through windows, to the colder exterior. The lower the U-value, the slower that flow. Therefore, the low U-values of Heat Mirror™ equipped

windows show up as reduced heating bills. In summer, heat flows from outside to inside, and a low U-value again indicates that less heat will pass through the window - hence reduced air conditioning costs.

Typical Glass U-values – Winter [1]

	Single Glass	Double Glass	Triple Glass
U-value	1.10	.49	.31
k-value	6.27	2.78	1.79

	Heat Mirror™ 88 Equipped Double Glass	Heat Mirror™ 77 Equipped Double Glass	Heat Mirror™ 55 Equipped Double Glass
U-value	.23	.23	.22
k-value	1.32	1.32	1.28

[1] Standard ASHRAE winter test conditions: 0°F (– 18°C) outdoor temperature, 70°F (21°C) indoor temperature, 15 mph (6.7 m/sec) wind velocity, no sun. For all glass: 1/2" (12.7mm) air gap, 1/4" (6mm) glass. English U-values represent Btu/hr./sq. ft./°F, Metric K-values represent W/(M^2K).

With Heat Mirror™, heating and air conditioning bills will be reduced - how much depends on the building, the climate, and the Heat Mirror™ product selected. Heat Mirror™ 88 is ideally suited for cold climates or heating load dominated buildings where it is important to have clear windows that are highly transparent to solar radiation. In contrast, Heat Mirror™ 55 provides shading by reflecting the invisible near infrared portion of the solar spectrum. This shading reduces air conditioning costs, making Heat Mirror™ 55 well suited to warm climates or cooling load dominated buildings. Heat Mirror™ 77, on the other hand, gives much of the shading protection of the Heat Mirror™ 55, while retaining most of the visible light transmission qualities of Heat Mirror™ 88.

Heating and Air Conditioning Annual Costs [1]

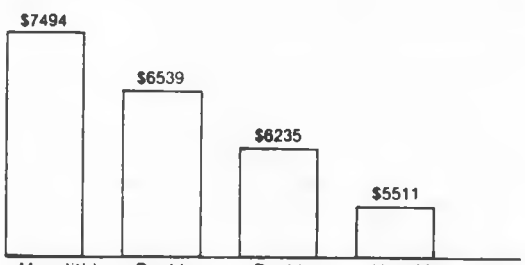

Monolithic Grey Reflective	Double Glass Tinted	Double Glass Reflective	Heat Mirror™ 55 Equipped Double Glass
U-value = 1.1	U-value = .58	U-value = .58	U-value = .22
Shading Coefficient = .46	Shading Coefficient = .54	Shading Coefficient = .39	Shading Coefficient = .39

[1] Light commercial building, 21,000 sq. ft., Dallas, Texas 1760 sq. ft. (169m^2) of windows, 2 floors, CALPAS computer simulation.

- High Daylight Transmission Provides Cool, Natural Lighting

Natural lighting is free and cool. In addition to heating and air conditioning savings, Heat Mirror™ decreases energy costs for lighting. More than half the energy consumed in a typical office building can be for artificial lighting, primarily during daytime hours. Using natural light can significantly cut costs. The problem, especially in cooling load dominated buildings, is that many glass technologies reject light in order to reject solar heat gain. Such windows appear dark, or reflective - like looking at the world through sunglasses. Heat Mirror™ 77 and 55 solve this problem by transmitting a high percentage of daylight, while rejecting a large portion of invisible near infrared.

Comparative Coolness of Natural Light

Glass Type	Visible Transmission Percent [1]	Relative Heat Gain [2]	Visible Energy As Percent of Total Energy Gain [3]
Open Window	100	248.2	49.5
Monolithic Clear	89	204	54
Double Clear	80	170	58
Triple Clear	72	146	61
Heat Mirror™ 77/ Clear	66	120	68
Heat Mirror™ 55/ Clear	48	82	72
Monolithic Green	75	166	56
Double Green	67	128	64
Heat Mirror™ 77/ Green	56	85	81
Heat Mirror™ 55/ Green	40	60	82
Monolithic Bronze	50	159	39
Double Bronze	45	122	45
Heat Mirror™ 77/ Bronze	37	79	58
Heat Mirror™ 55/ Bronze	27	56	59
Incandescent Lights			6-13
Fluorescent Lights			22-40

[1] All glass 1/4", all inboard lights clear, all airspaces 1/2".
[2] Based on ASHRAE solar heat gain factor of 200 Btu/hr./sq. ft. and an outdoor temperature of 14°F higher than indoor.
[3] Calculation based on 49.5% of solar radiation being visible (123 BTU/hr./ft.^{2}). Percent visible energy = (Visible Transmission) x 123 ÷ (Relative Heat Gain) x 100.

- Warmer Glass Surface - Less Condensation

The colder a surface, the more readily condensation collects on it. During cold weather, the interior surface of window glass is one of the first places condensation forms. Besides being unsightly, condensation increases operating costs by damaging window frames, walls, drapes and carpets; and by increasing heat loss through the window. A Heat Mirror™ equipped window has a warmer interior glass surface temperature in winter - therefore less condensation for a given outside temperature. The figure below illustrates how

Heat Mirror™ provides condensation protection.

Effect of Heat Mirror™ on Condensation[1]

Exterior temperatures that cause condensation to form on the interior glass:

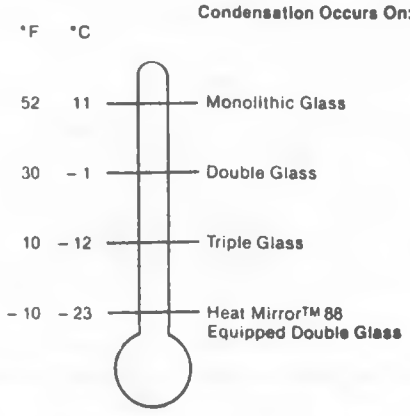

3. Increased Aesthetic Design Freedom

   - High performance without aesthetic compromise
   - Variety of performances - one appearance

- High Performance Without Aesthetic Compromise

  Heat Mirror™ transparent insulations allow the architect or designer to separate the glass appearance choice from the glass performance choice. Since Heat Mirror™ is suspended in the airspace of double insulating glass and is independent of the glass, it is possible to combine Heat Mirror™ performance in combination with any color of tinted or reflective glass. Conversely, if color or reflective appearance is objectionable, Heat Mirror™ makes it possible to achieve high performance in a clear unit - a particularly desirable quality in traditional architectural styles.

- Variety of Performance - One Appearance

  One additional benefit occurs in buildings where windows must have the same appearance but perform differently. For example, in a climate with cold winters and hot summers, the ideal window for the south elevation has a high shading coefficient to admit the low winter sun and a high insulation value to prevent heat loss. Conversely, windows with a lower shading coefficient but high insulation value are needed on the east and west to reduce unwanted summer solar heating. Windows with Heat Mirror™88 for the south and Heat Mirror™77 for the east and west accomplish these goals in visually indistinguishable clear windows.

BENEFITS OF HEAT MIRROR™ TO DIRECT GAIN PASSIVE SOLAR

By using the appropriate equations, it is possible to calculate the efficiency of Heat Mirror™88 equipped glass compared with other glazing configurations for any given passive solar project. The heat loss is subtracted from the gain to yield a net energy contribution to help heat the building. Naturally certain assumptions will have to be made about climate, occupant behavior, thermal mass, etc. In such analyses, Heat Mirror™ equipped windows will often be the largest net contributors of energy, but also often other glazing alternatives will have a slight Btu advantage.

This brings us to the concept of practical, livable, affordable passive solar rather than necessarily energy optimal passive solar.

The many advantages of Heat Mirror™88, both economic and practical, to passive solar designs bring a new, broader focus to the viability of passive solar.

To touch on this subject, consider the following:

- The ability of Heat Mirror™ to insulate glass to the R-4.3 level can make movable insulation systems unnecessary, ushering in the truly passive, passive home. No longer do passive homes require active, constantly present occupants.

- Heat Mirror™, mounted between the glass of double pane windows, is a truly maintenance-free feature.

- In most cases, the cost of Heat Mirror™ above and beyond double glass is cheaper than movable insulation systems.

- The higher insulation value of Heat Mirror™ equipped glass reduces the design need for thermal mass, a potential cost saver. It is well recognized that many homes with passive solar features lack adequate thermal mass to truly utilize the available sunlight on bright days.

- As envisioned earlier, occupant comfort is significantly affected by the inside surface temperature of windows. In passive solar buildings with large expanses of glass, the need for more moderate inside temperatures is very pronounced.

- As with the comfort issue, the greater use of glass in passive solar buildings makes the condensation resistance feature of Heat Mirror™ very important with passive solar designs.

REDUCTION OF GLARE IN DIRECT GAIN PASSIVE SOLAR

Glare is a problem in direct gain passive solar designs. Glare results from the contrast between daylight transmitted through the windows and the darker interior. Large amounts of visible light from the sun on a cold, winter day represent welcome Btu's of energy, but they can make the glare in a living space unbearable.

The selective transmission characteristic of Heat Mirror™, combined with conventional heat absorbing or tinted glass, offers a unique solution to this problem.

Preventing Glare in Direct Gain Passive Solar

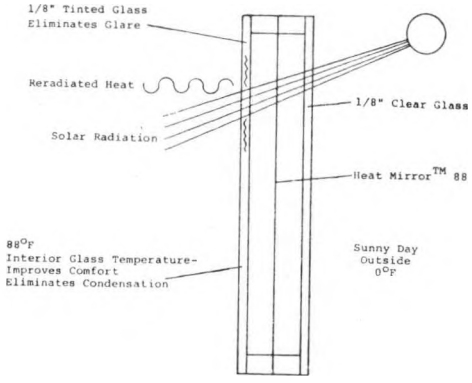

The concept is to glaze the south facing glass with clear glass on the outside, Heat Mirror™ in the middle, and tinted glass on the inside. Normally one would think that dark glass would radically reduce transmission and defeat the whole purpose of passive solar heating. One must remember, however, that tinted glass blocks by absorption. The sunlight passes through the clear exterior pane and the Heat Mirror™ and is greatly absorbed by the tinted glass. The tinted glass in turn reradiates the energy in the form of far infrared or heat radiation. The energy is now in the wavelengths that are reflected by Heat Mirror™. In other words, much of the energy absorbed and seemingly blocked by the tinted glass is forced to end up in the building because it is prevented from escaping by the Heat Mirror™.

To illustrate this point, compare the values in the chart below. The relative heat gain of bronze interior Heat Mirror™ unit (118) is only 3 less than the relative heat gain of a clear Heat Mirror™ unit (121).

Glass Type	Winter Values U Value	R Value	Interior Glass Surface Temperature °F Night	Day	Night Condensation Point (% R.H.)	Relative Heat Gain Btu/hr/sq. ft.
Heat Mirror™ 88 Clear Exterior, Bronze Interior	.23	4.3	57	88	64	118
For Comparative Purposes						
Heat Mirror™ 88 Bronze Exterior, Clear Interior	.23	4.3	57	69	64	92
Heat Mirror™ 88 Clear Exterior, Clear Interior	.23	4.3	57	69	64	121
Conventional Double Clear Exterior, Clear Interior	.49	2.0	46	52	42	141

Notes

* All glass 1/8", all air spaces 1/2".
* U-values shown represent Btu/hr/sq. ft./°F. 0°F outside, 15 mph wind, 70°F inside, no wind, no sun.
* Interior glass surface temperature and condensation point calculated for 0°F outside with 15 mph wind, 70°F inside temperature. Day values calculated for solar intensity of 248.2 Btu/hr,/sq. ft.
* Relative heat gain based upon a solar intensity of 248.2 Btu/hr./sq. ft., 0°F outside, 15 mph wind, 70°F inside.

It is the transformation of daylight to heat, before it enters the building, that minimizes glare problems.

CONCLUSION

The Heat Mirror™ family of transparent insulations from The Southwall Corporation today makes possible a new generation of high performance glazings for passive solar and energy conservation usage. Everyday architects, designers, builders, and energy consultants are exploring with their imaginations and their projects new ways Heat Mirror™ can advance their work. The reality of high performance Heat Mirror™ equipped glass is here.

PROJECT SUMMARY

Project Title: Development of Radiative Cooling Materials--Phase III

Principal Investigator: John R. Brookes

Organization: Energy Materials Research Company
2547 Eighth Street
Berkeley, CA 94710

Project Goals: Primary project focus is on development of polymer based IR (InfraRed) transparent solar reflective glazings for use in radiative cooling applications. Secondary focus is on development of selective emitter materials.

Project Status: Project is midstream.

A computer simulation was developed in order to carefully identify the minimum product property levels necessary for daytime cooling to occur. Variable glazing, emitter, insolation, and environmental parameters were used to determine the appropriate conditions.

Results of this computer study show that a range of glazing and radiator parameters are available for daytime radiative cooling. For "real" polyethylene glazings with non-selective IR transmittances of between 0.75-0.80, minimum glazing solar reflectances of 0.60-0.93 can produce daytime cooling when using solar absorptive IR non-selective radiators. The drawback for these emitters is that the total glazing solar transmittance must be between 0.90-1.0. Solar reflective IR non-selective radiators produce a minimum glazing reflectance range of between 0.60 and 0.84 with much greater lattitude in the permissable glazing solar absorptance. Non-uniform glazings (where bottom surface is solar absorptive) exhibit similar minimum glazing reflectance ranges yet show more favorable solar reflectances (i.e. lower) at medium glazing solar absorptance values when solar reflective radiators are used.

As would be expected, an increase in glazing IR transmittance increases daytime cooling capacity. In addition, use of IR selective radiators decreases the necessary glazing solar reflectance when glazing is solar absorptive. This later effect, however, decreases as glazing IR properties approach "ideal" (1.0 IR Transmittance).

Materials selection and aquisition for sample fabrication is nearly complete. Previous research determined ZnO & ZnS powders are best IR transmissive solar reflective pigment candidates with ZnO being excellent for material lifetime enhancement. Large particle size ZnO & ZnS powders (the former developed especially for the space program) will be employed. The increased particle size allows greater solar reflectance with the same pigment loading. Titanate surface treatments will be used to allow higher pigment loadings.

Contract Number: DE-FC03-80SF11504

Contract Period: March 1, 1982 thru February 28, 1983

Funding Level: $109,570

Funding Source: Materials & Components Div. of the U.S. Department of Energy, Chicago Office.

PRODUCT PERFORMANCE GOALS FOR THE DEVELOPMENT OF RADIATIVE COOLING MATERIALS--PHASE III

John A. Compton
Energy Materials Research Company
2547 Eighth Street
Berkeley, CA 94710
(415) 644-2244

ABSTRACT

This paper represents a summary of the first half of the current contract. The cooling performance of horizontal radiative cooling panels is analyzed via simple BASIC computer programs. Emphasis is placed on determining minimum properties of glazing materials which will allow "daytime" cooling. The "Zero Point" is defined as the magnitude of insolation necessary to exactly counteract a panel's cooling power. Plots of the "Zero Point" vs various material properties will then show which material combinations allow daytime cooling. Conclusions: Necessary solar reflectances for polyethylene glazings range beween 0.60-0.93 depending on glazing infra-red (IR) properties, glazing solar absorptance and solar properties of radiator (emitter). IR selective radiators significantly reduce (below range listed above) necessary glazing solar reflectance when glazing is also solar absorptive.

INTRODUCTION

The basis for radiative cooling is the spectral radiance of the atmosphere. Figure 1 shows the zenith atmospheric spectral radiance published in 1978 by Berdahl and Martin (1). Inspection of this figure shows that the radiance is depressed in the interval 8-13 microns compared to a black body. The magnitude of the depression correlates inversely with the amount of water vapor present. If a black body is placed on a horizontal surface at night, it will cool below ambient temperature because it initially emits more radiation than it absorbs. The difference is simply the difference in area under the black body curve and under the appropriate atmospheric radiance curve. 'Selective' radiative cooling occurs when special emitter materials are used to take specific advantage of the 8-13 micron atmospheric window.

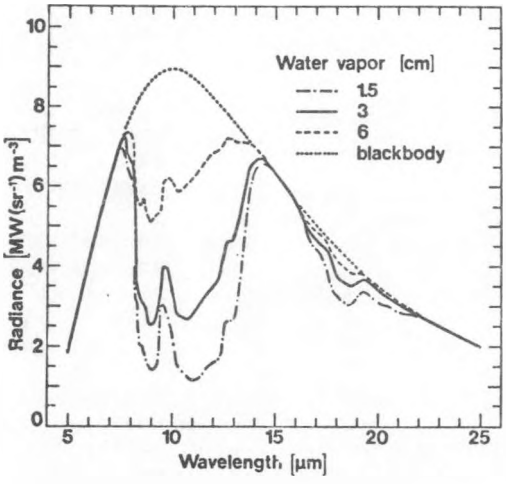

FIGURE 1
Spectral Radiance of the Atmosphere

The current program involves advanced research and development on polymer glazing and emitter materials for sky radiative cooling. The major focus is development of longlife glazing materials which will enhance 'daytime' cooling. This necessitates that the system be able to shed solar radiation for cooling to take place. Glazing materials should be:

1) Transparent to IR radiation between 8-13 microns (for IR radiative exchange to take place)

2) Absorbing or reflective to ultraviolet solar radiation between .25-.4 microns (to prevent photodegradation of polymer materials)

3) Reflective to the visible and near IR portions of solar spectrum (limits radiator solar uptake)

This computer study attempts to identify the minimum glazing properties (#1 and #3 from above) necessary for daytime cooling to take place. This task was accomplished by performing radiative cooling calculations of the emitter-glazing-sky system. BASIC computer programs were developed for this purpose. This report describes the methods and results of those calculations. Computer program listings are not included here due to limited available space.

The calculation model employed is based on that developed by Berdahl*, Martin, and Sakkal for their computer studies of radiative cooling without insolation (3). Though the computer program developed in that study is very exact, it is also very large and costly to run. Thus, modification of that program to include insolation effects was not considered practical for the parametric analysis currently needed. The programs developed in the current study are simple BASIC language routines which use the Micro Soft BASIC interpreter (1977) (Other BASIC interpreters may be used with some modifications being necessary).

* Special acknowledgement goes to Paul Berdahl of Lawrence Berkeley Laboratory whos aide was indispensible.

FORMULAE DERIVATION FOR HORIZONTAL DAYTIME RADIATIVE COOLING

In describing the heat balance between two surfaces one begins with the difference between their black body IR radiative heat flux. This difference is then modified by factors which describe the deviations of each material's properties from that of a black body and any multiple reflections which may occur between surfaces. Next, the solar uptake is evaluated. The insolation is modified in much the same way as the IR radiation. Finally, the non-radiative components such as convection and conduction, are considered.

For the purpose of simplicity, angle dependencies of optical properites (transmittance, absorptance, reflectance, and emittance,--t,a,r,e) have been ignored. As well, wavelength dependency is limited to the following three groups: 1) Solar, 2) IR inside the 8-13 micron window (IR_w), and 3) IR outside the 8-13 micron window (IR_o). The small error these assumptions introduce does not significantly hinder the use of the results in parametric analysis though caution should be used when referring to specific numeric results. With these assumptions and definitions the following equations have been derived. References to emittance (e) have been replaced by the absorbance (a) using Kirchoff's law.

A. Using Single Uniform Glazing Layer

In the equations below Q, S, H, & N are partial heat transfer sums in W/m^2, A & B are dimentionless multipliers, I is the insolation in W/m^2, T is the temperature in ^oK, R is the unmodified radiance in W/m^2 and h is the non-radiative heat transfer constant in $W/(m^2K)$. The numeric subscripts refer to the individual surfaces in the diagram at right, 'z' is the wave band reference, 'y' is the surface ref. #, 'σ' is the Stefan-Boltzman Constant, and F is the black body energy fraction.

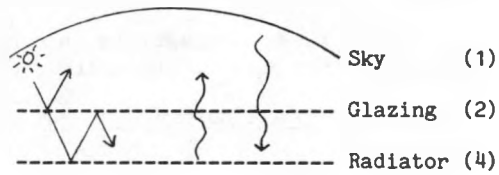

DIAGRAM OF UNIFORM GLAZING MODEL

Radiator Heat Balance

$Q_{4w} = A_w*(R_{4w}-R_{1w}) + B_w*(R_{4w}-R_{2w})$	IR_w exchange	Where: $A_z = t_2*a_4*X_z$
$Q_{4o} = A_o*(R_{4o}-R_{1o}) + B_o*(R_{4o}-R_{2o})$	IR_o exchange	$B_z = a_2*a_4*X_z$
$S_4 = A_s*I$	Solar uptake	$R_{yz} = \sigma*T_y^4*F_z$
$H_4 = h_{41}*(T_4-T_1) + h_{42}*(T_4-T_2)$	Non-radiative uptake	
$N_4 = N_{4w} + N_{4o} - S_4 + H_4$	Net cooling	and $X_z = 1/(1-(r_4*r_2))$

The above model assumes that temperatures for each material may be determined. This is not directly possible for the atmosphere as a very large thickness (and thus a wide range of temperature) is involved. The equation for R_1, then, must be modified. This is accomplished by assuming: 1) the sky is at a uniform temperature equal to ambient near the ground, and 2) the 'apparent' sky emissivity (a_1) is such that the calculated sky radiance equals the empirical value. We have then:

$$R_1 = a_1*\sigma*T_1^4$$

Next we must separate the contributions inside and outside the 8-13 micron window. Berdahl and Fromberg (2) derived a set of equations by assuming that the effective sky emissivity is 1.0 outside the 8-13 micron range (see Figure 1). The results are:

$$R_{1w} = (a_1-(1-f_w))*\sigma*T_1^4$$
$$R_{1o} = R_1-R_{1w}$$

Finally, the only value that cannot be independently fixed is the glazing temperature. Assuming that the heat capacity of the glazing is zero (reasonable for a 2 mil polyethylene film) the appropriate value of the glazing temperature will give a heat balance of zero. This assumption would need to be altered if other materials were used. With the glazing temperature at hand, all values are definable and the net cooling power of the radiator (N_4) may be calculated. With all constants as previously defined, the glazing heat balance equations are:

Glazing Heat Balance

$Q_{2w} = C_w*(R_{2w}-R_{1w}) + B_w*(R_{2w}-R_{4w})$	IR_w exchange	Where: $C_z = a_2*(1+t_2*r_4*X_z)$
$Q_{2o} = C_o*(R_{2o}-R_{1o}) + B_o*(R_{2o}-R_{4o})$	IR_o exchange	
$S_2 = C_s*I$	Solar uptake	
$H_2 = h_{42}*(T_2-T_4) + h_{21}*(T_2-T_1)$	Non-radiative uptake	
$N_2 = N_{2w} + N_{2o} - S_2 + H_2$	Heat balance	

B. Using Single Non-Uniform Glazing Layer

When evaluating solar reflective glazing materials one may also consider the case where the top and bottom surfaces of the glazing have different optical properties. For example, if the bottom surface of the glazing is more solar absorptive than solar reflective, one will get less solar radiation reflected back to the radiator.

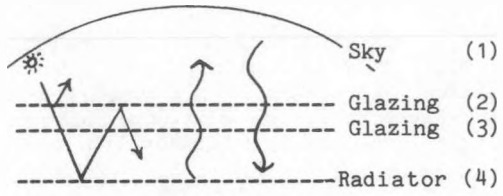

DIAGRAM OF NON-UNIFORM GLAZING MODEL

The model used for single non-uniform glazings is diagramed at right. In this model the glazing's bottom surface (surface #3) is assumed to have no independent solar reflectance. Next, it is assumed that the two layers are in complete thermal contact. There is no air gap imbetween the surfaces in this model. This means that the two surfaces act like opposite sides of a single film. Therefore, the total glazing solar uptake is equal to the sum of the uptakes of the two surfaces. Finally, it is assumed that the glazing's overall IR properties are independent of changes in the solar optical properties.

With these assumptions the only changes necessary in the previously derived equations are in the values for the A_s & C_s multipliers (IR properties remain as in the uniform glazing).

Solar Uptake Multipliers for Non-uniform Glazing

$$A_s = a_4 * t_2 * t_3 * X_z$$
$$C_s = a_2 * (1 + t_2 * t_3^2 * r_4 * X_z) + a_3 * t_2 * X_z * (1 + t_3 * r_4)$$
and $$X_z = 1/(1 - (t_3^2 * r_4 * r_2))$$

PARAMETER RANGES

A. Environmental Parameters

Sky Emissivity. We need to know the range that the total hemispherical sky emissivity actually takes. The empirical formulas developed by Berdahl and Fromberg (2) indicate that summer a_1 values range somewhere between 0.74-0.88 (night) and 0.73-0.86 (day) with average values close to 0.80.

Insolation. The magnitude of solar radiation on the earth's surface is a function of zenith angle and atmospheric conditions. Zenith angle is dependent on season, latitude, and time of day. On a diurnal basis the incident radiation is at its peak at solar noon falling off on either side toward zero. With the sun at solar noon (zenith angle of 0^o) Meinel & Meinel defined the direct insolation as 930 W/m^2 for a standard summer atmosphere containing 20mm of water vapor (4). When combined with the scattered solar component, the value is close to 1000 W/m^2. Weather and pollution are the major atmospheric conditions affecting insolation. As an example, measurements reported by Meinel & Meinel for an 'urban' summer atmosphere on the east coast of the U.S. set the noon time insolation (total) value at just above 800 W/m^2. Thus, 1000 W/m^2 will be the maximum insolation value considered in this study with the range 800-1000 W/m^2 being 'solar noon'.

Ambient Temperature. The ambient temperature range considered is 290-320 ^oK (62.6-116.6 ^oF). This range was chosen as cooling is rarely desired below 290 ^oK and few locations experience temperatures above 320 ^oK.

Non-Radiative Constants. The following non-radiative constants are used (3):

Symbol	Value ($W/(m^2*K)$)	Description
h_{41}	0.3	Radiator-to-air losses through back of 10 cm plastic foam.
h_{42}	0.9	Radiator-to-cover loss through 2.7 cm air gap between radiator and cover, $T_2 > T_4$.
h_{42}	$1.3*(T_4-T_2)^{.25}$	Radiator-to-cover loss through laminar convection, $T_4 < T_2$.
h_{21}	5.4	Cover-to-air loss through forced convection with wind speed = 2 m/sec. Length scale = 1m.
h_{21}	17.0	Cover-to-air loss through forced convection with wind speed = 10 m/sec. Length scale = 1m.

Window Fraction. The value of F_w is both wavelength and temperature dependent. Values range from 0.28 to 0.35 for temperatures of 260 ^oK to 320 ^oK inside the 8-13 micron window. The equations as written are not very sensitive to small changes in the value of F_w and so an average value is permissable. A value of 0.31 was chosen for this study. This value is compatable with the lower limits of the emissivity defined above. In the equation defining R_{1w} it can be shown that with a fraction value of 0.31 the minimum permissible value for the sky emissivity is 0.69 (if lower values are used the equations breakdown). Finally it should be noted that defining the window as 8-13 microns is accurate only where surface dewpoint temperatures are above 0^oC (typically summer months)(2).

B. Material Parameters

All materials must follow the law: Transmittance + Absorptance + Reflectance = 1.0

Each wave band's set of constants are considered independent of the other wave bands. Finally, as all angle dependencies are being ignored, the diffuse or hemispherical spectral properties are the most appropriate to use.

Radiator (Emitter). Other than the limits set above, the radiator will be considered to have a transmittance of zero in all wavelength bands. A 'selective' emitter will have a greater absorbance in the 8-13 micron IR region than in the IR outside that region. Caution should be exercised when dealing with specific numeric results obtained using selective materials as a somewhat greater error is inherent in their calculation (Probably no more than +/- 10%). This should not hinder their use in parametric analysis.

Glazing. The glazing material will have no specific limits other than those mentioned above. One should keep in mind, however, that there are some "real" limits that may not be apparent when inspecting "Zero Point" graphs or "Performance Maps". One such case is that highly solar absorptive glazing materials that have low IR emissivities will exhibit very large temperature increases (over 50 ^{o}K in the "ideal" case). These temperatures would cause destruction of the glazing material. Two reasonable scenarios for 2 mil polyethylene films (5) are used in this study for comparison to the ideal.

RESULTS

A. Set-Up

Because 'solar noon' has the highest level of solar radiation, if a radiative cooling device can produce any cooling at that time, cooling would be possible during any other portion of the day (and night assuming the same environmental conditions). The term "Zero Point" will be defined as the level of insolaton which produces exactly zero cooling given a particular set of environmental conditions and material properties (Radiator temperature equals ambient). If the "Zero Point" is equal to the solar noon insolation, that set of parameters would produce some cooling during the entire day. A parameter's effect on the "Zero Point" may be determined by plotting it against the "Zero Point" values. As discussd in the section on Parameter Ranges, solar noon insolation will be defined as between 800-1000 W/m^2.

The other environmental conditions (sky emissivity, ambient temperature, non-radiative heat transfer constants) can greatly effect the outcome of an analysis and so must be chosen carefully. In an effort to see an average to poor case, the following values have been chosen:

1) An average sky emissivity of 0.80 (according to Berdahl and Fromberg's studies (2)).

2) An ambient temperature of 300 ^{o}K (80.6 ^{o}F)(higher ambient temperatures allow for greater cooling power).

3) The standard non-radiative heat transfer constants with wind speeds assumed to be 2 m/sec. Unlike night cooling, high rates of convection are beneficial during the day as the glazing material heats up in the sun.

The remaining discussion describes those plots. Please refer to the section "Figure Information" for figure specifics (Figures 2-9 are located at end of report).

B. Figure Analysis

Figures 2-4 show how the "Zero Points" of a radiative cooling device using a single uniform glazing (SUG) change with alterations in either the glazing or radiator solar reflectance and absorptance. Figure 2 shows that when a solar absorptive IR non-selective radiator is used any increase in either glazing solar reflectance or absorptance is advantageous. Figure 3 represents the case of a solar reflective IR non-selective radiator. As in Figure 2, Figure 3 shows that any increase in glazing solar reflectance is advantageous. Increases in glazing solar absorptance, however, are beneficial only after a certain value of glazing solar reflectance has been reached.

Figure 4 shows a comparison between the solar relective and solar absorptive radiator types. It is important to note that the line representing "Solar Refl. + Solar Abs. = 1.0" (or Solar Trans. = 0.0) is independent of radiator solar properties. The shape and placement of this curve is dependent only on the IR properties of the glazing and radiator.

An alternative means of representing the effect of glazing properties on the "Zero Point" is the "Performance Map" as shown in Figure 5-7. Here we see curves showing the combined relationship between glazing solar reflectance, solar absorptance, and insolation. Figures 5 & 6 compare the results of SUGs using dfferent IR properties for the two radiator types previously mentioned. The solar absorptive

radiator (Figure 5) produces fairly stringent requirements on the glazing properties. In general, the glazing solar transmittance must be very close to zero in that case. The solar reflective radiator (Figure 6) allows much more lattitude in glazing properties.

Figure 7 shows how an IR selective radiator enhances the cooling ability of the panel. As the glazing solar absorptance increases, the IR selective nature of the radiator rejects much of the IR radiation emitted from the glazing. This is note worthy as IR selective radiators do not typically give as good performance as IR non-selective radiators when the radiator temperature is close to that of ambient and there is no insolation. It should also be noted that use of an "ideal" glazing (1.0 IR transmittance) eliminates any comparative benefits from the selective radiator as the glazing does not emit IR radiation.

Next we consider the case of a single non-uniform glazing (SNUG) where the bottom surface can have increased solar absorptance. Figure 8 shows a set of "Zero Point" curves for a device using a glazing with top surface solar absorptance of 0.0, IR properties as in the previous examples of SUGs, and solar reflective IR non-selective radiator. Note how there are no absolute insolation limits for these curves as there were for those representing uniform glazings (see Figure 3). This is true because of the independent nature of the top and bottom properties. Figure 9 is the performance map of the non-uniform single glazing. Note that the top surface solar absorptance has little effect on the overall performance. Also note that these are merely flattened SUG curves as the end points (reflectance values) are identical.

CONCLUSIONS

A range of glazing and radiator parameters are available for daytime radiative cooling. For "real" polymer glazings with non-selective IR transmittances of between 0.75-0.80, minimum glazing solar reflectances of 0.60-0.93 produce solar noon zero points when using solar absorptive IR non-selective radiators. Solar reflective IR non-selective radiators produce a minimum glazing reflectance range of between 0.60-0.84 with much greater lattitude in the permissable glazing solar absorptance. When glazing is solar absorptive, use of IR selective radiators decreases the necessary glazing solar reflectance. Non-uniform glazings exhibit similar "Zero Point" property ranges yet show more favorable solar reflectances (i.e. lower) at medium absorptances when solar reflective radiators are used. Glazing IR properties have a significant impact on the necessary solar properties. The beneficial effect of IR selective radiators decreases as glazing IR properties approach "ideal" (1.0 IR Trans.).

Finally, several points of further study present themselves:

1) First, a careful error analysis of this method should be undertaken. In general the error is small, however, there are two areas that need direct attention:

   a) It is unclear exactly how far the standard convection coeficients produce reasonable results (partiucularly at high glazing temperatures)

   b) The extent of the error in the calculations involving IR selective radiators is unknown.

2) Secondly, it would be interesting to determine the effect of various glazing solar property changes on the slope of the standard cooling curve (Cooling Power vs Radiator Teperature Drop).

3) Thirdly, a program integrating the total cooling during a day could be developed.

FIGURE INFORMATION

All Zero Point and Performance Map figures have the following environmental parameters:

Sky Emissivity	0.80
Wind Speed	2 m/sec (h_{21}=5.4 W/(m^2*K))
Ambient Temperature	300 ^{o}K
IR Window Fraction	0.31

The following are the material property ranges depicted and their reference codes.

Radiators: Black (R-B), Selective Black (R-SB), White (R-W), & Selective White (R-SW)

	SOL		IR_W		IR_O	
CODE	Refl	Abs	Refl	Abs	Refl	Abs
R-B	0.10	0.90	0.10	0.90	0.10	0.90
R-SB	0.10	0.90	0.10	0.90	0.90	0.10
R-W	0.90	0.10	0.10	0.90	0.10	0.90
R-SW	0.90	0.10	0.10	0.90	0.90	0.10

Glazings: Ideal (G-I), Polymer #1 (G-1), Polymer #2 (G-2)

	SOL*	IR**		
CODE		Refl	Abs	Tran
G-I	Var.	0.00	0.00	1.00
G-1	Var.	0.08	0.12	0.80
G-2	Var.	0.10	0.15	0.75

* These values vary in the graphs.

** These are IR non-selective glazings

FIGURE 2: ZERO POINTS of Single Uniform Glazing Layer

Glazing = G-2
Radiator = R-B
Solar Abs.:
a = 0.0
b = 0.1
c = 0.3
d = 0.5
e = 0.7
f = 0.9

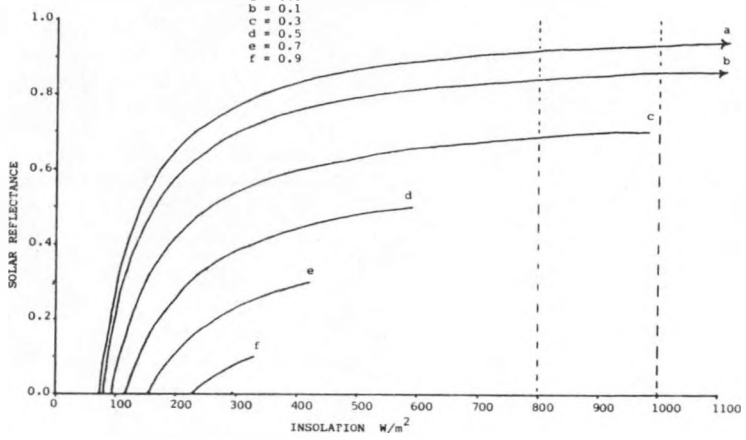

FIGURE 3: ZERO POINTS of Single Uniform Glazing Layer

Glazing = G-2
Radiator = R-W
Solar Abs.(Glazing)
a = 0.0
b = 0.1
c = 0.3
d = 0.5
e = 0.7
f = 0.9

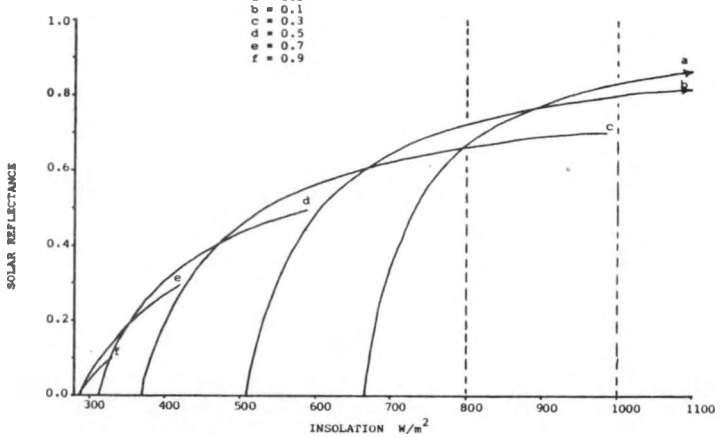

FIGURE 4: ZERO POINTS of Single Uniform Glazing Layer

Glazing = G-2
Radiators:
a = R-B
b = R-W
c = R-B or R-W

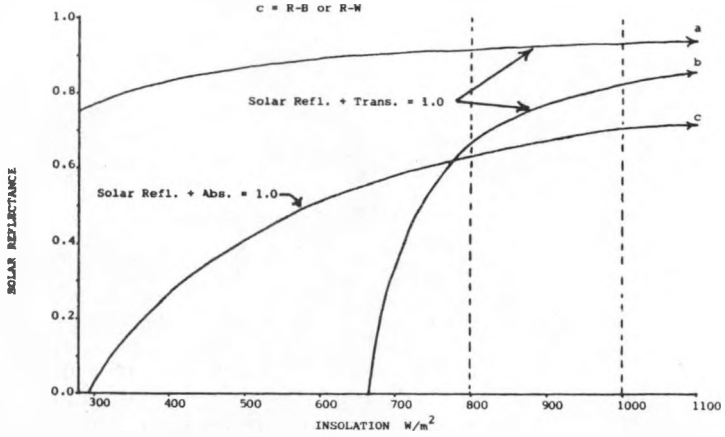

FIGURE 5: PERFORMANCE MAP

Single Uniform Glazing Layer

Glazings:
a = G-2
c = G-1
Radiator = R-B
- - - - - = 1000 W/m2 Insolation
——— = 800 W/m2 Insolation

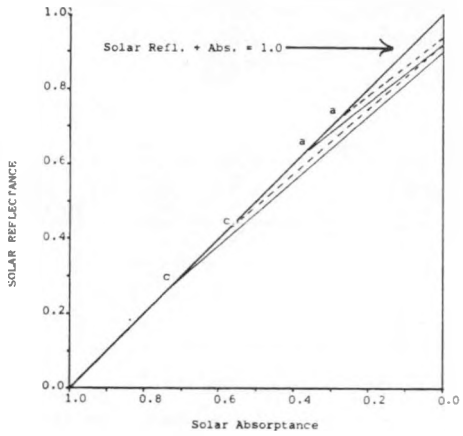

FIGURE 6: PERFORMANCE MAP

Single Uniform Glazing Layer

Glazings:
a = G-2
b = G-1
c = G-I
Radiator = R-W
- - - - = 1000 W/m2 Insolation
——— = 800 W/m2 Insolation

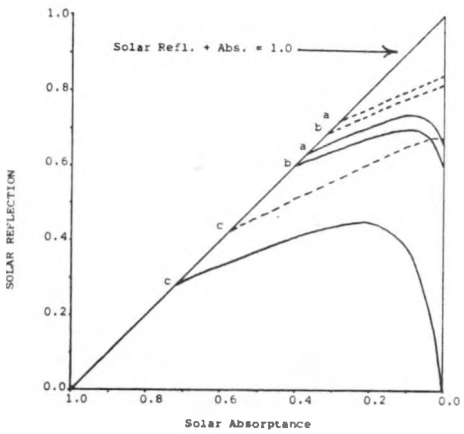

FIGURE 7: PERFORMANCE MAP

Single Uniform Glazing Layer

a = G-2, R-W
b = G-2, R-SW
c = G-I, R-W or R-SW
- - - - = 1000 W/m2 Insolation
——— = 800 W/m2 Insolation

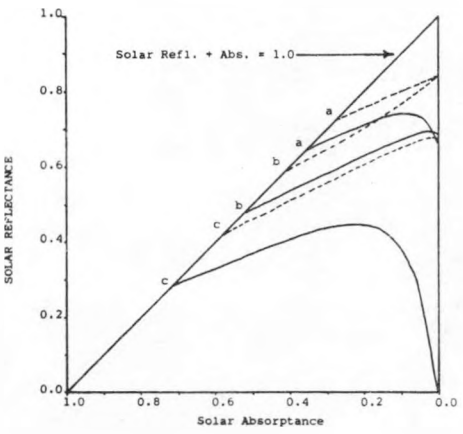

FIGURE 8: ZERO POINTS of Single Non-Uniform Glazing Layer

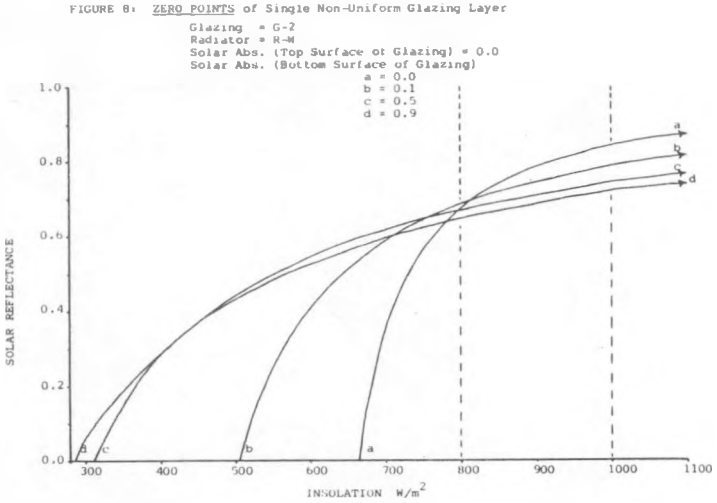

FIGURE 9: PERFORMANCE MAP

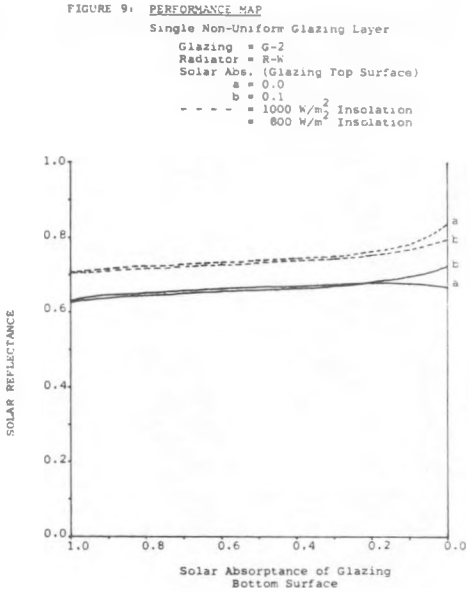

REFERENCES

1. P. Berdahl and M. Martin, Proceedings of the Second National Passive Solar Conference, (editors: D. Prowler, I. Duncan, and B. Bennett, American Section of the International Solar Energy Society, Newark Delaware, 1978), Vol. 2, p. 684.

2. P. Berdahl and R. Fromberg, An Empirical Method for Estimating the Thermal Radiance of Clear Skies, Lawrence Berkeley Laboratory, Report #LBL-12720, May 1981. (Submitted to Solar Energy).

3. P. Berdahl, M. Martin, and F. Sakkal, Thermal Performance of Radiative Cooling Panels, Lawrence Berkeley Laboratory, 1982.

4. A. Meinel and M. Meinel, Applied Solar Energy, An Introduction, Addison-Wesley Publishing Co., 1976.

5. Energy Material Research Company, Development of Radiative Cooling Materials--Phase II Technical Report, 1981. DOE Contract #DE-FC03-80SF11504. Address: 2547 Eighth Street, Berkeley, CA 94710.

PROJECT SUMMARY

Project Title:	Thermal Test Methods - Passive Components
Principal Investigator:	Michael E. McCabe
Organization:	National Bureau of Standards Building Physics Division Washington, D.C. 20234
Project Goals:	To develop standard thermal performance test procedures for various generic classes of passive/hybrid solar components.
Project Status:	A survey of passive/hybrid solar products resulted in an interim classification system consisting of ten generic groupings for purposes of thermal testing. Ten representative products for two of the generic classifications have been or will be purchased and prepared for field testing in FY82-83. Thermal performance testing has been completed in two commercial testing laboratories using four of the test articles and simulated outdoor conditions to measure overall thermal transmittance (U-Factor). Each laboratory performed the U-Factor tests on the same test articles for the same test conditions; however, different methods of simulating wind were used. Significant differences between the U-Factors were noted due to the different wind simulations. A test facility has been constructed to measure thermal performance of the test articles under conditions of controlled interior and actual exterior thermal environments. Comparison of test results between the field and laboratory conditions will provide the technical basis for a recommended laboratory based test procedure for U-Factor measurement. The test facility is specifically designed to measure both the solar radiative gain and thermal energy loss or gain through passive/hybrid solar components installed in either vertical or horizontal orientations in buildings, thereby permitting more quantitative evaluation of thermal performance of under field conditions.
Contract Number:	DE-A1101-76PR06010
Contract Period:	October 1, 1981 to September 30, 1982
Funding Level:	200 K
Funding Source:	DoE Passive and Hybrid Solar Energy Division

THERMAL TESTING OF PASSIVE/HYBRID SOLAR COMPONENTS

Michael E. McCabe
Building Physics Division
Center for Building Technology
National Bureau of Standards
Washington, D.C. 20234

ABSTRACT

Studies of thermal performance of passive solar buildings have indicated a need for precise field measurement of solar heat gain and thermal heat loss or gain for modular passive/hybrid solar components. A description of the conceptual design and the major assemblies and subsystems for a new calorimetric test facility is presented. The facility is designed for field testing of passive solar components at the National Bureau of Standards in Gaithersburg, Maryland. The test facility metering chamber can accommodate test articles having nominal dimensions up to 1.26 x 2.09 m (49 1/2" x 82 1/2") corresponding to a standard sliding door, with thicknesses up to 410 mm (16 in). The test articles are installed in the building envelope and can be oriented either to the vertical-south, or to the horizontal-upward facing direction. The metering chamber is designed to simulate an ideal indoor thermal environment by absorbing all the solar energy transmitted by the test article and by maintaining the indoor air and surface temperatures at controlled values between 15.6 and 26.7°C (60 and 80°F). A description of the passive/hybrid solar components proposed for testing in the calorimeter during the winter season of 1982-1983 is provided.

INTRODUCTION

A comprehensive evaluation of the transfer of thermal energy through a non-energy storing passive/hybrid solar component should consider the simultaneous effects of radiative heat transfer due to solar irradiation of the exterior surface, conductive heat transfer[1/] due to inside-to-outside air temperature difference, and mass transfer (air leakage) due to inside-to-outside pressure difference. Simplified evaluation procedures generally assume that the radiative, conductive, and mass transfer processes are parallel mechanisms, and therefore, the effect of each process can be measured separately and the results added.

These simplified evaluation procedures have led to the development of test methodology for conventional building components, such as insulation batts, windows, doors, and wall or roof sections, involving measurement of one or more of the following characteristics:

- Shading Coefficient
- U-Factor
- Infiltration Coefficient

The capability of a passive solar building space to accept thermal energy without overheating, however, is dependent in part on whether the energy transfer into the space is conductive or radiative. Therefore, the existing test methodology of separately measuring Shading Coefficient, U-Factor, and Infiltration Coefficient may not be sufficiently accurate to characterize the thermal performance of passive solar components. Furthermore, the storage of solar energy in a direct gain space occurs primarily from the radiative contribution (transmitted solar and re-radiated infrared), while the conductive portion is immediately available for heating the room air. However, Shading Coefficient characterizes the total energy transfer due to solar irradiation including both conductive and radiative components. Shading Coefficient, therefore, may not be the most appropriate parameter to characterize the solar gain through passive solar components installed in buildings.

Test methods for passive solar systems and components have evolved differently from test methods used for conventional building components. Most often, testing was performed on passive solar systems installed in small outdoor test rooms or cells using the naturally occurring weather conditions and with the test room air allowed to vary over a wide range of temperature. Although the results of the passive solar testing programs have yielded significant information on the operating principles and the relative thermal performance of alternative passive solar systems and components, the use of such test rooms with uncontrolled indoor air temperature is not recommended for standard testing of modular passive/hybrid components [1]. In the uncontrolled test rooms, the room air temperature is sensitive to such test room characteristics as

---

1/ The term conductive heat transfer in this paper is assumed to include both conduction across solid surfaces and convection across air spaces.

insulation thickness, surface area and thermal mass. Uncontrolled air temperature in the test room tends to modify the temperature-dependent heat transfer mechanisms such as free convection and infrared radiative transfer that normally occur. This results in performance data that are strongly facility dependent - a highly undesirable characteristic for a standard test procedure.

It appears that a more appropriate thermal boundary condition for standard testing of passive solar components is to establish fixed conditions of indoor air temperature and room surface temperature, and to accurately measure the rate of heat transfer that occurs between the outside and the inside, through the passive solar component. The remainder of this report discusses the conceptual design and the major assemblies and subsystems for a calorimetric test facility designed for field testing of passive/hybrid solar components. Additional details of construction and performance specifications are given in reference 2. It is anticipated that the test facility will provide a substantial improvement in the field measurement techniques for passive/hybrid solar components and thus provide a firm technical basis from which laboratory test procedures can be evaluated.

DESCRIPTION OF PASSIVE SOLAR CALORIMETER TEST FACILITY

The Passive Solar Calorimeter has been installed in the NBS/DoE Passive Solar Test Building which is located at the NBS Annex (Nike Site) immediately south of the main NBS campus in Gaithersburg, Maryland. An exterior view of the test building, which was completed in 1981 to test full-scale passive solar systems integrated into buildings, is shown in figure 1. Figure 2 shows the interior layout of the building experiments and calorimeter in the test building. An advantage to locating the calorimeter in the Passive Solar Test Building is the opportunity for simultaneous thermal testing of two identical passive solar components; one in the idealized room environment provided by the calorimeter, and the other in the more realistic full-scale room environment provided by one of the test cells. This will enable qualitative assessment of the effect of the calorimeter environment on component thermal performance.

The passive solar calorimeter facility consists of the following major assemblies and subsystems:

- metering chamber assembly
- fluid conditioning subsystems
- data acquisition and control subsystem
- building - test article interface.

A description of the major assemblies and subsystems is given in the following sections.

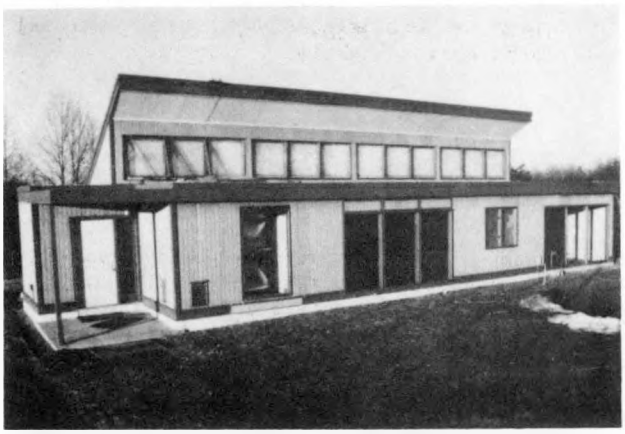

FIG. 1. PHOTOGRAPH OF NBS/DOE PASSIVE SOLAR TEST BUILDING

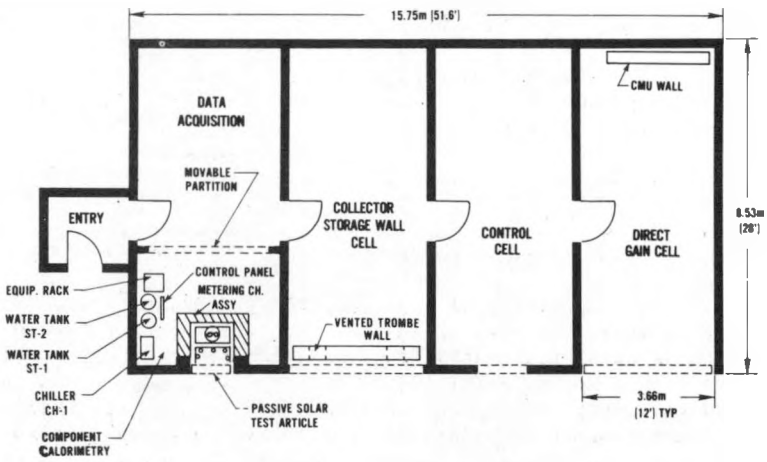

FIG. 2. FLOOR PLAN PASSIVE SOLAR TEST BUILDING

METERING CHAMBER ASSEMBLY

The metering chamber assembly, shown schematically in figure 3, includes the five-sided metering chamber constructed of rigid polyurethane foam insulation 150 mm (6 in) thick, which completely encloses the interior of the passive solar test article, and which can be mounted either vertically against the south wall or horizontally against the ceiling of the calorimeter room. The metering chamber is sealed against the interface surface of the test building by a clamping and gasket arrangement to minimize infiltration air exchange with the test building. A small charge of dessicant is placed in a pan near the return duct to dehumidify the metering chamber air. The dessicant is replaced at the completion of each test in order to prevent

condensation on cold surfaces of the test article. Temperature control of the metering chamber assembly is provided by the solar absorber panel and by the air conditioning unit.

A uniform surface temperature is maintained in the calorimeter by forced circulation of water through the solar absorber panel. The panel is constructed of a soldered assembly of copper sheets and tubes which are painted with a highly absorbing black paint. The panel is designed to absorb almost all of the solar energy transmitted by the test article and to provide a controlled, nearly-isothermal, radiative heat sink (or heat source) for the test article. Temperature control is achieved by sensing the average surface temperature of the panel with a six-junction thermopile used to control the duty cycle of the water heater located at the absorber panel inlet.

A uniform air temperature is maintained in the calorimeter by forced circulation of air at low velocity between the test article interior surface and the absorber panel. Temperature control is achieved in the air conditioning unit by removing heat and adding heat to the circulating air using the water-cooled heat exchanger and a two-stage electric heater, respectively. A reversible fan directs the air flow over the test article in the downward direction in the winter and upward direction in the summer to avoid interference with the free convection flow patterns that occur due to seasonal reversal of heat flow direction.

FLUID CONDITIONING SUBSYSTEMS

The test facility uses distilled water for the heat transfer medium in the fluid conditioning subsystems. Figure 4 shows a schematic drawing of the solar absorber panel fluid conditioning loop which contains the primary coolant circulating pump, emergency pump, heat rejection pump, storage tank, immersion heater, solid state temperature controller, and an air-cooled water chiller. Solar energy from the absorber panel is transferred to the storage tank from which it is rejected to ambient air by the water chiller. Emergency coolant circulation is provided by a battery-operated, low capacity pump to prevent freezing of the absorber panel due to a loss of power. The thermal energy contained in the storage tank will maintain the temperature of the absorber panel above freezing for at least 24 hours. The emergency coolant pump storage battery is kept on a trickle charge using a small photovoltaic array.

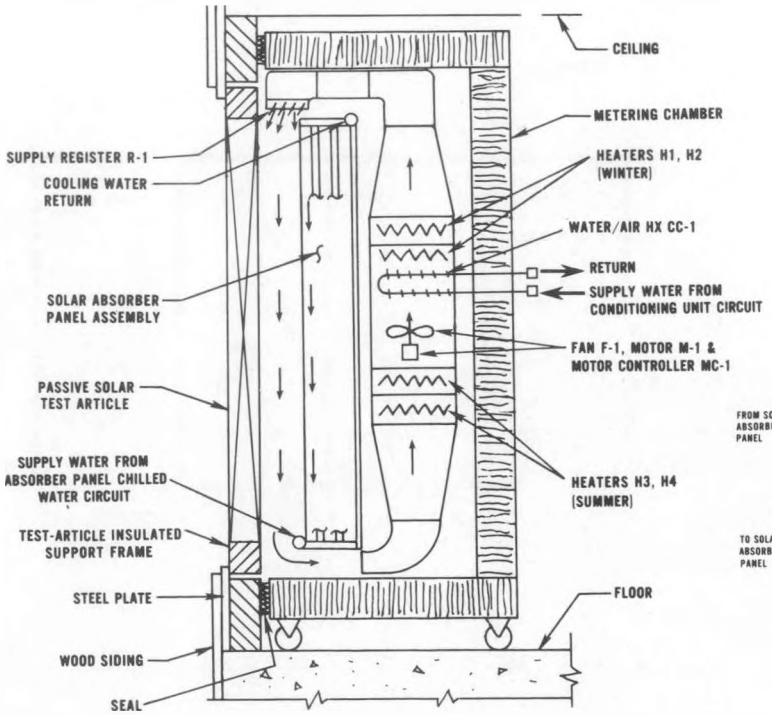

FIG. 3. METERING CHAMBER ASSEMBLY SCHEMATIC

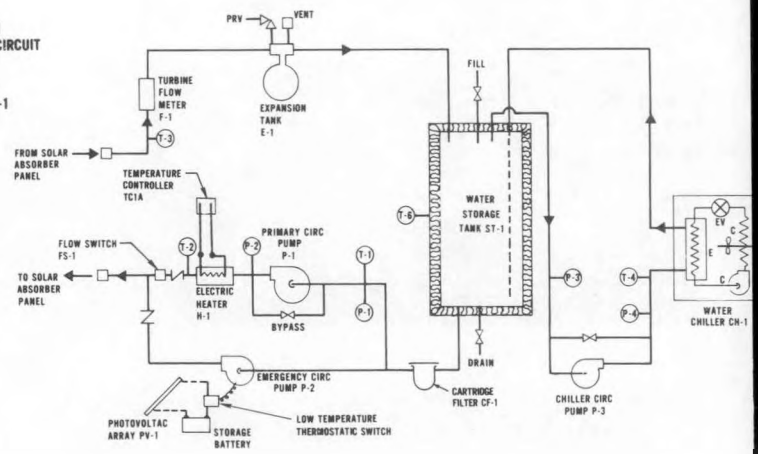

FIG. 4. ABSORBER PANEL CHILLED WATER CIRCUIT

A similar arrangement of pumps, electric heaters and a water chiller is used in the fluid conditioning loop (not shown) to remove heat from the metering chamber air circulation loop through the water/air heat exchanger. Thermal energy absorbed in the metering chamber air loop is rejected to the calorimeter room using the water chiller. Final control of the metering chamber air temperature is provided by a two stage electric heater located in the air conditioning unit downstream of the water/air heat exchanger. The heat exchanger coil operates at a constant flow rate and pre-selected cooling water supply temperature in

conjunction with the proportionally controlled electric heaters to provide the desired air temperature in the metering chamber.

DATA ACQUISITION AND CONTROL

Data acquisition and facility control will be performed separately during the initial phase of operation of the test facility with the intention of combining both functions in the future using a microprocessor. The test facility has a 60 channel data logger to scan and print the temperature and millivolt sensor readings and a 9 track tape recorder to store data on magnetic tape. The sensor readings are converted to engineering units using individual sensor calibration data, and heat balance calculations are performed using an off-line minicomputer. Further evaluation of the test results is performed using graphics plotting packages and statistical analysis programs. The data logger has the capability of reading 40 type-T thermocouple channels for surface and air temperature measurement and 20 channels for other analog voltage measurements including solar radiation, outside wind velocity, metering chamber air velocity, water flow rate and electric power consumption.

Initially, temperature control of the metering chamber air temperature and absorber panel will be provided by manually-set, solid-state temperature controllers. Future improvements in the test facility will replace the manual controllers with programmable controllers, so that any desired time-temperature profile can be obtained.

BUILDING - TEST ARTICLE INTERFACE

The passive/hybrid solar component to be tested is assembled in a suitable support structure and installed in either the vertical-south facing, or the horizontal aperture of the NBS Passive Test Building. The purpose of the building interface is to provide structural support for the test article and for thermal isolation from the building. Undesired heat flow paths between the metering chamber and outside are minimized by careful sealing of joints against air leakage and provision of a substantial thickness of rigid insulation to reduce heat conduction. Figure 5 shows details of the vertical aperture building interface. Modular passive solar components that are provided with a self-contained glazing system can be readily accommodated by removing the double-glazed window that is provided for non-glazed components. Figure 6 shows the installation of a skylight/shutter test article in the horizontal aperture building interface.

FUTURE ACTIVITY

The test program planned for the December 1982 to March 1983 winter season includes the re-testing of two direct gain fenestration (DGF) test articles which were previously tested in commercial testing laboratories, and the testing of two new DGF test articles and four new collector-storage wall (CSW) test articles. Two of the CSW test articles will contain water storage modules and the other two will contain hydrated-salt, phase change storage modules. Also, it is planned to test simultaneously one of the new DGF test articles in the calorimeter with a larger-sized unit of identical construction installed in the Direct Gain Cell of the Passive Solar Test Building.

The results of the 1982-1982 winter test program will be correlated with previous laboratory test results for DGF components and a draft standard recommended practice addressing U-Factor measurements will be prepared. Test results for the CSW modules will form the basis for a new test procedure for this group of products. In addition, all test data will be archived and made available to interested parties for further evaluation.

ACKNOWLEDGMENT

The author wishes to thank all persons who contributed to the design and construction of the test facility. In particular, continued financial and management support from the U.S. Department of Energy, Passive and Hybrid Solar Energy Division is acknowledged.

REFERENCES

1. M. McCabe, W. Ducas, M. Orloski, and K. DeCorte, "Passive/Hybrid Solar Components-An Approach to Standard Thermal Test Methods," NBSIR 81-2300, July 1981.

2. M. McCabe, M.S. Bushby, and W. Ducas, "Conceptual Design and Performance Specification for the Passive Solar Component Calorimeter," Letter Report from NBS to DoE, March 1982.

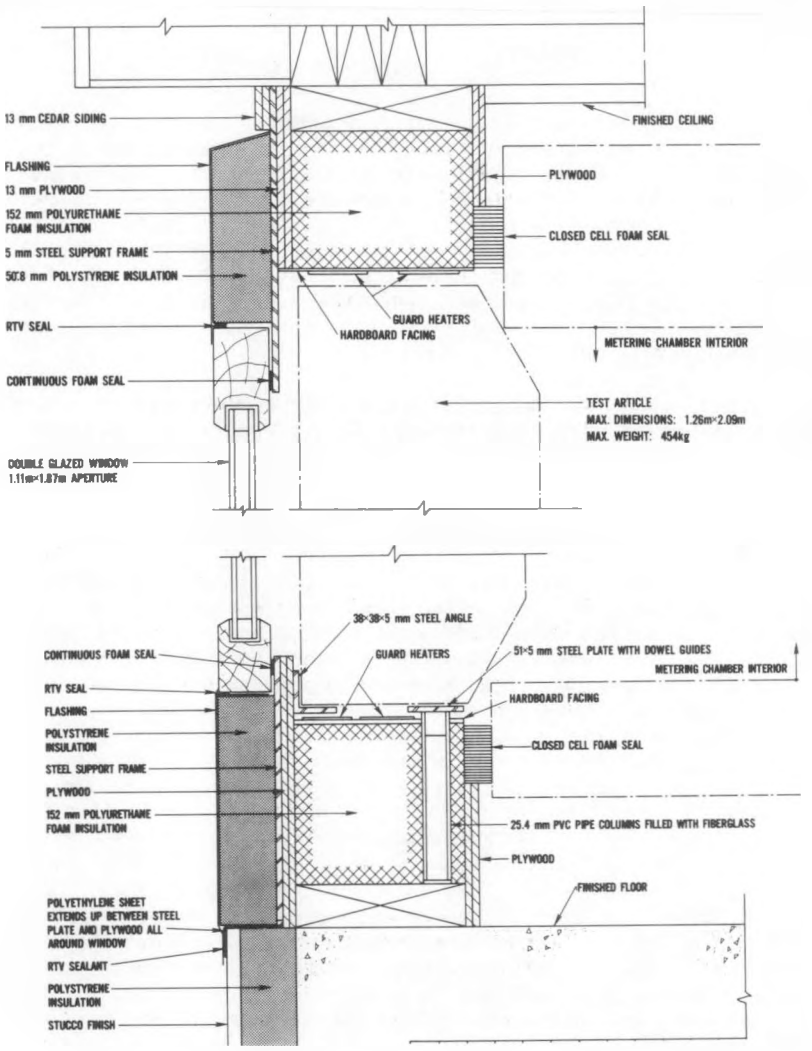

FIG. 5. TEST ARTICLE-VERTICAL APERTURE INTERFACE

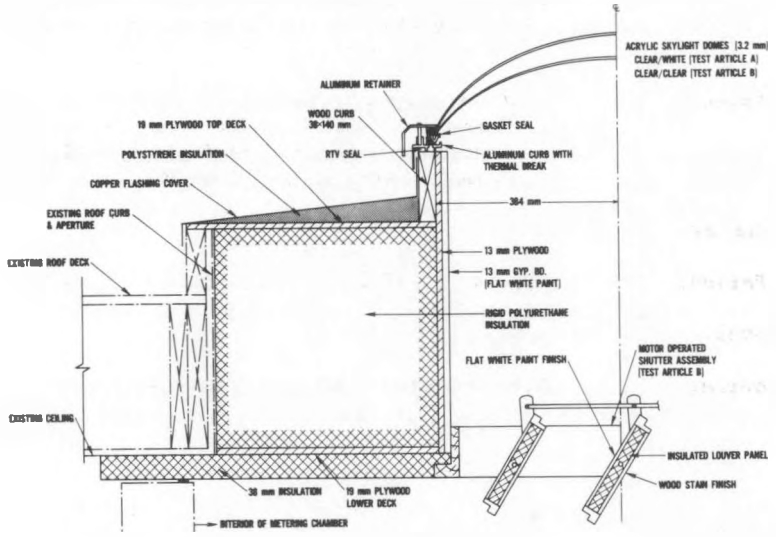

FIG. 6. SKYLIGHT/SHUTTER TEST ARTICLE-HORIZONTAL APERTURE INTERFACE

PROJECT SUMMARY

Project Title:	Advanced Optical and Thermal Technologies for Aperture Control
Principal Investigator:	Stephen E. Selkowitz
Organization:	Energy and Environment Division Lawrence Berkeley Laboratory University of California Berkeley, CA 94720
Project Goals:	Investigate fundamental physical processes, materials, and devices having a high potential for increasing the energy efficiency of glazed apertures in buildings. Emphasis will be placed on applications of modern optical technologies--for example, interference coatings, microstructural surfaces, scattering media, transparent aerogels, optically active materials, holography, and guided-wave optics. Applications fall into four major areas: Low-conductance, high-transmittance glazing: systems that minimize conducted, convected, and radiated (IR) transmission while maximizing solar transmittance. Optical switching materials: materials that actively modulate transmission of solar radiation on the basis of environmental conditions and building requirements. Selective transmittance glazing: materials that control transmittance (a) as a function of incident angle or (b) as a function of wavelength in order to enhance daylight transmission. Daylight enhancement: materials that provide for optical collection, transmittance, and distribution to enhance daylight utilization.
Project Status:	State-of-the-art reviews and technology assessments are underway in each major area. Analytical studies to estimate potential savings as well as detailed experimental studies are planned.
Contract Number:	
Contract Period:	October 1, 1981, through September 30, 1982.
Funding Level:	
Funding Source:	U.S. Department of Energy through Lawrence Berkely Laboratory

ADVANCED OPTICAL AND THERMAL TECHNOLOGIES FOR APERTURE CONTROL

Stephen E. Selkowitz
Carl M. Lampert
Michael Rubin

Energy Efficient Buildings Program
Lawrence Berkeley Laboratory
University of California
Berkeley, California 94720

INTRODUCTION

The energy-related performance of glazed apertures is generally seen as a major consideration in building energy use. These apertures have potentially positive and negative attributes with respect to heating loads, cooling loads, and lighting loads in buildings. As a basic approach, one would like to reduce undesirable heat losses and cooling loads to an absolute minimum. A better strategy is to balance useful gains against unavoidable losses so that the apertures make no net contribution to the energy cost of operating the building; that is, the gains and losses balance. Achievement of this goal would allow the major determination of the role of apertures to be based upon non-energy architectural and design constraints. The optimal use of a glazed aperture, however, would be to maximize the net energy benefits so that thermal gains and daylighting benefits can fulfill energy requirements elsewhere in the building. The identification of specific attributes of aperture systems that either minimize losses, break even, or maximize net energy benefits will be a sensitive function of climate, orientation, building type, and related operational parameters.

Most previous considerations of aperture performance have viewed the aperture as a static device having optical properties that are to be selected to optimize energy use in response to climate, building type, etc. But selection of this optimum level of performance based upon fixed thermal and optical properties almost always involves selecting a compromise solution, and the compromise will rarely be the solution that minimizes non-renewable energy consumption.

Aperture designs that minimize non-renewable energy consumption must be responsive to the hourly, daily, and seasonal climatic cycles that influence building energy consumption. The properties of elements of the ideal aperture system can be varied in response to climatic conditions, and the net performance of the total system can thus be timed to respond to thermal control and daylighting requirements. The aperture acts as an energy modulator, or controller, in the envelope of the building by rejecting, filtering, and/or enhancing energy flows, both thermal and daylighting. The functional role of the aperture at any given time is determined by intrinsic properties of the glazing elements, environmental conditions, and control responses by occupants.

Although a wide variety of specific functions can be assigned to any aperture, desirable performance characteristics can be organized into four broad functional categories.

1. Low-conductance, high-transmittance glazing.

These systems minimize conducted and convected heat transfer while maximizing radiant transmission. These are the dominant desirable attributes of most passive solar heating systems.

2. Optical switching materials.

These devices modulate daylight and/or total solar radiation on the basis of environmental conditions and building requirements. The significant feature of these materials is that they are active, changing properties over time.

3. Selective transmittance glazing.

There are two categories of materials that control sunlight and daylight through selective transmittance. The first category contains angle-selective glazings that use optical techniques to control transmittance as a function of incident angle. These are designed to control undesired solar gain. The second category includes materials that are selective in a spectral mode, transmitting in some portion

of the spectrum while reflecting or absorbing in other portions. These systems provide high daylight transmittance while minimizing total solar gain.

4. Daylight enhancement.

These systems provide optical collection, transmission, and distribution to enhance daylight utilization within a building.

For each of these four functional concepts we can identify a number of existing glazing options that provide some limited portion of the required control function. These options rely primarily on incremental improvements to existing glazing systems or on the addition of mechanically complex devices such as movable insulation. Even the new generation of heat-mirror coatings now entering the marketplace only begins to hint at potential improvements. Although new discoveries in optical sciences and engineering have advanced rapidly in some commercial fields, the architectural impacts have been limited. A broad range of advanced optical and thermal technologies has been largely unexplored in terms of ultimate application to building apertures.

Research on many elements of this program has been supported throughout the past six years by the Office of Buildings Energy Research and Development, Assistant Secretary for Conservation and Renewable Energy. The current program, initiated late in FY 82, builds upon this prior work and expands the scope and depth of these investigations. In each area detailed state-of-the-art reviews and technology assessments are underway. Results of these research overviews will be used in developing a comprehensive research plan to guide research activities in this field. The more promising technologies are being identified and will become the subject of new research investigations during the coming year.

The following discussion reviews preliminary results in three technical areas to suggest the importance and potential impact of these studies.

LOW-CONDUCTANCE, HIGH-TRANSMITTANCE GLAZINGS: HEAT MIRRORS

Coatings classified as heat mirrors, or transparent conductors, can be used to reduce radiative losses through architectural windows (1-3). Numerous thin-film systems exist which exhibit the potential for inclusion in energy-efficient glazings (4). Some of these coatings have been used as transparent electrical conductors and, to a lesser extent, as infrared radiation reflectors.

For our purposes a "heat mirror" is defined as a coating that is predominately transparent over the visible wavelengths (0.3 - 0.77 microns) and reflective in the infrared (2.0 - 100 microns). For the near-infrared (0.77 - 2.0), the material may exhibit combined properties depending upon design and end use. Heat mirrors fall into two classes based on design: single-layer doped semiconductors, and metal/dielectric interference films. Examples of the former are SnO_2:F, In_2O_3:Sn, Cd_2SnO_4, and CdO. Illustrative systems of the latter might be based on TiO_2/metal, Al_2O_3/metal, or ZnS/metal alternations.

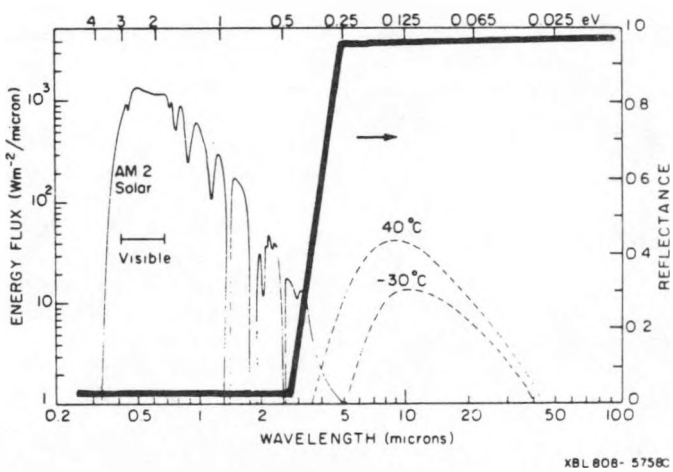

Figure 1. Solar irradiance (airmass 2) with two blackbody distributions (40°C, -30°C). Superimposed is the idealized reflectance of a heat-mirror coating.

Idealized properties of a heat mirror are shown schematically in Fig. 1 along with the solar (airmass 2) and blackbody spectra. With heat mirrors for windows, the coating's infrared reflectance provides a low-emittance (E) surface. The lower the emittance, the less the magnitude of radiative transfer by the window. Hence by using these nearly transparent coatings on a window surface, the thermal characteristics can be dramatically altered and energy can be more efficiently managed.

Figure 2 shows a triple- and a double- glazed window incorporating heat mirrors. In the separation between the glazing sheets a low-conductivity gas or vacuum may be used to further reduce convective heat transfer (2). Figure 3 shows the effect of multiple glazing and coating placement on overall thermal conductance, or U-value. Results were derived by computer modeling (5). For comparative purposes, a nonglass insulated wall has U = 0.6 W/m^2K (R-11) to 0.3 W/m^2K (R-19). New developments should make it possible to build R-5 to R-15 windows having a solar transmittance of 50 to 60%. Such windows would outperform insulated walls in any orientation for most climates.

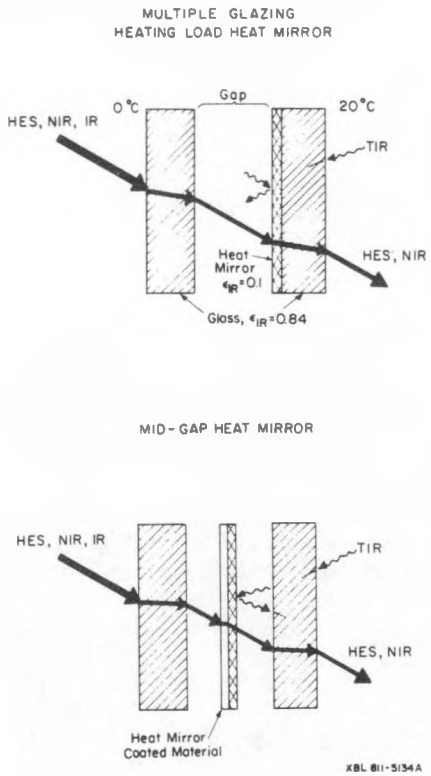

Figure 2. Multiple glazed windows employing heat-mirror coatings.

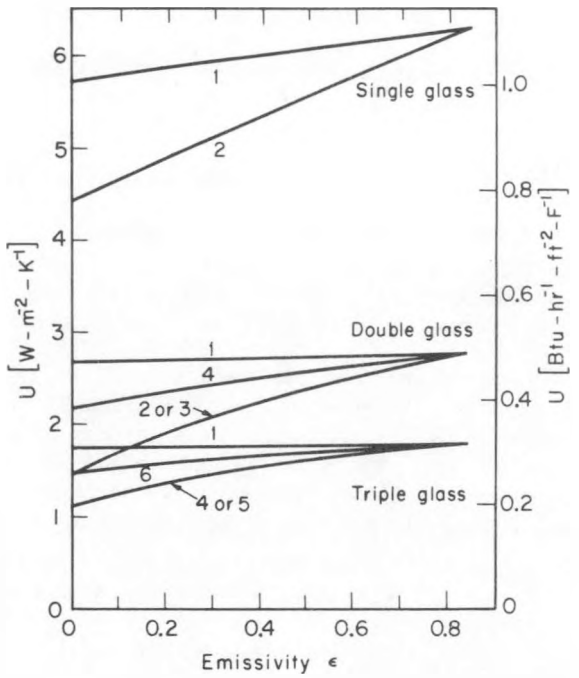

Figure 3. Modeled thermal conductance (U) for various window designs (5) using ASHRAE Standard winter conditions (T_{out} = 18°C, T_{in} = 18°C, wind speed = 24 km/hr). The effect of lowering the emittance of a single surface by the addition of a heat mirror. The surfaces on which the heat mirror appears are given as consecutive numbers, starting from the outside surface labeled 1. Air gap is 1.27 cm.

Active materials research centers around deposition processes and materials microstructural-property relationships. Development of cost-effective techniques to deposit such films on glass and plastic film materials is a major concern. Eliminating post-annealing treatments (to increase conductivity) would reduce expense. Improvement in chemical dip-coating processes and understanding of hydrolysis (CVD) chemistry as it relates to film properties are important research areas. Further development of plasma-assisted physical vapor deposition (PVD) is critical to room-temperature deposition on thin plastic film substrates. Lower deposition temperatures, along with near-atmospheric pressures, should be utilized for refined coating processes. An understanding of doping and defect properties in semiconductor films is necessary, with emphasis on durability and stability. There is also room for basic materials research of new binary and ternary compounds including boride, nitride, oxide, and carbide systems which may be better suited to simple deposition.

LOW-CONDUCTANCE, HIGH-TRANSMITTANCE GLAZINGS: TRANSPARENT AEROGELS

Transparent silica aerogels can be formed by supercritcially drying a colloidal gel of silica. The resulting material is highly transparent because the silica particles are much smaller than a wavelength of visible light. It is also an excellent thermal insulator because the material consists of 97% air trapped in pores smaller than the mean free path of air molecules. Basic studies of aerogel properties were initiated to determine its suitability for window glazing applications (6).

Aerogel Windows

For use in window systems, aerogel must be protected from moisture, shock, and handling. Although it can be fractured quite easily, aerogel is surprisingly strong in compression. Thus it can be protected by rigid glass panes on either side and should be sealed at the edges. Schmitt produced such a window by forming aerogel between panes of glass and drying through the edges (7). Even a large window can be dried by this method because the aerogel has a high permeability for ethanol under supercritical conditions. Other methods for protecting the aerogel should be investigated.

The thickness of glass in an ordinary window is determined by the size of the unsupported area. The sandwich structure of an aerogel window undoubtedly will permit thinner glass based on structural requirements alone. However, tests are needed to determine the thickness of glass required to protect the aerogel from damage. This thickness may prove to be greater than that required for standard windows unless transparent spacers are used.

Aerogel appears slightly yellow when viewed against a bright background, such as the sky or a white wall, because the blue light is scattered most efficiently. Against a dark background, the aerogel appears milky blue because the light is backscattered from the aerogel itself.

We have used the procedures of (8), together with optical measurements of aerogel samples, to calculate normal-hemispherical transmittance, T_h, for aerogel windows. Figure 4 shows the effect on aerogel thickness on T_h, averaged over the air-mass-2 solar spectrum. Aerogel by itself, despite scattering losses in the visible and O-H absorption in the infrared, has a higher transmittance than does window glass of equal thickness. The transmittance of an aerogel window made with low-iron glass and an aerogel thickness of 6 mm equals that of double glass. Doubling the thickness of aerogel reduces T_h to about 0.6, equal to triple glass. Increasing aerogel thickness reduces transmittance but also lowers the thermal conductance, U, of the aerogel window, while U for the double-glass window rapidly reaches a limiting value.

Using the measured thermal conductivity of aerogel, 0.019 $Wm^{-1}K^{-1}$, and the methods of (9), we can predict the heat transfer through an aerogel window. Figure 5 compares the thermal conductance of aerogel windows to that of ordinary double-glass windows as a function of the space between panes, D. At D = 0 the panes of glass touch, effectively becoming a single sheet of glass having U only slightly lower than for a single glass pane. For low D, heat flows only by conduction and radiation. The radiative term in U is much larger for the double-glass window, however, because the air is transparent to infrared radiation. As D increases further, convection heat transfer increases in the double-glass window but not in the aerogel window, so the overall conductance of the aerogel window continues to drop. Even lower conductance values can be achieved using low-conductance gases such as CO_2 and CCl_2F_2. The lowest reported heat transfer value is 0.011 $W^{-1}K^{-1}$, with CCl_2F_2. For this value, a window with 20 mm of aerogel would have a thermal conductance less than 0.5 $Wm^{-2}K^{-1}$.

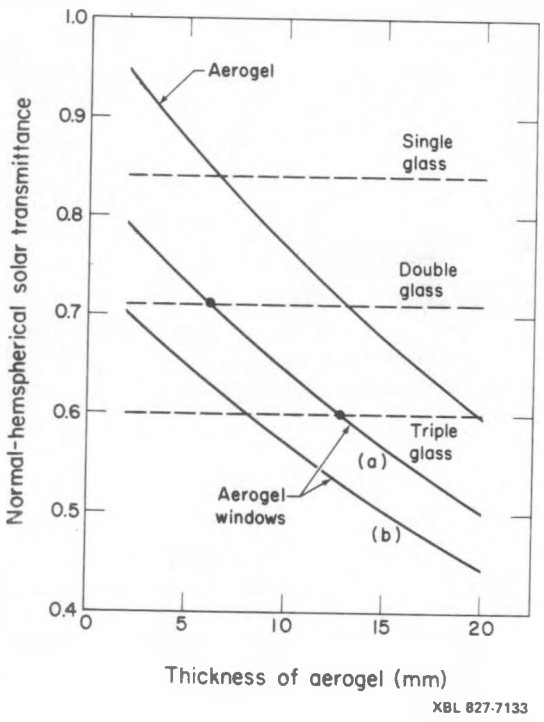

Figure 4. Calculated solar transmittance of aerogel windows vs. aerogel thickness compared to solar transmittance of conventional glass except for the 3-mm windows. All glass is 3-mm clear float glass except for the low-iron glass of aerogel window (a).

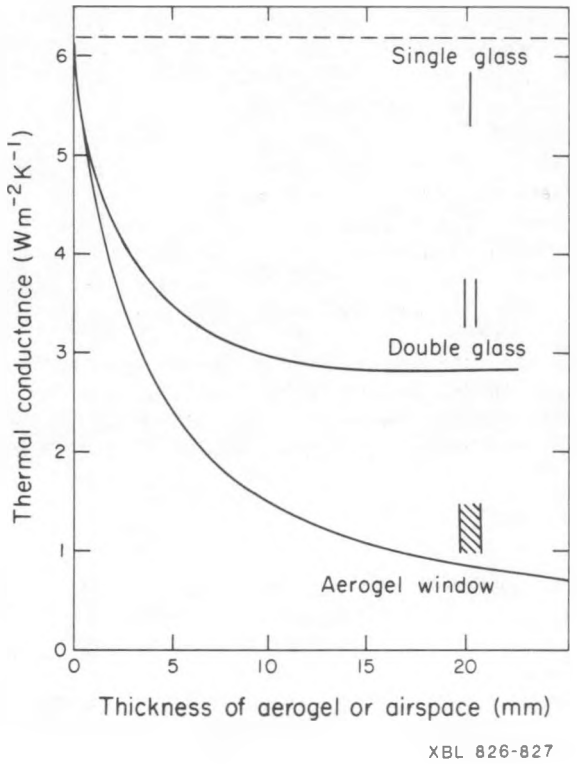

Figure 5. Calculated thermal conductance of aerogel window and of conventional single- and double-glass windows vs. spacing between glass panes.

In principle, we could increase the thickness of the aerogel until reaching the desired conductance, but unless scattering can be reduced, the solar transmittance and optical quality degrade to unacceptable levels for thickness greater than a few centimeters. In any case, it may not be possible to make layers thicker than a few centimeters by the process described above; experiments with tall columns of aerogel produced defects at the base of the column. The optimum thickness in window systems will depend on climate, building type, and window orientation.

OPTICAL SWITCHING MATERIALS

Optical switching materials or devices can be used for energy-efficient windows or other passive solar devices. An optical shutter provides a drastic change in optical properties under the influence of light, heat, or electrical field or by their combination. The change can occur as a transformation from a material that is highly solar transmitting to one that is reflecting either totally or partly over the solar spectrum. A less desirable alternative might be a film that converts from highly transmitting to highly absorbing. An optical shutter coating would control the flow of light and/or heat in and out of a building window, thus performing an energy management function. Phenomena of interest to optical shutters are electrochromic, photochromic, thermochromic, and liquid crystal processes (10).

Electrochromic Devices

Electrochromism is exhibited by a large number of inorganic and organic materials. The electrochromic effect is of current research interest mainly because of its application to electronic display devices, although some studies for window applications have been completed (11). An electrochromic material exhibits intense color change due to the formation of a colored compound formed from an ion-insertion reaction induced by an instantaneous applied electric field. The reaction might follow: $MO_x + yA^+ + ye \longleftrightarrow A_yMO_x$.

There are three categories of electrochromic materials: transition metal oxides, organic compounds, and intercalated materials. The materials that have attracted the most research interest are WO_3, MoO_3, and IrO_x films. Organic electrochromics are based on the liquid viologens, anthraquinones, diphthalocyanines, and tetrathiafulvalenes. With organics, coloration of a liquid is achieved by an oxidation-reduction reaction, which may be coupled with a chemical reaction. Intercalated electrochromics are based on graphite and so are not useful for window applications.

A solid-state window device can be fabricated containing the elements shown in Figure 6: transparent conductors (TC), an electrolyte or fast-ion conductor (FIC), counter electrode (CE), and electrochromic layer (EC). Much research is needed to develop a usable panel and better electrochromic materials having high cycle lifetimes and short response times. Fast-ion conductors and electrolytes also require further study.

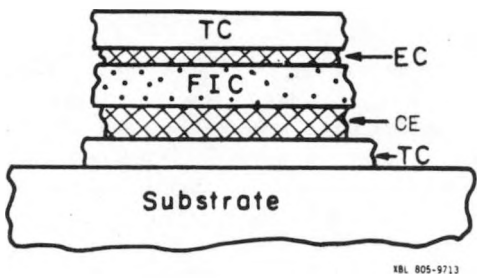

Figure 6. Model of solid-state electrochromic cell.

Photochromic Materials

Photochromic materials change their optical properties or color with light intensity. Generally, photochromic materials are energy-absorptive. The phenonemon is based on the reversible change of a single chemical species between two energy states having different absorption spectra. This change in states can be induced by electromagnetic radiation. Probably the best known application is photochromic glass used in eyeglasses and goggles. Photochromic materials are classified as organics, inorganics, and glasses. The organics include stereoismers, dyes, and polynuclear aromatic hydrocarbons. The inorganics include ZnS, TiO_2, Li_3N, HgS, HgI_2, HgCNS, and alkaline earth sulfides and titanates, with many of these compounds requiring traces of heavy metal or a halogen to be photochromic. Glasses that exhibit photochromism are Hackmanite, Ce, and Eu doped glasses (which are ultraviolet sensitive), and silver halide glasses (which include other metal oxides). The silver halide glasses color by color-center formation from an AgCl crystalline phase.

For windows, development work is needed to utilize commercially available silver halide glasses. Deposition of such glasses as film compounds requires more research for possible utilization as films and suspensions in polymeric materials.

Reversible Thermochromic Materials

Many thermochromic materials are used as nonreversible temperature indicators, but for an optical shutter one can consider only the reversible materials, although their cyclic lifetime is limited by nonreversible secondary reactions. Organic materials such as spiropyrans, anils, polyvinyl acetal resins, and hydrozides are examples of thermochromic materials. Inorganic materials include HgI_2, AgI, Ag_2HgI_4, $SrTiO_3$, Cd_3P_3Cl, and Copper, Tin, and Cobalt complexes. Work is suggested on compounds that exhibit both photo and thermochromism. Identification of limiting reactions, development of film materials, and polymeric and glassy dispersions are necessary.

Liquid Crystals

Liquid crystals have been extensively researched for use as electronic and temperature displays. Liquid crystals are characterized as one of three structural organic mesophases: smectic, nematic, or twisted nematic (cholesteric). The most widely used is the twisted nematic. From a materials standpoint, liquid crystals are based on azo-azoxy esters, biphenyls, and Schiff bases. Passive liquid crystal films can be solidified into solid films by polymerization, giving preset optical properties. A liquid crystal in the form of a light valve could be used to modulate transmittance and reflectance of light. Unlike the electrochromic device, a liquid crystal would require continuous power to stay reflective. Both cost and fabrication problems must be considered for large-area liquid crystal optical shutters.

SUMMARY

The research program described above is designed to identify, develop, and evaluate new optical technologies that promise to increase the energy efficiency of building apertures and enhance the performance of all passive systems in buildings. Although the program started late in FY 82, it builds upon six years of prior work on aperture performance so that we expect additional results to emerge quickly in FY 83. New state-of-the-art reviews have already identified promising technical concepts in each of the four major areas of aperture function that will be further explored in FY 83.

ACKNOWLEDGEMENT

This work was supported by the Assistant Secretary for Conservation and Renewable Energy, Office of Building Energy Research and Development, Buildings System Division and the Office of Solar Heat Technologies, Passive and Hybrid Solar Energy Division of the U.S. Department of Energy under Contract No. DE-AC03-76SF00098.

REFERENCES

(1) S. Selkowitz, "Transparent Heat Mirrors for Passive Solar Heating Applications," Proceedings of the Third Passive Solar Conference, San Jose, CA, Jan. 1979, pp. 124-132. Lawrence Berkeley Laboratory Report LBL-7833.

(2) S. Selkowitz, "Thermal Performance of Insulating Window Systems," ASHRAE Transactions Vol. 85, No. 2, p.669 (1979). Lawrence Berkeley Laboratory Report LBL-8835.

(3) R. Johnson, S. Selkowitz, F. Winklemann, and M. Zenter, "Glazing Optimization Study for Energy Efficiency in Commercial Office Buildings," presented at the Third International Symposium on Energy Conservation in the Built Environment, Dublin, Ireland, March 1982. Lawrence Berkeley Laboratory Report LBL-12764.

(4) C.M. Lampert, "Heat Mirror Coatings for Energy Conserving Windows," Solar Energy Materials, Vol. 6, No. 1, pp. 1-42 (1981). Lawrence Berkeley Laboratory Report LBL-11446.

(5) M. Rubin, R. Creswick, and S. Selkowitz, "Transparent Heat Mirror for Windows: Thermal Performance," Proceedings of the Fifth National Passive Solar Conference, Amherst, MA, October 1980. Lawrence Berkeley Laboratory Report LBL-11408.

(6) M. Rubin, and C. Lampert, "Transparent Silica Aerogels For Window Insulation," to be published in Solar Energy Materials Lawrence Berkeley Laboratory Report LBL-14462 (1982).

(7) W.J. Schmitt, presented at the Annual Meeting of the AIChE, New Orleans, LA (1981).

(8) M. Rubin, "Solar Optical Properties of Windows," Energy Research Vol. 6, p. 123 (1981). Lawrence Berkeley Laboratory Report LBL-12246.

(9) M. Rubin, "Calculating Heat Transfer through Windows," to be published in Energy Research, Vol. 6, No. 4 (1982). Lawrence Berkeley Laboratory Report LBL-12486.

(10) C.M. Lampert, "Thin Film Electrochromic Materials for Energy-Efficient Windows," Lawrence Berkeley Laboratory Report LBL-10862 (1980).

(11) C.M. Lampert, "Durable Innovative Solar Optical Materials--The International Challenge," presented at the SPIE Technical Symposium, Los Angles CA, January 1982. Lawrence Berkeley Laboratory Report LBL-13753.

PROJECT SUMMARY

Project Title:	Variable Transmittance Electrochromic Windows
Principal Investigator:	R. David Rauh
Organization:	EIC Laboratories, Inc. 111 Chapel Street Newton, Massachusetts 02158
Project Goals:	Development of variable aperture windows based on reflective electrochromic thin films. The project entails evaluation of deposition methods for large areas of electrochromic WO_3 onto conductive glass substrates, and incorporation of thin film electrodes into a window structure containing a solid or semisolid electrolyte and suitably chosen counter electrode reaction.
Project Status:	This is a new project. RF sputter deposition of WO_3 films has been achieved from a hot pressed WO_3 3" target onto indium/tin oxide (ITO) coated (conductive) glass. Rapid coloration is observed for films produced at high rates. This method can be scaled to high areas. Other techniques under investigation for producing large area films are spray pyrolysis and coating substrates from an oxide gel suspension. While WO_3 deposition methods are being evaluated, window structures and electrolytes are being tested with Prussian blue (PB) coated electrodes. PB is easily deposited from solution and can be oxidized or reduced to colorless forms (PB^+, PB^-), making symmetrical window structures feasible. Total windows of structure ITO|PB|electrolyte|PB|ITO (blue) have been prepared and converted to ITO|PB^+|electrolyte|PB^-|ITO (colorless) at less than 2V polarization. Liquid, semisolid and solid polymer electrolytes have been tested in these cells. In future designs, PB may be used as a counter electrode with WO_3.
Contract Number:	DE-AC02-82CE30746
Contract Period:	July 26, 1982 through July 25, 1983
Funding Level:	$145,997
Funding Source:	U.S. Department of Energy, Chicago Operations Office

VARIABLE TRANSMITTANCE ELECTROCHROMIC WINDOWS FOR PASSIVE SOLAR APPLICATIONS

R. David Rauh
EIC Laboratories, Inc.
111 Chapel Street
Newton, Massachusetts 02158

ABSTRACT

Electrochromic windows can be used for linear variation of transmission and/or reflection of light. Such windows can be useful in passive solar space conditioning, as the entering sunlight can be subjected to thermal or optical feedback control. The present work describes window structures comprised of WO_3 and/or Prussian blue electrochromic elements combined with thin layer solid or semisolid electrolytes.

INTRODUCTION

One of the most important factors governing the successful application of passive solar space conditioning is the timing of sunlight transmission through windows. Although in colder climates and seasons a high solar transmission is desired, in warm and variable outside climates, overheating and thermal stability of interior space become problematic. In large modern office buildings with extensive window areas, air conditioning losses can be substantial on sunny days due to "greenhouse" heating. Yet on cold or cloudy days, the day lighting from these windows is desired. In addition, in passive solar structures with large south facing glass windows, a mechanism for controlling glare in the daytime and for insuring privacy at night is needed. Some of these problems can be solved with various forms of mechanical aperture control over glazed areas. Shades, shutters and curtains restrict vision through the windows, and must be either mechanically controlled (requiring continued personal attention) or auto-mechanically controlled, which could require a complex and cumbersome series of motors and relays.

In this program, we are investigating a new type of aperture control based on electrochromic coloration of the window structures. The window would function by changing its light transmission and reflectivity over a linear range through the application of a DC electrical current, lightening or darkening depending on the direction of current flow. A favorable aspect of electrochromic devices is that, once the current is interrupted, the coloration persists until current flow is resumed. Since electrochromic displays have been extensively investigated (1), we know that they are inherently low power devices, consuming <1 mW/cm^2 during a full coloration cycle ($\sim$1 min). One particular advantage to a window that can be electrically tinted and bleached is the possibility of feedback control. An interior thermostat sensor could be used to trigger the coloration of the glass panel, for example. In this way, the temperature control could be automated in a passive structure based on large solar windows, with a manual override or secondary photocell sensor to provide nighttime privacy.

A schematic view illustrating the operation of this kind of window, as well as the associated heat flows, is presented in Fig. 1. Some heating will occur in the colored glass, due to absorption, and a fraction of that heat will be transferred into the living space, that fraction depending on the placement of the colored element within the glass structure. This kind of unwanted heat transfer is reduced because the structure also increases its reflectance when electrically colored. Furthermore, when used as thermopane, the windows will have a higher than normal "R" value. First, since they are comprised of two glass sheets sandwiching thin film electrochromic elements, their insulation should approach that of conventional double glazing. Also, infrared reflectance is increased on coloration, making the window a partial heat mirror, which should reduce interior heat losses in winter.

ELECTROCHROMIC WINDOW STRUCTURES

A cross section of a hypothetical electrochromic window is shown in Fig. 2. It consists of three major parts: 1) glass coated with transparent electrodes, such as reduced SnO_2, about 0.1 μm thick; 2) an electrochromic layer, here WO_3, also $\sim$0.1 μm thick, containing H^+ or alkali metal ions and an oxidizable species (e.g., I^- or $S^=$). Making the WO_3 the cathode, passage of an electrical current converts it to a colored "tungsten bronze", a nonstoichiometric compound of general formula M_xWO_3 ($x < 1$), where M = H, Li, Na, etc. The oxidizable species will be oxidized at the other electrode, balancing the net ionic charge. If the WO_3 layer is amorphous, then M_xWO_3 is blue, darkening as x increases. If the WO_3 is crystallized, the M_xWO_3 appears blue to transmission, but also takes on a metal-like bronze reflective property due to the delocalization of electrons in the extended crystal lattice (2). This reflectance would be desirable in a window, to prevent overheating (see above). The electrochemical reaction is extremely reversible, so that the transmission of the WO_3 can be adjustable at will.

Monolithic light valve structures like that in Fig. 2 have not been reported previously, and the present program is aimed at their demonstration and research on each of the individual components.

Preliminary results have been obtained on deposition of WO_3 by rf sputtering, a process that can be economical and scaled to large area production. Conditions have been selected to produce films which are fully oxidized and colorless (blue WO_{3-x} cannot be bleached electrochemically), and of high surface area microcrystalline morphology. The latter appears necessary to ensure rapid rates of electrocoloration/bleaching. The absorption spectra of the sputtered films WO_3 and Li_xWO_3 (prepared electrochemically in $LiClO_4$, propylene carbonate) are shown in Fig. 3. Preliminary results also indicate the expected bronze-like reflectance for these colored films.

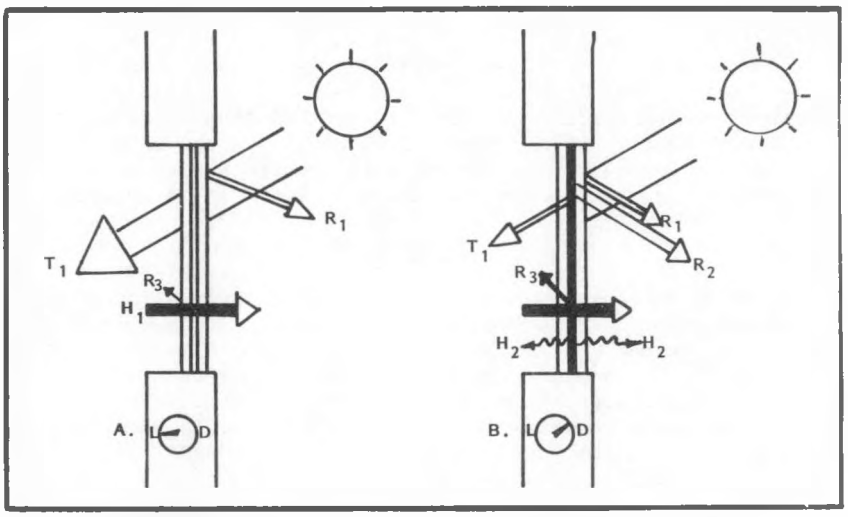

Fig. 1. Schematic representation of electrochromic window in (A) bleached and (B) partially darkened state, showing radiation and thermal flow: T_1, visible sunlight transmission; R_1, reflection from glass; R_2, visible light reflection from tungsten bronze; R_3, heat (infrared) reflection from bronze; H_1, combined convective heat loss through glass; H_2, heat flow due to heating in colored window.

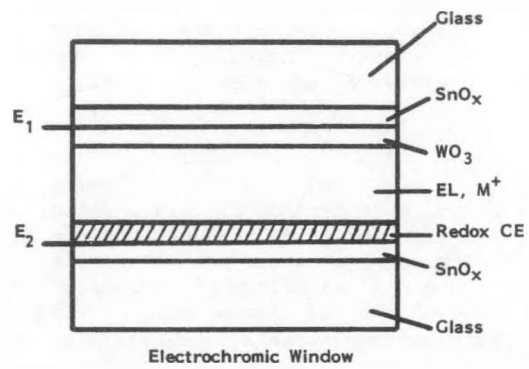

Fig. 2. Cross section of an electrochromic window (not to scale). E_1, E_2 are electrodes addressing the conductive SnO_x layers. The electrochromic layer WO_3 is colored when reduced in the presence of M^+ from the electrolyte (EL) to form M_xWO_3. The circuit is completed by oxidation of the counter electrode (CE) species, which must be colorless in the reduced form.

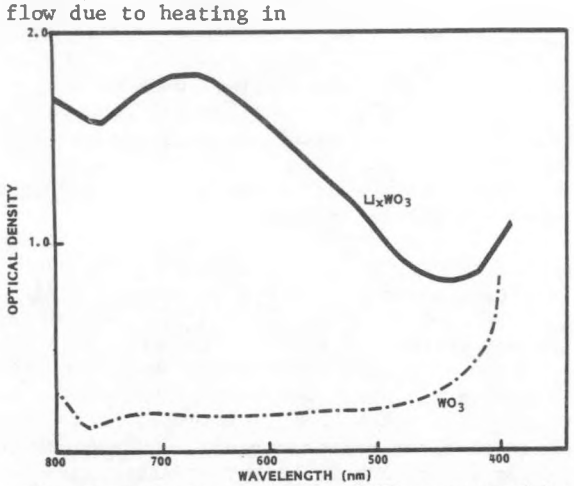

Fig. 3. Absorption spectrum of WO_3 prepared by rf sputtering onto glass coated with conductive In, SnO_x. Dashed line, as deposited (1.4 μm thick); solid line, after electrochemical introduction of 86.5 mCoulombs/cm^2 of Li from 1M $LiClO_4$ in propylene carbonate.

THE PRUSSIAN BLUE WINDOW

Prussian blue (PB) may be readily immobilized on transparent conductive oxide electrodes to form a three-state electrochromic system (3). Although it is not reflective on coloration, it does provide an easily prepared system for demonstrating window structures and evaluating electrolytes.

Immobilized Prussian blue is prepared by electrochemical reduction of $FeCl_3$ and $K_3Fe(CN)_6$ from an aqueous solution onto the desired substrate. The mixed-valence compound undergoes the following series or redox reactions:

$$\underset{PB^+}{Fe_4^{III}[Fe^{III}(CN)_6]_3} \xrightarrow{+3e^-} \underset{PB}{Fe_4^{III}[Fe^{II}(CN)_6]_3} \xrightarrow{+4e^-} \underset{PB^-}{Fe_4^{II}[Fe^{III}(CN)_6]_3}$$

(very light green) (dark blue) (colorless)

Hence, two transparent electrodes initially prepared with equal amounts of PB can be combined into an electrochromic window with two states - a colored form (PB|electrolyte|PB) and a bleached form (PB^+|electrolyte|PB^-). In our laboratory, single electrodes could be reduced and oxidized reversibly for many cycles in an aqueous electrolyte, under either current or voltage control. Electrodes of 4 cm^2 area could be completely colored ($OD_{720\ nm} \approx 1$) or bleached in 1-2 sec.

Window structures were prepared from these PB electrodes employing a geometry like Fig. 2. The two electrodes were separated by a water permeable cellophane laminate (Acroshield, Gelman Sciences Inc.) which provided an optically clear path. The separator was swelled with aqueous KCl electrolyte. These structures were cycled under constant current. In Fig. 4, the OD at 750 nm is followed as a function of injected charge in one of these structures at 40 $\mu A/cm^2$, first through a bleached cycle, and then for a coloring cycle.

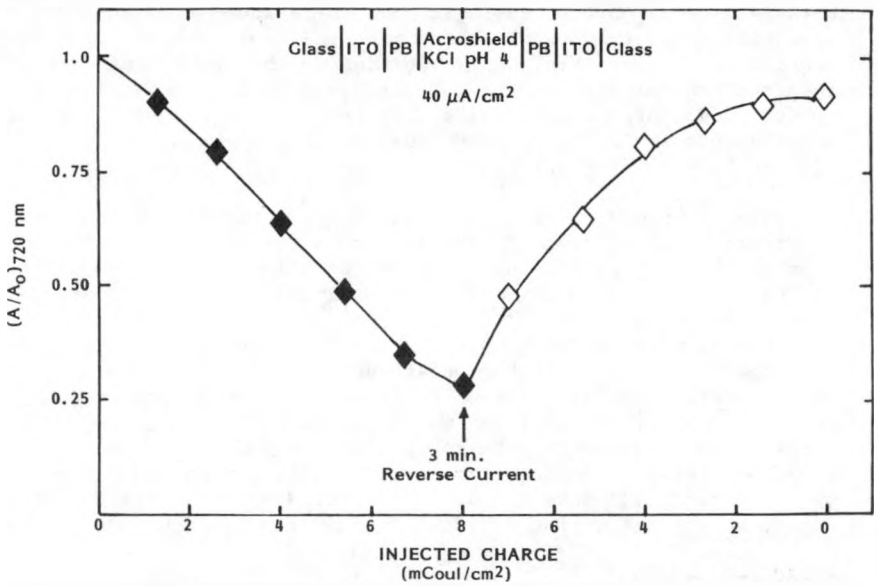

Fig. 4. Change in optical density vs. total injected charge for an electrochromic window based on Prussian blue. One complete cycle is shown, under constant current. Total device area = 3 cm^2.

CONCLUSIONS

Initial experiments on electrochromic window structures have demonstrated the feasibility of an electrically driven electrochromic "light" valve with a semisolid electrolyte. Replacement of one of the PB electrodes with sputtered, crystallized WO_3 will permit a reflective colored state to be achieved. Counter electrode reactions other than PB/PB^+ will also be considered, since PB^+ is a light green and not truly colorless. Possibilities include IrO_2/Ir_2O_3, viologens, and I_3^-/I^-. Furthermore, removal of the aqueous phase of the electrolyte is desirable, either by going to an ion-conducting polymer such as polyethylene oxide, or by using thin film crystalline or glassy inorganic ion conductors such as sputtered Na-beta alumina.

REFERENCES

1. I. F. Chang, "Electrochromic and Electrochemichromic Materials and Phenomena," in Nonemissive Electrooptic Displays, A. R. Kinetz and F. K. von Willisen, eds. (New York: Plenum Press, 1976).

2. O. F. Schirmer, V. Wittwer, G. Baur and G. Branett, "Dependence of WO_3 Electrochromic Absorption on Crystallinity," J. Electrochem. Soc., 124, 749 (1977).

3. K. Itaya, H. Akahoshi and S. Toshima, "Electrochemistry of Prussian Blue Modified Electrodes: An Electrochemical Preparation Method," J. Electrochem. Soc., 129, 1498 (1982).

PROJECT SUMMARY

Project Title:	Optics and Materials Research Applied to Controlled Radiant Energy Transfer Through Building Envelopes
Principal Investigator:	Professor Ronald B. Goldner
Organization:	Department of Electrical Engineering Tufts University Medford, Massachusetts 02155
Project Objectives:	To identify the fundamental optical and materials problems associated with, and determine the feasibility of, designing and fabricating envelopes with switchable optical properties.
Project Status:	The project started 8 August 1982. The general study has been initiated. We are searching for and studying classes of materials and materials systems which appear to be potentially useful for switchable glazings. We are attempting to determine the associated critical materials research problems that need to be addressed. As part of this global investigation, attempts are being made to identify basic principles and fundamental constraints. Currently, we are working on the problem of transforming the required transmissivity/reflectivity properties into requirements on the effective optical constants of materials. This approach fits naturally with the optical measurements and analysis techniques which we have developed, are presently using, and are further developing. The specific study, aimed at identifying and characterizing the most promising candidate materials and structures for solid-state electrochromic cells, has also been initiated. Electrochromic tungsten trioxide films have been vacuum deposited by thermal evaporation. Several optical and charge transport measurement techniques are being used and further developed as precision diagnostic tools, and comparisons with existing models are being made. A similar approach will be taken for other materials with the objective of evaluating asymmetric structures. One such structure which we intend to investigate is a complementary electrochromic cell composed of one material which colors anodically, and one which colors cathodically, analogous to a semiconducting p-n junction. Another such structure would be similar to a Schottky barrier cell, whereby only one electrochromic material would be used, and only one of the electrodes would be electron injecting. In all cases, we are attempting to identify fundamental mechanisms and constraints.
Contract Number:	DE-AC02-82CE30753
Contract Period:	8 August 1982 - 7 August 1983
Funding Level:	$95,000
Funding Source:	U.S. Department of Energy

OPTICS AND MATERIALS RESEARCH APPLIED TO CONTROLLED RADIANT ENERGY TRANSFER THROUGH BUILDING ENVELOPES

Ronald B. Goldner

Department of Electrical Engineering
Tufts University
Medford, Massachusetts 02155

ABSTRACT

A dual set of basic optics and materials research studies is under investigation. The studies are focused on the problem of having buildings significantly increase the economical use of available solar energy to meet most of the energy needs for control of the building climate. One means by which this may be accomplished is through the use of controlled radiant energy transfer (CRET) through the entire building envelope. One set of research studies is a general, but basic, theoretical study. Its purpose is to identify the fundamental optical and materials science principles associated with choosing and synthesizing such envelopes. The other set of studies is focused, experimentally and theoretically, on identifying and solving the basic optical and materials design problems associated with a specific approach for achieving the CRET envelopes: the use of solid-state electrochromic (EC) cells. In this specific study the basic materials research and design problems are being identified and evaluated by fabricating and characterizing prototype EC cells. The cells are of the type recently or currently being investigated for display devices purposes, using known and/or new materials and techniques. Such cells serve also as proof of concept and as test cells for providing valuable feedback information for the general study and for other systems studies.

PROJECT SUMMARY

Project Title:	Thermal Properties of Soils and Soils Tests
Principal Investigator:	Surendra K. Saxena
Organization:	EarthTech Research Corporation 6655 Amberton Drive Baltimore, Maryland 21227
Project Goals:	To develop and test a methodology and appropriate instrumentation for obtaining data related to the thermal conductivity of various soils at various levels of moisture content for use by designers interested in real-world application of earth contact concepts.
Project Status:	The program began with a state-of-the-art review indicating that numerous laboratory studies in soil thermal properties, in both saturated and dry soils had been conducted. However, the literature revealed that no large-scale field tests had been conducted, nor had laboratory tests on unsaturated soils with a variety of moisture content been conducted. Therefore, it was decided to conduct comparisons of laboratory data to large-scale tests in the field. Instrumentation was developed to measure thermal conductivity and moisture content in-situ; however, the first generation of equipment had problems, including soil stratification over the measurement length, air voids adjacent to the heater wall, absence of guard heaters allowing vertical heat flux, and emplacement of heat measurement probes at too great a distance from the heater. This experience lead to the development of a second generation system described in this paper which overcomes these problems. Field testing of the equipment is currently underway.
Contract Number:	DE-AC03-80SF11509
Contract Period:	September 30, 1980 through December 30, 1982
Funding Level:	$254,000
Funding Source:	U.S. Department of Energy, San Francisco Operations Office

IN-SITU MEASUREMENT OF SOIL THERMAL CONDUCTIVITY AND SOIL MOISTURE MOVEMENT

Jeffrey A. Bloom Muriel J. Waller
EarthTech Research Corporation
6655 Amberton Drive
Baltimore, Maryland 21227

ABSTRACT

Instrumentation procedures and analysis techniques have been developed for the measurement of soil thermal conductivity and soil moisture migration adjacent to earth-sheltered structures and buried heat exchangers. The equipment will be used for developing data for use by designers of earth contact concepts. The instrumentation can be utilized with a minimal disturbance to the existing site. The instruments have been laboratory tested prior to field installation in order to assess performance and develop operational techniques.

INTRODUCTION

Developing a methodology for obtaining data on the thermal conductivity of soils in-situ is an important element in the design of earth-sheltered structures, thermal storage systems, underground heat exchangers and underground nuclear waste storage facilities. Previously, soil thermal conductivity measurement had been limited to controlled laboratory testing of soil samples. While adequate for measurements required to model dwellings, data from in-situ soils, which are subject to moisture level changes and seasonal variations, was not available. Previously designed laboratory instruments were not suitable for the heat flux levels required to simulate buried heat exchangers. This contract has developed specialized instrumentation that can measure the thermal conductivity at representative construction sites. This allows site specific seasonal variations and moisture content changes to be assessed. In addition to the measurement of thermal conductivity the equipment measures moisture content and monitors its changes due to heat flux. Heat can drive out moisture and thus affect the thermal conductivity since moisture content has a strong effect on thermal conductivity.

MEASUREMENT METHODOLOGY

Thermal conductivity of the soil is measured utilizing a vertical thermal needle placed in the soil which heats the surrounding soil. The ability of the soil to remove heat from the heater surface as well as the radial temperature change with time are measured by the system and used to calculate thermal conductivity. Time-domain reflectometry (TDR) is used to measure the moisture content of the soil surrounding the needle to determine if changes in moisture content and moisture migration occur as a result of the heat. Soil moisture content is an important parameter affecting thermal conductivity and must be quantified if meaningful data is to be obtained.

The field test set-up is shown in Figure 1. The set-up consists of a central thermal needle soil heater, 6 soil temperature monitor (STM) probes, and 6 TDR probes. The STM and TDR probes are situated at three radial distances from the heater; i.e., two probes of each type at each radius. The positions of the probes are arranged along four radial lines 90° apart as shown. This provides a check of the data in two directions to assure that the heat flows uniformly in all radial directions as is assumed. It also provides redundant data for quality control purposes.

The soil heater needle has three heater elements. The top and bottom elements are called guard heaters and are designed to keep the heat flux from the center or test heater from flowing in the vertical or "Z" direction. The temperature of the guard heaters must be maintained at the same temperature as the test heater or else heat can flow in the "Z" direction.

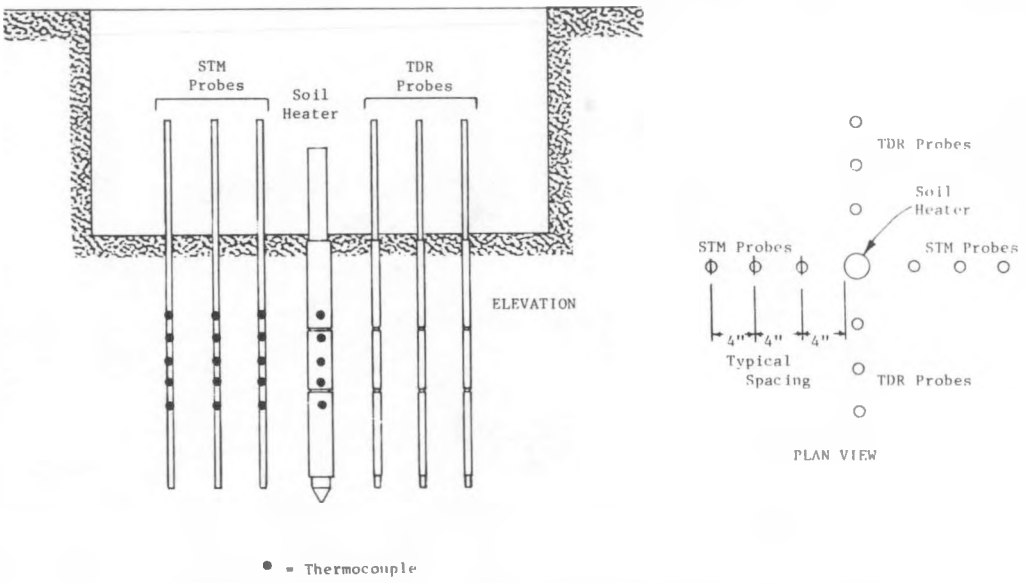

Figure 1. Field test set-up plan and profile view of the central thermal needle soil heater, STM probes and TDR probes

Two types of tests were conducted to determine thermal conductivity (K), constant power and constant temperature. The two methods are described as follows:

1) Constant power - in this test constant power is maintained in the test heater and power in the guard heaters is varied to maintain the same temperature in all three heater elements. The thermal conductivity (K) is found utilizing the work of Carslaw and Jaegar[1] and Woodside and Messmer[2]. They assumed an infinite mass of soil and a perfect line source. This system should approach these assumed conditions.

   From this work it is determined that the governing equation for thermal conductivity is:

$$K = \frac{Q}{4\pi\Delta\theta} \ln\left(\frac{t_2}{t_1}\right)$$

   Where Q = Power input per unit length of source, cal/cm. sec.

   K = Thermal conductivity of material, cal/cm. sec. ^{o}C

   $\Delta\theta$ = Temperature change of test heater between t_2 and t, ^{o}C

   t = Time from start of heating, sec.

   The constant power method essentially measures the soil's ability to carry off heat with time and does not require use of the soil temperature monitor probes. During constant power tests, only the power in the test heater is held constant and the power to the guard heaters is varied to maintain the same temperature in all three heaters.

2) Constant temperature - the constant temperature method essentially measures conductivity by observing the rise in temperature with time and distance from the source. The STMs are used to measure this heat flux while the thermal needle is held at a constant surface temperature. The soils to be tested are considered isotropic and homogeneous. The heat transfer is considered to be symmetric about the heater. The equation of heat transfer, assuming no vertical heat flux, is:

$$\frac{\partial\theta}{\partial t} = \alpha \left(\frac{\partial^2\theta}{\partial r^2} + \frac{1}{r}\frac{\partial\theta}{\partial r}\right)$$

Where α = Thermal diffusivity of material, cm^2/sec.

r = Radial distance of measurement point from heat source, cm.

Thermal conductivity (K) can be calculated by using thermal diffusivity (α), the specific heat of dry soil (C_{md}) and the moisture content of soil by dry weight (w).

INSTRUMENTATION

The soil heater is a vertical thermal needle type of device. A portion of the device is shown in Figure 2. The size of the heater has been kept short in order to eliminate the affects of soil stratification and moisture variations. The soil heater has a two-foot long heated section consisting of three heater elements. The center or test heater element is nominally 6 inches long. Above and below this heater are guard heater elements which are nominally 9 inches in length. The ratio of guard heater length to test heater length was designed to eliminate any vertical heat flow.

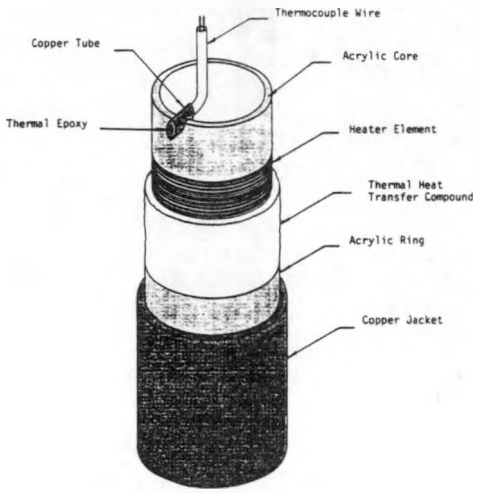

Figure 2. Portion of soil heater element showing construction

The outside diameter of the soil heater is only 2 1/8 inches, in order to closely approximate a line source. The heater is constructed with a core made of 1 3/4 inch OD x 1/4 inch wall acrylic plastic tube which is 33 inches in length (9 inches extends above the ground). Four small rings made of 2 inch OD x 1/8 inch wall acrylic tube are located along the core to act as heater element separators. These rings are cemented to the core. The heater elements are made by winding a pair of 24 gauge lacquered copper wires around the core in two layers. This results in a resistance of 9.1 ohms for each of the guard heater elements and 5.2 ohms for the test heater element. Each heater element is jacketed using 2 inch copper tubing (which has an outer diamter of 2 1/8 inches). The copper tubing serves as a heat transfer surface and also forms a strong outer jacket to allow the heater to be pushed into the soil without damaging the heater wires or thermocouples. The space between the heater wires and the copper tubing is filled with a thermal heat transfer compound as used between semiconductors and heat sinks. Each heater section has a separate copper jacket which does not touch the adjacent jacket.

The heater connection wires (16 gauge copper) are fed through holes in the core and up the core center. The thermocouples attach to the copper jackets through 1/4 inch OD copper tubing which runs through holes in the core. Thus the thermocouples are actually located inside the core and thermally connected using the copper tubes. Five thermocouples read outer jacket temperature as shown in Figure 3. One additional thermocouple is placed inside the core to monitor heat flow from the core.

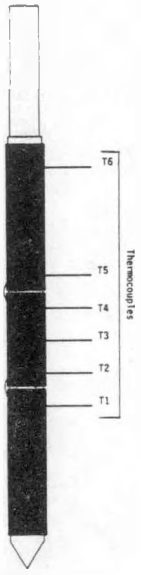

Figure 3. Central thermal needle soil heater with thermocouples T1-T6

The soil temperature monitor probes are also vertical needles shown in Figure 4. The core consists of a 1/2 inch diameter wood rod. The upper 12 inches of the 36 inch rod projects above the ground. Five thermocouples are attached to the outside of the rod at vertical positions that correspond with the heater thermocouples. The entire assembly is covered with a jacket made of polyolefin heat shrink tubing for protection.

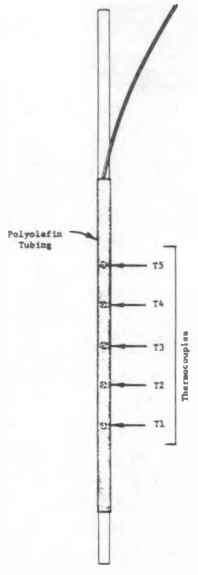

Figure 4. Soil temperature monitor probe with thermocouple locations

The TDR probes shown in Figure 5 have a 1/2 inch diameter wooden center core, 36 inches in length. The diameter of the probes was kept small in order to prevent heat flow disruption found in an earlier prototype design. Three 1/2 inch nominal copper pipe sleeves are attached to each core with lengths and positions that correspond to the copper heater sleeves. The copper sleeves are electrically connected by a small piece of buss wire as is also done on the copper heater jackets. These discontinuities provide a means for identifying positions on the TDR output trace. Moisture measurements are made by holding a wedge-shaped connector (Figure 6) between the TDR probes (the heater is also a TDR probe) and measuring reflection time which is a function of soil dielectric constant. Soil dielectric constant is in turn directly proportional to moisture contents with very little variation for soil type, as shown by Topp, et. al.[3]

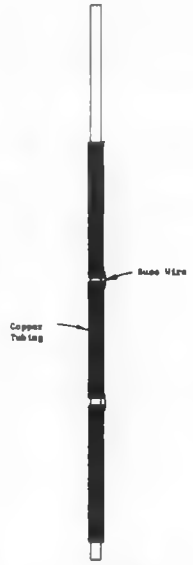

Figure 5. Time-domain reflectometry probe

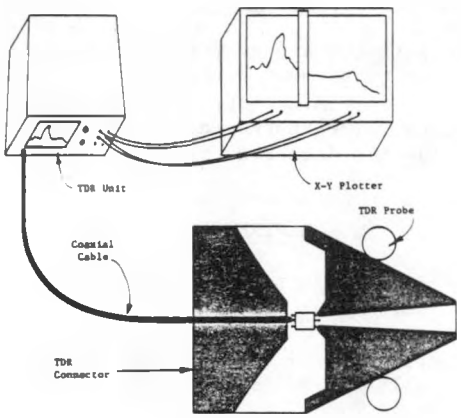

Figure 6. TDR connector for quick coupling to probes

FIELD TESTING

Prior to emplacing the soil heater and temperature monitor probes in the ground, a 2-foot deep (or deeper) trench is dug. This trench enables the hardware to be placed below the top soil insuring a more homogeneous soil consistency for the tests. The devices are emplaced by coring holes which are slightly smaller in diameter and then pushing the devices into these holes. Standard steel pipe in 3/8 inch and 1 1/2 inch nominal sizes are used for the coring tubes. This method of emplacing the heater and temperature monitoring probes insures a snug fit without voids and without disturbing the native soil.

The following additional equipment is used to run the field tests:

- Power Unit: The power unit is composed of three AC variacs, each one in parallel with a temperature controller to supply power for the top, middle and bottom heaters. The AC variacs are capable of applying voltage inputs within the range of 0 to 120 volts. The temperature controller can hold a constant temperature with a resolution of $\pm 5^{\circ}$ C.

- Data Reading Equipment: The temperatures and voltage inputs are read by a Monitor Laboratory 9300 Data Logger, with a capacity to read up to a total of 80 channels. Forty of these channels are suitable for temperature reading.

- Moisture Migration Monitoring Equipment: A Tektronix 1502 TDR unit is used to measure the velocity of an electromagnetic wave propagating along a pair of parallel transmission lines. This rate of propagation or velocity is directly proportional to the dielectric constant of the material located between the transmission lines, which in the case of soil is strongly dependent on the soil water content. The dielectric constant for dry soils is on the order of 4 to 9 depending on the type of soil. Water on the other hand, has a dielectric constant of 80. Therefore, a significant contrast from dry to wet can be easily observed and quantification of bulk moisture content accomplished. The output from the TDR is a two-dimensional trace which is analyzed to determine signal propagation time along the known length of the parallel transmission line. This trace is recorded on an X-Y plotter for later analysis.

The tests were started by monitoring the initial condition of the soil at the outset. This portion of the test, which will last about 48-72 hours, reads the soil temperature before the application of any heat.

Simultaneously, TDR tests are performed for monitoring the dielectric constant of soil in-situ, thereby determining the initial moisture content of the soil. The first heater tests are short-term constant voltage and last about 45 minutes. Moisture migration is assumed very small in this test, however, it is monitored to verify this assumption. Following this test a series of long-term constant temperature tests are run at various temperatures while also monitoring moisture movement.

CONCLUSION

The second generation of in-situ soil termal conductivity and moisture content instrumentation appears to overcome the problems found in the original prototype. The equipment has been found to be rugged and easily field installed. Initial laboratory evaluations indicate a sensitivity to variations in soil thermal properties and moisture contents. The instruments described here are currently being field tested and will be valuable tools in developing the data required by designers of earth contact devices and structures.

REFERENCES

1. H. S. Carslaw and H. C. Jaeger, "Conductivity of Heat in Solids", Clarendon Press, Oxford, England, 1959 , 2nd Ed.

2. W. Woodside and J. H. Messmer, "Thermal Conductivity of Porous Media, I., Unconsolidated Sands", Journal of Applied Physics, Vol. 32, No. 9, September, 1961.

3. Topp, G. C., Davis, J. L., and Annan, A. P., "Electromagnetic Determination of Soil Water Content: Measurement in Coaxial Transmission Lines", Water Resources Research, Vol. 16, No. 3, June, 1980.

PROJECT SUMMARY

Project Title:	Preferred Practices Instrumentation Guidelines Manual for Solar Passive Test Facilities R&D
Principal Investigator:	W. B. Ingle/ A. J. Darnell
Organization:	Rockwell International Energy Technology Engineering Center Canoga Park, California 91304
Project Goals:	To promote uniformity in the procurement, calibration, and installation of instrumentation used in monitoring the performance of passive solar installations. In FY 1982, this will include studies on three of the eleven instrumentation areas, i.e., heat flux sensors, mean radiant temperature, and relative humidity.
Project Status:	A literature search has been conducted to collect the published literature on the underlying theory, calibration, and use of heat flux sensors, mean radiant flux thermometers, and relative humidity-measuring devices. Heat flux sensors have been procured from two suppliers and subsequently calibrated by a commercial testing laboratory to verify the manufacturers' calibration. Methods are being investigated to stabilize or "age" Styrofoam board materials currently being used as thermal conductivity standards for testing of insulation materials. A guarded hot box apparatus was constructed for the testing of heat flux sensors. This will be used in conjunction with calibrated insulation "beadboard" to simulate conditions existing in the field during the course of thermal performance evaluation of passive solar buildings. A manual is being prepared which gives recommended practices to be used in the calibration, installation, use, and maintenance of heat flux sensors.
Contract Number:	DE-AM03-76-SF00700
Contract Period:	FY 1982
Funding Level:	$120,000
Funding Source:	U.S. Department of Energy

INSTRUMENTATION GUIDELINES MANUAL FOR PASSIVE SOLAR TEST FACILITIES: HEAT FLUX SENSORS

A. J. Darnell, W. B. Ingle, and L. R. McCoy
Rockwell International
Energy Technology Engineering Center
Canoga Park, California 91304

ABSTRACT

The published literature has been searched concerning the theory, construction, calibration, and use of heat flux sensors. These data were examined in respect to their use in the measurement of heat flux for the evaluation of passive solar structures. Six heat flux sensors were purchased and subsequently calibrated by an independent testing laboratory. The results showed significant differences in sensitivity (10-30%) from the manufacturers' data. A method has been designed for the "aging" and stabilization of polystyrene beadboard, commonly used for insulation calibration standards. A guarded hot box apparatus was constructed to study the factors affecting the mounting and use of heat flux sensors.

INTRODUCTION

Characterization and evaluation of passive solar installations involves the measurement of the heat transport through components of the structure, i.e., walls, ceilings, floors. This is done with heat flow sensors placed at selected locations in the structure. However, measurement of this parameter is not an easy task. The purpose of this work is to promote uniformity in the procurement, installation, and calibration of heat flux sensors used in passive solar applications in order to improve the quality and uniformity of heat flux measurements. Highlights of the features discussed in preparation of the Instrumentation Manual for Heat Flux Sensors are discussed.

THEORY AND CONSTRUCTION OF HEAT FLUX SENSORS

The heat flux sensor is based upon the principle that heat flux may be determined from the temperature difference across a layer of material of known thermal resistance. The heat flux sensor typically consists of a thin plate in order to minimize edge effects and to minimize the effect of thermal mass of the heat flux sensor upon the measurement. The plate is usually made of a highly conducting material such as aluminum, glass-phenolic, paper-phenolic, or polyamide-glass. The combination of these factors, i.e., thinness and high thermal conductivity, produces a small temperature differential across the gauge. This temperature difference is measured by multi-junction thermopiles having alternate junctions on each side of the plate. The thermopile materials are typically copper-constantan or silver-constantan. The output signal is increased by use of multiple thermocouple junctions in each sensor (sometimes up to a hundred or more). When placed in a system perpendicular to the heat flow, the temperature gradient across the sensor plate generates a signal which is directly proportional to the heat flux through the sensor. Typical output of several of the currently (1982) available commercial units is of the order of 0.1-1 millivolt per Btu/ft^2-hr heat flux through the sensor.

CURRENT STATE OF THE ART IN HEAT FLOW MEASUREMENT

Although the heat flux sensor is a relatively simple device, its calibration, installation, use, and interpretation of results can be a difficult task. Principal sources of potential error include the following:

1) Features inherent in the construction of the sensor

2) Calibration procedures

3) Location and mounting the sensor to the substrate

4) Distortions in the heat flow induced by presence of the sensor

5) Effects of the surrounding environment such as air currents, radiation/emission, thermal conductivity of the substrate

6) Nonsteady-state conditions at time of measurement

7) Instrumentation errors.

Inherent errors due to construction of the heat flux sensor are minimized if the sensor is made as thin as possible and its thermal conductivity is as great as possible. Practical considerations of physical size and sensitivity of the thermopile elements place limits on its construction. The sensor should be made as

homogeneous and simple as practical to enhance a uniform thermal conductivity over its surface. In current practice, many of the commercially available sensors are constructed from materials with high thermal conductivity of dimensions approximately 1 to 2 mm thick and from 25 to 150 mm width and length.

Many procedures have been proposed in the literature for calibration of heat flux sensors (references 1 and 2). These include comparative methods in which the same heat flux is passed through a standard or reference sensor and the sensor being calibrated. More elaborate devices include use of guarded test plates utilizing two constant-temperature liquid baths or the use of thermostated enclosures.

For optimum results, the sensor should be calibrated at a heat flux comparable to or in the range of the flux to be measured in actual practice. Heat flow is generally quite low for passive solar applications, on the order of 2-10 W/m^2. Calibration of the sensor should be made at temperatures within the range usually encountered in passive solar applications, i.e., between 30 and 120°F. Calibration should be made in both directions through the sensor since, in many passive solar applications, bidirectional heat flow measurements are made.

For practical and economic reasons, heat flow sensors are of relatively small dimensions (i.e., 2 in. by 2 in.) compared to the dimensions of the substrate surface, i.e., wall, floor, ceiling, which is being measured in passive solar applications. The heat flux sensor should be located at a position representative of the entire surface. A temperature sensor should be located in close proximity to the heat flux sensor. Exposure to drafts, and from direct sources of radiation, should be minimized. If, during data reduction, an attempt will be made to separate out the convective and radiative effects (based upon other measurements), the location of the heat flux sensor should take this into account. Placement of the sensor directly over beams, girders, and water pipes will give distorted values of the heat flux for the representative sample.

It is important that the heat flux sensor be installed in a manner to present minimal disturbance of the convective air flow in the boundary layer adjacent to the substrate surface (references 3 and 4). The sensor should preferably be flush-mounted onto the substrate surface. If this is not possible, then the areas around the edges of the sensor should be tapered or flared to minimize disturbance of convective air flow over the substrate. The blending material should match the heat transfer characteristics of the mounting surface to the maximum extent practical, such as using dry wall joint compound, spackle, or plastic wood, unless the mounting surface has a high heat transfer coefficient, such as metal wall.

The heat flux gauge should be oriented so that the electrical leads present minimal disturbance of the convective air flows. For example, on vertical surfaces, the gauge should be oriented so that the electrical leads are on the side (horizontally), rather than the bottom or top. If the leads are buried or blended into the wall surface, the above precautions are not necessary.

If the surface on which the gauge is to be mounted is reasonably flat and smooth, no surface treatment is required. On new construction, the surface should not be textured or painted before installing the gauges. If the surface is textured or uneven, the location where the gauge is to be installed should be sanded smooth and flat to provide good contact with the surface. If the surface is hard, such as concrete, fill voids with dry wall joint compound or heat transfer paste.

A thin film of heat transfer compound which is free of air bubbles should be applied between the heat flux gauge and the surface to which it is mounted; installation of the sensor should be done using sufficient pressure to remove air bubbles. Omegatherm 201 (Omega Engineering, Box 4047, Stamford, Connecticut 06907) or Dow Corning 342 Heat-Transfer Compound (Dow Corning Corporation, Midland, Michigan 48640) are the recommended heat transfer pastes because they resist hardening and are sufficiently "tacky" to hold heat flux gauges to the bottom of a horizontal surface if the corners are bonded. The mechanical attachment of the heat flux gauge should be accomplished by bonding the corners of the gauge to the mounting surface with either a small quantity of epoxy cement or quick-bonding cyanoacrylates.

The final surface finish should be the same for the heat flux gauge and blending material as for the remainder of the wall, which normally means painting to obtain the surface original infrared emissivity. However, there may be instances where the blending material and surface finish are the same, such as a mud, stucco, adobe, plaster, etc.

If the heat flux sensor has thermal properties different from the substrate upon which it is mounted, the sensor will interfere with the natural heat transfer and an error in measurement will occur. Portman (reference 5) has developed a model for use under steady-state conditions which derives a correction coefficient based upon two parameters: (1) the ratio of transducer thermal conductivity to substrate thermal conductivity and (2) the ratio of transducer thickness to transducer width.

Since the electrical output of the heat flux gauge is a few millivolts, at most, the electrical connection technique is critical to preventing the generation of erroneous data. All connections in the leadwire system should be soldered or bolted. The leadwire used should be a two-conductor, tinned, stranded, copper-twisted and shielded cable utilizing an aluminized Mylar shield with a tinned-copper shield drain wire. A suitable shielded, two-conductor cable of this type is Beldon 9501. If multi-pair cables are used,

each cable pair should have a separate shield and drain wire. The shields of these cables should be grounded at one point only and should be connected to the data acquisition system (DAS) in accordance with the DAS manufacturer's instructions. Depending on the design of the DAS, the shield may or may not be grounded at the DAS; if not, it should be grounded as near the heat flux gauge as practical. Since the impedance of the heat flux gauge is low and the impedance of the DAS is large, long-lead lengths do not present a measurement problem, provided the shielding and grounding practices are followed.

CALIBRATION RESULTS

Heat flux sensors were purchased from two sources (Hy-Cal Engineering, Santa Fe Springs, California, and International Thermal Instrument Company, Del Mar, California).

These heat sensors are approximately 2 in. by 2 in. in dimension; they are equipped with internal copper-constantan thermocouples. Three sensors from each of these sources were, in turn, calibrated by a commercial laboratory (Dynatech R/D Company, Cambridge, Massachusetts) using ASTM Procedure C177-76. Calibration was made at 50° and 100°F at two heat flux rates, 10 and 35 Btu/ft^2-hr. Sensor sensitivities at the two temperatures showed, on the average, about 2% higher value at 50°F; thus, the sensors are not very temperature-dependent. Average sensitivity at the 10-Btu/ft^2-hr rate was about 1.7% higher than at 35 Btu/ft^2-hr, thus indicating there was no substantial zero crossing.

The sensitivity of the sensors from this calibration were averaged and compared against the manufacturers' data. The sensitivities reported by Hy-Cal were 21, 26, and 30% higher than Dynatech's calibration data; the data supplied by ITI were 10, 14, and 15% higher. This indicates there are significant differences between the manufacturer's calibration data and the data reported by the testing laboratory. However, these sensors should, in turn, be calibrated by another laboratory to confirm these results.

GUARDED HOT BOX APPARATUS

A guarded hot box apparatus was constructed following the recommendations described in ASTM C-236-80. A drawing of this apparatus is shown in Figure 1. The structural walls of the apparatus are made of 2-in.-thick polystyrene "beadboard." The two components of compartments making up the hot box are shown in Figure 2. On the left, is the cold compartment which contains a refrigerated-coil heat exchanger and bucking heaters to maintain constant temperature below ambient. Thermocouples for measuring the air temperature and surface temperature of the substrate panel are provided. The guard box containing the metering box is shown on the right. The cold and hot compartments are separately thermostated and controlled to within 0.05°C. The two compartments are separated by the material to be tested for thermal conductivity. Thus, the temperature differential, specified emissivity, air flow, position, etc., represent a controlled environment which can be maintained in a constant or steady-state condition. This apparatus will be used to simulate measurement of thermal conductivities of materials using calibrated heat flux sensors. In this manner, the various factors affecting the mounting and use of heat flux sensors can be studied under controlled conditions.

INSULATION STANDARDS

Slabs of polystyrene "beadboard" insulation with a density of 1.58 lb/ft^3, 2 in. thick by 2 ft^2 were "aged" by heating in a drying oven at $130\text{-}140^{\circ}$F until constant weight was obtained. Four slabs were treated in this manner. Weight losses ranged from 0.46 to 0.52% of the original weight. Two of these slabs were then given two coats of vinyl latex paint and again brought to constant weight. Application of this coating raised the apparent or average density to 1.98 lb/ft^3. These slabs were placed in sealed polyethylene bags and shipped to a commercial laboratory for measurement of their thermal conductivity. The specimens were tested in accordance with ASTM C518-76. The apparent thermal conductivities of the uncoated slabs were 0.0357 and 0.0351 Wm^{-1} K^{-1}; for the coated slabs, it was 0.0358 and 0.0356 Wm^{-1} K^{-1}. Thus, the vinyl latex protective coating had no detectable effect upon the thermal conductivity of the polystyrene test slabs.

These slabs will be used in conjunction with the guarded hot box apparatus and calibrated heat flux sensors to evaluate the factors affecting installation and use of heat flux sensors.

CONCLUSION

Heat flux sensors are in theory and construction relatively simple; however, there are many factors which can affect the results of the quantity they are attempting to measure. Calibration data supplied by the manufacturer has been shown to differ from 10 to 30% from values measured by an independent testing laboratory. An "aging" technique was developed to stabilize the thermal conductivity of polystyrene beadboard used as calibration standards. A protective coating against change in moisture content was also developed.

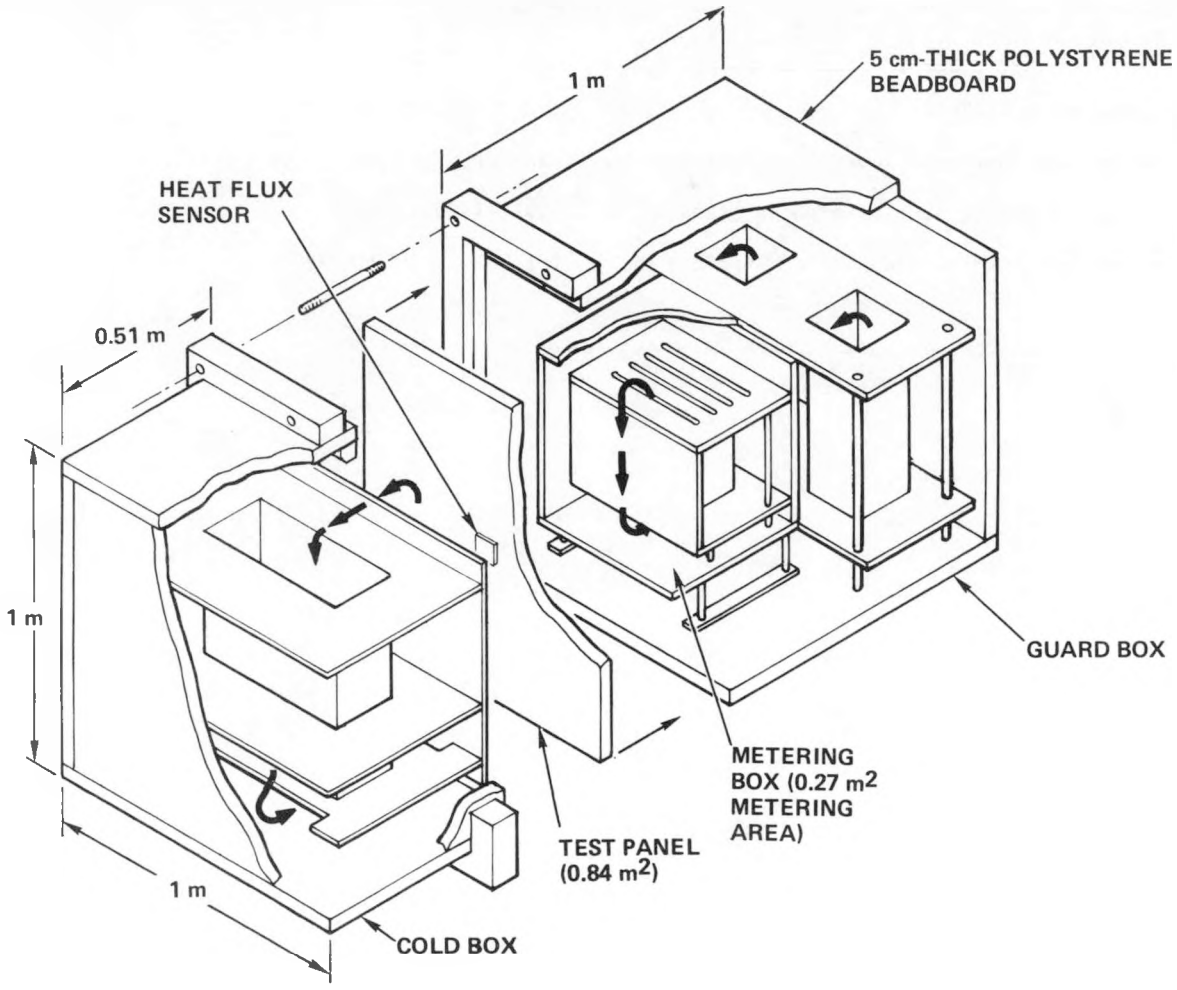

Figure 1. Guarded Hot Box Apparatus

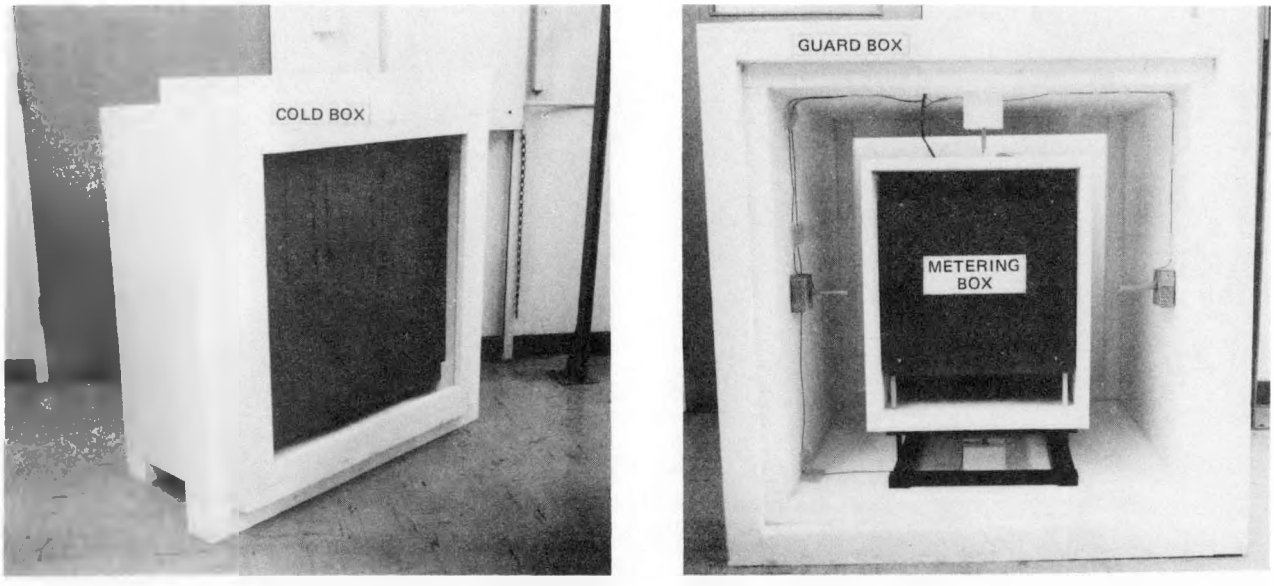

Figure 2. Separated View of Guarded Hot Box Apparatus

REFERENCES

1. C. F. Gilbo, Conductimeters, Their Construction and Use. ASTM Bulletin No. 212 (1956).

2. ASTM Procedure C177-76.

3. A. Bejan, International Journal of Heat and Mass Transfer, Vol. 24, p 1611 (1981).

4. Anderson and Bejan, Journal of Heat Transfer, Vol. 102 (1980).

5. D. J. Portman, Transactions of Geophysical Union, Vol. 39, p 1089 (1958).

PROJECT SUMMARY

Project Title:	A Modular Passive Solar Home
Organization:	Dynamic Homes, Inc. 525 Roosevelt Avenue Detroit Lakes, Minnesota 56501
Project Goals:	To design and market an affordable line of passive solar homes. To design, construct, and monitor a solar prototype.
Project Status:	Three passive solar models have been designed and are being marketed along with our present product line. A prototype home was built in our factory and set in Fargo, North Dakota. S.E.R.I. performed one-time measurements and then installed data acquisition equipment to provide Class B passive solar thermal performance monitoring. This monitoring continues at the present time.
Contract Number:	D2-FC02-80CS-30
Contract Period:	October 1, 1981 - October 1, 1982
Funding Level:	$15,000
Funding Source:	United States Department of Energy

A MODULAR PASSIVE SOLAR HOME

Dynamic Homes, Inc.
Modular Home Manufacturer
Detroit Lakes, Minnesota

ABSTRACT

Due to the dramatic rise of energy prices in the 1970's and the fact that Dynamic Homes' market is in the upper midwest, energy conservation has always been an important priority in the design and construction of their homes. Solar energy rose in popularity in the 1970's and seemed to be an ideal compliment to the already energy efficient Dynamic Home. All that was needed was a boost to get started. This paper describes the program that got Dynamic Homes started into marketing solar homes.

INTRODUCTION

In 1979 Dynamic Homes submitted a winning proposal in a Department of Energy passive and hybrid solar manufactured housing competition in the modular construction category. This provided an opportunity to participate in a cost sharing grant through the manufactured buildings program developed by the Department of Energy (D.O.E.) and the Solar Energy Research Institute (S.E.R.I.).

DESIGN DEVELOPMENT

Dynamic Homes hired the consultation of the architectural firm of Ritter, Suppes, Plautz, LTD, of Minneapolis, Minnesota. They developed a set of preliminary designs for various housing types (ramblers, split entries, split levels, and two-stories). The split entry designs seemed most feasible. They provided a good product at a price that could be marketable. It was decided to proceed with the split entry designs and three models were developed - two single-family and one duplex.

A prototype of the smaller single-family model (model SH-2SE36-A) was constructed in the factory and transported to and set on a site in Fargo, North Dakota. This split entry home contains 1810 square feet of living space on two levels. It is well insulated, with the roof at R-50, walls at R-21, and floor slab R-12. South exposures have double-glazed casement windows with movable insulation (R-5). Windows not facing South are triple-glazed. The home has a low infiltration rate due to the use of quality materials and careful construction techniques, including the use of a continuous polyethylene vapor barrier in exterior walls and ceiling, and extensive caulking. An insulated vestibule acts as an air lock entry between outdoors and indoors.

Coniferous trees to the North and West buffer against cold Northwesterly winds. Deciduous trees to the South shade in the Summer but allow the sun to penetrate in the Winter. Berms on the North and East reduce exposed wall area, thus reducing heat loss and infiltration. Natural ventilation occurs through the opening of lower level windows to let in air and opening upper level windows to exhaust warm air.

The garage and entry vestibule are located to the North and West to serve as protection against Winter winds. Living spaces are arranged such that the most frequently occupied spaces are on the South side and less occupied spaces to the North. The house is elongated on the East-West axis with major glass (collector) areas to the South.

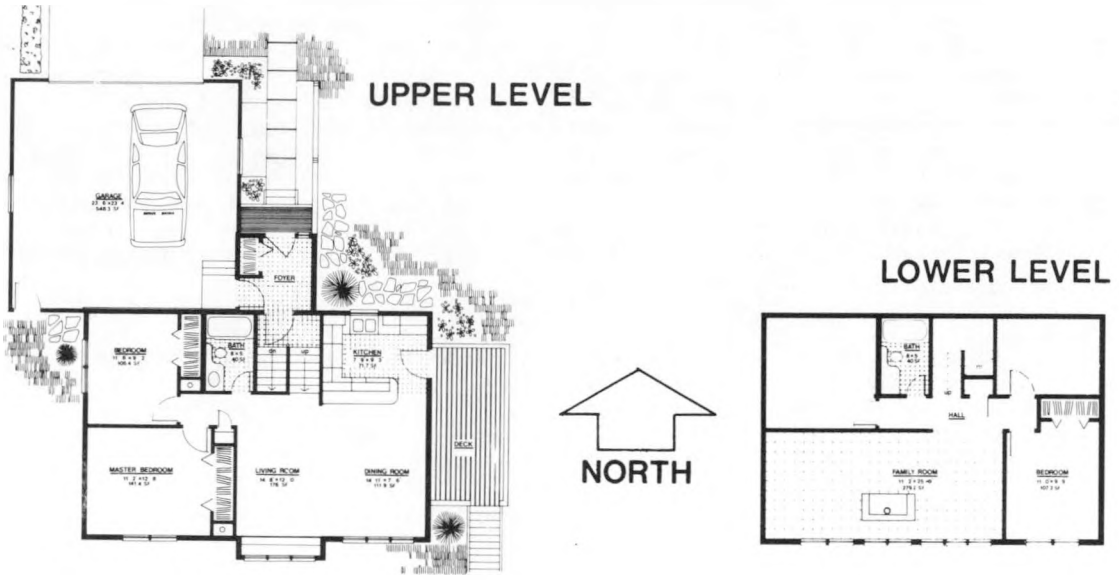

FIGURE 1. FLOOR PLANS (model SH-2SE36-A)

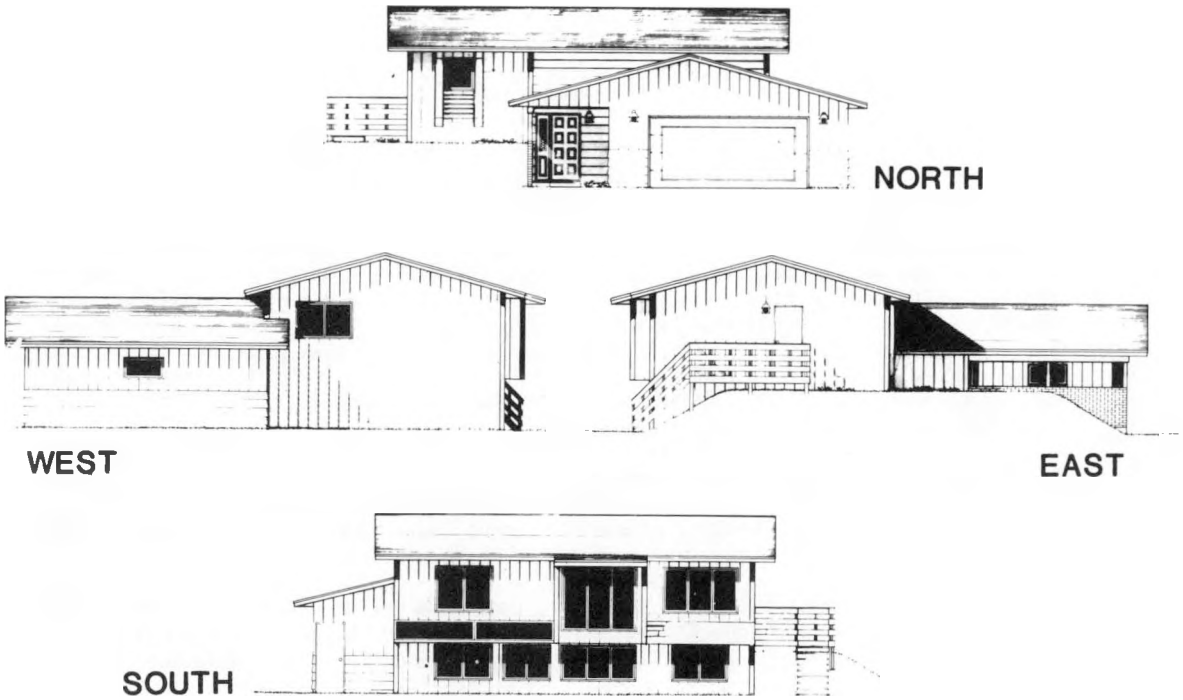

FIGURE 2. ELEVATIONS (model SH-2SE36-A)

The passive solar heating occurs in a direct gain fashion. The solar heat gained through the South facing windows is stored in phase change material in the shape of coffee cans. These cans are stacked behind a louvered wooded bench, the back of which is open to the sun. This bench is located in the living room. In the lower level the solar heat is stored in the masonry hearth of the wood burning stove and the floor slab of the family room. A two foot roof overhang helps shade the upper level windows from the Summer sun. The lower level windows are shaded by the two foot cantilever on the upper level and a shading trellis and optional solar d.h.w panels. A low energy paddle fan circulates air reducing statification. An air-to-air heat exchanger provides tempered fresh air intake. Electric baseboard provides required auxiliary heat. (forced-air heat is optional)

THERMAL PERFORMANCE/COST SAVINGS

After construction was completed on the solar prototype in January 1982, S.E.R.I. performed one-time measurements then installed data acquisition equipment which is currently providing Class B passive solar thermal performance monitoring. Items being monitored include: solar radiation, indoor and outdoor temperatures and auxiliary electric heating requirements.

S.E.R.I. is calculating daily and monthly functions such as solar, auxiliary and internal contributions to the total heating load of the house and measuring overall heat loss coefficients and air infiltration rates.

Using the residential energy simulator, S.E.R.I. estimated the building energy use of the solar prototype then compared that to the energy use of a home built to U.S. Housing and Urban Development Minimum Thermal Requirements (HUD/MTR) and also to a typical non-solar Dynamic Home.

S.E.R.I. predicted the solar prototype will conserve up to 36% of the auxiliary fuel use of Dynamic's present product line and 47% of the HUD/MTR building's auxiliary load.

Solar and energy conservation measures add about 6.5% to the cost of a home when compared to a standard Dynamic model.

MARKETING

Dynamic Homes, Inc. currently markets its homes through a builder/dealer network in seven upper-midwest states. The builders are supplied with product brochures and information, pricing, construction and marketing manuals, floor plan books, samples and various other marketing tools to enable them to sell the many Dynamic Homes designs and concepts. The 90+ floor plans are broken down into "collections" which typify the style of the homes: i.e., two and three-bedroom ramblers, two and three-bedroom split entries, two-story and split level designs. This enabled an easy addition of a solar collection of homes.

The greatest emphasis to Dynamic Homes customers thus far is in utilizing passive solar concepts - - what energy savings can be gained by (1) finding the right home site and orienting the home to the South, (2) triple-glazing the North, East, and West windows, proper garage placement, etc. We have found most people to be interested in those concepts and willing to implement them when possible.

The monitoring of the solar model in Fargo, North Dakota is still in process, and therefore we do not know the extent of energy savings. We have learned that the products used are not the quality that we had hoped for and will have to use others in the future.

We predict that our market will continue to be energy conscious. When energy cost savings can be shown to outweigh the added cost of passive solar hardware, our product will be readily accepted.

CONCLUSION

S.E.R.I., in their evaluation of the solar prototype came to several valuable conclusions: the house was slightly oversized for the existing thermal storage. This caused overheating in some rooms. The phase change material and movable insulation used were found to be expensive and relatively ineffective.

These comments will be evaluated and design modification and/or revised product selections may have to be implemented to remedy the situation.

The experience Dynamic Homes has received in this project has provided a valuable insight into solar energy and has allowed us to establish a passive solar product line. Principles learned here will help us to modify and add to our product line as the need arises.

REFERENCES

1. Robert deKieffer, Robert Taylor, Steven Brant, David Simms PASSIVE SOLAR MANUFACTURED BUILDINGS DEVELOPMENT AND ANALYSIS. TP-1643 Solar Energy Research Institute.

INITIAL PERFORMANCE OF THE MIT CRYSTAL PAVILION

by

Timothy E. Johnson
Brian Hubbell
Department of Architecture
Massachusetts Institute of Technology
Cambridge, Massachusetts

ABSTRACT

Many winter climates in the U.S. and Europe can be characterized as 'benign', where most of the days are cloudy, yet air temperatures rarely go below 6°C (42°F). The MIT Crystal Pavilion has been built to demonstrate 100% solar heating can be accomplished in these climates using the diffuse radiation that filters through the clouds. The vertical surfaces on the 46 m^2 (490 ft^2) addition to the MIT Solar Building No. 5 are glazed with double glass filled with argon and coated on one side with a transparent low emissivity layer that gives an overall average solar transmission of 63% and a nighttime U value of 1.24 $w/m^2°C$. The roof is double glazed with a low emissivity reflective glass and a laminated glass to reject summer solar gains. The floor is veneered with tiles filled with phase change material to store any beam energy that is available.

The building was completed for monitoring during February 1982. Initial measurements showed the building experiences a daily average lift of 10.3°C above ambient outdoor air temperatures during cloudy days. (Internal gains account for 4.1°C of this lift.) Summertime indoor air temperatures do not exceed ambient temperatures by more than 0.6°C on sunny days. The Pavilion thermal performance for the spring heating season is summarized.

1. INTRODUCTION

The Crystal Pavilion is the latest in a series of experimental solar buildings developed at the Massashusetts Institute of Technology. The Pavilion, which was funded by the U.S. Department of Energy and the MIT Cabot Fund and built by MIT architecture students, is an addition to the Solar 5 building on the MIT campus in Cambridge, Massachusetts. Although primarily constructed for experimental and demonstration purposes, both buildings are also used for architectural studios and lecture space.

The initial concept was to design a building which demonstrates the feasibility of passive space heating using diffuse sunlight directly gained through glass selective transmitters which also serve as windows. While not intended to be prototypical, the Pavilion demonstrates a system which can be used in overcast climates such as the Pacific northwest and northern Europe which are characterized by extended cloudy periods, yet experience 'benign' winter ambient air temperatures which rarely drop below 6°C. In addition, the building shows that significant solar heating can be accomplished in many building types without the necessity of a southern exposure as previously dictated by conventional solar designs. The specific design is intended to illustrate some of the architectural flexibility available through the use of these new materials.

2. BUILDING DESCRIPTION

The 46 m^2 (490 ft^2) building has 52 m^2 (563 ft^2) of vertical double-glazing which is attached to a steel super structure by a redwood batten system of thermal breaks (See Fig. 1). The vertical glazing units, provided by Airco-Temescal and Guardian Industries, are two 0.32 cm (1/8") lights of clear glass spaced 0.64 cm apart with a thin transparent coating of copper-tin-oxide (CTO) on the exterior side of the interior lite. The units also contain argon gas to minimize convective heat transfer between the lites. The glass edges are sealed with a standard polysulfide and metal edge spacer system

The low-emittance coating combined with the hermetically sealed argon filled space yield a measured nighttime U value of 1.24 $W/m^2°C$ (0.22 BTU/hr-°F) or nearly one third that of conventional double glazing while maintaining an average effective solar transmission of 63%. This means that on a typical cloudy day when 568 Wh/m^2 (180 BTU/ft^2-day) are incident on a vertical surface, 356 Wh/m^2 (113 BTU/ft^2-day) are gained for heating purposes while 20 $Wh/m^2°C$ (5.3 $BTU/ft^2°F$-day) are lost through the glass. Since most of the Pavilion is glazed, this small heating profit adds to a total which meets the daily conduction heat losses and building infiltration load whenever the outdoor air temperature exceeds 7°C (44°F) on a cloudy day (assuming normal internal gains for a residence are present). When outdoor air temperatures are colder the building draws additional heat from either the electrical auxiliary system or the phase change and masonry thermal storage elements which are charged on sunny days.

The 51 m^2 (540 ft^2) roof is also double glazed with a 0.48 cm (3/16") stainless steel coated reflective glass on the exterior and a 0.64 cm laminated glass on the interior. The stainless steel coating reflects 60% of the unwanted summer solar gain. The roof lights are separated by a 2.5 cm (1") air space which is seasonally vented to the outside to remove the remaining solar energy absorbed by the coating. The roof has an unusually low U value of 1.82 $w/m^2°C$ because the stainless steel is not heavily over-coated so the emissivity remains low at 30%.

In the winter (unventilated) mode the roof absorbs [redacted]% of the incident solar radiation which increases the roof temperature, and nearly eliminated daytime heat losses through the roof. In the summer, extensive natural air flow through the two roof top ventilators

Fig. 1. Southeast view of Crystal Pavilion and MIT Solar Building No. 5

and the east and west casements and doors provides enough cooling to maintain a peak interior air temperature only 1°C above the outdoor ambient temperature (assuming a 3 mph breeze).

Thermal storage is provided primarily by 25 m^2 (270 ft^2) of Glauber's salts within 51 cm x 51 cm (20" x 20") polymer concrete floor tiles furnished by the Architectural Research Corporation (Fig. 2). The tiles and salts are similar to those used in the ceiling of the MIT Solar No. 5 building. Two adjacent 1 cm (3/8") layers of Glauber's salts form the phase change core. This core is encapsulated with 0.64 cm (1/4") polymer concrete which also constitutes the finish surface. The tile stores 694 Wh/m^2 (220 Btu/ft^2) at a phase change temperature of 23°C (74°F). Additional sensible storage is provided by the masonry planters and seating seen in Figs. 2 & 3.

3. BUILDING HEAT LOSS

Roughly two-thirds of the Pavilion's floor area is .61 m (2 ft) below grade, and all exterior retaining walls are sheathed with 5 cm (2") of rigid Styrofoam^R SM type insulation (See Fig. 4). A perimeter tongue of this insulation also extends .61 m (2 ft) horizontally from the top of the wall footings to prevent edge heat losses. The concrete floor slab is also insulated with 2.5 cm (1") of Styrofoam^R. The combined heat loss coefficient of the slats and perimeter masonry walls is 14.5 W/°C (28 BTU/hr°F).

The air infiltration rate averages 3/4 or an air change /hr with a 2.2 m/s (5 mph) wind as determined by several experiments using sulfur hexaflouride as a tracer gas. The heat loss coefficient due to this infiltration is 29.5 W/°C (56 BTU/hr°F).

The heat loss coefficient for the reflective glass roof (including framing and opaque areas) is 78 W/°C (148 Btu/hr°F). The coefficient for the special windows and all other vertical surfaces is 65 W/°C (124 Btu/hr°F);these total a theoretical building heat loss coefficient of 187.8 W/°C (356 Btu/hr°F). This compares to a measured value of 175 W/°C (332 Btu/hr °F). The building heat loss rate was experimentally determined by measuring the ΔT sustained by internal gains from 820 Watts of lighting on a calm, February night after two cloudy days' operation had completely discharged the building's thermal storage.

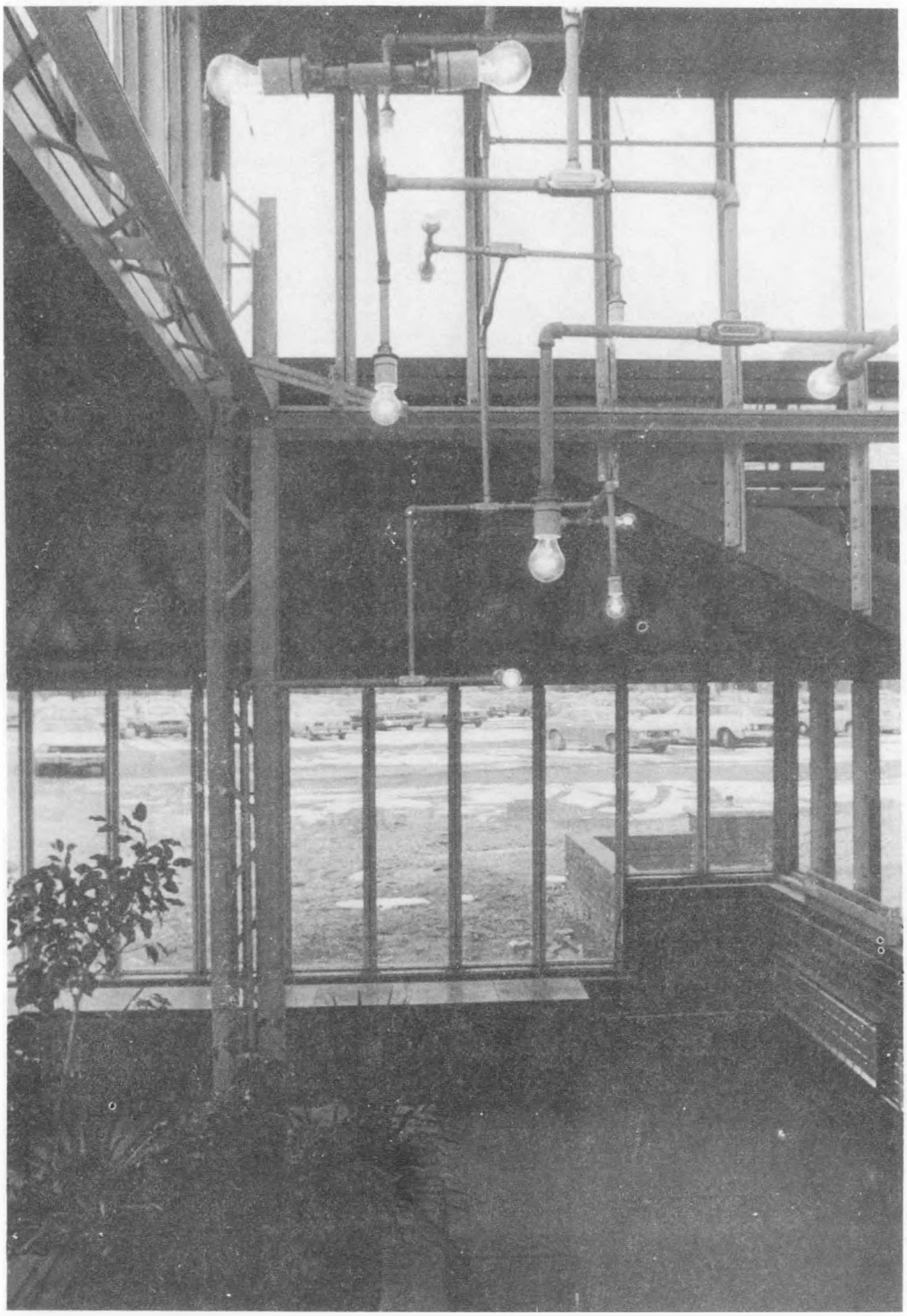

Fig. 2. Interior view of the Crystal Pavilion lower level looking towards south

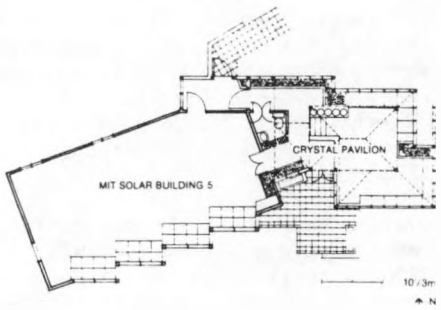

Fig. 3. Floor plan of Crystal Pavilion and Solar 5 Building

4. SPECIAL GLAZING PERFORMANCE

The U value for all glazing systems varies throughout the day as the wind and sun add or subtract energy. This variation in ordinary double glazed systems is not significant on cloudy days. However, this variation for superinsulating glazing systems can be so large that the U value can become negative during a winter day for north facing windows. This effect can be readily seen in Fig. 5 which shows the U value for the Crystal Pavilion north facing, vertical glazing during a 24 hour period in early April,1982. The curve begins on an average cloudy afternoon and ends on a sunny morning. The curve can be best understood by accounting for the absorption heating effect. The average solar transmission of the Argon filled, double 0.32 cm (1/8") glass assembly with copper-tin-oxide coated on surface No. 3 (the protected surface of the inside lite) is 48% (approximately 30% of the incident solar energy is absorbed in the system, mostly in the CTO coating). Since the coating is not on the glass exposed to the wind, half of the absorbed energy will, in effect, be deposited in the building. Measurements with a radiant flux meter confirm the sum of the solar transmission (at a 45° angle of incidence) and the absorption component deposited in the building is 63%. This sum is known as the effective transmission.

Fig. 5 shows the average nighttime U value for the special glazing is 1.24 $W/m^2°C$ (0.22 $Btu/hr°Fft^2$). As soon as daylight falls on the vertical north facing glass, the U value drops quickly to near zero and actually becomes negative for a short time on cloudy days due to the absorption heating effect.

Although one should idealistically use a dynamic U value for windows similar to these when predicting building performance, it is more realistic to use the nighttime 'U' value for super insulating glass to compute losses and the effective solar transmission to compute gains. Notice the solar gains through [illegible]th glazin[illegible] not be ignored when using these types of gl[illegible]tems.

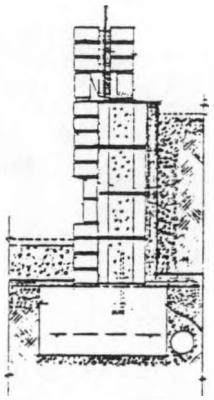

Fig. 4. Typical exterior retaining wall

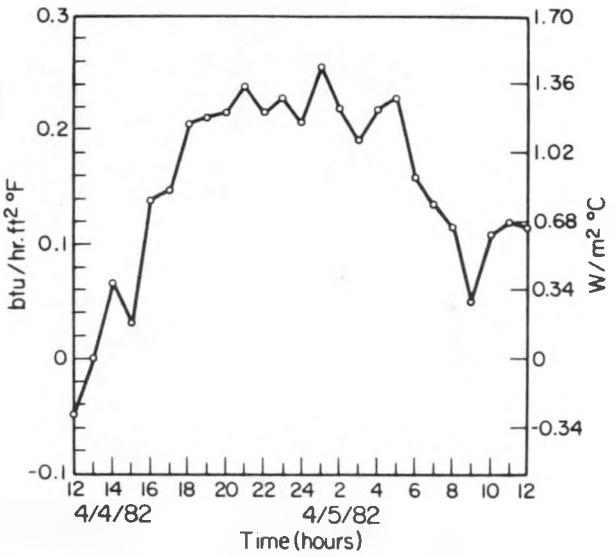

Fig. 5. Cloudy day U values for CTO coated, Argon filled,double glazing spaced 0.64 cm (1/4") apart (by Hisaya Sugiyama).

The dynamic U value of a north facing, 1.83 m (6') high window was indirectly measured by recording the temperatures of glass surfaces no. 1 and 4 with thermistors epoxied to the glass at the 1.52 m (5') level, and by measuring the indoor and outdoor air temperatures with thermistors placed 2.5 cm away from the respective surfaces. The temperatures were recorded on a 30 channel Precision Digital printing data logger. These hourly values are shown in Fig. 6 which includes the same time period displayed in Fig. 5.

The U value is related to the ratio of the temperature differences by the following equation:

$U=h_i (T_{inside}-T_{glass})/T_{inside}-T_{outside})$ where h_i is the combined film conductance due to free convection and radiation. The value for h_i only varies with the mean temperature, the average of the room air (T_{inside}) and the inner glass surface temperature, since no wind is present in the building. Also, the value of h_i does not vary significantly with height once the window height exceeds 0.2 m (2'). (1). The value of h_i *vs.* mean temperature is well documented in the literature alghouth some disagreement exists. Reference 2 closely duplicates the conditions encountered in the Crystal Pavilion, although the values used, 8.85 $W/m^2°C$ (1.56 $Btu/hrft^2°F$) at a mean temerature of 10°C (50°F) for example, are slightly higher than the single value of 8.28 $W/m^2°C$ (1.46 $Btu/ft^2°F$) published by ASHRAE (3). The values of h_i used to compute Fig. 5 are at most 6% too high.

5. BUILDING PERFORMANCE ON AVERAGE CLOUDY DAYS

Fig. 6 gives the temperature variation of several Pavilion building components over nearly a two day period with 820 W of lighting burning continuously Several building thermal performance features can be inferred from this representative data.

The previous two days were cloudy so any solar energy stored during clear days had already dissipated. This is evidenced by the constant temperature of the brick and tile thermal storage elements during the night of April 4. The following day brought cloudy weather of average intensity as indicated by a recording pyranometer mounted vertically behind the north facing glass (these data have not been calibrated yet). The outdoor air temperature continued to fall until April 5 dawned with sunny weather. The radiation trapped during the cloudy day was sufficient to raise the temperature of the brick and tile thermal storage slightly while maintaining the Pavilion indoor air temperature near 16°C (60°F) in face of outdoor air temperatures near 4°C (40°F). Notice the tiles never reach their phase change temperatures of 23°C so heat is only stored sensibly.

The average day-night indoor-outdoor temperature difference for a 24 hour period beginning at midnight on April 4 was 10.3°C (18.5°F) with a daytime peaking temperature difference of 1.29°C (23.3°F). Internal gains of 820 W accounted for 4.1°C (8.4°F) of these temperature differences. These temperature differences generated by the diffuse solar energy filtering through the clouds proved to be average during the February to June monitoring period. Increased ground reflectance due to snow raised the cloudy day average sustained temperature difference to 11.1°C (20°F).

Fig. 6 also shows the hours when the special glass U value goes negative on a cloudy day. This begins approximately 11:30 on April 4, as evidenced by the indoor air temperature lowering below the inside glass surface temperature, and continues until approximately 14:00 while the outdoor air temperature was averaging 6°C (42.5°F).

The evening of April 4 was windy as shown by the near convergence of the outdoor air and outdoor glass surface temperature curves. The wind greatly increases the heat conductance at the outside glass surface.

The outside air temperature drops sharply after sunset of April 4, going below the design conditions of 6°C (42.5°F). This drop generated a large load on the thermal storage which drops in temperature to meet the demand. Although the indoor air temperature drops below 15°C (59°F), the air temperature difference between indoors and outdoors remains steady at 11°C (19.8°F) during the late night hours. All temperature levels recover during the sunny morning of April 5.

6. CONCLUSIONS

Measurements show the Crystal Pavilion can sustain nearly an 11°C (19°F) 24 hour average indoor-outdoor air temperature difference during an average cloudy day occuring near the Equinox. This difference will

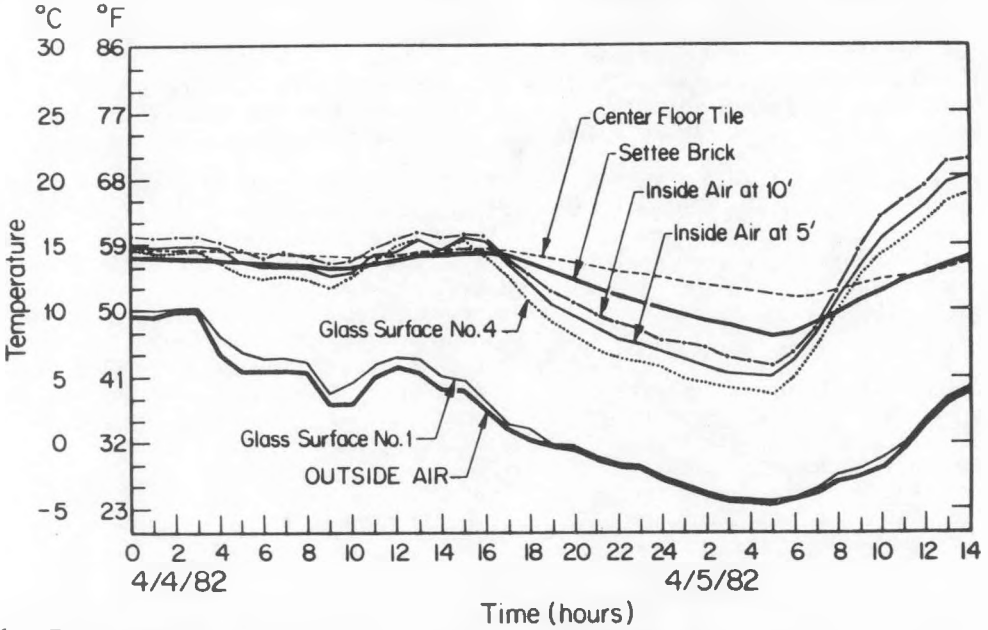

Fig. 6. Temperature *vs.* time for several Crystal Pavilion building components (by Hisaya Sugiyama).

wer during December and January when the days re shorter. This means the building can provide 100% solar heating during most winter periods, even on cloudy days, provided the outdoor air temperature remains above 7°C (44°F). The U.S. Pacific northwest and many parts of the United Kingdom have winter climates similar to this.

The Pavilion is nearly 100% glazed in order to multiply the small solar profit available on cloudy days. Detached residences could not readily be built this way because visual privacy would suffer. Expected advances in coating and gas fill technology should ease this problem, but the special glass could be used in multiple family housing now since thermal loads are lower, so much less glass would be required. This means solar heating in cities will be easier to accomplish because only diffuse solar radiation is required, not direct beam solar energy. Setbacks would be eased and north facing apartments could be solar heated.

Data logging will continue for another year, while the building is tightened to lower the infiltration rate to below 0.5 ac/hr. A full MIT report will be available next year documenting the entire performance of the building.

7. REFERENCES

1. Introduction to Heat Transfer, Brown and Marco.

2. "Surface Conductances as Affected by Air Velocity, temperature and Character of Surface", F. B. Rowley, A.B. Algren, J.L. Bolckshaw, ASHRAE Transactions, Vol. 36, 1930.

3. ASHRAE, Handbook of Fundamentals, 1972.

PHASE CHANGE THERMAL STORAGE: A BUILDING INDUSTRY PERSPECTIVE

Paul F. Kando, NAHB Research Foundation

1. The Market Potential

The NAHB Research Foundation is the research arm of the National Association of Home Builders, the over 100,000 member trade association of the home building industry. For the last several years, the Foundation has been engaged in phase change thermal storage research in response to the generally recognized need for residential buildings to be (1) more affordable, (i.e., lighter weight, higher productivity construction methods, shorter construction time, component construction, etc.); and (2) energy efficient. Phase change thermal storage holds the promise of allowing significant thermal mass to be introduced into light weight structures, without disruption to the customary construction process, thereby providing them with the comfort and energy efficiency of more massive buildings but without their massive price tag.

The Foundation sees a significant potential market for properly designed and priced building products which contain high heat storage capacity phase change materials. Some relevant facts:

- Recent NAHB Research Foundation housing data indicate that nationwide over 90% of all new housing units are constructed using a wood frame. Without significant disruption of the usual building process and therefore additional expense, the only realistic way to introduce an appropriate amount of thermal mass into these buildings is by means of phase change materials.

- Assuming a return to normal economic conditions, NAHB Research Foundation estimates call for the construction of over 500,000 passive solar housing units annually by the year 1987. If appropriate phase change thermal storage products are available by then, these should capture at least half of this market, or 250,000 units.

  An estimated average of 1000 lbs. of phase change material per housing unit translates to an annual production volume of 250,000,000 lbs. of phase change materials annually. We estimate an average price of $1000 per housing unit. This means a business volume of $250,000,000.

- The retrofit market traditionally follows the new home market in the introduction and acceptance of new building products. If, by 1987, we assume this market to be equal to 10% of the new home market, we are speaking of an additional $25,000,000 business volume. However, the retrofit market could easily outdistance the new home market. After all, most of the homes of the year 2000 are already standing today. The Foundation's Market Research Department estimates that there are now some 81,8 million existing housing units in the United States.

- Thermal storage that allows the off-peak use of air conditioning equipment is another vast potential market for phase change thermal storage products. As summer electric power costs rise, peak demand increases, and peak load problems of utility companies multiply, this may well develop into a market equal to or larger than the passive solar market. Obviously the products will have to be different than those designed for heating. Nevertheless, the addition of another $250,000,000 annual business volume by 1987 is a reasonable projection.

  Thus we are speaking of a combined total annual business volume of over $500,000,000 by 1987. This is an attainable goal. The key is the development of the right products for the builder and an effective marketing strategy for their introduction to the building industry.

- One reason for the great promise phase change materials have for building applications is this: In a typical solar application, for each square foot of south facing glazing the corresponding amount of thermal mass is approximately the equivalent of 150 bricks (785 lbs.) or 4 gallons of water. However, the same amount of heat storage can be provided with less than 8 lbs of phase change material. This is only a 3/4" thick layer of material of a one square foot area.

2. State of the Art

Phase change thermal storage research has been ongoing since the 19th century when the first theoretical investigations began. In more recent times, it was successfully applied at various temperatures in military, space and medical applications. In a house it was first used in 1949 as a part of an experimental solar heating system.

Today there are a number of containerized phase change materials available on the market. However, none of these are truly home building products. To use these products in their current state of sophistication, a builder would have to design and build a heat exchanger system. This is certainly not economic, nor practical. Also, many of the available containers are cylindrical, a shape not ideal from the heat exchange standpoint because the ratio of surface area to volume is too low.

There are good reasons why, after all these years, there are still no real building products available that contain phase change thermal storage materials. The main one is that research to date has almost exclusively concentrated on developing the materials themselves. As a result, we are confident that materials problems are either already solved or solvable without undue difficulty. These problems include performance degradation after repeated thermal cycling, nucleation problems, and container failures of various kinds.

The material scientist now can concentrate on the few, well defined, remaining problems, like stabilizing the performance of incongruently melting phase change materials systems in containers with large vertical dimensions. Most definitely they must focus on cost reduction. But even if all these problems were solved, we still would not have a single suitable building product on hand to utilize phase change materials. To succeed in developing such products, we are convinced that:

- Phase change material research must be extended beyond the chemist's laboratory.
- The remaining problems require the collaboration of many disciplines and capabilities.
- Phase change material product manufacturing is not, for the foreseeable future, in the realm of either the small garage style cottage industry, or the do-it-yourselfer. It requires significant investment, know-how and industrial capability.

In the recent past, the NAHB Research Foundation held conversations with many individuals representing a cross section of industry interested in phase change thermal storage products for buildings: chemical manufacturers, the packaging industry, building products manufacturing and distribution, builders and home manufacturers. We have come to the following conslusions:

1. There are at least two materials which are at present technically and economically suitable as phase change thermal storage products for passive solar and off-peak cooling applications. These are Calcium Chloride Hexahydrate, with a melting point of 81°F; and Sodium Sulfate Decahydrate, with a melting point of 89°F. There are also a number of eutectic mixtures of the latter which provide an array of melting points from 45 to 75°F. Other materials are either in various stages of development or are available only at much higher prices.

2. Product design limitations imposed by the chemical and physical behavior of these materials are known, a range of containment materials have been found, and the remaining technical problems are fairly well defined.

3. A product must be designed for a specific system application. This involves both technical and aesthetic design considerations.

4. The phase change products which will eventually sell will have to be functional, attractive building components, which in addition to their normally expected features offer maximum thermal capacity. These newly developed building components must be able to be applied by ordinary builders, using normal tools and skills.

5. Before phase change thermal storage building products can be developed for the home building industry, more must be known about:

- generic information on the thermal performance of homes and apartments, especially indoor temperature variations. The new products must both functionally and aesthetically blend with the home. The specific thermal behavior of buildings and the compatibility of candidate building products with phase change materials must be determined;
- cost and performance data, based on actual measurements;
- the market, overall and in terms of its primary segments, such as regional sub-division, custom or mass builders, manufactured homes, retrofit and remodeling;
- product design which must insure simplicity of installation, utilizing customary tools, methods and labor skills.

SPECIFIC PRODUCT DESIGN ISSUES:

1. Thermal storage location in the building. It probably must be hidden from view since it has little visual appeal, but this is not certain.

2. Container shape (heat transfer, structure, aesthetics)

3. Heat transfer in/out of storage (passive/hybrid methods)

4. Containers must be vapor impermeable

5. Shelf lift (15 years or more) and replaceability

6. Identify optimum operating temperatures and fail safe mechanisms for various likely applications

7. Ease of installation (self contained units; semi-skilled labor)

8. Define maximum size and unit weight for specific applications

9. Abuse in handling and safety considerations

10. A means to show the consumer that the system is working (indicator lights, meters, etc.) is probably a good idea.

6. There is also a need to develop performance standards (not codes) and standard test methods. Products must be demonstrated in homes. Builders must be educated about using them. A coordinated effort between materials suppliers, packagers and builders, especially during the initial phases of development is essential.

3. A Multi-Client Research Approach

The conclusions and design related issues identified indicate a need for many experts to undertake the more generic activities necessary to bring phase change thermal storage products to the builder. This research is logically funded by a combination of two sources:

(1) Government R&D programs; and (2) Multi-client R&D efforts in which a number of corporations share the cost of generating the needed information. Once sufficient generic information exists to undertake meaningful proprietary development work, the market potential will provide the needed motivation for individual corporations to continue with such efforts.

The Federal Government, primarily through the Department of Energy, has been sponsoring research in phase change materials for the past several years. As a result, a number of materials have been identified as technically promising for applications in heating and cooling indoor space. The Research Foundation has and will continue to keep abreast of developments in this area. Additionally, under a recent contract with the Department of Energy, the Foundation will conduct research to select promising phase change materials for building applications, evaluate their feasibility in various generic system configurations, develop the necessary heat transfer mechanisms for passive solar applications, examine safety, manufacturability, reliability and related issues and disseminate the resulting information through industry channels.

However, currently there is no Federal funding available to cover the cost of analyzing and characterizing the buildings and building components with which phase change products must successfully integrate to form a working system. Neither is there a current Federal program to help assess the general and specific markets for phase change thermal storage products or to develop a given product type and assess its market potential. Likewise, performance monitoring, testing and demonstration of any potential or real products are not covered by Federal programs.

The NAHB Research Foundation therefore conducts this part of its research leading to phase change thermal storage product development under a multi-client sponsorship arrangement.

4. The Scope of the Multi-Client Work

Under multi-client, private sector sponsorship the Foundation conducts the following major activities:

1. Building thermal performance studies, especially indoor temperature variations

2. Builder practices and market studies

3. Phase change materials selection, testing and evaluation for specific products

4. Produce specific performance monitoring and test method development

a. Building Thermal Performance Studies

Phase change materials, in addition to their large heat storage capacity, have the added advantage of providing storage at a fixed temperature. To be able to fully capitalize on these features, a phase change thermal storage product must be thermally well integrated with the building structure. Comfort conditions within an occupied building require that temperature fluctuations be kept within a small range. Consequently, a thermal storage device must function within a very narrow temperature band. To permit sufficient heat transfer under these conditions, the functional temperature of the phase change material must be just right in relation to the indoor ambient and surface temperatures, and the heat transfer mechanisms must be specifically designed to permit efficient charging and discharging cycles. These must be coordinated with the diurnal solar cycles at the installation site, as well as with the appropriate heating and cooling systems. For such designs we must have much more detailed, measured dynamic temperature profiles for occupied buildings than are currently available.

In order to provide this information, we collect and analyze building temperature profiles. We analyze data from a number of currently monitored buildings across the country and data from instrumented research homes. We also perform detailed temperature measurements in test structures specifically developed for this project.

The results will provide guidance for product design with respect to optimum operating temperatures, the geometric shape of prospective products/components, surface configurations and treatments, the mechanisms needed to prevent heat losses from storage back to the environment, etc.

b. Builder Practices and Market Studies

In home building, it is the builder who makes product decisions. It is therefore essential than any new or improved building product fit in with current builder practices and coordinate well with other popular building products.

The NAHB Research Foundation annually surveys the nation's builders. The results of these surveys cover in detail over 100,000 homes and small commercial buildings. Utilizing this vast data base and survey capability, and with active client involvement, this project will define the marketplace, and describe the kinds of products the builder or remodeler may actually buy. The work covers only the pre-proprietary phase of this research; i.e., it will provide both a good picture of the marketplace, and generic performance, cost and system integration information. This information is needed by corporations intent upon developing suitable products before they are in a position to invest in their our product development efforts.

c. Materials Selection Testing and Evaluation

The Research Foundation has unique capabilities to test building products and components of all kinds, ranging from windows and insulation to full truss systems up to 74 feet long.

Our Phase Change Materials Laboratory is capable of performing continuous thermal cycling tests both on material samples and on full scale containers and modules. This laboratory capability will be augmented by full scale, single room housing structures, developed expressly for the purpose of evaluating thermal storage product prototypes in actual installations. These test structures will be constructed according to the prevailing practices of the home building industry. They will be instrumented one room structures with modular, replaceable components, like south facing walls, ceilings and floors.

The Foundation is evaluating promising phase change materials and additives from both the cost effectiveness and performance standpoints. Tentative selections of specific materials for specific purposes and configurations within buildings will be evaluated.

d. Performance Monitoring and Test Method Development

Utilizing the full scale test structures, the Foundation will assemble and test a number of generic prototype thermal storage devices and report on the results.

We also conduct confidential individual tests on proprietary products for manufacturer clients, utilizing similar test facilities. Tests on such proprietary products are, of course, not a part of multi-client research, but are performed on a basis negotiated with individual clients.

5. Prototype Product Demonstration and Market Feedback

The Research Foundation also provides demonstration sites in test structures for various product prototypes and report on initial builder reaction and other items of market feedback. Such informal feedback from the marketplace reduces both the costs and the risk of new development to a manufacturer. Hence it is a viable preliminary to full scale demonstration in a research home.

In summation, the Research Foundation sees phase change materials as an important potential component of future light weight housing. Much needs to be done before commercial products useable by a builder will enter the marketplace. The Foundation follows a product development process essentially similar to one all new ideas in building science undergo. Some building products which were developed with the Research Foundation's direct involvement are shown on Table 1.

Table 1

Examples of Products Developed with NAHB Research Foundation Assistance for the Home Building Industry

Textured hardboard
Textured plywood
Texture 111 and variants
Foam-core steel doors, pre-hung and weatherstripped
Add-on, plug-in A/C units for central system
Treated wood foundation system
Floor-to-ceiling closet-panel system
Wall-hung water closets
Hardwood flooring system
Perforated soffits for ventilation
Open web steel bar joist system
Sashless window
Latex breather paints
Metal plate connected truss
Plywood glue-nailed truss
Prefabricated split-block wall panels
Engineered design, concrete and steel foundation system
Component wall panel system
Raised bottom bath tubs
One piece bath tub with integral wall sorround
Foam-backed sheet goods for flooring
Tight fitting, low infiltration aluminum window (1956)
Modular fiberglass manholes and related products
Modular built-in cabinet system
Foil-faced insulation
Pre-wired, pre-finished exterior wall panels
Plastic water pipes and fittings
Double access bath tubs
Decay-resistant post anchorage and pier system
Glue-nailed beam and headers
Textured aluminum roofing system
A-frame construction system
Foam-core stress skin panel
Grade beam construction
Prefabricated brick panels
Hard thin coat plaster
One piece sink and countertop vanities
One piece flashing, gutter, fascia product
Manufactured slate flooring for adhesive application

PROJECT SUMMARY

Project Title: Passive Cooling Experimental Facility - Hot/Arid Climate

Principal Investigator: John F. Peck

Organization:
University of Arizona
Environmental Research Laboratory
Tucson International Airport
Tucson, AZ 85706

Project Goals:
Bring the state of the art of passive cooling in hot arid climates up to that of passive solar heating. Build several test structures with a comprehensive data acquisition system in order to collect enough data to validate computer models and verify the performance of a large number of passive cooling strategies. Provide design data to users of passive cooling systems in architectural projects.

Project Status:
Three test structures and the data acquisition building have been completed and monitoring equipment has been installed. Data has been continuously collected since early March, 1982 at 413 data points. Collected data includes dry bulb and wet bulb temperatures, wall temperatures, heat flow, ground temperatures, insolation through windows and ambient conditions. Manual data including electrical usage and water consumption have also been collected.

During winter monitoring (under Arizona Solar Energy Commission funding), testing of two solar heating devices, the solar/screen porch on structure one and the solar heated attic on structure three, were carried out.

Since March, structure two, which is partially earth integrated, has been monitored. The inside temperature has been kept constant with an air conditioner/heat pump. To reduce outside influences, windows were insulated with 1" of polystyrene. Data has been sent to the University of Minnesota for analysis.

Between May and July the nocturnal radiation roof of structure one was in operation. After mid-July, the building was evaporatively cooled 24 hours per day for two weeks. Since then it has been cooled at night and allowed to coast through the day on coolth stored in the massive adobe walls.

Structure two and structure one have outdoor living spaces including a roof porch, a roof deck and a solar/screen porch (screened in summer). These are being monitored for comfort. Different roofing surfaces are being experimented with on the roof deck.

Structure three has been operated using the rockbed for various forms of two stage and indirect evaporative cooling throughout the summer.

In addition to the standard instrumented data, ERL staff have on occasion been sitting inside the test structures and recording their own comfort perceptions. These will be compared to the instrumented comfort data (the Predicted Mean Vote (PMV)).

Analysis of the data from the facility will begin in the fall of 1982 pending sufficient funding.

A document describing the design, instrumentation and construction of the facility together with the summer data is being written for DOE.

Contract Number: DE-AC03-80SF10816

Contract Period: August 18, 1980 through September 30, 1982

Funding Level: $750,615

Funding Source: U.S. Department of Energy

PASSIVE COOLING FOR HOT ARID REGIONS

Helen J. Kessler
University of Arizona
Environmental Research Laboratory
Tucson International Airport
Tucson, Arizona 85706

ABSTRACT

A Passive Cooling Experimental Facility for a Hot/Arid Climate has been constructed. It has been designed to test a large number of passive cooling strategies in order to bring the state of the art of passive cooling up to that of passive solar heating. Three test structures and a data acquisition building have been built and are fully instrumented. Ambient weather conditions are also monitored. Passive cooling strategies being studied include both traditional and new concepts and are based on the basic passive sources of coolth: ventilation, evaporation, nocturnal radiation and earth contact.

INTRODUCTION

Passive cooling had until recently been generally neglected in both solar research and in actual building designs. Passive solar heating on the other hand is quite well understood and is more commonly used in new and existing homes. Unfortunately, in many solar designs, passive solar has produced an overabundance of heat and has caused a cooling problem. Thus the objective in studying passive cooling is two fold—to reduce unwanted heat gains and to provide cooling at a much lower cost than refrigerated air conditioning.

The Passive Cooling Experimental Facility for a Hot/Arid Climate was constructed to test a large number of passive cooling strategies in a relatively short period of time in order to bring the state of the art of passive cooling up to that of passive solar heating.

Four test structures were originally planned. Three plus a data acquisition building were built. The three buildings illustrate high mass and low mass construction techniques as well as ways to use each passive source of coolth - ventilation, evaporation, nocturnal radiation and earth contact.

The facility will be used to validate computer models and develop design guidelines. The data will also be used to test comfort in each structure during various ambient conditions and when different passive cooling strategies are used.

TEST STRUCTURE DESCRIPTION

Structure One - Structure one is built of stabilized mud adobe. See Figure 1. Its walls are 16-17" thick and uninsulated. The roof of structure one is a corrugated metal roof decking through which air may be blown. It is used to test the effectiveness of nocturnal radiation. A solar/screen porch with removable glazing is used as a solar collector, sunroom or solar greenhouse during the winter and as a low mass screened porch in the summer. The comfort on this screen porch is being compared to that on the above grade screened porch of structure two. Nocturnal evaporative cooling is also being tested. The building is evaporatively cooled at night and then allowed to coast through the day on coolth stored in the walls. Other testing will be done in future years. A ramada has been built onto the north side of structure one. It will soon be covered with vines to test its effectiveness as a summer outdoor living space.

Structure Two - Structure two is a multi-story building with a basement, a half-basement, a level on grade, a roof porch and a roof deck. See Figure 2. Its walls are eight and twelve inch solid concrete block (12" in the basement) and are insulated on the exterior to four feet below grade. Data has been gathered since March with the basement closed up and air conditioned. The windows are covered with one inch of polystyrene and the temperature inside the structure is kept at a steady 74F. This is to limit the parameters in order to provide data for the University of Minnesota Underground Space Center to validate their computer models for hot arid climates. (The temperature inside the structure rose to 84F for a short time during the summer of 1982 when the air conditioner failed.)

The roof porch is both a daytime and a nighttime living area - a low mass adjunct to a high mass building. Comfort parameters including wet bulb, dry bulb, globe thermometer and air velocity are being measured. It is about five feet above grade and is open and screened on four sides to allow breezes to pass through. The roof is insulated with R-30 fiberglass batts.

The roof deck is a nighttime living area. A person sitting or sleeping there will radiate heat to the night sky and thus be cooled. Different flooring materials are being used to determine their effects on the mean radiant temperature at night.

Structure Three - Structure three is the only low mass building. See Figure 3. Constructed of wood, it uses a rockbed below the floor to store heat and coolth. Water walls (water may be added and removed as

desired) have also been installed inside the building for thermal storage during periods when the rockbed is not being used. Various evaporative cooling systems are designed into structure three, including two stage and indirect evaporative cooling systems using the rockbed. Other advanced evaporative cooling systems could be retrofitted and tested later. Numerous solar heating systems are also built into structure three, including an attic solar collector and a ClearView Solar Collector. The attic was tested with an opaque dark metal roof during winter 1982.

Data Acquisition Building - The data acquisition building was also designed as a test structure although its main purpose is to house the computers and their operators. See Figure 4. All instrumentation wiring enters the data building and the measurements are recorded there. The building is air conditioned so that it stays at a fairly constant temperature and does not perturb the data. The building is of high mass construction - 8" solid concrete block with outside insulation. It may be bermed to 7 feet at a later date. Off peak electrical use may also be tested.

All of the test structures have Klos windows. They consist of two single sliding windows which open in opposite directions and which have a venetian blind installed in between. These windows may be used as solar collectors in the winter if they are located in a south wall and as heat rejectors when the evaporative coolers are in use during the summer.

During appropriate periods, researchers will occupy the buildings and record their comfort perceptions. These perceptions will be compared to the instrumented comfort data - the PMV (Predicted Mean Vote).

Figure 1. North side of structure one - adobe building. The ramada will be covered with vines during the next couple of years.

Figure 2. South side of structure two. The windows have been insulated with 1" polystyrene to reduce the outside influences on interior temperatures.

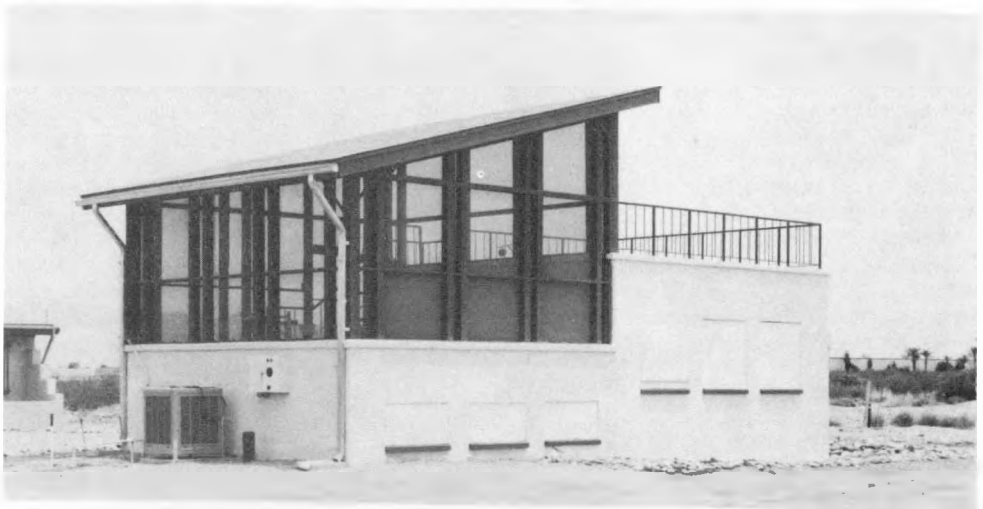

Figure 3. South side of structure three - wood frame construction.

Figure 4. Data acquisition building with weather station in foreground.

SELECTED DATA

It is always awkward reporting on experiments one has just carried out and data one has just collected without having time to fully analyze the results. In the case of a summer cooling program and an early fall deadline, this will naturally occur. Thus, the items in this discussion will not have been carefully analyzed. Graphs produced with the HP9845 computer are shown. The days shown in the graphs were not chosen based on any special significance in terms of results we wanted to show. They were essentially randomly chosen. However, they do show some trends and typical data that have been collected.

Structures one and two are both high mass buildings with different but typical wall construction. One is uninsulated approximately 17" thick mud adobe and the other is 8" solid filled concrete block with 2" of exterior polystyrene insulation. Typical temperatures from the two buildings are illustrated in Figures 5, 6, 7 and 8.

Figures 5 and 6, which illustrate the wall temperature rakes in the adobe building, show that the peak of the heat wave appears to be passing through the wall from outside to inside at about 2" per hour. It

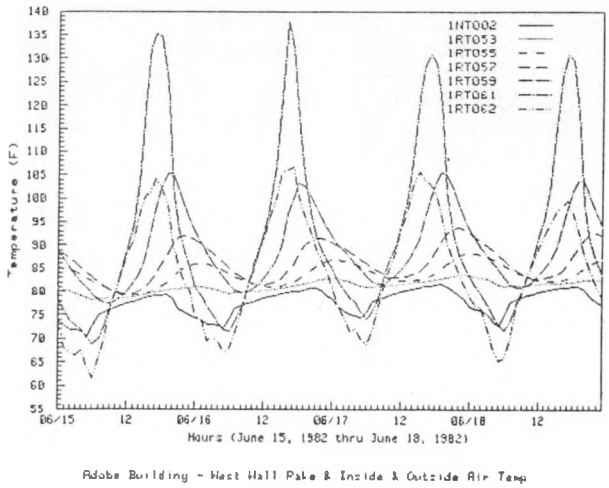

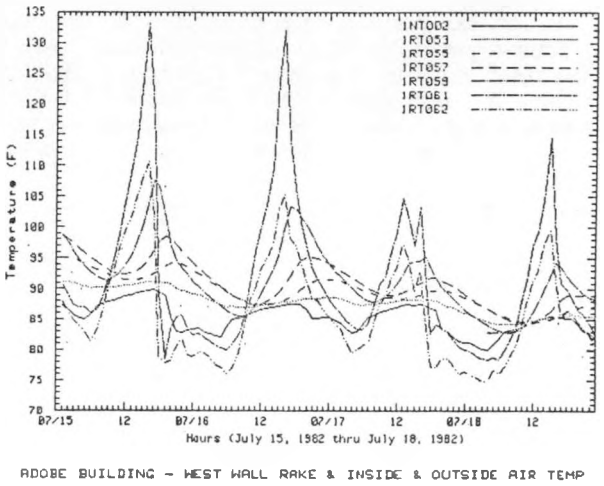

Figures 5 and 6. Thermocouple rakes through west adobe walls in June and July 1982. Sensor notation: 1NT002 - inside air temperature, 1RT053 - 1RT059 - thermocouples at 4" intervals through adobe wall from inside to outside, 1RT061 - outside adobe surface temperature, 1RT062 - outside air temperature approximately 2" from wall.

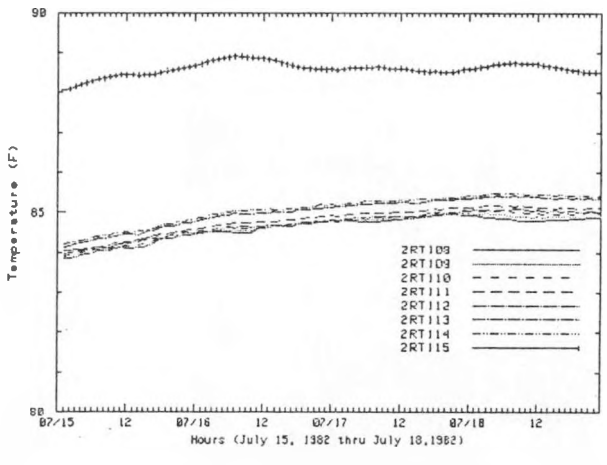

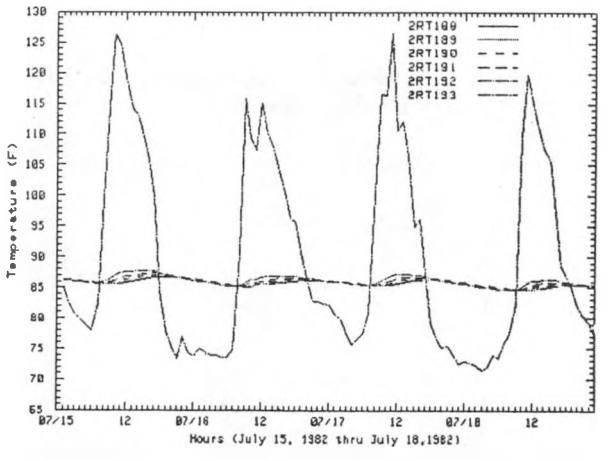

Figures 7 and 8. Thermocouple rakes through east walls in structure two. Rake on left is six feet above basement floor level. Sensor notation: 2RT108 - 2RT114 - thermocouples at 2" intervals through 12" concrete block wall from inside to outside. Sensors are located within solid grouted core of block. 2RT115 - thermocouple between polystyrene insulation and earth. Rake on right is four feet above ground floor level. Sensor notation: 2RT188 - 2RT192 - thermocouples at 2" intervals through 8" concrete block wall from inside to outside. Sensors are located within solid grouted core of block. 2RT193 - thermocouple on outside surface of 2" polystyrene insulation.

might also be noted that the surface temperature on the outside is considerably higher than the air temperature near the surface. The difference between outside surface and inside surface temperature is as much as 50F. The air temperature inside the structure is lower than the surface temperature indicating that the cooler air inside the building may also be affecting the wall temperature.

In both June and July the adobe building was cooled with the night sky radiation roof. From the wall rake graphs it can be seen that the roof is able to keep the tempertures inside the building within a comfortable range in June but not in July. In July, the afternoon weather tends to be stormy. This helps lower the temperatures on the surface of the west adobe wall and tends to help keep the wall and thus the air temperature inside the building cooler. Ambient wet bulb and dry bulb conditions in June and July are shown in Figures 9 and 10 for comparison. Wind speed and direction are shown in Figures 11 and 12, and horizontal insolation and diffuse radiation are shown in Figure 13 for July only.

Figures 7 and 8, which illustrate wall temperature rakes in structure two, show the stabilization effect of the 2" styrofoam insulation on the exterior of the block walls. During this period, the air conditioner was not operational (a repair man worked in the building on July 16). Thus the wall temperatures rose from about 74F when the air conditioner was on to around 84-85F in the basement and 85-87F on the ground floor. Air was continuously being circulated from the ground floor to the basement in order to prevent hot air pockets from forming. The average wall temperature in the basement rose about one degree in this four day time period, but stayed relatively level. There were some increases in temperature during day time peak loads at the ground floor, but the average temperature in the wall did not rise over the four day period. The increase in the basement wall temperature may have been due to a slight increase in the earth temperatures. While the earth temperatures significantly stabilize the below grade wall temperatures, it appears to be the insulation that does the most amount of good both above and below grade.

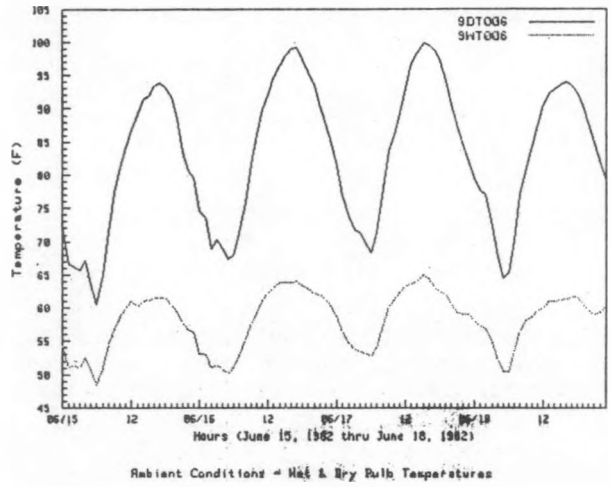

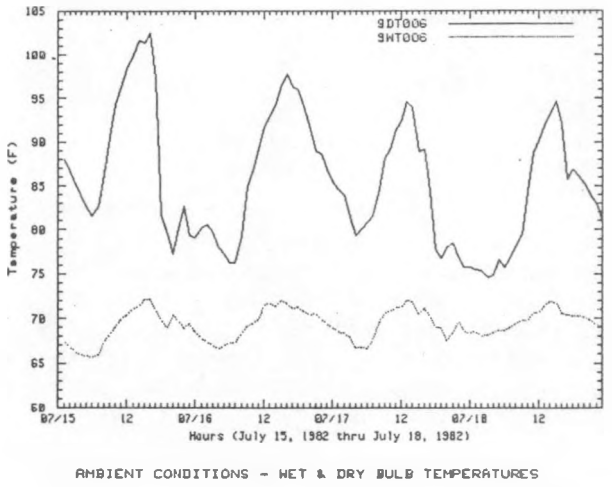

Figures 9 and 10. Ambient temperatures during June 15 - 18 and July 15 - 18, 1982. Sensor notation: 9DT006 - dry bulb, 9 WT006 - wet bulb.

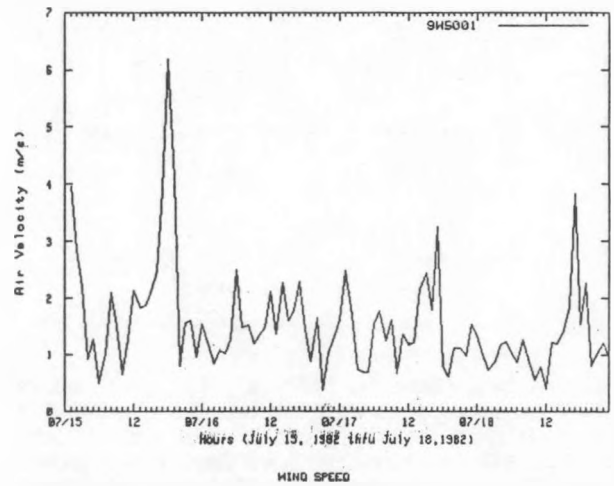

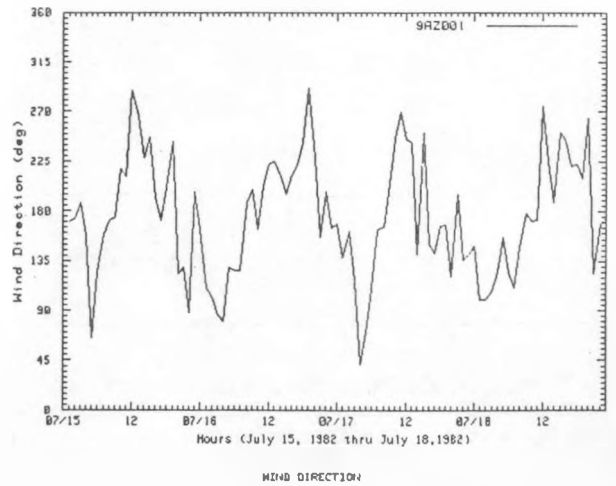

Figures 11 and 12. Wind speed and direction during July 15 - 18, 1982.

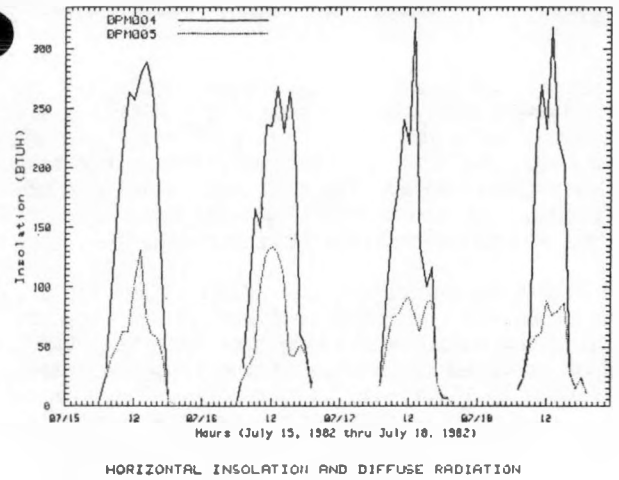

HORIZONTAL INSOLATION AND DIFFUSE RADIATION

Figure 13. Horizontal insolation (0PM004) and diffuse radiation (0PM005) during July 15 - 18, 1982.

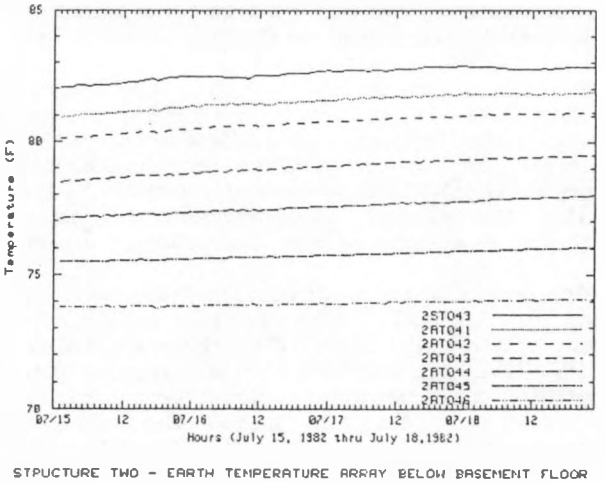

STRUCTURE TWO - EARTH TEMPERATURE ARRAY BELOW BASEMENT FLOOR

Figure 14. Temperatures below center of basement floor. Sensor notation: 2ST043 - surface of basement floor, 2AT041 - 4 1/4" below surface, 2AT042 - 8 1/4" below surface, 2AT043 - 16 1/4" below surface, 2AT044 - 27 3/4" below surface, 2AT045 - 47 3/4" below surface, 2AT046 89 1/2" below surface.

Earth temperatures are also a major part of the data being collected at the PCEF. With structure two closed up and kept at a constant temperature, the effect of ground temperatures on the building may be studied and computer models validated. Figure 14 shows some typical earth temperatures below the basement floor of structure two.

Ambient earth temperatures are shown in Figures 15 and 16. The earth temperature at 7' - 4" below the ground is constantly rising as the summer progresses, eventually to a level where it will be too high to provide comfort completely passively. However, even a stable ground temperature in the 80's can lower cooling bills, especially when small fans are used to increase air motion in relatively warm spaces.

Greg Lansdon of ERL installed thermocouples at various depths below the ground two years ago in order to study the earth temperatures. During July 1981 he placed 8" of rock mulch over one of the two test sites to determine what effect it would have on the earth temperatures. Although it does not appear to greatly affect the earth temperature at seven feet below grade, it lowers the temperatures of the earth near the surface to about 89-90F as compared to 97F at the exposed site in July. Even this small modification may

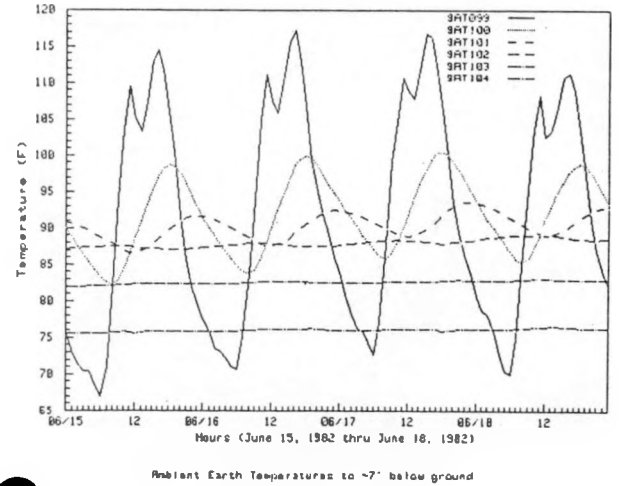

Ambient Earth Temperatures to -7' below ground

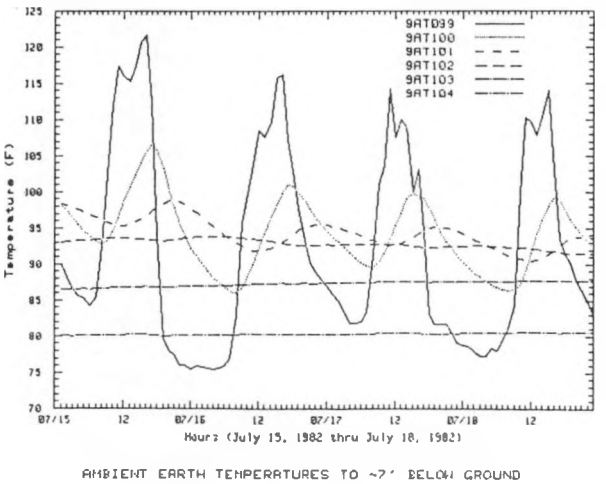

AMBIENT EARTH TEMPERATURES TO -7' BELOW GROUND

Figures 15 and 16. Earth temperatures at weather station. Sensor notation: 9AT099 - surface temperature, 9AT100 - 4" below surface, 9AT101 - 12" below surface, 9AT102 - 24" below surface, 9AT103 - 48" below surface, 9AT104 - 88" below surface. Surface temperature decrease occurs in early afternoon when adjacent pole shades thermocouple.

make rock mulches adjacent to earth integrated homes in arid regions desirable. This effect was originally suggested by Baruch Givoni of Israel.

The bottom line in any heating or cooling system is comfort. In order to determine comfort, the following data is gathered: dry bulb, wet bulb, and globe temperatures, and air velocity. Clothing and activity levels (external work and metabolic rate) are assumed given the time of year; and mean radiant temperature and vapor pressure are calculated by the computer. The PCEF data analysis system has been programmed to calculate comfort using Fanger's Predicted Mean Vote (PMV) scale. The PMV was developed by recording the comfort perceptions of a large number of people. It thus gives a general estimation of comfort for an average person and provides a comfort range. The PMV is described in reference 1.

PMV data together with wet bulb, dry bulb and globe temperatures for structure one is shown in Figures 17 and 18. Since this data was taken during a period when the night sky radiation roof was being used, the building stayed quite warm. When there was no air movement inside the building, it was generally too warm. However, if an air velocity of 1 m/s were assumed (this could be provided by an oscillating propeller fan), the building could be brought closer to a comfortable level as shown in Figure 18. Figures 19 and 20 show temperatures and the PMV inside the adobe building a couple of days later when the evaporative cooler (standard single stage) was run day and night. As can be seen from the graphs, the cooler provides considerably more cooling than the radiative roof does.

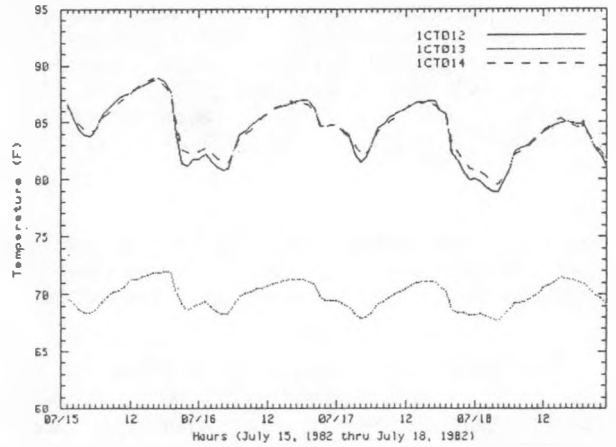

ADOBE BUILDING - LIVING ROOM - WET BULB & DRY BULB & GLOBE TEMP

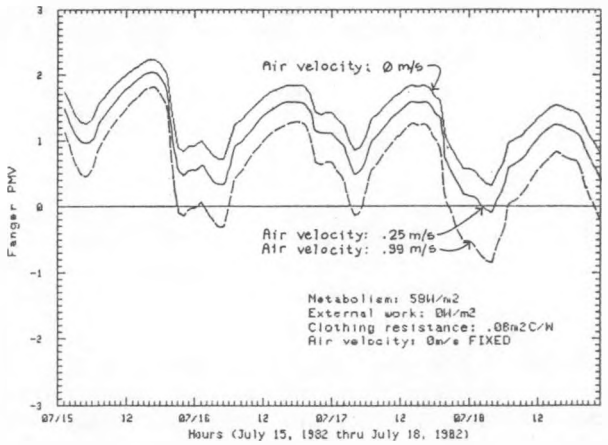

ADOBE BUILDING - LIVING ROOM - FANGER PMV

Figures 17 and 18. Wet bulb, dry bulb, globe temperatures and PMV's inside the south room (or living room) of structure one with radiative roof used for cooling at night only. Sensor notation: 1CT012 - dry bulb temperature, 1CT013 - wet bulb temperature, 1CT014 - globe temperature. Note changes in PMV as air velocity is increased.

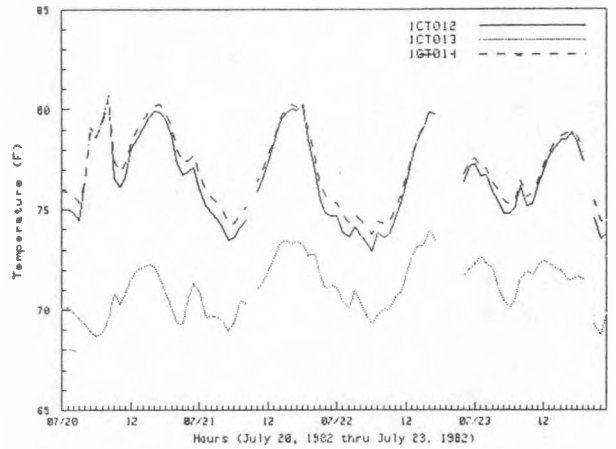

Adobe Building - Living Room - Wet Bulb & Dry Bulb & Globe Temp

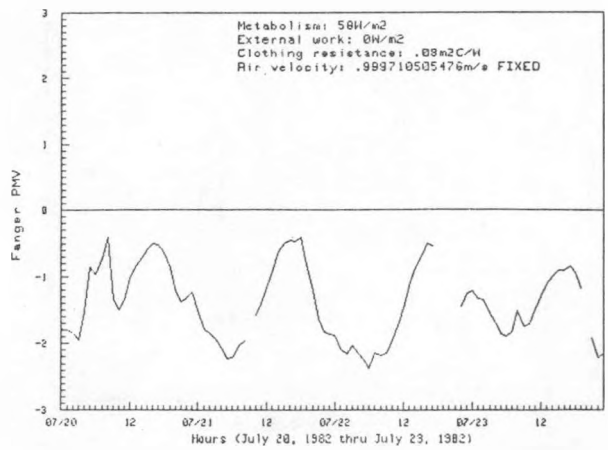

Adobe Building - Living Room - Fanger PMV w/ air vel at 1 m/s

Figures 19 and 20. Wet bulb, dry bulb, globe temperatures and PMV's inside south room (or living room) of structure one with one stage evaporative cooling 24 hours per day. Sensor notation: 1CT012 - dry bulb temperature, 1CT013 - wet bulb temperature, 1CT014 - globe temperature. The PMV has been calculated with an air velocity of approximately 1 meter/second.

Figures 21 and 22 show wet bulb, dry bulb and globe temperatures as well as the PMV in structure three. During this period, two stage evaporative cooling was used from mid-morning until about 5:00 p.m. and single stage cooling was used thereafter. This system provided cool comfort throughout the summer. It is interesting to note that the globe temperatures in this low mass wood frame building are considerably higher than those in the adobe building during the day.

The roof porch and roof deck of structure two also have comfort sensing devices. These are traditional types of spaces where people used to find comfort at night before mechanical cooling was available. As can be seen from the data in Figures 23, 24, 25 and 26, both spaces are cool at night and unbearably hot during the day.

Although it was nearly impossible to use the roof deck during the day due to the extremely high mean radiant temperature as well as the blinding glare from the white roof, the roof porch turned out to be much more comfortable than the PMV's might indicate. Most people who spent any time on the roof porch found that as long as a breeze was blowing, their perception was that the temperature was as much as 15-20F lower than the actual temperature. Although still warm, it was not perceived as unbearable. In this case, air motion was the key to comfort.

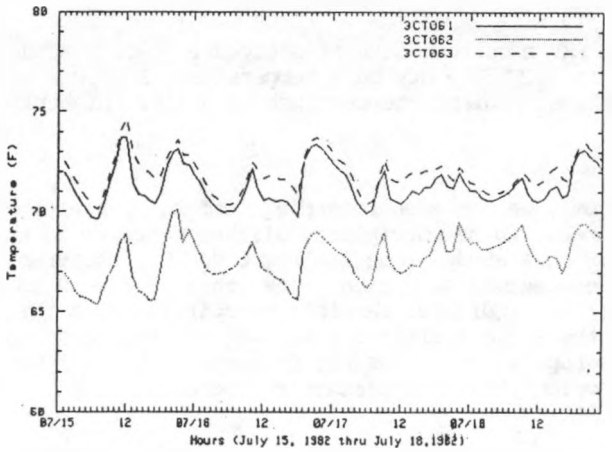

STRUCTURE THREE - SOUTH ROOM - DRY BULB & WET BULB & GLOBE TEMP

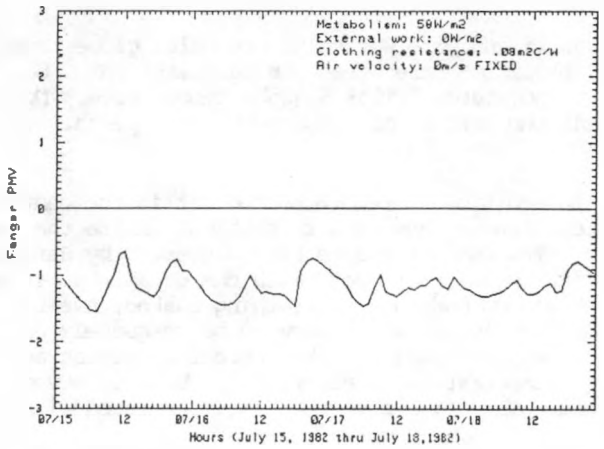

STRUCTURE THREE - SOUTH ROOM - FANGER PMV

Figures 21 and 22. Wet bulb, dry bulb, globe temperatures and PMV's inside south room of structure three. Two stage evaporative cooling is used from mid-morning until about 5:00 p.m. and single stage evaporative cooling is being used during all other times. Sensor notation: 3CT061 - dry bulb temperature, 3CT062 - wet bulb temperature, 3CT063 - globe temperature. The PMV has been calculated with an air velocity of 0 meters/second. Since the cooler is on, calculating in some air velocity would be more accurate.

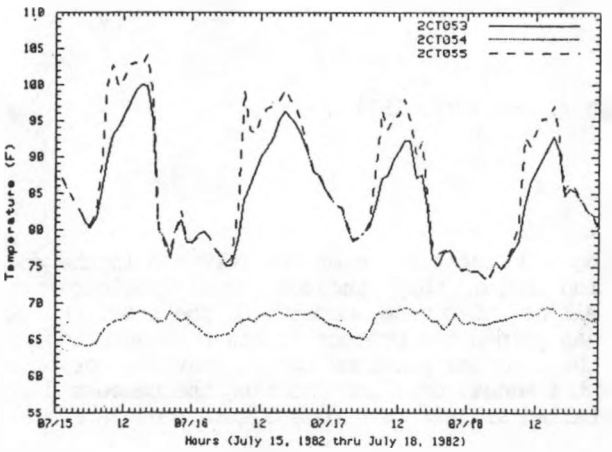

STRUCTURE TWO - SCREEN PORCH - DRY & WET & GLOBE TEMP

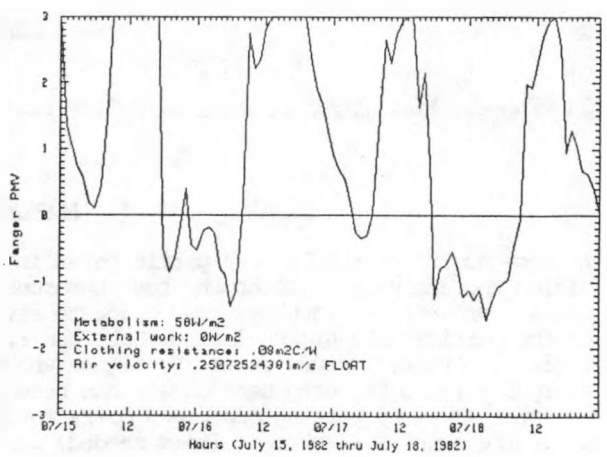

STRUCTURE TWO - SCREEN PORCH - FANGER PMV

Figures 23 and 24. Wet bulb, dry bulb, globe temperatures and PMV's on above grade screen porch of structure two. Actual air velocities are used to calculate PMV. Sensor notation: 2CT053 - dry bulb temperature, 2CT054 - wet bulb temperature, 2CT055 - globe temperature.

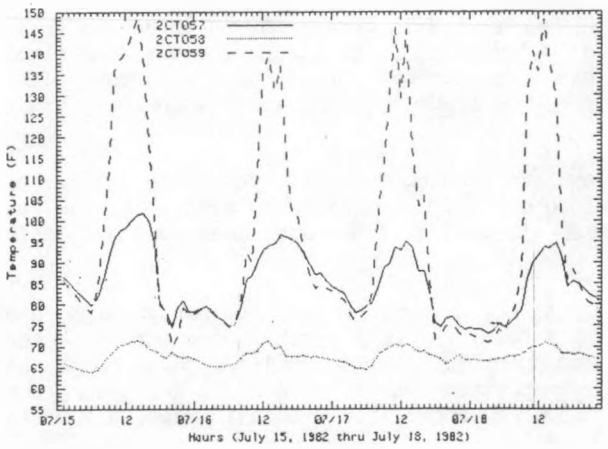

STRUCTURE TWO - ROOF DECK - DRY & WET & GLOBE TEMP

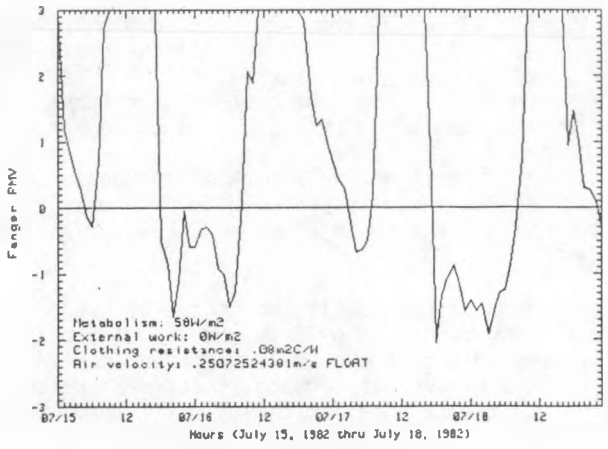

STRUCTURE TWO - ROOF DECK - FANGER PMV

Figures 25 and 26. Wet bulb, dry bulb, globe temperature and PMV's on roof deck of structure two. Actual air velocities are used to calculate PMV. Sensor notation: 2CT057 - dry bulb temperature, 2CT058 - wet bulb temperature, 2CT059 - globe temperature. Note high daytime radiant temperature and low nighttime radiant temperature as compared to roof porch.

In addition to recording comfort in the conventional manner, we are also recording comfort perceptions of researchers and staff sitting inside the test structures. These perceptions will be compared to the PMV's. Two comfort scales were suggested by Baruch Givoni for this study. One is from 0 to 9 (unbearably cold to unbearably hot with comfortable at 4) and indicates thermal sensation. The other is from 0 to 6 (forehead and body dry to clothing soaked, sweat dripping off) and indicates sensible perspiration. A third sensation which does not seem to be adequately documented in these two scales is a measure of stuffiness or air movement. Based on the thermal sensation and sensible perspiration scales the occupant might feel that the air temperature is acceptable. But air movement might provide the extra parameter necessary for true comfort. This data has yet to be correlated with the PMV's.

CONCLUSIONS

The above illustrated data shows that useful information is being obtained at the Passive Cooling Experimental Facility for a Hot/Arid Climate. Further work developing and validating computer models and developing design tools is needed and is being carried out in order to use the facility to its full potential.

REFERENCES

1. Fanger, P.O., Thermal Comfort, McGraw Hill Book Company, New York, 1970.

ACKNOWLEDGEMENTS

A large number of people have participated in the planning and construction of the PCEF and in the data acquisition and analysis. Although too numerous to mention here, they include local builders and architects, university faculty and graduate students as well as, of course, members of the staff at ERL. Some of the participants at ERL include Dr. John F. Peck who has guided the project in his role as principal investigator. Others include George V. Mignon who developed the computer programs for archiving, graphing and analyzing the data, Greg Lansdon who has been collecting the manual data and checking the sensors daily to make sure all is in working order and Barry Anthis who installed all six hundred and some sensors as well as most of the special electronic items needed.

PROJECT SUMMARY

Project Title:	Models for Generating Daylight and Sunlight Availability Data for the United States
Principal Investigator:	Claude L. Robbins
Organization:	Solar Energy Research Institute 1617 Cole Blvd. Golden, CO 80401
Project Goals:	Develop mathematical models suitable for generating daylight and sunlight availability for cities in the United States. Generate data for 80 U.S. cities.
Project Status:	Data for 80 U.S. cities have been generated and the final report is in preparation.
Contract Number:	EG-77-C-01-4042
Contract Period:	October 1, 1981, through September 30, 1982
Funding Level:	Subtask of task 1134: Daylighting Research
Funding Source:	U.S. Department of Energy

MODELS FOR GENERATING DAYLIGHT AND SUNLIGHT AVAILABILITY DATA FOR THE UNITED STATES

Claude L. Robbins Kerri C. Hunter

Solar Energy Research Institute
1617 Cole Boulevard
Golden, Colorado 80401

ABSTRACT

Little rigorous daylight and sunlight availability data have been established for the United States in a useful format for lighting designers. The most commonly used daylight data, found in the Illumination Engineering Society Handbook (reference 1), are based on work conducted in Washington, D.C., during the early 1920s (references 2 and 3). Durations of sunlight are based on weather station data published as monthly percentages of sunshine.

The exterior illuminance level and the frequency and duration of sunlight are important elements in the design, analysis, and evaluation of daylighting systems in buildings.

The daylighting laboratory of the Solar Energy Research Institute (SERI) is establishing daylight and sunlight availability data for select U.S. cities. This paper presents an overview of the mathematics and a sample of the daylight and sunlight availability data.

INTRODUCTION

The need for daylight and sunlight resource data has been recognized as a major issue in the design and analysis of daylighting systems. Many researchers have established exterior natural illuminance data based on empirical or analytical mathematics for a given locale. However, few attempts have been made to generate daylight and sunlight data based on empirical relationships between daylight and other weather variables for a wide range of climatic regions.

Used to generate hourly daylight availability data, the method is based on a modified version of the Solar Irradiance Model (SIM), called the Solar Illuminance Model (SIM2). Model output from SIM2 is total global illuminance E_G on vertical and horizontal surfaces on clear and overcast days, diffuse illuminance E_d on vertical and horizontal surfaces on clear and overcast days, and direct normal illuminance E_{DN}.

The method used to generate hourly sunlight availability data is based on the hourly solar radiation surface meteorological (SOLMET) observations (references 4 and 5) from the National Oceanic and Atmospheric Administration (NOAA). Model output is a percentage of average hourly sunlight availability.

THE ROBBINS AND HUNTER MODEL FOR GENERATING DAYLIGHT AVAILABILITY DATA

The General Model

We based the method used to generate hourly daylight availability data on computing exterior natural illuminance data on a surface of any orientation as a function of location (longitude and latitude), cloud cover, sky clearness, turbidity, altitude, and extraterrestrial illuminance for any of the Typical Meteorological Year (TMY) and Estimated Typical Meteorological Year (ETMY) weather stations.

The total instantaneous natural illuminance E_G on a surface is made up of three components: (1) the direct illumination E_D; (2) the diffuse sky illuminance E_d, and (3) the reflected ground illuminance E_g. These components make up the total illuminance, as given by

$$E_G = E_D + E_d + E_g \tag{1}$$

In the following sections we briefly describe the specific mathematical relationship used to derive these quantities for clear and overcast conditions, based on high and low turbidity climates.

Total, Direct, and Diffuse Illuminance for Clear Conditions

We calculated the direct normal illuminance E_{DN} using the equation

$$E_{DN} = E_{SC} e^{-\alpha} \tag{2}$$

where

E_{SC} = apparent extraterrestrial illuminance constant

α = atmospheric condition.

The atmospheric condition α varies in Eq. 2 with atmospheric turbidity.

For low turbidity conditions we see

$$\alpha_1 = \tau \sec \theta_o \tag{3}$$

where

α_1 = atmospheric condition, low turbidity

τ = total atmospheric optical depth

θ_o = solar zenith angle

The total atmospheric optical depth is made up of components because of the atmospheric attenuation of molecular scattering, aerosol/particulate scattering, and atmospheric turbidity. A monthly constant was used for τ for low turbidity climate conditions (reference 6).

For high turbidity conditions, we see

$$\alpha_2 = BmT \tag{4}$$

where

α_2 = atmospheric condition, high turbidity atmosphere

B = atmospheric extinction coefficient

m = optical air mass

T = turbidity factor.

The turbidity factor is given as

$$T = \frac{h + 85}{39.5\ e^{-w} + 47.4} + 0.1 = (16 + 0.22w)\beta \tag{5}$$

where

h = solar altitude

w = precipitable water in the atmosphere

β = turbidity coefficient.

The distribution of low and high turbidity areas in the United States is shown in Fig. 1.

The direct illuminance on a clear day ($E_{D,c}$) can be determined from

$$E_{D,c} = E_{DN} \cos \theta \quad , \tag{6}$$

where cos θ is the solar incident angle between the surface and the sun. For a horizontal surface, $E_{DH,c}$ would be

$$E_{DH,c} = E_{DN} \cos \theta_o \quad , \tag{7}$$

where θ_o is the solar zenith angle. The diffuse luminance on a horizontal surface on a clear day ($E_{dH,c}$) is

$$E_{dH,c} = (C)(E_{DN})/(CN_d)^2 \quad , \tag{8}$$

where C is the ratio of diffuse luminance to direct normal illumination, from Table 2, and CN_d is the sky-clearness number for daylight. Recent work done at SERI indicates that the sky-clearness number for daylight is approximately equal to the more commonly used clearness number CN.

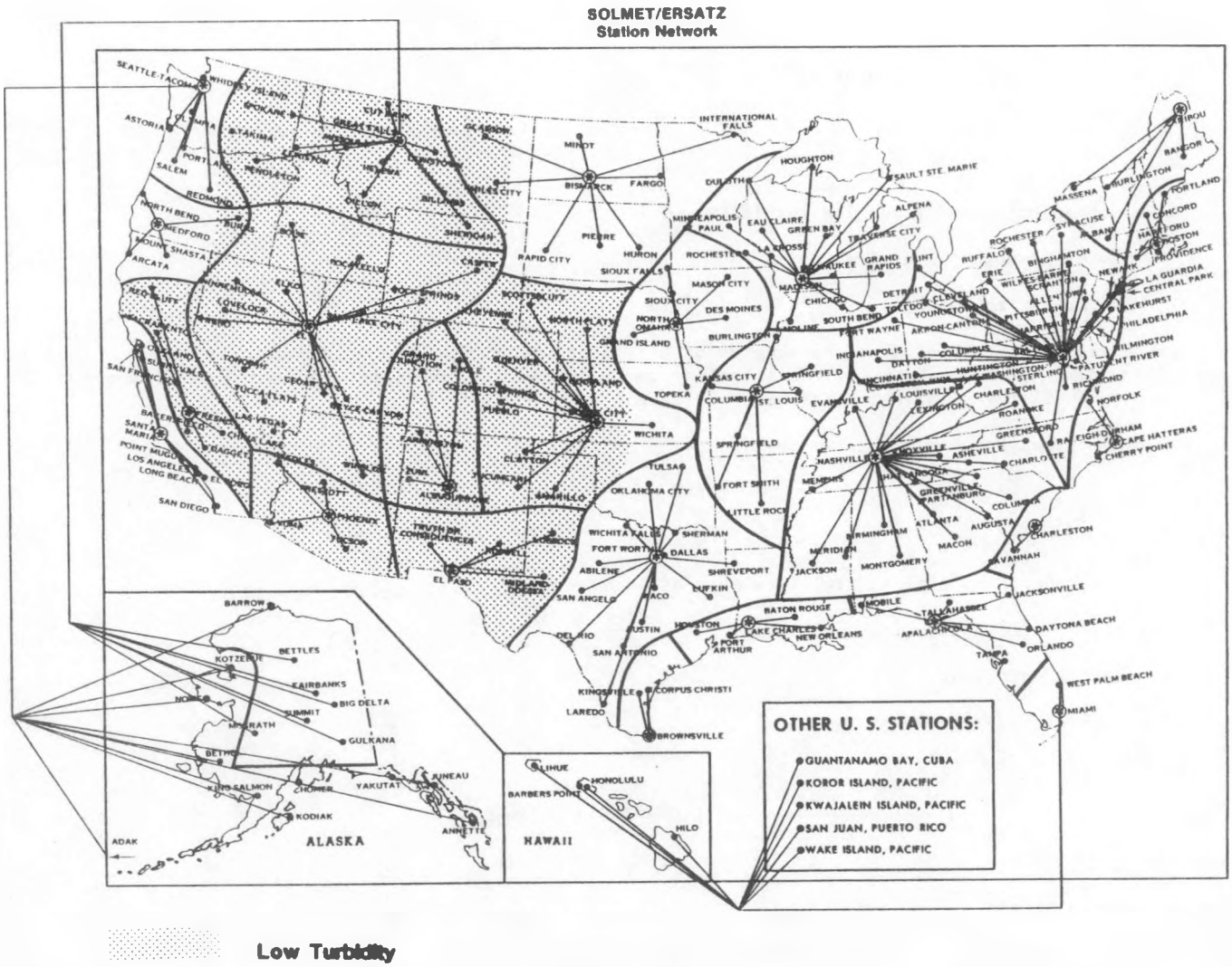

Figure 1. Distribution of Low and High Turbidity Areas

The ground-reflected component of daylight on a clear day is described as

$$E_{g,c} = (E_{GH,c})(F_g)(\rho_g) \quad , \tag{9}$$

where $E_{GH,c}$ is equal to the total illuminance falling on a horizontal surface on a clear day, F_g is the angle factor between the surface and the ground, and ρ_g is the reflectivity of the ground. The angle factor between the surface and the ground is

$$F_g = (1 - \cos \psi)/2 \quad , \tag{10}$$

where ψ is the angle between the surface and the ground. When the surface is horizontal, ψ equals 1, and the factor F_g equals 0. Therefore, the total global illuminance on a horizontal surface $E_{GH,c}$ is

$$E_{GH,c} = E_{DH,c} + E_{dH,c} \quad ,$$

where the direct and diffuse components are described by Eqs. 7 and 8, respectively.

The total global illuminance on a vertical surface, on a clear day is described by

$$E_{GV,c} = E_{DV,c} + E_{dV,c} + E_{gV,c} \tag{12}$$

where E_{DV}, E_{dV}, and E_{gV} are the direct, diffuse and ground reflected components on a vertical, respectively.

The direct illuminance is described by Eq. 6, while the diffuse component is described by Eq. 8 modified by the angle factor between the surface and ground, that is:

$$E_{dV,c} = (E_{dH,c})(1 - \cos \psi)/2 \tag{13}$$

When the angle factor between the surface and the ground is determined for a vertical surface, ψ equals 0 and the factor F_g equals 0.5. Thus, the total global illuminance on a vertical surface on a clear day, $E_{GV,c}$, is

$$E_{GV,c} = (E_{DN} \cos \theta) + (0.5\ E_{dH,c}) + \rho g(E_{dH,c} + E_{DN} \cos \theta_o)\ (0.5) \ . \tag{14}$$

Using a standard ground reflectivity of 0.2, Eq. 10 can be rewritten as

$$E_{GV,c} = (E_{DN} \cos \theta) + (0.5\ E_{dH,c}) + (0.1)\ (E_{dH,c} + E_{DN} \cos \theta_o) \ . \tag{15}$$

Calculations for vertical surfaces under clear skies were made for the primary (N,E,S,W) and secondary (NE,SE,SW,NW) compass headings.

Direct and Diffuse Illuminance for Overcast Conditions

The general equation for illuminance on a surface of any orientation under an overcast sky is

$$E_{G,o} = E_{D,o} + E_{d,o} + E_{g,o} \ , \tag{16}$$

where E_D, E_d, and E_g are the direct, diffuse, and ground-reflected components, respectively. Overcast values for illuminance can be determined from clear-sky values that have been modified for the cloud cover. Therefore, the total global illuminance on a horizontal or vertical surface for an overcast day is

$$E_{GH,o} = E_{DH,o} + E_{dH,o} \tag{17}$$

and

$$E_{GV,o} = E_{DV,o} + E_{dV,o} + E_{gV,o} \ . \tag{18}$$

The direct illumination on a horizontal surface under an overcast sky is

$$E_{DH,o} = E_{DH,c}\ K\ (1 - CC/10) \ , \tag{19}$$

where K and CC are cloud-cover modifiers developed by Kimura and Stephenson (1969).

The diffuse luminance on a horizontal surface for overcast conditions is

$$E_{dH,o} = E_{dH,c}\ [CCF - K\ (1 - CC/10)] \ , \tag{20}$$

where CCF is the cloud-cover factor described in reference 6. The direct illumination on a vertical surface for overcast conditions is calculated by

$$E_{DV,o} = E_{DV,c}\ \frac{E_{DH,o}}{E_{DH,c}} \tag{21}$$

where $E_{DV,c}$, $E_{DH,o}$, and $E_{DH,c}$ were calculated from Eqs. 6, 19, and 7, respectively.

The diffuse luminance on a vertical surface $E_{dV,o}$ with overcast conditions is determined from

$$E_{dV,o} = E_{dV,c}\ \frac{E_{dH,o}}{E_{dH,c}} \ . \tag{22}$$

The ground-reflected luminance on a vertical surface under an overcast sky, where $\rho_g = 0.20$, is

$$E_{gV,o} = (0.1)(E_{DH,o} + E_{dHo}) \ . \tag{23}$$

Using Eqs. 20, 21, and 23, Eq. 18 can be rewritten as

$$E_{GV,o} = [E_{DV,c}(E_{DH,o}/E_{DH,c})] + [E_{dV,c}(E_{dH,o}/E_{dH,c})] + (0.1)(E_{DH,o} + E_{dH,o}) \quad . \tag{24}$$

Assuming a uniform sky, illuminance distribution from an overcast sky is independent of orientation.

Model Output

For each hour on the 21st of the month we computed the following illuminance data:

- direct normal illuminance (E_{DN})
- total global illuminance, clear sky, vertical surface ($E_{GV,c}$) (for the primary and secondary compass orientations N, NE, E, SE, S, SW, W, NW)
- diffuse illuminance on a vertical surface ($E_{dV,c}$)
- total global illuminance, overcast sky, vertical surface ($E_{GV,o}$)
- total global illuminance, clear sky, horizontal surface ($E_{GH,c}$)
- diffuse illuminance, clear sky, horizontal surface ($E_{dH,c}$)
- total global illuminance, overcast sky, horizontal surface ($E_{GH,o}$).

A typical model output is illustrated in Table 1 (see references 7 and 8).

Table 1. Typical Model Output

LEXINGTON ,KY

	TIME	DIRECT NORMAL CLEAR (LUX)	NORTH VERTICAL GLOBAL CLEAR (LUX)	NORTHEAST VERTICAL GLOBAL CLEAR (LUX)	EAST VERTICAL GLOBAL CLEAR (LUX)	SOUTHEAST VERTICAL GLOBAL CLEAR (LUX)	SOUTH VERTICAL GLOBAL CLEAR (LUX)	VERTICAL DIFFUSE CLEAR (LUX)	VERTICAL GLOBAL OVERCAST (LUX)	HORIZONTAL GLOBAL CLEAR (LUX)	HORIZONTAL DIFFUSE CLEAR (LUX)	HORIZONTAL GLOBAL OVERCAST (LUX)	
	8	43855	3221	10598	36069	42298	25636	2090	2953	11303	4181	4921	16
	9	67072	5956	5956	46975	64435	47639	3197	7376	27585	6394	12293	15
	10	75780	7622	7622	40393	68633	61134	3612	10837	40094	7224	18062	14
	11	79486	8583	8583	26376	63846	68943	3789	13022	47941	7578	21704	13
JAN	12	80546	8901	8901	8901	53185	71528	3839	13768	50615	7679	22947	12
	13	79486	8583	8583	8583	38682	68943	3789	13022	47941	7578	21704	11
	14	75780	7622	7622	7622	22288	61134	3612	10837	40094	7224	18062	10
	15	67072	5956	5956	5956	6425	47639	3197	7376	27585	6394	12293	9
	16	43855	3221	3221	3221	3221	25636	2090	2953	11303	4181	4921	8
	7	19934	1292	9191	17712	16615	6541	934	923	3574	1869	1538	17
	8	63220	5277	20857	51969	55729	29936	2963	6160	23136	5927	10267	16
	9	76914	7653	13318	54034	67580	46022	3605	10948	40474	7211	18246	15
	10	82798	9257	9257	44562	68317	57474	3881	14649	53754	7762	24416	14
	11	85463	10215	10215	29079	61918	64470	4006	16982	62091	8012	28303	13
FEB	12	86244	10536	10536	10536	50343	66831	4043	17778	64934	8085	29629	12
	13	85463	10215	10215	10215	35241	64470	4006	16982	62091	8012	28303	11
	14	82798	9257	9257	9257	18387	57474	3881	14649	53754	7762	24416	10
	15	76914	7653	7653	7653	7653	46022	3605	10948	40474	7211	18246	9
	16	63220	5277	5277	5277	5277	29936	2963	6160	23136	5927	10267	8
	17	19934	1292	1292	1292	1292	6541	934	923	3574	1869	1538	7
	7	50597	4237	30985	49543	41561	11716	2671	4114	15658	5343	6857	17
	8	73186	7519	34287	66273	63842	28417	3864	9821	36552	7728	16368	16
	9	82188	9785	24410	63658	71348	42975	4339	14793	54456	8678	24655	15
	10	86523	11384	11384	51487	70001	54177	4568	18621	68158	9136	31034	14
	11	88594	12354	12354	33609	61941	61225	4677	21029	76761	9355	35049	13
MAR	12	89215	12680	12680	12680	48707	63630	4710	21851	79694	9420	36419	12
	13	88594	12354	12354	12354	31881	61225	4677	21029	76761	9355	35049	11
	14	86523	11384	11384	11384	13286	54177	4568	18621	68158	9136	31034	10
	15	82188	9785	9785	9785	9785	42975	4339	14793	54456	8678	24655	9
	16	73186	7519	7519	7519	7519	28417	3864	9821	36552	7728	16368	8
	17	50597	4237	4237	4237	4237	11716	2671	4114	15658	5343	6857	7

	TIME	NORTHWEST VERTICAL (LUX)	WEST VERTICAL (LUX)	SOUTHWEST VERTICAL (LUX)	
	8	10598	36069	42298	16
	9	5956	46975	64435	15
	10	7622	40393	68633	14
	11	8583	26376	63846	13
JAN	12	8901	8901	53185	12
	13	8583	8583	38682	11
	14	7622	7622	22288	10
	15	5956	5956	6425	9
	16	3221	3221	3221	8
	7	9191	17712	16615	17
	8	20857	51969	55729	16
	9	13318	54034	67580	15
	10	9257	44562	68317	14
	11	10215	29079	61918	13
FEB	12	10536	10536	50343	12
	13	10215	10215	35241	11
	14	9257	9257	18387	10
	15	7653	7653	7653	9
	16	5277	5277	5277	8
	17	1292	1292	1292	7
	7	30985	49543	41561	17
	8	34287	66273	63842	16
	9	24410	63658	71348	15
	10	11384	51487	70001	14
	11	12354	33609	61941	13
MAR	12	12680	12680	48707	12
	13	12354	12354	31881	11
	14	11384	11384	13286	10
	15	9785	9785	9785	9
	16	7519	7519	7519	8
	17	4237	4237	4237	7

TIME

DESCRIPTION OF THE MODEL FOR GENERATING SUNLIGHT AVAILABILITY DATA

General Model

As part of the analysis and establishment of rehabilitated hourly SOLMET data, the Air Resources Laboratory established a series of polynomial equations to determine solar radiation based on (1) the solar zenith angle; (2) the opaque cloudiness, or sky cover; (3) the minutes of sunshine; and (4) a precipitation counter. Based on measured minutes of sunshine SS from Campbell-Stokes recorders and solar radiation from a clear sky SRCS, solar radiation SR can be expressed by the following regression equation (see reference 9).

$$SR = SRCS\ (b_0 + b_1SS + b_2RN) \tag{25}$$

where RN is the precipitation counter data from the SOLMET control stations. If both sunshine and opaque cloudiness observations were available, then

$$SR = SRCS\ (d_0 - D_1SS - d_2OPQ - d_3OPQ^2 - d_4OPQ^3 - d_5RN) \tag{26}$$

where OPQ is the opaque cloudiness value from the SOLMET control station data. The values of the regression coefficients b and d for each of the control stations for which they are available are given in Tables 2 and 3.

Because SR data are available for each SOLMET station, using either Eq. 25 or 26 and solving for the minutes of sunshine, we can estimate sunlight availability for the SOLMET control stations and the derived SOLMET stations.

Control Cities for Which b and d Coefficients Exist

ARL used 25 of the 26 SOLMET control cities to generate SR data for the country. However, actual minutes of sunshine data were collected at only 15 of the 26 stations. Because of this, the b and d coefficients required for equations 25 and 26 were available for only 15 stations. These stations are

Albuquerque, NM,
Apalachicola, FL
Bismarck, ND
Boston, MA
Brownsville, TX
Cape Hatteras, NC
Columbia, MO
Dodge City, KS
El Paso, TX
Ely, NV
Fresno, CA
Great Falls, MT
Madison, WI
Nashville, TN
New York, NY

Table 2. Regression Coefficients for Sunlight Equation

Station	b_0	b_1	b_2
Albuquerque, N. Mex.	0.413	0.563	-0.212
Apalachicola, Fla.	0.375	0.552	-0.201
Bismarck, N.D.	0.371	0.598	-0.247
Boston, Mass.	0.257	0.655	-0.140
Brownsville, Tex.	0.359	0.585	-0.187
Cape Hatteras, N.C.	0.345	0.609	-0.178
Columbia, Mo.	0.347	0.609	-0.181
Dogde City, Ks.	0.351	0.592	-0.228
El Paso, Tex.	0.399	0.577	-0.207
Ely, Nev.	0.431	0.512	-0.287
Fresno, Calif.	0.294	0.680	-0.151
Great Falls, Mt.	0.408	0.504	-0.261
Madison, Wis.	0.342	0.597	-0.215
Nashville, Tenn.	0.302	0.648	-0.153
New York, N.Y.	0.250	0.703	-0.138

Table 3. Regression Coefficients for Sunshine and Opaque Cloud Equation

Station	d_0	d_1	d_2	d_3	d_4	d_5
Albuquerque, N. Mex.	0.666	0.337	-0.065	-0.167	-0.088	-0.145
Apalachicola, Fla.	0.568	0.440	-0.186	0.253	-0.344	-0.079
Bismarck, N.D	0.671	0.329	-0.166	0.411	-0.568	-0.215
Boston, Mass.	0.696	0.308	-0.531	0.647	-0.560	-0.121
Brownsville, Tex.	0.737	0.267	-0.237	0.676	-0.850	-0.170
Cape Hatteras, N.C.	0.640	0.360	-0.096	0.036	-0.252	-0.156
Columbia, Mo.	0.707	0.296	-0.395	0.850	-0.850	-0.141
Dodge City, Ks.	0.778	0.224	-0.245	0.455	-0.666	-0.180
El Paso, Tex.	0.648	0.354	-0.137	0.189	-0.343	-0.154
Ely, Nev.	0.798	0.201	-0.091	-0.018	-0.312	-0.179
Fresno, Calif.	0.706	0.295	-0.363	0.048	-0.005	-0.106
Great Falls, Mt.	0.828	0.173	-0.280	0.180	-0.404	-0.146
Madison, Wis.	0.808	0.198	-0.312	0.654	-0.833	-0.164
Nashville, Tenn.	0.664	0.344	-0.350	0.749	-0.768	-0.138
New York, N.Y.	0.503	0.502	-0.365	0.690	-0.604	-0.106

Control Stations for Which No b and d Values Exist

We merged the 11 control stations and accompanying regions for which no b values were generated into surrounding regions for which these values had been computed.

We used two tests to establish which regions should be merged:

- similar patterns of sunshine using NOAA data
- similar patterns of cloudiness using cloudiness index $\overline{K}_t$ data.

We allowed a deviation of ±5% for monthly values and ±3% for annual values in establishing the new regions, as this deviation already existed in each region. The new regions are shown in Fig. 2.

MODEL OUTPUT

Hourly Sunlight Availability

Using the calculated SS values, the sunlight availability SA is expressed as $SA_H = SS_H/SM_H$, where SM is the maximum number of minutes of sunlight in a given hour H. The sunlight availability for 0800 is based on data for the hour 0700 to 0800. The average sunlight availability for a given month (SA_M) is expressed as

$$SA_M = \frac{\sum_{i=1}^{n} SS_H/SM_H}{n} \tag{27}$$

where N is the number of days in the month the sun is shining during hour H. Data for Denver, Colo., is illustrated in Table 4 (reference 10).

Sunlight Availability by Standard Work Year

A standard work year is defined as 365 days from 0800-1700 hours for a yearly total of 3285 hours. However, many buildings operate on schedules other than the 0800-1700-hour work day. Table 5 lists a series of alternative standard work years, based on different operating schedules and associated total yearly hours of operation.

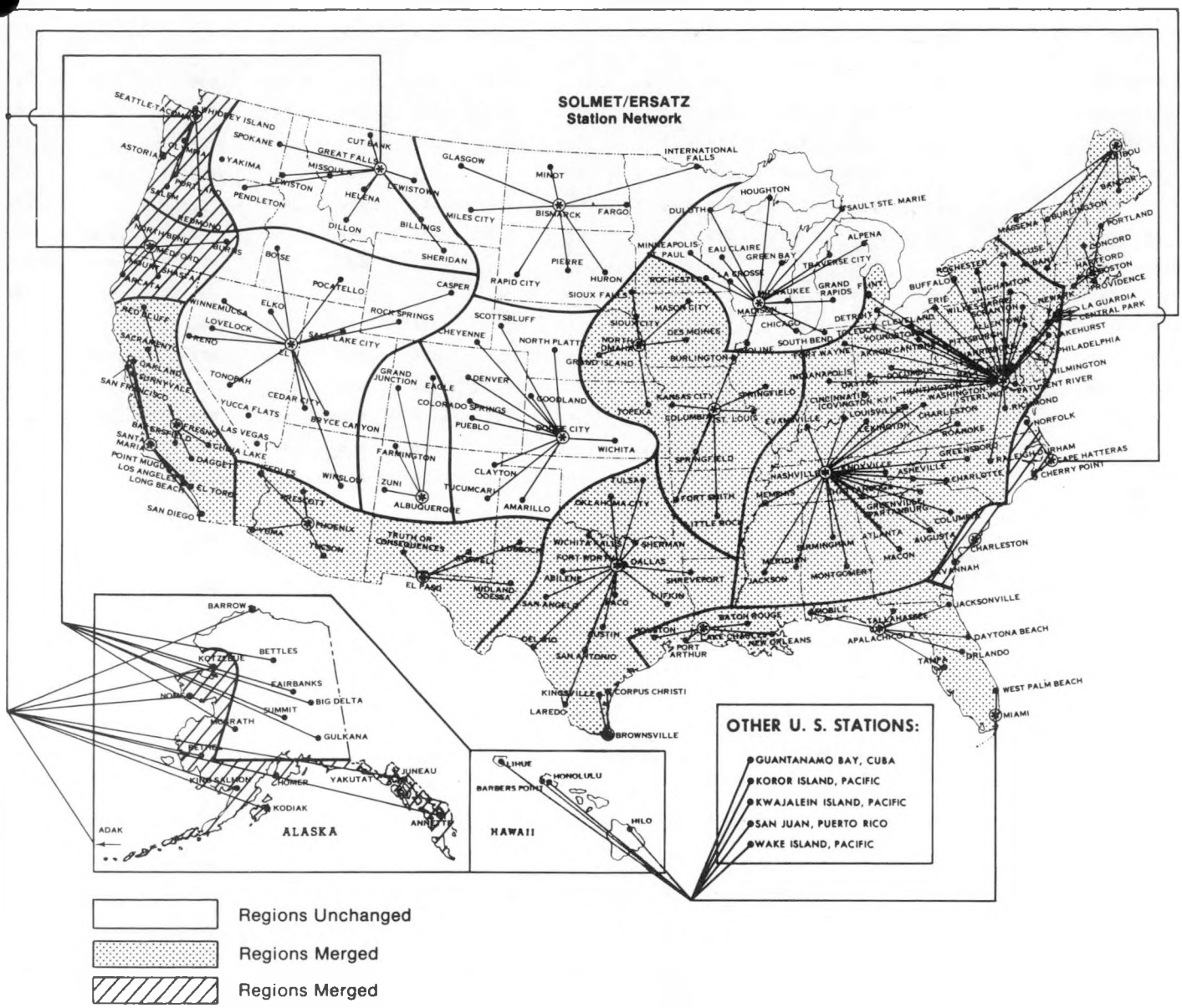

Figure 2. New Regions

The average sunlight availability for a given standard work year (SA_s) is expressed as

$$SA_s = \sum_{i=1}^{P} \frac{\sum_{i=1}^{n} SS_h/SM_h}{m} \Big/ p \qquad (28)$$

where m is the number of days in the year the sun is shining for each hour p in the standard work year chosen.

Typical sunlight availability data is illustrated in Table 6.

Table 4. Sunlight Availability for Denver, Colo.

HOUR, SOLAR	JAN	FEB	MAR	APR	MAY	JUN	JUL	AUG	SEP	OCT	NOV	DEC	ANNUAL FRACTION	ANNUAL HOURS
05:00-06:00	0.000	0.000	0.000	.339	.636	.782	.875	.376	0.000	0.000	0.000	0.000	.537	96.3
06:00-07:00	0.000	.146	.792	.754	.804	.790	.894	.823	.649	.288	0.000	0.000	.672	187.5
07:00-08:00	.621	.627	.805	.761	.790	.810	.911	.824	.822	.853	.729	.752	.777	283.8
08:00-09:00	.732	.642	.811	.755	.804	.818	.913	.830	.831	.860	.749	.798	.797	290.8
09:00-10:00	.754	.678	.843	.758	.786	.821	.896	.836	.846	.864	.744	.772	.801	292.3
10:00-11:00	.775	.750	.872	.764	.792	.823	.877	.852	.871	.851	.784	.784	.815	297.8
11:00-12:00	.818	.711	.829	.766	.796	.837	.864	.791	.866	.847	.812	.810	.813	296.7
12:00-13:00	.839	.721	.789	.734	.758	.794	.879	.754	.859	.852	.778	.822	.799	291.8
13:00-14:00	.854	.739	.745	.707	.717	.769	.814	.752	.861	.860	.763	.845	.788	286.8
14:00-15:00	.829	.716	.728	.675	.684	.774	.741	.710	.821	.854	.748	.878	.784	278.7
15:00-16:00	.831	.715	.704	.649	.649	.715	.641	.711	.797	.865	.747	.861	.741	270.3
16:00-17:00	.736	.731	.693	.623	.627	.694	.662	.724	.748	.855	.760	.818	.723	263.8
17:00-18:00	0.000	.150	.679	.639	.618	.712	.756	.718	.774	.278	0.000	0.000	.582	182.4
18:00-19:00	0.000	0.000	0.000	.227	.618	.699	.796	.335	0.000	0.000	0.000	0.000	.448	82.0
MONTHLY AVERAGE	.779	.610	.774	.654	.734	.774	.823	.717	.829	.760	.759	.814		
MONTHLY FRACTION	.779	.618	.735	.654	.669	.677	.720	.713	.746	.760	.721	.814		
MONTHLY AVG. HOURS OF SUNLIGHT PER DAY (HR)	7.8	7.3	9.3	9.2	10.3	10.8	11.5	10.0	9.9	9.1	7.6	8.1		

Table 5. Alternative Standard Work Years

Standard Work Year	Total Yearly Hours of Operation
0700-1600	3285
0700-1700	3650
0700-1800	4015
0700-1900	4380
0800-1600	2920
0800-1700[a]	3285
0800-1800	3650
0800-1900	4015
0900-1600	2555
0900-1700	2920
0900-1800	3285
0900-1900	3650

[a]base standard work year

Table 6. Sunlight Availability by Standard Work Year for Denver, Colo.

STANDARD WORK YEAR	JAN	FEB	MAR	APR	MAY	JUN	JUL	AUG	SEP	OCT	NOV	DEC	ANNUAL (SA_S)
07:00-16:00	.705	.644	.792	.732	.758	.795	.843	.788	.842	.799	.683	.732	.760
07:00-17:00	.708	.652	.783	.722	.746	.786	.827	.782	.834	.804	.690	.740	.756
07:00-18:00	.649	.610	.774	.716	.735	.780	.821	.777	.829	.760	.632	.678	.730
07:00-19:00	.599	.564	.715	.678	.726	.774	.819	.743	.765	.702	.584	.626	.691
08:00-16:00	.784	.700	.792	.730	.753	.796	.837	.784	.842	.856	.759	.814	.787
08:00-17:00	.779	.703	.782	.719	.740	.786	.820	.778	.832	.856	.759	.814	.781
08:00-18:00	.708	.653	.773	.712	.729	.779	.814	.773	.827	.803	.690	.740	.750
08:00-19:00	.649	.598	.708	.672	.720	.772	.813	.736	.758	.736	.632	.678	.706
09:00-16:00	.804	.709	.790	.726	.748	.794	.828	.779	.844	.857	.763	.821	.789
09:00-17:00	.796	.711	.779	.715	.735	.783	.810	.773	.833	.856	.762	.821	.781
09:00-18:00	.717	.655	.769	.707	.723	.776	.804	.768	.827	.798	.686	.739	.747
09:00-19:00	.652	.598	.699	.663	.714	.769	.804	.728	.752	.726	.624	.672	.700

CONCLUSION

We have used the preceeding models for generating sunlight and daylight availability data to establish data for 80 cities in the United States. The data is presented in a format useful to designers in designing and analyzing daylighting systems in buildings. The data can be used to:

- establish absolute illuminance in a space using the daylight factor method of analysis;
- establish absolute illuminance in a space using the lumen input method of analysis;
- establish absolute illuminance in a space for direct beam daylighting systems;
- predict energy savings in buildings using daylight availability (reference 11);
- determine the impact of daylight on the thermal interactions of a building using hourly daylight availability data or the Robbins and Hunter model with hourly thermal simulation computer codes; and
- determine the fraction of a workday that a given daylighting system is in operation.

REFERENCES

1. Illuminating Engineering Society, IES Handbook, Reference Volume (1981).

2. H. H. Kimball, I. F. Hand. "Sky Brightness and Daylight Illumination Measurement." Monthly Weather Review. Vol. 48: pp. 481 (1921).

3. H. H. Kimball. "Variations in the Total and Luminous Solar Radiation with Geographical Position in the United States. U.S. Weather Review. Vol. 47: pp. 769 (1919).

4. U.S. Department of Commerce. Hourly Solar Radiation-Surface Meteorological Observations. Vol. 1 Report No. TD-9724 (1978).

5. U.S. Department of Commerce. Hourly Solar Radiation--Surface Meteorological Observations. Vol. 2 Report No. TD-9724 (1979).

6. Tamami Kusuda. Heating and Cooling Loads Calculation Program. National Bureau of Standards, Thermal Engineering Systems Section, Building Environment Division, Center of Building Technology, Institute of Applied Technology. (1979)

7. C. L. Robbins, K. C. Hunter. Daylight Availability Data for Selected Cities in the United States. Solar Energy Research Institute, Golden, CO. (1982) SERI/TR-254-1696.

C. L. Robbins, K. C. Hunter. A Model for Generating Illuminance Data on Horizontal and Vertical Surfaces. Solar Energy Research Institute, Golden, CO. (1982) SERI/TR-254-1703.

9. G. F. Cotton. "ARL Models of Global Solar Radiation." Appendix VI. SOLMET User's Manual. Air Resources Laboratory, TD-9724. (1979).

10. C. L. Robbins, K. C. Hunter. Sunlight Availability Data for Select U.S. Cities. Solar Energy Research Institute, Golden, CO. (1982), SERI/TR-254-1687.

11. C. L. Robbins. A Method for Predicting Energy Savings Attributed to Daylighting. Solar Energy Research Institute, Golden, CO, SERI/TR-254-1664

NOMENCLATURE

$b_{0,1,2}$	regression coefficient
B	atmospheric extinction coefficient
C	ratio of diffuse luminance to direct normal illumination
CC	cloud cover modifier
CCF	cloud cover factor
CN_d	sky clearness number for daylight
$d_{0,1,2,3,4,5}$	regression coefficient
E_d	diffuse illuminance
E_D	direct illuminance
$E_{D,c}$	direct illuminance, clear day
$E_{d,o}$	diffuse illuminance, overcast day
$E_{D,o}$	direct illuminance, overcast day
$E_{dH,c}$	diffuse illuminance on a horizontal, clear day
$E_{DH,c}$	direct illuminance on a horizontal, clear day
$E_{dH,o}$	diffuse illuminance on a horizontal, overcast day
$E_{DH,o}$	direct illuminance on a horizontal, overcast day
E_{DN}	direct normal illuminance
$E_{dV,c}$	diffuse illuminance on a vertical, clear day
$E_{DV,c}$	direct illuminance on a vertical, clear day
$E_{dV,o}$	diffuse illuminance on a vertical, overcast day
$E_{DV,o}$	direct illuminance on a vertical, overcast day
E_g	ground reflected illuminance
E_G	total global illuminance
$E_{g,c}$	ground reflected component of daylight, clear day
$E_{g,o}$	ground reflected illuminance, overcast day
$E_{G,o}$	illumination on a surface of any orientation, overcast day
$E_{GH,c}$	total global illuminance on a horizontal, clear day
$E_{GH,o}$	total global illuminance on a horizontal, overcast day
$E_{gV,c}$	ground reflected illuminance on a vertical, clear day
$E_{GV,c}$	total global illuminance on a vertical, clear day
$E_{gV,o}$	ground reflected illuminance on a vertical, overcast day
$E_{GV,o}$	total global illuminance on a vertical, overcast day
E_{SC}	extraterrestrial illuminance constant
F_g	angle factor between the surface and the ground
h	solar altitude (degrees)
H	hour
K	cloud cover modifier

$\bar{K}_t$	cloudiness index
	optical air mass
M	month
N	number of days in month the sun is shining during hour H
OPQ	opaque cloudiness value
p	hour in a standard work year
RN	precipitation counter
SA	sunlight availability
SA_s	average sunlight availability for a given standard work year
SM	maximum minutes of sunshine possible
SR	solar radiation
SRCS	solar radiation from a clear sky
SS	sunlight observations
T	turbidity factor
w	precipitable water in the atmosphere
α	atmospheric condition
α_1	atmospheric condition for low turbidity
α_2	atmospheric condition for high turbidity
β	turbidity coefficient
θ	relative air mass
$\cos \theta$	solar incident angle between the surface and the sun
θ_o	solar zenith angle
p_g	reflectivity of the ground
τ	optic depth as a function of turbidity, molecular scattering, and particulate/aerosol scattering
ψ	angle between the surface and the ground

IOWA-PROJECT PASSIVE: A PROGRAM TO ACCELERATE PASSIVE SOLAR CONSTRUCTION IN IOWA

Philip H. Svanoe
Iowa Energy Policy Council
Des Moines, Iowa

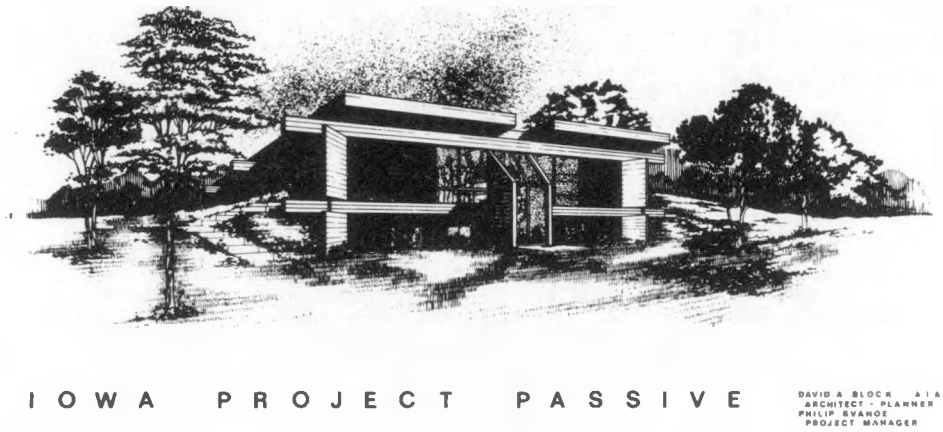

Figure 1

ABSTRACT

This paper describes a program of the Iowa Energy Policy Council (state energy office) to introduce passive solar technology into community college building trades curricula. The center of this program is a passive solar house design which has been built in four community colleges in Iowa in lieu of a more typical design. A description of the energy related features and preliminary data pertaining to performance of the passive solar house is presented. Also described are additional aspects of this program which include development of curriculum material and outreach programs to home building industry professionals throughout Iowa.

INTRODUCTION

It is the expressed goal of the Governor of Iowa and the Iowa Energy Policy Council to see a greater degree of passive solar technology incorporated in all new residential construction. The state of Iowa has adopted a goal of reducing 1985 residential energy consumption in new construction by fifty percent compared with 1979 Iowa thermal performance standards. It is believed that this goal is attainable in a cost effective manner by using known passive solar techniques.

The Iowa Energy Policy Council has developed a comprehensive passive solar information program which includes development of literature, seminars, design services, and demonstration projects. However, this paper will discuss only one component of the comprehensive program, Iowa-Project Passive.

PROGRAM DESCRIPTION

The Iowa-Project Passive Program was conceived in 1978 to introduce passive solar design and construction techniques to Iowa's future builders and contractors. Significant aspects of the program were to provide both tangible demonstrations of the technology via student construction of a passive solar house and to provide focal points for the distribution of information to the existing building industries and general public in the communities surrounding each school. It was the responsibility of each school in this program to hold seminars for builders, bankers, appraisers, and realtors as well as hold and publicize open houses for the general public. Energy usage is to be monitored and reported on over a period of three years.

DESCRIPTION OF HOUSE DESIGN

The house has two levels with 83.5 m^2 (899 ft^2) of living area on the lower level and 8.7 m^2 (94 ft^2) on the upper level for a total inside area of 171 m^2 (1,840 ft^2). Referring to Figure 2, you can see how the interior spaces have been designed to exploit the advantages and minimize the disadvantages of natural temperature variations. Sleeping rooms have been placed on the lower level which is anticipated to be cooler. The garage, utility spaces, closets and bathrooms are placed as buffers on the colder north side. All living spaces have a warm south exposure. The main entry is protected by the garage from the predominantly northwestern winter winds. In addition, this entry uses two doors as a "airlock" to reduce the introduction of outside area. Similiarly, small wing walls shield doors from north winds at the south end of the east and west elevations. As a further means of saving energy, the east, west, and north walls have earth-sheltering berms extending halfway to the eaves as can be seen in the elevations., Figure 2 .

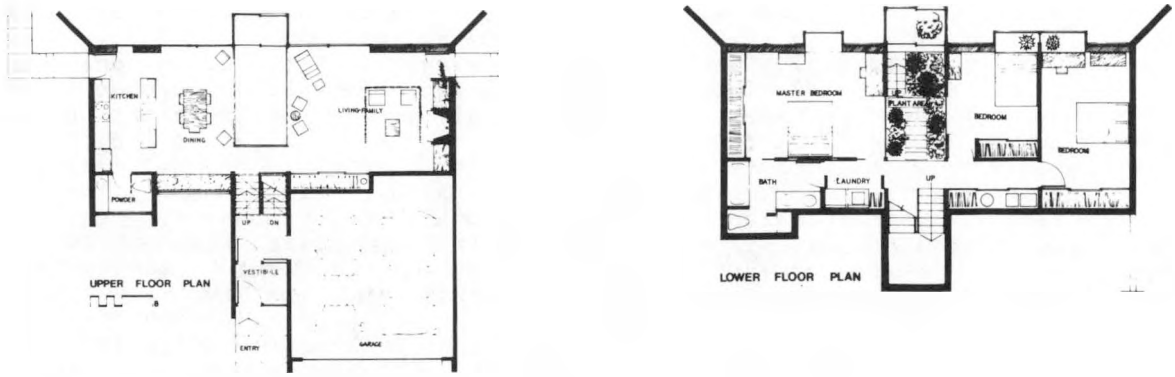

Figure 2

The objectives of the energy efficient design approach used for this building were to: 1) reduce the need for heating energy by cost-effective energy conservation measures, 2) supply a significant fraction of the required heating energy by passive solar techniques, 3) use an efficient means of supplying the remaining auxiliary heating energy, and 4) minimize the requirement for other uses of energy by the use of an active solar domestic hot water heater and energy efficient appliances.

The principle energy conservation measure used was to reduce the heat loss of the envelope. The envelope of this house is insulated significantly better than required by Iowa's thermal efficiency standards (which are based on ASHRAE standard 90-75). The above grade walls are insulated to R30 and below grade walls and the perimeter of the lower

The objectives of the energy efficient design approach used for this building were to: 1) reduce the need for heating energy by cost-effective energy conservation measures, 2) supply a significant fraction of the required heating energy by passive solar techniques, 3) use an efficient means of supplying the remaining auxiliary heating energy, and 4) minimize the requirement for other uses of energy by the use of an active solar domestic hot water heater and energy efficient appliances.

The principle energy conservation measure used was to reduce the heat loss of the envelope. The envelope of this house is insulated significantly better than required by Iowa's thermal efficiency standards (which are based on ASHRAE standard 90-75). The above grade walls are insulated to R30 and below grade walls and the perimeter of the lower level slab are insulated to R15. The ceiling/roof structure is 35 cm (14 in) deep flat trusses insulated to R45. A skylight is formed over the entry stairs for daylighting and heat gain. The opaque frame of this skylight is insulated to R21 and a R10 insulated flap closed the skylight well at night. Attention has been paid to insulating details to assure that there are no direct paths for heat leaks. Examples of this are polystyrene thermal breaks between the unheated garage foundation and the house and hollow headers and beams filled with insulation.

To minimize infiltration and water vapor transmission, all interior surfaces of exterior insulated wall assemblies are covered with a 6 mil polyethylene vapor barrier with joints caulked and taped. Small self-contained air to air exchangers are used to assure proper ventilation to control indoor air quality. These are multi-speed to allow 1/2, 3/4, and 1 air changes per hour with a 70% efficiency of total (sensible and latent) heat recovery from the exhaust air to the outside air.

The result of these energy conservation measures is a residence with a calculated 14.8 GJ/^{o}C-day (7,800 BTU/^{o}F-day) gross load (including south glazing losses). This is less than half of the gross load of a building of comparable size insulated to comply with current Iowa thermal efficiency standards.

Three passive solar techniques are used to supply heat energy. These are: 18.6 m^2 (200 ft^2) of direct gain, 7.4 m^2 (80 ft^2) of isolated gain, and 20.4 m^2 (220 ft^2) of thermal mass wall. By referring to Figures 1 and 2, you can see the arrangement of these. The direct gain consists primarily of fixed glass with several operating awning units for ventilation and emergency egress. Twenty cm (8 in) thick, precast, hollow core concrete slabs covered with 5 cm (2 in) of concrete topping and quarry tile are used behind the direct gain apertures on the upper level for thermal storage. A two story sunspace is used in the center of the house for isolated gain. Interior walls and the floor of this sunspace are covered with 10 cm (4 in) masonry units to serve as thermal mass and are in direct thermal contact with the rest of the house. Sliding glass doors allow the sunspace to be connecting with the interior spaces and the outdoors for convective heat transfer. Thermal walls are divided into 6.7 m^2 (72 ft^2) on the lower level and 13.7 m^2 (148 ft^2) on the upper level. They are formed from 25 cm (10 in) thick concrete blocks with the cores grouted solid and fixed glazing installed in site-built mullions.

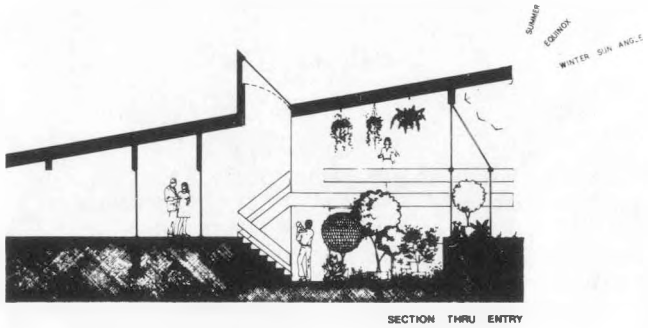

Figure 3

Two rather unusual features of these walls are that they are unvented to the inside and they have a selective outer surface. They are not vented to the inside because the direct gain aperture supplies the heat needed during the day and hence there is no need for convective vents. By not installing vents, the installation was simplified and the possibility of dust and insects entering the air gap was avoided. The air gap between the glass and the wall is vented to the outside during the summer to avoid overheating.

In an effort to improve the net output of the mass walls, the use of movable insulation, triple glazing, and a selective surface was investigated. It was decided to use a selective surface based on the expectation of higher performance and a lower first cost.

Berry Solar Products was contacted for a sample sheet of theird SolarStrip which is a black chrome over bright nickel selective surface applied to a .012" copper foil substrate. This has a high absorptivity of 0.95 and a low emissivity of 0.10. In addition, the 3M Corporation was asked for their recommendation of an adhesive suitable for adhering the foil to a concrete block wall. They sent samples of thier Isotak Y9469 and Veristrate SJ8056 double sided sheet adhesives. They are both similar with Isotak having better strength of high temperatures and Veristrate being less expensive.

Summer overheating is further avoided by the use of a roof overhand. In addition, canted front walls at the east and west side protect the glass from the low morning and evening summer sun.

The auxiliary heat requirement is supplied by a high efficiency (80%) downflow gas furnace. The furnace blower can be used as a heat distribution mechanism without the furnace turning on. An inlet grill picks up heat at the high ceiling level on the south side. This heat, which otherwise may have been vented and wasted, is pulled through a duct and injected into a plenum formed by raising the lower level subfloor 15 cm (6 in) above the slab. Some of the beat is stored in the slab and the rest heats the lower floor giving a radiant effect. The air leaves the plenum through perimeter slots.

PERFORMANCE PREDICTION

The predicted thermal performance of the project house was compared to that of an assumed reference house. This reference house, typical of speculatively built homes in Iowa, was of a similar size and configuration but did not have the passive solar features and was insulated to comply with the ASHRAE 90-75 standard. With all south facing glass on the reference house assumed to be adiabatic, its gross heaing load would be 111 GJ (105 MM BTU) annually in a 3667°C-day (6600°F-day) climate.

The thermal performance of the passive solar deisgn was estimated using the Solar Load Ratio method. A summary of the result of this is shown in Table 1. The predicted annual auxiliary energy requirement of 12.7GJ (12.1 MM BTU) would require 487 m^3 C172 CCF) of natural gas worth $86 at the current price of $0.50 per 2.8 m^3 (CCF). This compares to an annual estimated heating bill of $525 for the reference house. As another measure of performance the energy utilization index of the passive design is .02 KJ/°C-day-m^2 (1 BTU/ F-day-ft^2) compared to .17 KJ/°C-day-m^2 (8.6 BTU/°F-day-ft^2) for the reference house.

TABLE 1-THERMAL PERFORMANCE PREDICTION

MONTH	HEAT LOAD GJ	SOLAR HEAT GJ	SHF	AUX. HEAT. REQ. GJ
Sept.	.48	.50	100	0
Oct.	2.88	2.90	100	0
Nov.	7.04	5.92	84	1.11
Dec.	10.60	6.83	64	3.78
Jan.	11.91	7.83	66	4.07
Feb.	9.82	7.45	76	2.37
Mar.	7.83	6.56	84	1.27
Apr.	3.56	3.44	97	.12
May	1.24	1.26	100	0
Jun	0	0	0	0
ANNUAL	55.37	42.67	77	12.72

PROJECT EXPERIENCE TO DATE

The Iowa-Project Passive house has been built by college trade school programs in four locations in Iowa. Aside from the typical disgruntlement between builder and architect regarding the level of detail and accuracy of plans, the construction progressed smoothly with completion occurring in the spring of 1982. Materials for the house averaged $46.069 (1979 dollars) and the 1979 estimated materials cost was placed at $40,000, representing a slight over-run. The performance of the Iowa-Project Passive home is being monitored wit the Aeolian Kinetics Data Acquisition System. Data will be collected during the 1982-83 winter and 1983 summer.

CONCLUSION

The major emphasis of this project is sociological, rather than technical in nature, however. The Iowa Energy Policy Council desired to influence the Iowa building trade toward a greater awareness of passive solar principles in an attempt to accelerate their incorporation into all residential construction in Iowa. The rather contemporary and protrusive display of the three major passive solar design techniques in the design was considered justified given this purpose. While this project has served to highlight passive solar techniques, experience by builders has taught them a more practical, moderated approach to the use of these design techniques. A well insulated, tight house with moderate amounts of south glazing and internal mass areas will in all cases more practically and economically achieve the same level of energy conserving performance. However the publicity value of this contemporary design has been instrumental in influencing the industry and general public. The participating schools have experienced unprecedented interest as evidenced by the attention given to them by the media and in attendance records in seminars and openhouses given as part of the outreach aspect of this project.

Project Summary

Project Title:	Construction, Instrumentation and Testing of the REPEAT facility.
Principal Investigator:	C. Byron Winn
Organization:	Colorado State University Mechanical Engineering Department Fort Collins, CO 80523
Project Goals:	Provide class A data for the validation of computer codes, developed under DOE contracts and elsewhere, for simulating passive solar heated buildings. Perform fundamental studies of heat transfer processes in passive buildings; apply parameter estimation techniques to the observed weather and building responses to facilitate the characterization of these processes.
Project Status:	The house electrical system has been modified extensively and numerous other improvements have been made to the structure to facilitate the installation of transducers and future changes in the building configuration. Installation of cables and transducers is about 60% complete. Over 200 data channels will eventually be installed. The real-time data reduction system is essentially complete except for the uninterruptible power supply. A second microcomputer for program development is being assembled. Many of the basic data handling programs and subroutines have been written and tested. Rudimentary data acquisition and reduction is now routinely performed in association with preliminary experiments. Some of the important initial testing has been completed. Infiltration rates have been characterized under steady uniform interior/exterior pressure differences. Experiments have been performed to establish the magnitude of transducer installation errors and errors due to inhomogeneity of building materials. Details of building components and construction, building dimensions, and transducer locations have been provided to Los Alamos National Laboratory for compilation of a site handbook.
Contract Number:	C00-30259-2
Contract Period:	January 1980 - December 1983
Funding Level:	$125,000
Funding Source:	U. S. Department of Energy

REPEAT Facility Status Report - September 1982

Doug Swartz, Ed Hancock, Peter Armstrong, C. Byron Winn
Colorado State University
Fort Collins, CO 80523

This report summarizes the current status and plans for the immediate future for the REPEAT facility at CSU. Progress is being made on a number of fronts which are described in separate sections below.

I. Building

Various measures have been taken to make the facility more workable and to prepare for the instrumentation installation and tests. A catwalk and ladder have been installed to give better access to the roof mounted instruments. Galvanized steel rain gutters have been suspended throughout the interior of the building to serve as low cost conduits for sensor leads. The gutters allow flexibility for future changes and also provide secondary electromagnetic shielding for the transducer leads. A well-insulated closet has been built to reduce the rates and amplitudes of temperature changes around the data logger's remote scanner box. This has reduced temperature gradients on the multiplexing boards to the point where channel offset errors agree to within 2 microvolts on any given scan for all 200 channels. Air-to-air heat exchangers have arrived but have not yet been installed. The entire building has been marked out in a metric coordinate system which can be used to unambiguously identify the location of transducers and other system components.

An 8 inch thick brick wall (bricks donated by Robco; skilled masonry labor donated by Soderberg Masonry) is about to be installed. This wall will span the interior of the building from east to west (40') and from the lower level floor to within 2' of the upper level ceiling (19'). The remaining 2' will be framed in. The wall will be situated 8' north of the principle solar gain aperture (the existing south wall of the building). A sunspace, coupled by a mass wall to the main space, will thus be created. This will be the first passive solar heating configuration to be monitored in the REPEAT building.

II. Instrumentation

Transducer locations were chosen and numbered according to a coordinate system defined for the building, so as to leave no ambiguity as to placement. Cables have been strung to transducer locations, with only a few remaining to be installed (primarily to outdoor locations). Careful attention is being paid to proper grounding and shielding techniques.

Transducers are currently being installed at most locations. Terminal strips where junctions occur between sensor and cabling are being enclosed in foam containers in order to provide spatially isothermal conditions; this is crucial to our goal of obtaining thermopile measurements to $\pm$(.25 Kelvin + 2% of reading) accuracy. We are experimenting with a variety of mounting techniques for the thermopile junctions and heat flux meters. Small diameter (#30 AWG) thermocouple wire is being used where conduction and radiation effects pose a problem.

Thermocouple junctions and heat flux meters were situated at a number of locations in the slab, and in the ground below, before the slab was poured. However, the contractor made some last minute changes which may affect the heat flux through these areas. No sensors were embedded in the concrete walls of the lower level when they were poured. In order to check the feasibility of installing thermocouples in the concrete walls, and in the concrete floor near one of the previously instrumented locations (as a back-up) two 8 inch cores were drilled, and small diameter (1/8 inch) holes drilled at right angles to these at the desired depths. Thermocouples have been installed in these holes. It appears that by drilling the 1/8 inch holes deep enough, and replacing the concrete core, the temperature profiles at the instrument locations are probably representative; i.e. undistorted by the installation. An experiment has been run to determine whether the measurements obtained in this type of installation are sufficiently representative of temperatures in the undisturbed slab. In this experiment a step change in temperature is imposed on the top suface of the slab by forming a pool of ice water there. The response of the slab/ground system to this step change is measured by both the originally embedded thermocouple junctions and by the subsequently installed thermocouple junctions. Temperature gradients parallel to the surface are also measured by recording temperatures at different distances outside the circumference of the 8 inch diameter access hole; i.e. at different depths into the 1/8 inch holes. After data from this experiment are analysed the decision will be made as to whether to drill similar core holes in other wall and slab locations, or whether to rely on existing slab instrumentation and, in the walls, to rely on surface transducers only.

Kipp and Zonen CM-5 (double domed) pyranometers are being used. These have been procured without base, shield, or thermal compensation networks, which are being fabricated here. A shadow band pyranometer stand has been built and installed. When the pyranometers arrive they will probably be sent to NOAA in Boulder, CO, for a doublecheck of the factory calibrations. Five pyranometers will be used; total horizontal, diffuse horizontal, total vertical, plus

two 'floaters' which will be used for a variety of things, including measuring transmitted radiation through the glazing.

Wind and outdoor temperature measurements will begin when the data logger's pulse counting interface has been modified to match the impedance and voltage of the anemometer signal. Barometric pressure and humidity measurements are also planned. Sensor calibrations and checks of the wiring will soon be undertaken, prior to the start of data collection. We plan to investigate the effects of changes in sensor placement in several cases; for example, of concern are variation in heat flux over and in the vicinity of the studs in a stud wall, and problems which will arise in trying to measure heat flux through, and temperature differences across, glazings in the presence of solar radiation.

III. Data Acquisition / Microcomputer System

One of the biggest holdups has been the Acurex Autodata Ten/10 data logger which is on loan from SERI. It suffered intermittent problems which made attempts at logging and recording data very unpredictable. A fault was found in one of the two CPU boards but some problems remained after exchanging this component. The entire data logger was then returned to the factory. The keyboard and motherboard were replaced and the data logger has been functioning properly since then. We are now able to use it with some confidence and to exploit more of its options, such as the GPIB and serial ports.

The microcomputer system is taking shape. It centers around a single board computer and S100 bus, with I/O provided via RS-232 ports, GPIB interface and tape interface to console, printer, data logger, floppy disk drives and tape drive. About one half of the equipment is here, the remainder being on loan by project personnel temporarily, for system development.

Program development is underway. Data logger communications are being handled through the serial ports until a GPIB software driver has been written. The I/O routines are being written, as well as auxiliary programs for general use and to handle basic data reduction tasks. The thermopile conversion routines for T and J thermocouple types are running. Routines have been written to assign labels, sort, and verify channel assignments. The basic program to log, convert to SI units, and display logged data has also been written. Most of the remaining real-time programming work will involve the calculation of hourly heat transfers and changes in stored energy within the building, and the calculation of heat balance closure errors. The programs for batch deferred processing must also be written. Batch processing will include programs that essentially duplicate the real-time data reduction programs and will also include programs for parameter estimation.

IV. Infiltration

Infiltration tests were performed on the building using a blower door loaned to us by the University of Colorado in Boulder. Initial runs revealed rates of about 0.6 air changes per hour (ACH) at 4 Pa pressure difference. By running in a subatmospheric pressure mode, it was possible to locate many places were air was entering and these were caulked and sealed in other ways (approx. 30-40 tubes of caulk were used!). The infiltration rate was gradually reduced to approximately .07 ACH at 4 Pa and 0.5 ACH at 50 Pa; further substantial reduction seems unlikely. It was noted that leakage around operable windows was not a major component in the remaining infiltration, which is somewhat surprising as leaks could be felt. The infiltration tests are discussed in greater detail in Appendix A.

Negotiations are underway to borrow tracer gas injection/monitoring equipment in order to verify these results and to gain further insight into the infiltration mechanisms. Continuous monitoring remains a possibility. Long term goals include developing a model based on wind velocity and temperature difference. The model may be used to predict infiltration rates, which, although small in this buildng compared to many other buildings, are still of sufficient magnitude to affect the energy balance significantly.

Appendix A
REPEAT Infiltration Studies - Blower Door Tests, May-June 1982

Introduction

Infiltration, (or uncontrolled air leakage through a building shell), can be responsible for a significant fraction of heating and cooling requirements in residential buildings. About 30% of space heating needs is a common estimate. But infiltration is a particularly difficult quantity to estimate because it depends upon such things as architectural design (especially structural and finish details) and the quality of workmanship in construction. In contrast, conduction heat losses depend upon relatively well known material properties. After a structure has been built, however, tests can be performed to estimate the crack leakage area of the building, and therein lies the usefulness of a "blower door"

A blower door typically consists of a panel containing a fan that can be sealed into an exterior doorway of the building. The fan is then used to depressurize the building relative to the outside and the mass flow of air exhausted by the fan, which is equal to the infiltration induced through cracks and vents, can be measured as a function of pressure difference. A description of infiltration characteristics is developed by making these measurements at different fan speeds.

It is especially important to use the blower door at the REPEAT Facility at this time because the major objective of tests at the facility will be to carefully measure all energy flows in the building. Since it is very difficult to make an a priori estimate of infiltration, the blower door tests provide the first information on the magnitude of infiltration heat transfer in the building. In addition, the blower door is extremely useful in locating cracks so that they can be repaired, and uncontrolled ventilation in the test facility can be reduced to a low level.

This report describes the procedures used in blower door tests at REPEAT and presents results to show how the building was progressively tightened. The infiltration characteristics of the building in its final state are also presented.

Equipment and Test Procedures

The equipment used for these tests was provided by Ener-Corp Management, Ltd., through the University of Colorado College of Environmental Design. The "infiltrometer" equipment includes an aluminum frame that is adjustable to fit standard door sizes, a door-size molded plastic panel that houses the fan and motor, and is held in the frame by four clamps, a venturi-nozzle to measure air flow, and a control panel cart that includes a programmable calculator. Two oil manometers are mounted on the door panel - one measures pressure difference across the building shell; the other is used to determine the velocity at the throat of the venturi.

A program for the TI-59 calculator is supplied by Ener-Corp to perform data analysis. Initial inputs to the program include the volume and surface area of the building, air temperature at the nozzle, and barometric pressure. The program calculates mass flow of air through the venturi from the manometer reading and is corrected for density changes due to temperature and atmospheric pressure. Pairs of manometer readings are entered into the program and from these data the program performs a least squares regression to determine parameters for the classical infiltration model

$$\dot{m} = C(\Delta P)^N$$

where:

$\dot{m}$ = infiltration mass flow rate

ΔP = pressure difference across building shell

C,N = empirical parameters.

The values of C and N that are determined by the least squares algorithm are the values that minimize the root-mean-square (RMS) deviation of the modeled value of $\ln(\dot{m}) = \ln(C) + N \ln(\Delta P)$ from the measured value of $\ln(\dot{m})$ at each of n data points, i=1,n. The RMS deviation is

$$\left[1/n \sum_{i=1}^{n} (\ln(\dot{m}_i) - \ln(C) - N \ln(\Delta P_i))^2\right]^{1/2}$$

This log transformation results in least squares parameter estimates that tend to reduce the percentage (rather than absolute) errors in $\dot{m}$, which is actually the more desirable criterion.

Other parameters calculated by the program include the equivalent total leakage area of the building, the air changes per hour at 4 Pa and 50 Pa, and the air leakage rate per unit of surface area. The correlation coefficient is also printed. A sample printout from a program run is shown in Figure A.1.

For a typical run of the infiltrometer, the fan is set to its maximum power, the two manometers are read and the data are entered into the calculator program. The fan speed is then reduced and more readings are taken.

This is repeated until a minimum of four approximately evenly spaced points are obtained, an entire run typically taking less than five minutes. For tests done at REPEAT, wind speed was always less than 2 m/sec and inside-outside temperature difference less than 10 Kelvins to give confidence that the only significant ΔP was that developed by the blower door fan.

Test Results

While the blower door tests were being conducted at REPEAT an effort was made to seal all major leaks. Most of these leaks involved construction details that might have been sealed during original construction with relative ease. Figure A.2 shows the general progress in tightening the building during the tests and indicates that the leakage area was reduced by nearly a factor of ten. To accomplish this, a total of 40 tubes of butyl, latex and silicone caulk were used along with 200 ft. of one inch diameter foam rubber and 10 square feet of styrofoam board. An estimated 80 person hours was spent in sealing the building.

The primary leaks mentioned in Figure A.2 are generally located where two building components intersect. Areas around the beams and columns were major leakage problems because cracks remained where the steel or wood intersected the wall board. Leakage associated with electrical fixtures appeared at the wall board penetrations. Even leakage associated with windows appeared to be due to spaces left between drywall and the manufactured window unit, and were not due primarily to cracks within the window unit. This result was a pleasant surprise because the windows are standard production units (donated by Marvin Windows) and a considerably larger infiltration rate was expected due to the large (60 m2) total window area and the large number (33) of operable units. The most unusual leakage site was around the perimeter of the basement where the concrete slab intersects the concrete basement walls. This is a particularly curious finding since most of the basement perimeter is six feet below grade.

After sealing of the building was completed, a series of tests was conducted to determine the effects of several important parameters. The infiltrometer was used to pressurize as well as depressurize the building to see if the remaining leakage behaved differently under these two conditions. Because the very high pressures used in most tests are not typical of weather induced infiltration, some tests were made at much lower pressures in an attempt to detect any difference in results. Another interesting test involved opening holes of known size and shape in the building shell to check the equivalent leakage area calculations of the Ener-Corp program. The most important effort was to determine the contributions of operable windows and electrical outlets to the total leakage area.

The results of these tests are presented in Tables A.1 and A.2. Here a difference in the building response to pressure as opposed to suction is apparent. The tests with known openings indicate that confidence can be placed in the equivalent area calculations. It can also be seen that tests at lower pressure differences did not produce significantly different results from those obtained with very high pressures differences. The tests in which window and electrical outlet cracks were taped show the interesting result that the two separate effects are of approximately the same magnitude but that neither accounts for more than 10% of total remaining leakage.

Discussion

The most important points observed from the blower door tests are noted as follows:

- Most of the leakage sites found at the REPEAT facility were due to lack of attention to construction details by both craftsmen and designers. Sealing the building better during initial construction would have taken much less time than was eventually spent on repairing leaks.
- It appears that the infiltration paths that remain in the REPEAT building must be very diffuse because it is very difficult to detect air flows even at high pessure differences (200 Pa).
- The windows in the facility were found to contribute very little to the total remaining crack area. This is an important observation on the general question of infiltration in passive solar buildings. Since it has been widely thought that windows contribute significantly to infiltration and since passive buildings may have more glazed area than the average building, there has been concern that infiltration rates would be higher. For the REPEAT facility at least, this does not seem to be the case.
- Many of the paths for air flow are very indirect and some leakage sites are counter-intuitive. The roundabout nature of air flow through the walls and beneath the slab floor very much complicates the prediction of actual wind and bouyancy induced infiltration rates based on internal and external pressure distributions on the walls of the building.
- The leakage characteristics of the building under uniformly imposed pressure differentials are now reasonably well known, but it is still not clear that long term building energy use can be adequately predicted based only on blower door tests.
- The effect of the infiltration reductions on the heating load of the REPEAT building is estimated below. The infiltration is expressed as a building load coefficient (BLC), that is, as a UA equivalent with units of W/K, at a particular wind speed.

Infiltration component of BLC (W/K)

wind speed	2 m/sec	8 m/sec
BLC before sealing	19.4	186
BLC after sealing	2.3	22

Conduction component of BLC (W/K)

night insulation	0 m2-K/W	1.5 m2-K/W
BLC	427	211

ENER-SEAL

VOL/AREA/TEMP/PRES

29535.	FT^3
4000.	FT^2
77.	TEMP
24.89	PRES

H.PRS/N.PRS/FLOW

60.	HP
67.257	NP
217.2647565	Q
49.	HP
47.329	NP
181.6687333	Q
44.	HP
41.1015	NP
169.0758887	Q
39.	HP
34.874	NP
155.5060358	Q
32.	HP
27.401	NP
137.5358798	Q
27.	HP
19.928	NP
116.9478591	Q
.9975475224	
17.15255442	INT2
.3810678458	50PA
.0578050559	4PA
10.09645447	C
.0141029364	FT/M
.7466760898	N

ENER-SEAL

VOL/AREA/TEMP/PRES

29535.	FT^3
4000.	FT^2
75.	TEMP
24.89	PRES

H.PRS/N.PRS/FLOW

146.	HP
246.609	NP
422.6087321	Q
132.	HP
206.753	NP
386.32747	Q
104.	HP
146.969	NP
324.6974438	Q
91.	HP
124.55	NP
298.4534142	Q
77.	HP
94.658	NP
259.5295613	Q
65.	HP
74.73	NP
230.0971122	Q
.9995026633	
17.38496219	INT2
0.384640369	50PA
.0587261078	4PA
10.29385773	C
.0142940235	FT/M
0.744111764	N

Figure A.1. Typical Infiltrometer printouts. Due to low flow rates a different manometer was used to measure nozzle pressures and the program modified to convert reading from inches to millimeters.

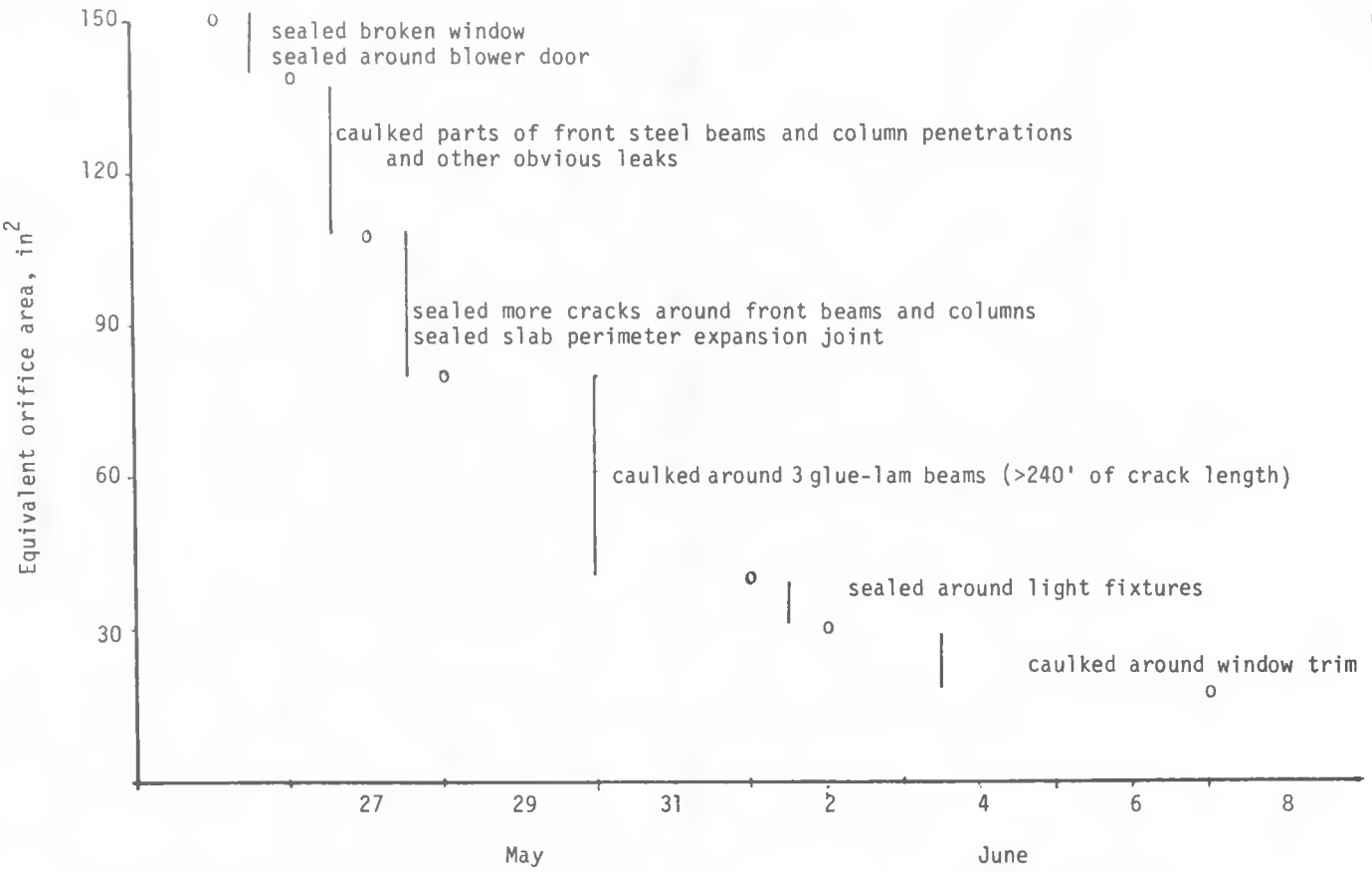

Figure A.2. Progress in the reductions of infiltration leakage area.

Table A.1 Parameters fitted to the infiltration model, $\dot{m} = C(\Delta P)^N$, to test sensitivity of different leaks to flow direction.

	ΔP range	Area, in^2	C	N
8 June tests.				
Depres., windows + outlets taped				
	228-65	18.7	10.80	.756
	66-234	21.4	13.78	.707
	232-70	19.8	11.98	.734
	228-67	19.3	11.60	.738
	65-225	20.0	12.24	.729
	225-63	20.1	12.44	.725
Depres., windows taped				
	226-61	22.8	14.75	.706
	67-228	22.3	14.26	.711
	226-66	21.6	13.48	.722
Depres., no tape.				
	228-72	20.5	12.00	.749
	216-60	23.5	15.07	.710
	63-203	23.3	14.80	.714
	206-57	22.5	13.89	.726
9 June tests.				
Depres. outlets taped				
	210-60	20.5	12.58	.729
	60-200	20.3	12.40	.731
	193-66	22.4	13.77	.728
	60-186	22.8	14.21	.722
	176-65	22.2	13.55	.731
Pres. outlets taped				
	52-200	16.6	6.34	.933
	180-50	22.6	10.67	.843
	49-245	21.1	9.54	.861
20 June tests				
Pres., Windows + outlets taped				
	185-63	17.6	9.30	.79
	59-18	16.6	8.74	.80
	18-65	18.6	10.28	.773
	64-19	15.1	6.49	.882
Pres., only outlets taped				
	60-17	17.9	8.81	.825
	170-63	18.4	9.15	.820
Pres., no tape - windows, outlets				
	167-58	19.3	9.47	.826

Table A.2 Parameters fitted to the infiltration model, $\dot{m} = C(\Delta P)^N$, during equivalent orifice area and low flow tests

	ΔP range	Area, in^2	C	N
18 June, Test openings of known area				
Depres., windows + outlets taped				
base case	179-70	18.1	11.02	.733
1 7.0 in^2 hole	162-62	25.4	17.69	.674
2 holes	155-55	31.5	22.99	.654
3 holes	156-47	40.2	31.84	.618
Pres.,				
base case	142-50	18.6	9.62	.802
1 7.0 in^2 hole	165-44	24.9	14.93	.738
2 holes	164-39	30.91	19.71	.712
3 holes	157-35	36.2	23.76	.700
17 June, low flow test windows + outlets taped				
	146-65	17.4	10.29	.744
	61-21	17.1	9.92	.753
	60-27	17.2	10.10	.747

PROJECT SUMMARY

Project Title:	Performance Evaluation of RPI's Campus Information Center
Principal Investigators:	Walter M. Kroner, John A. Tichy
Organization:	Rensselaer Polytechnic Institute Troy, New York 12181
Project Goals:	Evaluate performance of RPI Passive Solar Visitors Information Center, by measuring end use energy consumption in various categories and comparing measured performance to predicted performance.
Project Status:	The performance evaluation of the RPI Passive Solar Visitors Information Center is proceeding smoothly. Data for January through June 1982 have been presented and extrapolated for the full year. The projected yearly total energy use is 59.6 MW-h/yr (202 MBtu/yr), or on a per unit floor area basis, 123 kW-h/m^2-yr (38.7 kBtu/ft^2-yr). These figures agree reasonably well with updated simulation provided realistic values for the interior thermostat set points are used.
Contract Number:	DE-FC02-80CS30350
Contract Period:	January 1, 1983 through December 31, 1982
Funding Level:	$29,620
Funding Source:	U.S. Department of Energy, Passive Solar Commercial Buildings Program

PERFORMANCE OF THE RPI PASSIVE SOLAR VISITORS INFORMATION CENTER BUILDING: PROGRESS REPORT

John A. Tichy
Department of Mechanical Engineering
Rensselaer Polytechnic Institute
Troy, New York 12181

ABSTRACT

The performance evaluation of the RPI Passive Solar Visitors Information Center is proceeding smoothly. Data for January through June 1982 have been presented and extrapolated for the full year. The projected yearly total energy use is 59.6 MW-h/yr (202 MBtu/yr), or on a per unit floor area basis, 123 kW-h/m^2-yr (38.7 kBtu/ft^2-yr). These figures agree reasonably well with updated simulation provided realistic values for the interior thermostat set points are used.

INTRODUCTION

Rensselaer Polytechnic Institute in Troy, New York began the Visitors Information Center project in May 1979. The building was to serve as a "front door" to the campus, i.e., to provide conference rooms and reception spaces for visitors, and to house the campus security office. In October 1979, RPI received notification that its proposal for a Design Assistance and Demonstration grant from DOE had been accepted. In January 1981, the building was completed. Since January 1, 1982 the building's thermal performance has been carefully monitored as part of the Performance Evaluation Phase of the DOE Passive Solar Commercial Buildings Program. In this paper, overall performance results to date are presented, along with a detailed look at several typical winter days. Comparisons are made to simulations based on original design assumptions of building use, and on updated information regarding actual building use. Results are extrapolated to a full year, based on the typical yearly degree-day distribution.

The present document is meant to be a progress report, presenting basic data with relatively little analysis and conclusions. The latter items will be addressed in the final project report after one full year's data.

BUILDING DESCRIPTION

A schematic of the VIC's floor plan is shown in Figure 1. The building's large south elevation accommodates a sunspace to collect and store solar energy in the sunspace floor slab and a system of mass wall segments. Infrequently used spaces, which do not have critical thermal requirements, are found along the earth-bermed northern perimeter. This region is called zone 2. Unfortunately, office space has recently been added to this north wall area, replacing previously thermally insensitive areas. The interior is a buffered central zone of thermally sensitive office spaces, zone 1. The thermally controlled floor area is 401 m^2 (4300 ft^2) and the total floor area, including the uncontrolled sunspace is 484 m^2 (5200 ft^2). The sunspace glazing area is 63 m^2 (680 ft^2). Further description of the building is contained in the final design report [1].

All auxilliary energy consumption is electric. A variable air volume system, integrated with an electrical resistance heating element and a cooling coil, provides for back-up heating and cooling. Individual spaces are supplied with radiant heating panels to provide supplemental heating when occupied. Movable insulation with controls in the sunspace are designed to maintain comfortable temperature in the sunspace, to prevent heat loss, and to provide shading in the summer. Stored energy in the mass walls transfers to the interior of adjacent spaces in the evening. Operable openings in the glass wall of the sunspace, the office windows, and the light tower (containing an exhaust fan) create a thermosiphoning effect for natural ventilation and space cooling during the summer.

DESCRIPTION OF THE MONITORING SYSTEM

Three types of variables are measured: temperature, solar irradiation, and electrical energy consumption. The temperature transducers are manufactured by Analogue Devices, Model AD590. They are integrated circuit devices with nominal output current of 1 $\mu A/^{\circ}K$. Measurement of insolation is done by the Li-Cor LI-200s calibrated Pyramometer sensor with 50 $\mu A/1000$ W-m^2 sensitivity, which uses a silicon detector in a corrected head. Energy consumption is determined by Ohio Semitronics PC5 series Hall Effect AC Watt Transducers. The monitoring system is controlled by the Aeolian Kinetics PDL-24 Data Logger. All variables are scanned each 30 s and the averaged results printed each hour. Energy (in kW-h) is determined by integration of the power consumption (in kW) over each hour interval. Hourly values are printed on paper tape and stored on tape cassettes.

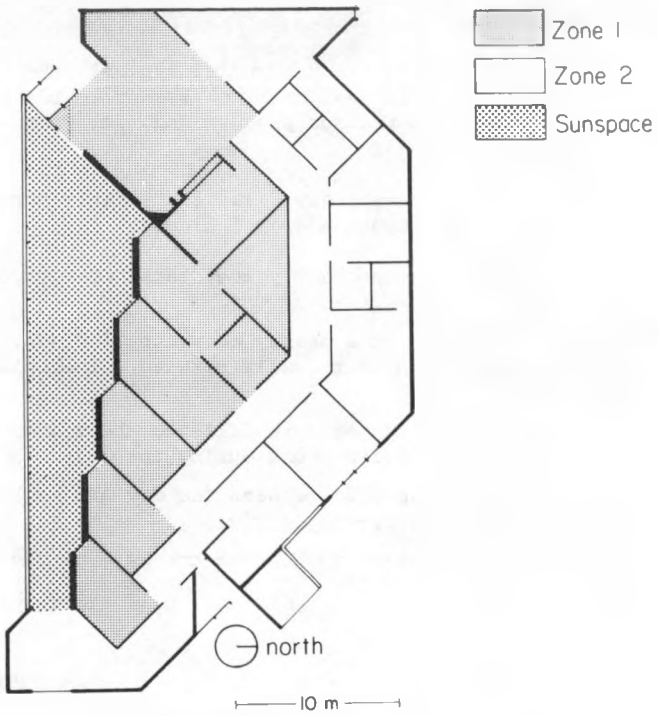

Figure 1 VIC Floor Plan Schematic

The following air temperatures are measured: outside environment, sunspace, two interior (zone 1) offices, and a north wall office (zone 2). Three mass wall temperatures are measured. Outside horizontal solar irradiation and vertical solar irradiation on the sunspace mass wall are monitored. Electrical energy consumption is measured for heating (the sum of the air duct coil, baseboard heaters and radiant panels), air conditioning, inside lighting, outside lighting, and HVAC/ventilation equipment.

The overall energy for any significant time period is known from the Niagara Mohawk Utility meter, as recorded by visual observation. Total building energy use is determined by subtracting the outside lighting from the utility meter reading. Prior to March 1982, the outside lighting was only estimated based on rated load and hours of daylight after which time a transducer was available for this variable. The January through March estimates were later revised slightly based on the subsequent outside lighting measurements.

OVERALL PERFORMANCE

Overall thermal performance for the first six months of 1982 is depicted in Figure 2. The increase in average outside air temperature and horizontal insolation from January through June is also shown. As a point of reference, the dotted line indicates the daily average equivalent to 50 kBtu/ft^2-yr, a commonly accepted standard for energy consumption in highly efficient nonsolar commercial buildings. The term "overall" is used to represent building behavior over relatively large increments of time (month-by-month), rather than detailed (hour-by-hour) behavior. The units shown are average daily consumption of energy (kW-h or Btu) per unit gross floor area (m^2 or ft^2) over the month shown.

Note that auxilliary heating is by far the largest component of total energy use, approximately 40% on a yearly average. Air conditioning is a very small part of the total, on a yearly average and is less than 30% even in the peak months. This is also borne out by the July and August data which has not yet been fully evaluated. Lighting and HVAC equipment are relatively constant throughout the year and typically comprise 10 - 30% of the total useage depending on the particular month.

Estimated yearly energy consumption is shown in Table 1. Results are also shown in a percent floor area basis. The estimates are made by scaling the heating and cooling measurements by degree-days. For January through June, typically 62.8% of the yearly 3780 heating °C-days (6800 °F have occurred, and 24.0% of the yearly 360 cooling °C-days (650 °F-days). The other energy use variables are assumed constant through the year.

TYPICAL HOUR-BY-HOUR PERFORMANCE

To better understand the building system performance, several typical days are selected from the peak winter heating season. Clearly the heating (rather than cooling) season is the greater determinant of the overall energy consumption. Data evaluation is a tedious process and must currently be done by pulling figures from paper tape by hand.

Typical behavior is plotted in Figure 3, for February 9-11, 1982. This period includes a very cloudy and a very sunny day. The most important observations are as follows:

1) Most heating energy consumption (and consequently most total energy consumption) occurs in surges during the morning.
2) The interior offices (zone 1) are kept at a nearly constant 23°C (73.6°F) all day and night. A brief drop to 21°C seems to occur in the very early morning. The building is in use by security personnel 24 hours a day.
3) In the north wall region (zone 2) the temperature falls to about 15°C (58°F) at night, then is brought up to about 20°C at least for a few hours during the day.
4) The sunspace temperature swings considerably between the day and night, but is generally inhabitable during daylight hours when visitors may arrive.
5) Lighting energy use is relatively constant throughout the 24-hour day other than a brief low period very early in the morning.

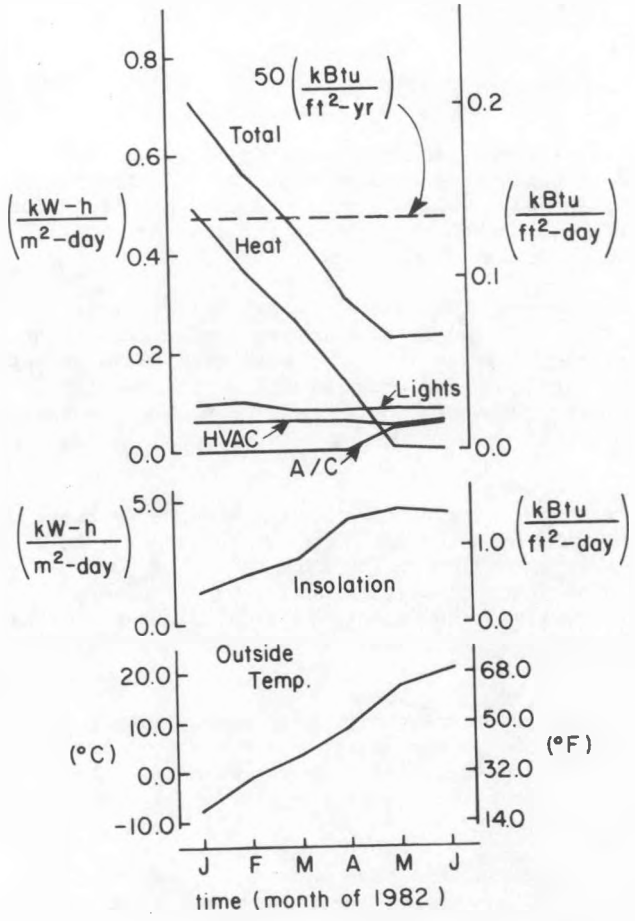

Figure 2 Overall Building Performance: Month-by-Month Energy Use for 1982

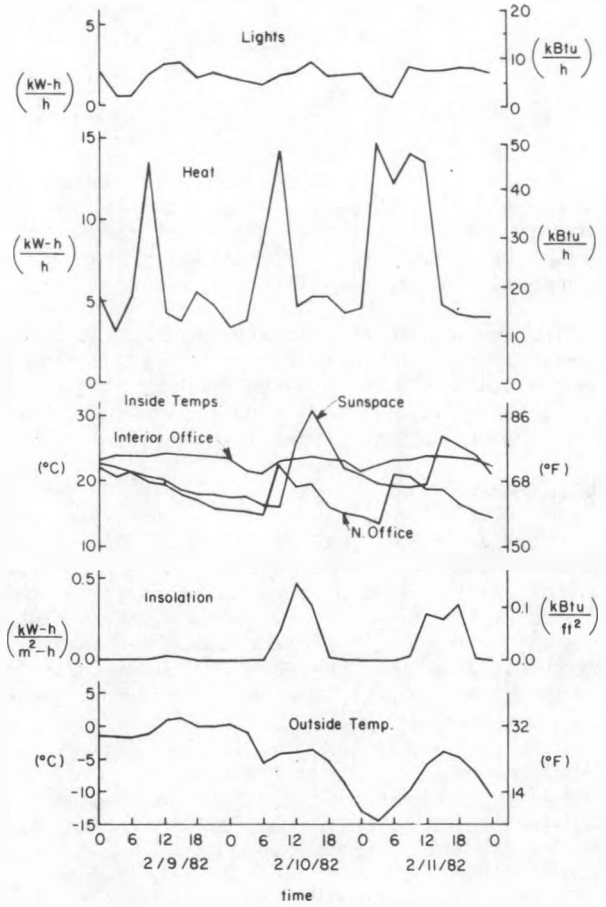

Figure 3 Hour-by-Hour Performance in Typical Winter Conditions

The thermostat settings for the air duct heaters are 20°C (68°F) day-zone 1, 12.8°C (55°F) night-zones 1 and 2, and 15.6°C (60°F) day-zone 2. These settings can (and by observation are) overridden by the building occupants by the use of the manually controlled baseboard heaters and radiant panels. It seems reasonable to assume that the large surges of heat in the morning hours are due to the building's temperature being raised both by the thermostatically controlled duct heaters and the manually operated heaters.

COMPARISON OF ACTUAL TO SIMULATED PERFORMANCE

During the design phase of the VIC project, an "in-house" computer simulation tool was developed, as described in Refs.[1,2]. The program solves 12 implicit one-dimensional energy balance equations hour-by-hour for a year using a simple matrix inversion algorithm. The following variables are treated as hour-by-hour program inputs: outside temperature, horizontal insolation, zone 1 and 2 thermostat set points, and energy loads due to lighting, occupants, HVAC equipment, and other miscellaneous equipment (computer hardware, soda machines, kitchenette, etc.). The weather inputs (outside temperature and insolation) are obtained from a specially prepared "design year" tape of average months in Albany, NY between 1970-1976 (January 1975, February 1973 .... etc.). Hour-by-hour program outputs are heating (or cooling) by zone, and temperature of the nodes.

During the design phase, the program was run with what turned out to be overly optimistic thermostat set points, see Table 2. Also an infiltration and ventilation rate of one-half air change/h was assumed, which now seems unrealistic in view of the fact that the outside door is constantly opening and closing due to ingress and egress of visitors and campus security personnel. Under these assumptions the total energy end use figure of 66.1 kW-h/m^2-yr (21.0 kBtu/ft^2-yr) was obtained, which is considerably too low.

Participants in the performance evaluation phase of the DOE Passive Solar Commercial Buildings Program were encouraged to update their simulation based on improved knowledge of building use and characteristics. Therefore, the infiltration/ventilation rate has been changed to one air change/h, and thermostat set points of 22.2°C (72°F) for zone 1 (day and night), 22.2°C for zone 2 (day), 12.8°C (55°F) for zone 2 (night) have been used. In this case the simulated energy use is brought much more into line with the measured (see Table 2); 115.7 kW-h/m^2-yr (36.7 kBtu/ft^2-yr) simulated, vs. 123.0 kW-h/m^2-yr (38.7 kBtu/ft^2-yr) actual. For these conditions, simulated and actual heating and total energy use are compared on Figure 4. The results are in substantial agreement. It is important to note that the weather used in the present simulation is the same as that used in the design simulation, which is, of course, not the same as the actual weather.

Figure 5 depicts some typical details of the present simulation versus measured performance. The same days depicted in Figure 3 were selected for the comparison. Note that although the exact details of the fluctuations of the simulated and measured performance differ (as they should, due to the weather differences), the basic character and magnitude of the variables correspond. Note particularly the similarity of the heating surges and of the rise and fall of temperatures in zone 2.

CONCLUSIONS

The RPI design team feels it is gradually coming to an understanding of the VIC's thermal behavior. Its performance is highly dependent on the manner in which it is operated, much more so than was anticipated. Although we are disappointed in the fact that energy use is greater than that projected in the design phase, the "bottom line" figure of 123 kW-h/m^2-yr (38.7 kBtu/ft^2-yr) is highly respectable. A case is made herein that this discrepancy is due to user operation variations: thermostat settings, manual control of heaters, infiltration due to increased building access and egress. These considerations will be more fully examined in the final report.

The building's yearly performance is dominated by heating season characteristics. The building has relatively low internal loads and is located in a severe winter climate region. This fact diminishes the importance of the lighting energy use. While lighting nominally accounts for 25% of the total yearly energy consumption, 14.8 MW-h/yr (50.6 MBtu/yr), at least half of the value occurs during periods of auxilliary heating. Hence a reduced yearly lighting load would not reduce total energy use by the same amount.

REFERENCES

1. Kroner, W.M., "RPI Visitor Center Final Design Report," DOE Contract DOE-PN-2-79CS-30142.
2. Tichy, J.A., Kroner, W.M. and Borton, D.N., "The Design Simulation and Performance of the RPI Passive Solar Campus Information Center Building," ASME paper 81-WA/Sol-9, November 1981.

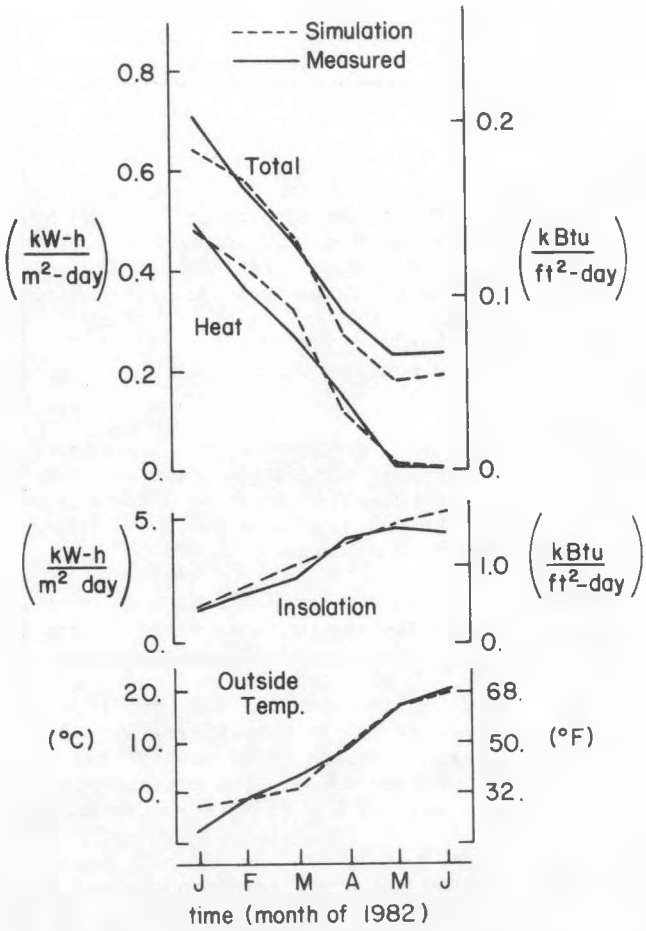

Figure 4 Comparison of Simulated to Measured Performance: Month-by-Month Energy Use for 1982

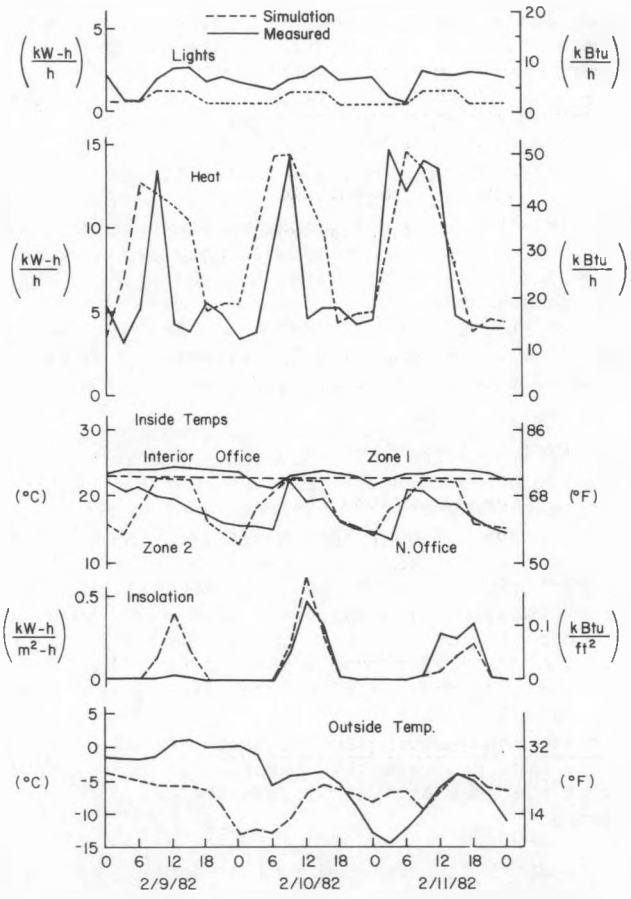

Figure 5 Comparison of Simulated to Measured Performance: Hour-by-Hour Behavior in Typical Winter Conditions

TABLE 1 ESTIMATED YEARLY ENERGY USE (BASED ON PERFORMANCE FOR JANUARY THROUGH JUNE 1982)

Energy Use Total			
Heating	76.0	MW-h/yr	(76 MBtu/yr)
Cooling	6.6	MW-h/yr	(22.4 MBtu/yr)
Lighting	14.9	MW-h/yr	(50.6 MBtu/yr)
HVAC	9.9	MW-h/yr	(33.7 MBtu/yr)
Total	202.	MW-h/yr	(202 MBtu/yr)
Energy Use Per Unit Gross Floor Area			
Heating	46.2	kW-h/m²-yr	(14.5 kBtu/ft²-yr)
Cooling	13.6	kW-h/m²-yr	(4.3 kBtu/ft²-yr)
Lighting	30.7	kW-h/m²-yr	(9.6 kBtu/ft²-yr)
HVAC	20.4	kW-h/m²-yr	(6.5 kBtu/ft²-yr)
Total	123	kW-h/m²-yr	(38.7 kBtu/ft²-yr)

TABLE 2 COMPARISON OF DESIGN PHASE SIMULATION TO PRESENT SIMULATION

Important Load Parameters - Overall Conductance (UA)		
Design Simulation		
Zone 1:	Transmission	UA = 124 W/°C = 234 Btu/°F-h
	Ventilation/Infiltration (One-half air change/h)	UA = 29.0 W/°C = 44 Btu/°F-h
Zone 2:	Transmission	UA = 133 W/°C = 252 Btu/°F-h
	Ventilation/Infiltration (One-half air change/h)	UA = 20.1 W/°C = 38 Btu/°F-h
Present Simulation		
Zone 1:	Transmission	UA = 124 W/°C = 234 Btu/°F-h
	Ventilation/Infiltration (One air change/h)	UA = 58 W/°C = 110 Btu/°F-h
Zone 2:	Transmission	UA = 136 W/°C = 257 Btu/°F-h
	Ventilation/Infiltration (One air change/h)	UA = 40.2 W/°C = 78 Btu/°F-h
Thermostat Heating Set Points		
Design Simulation		
Zone 1	18.3°C (65°F) day	12.8°C (55°F) night
Zone 2	15.5°C (60°F) day	12.8°C (55°F) night
Present Simulation		
Zone 1	22.2°C (72°F) day	22.2°C (72°F) night
Zone 2	22.2°C (72°F) day	12.8°C (55°F) night
Results - End Use Energy		
Design Simulation		
Heat	20.4 kW-h/m²-yr = 6.5 kBtu/ft²-yr	
Total	66.1 kW-h/m²-yr = 21.0 kBtu/ft²-yr	
Present Simulation		
Heat	61.3 kW-h/m²-yr = 19.5 kBtu/ft²-yr	
Total	115.7 kW-h/m²-yr = 36.7 kBtu/ft²-yr	

DRAIN-DOWN FREEZE PROTECTION FOR THERMOSYPHON SOLAR WATER HEATERS

by H.T. Whitehouse

Introduction

Historically, natural market selection processes have tended to favor thermosyphon water heating systems in countries which have pioneered solar applications -- such as Australia, Japan and Israel. The dominance of thermosyphonic equipment in these countries testifies to the inherent simplicity, low cost and excellent thermal performance of this generic system type. And, while their widespread adoption in these areas may be partly attributed to unique climatological, sociological or technical factors, it is possible that history will be repeated as the United States' solar market matures. Aggressive marketing of Australian (Shell/Solahart), Japanese (Yazaki) and Israeli (Amcor) thermosyphonic equipment is already under way in the continental U.S., and a few American manufacturers are now offering their own versions of thermosyphon systems.

U.S. solar water heater designers have almost unanimously opted for systems employing active control for circulation and freeze protection. There are several reasons behind the limited adoption of thermosyphon systems in the United States. Perhaps foremost is the relatively meager experiential base shared by those in the solar industry and the end user community. Further, geometric constraints imposed by the physics of thermosyphon systems represent a significant barrier to market acceptance. Because the solar storage tank must be placed above the collector array to insure thermosyphon circulation, and because the most logical collector position for maximum solar access is generally atop a roof structure, one invariably ends up with a heavy cylindrical storage tank in or on the roof. This situation poses both aesthetic and structural problems.

There is yet another obstacle to widespread adoption of most thermosyphon systems -- the absence of a fail-safe method of collector freeze protection. Ironically, thermosyphon systems are especially susceptible to debilitating collector freeze damage since they lack even the most rudimentary protective controls. This paper discusses the thermal mechanisms of collector freezing and describes a simple extension of "active" drain-down freeze protection technology which can be applied to "passive" or thermosyphon systems.

Radiation Losses to the Night Sky

Designers and installers frequently gauge the potential for collector freeze damage in a given locale by reviewing the historical records of measured air temperature. It is reasoned that no freeze protection apparatus will be necessary if the recorded extremes seldom, if ever, fall below 32°F (0°C). The error in this simple line of reasoning is tied to radiation heat transfer -- an often misunderstood and, in this case, underestimated factor in collector freezing events. Paradoxically, radiation losses to a cloudless night sky can depress the temperature of an absorber plate by 10°F (5.5°C), or more, below the surrounding air temperature. Thus, a "mild" 40°F (4.4°C) night can set the stage for a disastrous freeze.

This subtle night sky radiation heat loss phenomenon is evident elsewhere in our surroundings. For instance, on an early fall morning the reader may have noticed what appear to be "shadows" under trees, tables and other objects on an otherwise open, frost-covered field (cf. Figure 1). This is caused by selective freezing of beads of dew which form on the grass. Those beads which have been optically exposed to the clear night sky will preferentially freeze and give the appearance of "frost", and those shielded from radiation losses by, say, a table, will not freeze. Importantly, this freeze-based patterning can develop even if the air temperature remains above 32°F all evening!

A parked car (cf. Figure 2) is another familiar example. In proper weather conditions, dew will begin to form on the body in the late evening. The dew forms when warm, moist air comes in contact with the cooler surfaces of the automobile. The uppermost surfaces -- those facing the sky -- typically are the first to show the dew droplets. This is because these surfaces are preferentially cooled by radiation losses to the sky above. In contrast, the sides of the automobile are in radiant communication with nearby buildings, the ground and other mass elements which still retain the day's heat. This radiant environment serves to keep the side of the car "warm" and, in a relative sense, delays the formation of dew droplets!

With an appreciation of night sky radiation phenomena, one can easily surmise why smudge pots are used as an "optical" barrier to protect citrus crops from frost damage on cool, clear nights in Florida (cf. Figure 3). However, understanding the effectiveness of motor-driven "wind machines" to mitigate frost damage in the vineyards of California (cf. Figure 4) will likely require the perusal of subsequent sections.

Examples aside, the fact remains that collector freeze protection is a major issue in most -- if not all -- of the continental U.S. Due to night sky radiant effects, air temperature statistics used alone severely underestimate the collector freeze potential of a given area. This oversight has had disastrous consequences, evidenced by the extensive solar equipment freezes in Los Angeles in the early 1900's, the recurrent system damage in Florida in the 1940's, and the widespread freezeups throughout Florida, Arizona, Colorado and California in recent years.

Radiation Losses as They Affect a Collector

Figure 5 depicts a small roof-mounted collector array in a clear evening environment. Not surprisingly, the collector array typically has an unobstructed "view" of the sky dome. On a cloudless evening, the sky will have an effective temperature given approximately by [1]:

$$T_{sky} = .0411\ (T_{air})^{1.5}$$

Where T_{sky} and T_{air} are in absolute Rankine degrees (°R). The effect of water vapor in the air has been neglected in this correlation, but this omission is acceptable in the (drier) winter months when freezing is most likely to occur [2]. The correlation predicts that the sky dome will have a substantially lower temperature than the surrounding air temperature. Using our previous example of a 40°F (4.5°C) air temperature, we find T_{sky} to be less than 0°F (-18°C).

The effective sky temperature can be used to compute the equilibrium, night-time absorber plate temperature. While a thorough quantitative analysis is beyond the scope of this paper, it is revealing to qualitatively examine the key energy flows in the collector as illustrated by Figure 6. Here, principal heat flow interactions between the glazing, the night sky, surrounding air and collector absorber plate are superimposed on a typical collector cross section.

The loss-related radiation heat flows are in the infrared spectrum, and thus the collector cover glass appears opaque to this radiation. Accordingly, the only energy transmitted through the glass is that which is conducted. Practically, the conduction resistance in a single-glazed collector is small, so one can assume that the inside and outside surfaces of the glazing are at approximately the same temperature.

The equilibrium temperature reached by the glass depends upon the relative rates at which energy is lost and gained at the glass surfaces. On a clear evening, the outside surface of the glazing will be losing energy to the night sky (Q_{sky}). Unfortunately, this radiation loss is encouraged by the high emissivity of glass in the infrared wavelengths. Simultaneously, the outside glass surface will be gaining energy from the surrounding air molecules in an attempt to compensate for the radiation losses to the sky (Q_{air}). Finally, the inside surface of the glazing will be receiving energy from the absorber plate (Q_{loss}) by radiation and convection.

As time passes and the absorber plate cools, the energy flows eventually cause the glass temperature to seek a level between the surrounding air temperature and the night sky temperature. A breezy evening will result in a glass temperature closer to the surrounding air temperature, since the moving air will increase the convective coupling to the glass and enhance energy gains. In contrast, a still evening will tend to drive the glazing closer to the night sky temperature since the radiation losses will dominate. (This competitive interplay between radiation losses and convective gains described here explains the rationale for the motorized wind machines in the vineyards of Figure 4. The wind machine improves the convective coupling between the grapes and the relatively warm air!)

As the glass temperature gravitates to equilibrium in its radiation/convective environment, the absorber plate temperature follows suit. This is because the absorber "sees" only the inside glass surface in its thermal communication -- the colder the glass surface, the colder the absorber plate. And, while the rates of energy flow involved are generally low, the non-circulating collector has only its low effective thermal mass to resist this cooling process. The absorber plate temperature is thus inexorably drawn towards the glass temperature, which itself is at the mercy of the radiant environment of the night sky. Thus, on a cloudless evening, we will eventually find the glazing and absorber plate at a lower temperature than the surrounding air!

(It should be mentioned that the rate of collector plate cooling can be reduced by employing double glazing on the panels, and/or by utilizing a selective surface coating on the absorber plate. The selective surface, with a purposely low emissivity in the infrared, reduces the rate of radiant energy transfer between the absorber plate and inside surface of the glass.)

Methods of Collector Freeze Protection

The available methods of collector freeze protection in solar DHW systems have been covered admirably in the recent literature [3]. Briefly, these methods include:

1. Pump-recirculation methods
2. Heat exchanger/anti-freeze systems
3. Drain-back methods
4. Drain-down methods
5. Electrical resistance heating

Due to the absence of a pump and controller, thermosyphon systems obviously cannot employ the pump recirculation methodology. Anti-freeze solutions often introduce increased fluid viscosity -- a factor which can affect the delicate flows nurtured by the thermosyphon potential. Heat exchanger systems also add substantially to the cost and complexity of the system and degrade thermal performance significantly due to the lack of forced circulation on either side of the heat exchanger surface. Electrical resistance heaters are, at minimum, a questionable appropriation of high-quality energy resources, and provide no protection in the not-so-unlikely event of coincident power failure and low ambient temperatures. Drain-back methods suffer most of the hardware disadvantages of heat exchanger systems, are further complicated by the geometric constraints of thermosyphon systems, and require the use of some form of pump.

The foregoing leads to the consideration of a drain-down approach for thermosyphon freeze protection. The drain-down approach is premised on the direct control of pressurized potable water by the appropriate hardware. In the shutoff or drain mode, all collectors and exposed piping are completely devoid of water. In the operate or fill mode, potable water is heated directly and circulated by the thermosyphon potential. Due to the nature of available valving hardware, such a system can easily be made fail-safe in the event of a power failure.

Drain-down Freeze Protection for Active Systems

To better appreciate the special requirements of a drain-down thermosyphon water heater, it is helpful to review drain-down techniques as they apply to active systems. Figure 7 presents an isometric of a typical active solar water heater employing drain-down freeze protection. The drain-down valve is interposed between the pressurized preheat tank and the collector array. Whenever power is removed from the valve, the city water pressure is isolated from the collector array and draining commences through a dedicated port of the valve.

Naturally, the drain-down valve must be installed in an area protected from freezing temperatures. In an active system, the valve is typically located in a utility room, basement or garage area adjacent to the storage tank, pump and controller. The collectors, most often mounted on the roof, drain down into this protected area -- usually into a service sink or other sanitary drain. The amount of water drained is typically on the order of one gallon.

It is important to note that the integral drain-down valve in an active system serves two distinct functions at a single point in the piping system. It first isolates the array from the pressurized water and then serves as the point of drainage.

Drain-down Configurations for Thermosyphon Systems

Figures 8 and 9 illustrate two possible piping arrangements for a drain-down thermosyphon water heater. In each case, in order to evacuate the water from the collectors and exposed piping, one must again isolate the city water pressure. This generally calls for some form of valving mechanism between the tank and the collector array. Naturally, one must locate this draining point opening below the collector array. Thus, the functions of pressure isolation and draining must be carried out by distinct and physically separated hardware elements. It is here that thermosyphon drain-down systems depart from their active counterparts.

Sunspool has addressed this conceptual problem with two simple plumbing permutations shown in Figures 8 and 9. Figure 8 illustrates a multi-component approach using a standard Sunspool drain-down valve in conjunction with a thermostatically- or pressure-actuated, single port valve positioned at the bottom of the array. A Sunspool valve is mounted in an inverted position in a thermally-protected area close to the storage tank. In this configuration, the Sunspool valve port normally used for draining becomes a point of air admission during the drain cycle. The independent single port valve is thermostatically (or hydraulically) controlled to open after the Sunspool valve completes the pressure isolation task. When the single port valve opens, only the small amount of water in the collector array and exposed piping flows over the roof surface.

When warmer ambient conditions return, the Sunspool valve begins filling both the supply and return lines of the array. When this relatively warm water comes in contact with, say, a thermostatic version of the single port valve, it quickly closes. The "staggered" operation of the two valves during fill provides for positive air elimination during fill and vacuum relief during drain. A similar air elimination procedure can be achieved with a pressure-actuated valve.

A second plumbing arrangement is depicted in Figure 9. Here the collector supply and return lines are routed into a protected attic or crawl space. At the low point of the piping -- purposely below the bottommost portion of the collector array -- a modified Sunspool valve is operated as a simple three port device. The remaining "two ports" of the standard Sunspool valve become a sensitive check valve positioned in the collector return line inside the protected area. A standard air vent/-vacuum breaker combination is included for air elimination during fill and vacuum relief during drain.

When the modified Sunspool valve in Figure 9 is energized, it admits pressurized water into the collector supply piping, automatically filling the collector array and associated piping. The air vent automatically eliminates the displaced air. The check valve then permits normal thermosyphon flow, while preventing reverse thermosyphon flow on those occasions when the collector temperature is below the tank temperature, and yet draining has not occurred.

When de-energized, the Sunspool valve isolates the tank pressure and connects the collector piping to the integral drain port. The pressure reduction in the collector array causes the check valve to firmly seat and isolate the return line. The vacuum breaker admits air during the draining process.

Both plumbing configurations (i.e., Figures 8 and 9) have been constructed and are in operation. The configuration of Figure 8 has successfully operated under field conditions since September, 1980 in a Northern California climate. The alternate configuration is located at Sunspool headquarters and has been functioning since March 1981. Figure 10 presents this heavily instrumented system in isometric view.

Powering and Controlling the Sunspool Valve

Both of the design concepts described above require some form of valve actuation for the necessary fill and drain operations. The direct-acting spool configuration of the Sunspool valve was chosen because of its specific design for and proven field performance in pressurized, potable hot water systems. Efforts have focused on developing a relatively modest permutation of the basic Sunspool design because, by using this baseline technology, it is more likely that the thermosyphon product can be brought to market at a competitive price and in a timely fashion.

The standard production version of the Sunspool valve, shown in Figure 11, is actuated by means of thermal "heat motors". When heated by a simple power resistor, these phase change devices expand against the spool and return spring. The heater operates in conjunction with a positioning switch, drawing an average power of less than 2 watts. Since the heating element is a simple resistor, the valve can be constructed to operate with any supply voltage.

The most obvious powering and control strategy for the thermosyphon drain-down valve employs a low voltage transformer and a temperature switch. An inexpensive "doorbell transformer" can supply a safe 24 or 12 VAC voltage. The snap-action or solid state thermostatic switch is located at the collector array. In either plumbing configuration, the interruption of the circuit by the temperature switch allows a powerful return spring to move the valve to the drain position. Both plumbing configurations are fail-safe in power outages, regardless of the temperature switch disposition.

A second, more self-sufficient powering approach has also been used with success. Here a 7 to 10 watt photovoltaic (PV) array is used to power a 12 volt version of the Sunspool valve driver. The DC output of the PV array need not be inverted, since the heating resistor's performance is insensitive to AC or DC waveforms. In the PV-powered arrangement, the valve is de-energized and returned to the drain position every evening. The daily draining has little impact on water consumption, since the water residing within a typical two panel array and its minimal ancillary piping is less than 1 gallon. A schematic of the factory-based test system employing the plumbing configuration of Figure 9 and 10 and a PV array is shown in Figure 12. Typical valve operating characteristics are shown in Figure 13.

A third approach under investigation eliminates all electrical components and instead drives the valve with

a bellows assembly as depicted in Figures 14 and 15. A refrigerant-filled sensing bulb located in the collector monitors temperature and transmits a corresponding pressure to the actuating bellows by means of a capillary tube. Below a certain temperature, there is insufficient pressure generated in the bulb assembly to overcome the valving mechanism's return spring and the valve remains in the drain position. When the bulb temperature increases to a level above freezing, the bellows expands and pushes the spool valve to the "fill" position. This control arrangement is, of course, completely immune to electrical failures, and can be used in either plumbing configuration. Figure 16 presents typical operating characteristics of the refrigerant-based drive.

A fourth approach under evaluation employs a large thermal heat motor which is remotely mounted in the collector array and connected to the Sunspool valve by means of a short push-pull cable. This is an inexpensive configuration but highly dependent on the long term performance of the cable drive. Figure 17 details one version of the cable drive concept.

The Future

Sunspool plans to continue research and development efforts on the two principal plumbing configurations and the various control/powering strategies. Additional field test installations are being established for the 1982-83 winter season, and an extensive computerized data logging system will continue to monitor the factory test facilities.

Sunspool gratefully acknowledges the cost-sharing and programmatic support given by DOE's Marketable Products for Passive Solar Applications Program, managed by the Chicago Regional Office of the USDOE [4].

Bibliography

1. ASHRAE Applications Handbook, Chapter 58, ASHRAE, New York, NY, 1978.

2. J.A. Duffie and W.A. Beckman, Solar Energy Thermal Processes, John Wiley, New York, 1974.

3. S.A. Schiller, "Freeze Protection", Solar Age, August 1981.

4. Final Technical Report for USDOE Contract No. DE-PN02-80CS30154, "A Passively Operated Spool Valve for Drain-down Freeze Protection of Thermosyphon Water Heaters", Palo Alto, CA, 1982.

Dr. Whitehouse is the president of Sunspool Corporation and a member of the Stanford University School of Engineering faculty.

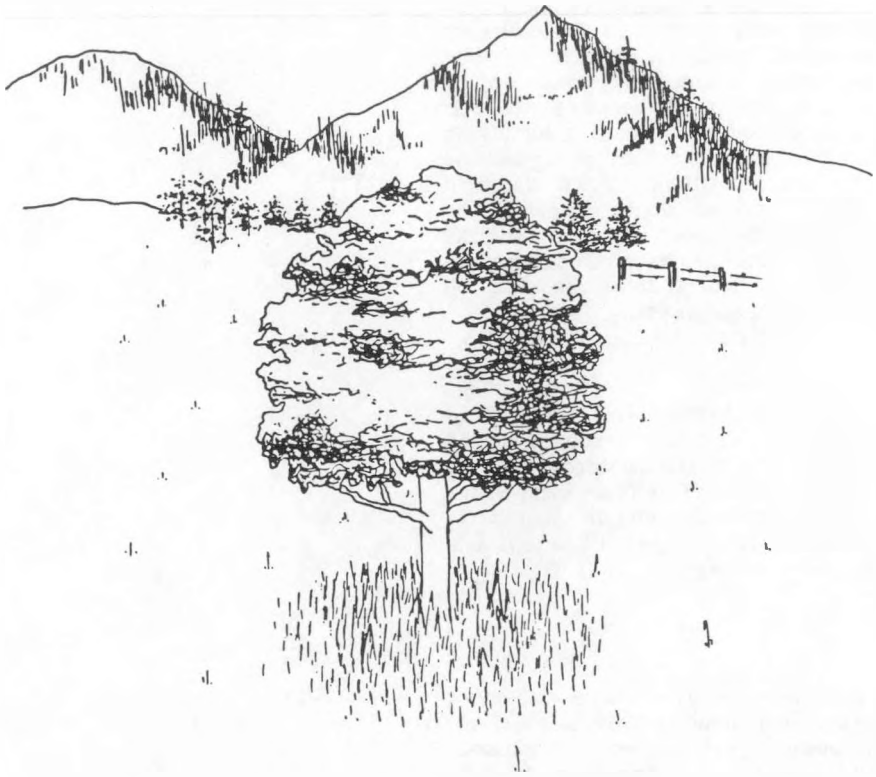

Figure 1. Dew-caused shadows on an otherwise frosty field.

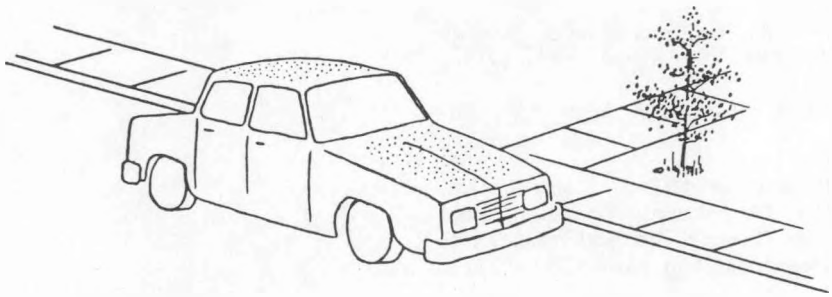

Figure 2. Dew patterns on an automobile first form on those surfaces facing the sky dome.

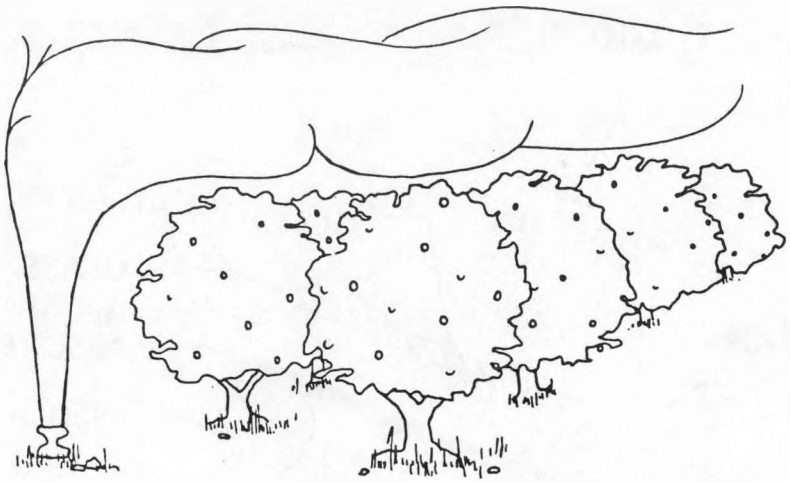

Figure 3. Smudge pots reduce radiation heat loss from crops.

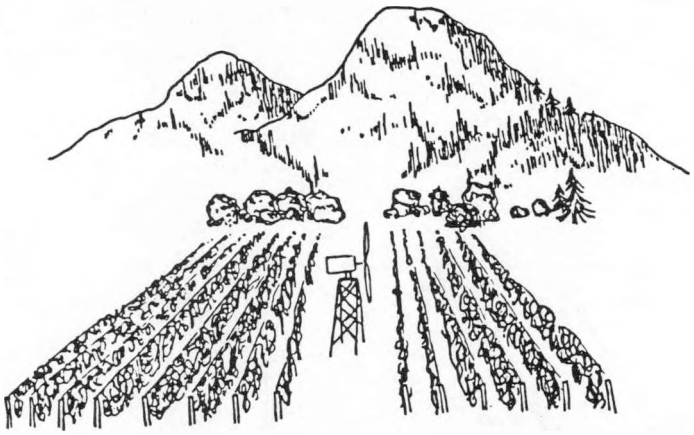

Figure 4. Wind machines in California vineyards.

Figure 5. A typical thermosyphon system on a clear night.

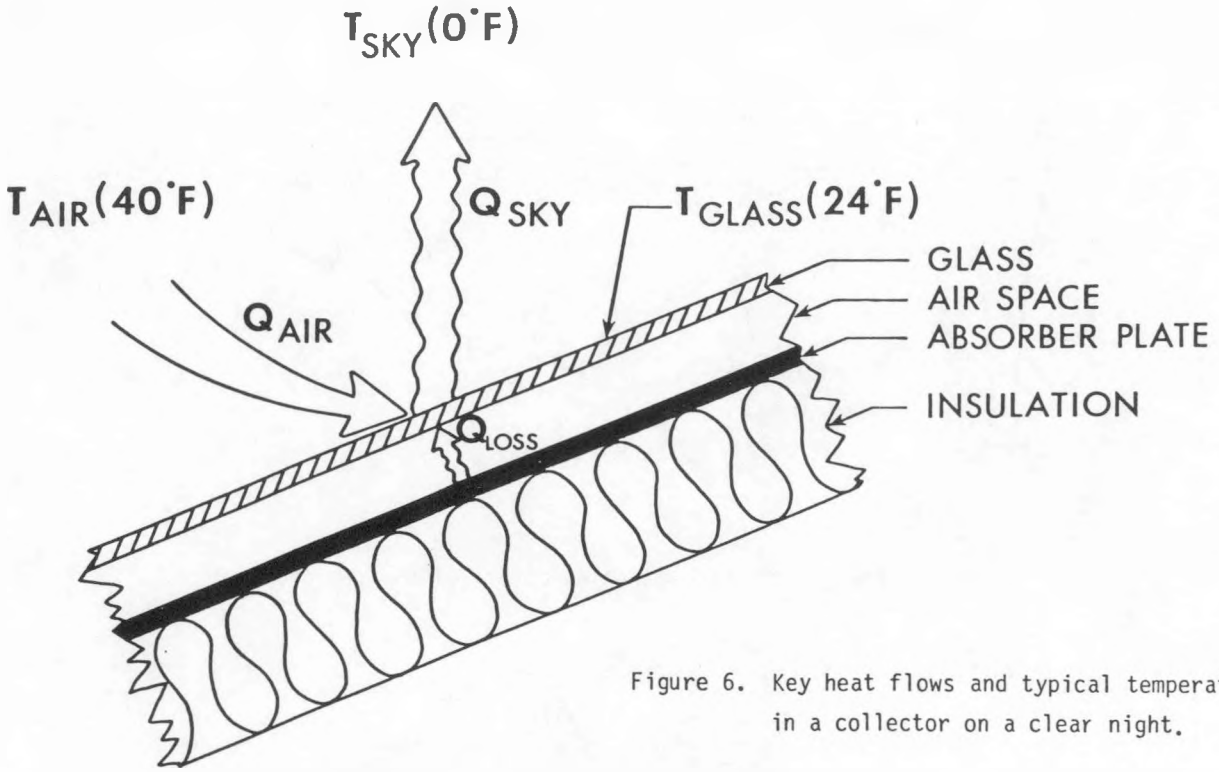

Figure 6. Key heat flows and typical temperatures in a collector on a clear night.

System Isometric

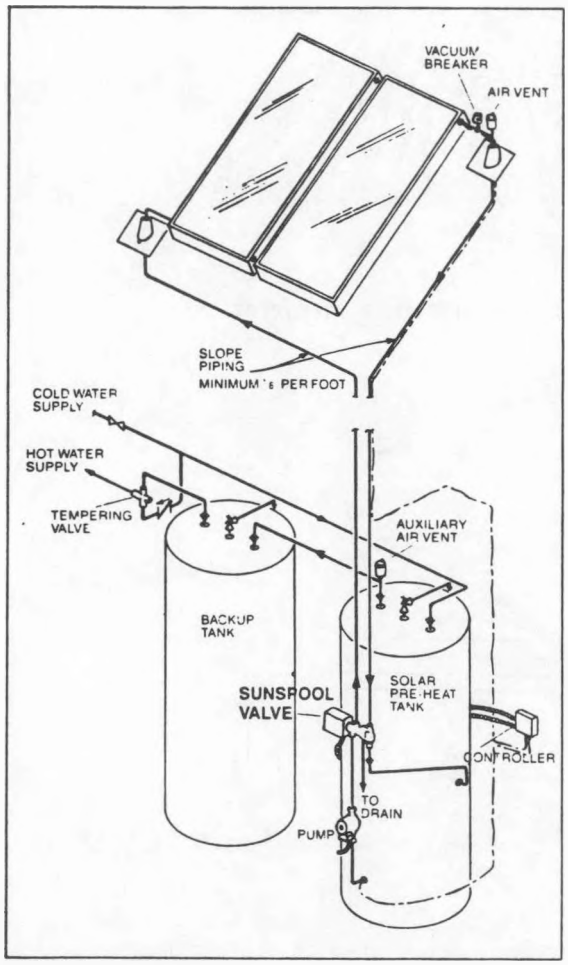

Figure 7. Active drain-down SDHW system.

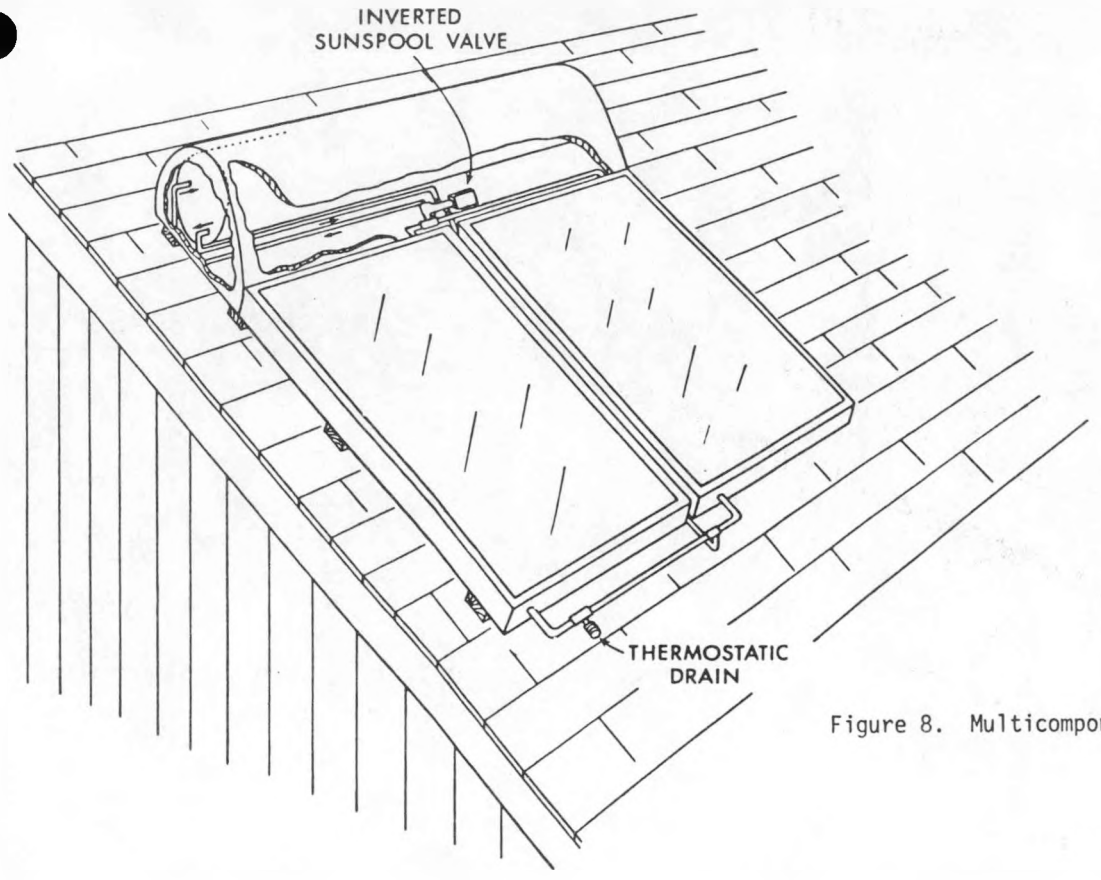

Figure 8. Multicomponent drain-down approach.

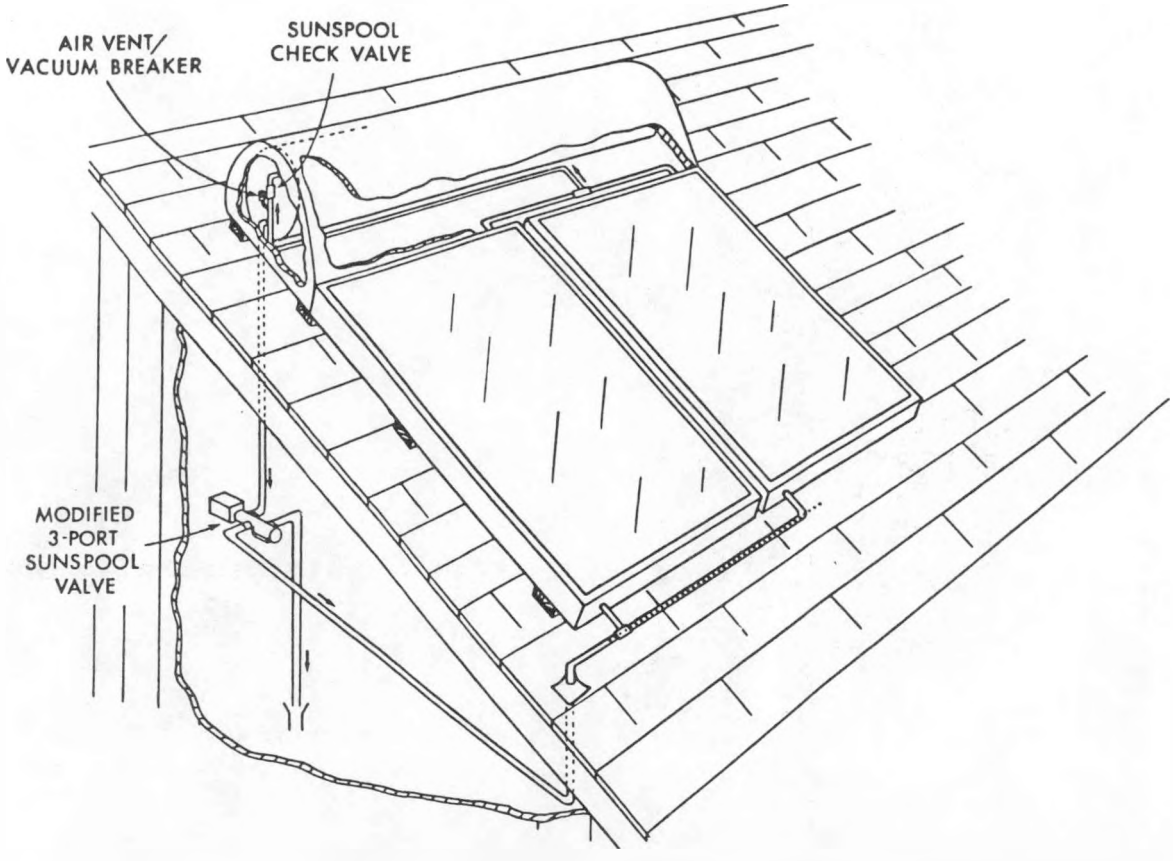

Figure 9. Modified three-port Sunspool valve arrangement

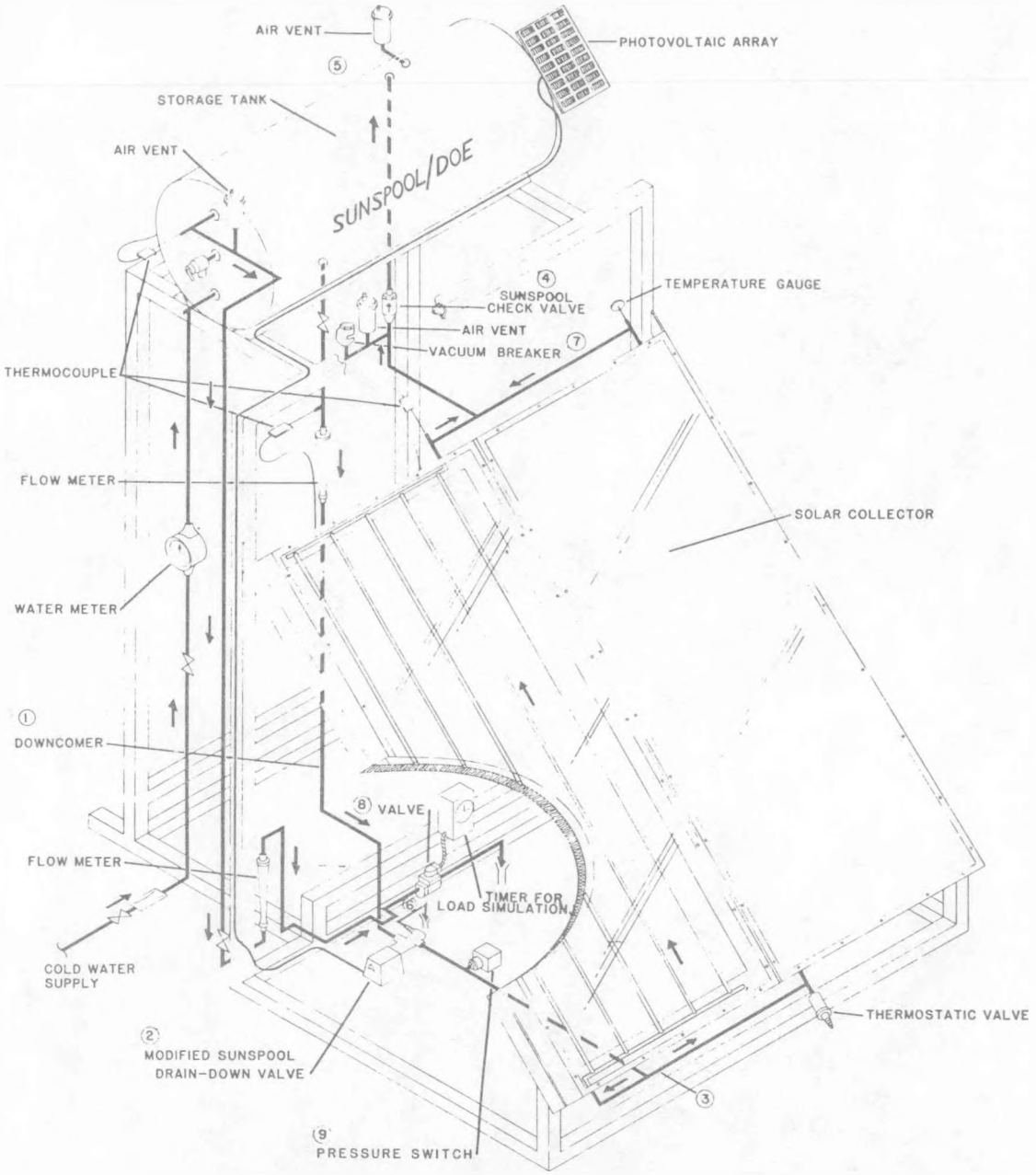

Figure 10. Isometric Drawing of Thermosyphon Test Stand

Cross Section

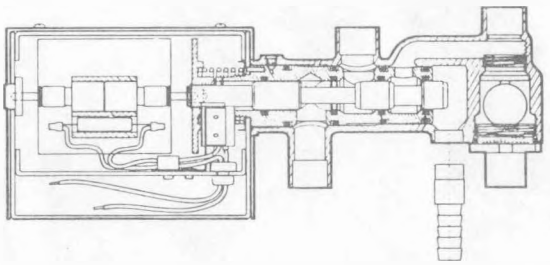

Figure 11. Cross section of standard Sunspool valve.

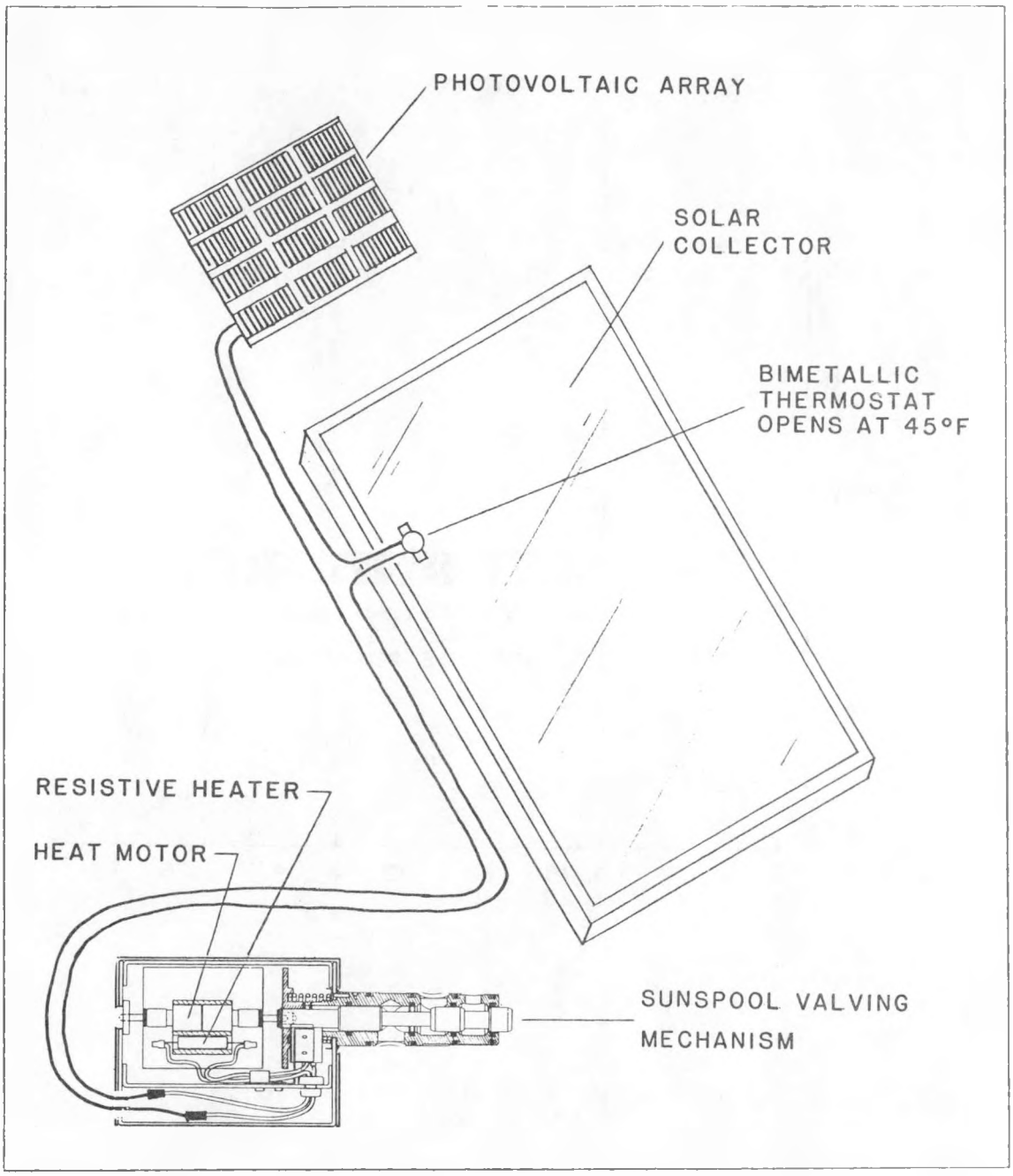

Figure 12. Photovoltaic-based Actuator Concept

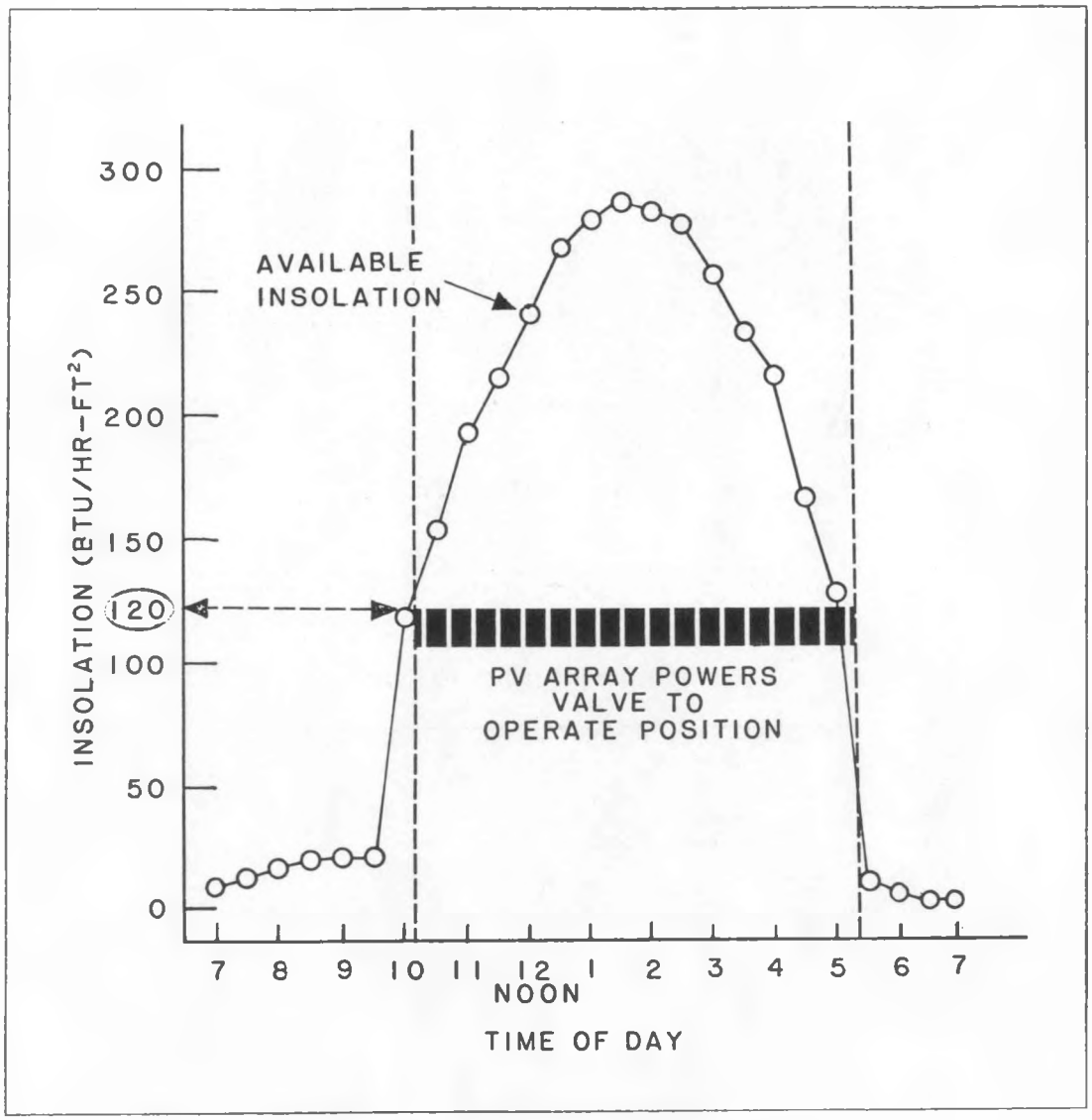

Figure 13. Operating Characteristics of Photovoltaic System

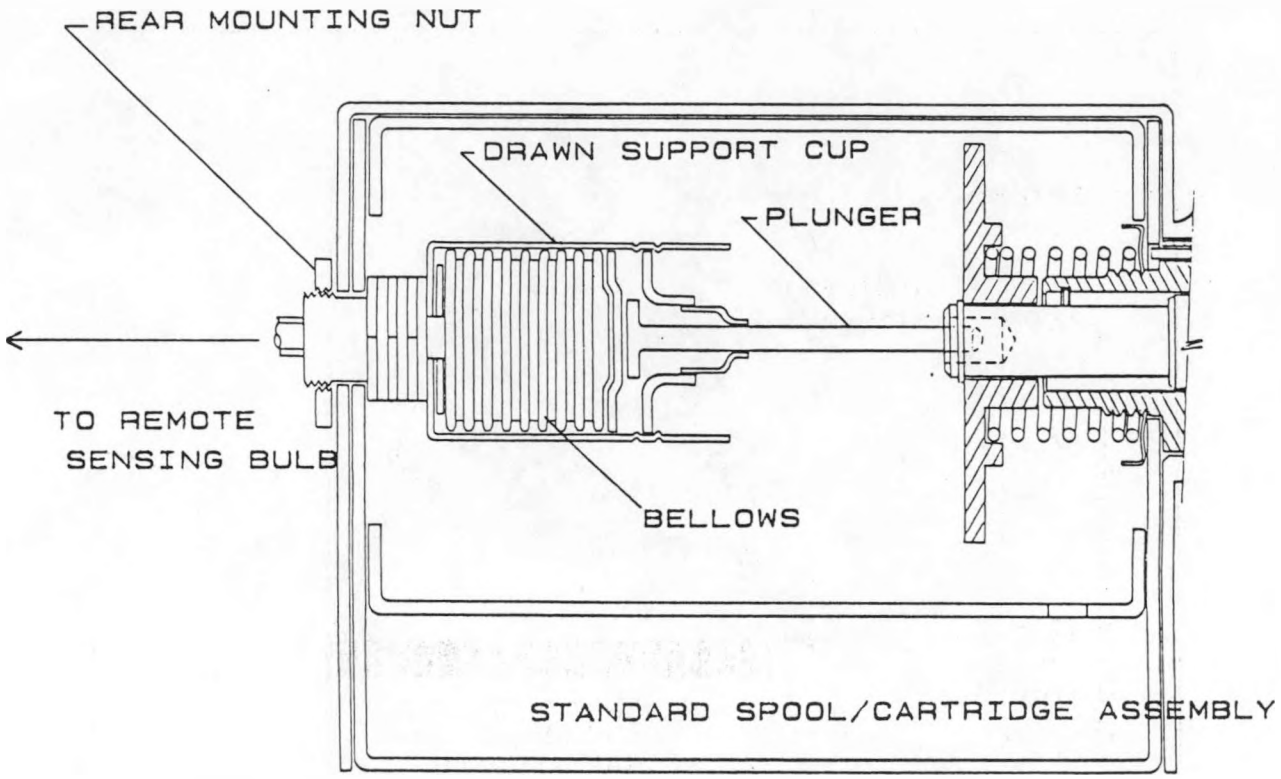

Figure 14. Preliminary Bellows Drive Assembly

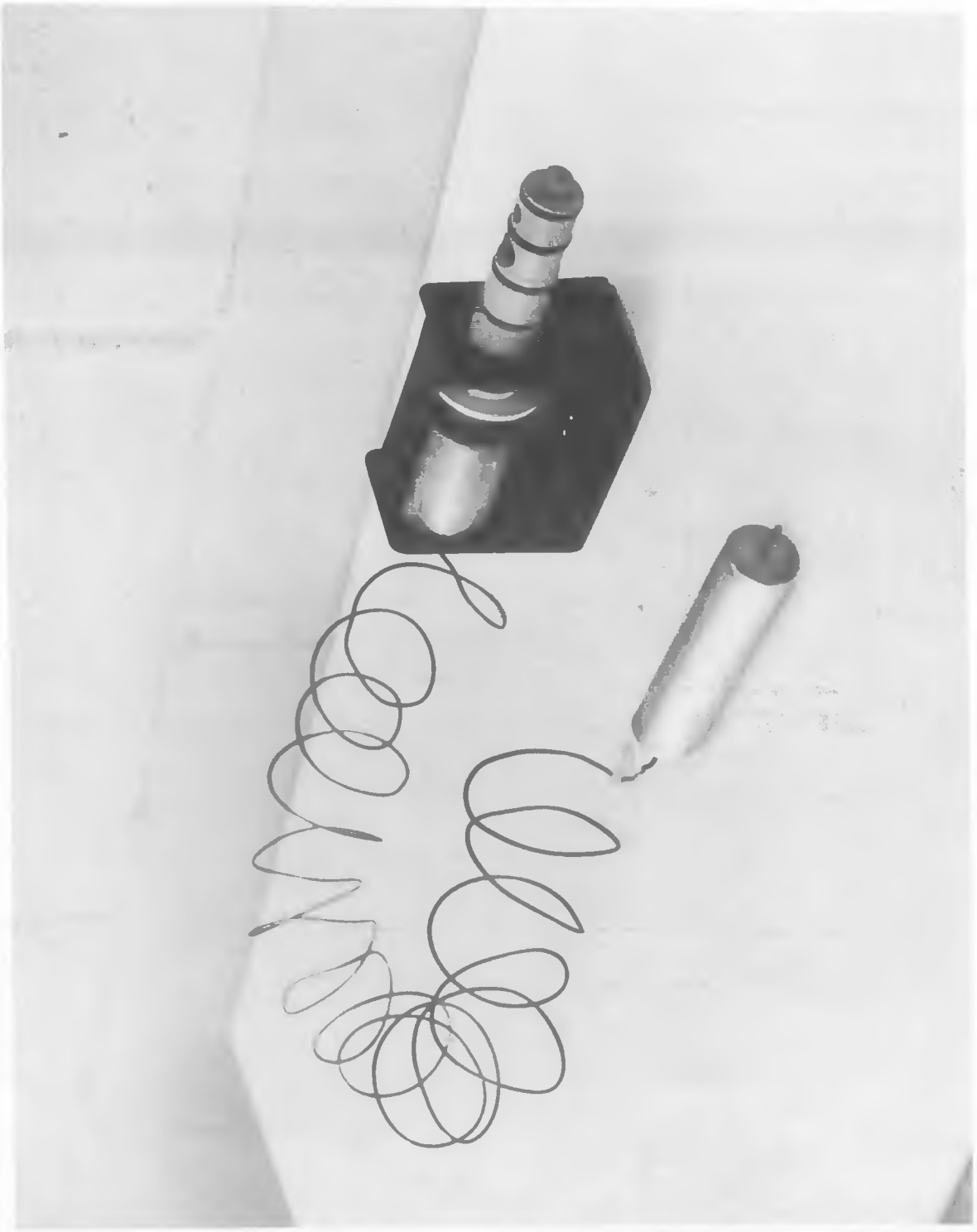

Figure 15. Prototype Bellows Assembly

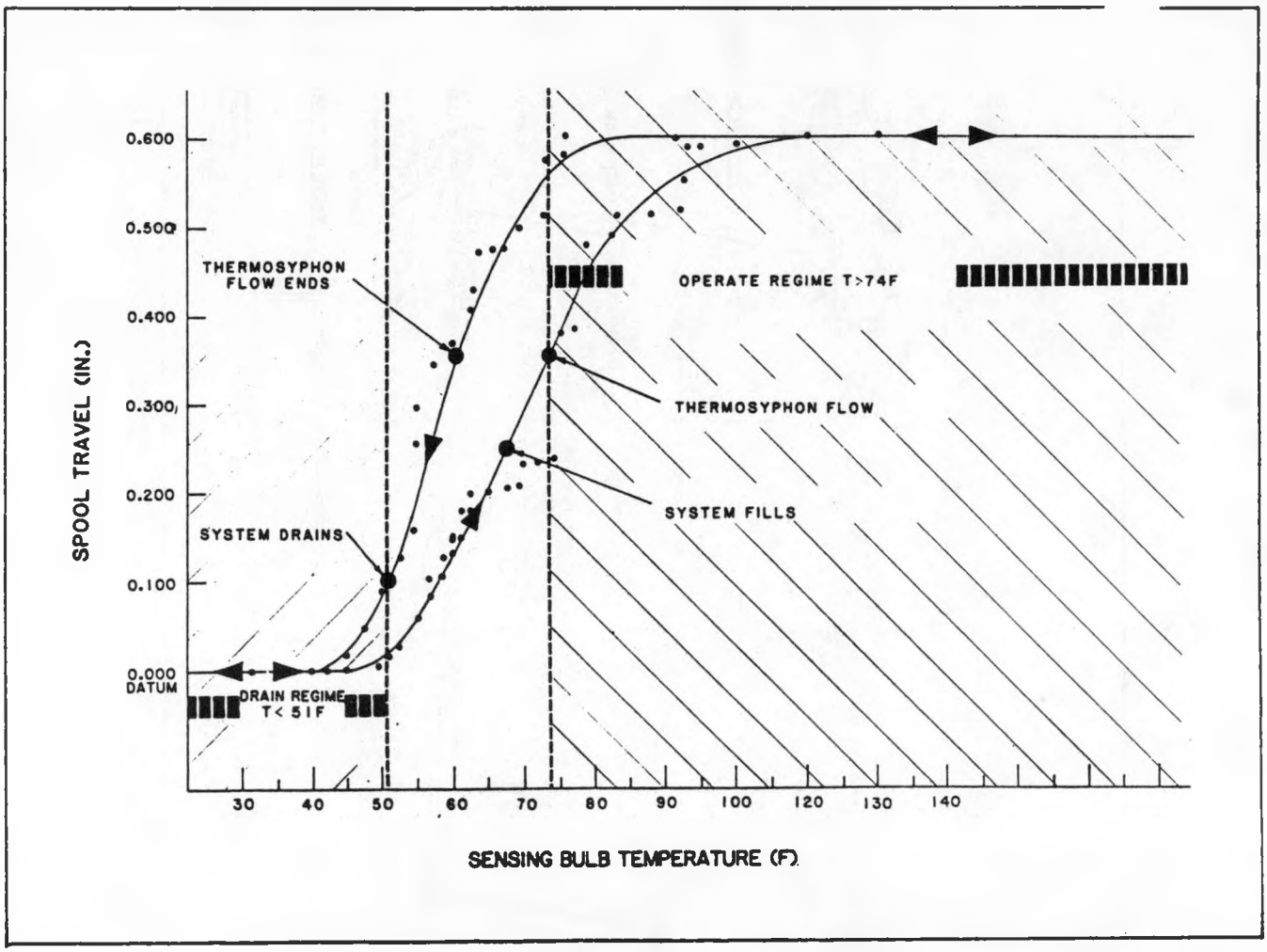

Figure 16. Plot of Spool Travel vs. Sensing Bulb Temperature

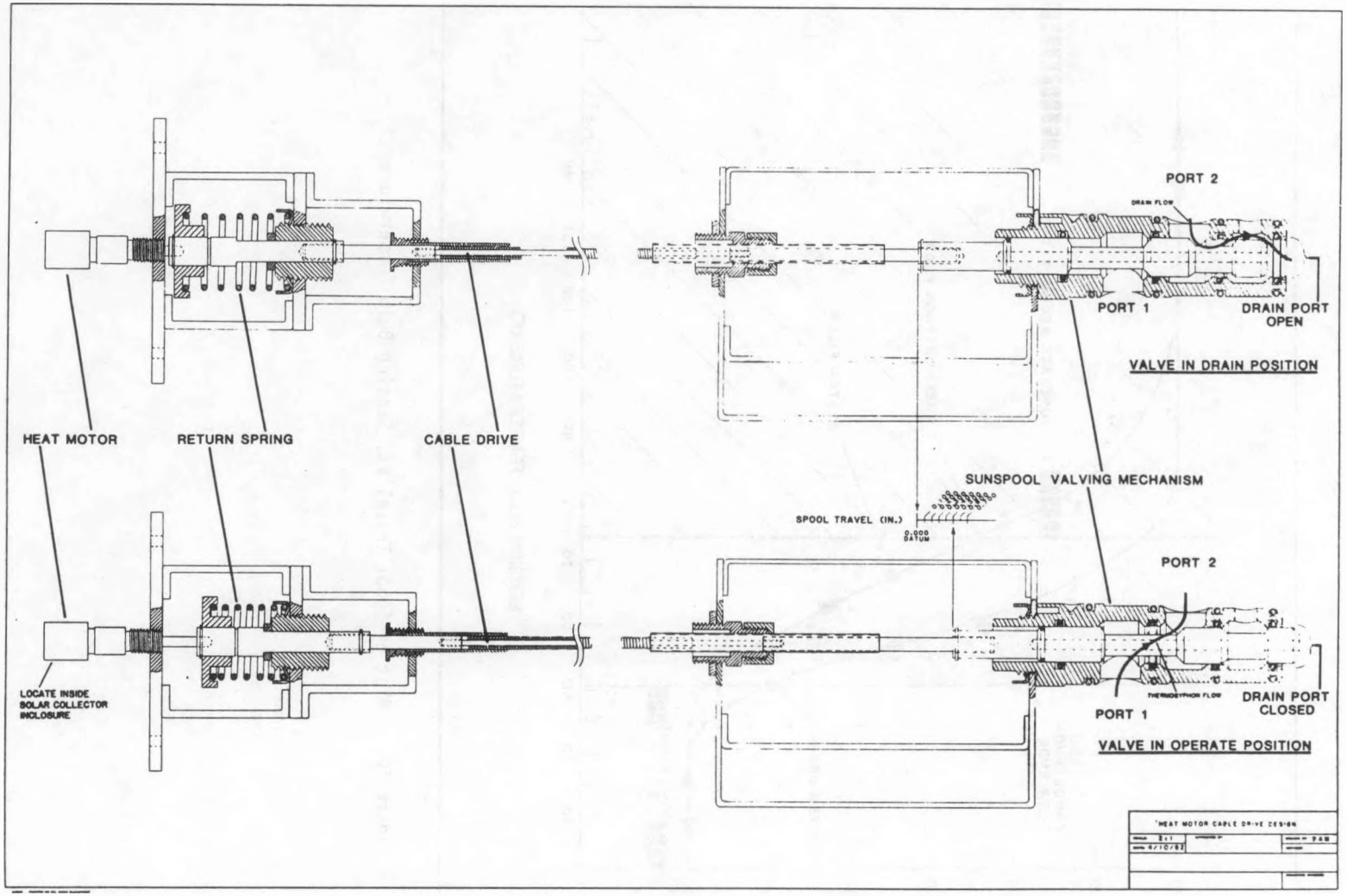

Figure 17. Heat Motor Drive Assembly Drawing

PASSIVE AND HYBRID SOLAR ENERGY UPDATE

Washington, D.C.
September 15 - 17, 1982

A G E N D A

TUESDAY, SEPTEMBER 14, 1982

6:00 - 8:00 pm REGISTRATION

WEDNESDAY, SEPTEMBER 15, 1982

7:15 - 8:00 am REGISTRATION (Cont'd)

SESSION I: OVERVIEW, ASSESSMENT, PLANNING
Robert Holliday (DOE-HQ) - Moderator

8:00 - 8:15 am "Welcome and Introduction"
Frederick Morse, U. S. Department of Energy

8:15 - 8:30 am "Planning Overview"
Robert Holliday, U. S. Department of Energy

8:30 - 9:00 am "Status of Passive Solar Industries"
Layne Ridley, Passive Solar Industries Council

9:00 - 9:30 am "Residential Passive Solar in the Marketplace"
Mike Bell, National Association of Home Builders

9:30 - 10:00 am "Potential Benefits of Fundamental Research for Passive Solar Heating and Cooling"
Don Neeper, Los Alamos National Laboratory

10:00 - 10:30 am COFFEE BREAK

10:30 - 11:10 am "Passive Cooling Assessment for Office Buildings"
William C. Carroll, Lawrence Berkeley Laboratory

SESSION II: DESIGN & ANALYSIS TOOLS
Janet Neville (DOE-SAN) - Moderator

11:10 - 11:30 am "Energy Performance Standards for New Buildings"
James Binkley, U. S. Department of Energy, Architectural and Systems Engineering

11:30 - 12:00 N "Building Energy Analysis: Simulation Validation"
Ron Judkoff, SERI
Bruce D. Hunn, Los Alamos National Laboratory

12:00 - 1:30 pm LUNCHEON
"Energy and Endowment: In the Evolution of Our Past, in the Myths of Our Present, in the Trajectories of Our Future"
David S. Scott, University of Toronto

1:30 - 2:00 pm "Passive Cooling by Natural Ventilation"
Subrato Chandra, University of Central Florida

2:00 - 2:40 pm "Earth Contact Systems"
George Meixel, University of Minnesota
Thomas Bligh, Massachusetts Institute of Technology

2:40 - 3:00 pm	"Skytherm Cooling Season Results" Thomas Mancini, New Mexico State University
3:00 - 3:30 pm	COFFEE BREAK
3:30 - 4:00 pm	"Summary of Results from the Spectral and Angular Sky Radiation Measurement Program" Marlo R. Martin, Lawrence Berkeley Laboratory
4:00 - 4:30 pm	"Natural Convection in Buildings" Ron Kammerud, Lawrence Berkeley Laboratory
4:30 - 5:00 pm	"Daylighting Strategies" Wayne Place, Lawrence Berkeley Laboratory

THURSDAY, SEPTEMBER 16, 1982

SESSION III: NON-RESIDENTIAL BUILDINGS
Ted Kurkowski (DOE-CHO) - Moderator

8:00 - 8:20 am	"The DOE Commercial Buildings Program" Harry T. Gordon, Burt Hill Kosar Rittelmann
8:20 - 8:50 am	"The Performance of the Johnson Controls Regional Office, Salt Lake City, Utah" John Schade, Johnson Controls, Inc., and California Energy Commission
8:50 - 9:10 am	"The Performance of the Security State Bank, Wells, Minnesota" John Weidt, John Weidt Associates, Inc.
9:10 - 9:30 am	"Advanced Performance Evaluation of the Security State Bank, Wells, Minnesota, and the Johnson Controls Branch Office, Salt Lake City, Utah" Tom Hartman, ESG, Inc.
9:30 - 10:00 am	"The TVA Passive Solar Commercial Buildings Program" Kaihan Strain, Tennessee Valley Authority "Design Guidelines for Commercial Buildings" Robert Floyd, Tennessee Valley Authority
10:00 - 10:30 am	COFFEE BREAK
10:30 - 10:55 am	"Design and Performance Evaluation of the Gunnison County Airport Terminal, Gunnison, Colorado" Leon Waller, Associated Architects of Crested Butte
10:55 - 11:20 am	"The Performance of the Community United Methodist Church Addition in Columbia, Missouri" Nicholas Peckham, Peckham & Wright Architects
11:20 - 11:45 am	"The Performance of a Retrofit Office/Store in Wausau, Wisconsin" Bruce D. Kieffer, North Design
11:45 - 12:10 pm	"Energy and Architecture: The AIA Professional Education Program" Huber Buehrer, Buehrer & Stough
12:10 - 1:30 pm	LUNCHEON

SESSION IV: RESIDENTIAL BUILDINGS
Ron Lutha (DOE-CHO) - Moderator

1:30 - 1:55 pm	"Manufactured Buildings Analysis" Rob DeKieffer, SERI
1:55 - 2:20 pm	"The Passive Solar Manufactured Residential Modular Buildings in Richmond, Virginia" J. Durwood Usry, Usry Inc.
2:20 - 2:45 pm	"The Passive Solar Manufactured Residential Panelized Buildings in Boulder, Colorado" Art Milliken and Jon Slote, Acorn Structures, Inc.
2:45 - 3:10 pm	"The National Solar Data Network (NSDN) Program" Edward Pollock, Vitro Laboratories
3:10 - 3:35 pm	COFFEE BREAK
3:35 - 4:00 pm	"The Consumer Perspective" Carol Ann Shindelar, Better Homes & Gardens
4:00 - 4:25 pm	"Residential Impact Analysis for Electric Utilities" Gary Purcell, Electric Power Research Institute Peter DeDuck, JBF Scientific Corporation
4:25 - 4:50 pm	"Passive Solar Technology Transfer" Peter Rush, Sumner, Rider and Associates
7:00 - 9:00 pm	BANQUET "Gentle Architecture" Malcolm Wells

FRIDAY, SEPTEMBER 17, 1982

SESSION V: MATERIALS AND COMPONENTS
Richard Schassburger (DOE-CHO) - Moderator

8:00 - 8:30 am	"Solid State Phase Change Materials Research" Dave Benson, SERI
8:30 - 9:00 am	"High Performance Windows for Passive Solar" Steve Brown
9:00 - 9:30 am	"Radiative Cooling Materials" John A. Compton, Energy Materials Research Co.
9:30 - 10:00 am	"Thermal Testing of Passive/Hybrid Solar Components" Mike McCabe, National Bureau of Standards
10:00 - 10:30 am	COFFEE BREAK
10:30 - 11:00 am	"Apertures" Carl Lambert, Lawrence Berkeley Laboratory
11:00 - 11:30 am	"Variable Transmittance Electrochromic Windows" R. David Rauh, EIC Laboratory, Inc. Ronald Goldner, Tufts University
11:30 - 12:00 N	"Coordinating Council for the National Program Plan for Thermal Envelope Systems and Materials: A Report" Jean Boulin, U.S. Department of Energy, Thermal Envelope Systems & Diagnostics
12:00 - 1:00 pm	LUNCHEON

SESSION VI: PANEL, DISCUSSION, SUMMARY

Paul Kando (National Association of Home Builders Research Foundation) - Moderator

1:00 - 2:00 pm PANEL DISCUSSION: PERSPECTIVES AND PROSPECTS IN PASSIVE & HYBRID SOLAR

Janet Neville, DOE-SAN
Ted Kurkowski, DOE-CHO
Bill Whiddon, Whiddon & Associates
Mike Bell, National Association of Home Builders
Richard Anderson, Flack and Kurtz
Walter B. Ingle, Rockwell International/ETEC
Earle Kennett, AIA Foundation
Ron Kammerud, Lawrence Berkeley Laboratory
Don Neeper, Los Alamos National Laboratory
Larry Flowers, SERI

2:00 - 2:30 pm Open Discussion (Questions to the Panel)

2:30 - 3:00 pm Summary and Closing Remarks
Lawnie Taylor, U.S. Department of Energy

PASSIVE AND HYBRID SOLAR ENERGY UPDATE

Washington, D.C.
September 15 - 17, 1982

P A R T I C I P A N T L I S T

FRED ABEL
U.S. DEPT. OF ENERGY
1000 INDEPENDENCE AVE SW
WASHINGTON, DC 20585
202/252-9417

ERV BALES
HAINES/LUNDBERG/WAEHLER
2 PARK AVENUE
NEW YORK, NY 10016
212/696-8588

MIKE BELL
NATL. ASSOC. HOME BUILDERS
15TH & M STS. NW
WASHINGTON, DC 20006
202/822-0246

THOMAS BLIGH
MASS. INST. OF TECHNOLOGY
77 MASSACHUSETTS AVE.
CAMBRIDGE, MA 02139
617/253-2018

STEVE BROWN
SOUTHWALL CORPORATION
3961 EAST BAYSHORE RD.
PALO ALTO, CA 94303
415/962-9111

ARNOLD P. CAPUTO
NATL. CONCRETE MASONRY ASS.
2302 HORSEPEN RD. BOX 781
HERNDON, VA 22043
703/435-4900

CLIFTON CARWILE
U.S. DEPT. OF ENERGY
1000 INDEP. AVE. CE311
WASHINGTON, DC 20585
202/252-8171

JOHNSON CHEN
PENNWALT CORP.
900 1ST AVE.
KING OF PRUSSIA, PA 19406
215/337-6735

KATHY CURLANDER
ROCKWELL INTERNATL/ETEC
P.O. BOX 1449 T487
CANOGA PARK, CA 91304
213/700-5347

ROB DEKIEFFER
SERI
1617 COLE BLVD.
GOLDEN, CO 80401
303/231-7062

WILLIAM ANCARROW
ONE DESIGN, INC.
MOUNTAIN FALLS RD.
WINCHESTER, VA 22601
703/877-2172

CALVIN BEATTY
BERRY SOLAR PRODUCTS
2850 WOODBRIDGE AVE.
EDISON, NJ 08837
201/549-3800

DAVE BENSON
SERI
1617 COLE BLVD.
GOLDEN, CO 80401
303/231-1162

SHEILA BLUM
TPI
5010 SUNNYSIDE AVE.
BELTSVILLE, MD 20750
301/345-5200

HUBER BUEHRER
BUEHRER & STOUGH
4246 SYLVANIA AVE
TOLEDO, OHIO 43623
419/473-2751

MEIR CARASSO
SERI
1617 COLE BLVD.
GOLDEN, CO 80401
303/231-1353

SUBRATO CHANDRA
UNIV. CENT. FLORIDA/FSEC
300 STATE RD. 401
CAPE CANAVERAL, FL 32920
305/783-0300

JOHN A. COMPTON
ENERGY MATERIALS RES. CO.
2547 EIGHTH ST.
BERKELEY, CA 94710
415/644-2244

ERROL DAVIS
U.S. DEPT. OF ENERGY
1000 INDEP. AVE. MS 5H-030
WASHINGTON, DC 20585
505/846-5221

HARRY A. DERDARIAN
DEPARTMENT OF ENERGY
1000 INDEP. AVE/CE311 MS5H030
WASHINGTON, D.C. 20585
202/252-5000

RICHARD ANDERSON
FLACK & KURTZ
475 FIFTH AVE.
NEW YORK, NY 10017
212/532-9600

E. W. BEHRENS
ARMSTRONG WORLD INDUSTRIES
2500 CLUMBIA AVE.
LANCASTER, PA 17604
717/397-0611 x5817

JAMES BINKLEY
U.S. DEPT. OF ENERGY
1000 INDEPENDENCE AV SW
WASHINGTON, DC 20585
202/252-9835

JEAN BOULIN
U.S. DEPT. OF ENERGY
1000 INDEPENDENCE AV SW
WASHINGTON, DC 20585
202/252-9187

CHARLES BURNETTE
CHARLES BURNETTE & ASSOC.
234 S. THIRD ST.
PHILA., PA 19106
215/925-0844

W. C. CARROLL
LAWRENCE BERKELEY LAB.
UNIV. OF CALIFORNIA
BERKELEY, CA 94720
415/486-4890

CECELIA CHANEY
MCC ASSOCIATES, INC.
8534 SECOND AVE.
SILVER SPRING, MD 20910
301/589-8130

CARL W. CONNER
U.S. DEPT. OF ENERGY
1000 INDEP. AVE. CE311
WASHINGTON, DC 20585
202/252-8156

PETER DEDUCK
JBF SCIENTIFIC CORP.
2 JEWEL DRIVE
WILMINGTON, MA 01887
617/657-4170

ROBERT D. DIKKERS
NATIONAL BUR. OF STANDARDS
BLDG. 226, RM B320
WASHINGTON, DC 20234
301/921-3285

Gene Doering
U.S. Dept. of Energy
1000 Independence Ave. SW
Washington, D.C. 20585
202/252-8150

Mary Ann Eichenberger
American Inst. of Architects
1735 New York Ave NW
Washington, DC 20016
202/626-7300

Frank H. Faust
ASHRAE
212 Daleview Lane
Louisville, KY 40207
502/896-9888

Robert N. Floyd
Robert N. Floyd AIA
3317 Crestone Circle
Chattanooga, TN 37411
615/624-5918

Ronald B. Goldner
Tufts University
Dept. of Elec. Engrng.
Medford, MA 02155
617/628-5000 x2492

Joan T. Grim
NRMCA
900 Spring St.
Silver Spring, MD 20910
301/587-1400

Joseph H. Hart
VEPCO
P.O. Box 26666
Richmond, VA 23261
804/771-4422

Harold R. Hay
Skytherm Processes & Engrng
2424 Wilshire Blvd.
Los Angeles, CA 90057
213/389-2300

Tom Holland
Honeywell Inc./Tech Strat.
1700 W. Highway 36
St. Paul, MN 55113
612/378-4267

Dick Holt
U.S. Dept. of Energy
1000 Indep. Ave. PE 35
Washington, DC 20585
202/252-6296

Norman Hughes
U.S. Dept. of Energy
1000 Independence Av SW
Washington, DC 20585
202/252-5000

Walter J. Draving
Phila. Electric Co.
2301 Market St. 518-1
Philadelphia, PA 19101
215/841-5613

Bruce Lloyd Eilert
Lowe's Companies, Inc.
Hwy 268E, Box 1111
North Wilkesboro, NC 28656
919/667-3111 x4551

Bill Fisher
Burt Hill Kosar Rittelmann
440 First St. NW
Washington, DC 20001
202/783-2866

Ernest C. Freeman
U.S. Dept. of Energy
1000 Ind. Ave. BERD/GH-067
Washington, DC 20585
202/252-9432

John C. Goldsmith
U.S. Dept. of Energy
1000 Independence Av/SF-044
Washington, DC 20585
202/252-8170

Blair Hamilton
Memphremagog Group
P.O. Box 456
Newport, VT 05855
802/334-8821

Tom Hartman
ESG, Inc.
61 Perimeter Park
Atlanta, GA 30341
404/458-8765

Steve Heibein
Innovative Design
4904 Waters Edge Drive
Raleigh, NC 27606
919/851-4572

William D. Holland
Central Pension Fund
4115 Chesapeake St.
Washington, DC 20016
202/362-1000

John K. Holton
Burt Hill Kosar Rittelmann
440 1st St. NW #500
Washington, DC 20001
202/783-2866

Bruce D. Hunn
Los Alamos National Lab.
Solar Energy Group Q-11
Los Alamos, NM 87545
505/667-6441

Gerald W. Duray
Decision Planning Corp.
c/o DOE, 9800 S. Cass St.
Argonne, IL 60439
312/972-2707

Guy Ervin, III
Rockwell Internatl/ETEC
P.O. Box 1449 MS T036
Canoga Park, CA 91304
213/700-5532

Larry Flowers
SERI
1617 Cole Blvd.
Golden, CO 80401
303/231-1081

David Gallagher
Architects Group Practice
P.O. Box 1264
Alexandria, VA 22313
703/549-0809

Harry T. Gordon
Burt Hill Kosar Rittelmann
440 1st St. NW #500
Washington, DC 20001
202/783-2866

G. Kimball Hart
Hart, McMurphy, & Parks
4330 East-West Hwy 914
Bethesda, MD 20914
301/656-0922

Robert Hassett
U.S. Dept. of Energy
1000 Independence Ave. SW
Washington, DC 20585
202/252-8163

Joseph W. Hobson
Asphalt Roofing Mfg. Assoc.
1800 Mass. Ave. NW
Washington, DC 20036
202/264-0464

Robert O. Holliday
U.S. Dept. of Energy
1000 Independ. Av MS 5H-030
Washington, DC 20585
202/252-2423

David Holzman
Solar Age Magazine
Church Hill
Harrisville, NH 03450
202/234-6799

Walter B. Ingle
Rockwell Internatl/ETEC
8900 De Soto Ave. Bldg T036
Canoga Park, CA 91304
213/700-5525

ARY-MARGARET JENIOR
U. S. DEPT. OF ENERGY
1000 INDEP. AVE. P&HSED/CE
WASHINGTON, DC 20585
202/252-2998

RON KAMMERUD
LAWRENCE BERKELEY LAB.
1 CYCLOTRON RD
BERKELEY, CA 94720
415/486-6620

HELEN KESSLER
UNIV. OF ARIZ/ENV RES LAB
TUCSON INTERNATL. AIRPORT
TUCSON, AZ 85706
602/626-2931

JERRY KLINE
ENERGY & HOUSING REPORT
1016 16TH ST. NW #225
WASHINGTON, DC 20036
202/659-0659

TED L. KURKOWSKI
DEPT. OF ENERGY/CHICAGO OPS.
9800 S. CASS AVENUE
ARGONNE, IL 60439
312/972-2028

TERRY LEVINSON
U.S. DEPT. OF ENERGY
1000 INDEP. AVE. SW
WASHINGTON, DC 20585
202/252-5000

JAMES D. LONG
NAVAL FACIL. ENGRNG. COMM.
200 STOVALL RD.
ALEXANDRIA, VA 22332
202/325-0057

BAL M. MAHAJAN
NATIONAL BUREAU STANDARDS
BLDG 226 RM B326
WASHINGTON, DC 20234
301/921-3293

TOM MANCINI
NEW MEXICO STATE UNIVERSITY
P.O. BOX 3450
LAS CRUCES, NM 88001
505/646-3501

MERLE F. MCBRIDE
OWENS-CORNING FIBERGLAS TC
P.O. BOX 415
GRANVILLE, OH 43023
614/587-7083

LARRY S. MCGEE
PPG INDUSTRIES, INC.
ONE GATEWAY CENTER
TSBURGH, PA 15222
/434-2298

EDWARD E. JOHANSON
JBF SCIENTIFIC CORP.
2 JEWEL DRIVE
WILMINGTON, MA 01887
617/657-4170

PAUL KANDO
NAHB RES. FOUNDATION
6509 SEVEN LOCKS RD.
CABIN JOHN, MD 20818
301/762-4200

BRUCE D. KIEFFER
BALL STATE UNIVERSITY
COLLEGE OF ARCHITECTURE
MUNCIE, IN 47306
317/285-4481

HALIM YAN KORZYBSKI
DESIGN CONSTRUCTION
6812 LITTLE RIVER TRNPK.
ANNANDALE, VA 22003

CARL M. LAMPERT
LAWRENCE BERKELEY LAB.
UNIVERSITY OF CALIFORNIA
BERKELEY, CA 94720
415/486-6093

EDWARD J. LISEE
ACEC RESEARCH & MGT. FOUND.
1015 15TH ST. NW
WASHINGTON, DC 20005
202/347-7474

PETER J. LUNDE
NEW ENERGY RESOURCES, INC.
4 DANIEL LANE
WEST SIMSBURY, CT 06092
203/658-5232

TIM MALONEY
ONE DESIGN, INC.
MOUNTAIN FALLS ROUTE
WINCHESTER, VA 22601
703/877-2172

MARLO R. MARTIN
LAWRENCE BERKELEY LAB.
UNIVERSITY OF CALIFORNIA
BERKELEY, CA 94720
415/486-5137

MICHAEL MCCABE
NATIONAL BUR. OF STANDARDS
BLDG 226 RM A319
WASHINGTON, DC 20234
301/921-2308

GEORGE D. MEIXEL, JR.
UNIV. OF MINNESOTA/USC
128 PLEASANT ST. SE
MINNEAPOLIS, MN 55455
612/376-1200

RON JUDKOFF
SERI
1617 COLE BLVD.
GOLDEN, CO 80401
303/231-1090

EARLE KENNETT
AIA FOUNDATION
1735 NEW YORK AVE. NW
WASHINGTON, DC 20016
202/626-7300

GLORIA N. KILBURN
BOOZ-ALLEN & HAMILTON
311 1ST ST. NW
WASHINGTON, DC 20001
202/624-0643

JAMES KOSINSKI
DOW CHEMICALS/U.S.A.
LARKIN LABS.
MIDLAND, MI 48640
517/636-1210

LOUIS H. LAYTON
ARMY CORPS OF ENGRS/HOUSING
6906 BEACON PLACE
RIVERDALE, MD 20737
301/459-0788

ELIZABETH LONG
ENERGY TODAY NEWSLETTER
233 NATIONAL PRESS BLDG.
WASHINGTON, DC 20045
202/393-0031

RON LUTHA
DEPT. OF ENERGY/CHICAGO OPS.
9800 SOUTH CASS AVENUE
ARGONNE, IL 60439
312/972-2323

HEIDI MALONI
MCC ASSOCIATES, INC.
8534 SECOND AVE.
SILVER SPRING, MD 20910
301/589-8130

MIKE MAYBAUM
COSENTINI ASSOCIATES
2 PENN PLAZA
NEW YORK, NY 10121
212/564-7200

MARIANNE B. MCCARTHY
MCC ASSOCIATES, INC.
8534 SECOND AVE. #400
SILVER SPRING, MD 20910
301/589-8130

JOHN MILLHONE
U.S. DEPT. OF ENERGY
1000 INDEPENDENCE AVE. SW
WASHINGTON, DC 20585
202/252-9444

ART MILLIKEN
ACORN STRUCTURES, INC.
P.O. BOX 250
CONCORD, MA 07142
617/369-4111

FREDERICK H. MORSE
U.S. DEPT. OF ENERGY
1000 INDEPENDENCE AV SW
WASHINGTON, DC 20585
202/252-5000

JANET NEVILLE
DEPT. OF ENERGY/SF OPS.
1333 BROADWAY
OAKLAND, CA 94612
415/273-7946

S. H. PANSKY
BATTELLE/PNL
P.O. BOX 999
RICHLAND, WA 99352
509/376-4665

WAYNE PLACE
LAWRENCE BERKELEY LAB.
ONE CYCLOTRON RD.
BERKELEY, CA 94720
415/486-5669

ARI RABL
PRINCETON UNIVERSITY

PRINCETON, NJ 08512
609/452-6422

KIRK RENAUD
BOOZ, ALLEN & HAMILTON
4330 EAST-WEST HWY
BETHESDA, MD 20814
301/951-2081

CLAUDE ROBBINS
SERI
1617 COLE BLVD.
GOLDEN, CO 80401
303/231-1090

SHERRY ROSSI
VITRO LABORATORIES
14000 GEORGIA AVE.
SILVER SPRING, MD 20910
301/871-5422

JOHN SCHADE
CALIF. ENERGY COMMISSION
922 VANDERBILT WAY
SACRAMENTO, CA 95825
916/924-2595

MICHAEL SEDMAK
BOOZ, ALLEN & HAMILTON
311 FIRST ST. NW
WASHINGTON, DC 20001
202/624-0610

JAMES S. MOORE, JR.
MUELLER ASSOC., INC.
600 MARYLAND AVE. SW
WASHINGTON, DC 20024
202/484-9484

HARRIET MURPHY
MCC ASSOCIATES, INC.
8534 SECOND AVE.
SILVER SPRING, MD 20910
301/589-8130

JOHN C. ODEGAARD
MAYHILL HOMES CORP.
P.O. BOX 1778 CANDLER RD.
GAINESVILLE, GA 30503
404/536-9871

NICHOLAS PECKHAM
PECKHAM & WRIGHT ARCHITECTS
1104 EAST BROADWAY
COLUMBIA, MO 65201
314/449-2683

EDWARD POLLOCK
VITRO LABORATORIES
14000 GEORGIA AVE.
SILVER SPRING, MD 20910
301/871-4522

R. DAVID RAUH
EIC LABORATORIES, INC.
111 CHAPEL ST.
NEWTON, MA 02158
617/965-2710

BRUCE RICH
VVKR INC.
1 EAST LEXINGTON ST.
BALTIMORE, MD 21202
301/621-4353

MICHAEL ROBERTS
AMER. STANDARDS TEST. BUR.
40 WATER ST.
NEW YORK, NY 10004
212/943-3156

PETER RUSH
SUMNER RIDER & ASSOC.
355 LEXINGTON AVE.
NEW YORK, NY 10017
212/661-5300

RICHARD J. SCHASSBURGER
DOE/CHICAGO OPERATIONS OFF.
9800 SOUTH CASS AVE.
ARGONNE, IL 60439
312/972-2570

JEFFREY M. SEISLER
ANALYTECH MGT CONSULTING
215 N. WEST ST.
ALEXANDRIA, VA 22314
703/836-7962

MILTON C. MORRISON
ARCH. ALUM. MFGRS. ASSOC.
4329 LOYOLA AVE.
ALEXANDRIA, VA 22304
703/370-4975

DONALD A. NEEPER
LOS ALAMOS NATL. LAB.
MAIL STOP 571
LOS ALAMOS, NM 87545
505/667-2242

JOHN C. O'NEILL
CHAS. E. SMITH MNGT.
1735 JEFF DAVIS HWY
ARLINGTON, VA 22202
703/920-8500

DAVID PELLISH
DEPT. OF ENERGY
1000 INDEPENDENCE AVE. SW
WASHINGTON, DC 20585
202/252-8110

GARY PURCELL
ELECTRIC POWER RES. INST.
P.O. BOX 10412
PALO ALTO, CA 94303
415/855-2168

J. W. REESE
J. W. REESE, CONS. ARCH.
8 BRIGHTON CT.
GAITHERSBURG, MD 20877
301/926-1113

LAYNE RIDLEY
PASSIVE SOLAR IND. COUNCIL
125 S. ROYAL ST.
ALEXANDRIA, VA 22134
703/683-5001

PETER G. ROCKWELL
BURT HILL KOSAR RITTELMANN
440 1ST ST. NW #500
WASHINGTON, DC 20001
202/783-2866

PAUL SABATIUK
MUELLER ASSOC.
1401 S. EDGEWOOD ST.
BALTIMORE, MD 21227
301/646-4500

DAVID S. SCOTT
U. OF TORONTO/HYD. SYST.
203 COLLEGE ST. #204
TORONTO, ONT. M5T 1P9 CAN
416/591-9367

ALEXANDER SHAW
AIA FOUNDATION
1735 NEW YORK AVE NW
WASHINGTON, DC 20006
202/626-7511

EDWARD M. SHIMAMOTO
DELAWARE ENERGY OFFICE
P.O. BOX 1401/ O'NEILL BLDG
DOVER, DE 19901
302/736-5644

JON SLOTE
ACORN STRUCTURES, INC.
P.O. BOX 250
CONCORD, MA 01742
617/369-4111

LINDA J. SMITH
MERIDIAN CORP.
5201 LEESBURG PIKE #400
FALLS CHURCH, VA 22041
703/998-0922

JOHN L. STOOPS
BATTELLE/PACIFIC NW LABS.
P.O. BOX 999
RICHLAND, WA 99352
202/785-8400

LAWNIE H. TAYLOR
U.S. DEPT. OF ENERGY
1000 INDEPENDENCE AV SW
WASHINGTON, DC 20585
202/252-8103

ANNE S. TOWNSEND
ANN TOWNSEND ASSOC., INC.
2772 S. RANDOLPH ST. #209
ARLINGTON, VA 22206
703/998-0552

LEON WALLER
ASSOC. ARCHS. CRESTED BUTTE
207 ELK AVENUE
CRESTED BUTTE, CO 81224
303/349-5353

JOHN L. WEIDT
JOHN WEIDT ASSOC., INC.
401 LAKE VILLAGE CENTER
CHASKA, MN 55318
612/448-6464

WILLIAM WHIDDON
W. I. WHIDDON & ASSOCIATES
4330 EAST-WEST HWY. #914
BETHESDA, MD 20914
301/656-8901

MARLENE ZALEZNICK
BURT HILL KOSAR RITTELMANN
440 1ST ST. NW #500
WASHINGTON, DC 20001
202/783-2866

CAROL ANN SHINDELAR
BETTER HOMES & GARDENS
LOCUST STREET
DES MOINES, IA 50309
515/284-2658

JIM SMITH
U.S. DEPT. OF ENERGY
1000 INDEP. AVE. SW CE111.1
WASHINGTON, DC 20585
202/252-9835

VERLYN SMITH
PMA
1700 17TH ST. NW #505
WASHINGTON, DC 20007
202/745-0500

KAIHAN STRAIN
TVA-SOLAR APPLICATIONS BR
715 MARKET ST.
CHATANOOGA, TN 37401
615/751-5252

DONALD D. TEAGUE
HOUSE SCI & TECH COMMITTEE
B 374 RAYBURN BLDG.
WASHINGTON, DC 20515
202/225-4494

J. DURWOOD USRY
USRY SOLAR CONCEPTS, INC.
P.O. BOX 27463
RICHMOND, VA 23261
804/321-4500

MURIEL JENNINGS WALLER
EARTHTECH RES. CORP.
6655 AMBERTON DR.
BALTIMORE, MD 21227
301/796-5200

STEPHEN D. WEINSTEIN
THE EHRENKRANTZ GROUP
19 WEST 44TH ST.
NEW YORK, NY 10036
212/730-1950

STEVEN WINTER
STEVEN WINTER ASSOC., INC.
6100 EMPIRE STATE BLDG.
NEW YORK, NY 10001
212/564-5800

EDWARD T. ZULKOFSKE
U.S. ARMY ENGR CORPS
20 MASS. AVE. (DAEN-MPE-E)
WASHINGTON, DC 20314
202/272-0428

MICHAEL M. SIZEMORE
SIZEMORE/FLOYD
ONE PIEDMONT CTR. #200
ATLANTA, GA 30305
404/233-7888

KAREN HAAS SMITH
CONSTRUCTION SPECIFIER MAG
6407 3RD ST. NW
WASHINGTON, DC 20012
202/726-6735

JAMES STEWART
ONE DESIGN, INC.
MOUNTAIN FALLS RD.
WINCHESTER, VA 22601
703/87-2172

PHILIP H. SVANOE
IOWA ENERGY POLICY COUNCIL
CAPITOL COMPLEX
DES MOINES, IA 50319
515/281-6682

JANET TERNER
MCC ASSOCIATES, INC.
8534 SECOND AVE. #400
SILVER SPRING, MD 20910
301/589-8130

GEORGE H. VERGINE
G.H. VERGINE, ARCH.
6700 BELCREST RD. #515
HYATTSVILLE, MD 20782
301/559-4898

GEORGE N. WALTON
NATIONAL BUR. OF STANDARDS
BLDG. 226 RM B114
WASHINGTON, DC 20234
202/921-3633

MALCOLM WELLS
MALCOLM WELLS, ARCHITECT
BOX 1149
BREWSTER, MA 02631
617/385-3576

WILLIAM O. WOODS
U.S. ARMY DARCOM
5001 EISENHOWER AVE.
ALEXANDRIA, VA 22301
703/274-8494

*U.S. GOVERNMENT PRINTING OFFICE : 1983 0-381-060/4138